Biological Electron Microscopy

Theory, Techniques, and Troubleshooting
2nd Edition

Biological Electron Microscopy

Theory, Techniques, and Troubleshooting
2nd Edition

Michael J. Dykstra and Laura E. Reuss
North Carolina State University

SPRINGER SCIENCE+BUSINESS MEDIA, LLC

Library of Congress Cataloging-in-Publication Data

Dykstra, Michael J.
Biological electron microscopy : theory, techniques, and troubleshooting / Michael J. Dykstra and Laura E. Reuss.-- 2nd ed.
p. cm.
Includes bibliographical references and index.
ISBN 978-1-4613-4856-6 ISBN 978-1-4419-9244-4 (eBook)
DOI 10.1007/978-1-4419-9244-4
1. Electron microscopy. 2. Scanning electron microscopy. 3. Transmission electron microscopy. I. Reuss, Laura E. II. Title.

QH212.E4D95 2003
570'.28'25--dc21

2003047709

ISBN 978-1-4613-4856-6

Originally published by Kluwer Academic Publishers/Plenum Publishers
Softcover reprint of the hardcover 2nd edition 2003
http://www.wkap.nl

10 9 8 7 6 5 4 3 2 1

Preface

Electron microscopy is frequently portrayed as a discipline that stands alone, separated from molecular biology, light microscopy, physiology, and biochemistry, among other disciplines. It is also presented as a technically demanding discipline operating largely in the sphere of "black boxes" and governed by many absolute laws of procedure. At the introductory level, this portrayal does the discipline and the student a disservice. The instrumentation we use is complex, but ultimately understandable and, more importantly, repairable. The procedures we employ for preparing tissues and cells are not totally understood, but enough information is available to allow investigators to make reasonable choices concerning the best techniques to apply to their particular problems. There are countless specialized techniques in the field of electron and light microscopy that require the acquisition of specialized knowledge, particularly for interpretation of results (electron tomography and energy dispersive spectroscopy immediately come to mind), but most laboratories possessing the equipment to effect these approaches have specialists to help the casual user. The advent of computer operated electron microscopes has also broadened access to these instruments, allowing users with little technical knowledge about electron microscope design to quickly become operators. This has been a welcome advance, because earlier instruments required a level of knowledge about electron optics and vacuum systems to produce optimal photographs and to avoid "crashing" the instruments that typically made it difficult for beginners.

There are many books and book series that deal with biological electron microscopy, but there are only few individual texts that give a comprehensive overview of preparative techniques and instrumentation that can answer the myriad questions posed by those pursuing structure–function relationships of cellular materials. Many students are taught to fear, rather than respect, electron microscopy instrumentation. In addition, many texts continue to teach that there is only one right way to fix and embed a given class of organisms, only one way to properly break a glass knife, only one side of a grid to use for section retrieval, and only one way to properly post-stain grids. After spending over 30 years reading about all the different types of approaches utilized to obtain publishable ultrastructural work, it is obvious that there are numerous equally valid methods to approach various questions, all of which will produce publishable results.

This textbook is an updated blend of technical approaches and didactic information found in the two books, *Biological Electron Microscopy: Theory, Techniques, and Troubleshooting* (Dykstra, 1992) and *A Manual of Applied Techniques for Biological Electron Microscopy* (Dykstra, 1993). This book is intended for a one-semester course that covers all the basic approaches to light microscopy, transmission electron microscopy, and scanning electron microscopy. Sections have been added to address photomicroscopy (including confocal scanning microscopy), digital imaging, and electron tomography utilizing intermediate voltage transmission electron microscopes.

A major component of this book is suggested by the subtitle: *Theory, Techniques, and Troubleshooting*. Too many electron microscopists have been trained with little theory beyond optical theory, too little about techniques except the ones used in their specific laboratory, and almost nothing about troubleshooting problems, particularly with regard to instrumentation. In a discipline with so many varied approaches from which to choose, learning how to apply

appropriate preparative techniques and choosing instrumentation for approaching questions concerning cell biology logically probably represent the highest aim of a course in electron microscopy.

This text is definitely not an in-depth compendium of all of the techniques and instrumentation capabilities currently available. Such an endeavor would occupy countless volumes (as exemplified by the excellent series edited by Audrey Glauert, *Practical Methods in Electron Microscopy*). What we have tried to accomplish is to put forth some basic tested techniques for common needs in the *Techniques* section at the end of various chapters, along with basic explanations of the different technical approaches and instrumentation employed, so that a student can see what is possible and can see what methods can be used to answer the variety of questions posed by cell biology in the cytological arena. To do this in one text suitable for a one-semester course necessitates brevity and superficiality in some areas, but the literature citations are intended to allow students to take their quest for knowledge in a specific area to a higher level.

A student who masters the concepts in this text will be capable, with continued practice on technical skills, to productively utilize electron and light microscopy techniques in his or her research. We hope that this text will also provide a sufficient foundation from which students can expand their horizons to numerous other specific areas of expertise within biological research.

Michael J. Dykstra
January 19, 2003

Acknowledgments

When the first edition of this book was written, acknowledgments were not included, which was an oversight corrected when *A Manual of Applied Techniques for Biological Electron Microscopy* (Dykstra, 1993) was published. Since the current textbook is a compilation of the materials found in both of these books, it seems appropriate to recap the acknowledgments from the manual and to include the acknowledgments that should have been in the first edition of this book.

Thus, this manual is dedicated to all of our friends, colleagues, technicians, and students who have helped us develop these approaches and have tested the various specific recipes and procedures to demonstrate that they generate reproducible results. We have been fortunate to have had a number of excellent technicians who have generated the bulk of the work coming out of our current laboratory (the Laboratory of Advanced Electron and Light Optical Methods, or LAELOM) and other laboratories which we have overseen over the years. We are particularly indebted to the following individuals who have made laboratory life instructive and easier than it would have been otherwise:

Sarah Bierley
Brendalyn Bradley-Kerr
Karen Greer
Jacqueline Lee
Nina Rodenroth
Robert Seiler

None of this work could have been accomplished without the formative 2 years that the senior author (Michael J. Dykstra) spent working as a post-doc for Dr. Henry C. Aldrich at the University of Florida. He introduced the concept that electron microscopes are not holy temples, but are just another type of machine that can be tinkered with, adjusted, and fixed. He also provided the concept that understanding the mechanism of fixation protocols and other methods makes it easier to make cogent choices when working with a new system or group of organisms. After two years with Dr. Aldrich, electron microscopy made much more sense and the intimidating aspects of earlier training were erased, which has made the ensuing 25 years in the field of electron and light microscopy much easier and more productive than it would have been otherwise.

Finally, Mary Born, the editor of the first two books that have been blended in this text, convinced the senior author to begin the daunting task of writing textbooks and helped him learn how to write more clearly. Without her encouragement, corrections, and helpful suggestions, the original books would not have come to be. Authors, in general, could not be what they are without the help of thoughtful editors. We were fortunate to walk the path that led to this book guided by such an inspiring soul.

Introduction to the Second Edition

Since the first edition of this book appeared in 1992, there has been an incremental improvement in most of the instrumentation utilized by electron microscopists. Conventional transmission electron microscopes (TEMs) operating in the 80–120 kV range and conventional scanning electron microscopes (SEMs) have generally been adapted to run in a Microsoft Windows™ environment. Specialized instrumentation, including intermediate voltage electron microscopes (IVEMs), high-resolution scanning electron microscopes, and environmental scanning electron microscopes (ESEMs) have become easier to use, more reliable, and are more commonly found on university campuses than in previous years. Advances in digital imaging and electron tomography techniques have changed our methods of image acquisition and storage and improved our understanding of complex three-dimensional structures. Finally, incremental advances in microanalytical packages (both in hardware and software), ultramicrotomes, cryoultramicrotomes, and various devices involved in preparing or viewing cryosamples have increased the ease of access to these techniques to biological researchers.

The transition from single department research electron microscopy facilities to multi-user service facilities serving campus-wide constituencies has been necessitated by the ever-increasing cost of instrumentation and maintenance. A fortuitous outcome of this shift in resource placement has been that the remaining facilities have greater pooled resources, allowing the purchase of more expensive and more broadly capable instrumentation in many cases.

Specimen preparation techniques have not changed much since the last edition of this book. The epoxide resins, acrylic resins, and fixatives used today were all available in 1992. The equipment for processing samples, both for conventional resin embedding and for cryotechniques, have improved, but no major breakthroughs have occurred. For this reason, the sections dealing with these subjects will be quite familiar to readers of the previous edition. The addition of a specific methods section at the end of selected chapters, however, is a major change from the first edition and we hope that this will help the reader to quickly jump from the didactic material to the direct application of techniques to their research problems.

Electron microscopy societies have, in general, broadened their bases by adding light microscopy approaches to their traditional interest in electron microscopy methodologies. In particular, the rapid rise in the importance of confocal microscopy to cytological investigations has filled in some visual gaps between light microscopy and electron microscopy, creating a fairly seamless path from images produced by compound light microscopes through those from confocal microscopes to those generated by transmission and scanning electron microscopes. To reflect this broadening, for example, the Electron Microscopy Society of America (EMSA) became the Microscopy Society of America (MSA). These changes seem fitting, particularly since electron microscopists have always used light microscopy methods during their investigations.

With that said, we asked ourselves why a new edition of our book(s) seemed sensible. As mentioned above, we decided that a new edition would allow us to merge the two original texts so that the didactic survey of different approaches to instrumentation and techniques could be immediately followed by specific techniques that we felt we could recommend, based on our years using them in our service laboratory. Having all of this material in one place, rather than in two separate volumes, was seen as a better package for the reader.

Some of the newer instruments gaining prominence in the 1990s such as IVEMs, low vacuum scanning electron microscopes (LV SEMs), FEG-equipped SEMs and TEMs, and ESEMs are now widely available and have increased the variety of capabilities for cytological observations considerably. The most notable advance has been the development of the discipline of electron tomography, which has produced scores of papers in the last 10 years and has allowed the characterization of the structure of macromolecules and cellular organelles as well as elucidating the three-dimensional relationships between cellular constituents with an ease and clarity only dreamed about by most electron microscopists in the 1980s.

The digital revolution that is affecting all aspects of visual communication has led to the digital control of microscopes, production of digital images, and the concomitant problems associated with producing appropriate digital files for their intended purposes, both from electron microscopes and from light microscopes. As you will see, we still believe film-based photography has a place with monochromatic images, though color digital images are a more pragmatic approach to producing printable color images.

We hope that the discussions of instrumentation and technical approaches available for cytological investigations will stimulate the reader to embark on the exciting adventure of studying cells and tissues. We are devoted to the concept that understanding structure/function relationships between what is in a cell and what the cell is doing are invaluable. We also encourage all students of cytological approaches to recognize that research should not be designed to use tools. Instead, tools should be chosen on the basis of the scientific questions being asked. Cytological, physiological, biochemical, and molecular tools should be used in concert, at a minimum, to study cellular behavior. Thus, it is appropriate for biologists utilizing electron microscopy to describe themselves from the standpoint of their biological discipline (e.g., botany, entomology, microbiology), rather than to describe themselves as electron microscopists. The physicists and electronics engineers, starting with Ernst Ruska, who have made possible the stunning array of electron microscopes available today are the true electron microscopists.

The purpose of this text is to help students see what is possible and to help them approach instrumentation and preparative techniques in a thoughtful, scientific way, so that they can solve microscopy and sample handling problems quickly and easily so that they can get on with their investigations of cells and tissues.

When exploring the technical approaches we recommend, we hope you realize that we are not trying to be encyclopedic. The techniques described are included because we *routinely* use them with great success. They will not fulfill every need for every sample, but they work for the vast majority of samples and they should serve as an excellent starting point, if no other specific approach has been gleaned from the literature pertaining to your specific biological model.

We hope that the journey through the myriad types of instrumentation and associated sample preparation procedures will serve to introduce you to a set of disciplines associated with cytological investigations that have kept the senior author fascinated with cellular structure and function for over 30 years as he has used electron microscopy to study aspects of protozoan and fungal development in his own research. Over the years, studies of bacteria, viruses, mammalian tissues, insects, fish, reptiles, amphibians, nematodes, and various types of cytopatholgy were added to the mix. In recent years, our laboratory has devoted a major amount of effort to the assessment of changes induced in animal tissues produced during drug development studies. There seems to be an infinite variety of biological questions that can be answered, at least in part, by cytological approaches.

We hope that the introduction to this discipline that is in your hands will lead you to cytological research and that it will give you as much thoughtful stimulation and entertainment as we have experienced during our years as biologists using electron and light microscopy.

Contents

1

Specimen Preparation for Electron Microscopy

The purpose of fixation is twofold: to bring about the rapid cessation of biological activity and to preserve the structure of the cell. Ideally, the colloidal suspension of the cytoplasm and organelles within a cell is turned into a gel that maintains the spatial relationship of the components while providing sufficient stability for them to survive the solvent action of aqueous buffers, dehydration agents, and plastic resins. The objective is to process tissues and cells without significant changes in size, shape, and positional relationships of the cellular components and to preserve as much of the biological activity and chemical nature of cellular constituents, such as enzymes and antigenic proteins.

I. PHYSICAL FIXATION TECHNIQUES

Physical fixation involves the application of either heat or cold to stabilize cellular components.

A. Heat

Heat fixation can be demonstrated simply by observing the changes that take place in an egg when it is fried: The translucent, colloidal proteinaceous material of the egg white becomes gelled into an opaque, rubbery solid. This material is truly fixed; however, it has been massively altered in structure. Heat fixing has also been used for decades to preserve blood smears in a clinical setting. Blood samples are smeared onto a glass slide and then passed through heat, such as a Bunsen burner flame, to affix the cells semipermanently to the slide and to stabilize their structure enough for rudimentary staining for further identification of cell populations. Neither of these techniques avoids serious precipitation of proteins and major changes in their tertiary structures. In addition, there is a rapid change in the states of hydration of cellular components. Various constituents, such as lipids, normally would not be well preserved by such methods. Thus, these techniques are grossly inadequate for ultrastructural preservation.

In recent years, *microwave* use (Giberson and Demaree, 2001; Leong *et al.*, 1985; Leong and Gove, 1990; Login *et al.*, 1990; Login and Dvorak, 1994) has resulted in some novel, extremely rapid fixation and staining techniques. They are not, however, solely heat fixation techniques. Cells or tissues may be fixed directly by microwaves (after suspension in a suitable fluid such as phosphate-buffered saline) or may be put into a fixative (aldehydes or osmium), which is then subjected to microwaves for a matter of seconds. In the latter case, this allows a much shorter time of fixation and is reported to result in better fixative penetration than conventional chilled or room-temperature fixation for an hour or two.

B. Cold

Cold, defined as the rapid freezing of cells or tissues, has been used effectively for preservation of cellular details. Cryofixation, in general, is restricted to much smaller sample sizes than needed for conventional chemical fixation. This is because heat must be removed from the specimen quickly enough to prevent ice crystal formation and consequent cellular damage. This is generally only possible near the surface of a specimen. Thus, with most techniques, an adequate freezing depth of about 10–15 μm is achieved. The more basal layers of the specimen have ice crystals large enough that ultrastructural detail is unacceptably distorted. There are three major variations on the theme of cryopreservation that will be elaborated:

1. Cryofixation followed by cryoultramicrotomy to produce ultrathin frozen sections, primarily for microanalysis and immunolabeling.
2. Cryosubstitution, wherein a specimen is quickly frozen and then dehydrated at reduced temperatures (−80°C), followed by infiltration with chemical fixatives that are inactive at the low temperature at which the sample is maintained. After diffusion of the fixation solution throughout the specimen, the temperature is raised in a controlled fashion. As the temperature increases, the fixative components become chemically active and stabilize all of the cellular components with which they react simultaneously (as opposed to normal chemical fixation, which involves diffusion of the fixatives from outside the tissues/cells to the interior, resulting in different areas of the sample becoming fixed at different times).
3. Freeze-drying, which involves cyrofixation followed by the removal of water by sublimation while the specimen is maintained at a low temperature under vacuum. See Chapter 2 for further information on cryotechniques.

II. TRADITIONAL CHEMICAL FIXATION

Before beginning this section, I want to recommend two texts by Hayat (1981, 2000), which are invaluable sources that contain information concerning all aspects of biological specimen preparation in much greater depth than can be provided in this text. The text by Glauert and Lewis (1998) also gives in-depth attention to all aspects of fixation and embedment of biological samples. In this chapter, the techniques will be discussed primarily in regard to preparing specimens for transmission electron microscopy (TEM), but many of the primary fixation suggestions pertain to preparing samples for scanning electron microscopy (SEM) as well. Techniques specific to preparing samples for SEM will be presented in Chapter 13.

A. Purpose; Killing versus Fixing

When preparing samples, one of the first concepts to consider is the difference between killing and fixing. Most of the time, the term *fixing* is used to include both processes, which sometimes leads us to forget that they are not one and the same thing. Most primary fixatives used today are aldehyde fixatives, and it is well documented that cells can have significant time periods during which they can respond to fixative solutions before death (Table 1). Slime mold amoebae

Table 1. Rates of Fixation (Gilkey and Staehelin, 1986; with permission)

I. CHEMICAL FIXATION
A. 3% glutaraldehyde/3% acrolein: *Pyrsonympha* axoneme moves for 2 seconds
B. 3% glutaraldehyde: chicken embryo fibroblast cytoplasmic inclusions move for 30–45 seconds
C. Tomato petiolar hair cell cytoplasmic streaming continues for:
1. 15 min with 0.5–5.3% glutaraldehyde
2. 9 min with 5% acrolein
3. 6 min with 2% glutaraldehyde + 5% acrolein
4. 15 min with 2% glutaraldehyde + 1% osmium
II. CRYOFIXATION: Movement ceases in 10 msec

grown to confluence on an agar surface can be seen to round up and develop intercellular spaces during the first 30 s after a glutaraldehyde mixture is poured onto them. If, instead, the Petri dish containing the cells is first inverted over a drop of 1% osmium tetroxide for 3 min, the addition of glutaraldehyde causes no obvious morphological change in the cells. Thus, the highly volatile and toxic osmium tetroxide vapor *kills* the cells, and the later addition of glutaraldehyde *fixes* the cells. It is important not to forget that these processes are not the same thing when evaluating the success or failure of your particular fixation regimen.

B. Methods

Chemical fixation has been the standard of the biological electron microscopy trade since its inception and, despite the advances in cryopreservation techniques discussed subsequently, continues to dominate the field. The fixatives commonly in use have been derived to a large extent from the leather-tanning industry. The advantages of chemical fixation are that the chemicals are generally fairly stable, the specimen-handling techniques are simple, materials can be stored in the solutions for some period of time, no significant equipment is needed, and the fixatives are relatively inexpensive.

It is important to remember that typical chemical fixation procedures involve chemical reactions that occur over time and that the process is dependent on the diffusion of fixative components into the samples. The samples and fixative solutions are continually changing during the initial period of fixation. With standard aldehyde fixation, the sample is immersed in a fixative solution containing a specific concentration of the fixative chemical in a buffering solution. At the outset of fixation, the surface of the sample is exposed to the full-strength fixative. As the solution diffuses to the interior of the sample, the aldehyde component becomes bound to sample constituents. As the sample components become cross-linked, the assemblages become partial barriers to further penetration of the sample by the fixative solution. In addition, as the aldehyde component becomes bound to sample components, the remaining solution diffusing more deeply into the sample contains less of the aldehyde. Thus, over time, fixative penetration from the sample surface slows down (due to partial aldehyde/tissue barriers) at the same time that the concentration of the fixative component (aldehyde) in the diffusing solution becomes weaker, since the aldehyde is being removed from the solution by the sample fixation process. The solution to the twin problems of ever-decreased speed of fixative penetration and ever-more-diluted fixative solution reaching the interior of the sample is to have a vast excess of fixative solution in which the sample is immersed (the fixative solution volume should be 5–10 times the volume of

the sample), along with a sample that is a millimeter or less in thickness in at least one dimension. If these rules are observed, although the rate of chemical fixative penetration is not particularly fast, and specimens must be made thin enough for rapid penetration of fixative solutions to prevent autolysis of structures deep within the sample, a relatively large sample can be adequately preserved. The general rule of thumb is that most fixatives will penetrate at least 0.5 mm into a sample within 1 hr such that if you could produce a 1-mm-thin slice through the center of a watermelon, it would be well fixed. Figure 1 shows one block that was less than 1 mm in the narrowest dimension during osmication, while the other block was approximately 2 mm^3 when osmicated. The center of the latter piece is still unblackened, since the osmium never penetrated to that area during the 1 hr step. Needless to say, softer samples, such as brain tissue, are resistant to being neatly sliced into 1-mm-thick portions without some sort of fixation. Vascular perfusion techniques are typically employed to address this problem (see specific techniques in Hayat, 1981, 2000).

Evidence of good fixation is based on a variety of criteria, including: (1) preservation of ground substance (a background density greater than that of non-tissue plastic areas outside the cells) in the cytoplasm and nucleoplasm, and membranes of the nuclear envelope virtually parallel, without significant swelling; (2) mitochondria that are not distended, and inner and outer membranes that are more or less parallel; (3) endoplasmic reticulum that is not swollen, and most membranes and cellular components are intact. If these three criteria are met, fixation is considered adequate in most cases. Figure 2 shows a slightly suboptimally fixed rat liver, with slightly inflated endoplasmic reticulum and slightly uneven spacing between the inner and outer nuclear envelope membranes. Cytoplasmic and nucleoplasmic ground substance is well represented, and mitochondria are dense. The sample was fixed in McDowell and Trump's (1976) 4F:1G fixative (4F:1G) utilizing the general processing schedule in the Techniques section at the end of this chapter. The area examined was apparently just a little too far from the sample surface so that either the primary fixative was diluted slightly too much when it interacted with the area shown, or it may have taken slightly too long to arrive at the site so that some minor autolytic changes occurred, as shown. The woodchuck cardiac muscle shown in Fig. 3 was fixed in buffered neutral formalin (BNF) and shows quite enlarged and leached out mitochondria, a swollen nuclear envelope, and various membrane discontinuities characteristic of fixation with BNF. In addition, however, after

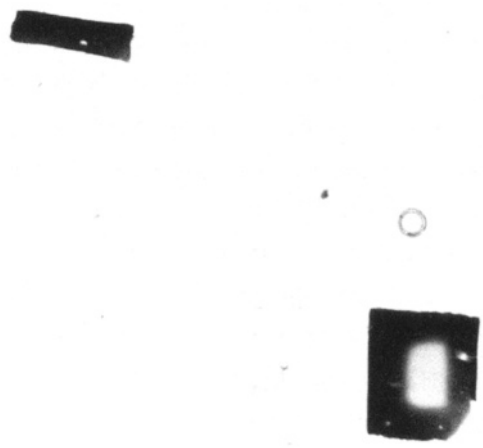

Figure 1. Rat liver. The smaller section is from a block of tissue that was 0.75 mm thick in the thinnest dimension. During the osmication step, osmium penetrated to the center of the sample. The larger section was cut from the center of a block that was 2 mm^3 when osmicated. The white central area did not react with osmium during the osmication step. 8.5×.

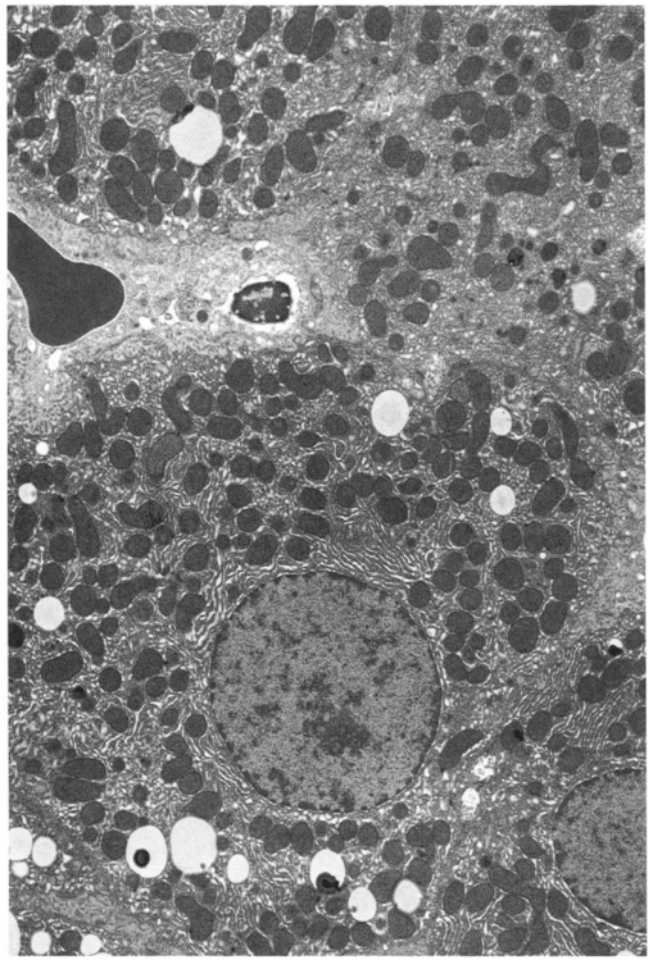

Figure 2. Suboptimally fixed rat liver (4F:1G primary fixation, followed by osmium postfixation). 4308×.

the sample was examined, it was discovered that the tissue was taken from an animal that had been found dead in its cage, and the animal care workers did not know how long it had been dead. Muscle tissue autolyzes more slowly than other types of tissues such as liver, kidney, and brain, so the overall preservation except for the mitochondria was not too bad.

Another factor that makes identification of good fixation of samples difficult is the recognition that cells grown in culture undergo a number of cytological changes when compared with the same cells fixed immediately after the tissue is removed from the living host. Franks and Wilson (1977) showed that one of the consistent changes that occur in cells grown in culture is apparent mitochondrial damage. The changes are typified by enlargement of mitochondria, an increase in "motheaten" mitochondria, and apparent degradation of cristal profiles. Figures 4–6 show three different cell types in culture that were healthy and growing well when fixed. As you will note, the mitochondria look damaged in a variety of ways.

Primary fixation is clearly a critical step in electron microscopy. If the samples are not well fixed, they will produce images that exhibit excessive contrast because cellular constituents

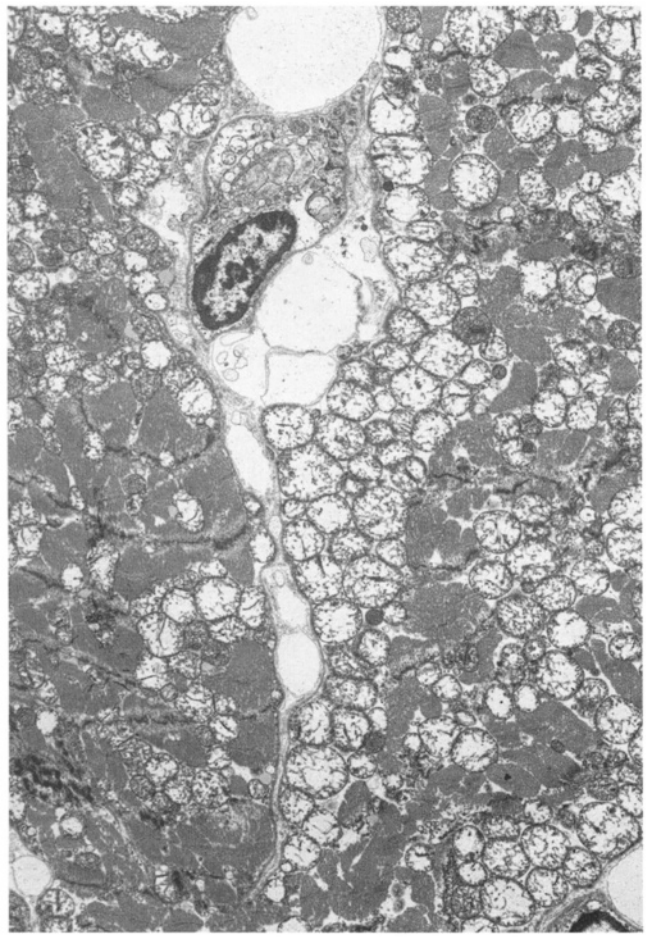

Figure 3. Woodchuck cardiac muscle fixed with buffered neutral formalin (BNF). The animal was found dead prior to excision and fixation of tissue. 4,308×.

that were poorly fixed become extracted during the various rinses in the processing schedule. Some components are also extracted during resin infiltration steps. Another problem with poor primary fixation is subsequent poor infiltration of resin. Thus, in addition to yielding sections with poor image quality, the blocks are frequently difficult to section. The hallmark of this problem is sections that are of uneven thickness when cut on the ultramicrotome. The interior, poorly fixed areas of tissue are softer than the exterior, more adequately fixed areas, resulting in a different section thickness in the two areas of the section.

In a general contemporary fixation schedule for straight structural examinations, tissues are fixed in a primary aldehyde fixative followed by rinses in an appropriate buffer. The samples are then postfixed in osmium, dehydrated, infiltrated with an epoxide resin, and the resin containing the sample is then put into molds and polymerized with heat.

We will now examine individual chemical fixatives and evaluate their effects on various cellular components. In addition, we will discuss their formulation, storage, and parameters of use.

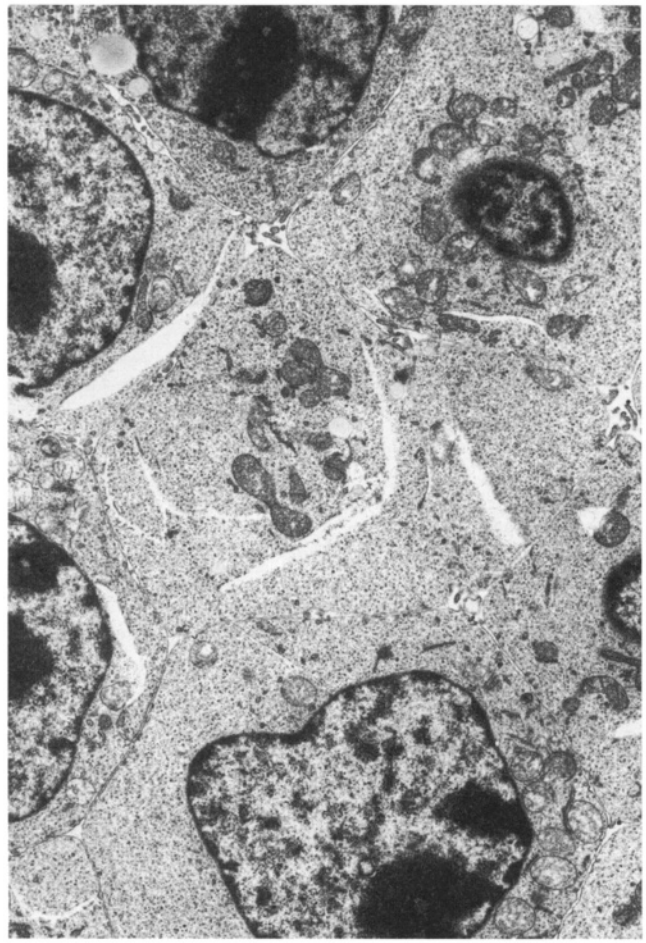

Figure 4. Mouse lymphoma cell line. 5,050×.

1. Osmium Tetroxide

Osmium tetroxide (osmium, osmium tetraoxide, OsO_4) has been used for over a century for the preservation of cellular detail. Botanists of the late 1800s would put a drop of osmium solution on a section of tissue on a glass slide and examine it avidly until sufficient darkening had occurred. These individuals often suffered from a certain haziness of vision, but it eventually resolved due to the sloughing of the old osmium-fixed corneal epithelium, followed by reepithelialization of the corneum. Osmium was the first successfully used fixative for the ultrastructural preservation of animal tissues (Glauert, 1975).

This fixative has a high vapor pressure, is highly toxic, and should be used under a fume hood at all times. An excellent rule to follow is that any detection of its acrid odor means you are working too close to this chemical. If osmium contacts skin, it will blacken it, and if you manage to cut yourself with an osmium-coated surface, the wound will heal more slowly than

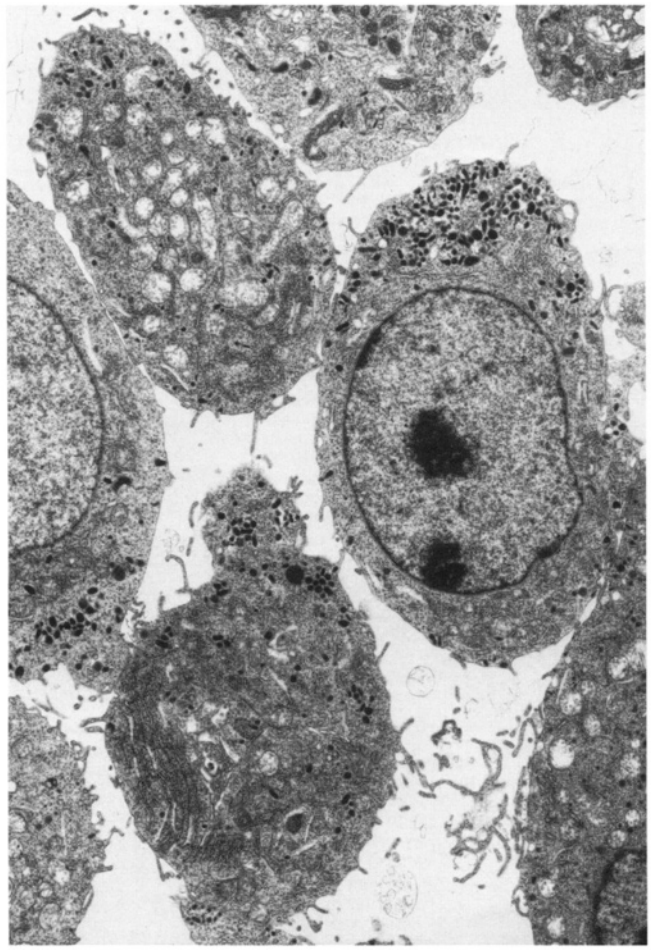

Figure 5. Rat pancreatic cell line. 5,050×.

usual because the cells lining the interior of the wound are killed by the fixative, delaying the normal controlled metastasis of cells during the healing process. Tissues generally turn black after osmication, but this is not the best judge of efficacy, since tissues low in lipids (such as highly proteinaceous scar tissues) will not blacken. In addition, lipids with different degrees of saturation reduce different amounts of osmium. If the unused aqueous osmium stock is straw-colored, it can be assumed to be chemically reactive. When the solution begins to gray or blacken, which indicates reduction of the osmium, it should be discarded.

As a primary fixative, osmium causes rapid gross permeabilization of membranes with cessation of cytoplasmic movement within seconds to minutes in most cases. It has been used as a vapor fixative to quickly stop biological processes in cell monolayers or cells suspended in small drops of growth medium. It has also been used to stabilize materials without the need for an aqueous phase. In the latter case, samples containing potentially soluble products have been prepared for X-ray microanalysis (energy dispersive spectroscopy, EDS) by exposing freeze-dried tissues to osmium crystals in a desiccator for 8 hr (Hayat, 1981).

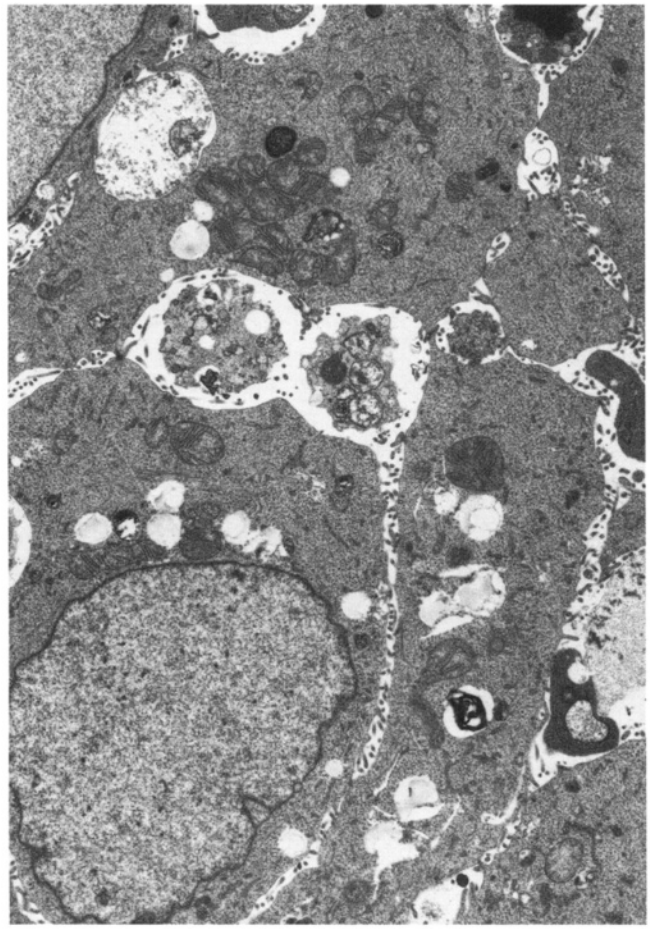

Figure 6. Human colon spheroids. 6,819×.

a. Disadvantages

Osmium is one of the most slowly penetrating fixatives we use and has no cross-linking capabilities for cellular components. When used as a primary fixative, it typically makes the nucleoplasm and cytoplasm look somewhat extracted, giving the material more contrast than when using better fixation techniques. As it is a strong oxidant, osmium profoundly inactivates virtually all enzymes and can be expected to damage many antigens.

b. Advantages

Osmium has nine different oxidation states (Hayat, 1981), and at least five of them are relatively stable and have different reactivity with cellular components. Osmium is soluble in both polar and nonpolar media, and thus can penetrate and fix both hydrophobic and hydrophilic domains in cells. Finally, when osmium reacts with cellular components in an oxidative fashion, it is concomitantly reduced. The reduced form is largely nonextractable and also has the added benefit of exhibiting electron density under an electron beam, since it is a heavy metal.

c. Specific Activity

Lipids. Osmium interacts directly with unsaturated lipids by oxidizing double bonds, leading to the formation of monoesters, diesters, and dimeric monoesters (Fig. 7). Saturated fatty acids are normally chemically unreactive with osmium, since they lack double bonds but often are preserved by an indirect route. As mentioned above, osmium is soluble in nonpolar materials such as lipids. Osmium can be taken up in an unreduced form by saturated lipids and then subsequently be reduced by organic solvents such as an ethanolic dehydration series. Thus, all classes of lipids are potentially preserved by osmication, either by a direct chemical reaction or indirectly in the case of saturated lipids.

Proteins. Prolonged osmium fixation results in the progressive denaturation of proteins, leading to the eventual extraction of the smaller peptides during buffer washes and the dehydration series. According to Hayat (1981), a weak osmium solution can produce gels with proteins such as albumin, globulin, and fibrinogen, possibly due to the presence of tryptophan residues with reactive double bonds. Osmium also reacts with a number of other amino acids, such as cysteine and methionine (at alkaline pH), with sulfhydryl, phenolic, hydroxyl, carboxyl, amino, and certain heterocyclic groups, and with disulfide linkages.

Nucleic Acids. Osmium can cause the formation of coarse aggregates of DNA. Some workers have added calcium to osmium to improve the stabilization of bacterial DNA. It is thought (Hayat, 1981) that chromosomal reactivity with osmium may be due to the presence of reactive amino acids in associated histones.

Carbohydrates. Osmium does not react with most pentoses and hexoses, though prolonged treatment of tissues with osmium at 50°C will cause glycogen blackening (Hayat, 1981). Most carbohydrates in osmium-fixed tissue are extracted during rinsing and dehydration.

d. Physical Changes

Osmium causes some swelling (30% in liver after 4 hr, 15% after 15 min, according to Hayat, 1981). This is normally counteracted to some extent by the consequent shrinkage encountered during dehydration. Some workers add calcium chloride or sodium chloride to osmium when using it as a primary fixative to help reduce the swelling. Nonelectrolytes, such as sucrose or glucose, have also been used in an attempt to alleviate the problem. This phenomenon is not a problem when osmium is used as a postfixative following aldehyde primary fixation. Some workers report that calcium added to osmium may cause a granular precipitate in tissue, while others claim that the calcium helps to prevent this artifact (Millonig and Marinozzi, 1968).

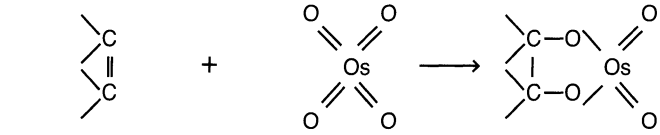

Figure 7. Osmium tetroxide (osmium, osmium tetraoxide).

Hardening. Hardening of tissues takes place as a result of osmium exposure. In most cases, this is a trivial problem, but in cases in which structures are fragile or when cells need to be centrifuged, this can cause severe problems. As discussed in the section on embedding media, cell suspensions are often embedded in molten water agar for subsequent ease of handling. If this is done after osmication, there is a great tendency for the cells to be sheared during centrifugation due to the hardening effects of osmium. This is not a significant problem with small cells such as bacteria, but with larger cells such as protozoa, it can be a serious problem.

e. Parameters

Concentration. Most workers utilize 1–2% osmium in buffers at slightly alkaline pH (7.2–7.4). It has been suggested that higher concentrations of osmium result in a greater conversion of polypeptides to soluble peptides, which can lead to cells with evident extraction of cytoplasmic components.

Temperature. Some workers insist on osmicating on ice or at 4°C, but other laboratories osmicate at room temperature with consistently good results. As with all chemical reactions and diffusion processes, lower temperatures can be expected to contribute to slower penetration of the tissue and reduced chemical reactivity of the fixative component.

Rate of Penetration. The addition of electrolytes or nonelectrolytes to osmium, as mentioned above, is said to decrease the rate of penetration (nonelectrolytes are said to reduce the rate of penetration more than electrolytes). At room temperature, the rate of penetration is no more than 0.5 mm/hr. Thus, a 1-mm-thick piece of tissue will be fixed to the center in 1 hr. After 1 hr, as mentioned before, fixation slows down because the fixed surface of the sample impedes the further incursion of fixative and the fixative that does reach the center is more dilute than the original fixative solution due to binding of the fixative to tissue components.

Duration. Fixation for 1–2 hr is usually sufficient for properly prepared samples (1 mm thin in at least one dimension) due to the penetration rate cited above, though some workers have utilized up to 12 hr with embryonic tissues or algae (Hayat, 1981).

Formulation and Storage. Osmium crystals can be melted by hot tap water. This allows the preparation of diluted osmium stocks from crystals, while avoiding the possibility of contamination, as described in the section Chapter 1 Techniques. Dilute aqueous stocks of osmium stored at 4°C are stable for 6 months or more. If the solution becomes gray or black, it is contaminated and should be replaced. Minute amounts of buffer or alcohol, as well as prolonged exposure to light are sufficient to begin the reduction of the osmium solution and its consequent darkening. Thus, it is always best to remove aliquots of the solution with a fresh Pasteur pipet and to keep the container in the refrigerator whenever it is not being used.

2. Permanganates

Permanganates were initially introduced to overcome some of the fixation problems encountered with walled organisms such as plants, as workers realized that osmium penetration was not adequate. Permanganates have now almost passed into history as primary fixatives,

though papers utilizing potassium permanganate are still seen periodically. Permanganates were introduced by Luft (1956) and were noted for their ability to penetrate tissue rapidly (approximately 1 mm/hr). Potassium, lithium, lanthanum, and sodium permanganates have all been used. They are all strong oxidants, like osmium, but they do not confer electron density to the cellular components with which they react. They preserve membranes well, but the rest of the cellular constituents are severely extracted. Ribosomes are lost, mitochondria and chloroplasts swell, and many lipids are lost, as are microtubules and microfilaments. Workers have generally used solutions containing 0.6–3.0% potassium permanganate buffered to pH 7.2–7.4. Fixation is usually on ice for about 1 hr, since higher temperatures and longer fixation times result in further cytoplasmic extractions.

3. Formaldehyde

Formaldehyde (Fig. 8) was used as a standard histological fixative component long before the advent of electron microscopy. It is the smallest and simplest aldehyde used, the formula CH_2O. It is available as commercial formalin (37–40% formaldehyde), which contains formic acid (less than 0.05%) and 6–15% methanol, the latter being added to prevent polymerization. When diluted to 2–4%, formaldehyde is primarily in monomeric form. Many electron microscopists prefer to make up formaldehyde fresh from the polymerized paraformaldehyde powder. Unfortunately, after paraformaldehyde is depolymerized to make pure formaldehyde, it immediately begins polymerizing again, leading to a limited shelf life. Do not be confused by literature stating that investigators "fixed with paraformaldehyde." What they mean is that they fixed with pure formaldehyde, freshly prepared from paraformaldehyde powder.

Formaldehyde is usually regarded as an inferior primary fixative for structural electron microscopy, because even though it penetrates rapidly due to the small size of the monomeric molecule, it does not cross-link strongly, and the fixation it achieves is reversible with sufficient washing in aqueous solvents (the formaldehyde can be washed out of the tissue). The pH of BNF solutions (4% formaldehyde in a phosphate buffer) made from 37% commercial formalin stocks and used in routine histological work frequently drops to 6.0–6.5 in a relatively short period of time on the shelf and causes poor ultrastructural fixation if not corrected. Carson *et al.* (1973) developed a formulation for phosphate-buffered 4% formaldehyde that produces acceptable ultrastructural preservation in many cases. It is generally accepted that the addition of methanol and other stabilizers to commercial-grade 37% formaldehyde makes it unsuitable for enzyme cytochemistry, but many procedures for light-level immunohistochemistry utilize BNF with great success, so this objection appears to be questionable. In addition, by the time the 37% stocks are diluted to 4% for fixation, the concentration of the stabilizers is not very significant.

We still make up fresh formaldehyde from paraformaldehyde for cytochemical procedures but utilize 37% formaldehyde stocks to prepare fixative solutions for conventional structural examinations. Numerous clinical samples submitted to our service laboratory in formaldehyde for

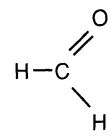

Figure 8. Formaldehyde.

ultrastructural study over the last 20 years have yielded images as good as glutaraldehyde-fixed tissues, while others have been so extracted and poorly fixed that they were virtually unusable. Clearly, the care with which formaldehyde is buffered and the handling of the tissue prior to fixation (i.e., not letting it sit on a counter at room temperature for 30 min prior to being put into the fixative) probably accounts for this observed variation. Ghadially (1985) illustrated his text on tumors exclusively with excellent photographs taken of formaldehyde-fixed tissues.

Poor fixation with formalin is characterized by numerous membrane discontinuities, nucleoplasmic and cytoplasmic areas with reduced ground substance (little gray background in an electron micrograph), and swollen endoplasmic reticulum and mitochondria. Nuclear envelopes often look fairly well preserved.

a. Disadvantages

As mentioned above, formaldehyde cross-links more weakly than other aldehydes and can be washed out of tissues by aqueous rinses. As with all aldehydes, it provides no electron density to tissues.

b. Advantages

The formaldehyde molecule is the smallest aldehyde and thus penetrates rapidly into samples. Being a small molecule, once it is bound to tissues or cells, it offers little steric hindrance to the interaction of biological molecules such as enzymes and antibodies with the samples, compared to the larger five-carbon glutaraldehyde molecule. Since it is not a strong cross-linker, it tends to leave most protein structures relatively unchanged and thus is a preferred fixative for various enzyme cytochemical procedures, as well as for immunocytochemical techniques.

c. Specific Activity

Lipids. Formaldehyde can react with the double bonds of unsaturated lipids, but various solvents in the processing series extract the lipids unless postfixation with osmium is added to stabilize lipids.

Proteins. Peptide chains are cross-linked, but the vast majority of the cross-links can be reversed by aqueous solutions. Using higher concentrations of the fixative causes increased formaldehyde binding. Higher temperatures and pH will also increase binding to proteins. Maximum binding to proteins is reported to be at pH 7.5–8.0 (Hayat, 1981).

Nucleic Acids. Formaldehyde reacts with nucleic acids and proteins without breaking the linear structure of either. The preservation of nucleic acids is probably due mostly to the interaction of formaldehyde with the protein component of nucleoproteins. As with pure proteins, the reaction of formaldehyde with nucleoproteins is reversible in aqueous solutions.

Carbohydrates. Small carbohydrate molecules are not preserved and are washed out during processing. Carbohydrate moieties complexed with other cellular components may be preserved. Mucoproteins are fixed, but acid mucopolysaccharides are not. Glycogen survives formaldehyde fixation, provided fixation times are not too long.

d. Physical Changes

Properly formulated formaldehyde solutions, such as that of Carson *et al.* (1973) applied to tissues less than 1-mm-thick in at least one dimension, should result in little appreciable shrinkage or swelling of tissues. Formaldehyde will toughen tissues, but they remain pliable (unlike osmium-fixed tissues, which become brittle). Cells can be easily pelleted through molten water agar without significant damage.

e. Parameters

Concentration. Most workers use 4% formaldehyde solutions, though some of the recent immunocytochemical procedures utilize as little as 2% formaldehyde made up from paraformaldehyde.

Temperature. Room-temperature fixation is successful, though some workers believe that ice-bath temperatures provide better fixation.

Rate of Penetration. Formaldehyde penetrates more rapidly than either osmium or glutaraldehyde due to the small size of the monoaldehyde and is thus the fixative of choice for large samples.

Duration. Many workers also warn that since the reaction of formaldehyde is slow and reversible, tissues should not be left in formaldehyde for very long. However, Ghadially has published two books (1975, 1985) illustrating numerous pathology samples that have been successfully fixed with BNF from histology labs, many of which have been stored in these solutions for extended periods of time. Generally, it would appear prudent to fix tissues for no longer than 1–2 hr in fixative solutions containing only formaldehyde and buffers before proceeding with the rest of the processing schedule.

Formulation and Storage. As mentioned previously, many electron microscopists believe that formalin (37–40% formaldehyde solutions containing stabilizers) is inappropriate for ultrastructural preservation. This is clearly not the case when one considers the numerous medical case reports illustrated with electron micrographs prepared from tissues fixed with BNF. However, poorly formulated BNF, particularly if the pH is below 7.0, is not recommended. If making fresh formaldehyde from paraformaldehyde powder, the monoaldehydes that are produced by putting the powder into heated water and raising the pH will begin repolymerizing immediately. Thus, most workers recommend utilizing freshly made formaldehyde immediately, or at least within a week or two. If the solution is being stored for a week or two, it should be refrigerated. Some investigators recommend freezing small aliquots for long-term storage. However, standard biological-grade formalin (37–40% formaldehyde sold by supply houses) has a storage life of years at room temperature. Buffered dilute stocks (4%) stored under refrigeration are presumed to be even more stable.

4. Acrolein

Luft first introduced acrolein (Fig. 9) as a primary fixative for electron microscopy in 1959. It is a three-carbon monoaldehyde (C_3H_4O) noted for its ability to penetrate tissues more

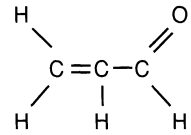

Figure 9. Acrolein.

rapidly than osmium, glutaraldehyde, or formaldehyde. It is more reactive than the other aldehydes and inactivates enzymes profoundly.

a. Disadvantages

Acrolein polymerizes rapidly upon exposure to air, light, and chemicals, and generates heat during the process. Commercial preparations usually contain 0.1% hydroquinone to prevent oxidation. Acrolein is flammable, and its vapors can be quite irritating to mucous membranes (it is a component of tear gas).

b. Advantages

Acrolein is more reactive with proteins than formaldehyde and penetrates tissues quite rapidly. It preserves microtubules better than either glutaraldehyde or formaldehyde alone.

c. Specific Activity (Glauert, 1975)

Lipids. Acrolein is reported to solubilize lipids.

Proteins. This aldehyde is more reactive with proteins than any of the other aldehydes. For enzyme or antigen localization, it is contraindicated as a fixative because of the chance for the severe denaturation of proteins.

Nucleic Acids. Acrolein is thought to be somewhat reactive with charged groups, but the primary fixation of nucleic acids is probably due to their association with well-fixed histone proteins.

Carbohydrates. These constituents are generally regarded as unreactive with acrolein.

d. Physical Changes

Acrolein causes a toughening of tissues without loss of pliability, a feature shared with the other aldehyde fixatives. The loss of lipids reported by some authors may be associated with changes in membrane permeability.

e. Parameters

Concentration. Some workers recommend 10% buffered acrolein, but others have used 3–4% with success.

Temperatures. Fixation at 4°C or at room temperature gives good results.

Rate of Penetration. Penetration of about 1 mm/hr has been reported for rat kidney tissue. This fixative has been recommended for large samples because of its excellent penetration capabilities.

Duration. Due to its rapid rate of penetration, 1 hr at room temperature is quite adequate for the sample sizes normally encountered in an electron microscopy laboratory.

Formulation and Storage. As previously mentioned, acrolein usually comes in concentrated form containing hydroquinone as a stabilizer. The presence of the stabilizer does not seem to adversely affect fixation. The shelf life of acrolein at room temperature is not long because of its propensity for auto-polymerization. Storage at 4°C is recommended. Diluted solutions will be less prone to polymerize. If a 10% solution in water has a pH below 6.4, or if there is turbidity in the concentrated solution from which the dilute solution is made, discard the solution. This fixative has a high vapor pressure and is extremely toxic, so always work carefully with it under a fume hood.

5. Glutaraldehyde

With the introduction of glutaraldehyde (Fig. 10) by Sabatini *et al.* (1963), a revolution in chemical fixation resulted because its capabilities were so much better than the preceding alternatives. The fact that it is a five-carbon dialdehyde ($C_5H_8O_2$) with two hydroxyl groups capable of binding proteins makes it an extremely good cross-linking fixative. This strong cross-linking is virtually irreversible, unlike the reversible cross-linking from formaldehyde.

a. Disadvantages

Glutaraldehyde penetrates tissues more slowly than formaldehyde or acrolein and inactivates some enzymes and antibodies. This is probably due to glutaraldehyde itself, or some of the nearby cross-linked proteins, sterically hindering access to reactive sites. Microtubules are depolymerized if they are exposed to cold fixative. No electron opacity is produced in the fixed tissue. Physiological activities of the cells are not stopped immediately, resulting in cells changing conformation in response to the fixative under some conditions. In addition, membranes become more permeable after primary glutaraldehyde fixation, and cellular compartments can subsequently leak. This will result in some hydrolytic enzymes escaping their normal cellular sequestration in lysosomes, which can cause some autolytic damage unless samples stored for prolonged periods are kept at temperatures considerably below the temperature at which the enzymes are most physiologically active (4°C is the temperature recommended for storing mammalian tissues that are normally at 36–38°C during life).

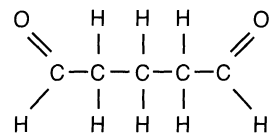

Figure 10. Glutaraldehyde.

b. Advantages

Even though this fixative affects the α-helix of proteins, the tertiary structure of proteins is unaffected. As previously mentioned, reactive moieties of proteins may be occupied by glutaraldehyde and thus be inaccessible to cytochemical procedures, though most proteins maintain a fair amount of their activity, which is useful for cytochemical or immunocytochemical procedures.

c. Specific Activity

Lipids. Glutaraldehyde probably reacts only with phospholipids containing free amino groups. If glutaraldehyde-fixed samples are not postfixed with osmium, most lipids are extracted during dehydration. Glutaraldehyde itself may make some phospholipids go into solution, which can result in the artifactual formation of myelin-like whorls of membranes that are stabilized by consequent osmication. This appears to be responsible for the formation of "mesosomes" in bacteria, since they are not found in cryopreserved materials (Aldrich *et al.*, 1987). Myelin figures are usually more abundant in large samples and are more common when extended glutaraldehyde fixation times are used. Some investigators add 1–3 mM $CaCl_2$ to glutaraldehyde to minimize this phenomenon.

Proteins. These are the main target of glutaraldehyde, which is most reactive with many free amino groups and cross-links proteins through this agency.

Nucleic Acids. As with the other aldehydes, most of the preservation of nucleic acids is considered to be due to the interaction of this fixative with the proteins associated with nucleic acids more than by any direct interaction between nucleic acids and glutaraldehyde.

Carbohydrates. Most carbohydrates are not fixed well and are lost during subsequent rinses. Glycogen is a major exception; 40–65% of the total glycogen remains in fixed tissues, according to Hayat (1981).

d. Physical Changes

Glutaraldehyde toughens tissues but does not impart electron density. It is known to cause shrinkage and so is generally made up in hypertonic solutions. Linear shrinkage in the realm of 5% is common for many tissues.

e. Parameters

Concentration. A high concentration (37%) causes profound shrinkage, while a low concentration (0.1–0.5%, as used in a number of immunocytochemical procedures) can result in severe extraction. Typically, solutions of 1.5–4% glutaraldehyde in an appropriate buffer are used. With larger sample sizes, some workers use higher concentrations of glutaraldehyde, since the solution becomes more dilute as it passes to the interior of a sample because the glutaraldehyde becomes bound and is no longer free in solution.

Temperature. Historically, it has been recommended that glutaraldehyde fixation be done on ice or at 4°C. At the same time, it was established early on that microtubules become depolymerized when held at such temperatures. Glutaraldehyde fixation at room temperature seems to give adequate results without causing microtubule depolymerization.

Rate of Penetration. Hayat (1981) reported that a 2% solution of glutaraldehyde at a tonicity of 200 mOsm penetrates liver to a depth of 0.7 mm after 3 hr at room temperature. Periodic acid–Schiff reagent staining to monitor the depth of penetration is effective, since the Schiff reagent will react with the two hydroxyls of glutaraldehyde.

Duration. Even though the fixative can reach depths in the tissue beyond 0.5 mm after 1 hr, most tissues will exhibit evidence of autolysis after an hour at room temperature. Thus, if the fixative does not penetrate all areas of the tissue after 1 hr at room temperature, most tissues will exhibit poorly fixed central areas.

Formulation and Storage. Glutaraldehyde is available in various forms, from a 70% aqueous solution stored under dry nitrogen gas in sealed ampules, to 50% or 25% aqueous solutions stored in 500-ml brown bottles, to 8% solutions in sealed ampules. Some users have redistilled their glutaraldehyde after the method of Smith and Farquhar (1966), but this is rarely necessary. Glutaraldehyde at high concentrations (over 25%) is subject to spontaneous polymerization if not stored under dry nitrogen. Heat can also adversely affect such stocks, though glutaraldehyde is not photosensitive. If stored under dry nitrogen in sealed ampules, glutaraldehyde should be stable indefinitely if stored at 4°C. Biological-grade glutaraldehyde (25%) stored in a refrigerator generally has a shelf life of several years. If glutaraldehyde stocks become yellowed, polymerization may be taking place. A more reliable indicator is pH. If the pH of 25% stocks is between 3 and 6, they are probably all right. If a spectrophotometric reading of the stock reveals a larger peak at 235 nm than at 280 nm, the stocks may be bad. A 1:1 or 2:1 ratio of 280-nm to 235-nm peaks is associated with good glutaraldehyde. After distillation, only the 280-nm (monomeric) peak should remain. Dimeric (235 nm) and higher polymeric forms are not considered good for fixation. Glutaraldehyde solutions mixed with buffer at working concentrations (2–4%) are good for at least a year at 4°C.

6. Fixative Supplements

Various agents have been previously mentioned, such as electrolytes, nonelectrolytes, calcium, and buffers that are added to fixatives to attempt to address the problems of tonicity and pH, and to help stabilize various cellular constituents. These agents usually deal broadly with cellular reactions rather than with a specific subset of cellular components.

A variety of other supplements (Hayat, 1981, 2000) have been utilized to stabilize specific compounds or structures. One of the most frequent problems addressed is that of lipid stability. Since the most commonly used primary fixatives, aldehydes, do not fix lipids, the lipids can undergo structural alterations and reconfigurations during the primary fixation period prior to osmium steps that will help to stabilize them. Thus, workers have added specific agents to aldehydes to help stabilize lipids until osmium can react with them. Glutaraldehyde containing digitonin has been used to specifically stabilize cholesterol and cholesterol esters, while glutaraldehyde containing malachite green has been used to preserve some lipid-containing granules in mammalian spermatozoa. A combination of glutaraldehyde fixation followed by osmium with added potassium ferricyanide has been used to help preserve phospholipids in central nervous system samples as well as the surfactant material in type II cells of the lung (myelin-like figures in vacuoles of type II cells).

Glutaraldehyde containing lead acetate has been used to preserve soluble inorganic phosphate, which would otherwise be washed out during fixation and buffer washes. Glutaraldehyde containing phosphotungstic acid applied to tissues pretreated with polyethyleneimine has been used to demonstrate anionic sites in basement membranes and collagen. Biogenic amines, such as adrenaline, have been demonstrated with a combination of glutaraldehyde and potassium dichromate.

Borrowing from light microscopy techniques, trinitro compounds, most notably, picric acid and 2,4,6-trinitrocresol, have been added to primary fixatives such as glutaraldehyde to better preserve smooth endoplasmic reticulum in interstitial cells of testes and other steroid-secreting cells, although microtubules are sometimes sacrificed in the process. Another attempt to produce better preservation of male reproductive tissues has utilized glutaraldehyde primary fixation followed by postfixation in osmium containing potassium ferrocyanide.

Tannic acid has been added to glutaraldehyde to help preserve various proteinaceous components of cells, such as microfilaments and microtubules, as well as cytomembranes. Its mode of action is purported to be a reaction with peptide bonds, amine, and amide residues present in side chains of polar amino acids.

Glutaraldehyde containing uranyl acetate has been utilized to preserve structures with a tendency to lose DNA because the mixture has been shown to gel DNA in minutes. Uranyl acetate is also frequently used as a separate incubation step (usually a 0.5% aqueous mixture) after primary aldehyde fixation and osmium postfixation. Samples are fixed overnight at 4°C in the uranyl acetate solution to help preserve phospholipids and to stabilize nucleic acids. The need for a uranyl acetate poststaining step is then considered by many workers to be unnecessary. Uranyl acetate reacts with phosphate groups of phospholipids and nucleic acids, and serves as an electron-dense stain after becoming complexed with these cellular constituents.

Finally, various workers have utilized alcian blue, ruthenium red, or cetylpyridinium chloride in aldehydes to help stabilize polysaccharide residues, particularly those on cell surfaces. In addition, ruthenium red has also been utilized for the same purpose as an additive during osmium postfixations. This area will be considered again in the section on cytochemistry, since the compounds are semispecific stains as well as fixatives.

7. Procedural Comparisons

a. Sequential Fixation

Sequential aldehyde/osmium fixation with a primary fixation for 1–2 hr in 2% glutaraldehyde in a 100 mM phosphate or cacodylate buffer at pH 7.2–7.4, followed by a postfixation in 1–2% osmium in the same buffer, is common in electron microscopy. As mentioned previously, lipids can sometimes migrate and/or change configuration in this type of fixation schedule.

b. Simultaneous Fixation

Simultaneous aldehyde/osmium fixation can be used successfully with various single-celled protozoans but can be expected to be most useful in a situation where lipid lability is of concern. It can exhibit penetration problems with blocks of tissue, resulting in only a superficial layer of adequate fixation. Customarily, quadruple-strength glutaraldehyde (8%) is mixed in equal volume with quadruple-strength buffer (0.4 M phosphate buffer, pH 7.2–7.4), and this combined mixture is added to an equal volume of double-strength aqueous osmium (4%) just before adding

tissues or cells. This results in a fixative containing 2% glutaraldehyde, 2% osmium, and 0.1 M phosphate buffer at pH 7.2–7.4. The various components can be easily made up far in advance of use and stored separately in the refrigerator. However, once they are mixed together, they begin reacting, with the glutaraldehyde reducing the osmium. At room temperature, the mixture will turn an opaque black within 1 hr after mixing. This is not of concern because there is such an excess of both fixative components. Some workers insist that this sort of procedure should be done at 4°C to minimize the fixative interactions, but it is unnecessary and theoretically would impede the interaction of the fixatives with the tissue to some extent. The whole point of this regimen is to be able to stabilize both proteins and lipids in the early moments of the fixation schedule, rather than waiting for 1–2 hr to stabilize the lipids with osmium. This technique is very effective for certain protozoans and seems to improve some neural samples.

c. Aldehyde Mixtures

Karnovsky first introduce aldehyde mixtures as primary fixatives in 1965. His original formula contained 5% glutaraldehyde and 4% formaldehyde made freshly from paraformaldehyde in 80 mM cacodylate buffer at pH 7.3 and included 5 mM $CaCl_2$. Various workers almost immediately modified this highly hypertonic medium (2,010 mOsm) by using it in a half-strength formulation. Over the years, some investigators have used phosphate buffer rather than cacodylate buffer, have used other percentages of the constituent aldehydes, or have omitted the calcium chloride. Thus, when reading the literature, beware of papers indicating that they used "Karnovsky's" fixative. Unless the authors specifically spell out the formulation they used, all you know is that they used some combination of formaldehyde and glutaraldehyde in some sort of buffer for their primary fixation.

Another major advance came in 1976 when McDowell and Trump examined a variety of aldehyde fixative combinations for kidney perfusions. They determined that 4F:1G (4% formaldehyde, 1% glutaraldehyde in a sodium phosphate buffer at pH 7.2–7.4) fulfilled their needs most completely. They were looking for a fixative of moderate osmolarity (760 mOsm) that could be made from commonly stocked chemicals with long shelf lives (25% biological-grade glutaraldehyde and 37–40% biological-grade formaldehyde) and that could be made into the final fixative solution and stored for some months before use (up to 3 months at 4°C). In addition, they wanted a fast-penetrating fixative that was suitable for perfusing kidneys. The formaldehyde component penetrated the tissue rapidly and was then followed by the more slowly diffusing glutaraldehyde, which stabilized the tissue more thoroughly and more permanently than the formaldehyde. This fixative was easier to formulate than Karnovsky's, since the formaldehyde was not made up fresh from paraformaldehyde powder and had a longer shelf life before application to tissues. They also determined that kidneys could be stored in the fixative for up to a year at 4°C without any serious structural changes. Finally, they noted that 4F:1G-fixed tissues embedded in paraffin still sectioned well and could be subjected to common histological staining techniques with excellent results. This contrasted significantly with the situation for most electron microscopy fixatives. Almost all procedures call for the use of at least 2% glutaraldehyde for fixing samples for ultrastructural examination. Tissues prepared in this fashion and then embedded in paraffin are typically brittle and hard to section. In addition, the excess glutaraldehyde in the samples with unbound hydroxyl groups makes them nonspecifically Schiff's reagent positive. As mentioned earlier, this is one way to monitor the depth of fixative penetration into tissues fixed with glutaraldehyde. By dropping the glutaraldehyde concentration to only 1%, most of the glutaraldehyde hydroxyl groups that could react with Schiff's reagent are cross-linked to proteins in the tissue and are thus unavailable to react with the stain.

d. Temperatures for Fixation

As mentioned previously, temperatures for fixation are variable in the literature. Many workers are convinced that fixing on ice or at 4°C is necessary. During fixation, various hydrolytic enzymes, such as acid phosphatases and esterases, begin leaking from their storage compartments (lysosomes) as membranes become partially solubilized during fixation. These enzymes can hydrolyze various cytoplasmic components, culminating in their removal during ensuing aqueous and other solvent washes. It is recognized that formaldehyde and glutaraldehyde, our most commonly used primary fixatives, do not completely inactivate a broad assemblage of enzymes (Hopwood, 1967, 1972). We make use of this knowledge when designing protocols for enzyme cytochemistry but frequently overlook it when questioning a partially unsuccessful fixation procedure. Maintaining a temperature considerably below the normal V_{max} range for these enzymes thus makes some sense. In addition, lower temperatures should also decrease the amount of cellular extractions possible during various fluid washes while tissues are being processed.

However, low temperatures will depolymerize microtubules and will cause vasoconstriction during perfusions of live animal tissues.

Our laboratory has used room-temperature fixation for 1 hr in 4F:1G fixative followed by postfixation for 1 hr in 1% osmium in a 0.1 M phosphate buffer, which is suitable for a variety of tissues from mammals, birds, fish, and plants, as well as for viruses, bacteria, fungi, and protozoans.

e. Storage

Storage of fixatives has been covered under the sections on individual fixatives, but a general recapping is in order. Most aldehyde fixatives diluted to working strength and appropriately buffered for use are stable for at least a year at 4°C. Aqueous osmium stocks are stable for months at the same temperature, provided that no dirt, buffer, or other reactive substances have been introduced and that they are stored in the dark.

Discussions on the pros and cons of storing EM samples in fixatives are relatively scarce in the literature (Bozzola and Russell, 1999; Flegler *et al.*, 1993; Robinson *et al.*, 1987). Glauert (1975) suggested, "... Fixation should not be prolonged since aldehydes do not stabilize lipid components and these may well be extracted during an extended fixation." Hayat (2000) says "The most desirable practice in the preparation of specimens for electron microscopy is to fix and embed them immediately after their collection." He gives no information concerning the outcome of long storage in fixatives but does say that storage of aldehyde-fixed samples in buffer "... is not recommended." In one of Hayat's earliest texts (1970), he discusses acceptable results reported in the literature in cases where samples had been stored in various aldehydes for several months or buffered formalin for up to 1 year. Chapter 5 in *Procedures in electron microscopy* (Robards and Wilson, 1993) provides a section on sample storage in fixatives and repeats the conventional wisdom that "... best preservation of biological specimens is achieved when processing immediately follows primary fixation." They next review reports that prolonged storage of perfusion-fixed liver, kidney, brain, and heart samples from rats fixed and stored at either 4°C or 21°C for up to 12 months produced rare myelin-like whorls of membrane in all of the tissues, but most prominently in the brain tissue at 6 months of storage. By 12 months, the whorls were associated with "areas of lucency," suggesting lipid leaching. Myelin-like whorls were also seen in skin samples stored for up to 4 weeks in phosphate-buffered 2.5% glutaraldehyde. In addition, storage of gastrin cells in 4% glutaraldehyde for 24 hr produced a marked decrease in dense-cored granules in the cells. Other workers insist that samples should never be stored in aldehydes because excessive protein precipitation will take place over time. Figures 11 and 12 compare a rat kidney sample

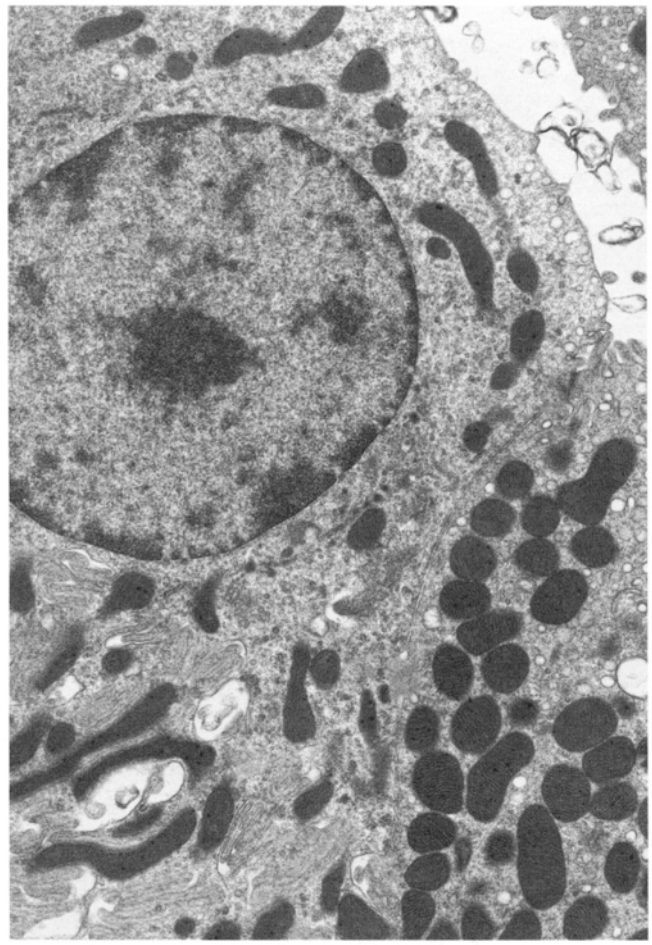

Figure 11. Distal convoluted tubule of a rat kidney fixed with 4F:1G and processed on the same day in 1985. 10,769×.

fixed and processed to resin on the same day in 1985 to a piece of the same sample of rat kidney stored in 4F:1G fixative at 4°C until final processing to resin in 2002. You will note that they are essentially indistinguishable and that long-term storage in aldehyde fixative produced a good publishable image. Long-term storage in other aldehyde fixatives has not been explored in our laboratory, but similar results would be expected. If the primary fixation is of a high quality, storage at 4°C in the fixative for long periods should not seriously degrade the samples.

However, it is generally agreed that long-term storage of samples in osmium solutions is not a good idea because within hours, polypeptides are cleaved into peptides, which are solubilized by the various washes, resulting in significant extraction of cellular contents.

f. Perfusion Methods

As mentioned before, perfusion methods for a variety of tissues are thoroughly discussed by Hayat (1981, 2000), and thus the technical aspects will be omitted here. Suffice it to say that if your research necessitates perfusion, it is best to consult recent literature in your area to

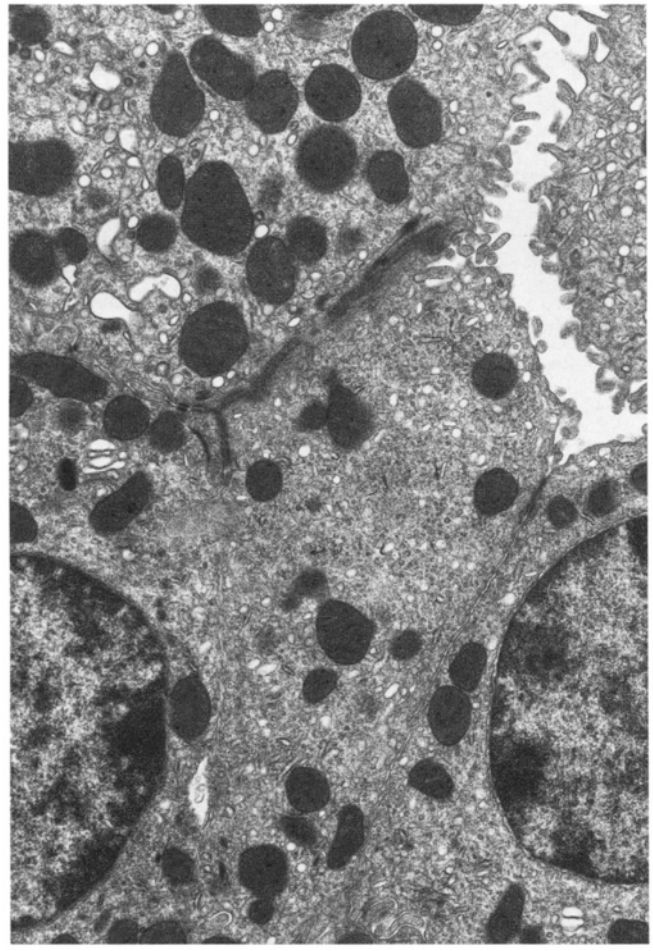

Figure 12. Distal convoluted tubule from the same rat kidney as shown in Fig. 11, except that it was fixed in 4F:1G in 1985 and subsequently stored at 4°C until further processing in 2002. 10,769×.

determine what your colleagues are doing with success. Perfusions are indicated when the tissue autolyzes quickly, changes structurally when vascular supplies are compromised (kidneys), or is deep within a large organism, necessitating lengthy dissection procedures before you can excise the small pieces mandated for good fixation, such as with brain. Clearly, utilizing the vasculature of an organism for the delivery of fixatives to all cells in a tissue is quicker than relying on diffusion of the fixative from the surface into a millimeter cube.

Most textbooks and manuals discount the need for any consideration of transport when working with plants or other nonvascular (in the circulating-fluid sense) organisms. There are exceptions to this concept, however. Dr. Gene Shih (personal communication) studied phloem in higher plants in the early 1970s and discovered that sieve-tube elements with plasmodesmata communicating with adjacent cells presented two different pictures depending on whether the stems were cut beneath fixative solutions or whether they were cut and then immersed into fixatives. He suggested that the image produced from stems sliced open under fixative solutions was less artifactual.

g. Marine Organisms

Marine organisms collected from nature or grown in complex artificial media can present special problems on occasion. Many ciliates and flagellates will continue swimming to the top of a tube while you are trying to spin them to the bottom prior to fixative addition. In these situations, it becomes necessary to mix a double-strength fixative in equal volume with the surrounding medium in the tube to kill them prior to centrifugation. If the medium contains significant amounts of reactive salts, such as calcium or magnesium, phosphate buffers will become coprecipitated with them, thus potentially putting precipitates into the tissue, as well as losing the buffering capacity of the medium and the fixative buffer. To avoid this problem, it is advisable to utilize cacodylate buffers, as will be detailed in the section on buffers.

Mixing double-strength fixative solutions with organisms contained in growth media is also necessary if the organisms have cellular projections, such as bacterial pili or flagella, which may be shed by the organisms if handled excessively. In many cases, once the fixative kills the cells, the structures will not be shed.

h. Anesthetics

Anesthetics are another often overlooked aspect of fixation. The various common anesthetics utilized in animal research affect some tissues in deleterious ways that must be considered when designing fixation protocols. A tissue such as liver can respond to certain classes of anesthetics such as barbiturates. Thus, if working with liver, other anesthetics should be considered. A more thorough discussion of this topic can be found in Hayat's works (1981, 2000).

i. Nutritional States

Nutritional states of some organisms can affect the perceived fixation quality. A liver from an animal fed right up to the moment of sacrifice is structurally different in terms of glycogen reserves and mitochondrial configurations from an animal taken off food 12 hr before sacrifice. Compare ultrathin sections from the liver of a well-fed rat (Fig. 13) with those from the liver of a fasted animal (Fig. 14). You will note that hepatocytes of the well-fed liver contain large cytoplasmic pools of dark, granular glycogen, while the hepatocytes from the fasted rat liver have dense cytoplasmic contents devoid of this material. This kind of change is important to consider when designing protocols and evaluating resulting photographs.

This whole section on fixation should make it clear that a variety of approaches can usually be taken to solve the same problem. If the initial simple attempts with general protocols fail, move on to more esoteric formulations to stabilize the samples in question. The approach in our laboratory is to try something like 4F:1G fixative first; we rarely have to move on to the more complicated procedures.

III. BUFFERS

A. Molarity/Molality/Osmolarity/Tonicity

Before any serious consideration of buffering systems can be undertaken, it is useful to review the various ways to discuss the concentration of solutions. When making up chemical

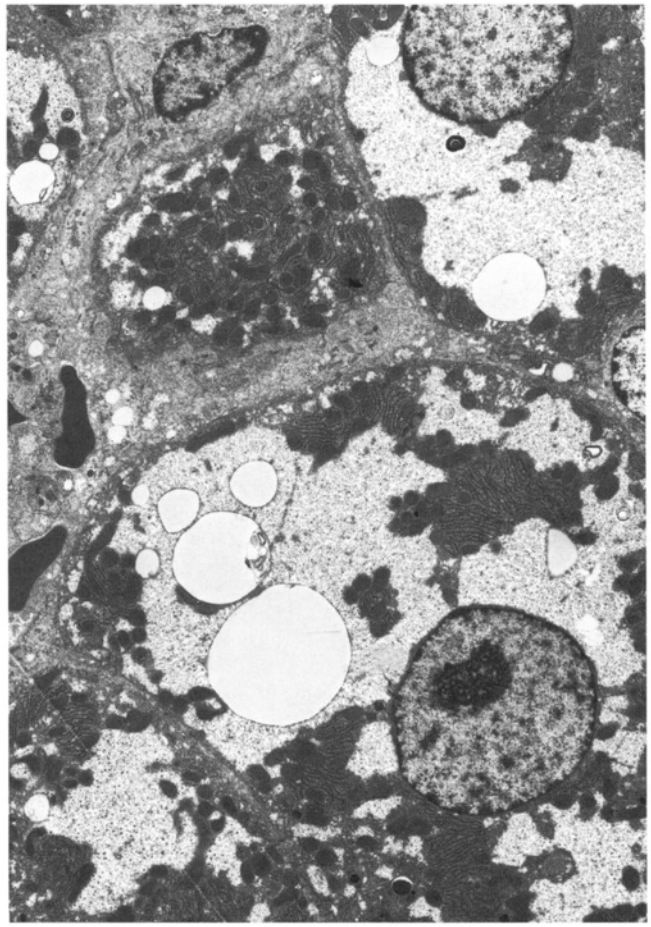

Figure 13. Rat liver from well-fed rat. 3,385×.

solutions, we normally talk in terms of molarity, wherein a 1.0 M solution is one molecular weight (MW) of solute brought up to 1 liter with solvent. Conversely, to make a solution with a molality of 1.0, 1 MW of the solute is added to sufficient solvent to produce a kilogram of solution.

A related concept used with acidic and basic solutions is normality (N). If the acid has only one hydrogen (HCl) or the base has only one hydroxyl group (NaOH), normality and molarity are identical. However, if there is more than one hydrogen or hydroxyl group in the formula, the normality and molarity are not identical, and the concept of equivalent weight must be considered. Equivalent weight is the molecular weight divided by the number of unit charges. Hydrochloric acid has a molecular weight of approximately 36.45, which means that a 1.0 M solution would contain 36.45 g of pure HCl, brought up to 1 liter with water. A 1.0 N solution would be formulated the same way, since the molecular weight divided by the number of unit charges (one hydrogen) is still 36.45 g/l. A 1.0 M solution of phosphoric acid (H_3PO_4), however, consists of 98 g/l, but only 32.67 g/l is needed to make a 1.0 N solution (98 MW/3 charges due to the three hydrogens = 32.67).

The term *osmolarity* (Osm/l) occurs frequently in discussions of buffers and fixative solutions. Tonicity and osmolarity are equivalent. An isotonic solution has the same osmotic

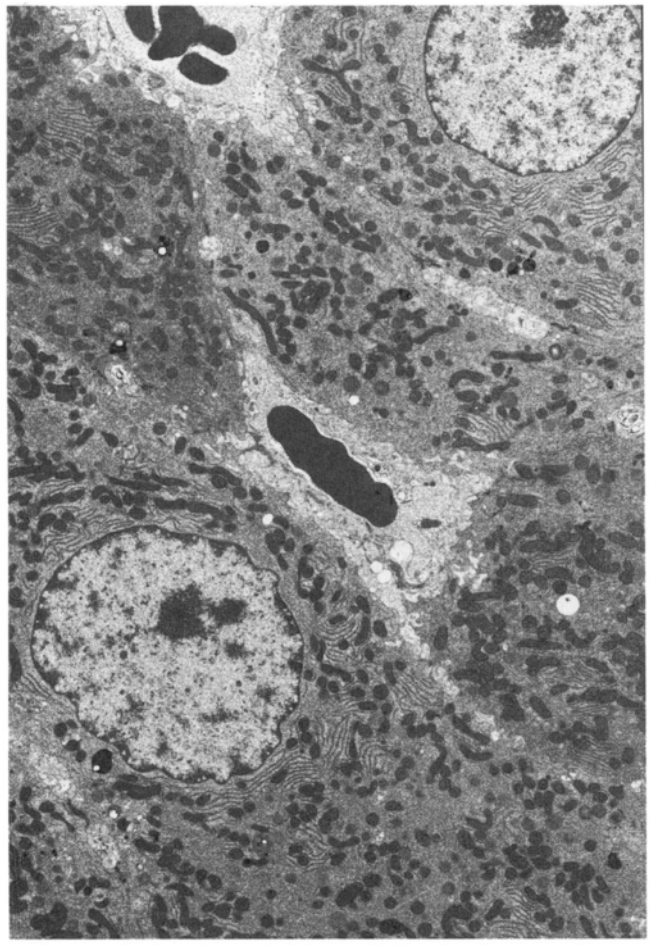

Figure 14. Rat liver from fasted rat. 3,385×.

potential as the cytoplasm of cells within it. If a nonelectrolytic solution is involved, molarity and osmolarity are the same. If a solution contains a dissociating electrolyte, the osmolarity is greater than the molarity (the osmotic pressure on the cells greater than it would be for a nonelectrolyte solution of the same molarity). Osmolarity is most frequently measured by freezing-point depression of a solution. Fixative solutions are typically either isotonic or slightly hypertonic (see Saito and Tanaka, 1980 for examples of the effect of different tonicities on cells).

Unfortunately, osmolarity of the cytoplasm of a living cell is not measurable. In practice, this means that fixatives with different tonicity have been tried on a variety of cell and tissue types. Some of those that have worked have had their osmolarity checked. Further studies can use an osmometer to ensure that all fixative solutions have the same osmolarity. Naturally, in a given organism such as a rat different tissues may have various osmolarities. It then becomes a task of empirically determining the best osmolarity for a fixative and buffering system. Once a suitable buffer strength is selected, an osmometer can be utilized to reproduce this osmolarity for ensuing studies. Thus, the osmolarity of a fixative or buffer can be measured, but the osmolarity of a cell is hard to determine. The best function of an osmometer is to measure the consistency of tonicity of solutions.

To formulate a glutaraldehyde fixative solution with the same osmotic potential as the osmium postfixative solution, it would be necessary to increase the tonicity of the vehicle (buffer) for the osmium because osmium has less osmotic potential than glutaraldehyde. A quick scan of the bulk of the electron microscopy techniques used in the literature makes it obvious that most investigators use the same buffer for both the primary and secondary fixative solutions, so absolute equivalencies in osmolarity are not necessary in customary practice.

B. Purpose

The purpose of buffers is threefold. First, the buffer serves as a solvent for the fixative constituents. Second, the buffer helps maintain a specified pH. Third, the buffer maintains tonicity, as described above. In the primary fixative, all three factors are important. However, after primary fixation in aldehydes, tonicity becomes a trivial concern because the cell membranes are no longer subject to osmotic potentials due to a major increase in permeability for small molecules conferred by primary fixation.

This is best exemplified by one of the major techniques utilized for the preparation of samples for cyroultramicrotomy (Tokuyasu, 1983). In this technique, cells are lightly fixed with aldehydes prior to being rinsed and placed in 2.3 M sucrose in phosphate buffer. If the cells were placed in sucrose *prior* to the aldehyde fixation, they would plasmolyze badly, but primary fixation prevents plasmolysis because of molecular changes in the plasmalemma induced by primary fixation.

Maintenance of pH is a significant activity of buffers, particularly if tissues are stored in the primary fixative or buffers for any period of time. As mentioned in the section on osmium, if osmium is the primary fixative, it tends to cleave polypeptides into their constituent peptide molecules. As the process continues, more and more carboxy terminals are exposed, causing a tendency for a decrease in pH that the buffer must resist. Tissues left in unbuffered osmium go from pH 6.2 to 4.4 in 48 hr (Hayat, 1981). Cellular necrosis itself can cause pH changes as the constituent proteins undergo autolysis, leading to the same potential for a drop in pH.

When designing buffering protocols, it is important to recognize that pH is somewhat dependent on temperature, so the buffer pH should be adjusted at the temperature at which the buffer is to be used. Another consideration is the effect of buffer concentration. A 0.2 M buffer diluted to 0.1 M by adding an equal volume of distilled water will still have the same pH, but its buffering capacity will be reduced.

C. Types, Characteristics, and Uses of Buffers

1. Phosphate Buffers

Phosphate buffers are probably the most widely used buffers in biological work. They are used for irrigation solutions for living tissues during surgical procedures (phosphate-buffered saline, or PBS), are used to make up immunologically active solutions during immunocytochemical staining procedures, and are used widely to buffer fixatives for light and electron microscopy preparations. They can be used to wash living cells in culture without inducing injury. The pH is maintained more effectively than with the other most commonly used buffer, sodium cacodylate.

In electron microscopy, phosphate buffers may be formulated from monobasic sodium phosphate (NaH_2PO_4), as in Millonig's phosphate buffer, or from a combination of monobasic and dibasic (Na_2HPO_4) sodium phosphate, as in Sorenson's buffer. Phosphate buffers are preferred by many workers, partially because of the lack of toxicity compared with the second most commonly used buffer, sodium cacodylate. However, the reactivity of phosphate groups must be considered when formulating solutions containing positively charged compounds, such as calcium or magnesium salts. It has been reported that the dibasic form of phosphate may cause protein precipitation and also can precipitate lead, uranyl acetate, and other polyvalent cations. Glauert (1975) has shown dog lung cells covered with a black precipitate that is said to be due to mixing phosphate buffer with osmium. Similar work in our laboratory has never produced this artifact. Phosphate buffers are best used either at physiological pH or in a slightly alkaline formulation (pH 7.2–7.4). Their buffering capacity drops dramatically when significantly above or below this range.

2. Sodium Cacodylate (Cacodylate) Buffer

Cacodylate buffer is the second most commonly used buffering material used in electron microscopy. Like phosphate buffer, it is used primarily at physiological pH or at slightly alkaline conditions, though it buffers effectively at pH 6.4–7.4. It lacks the strongly reactive character of phosphate solutions and thus can be used in cytochemical reaction mixtures and with media containing various ions without fear of coprecipitation with other solution components. If, for example, you are faced with fixing a marine protist that cannot be centrifuged easily in a living state because the organism swims to the top of the tube, it is often advisable to mix double-strength buffered fixative in equal volume with seawater containing the organism. However, seawater contains numerous salts that can be precipitated by phosphate buffers with consequent drastic changes in pH. Cacodylate buffers will avoid this problem, but this will precipitate uranyl acetate. Furthermore, sodium cacodylate contains arsenic and can produce arsenic gas when exposed to acids. It is toxic to the user and can cause dermatitis, so it must be handled with care. Sodium cacodylate is more toxic to cells than phosphate buffers. Finally, sodium cacodylate is also considerably more expensive than phosphate buffer components.

3. Collidine Buffer

Collidine buffer has mostly historical significance at this time. It was used as a buffer for osmium when used as a primary fixative. It was originally used because it had an effective pH range of 6.0–8.0, but it caused significant extraction of proteins in some tissues and was not compatible with formaldehyde, leading to membrane damage. It is also a relatively toxic compound.

4. Veronal Acetate

Veronal acetate buffer works most effectively at pH 4.2–5.2, is ineffective at physiological pH, and is reactive with aldehydes. It is thus contraindicated as a buffer for electron microscopy. Veronal acetate was first used as a buffer when osmium was being used as a primary fixative (Palade, 1952). Hayat (2000) states that it produces better membrane preservation than other buffering systems used with osmium. Veronal acetate is useful for cytochemical procedures that require maintenance of slightly acidic conditions.

5. Tris

Tris buffer is most effective above pH 7.5 and thus finds most use in cytochemical incubation solutions for demonstrating enzymes with activity under alkaline conditions. It may react with glutaraldehyde, so washing after primary fixation must be thorough.

6. Sodium Bicarbonate

Sodium bicarbonate is frequently encountered in buffers prepared for physiological studies but is not commonly recommended for electron microscopy fixative preparation. Salema and Brandao (1973) suggested that it was superior to phosphate buffers for the preservation of plant tissues.

7. Zwitterionic Buffers

The zwitterionic buffers PIPES, HEPES, and MOPS are a class of buffers little used in electron microscopy that are either amines or N-substituted amino acids. They have been used in tissue culture media, indicating their lack of toxicity and their effective buffering capabilities. Hayat (1981) states that they might find utility in microanalytical studies because they do not contain ions that might compromise elemental analysis. He also suggests that they produce a relatively high cellular density because of increased retention of proteins and phospholipids.

8. Miscellaneous Buffers

Various enzymatic localization protocols require maintenance of either high or low pH, so miscellaneous buffers are used for these specific purposes. It is helpful to recognize that many of these buffers have incompatibilities with common components of fixative solutions, and appropriate washes need to be employed to prevent inappropriate interactions between the constituents of these different solutions.

IV. DEHYDRATION

A. Purpose

The purpose of dehydration agents is to remove water from samples so that they can be infiltrated with the most widely used embedding media that are typically immiscible with water. Dehydration is also important for the preparation of materials for SEM, removing water from the specimen, and typically replacing it with ethanol, which then can be exchanged with liquid carbon dioxide during the critical-point drying process.

B. Agents

Ethanol and acetone are the two most commonly used dehydration fluids, with propylene oxide frequently recommended as a final transition solvent used to make up diluted epoxide

mixtures during the initial resin infiltration. Many of the electron microscopy texts and laboratory manuals suggest that propylene oxide is necessary for epoxide resin infiltration or that it is in some way superior to acetone as a transition solvent. This is neither borne out in practice nor mandated by the resin manufacturers' and vendors' instructions. The standard epoxide resins in use today (Spurr's resin, Poly-Bed 812, LX-112, SPI-Pon 812) are easily mixed with acetone, and infiltration is excellent with this transitional solvent. In addition, these resins are also miscible with ethanol and the resulting blocks section well, though the blocks are usually somewhat tacky on the surface. Despite its long record in the literature, because propylene oxide is the most toxic of the three solvents, has the highest vapor pressure, and confers no discernible advantage to infiltration processes for epoxide resins, it can no longer be recommended.

1. Ethanol

Ethanol continues to see the widest application as a dehydration agent. It is the most benign of the solvents used for dehydration because it is not as strong an organic solvent as acetone and thus is potentially less injurious to the user. In addition, it exhibits less flammability than acetone. However, Luft and Wood (1963) reported that 4% of proteins were extracted during dehydration following primary fixation in osmium, with the majority being lost in the more dilute ethanol steps. None were lost in 95–100% ethanol rinses or in the propylene oxide step. A study by Hanstede and Gerrits (1983) described linear shrinkage of about 9.3% in liver dehydrated with ethanol, mostly in ethanol concentrations above 95%.

2. Acetone

Acetone has been used as the sole dehydration agent in some protocols and appears to cause less tissue shrinkage than an ethanolic series. An early study by Page and Huxley (1963) determined that while 10% linear shrinkage in skeletal muscle occurred with ethanol dehydration, none was noticeable with an acetone series. Phospholipids stabilized by *en bloc* uranyl acetate treatment should be relatively unextracted by acetone dehydration, while the more hydrophobic lipid entities such as sterols and glycerides can be expected to be significantly extracted.

3. Dimethoxypropane

Dimethoxypropane (DMP) has been recommended as a superior dehydration agent compared to acetone or ethanol because more water-soluble entities remain in place (Thorpe and Harvey, 1979). Other workers (Beckmann and Dierichs, 1982) have suggested that DMP treatment extracts more lipids than ethanol or acetone. Due to the relatively limited application of DMP for dehydration in comparison with the other two solvents listed, it is still difficult to make a strong argument for the use of DMP.

C. Parameters

It should be evident from this brief discussion that shrinkage and extraction of various cellular components are to be expected with any dehydration series. It is thus important to consider

ways to minimize this effect. Employing a protocol that provides the least amount of time in solvents, including the eventual infiltration of resins (which are also solvents) is clearly the best plan. A brief scanning of the literature will reveal that there are proponents of cold dehydrations to minimize extractions, while other workers routinely dehydrate at room temperature. If refrigerated dehydration series are used, they will tend to develop increased water content after each exposure to room-temperature air as they come out of the refrigerator due to condensation of moisture from the air as it contacts the cold solvent. This can compromise the "dryness" of the final dehydration steps (100% ethanol, 100% acetone). As you will see in the section on resins, this is of extreme importance, because any residual water in the specimen or transition solvent can ruin the polymerization capabilities of most epoxide resins.

There are various approaches to dehydration, some involving more incremental steps and some involving fewer steps. If speed is the most important consideration, as might be expected in certain clinical settings, extremely rapid dehydration can be accomplished if the tissue samples are kept small (0.25 mm^3). Coulter (1967) completed a successful dehydration using ethanol followed by propylene oxide in under 30 min utilizing such small pieces of tissue and constant agitation. Under most circumstances, however, it is more convenient to dehydrate at a more leisurely pace. In our laboratory, we remove our osmium postfixative with two quick distilled water rinses followed by room temperature washes in 50% ethanol (15 min), 75% ethanol (15 min), 95% ethanol (two 15-min washes), 100% ethanol (two 30-min washes), and finish with two 10-min washes with 100% acetone before beginning our epoxide resin infiltration steps. We have never encountered any problems with insufficient dehydration or any appearance of excessive extraction. This procedure has been used with organisms from the five major kingdoms of life with equally good results.

V. EMBEDDING MEDIA

A. Ideal Qualities

Ideal qualities of embedding media include uniformity of batches of resin components, good solubility in dehydration agents, and low viscosity as a monomer, along with minimal shrinkage, stability under the electron beam, minimal granularity, and good sectioning characteristics. Unfortunately, some of these goals are mutually exclusive. For example, resins with low viscosity tend to shrink significantly during polymerization (see Table 2 for a listing of resins and resin viscosities). In addition, certain sacrifices are made when cytochemical or immunocytochemical methods are employed. Methods and media designed for the preservation of chemical reactivity often lead to muddier images than seen with samples prepared for strictly structural studies.

B. Classes and Characteristics of Resins

1. Acrylic Resins

The use of acrylic resins, primarily for immunocytochemical procedures, is predicated on the fact that these resins are more hydrophilic than the highly hydrophobic epoxide resins utilized

Table 2. Selected Resin Embedding Media

Acrylic
- Hydrophilic (polar): used primarily for immunocytochemistry
  - Lowicryl K4M (polymerizes with UV at −35°C)
  - Lowicryl K11M (polymerizes with UV at −60°C)
  - LR White (polymerizes at room temperature with added accelerator; at 60°C overnight without accelerator)
  - LR Gold (polymerizes at −25 °C with UV)
- Hydrophobic (apolar): good for lipid retention
  - Lowicryl HM20 (polymerizes with UV at −70°C)
  - Lowicryl HM23 (polymerizes with UV at −80°C)

Epoxy (viscosities in centipoises [cP] at 25°C)
- Water-immiscible
  - Epon 812 (150–210 cP; manufacture discontinued by Shell Oil Co. in 1979)
  - Epon 812 Replacements:
    - Medcast (Pelco)
    - Eponate 12 (Pelco)
    - SPI-pon 812 (SPI)
    - Poly/Bed 812 (Polysciences; somewhat water miscible)
    - EMbed 812 (EMS)
    - LX-112
  - Araldites
    - 502 (3,000 cP)
    - 6005 (1,300–1,650 cP)
  - Maraglas 655 (500 cP)
  - Spurr (60 cP)
  - HXSA-based Low Viscosity (21 cP; similar to Spurr except NSA replaced with Hexenyl Succinic Anhydride [HXSA]; Pelco)
- Water-miscible
  - Durcupan
  - Quetol 812 (140 cP; Kushida, H. 1983. *J. Electron Microsc.* 32: 65)
  - Quetol 651 (15 cP; Fujita *et al.* 1977. *J. Electron Microsc.* 23: 165)
  - Quetol 653 (60 cP; Kushida, H. 1980. *J. Electron Microsc.* 29: 193)

Melamine
- Nanoplast (water-miscible, no dehydration necessary; good for LM and EM; 8 to 10 times more expensive than resins such as Spurr's)

Polyester
- Vestopal-W

for standard structural studies. This allows sections of acrylic resin embedded materials to be probed with a variety of aqueous reagents with great success.

Acrylic resins were first used in the form of glycol methacrylates (Newman *et al.*, 1949). The glycol methacrylates have proved inadequate for ultrastructural examination because of their lability under the electron beam but have remained important for light microscopy studies, primarily in the form of JB-4™ resin. Acrylics, in general, are prone to uneven polymerization, which can be due to impurities in the resin or to the specimen itself catalyzing polymerization. Acrylics are strong lipid extractors as well as being more unstable under the electron beam than the epoxide resins. They must be polymerized in the absence of oxygen, so specimens are usually placed into resin-filled gelatin capsules, which are capped to exclude excess oxygen. Acetone also prevents polymerization, so the typical dehydration series is ethanolic, culminating in 95–100% ethanol for the water-miscible acrylics such as Lowicryl K4M, and LR White. Osmium in tissues can lead to inadequate polymerization in some cases, notably with the glycol methacrylates used

for light microscopy. Osmium also renders tissues opaque, thus preventing proper polymerization if ultraviolet (UV) light is used. Lowicryl resins will polymerize at room temperature with their catalyst, but the reaction is exothermic and produces an unacceptable increase in temperature unless polymerized at lower temperatures (on ice, typically). LR White resin sections can be usually picked up on uncoated grids, though they will respond to the electron beam by drifting initially. However, Lowicryl sections generally need a support film such as Formvar to prevent excessive movement under the beam. See Table 2 for brief descriptions of some of the acrylic resins currently in use.

2. Polyester Resins

Polyester resins were introduced by Kellenberger *et al.* (1956). The most commonly available resin is Vestopal W. It is more immune to beam damage than the methacrylates that it replaced, shrinks less, and polymerizes more evenly. The presence of air results in uneven polymerization. Polymerized blocks are harder than epoxy resin blocks. Two of the three components, benzoyl peroxide and cobalt napthenate, are unstable even if held at 4°C, and benzoyl peroxide must be mixed with Vestopal W prior to the addition of cobalt napthenate or a strongly exothermic reaction may take place. Heat may be used to polymerize the resin, eliminating the need for cobalt napthenate. The polymerized resin has excellent sectioning characteristics, low background, and consequent high contrast.

3. Epoxide Resins

Epoxide resins (see Table 2 for brief descriptions of readily available types) were introduced in 1956, with the Araldites (Glauert *et al.*, 1956) finding wide use despite their high viscosity. Luft (1961) published a seminal paper utilizing Epon 812 from Shell Oil Co., which had considerably less viscosity than the Araldites. Several authors then formulated mixtures of Epon and Araldites (Mollenhauer, 1964) that yielded blocks with the excellent sectioning characteristics of Araldites, along with a lower viscosity than found with Araldites used alone.

Epon was often used as the sole embedding medium because of its relatively low viscosity, minimal shrinkage, excellent sectioning and staining characteristics, and the low granularity of resulting images. Unfortunately, Shell Oil Co. stopped producing Epon in 1979, and the various Epon substitutes subsequently marketed are not exact replacements for Epon in all of the characteristics mentioned. Be aware that contemporary literature frequently mentions that samples were embedded in Epon (which was a specific trade name for the Shell Oil Co. product), but the investigators are invariably using one of the substitutes. Since the various Epon substitutes available from different vendors are not identical, it is useful to ascertain *which* Epon substitute they are actually using.

Most of the epoxides are extremely intolerant of the presence of water and will fail to polymerize properly if the tissue is not totally dehydrated, resulting in extremely rubbery blocks from which tissues cannot be rescued. As mentioned in the dehydration section, the epoxides are soluble in ethanol, acetone, and propylene oxide, though most schedules suggest passage through acetone or propylene oxide. These *transitional* solvents are better solvents for the resins than straight ethanol, though propylene oxide is more toxic than acetone and has no features to recommend its use. A few of the more recently derived resins are water miscible (see Table 2). Resins with viscosities higher than about 150 cP benefit from longer infiltration times, more gradual steps involving diluted resins, and rotation or tumbling of the specimens during infiltration.

Mollenhauer (1986) suggested the addition to Spurr resin of 0.1–0.4 g of lecithin dissolved in 0.1–0.4 g of peanut oil to improve sectioning characteristics with glass knives. This technique may be applicable to other epoxide resins.

Spurr resin (Spurr, 1969) is an excellent all-purpose epoxide resin that penetrates most tissues easily, stores for up to 2 months at −20°C, and has a short infiltration series (30 min in 50% Spurr/50% acetone; two 60-min steps in 100% Spurr; transfer samples to new Spurr in molds and polymerize overnight to 3 days at 70°C). If stored frozen, Spurr resin must be warmed to room temperature before opening to prevent water condensation, which would prevent proper polymerization of the resin. It has been our experience that vigorous conversation while changing resins or introducing samples into resin in molds is enough to produce rubber blocks, presumably due to a fine saliva spray being added to the liquid resin. The low viscosity of the monomer is associated with visible shrinkage in molds during polymerization. In addition, the resin chemically interacts with commonly used silicon embedding molds, unlike the other epoxides, resulting in premature failure of the molds (pieces of the silicon are pulled from the molds during block removal and cracking of the mold chambers is common over time). Spurr resin also does not stain effectively with aqueous uranyl acetate, so a 5% methanolic stain is usually employed, which can result in extensive wrinkling of sections if they are not dried properly (see the comments on section staining at the end of Chapter 4).

4. Polyethylene Glycol

Polyethylene glycol (PEG) was introduced as an embedding medium for producing sections for high-voltage electron microscopy (Wolosewick, 1980). The technique involves dehydrating normally fixed tissues to 100% ethanol, followed by placing the samples into a 1:1 mixture of 100% ethanol and PEG 4000 overnight at 60°C in uncapped vials, to let the alcohol evaporate. The tissues are then removed, briefly blotted dry, and placed in predried gelatin capsules filled with fresh PEG 4000. When the specimen has sunk to the bottom, the capsule is rapidly immersed in liquid nitrogen. Ultrathin sections are then cut (though the blocks are extremely hydrophilic and must be blotted dry frequently during sectioning) and placed on Formvar and poly-L-lysine-coated grids (the latter to keep the sections attached to the plastic film). They are next dehydrated again to remove the PEG and critical-point dried. This results in critical-point dried sections on grids without any surrounding medium, which thus have sufficient contrast to eliminate the need for poststaining. Samples embedded in PEG are relatively difficult to produce, so this technique has been largely limited to high-voltage electron microscopy preparations.

5. Miscellaneous Water-Miscible Media

Before the introduction of modern water-miscible acrylic resins in the form of the Lowicryls and the LR resins, media such as urea–aldehdye (Pease and Peterson, 1972) and Heckman and Barrnett's (1973) glutaraldehyde–carbohydrazide (GACH) were introduced to increase lipid retention and to produce sections that could be used for cytochemistry. These were innovative and useful in their day, but more difficult to handle than the acrylics, and so they have faded into history.

6. Health Hazards

All resins and their associated solvents present potential hazards. As mentioned previously, many workers still utilize the epoxide, propylene oxide, as a transitional solvent for epoxide resins. This is unnecessary and contraindicated due to its toxicity. We deal with a significant number of toxic substances during sample preparation and any that can be, should be eliminated. All epoxide resins should be treated with respect, but the vinylcyclohexene dioxide found in Spurr resin has been singled out for particular caution. It has been reported that, in addition to being potentially carcinogenic in liquid or vapor form, it is even dangerous after polymerization (Causton, 1981), suggesting that block trimming that produces chips of resin is a procedure that requires careful monitoring and cleanup. Acrylic resins are reputed to be less toxic than epoxides, but all resins and most of their solvents can cause dermatitis, so repeated contact with them may produce hypersensitivity. There are no readily available gloves guaranteed to be impervious to penetration by these substances. Double-gloving, wearing nitrile-based gloves, and keeping exposure times short may help, but the best policy is to prevent contact with these media in any way at any time.

C. Embedding Mold Types

Choice of Molds

The choice of molds is determined by the characteristics of the embedding medium employed and the need for specific specimen orientation. If an acrylic or polyester medium is used, air must be excluded, so gelatin capsules are commonly used. Polyethylene molds such as BEEM™ capsules are sometimes incompatible with acrylic resins polymerized with heat because they can partially dissolve. Flat embedding molds made of silicone rubber permit sample orientation. These molds come in a variety of colors and shapes, and are designed for different widths, lengths, and depths of resulting resin blocks. Some ultramicrotome chucks, in particular those used with Reichert and Leica ultramicrotomes, work best with flat blocks of a specific width that span the stepped ledges in the chucks. Experimentation with different mold configurations from different suppliers will reveal which ones work best for a specific ultramicrotome. The depth of the mold chambers also can be critical for some of the more brittle resins. Spurr resin blocks tend to break during trimming if too thin, so we use relatively deep molds to minimize this problem. One type of BEEM™ capsule has an extremely narrow attenuated tip that is not recommended for general use because they have a tendency to show chattered sections due to flexing. However, they permit good orientation of long, thin samples such as peripheral nerves or optic nerves, for transverse sections.

Specialized molds have been developed to embed cells grown on coverslips (Chang coverslip molds) or to serve as a substrate on which cells can be grown, fixed, dehydrated, and embedded, resulting in a 1×3 in. (2.5×7.6 cm) slide that has excellent optical characteristics for selecting individual cells to section (Hanker-Giammara mold). Consult the catalogs from electron microscopy supply houses listed at the back of this text for details concerning the different types of embedding molds manufactured.

Another approach to achieving desired sample orientation is to flat-embed tissues, cut out areas of the blocks and reorient them by gluing them to previously polymerized resin blocks containing no samples. Pieces of tissue can also be removed from polymerized resin blocks with

a jeweler's saw and oriented in empty flat-embedding molds, which then can be filled with fresh liquid resin and polymerized.

D. Agar Embedment

Agar embedment is a useful method for turning suspensions of cells, particulates such as mitochondria and microsomal preparations, or small metazoans such as shrimp embryos into tissue-like blocks for ease of handling during processing. Typically, cells are placed in primary fixative and rinsed several times in buffer before being immersed in molten water agar (at 45–50°C) and immediately centrifuged to bring the sample into the tip of the centrifuge tube (see the detailed instructions in the section Chapter 1 Techniques).

Another use of agar for specimen handling is the agar-peel technique for cells *in situ*. In this procedure, adherent cells in flasks or Petri dishes are rinsed free of growth medium with PBS to remove media proteins that otherwise would be fixed by aldehyde fixatives. The culture is then covered with the appropriate aldehyde fixative. After 30–60 min, the primary fixative is removed from the culture by several rinses with an appropriate buffer, and the cells are osmicated for an appropriate period of time and rinsed several times with distilled water. Molten 3–4% water agar is then gently poured onto the surface of the culture and allowed to harden. The culture is then dehydrated in a normal fashion. During the 100% acetone steps, the agar should come away from the dish, hopefully with the cultured cells attached to it. At that point, the agar with the cells can be cut into strips for further processing in vials and then finally flat embedded. On some occasions, the agar lifts off without removing the cells from the plate. If this occurs, put the plate back into 100% ethanol, so the plate will not be totally dissolved by the acetone. Then, go directly into a mixture of plastic resin and 100% ethanol after several rinses in 100% ethanol. After polymerization, pieces of the dish containing cells can be cut out with a jeweler's saw and glued to other blank blocks for sectioning. A method utilizing Permanox™ Petri dishes for growing, fixing, and embedding cells without using the agar-peel technique is described in the section Chapter 1 Techniques.

VI. EXAMINATION OF TISSUES PREPARED WITH A VARIETY OF FIXATIVES AND BUFFERS

We have already discussed various types of aldehyde fixatives and their combinations, as well as different buffers that can be used, and mixtures of aldhehydes and osmium for primary fixations. At this point, it would be useful to compare the effect of different protocols on a set of tissues. We have chosen three mouse tissues (kidney, liver, and small intestine). All the tissues were collected at the same time from the same animal and immediately placed in the various fixatives. Primary fixation was for 1 hr at room temperature, and in the cases where osmium was used as a postfixative, that step also lasted for 1 hr at room temperature. All tissues were rinsed in the same buffer used during primary fixation, rinsed in distilled water after osmium treatment, dehydrated in an ethanolic series, and embedded in Spurr resin as described in the section on routine processing of TEM samples in the Techniques section of this chapter. The figure legends describe the fixation protocol for each sample.

Figures 15–24 illustrate mouse kidney fixed in a variety of solutions. No totally unacceptable images appear, except in two cases. Figure 21 from a kidney fixed simultaneously with glutaraldehyde and osmium shows mitochondria almost in negative contrast and an overall muddiness of preservation, while the kidneys fixed in glutaraldehyde without osmium post-fixation

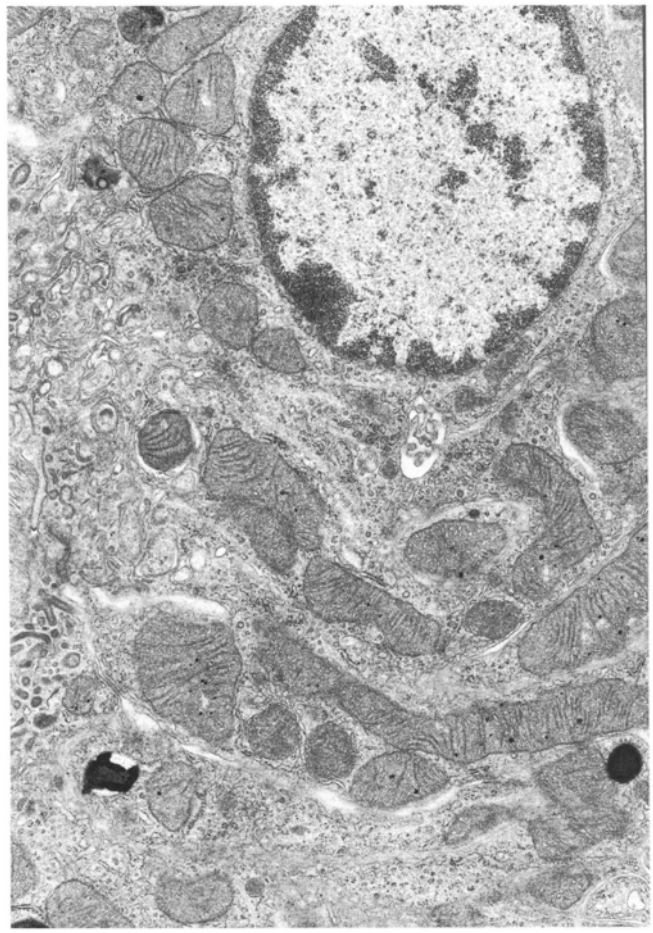

Figure 15. Mouse kidney fixed with Carson's fixative (4% formaldehyde in a phosphate buffer, pH 7.28. Postfixed in 1% osmium in the same buffer (Fix #1). 10,923×.

(Fig. 24) has indistinct membranous profiles, as well as electron-lucent areas where materials were extracted. The image shows a general granularity and muddiness. There are variations between the other preparations from the standpoint of mitochondrial density and nuclear and cytoplasmic extraction, but there is nothing in the series that is clearly unacceptable. In normal practice, samples prepared in exactly the same way with the same fixatives will show variation in the same range as seen in these samples.

Examination of the liver samples (Figs. 25–34) reveals more variation than found with the kidney samples. The Carson's-fixed sample (Fig. 25) had very irregular nuclear outlines and poorly differentiated glycogen. The full-strength Karnovsky's sample (Fig. 27) showed marked distension of endoplasmic reticulum, along with an apparent leaching of cytoplasmic materials. The material exposed to half-strength Karnovsky's (Fig. 28) showed some dilation of endoplasmic reticulum, along with a swollen and ruffled nuclear envelope profile. Tissues treated with osmium as a primary fixative (Figs. 32 and 33) showed some cytoplasmic extraction and damaged mitochondria. Finally, the liver fixed with glutaraldehyde, but without osmium postfixation (Fig. 34), had large extracted areas and indistinct membranous profiles.

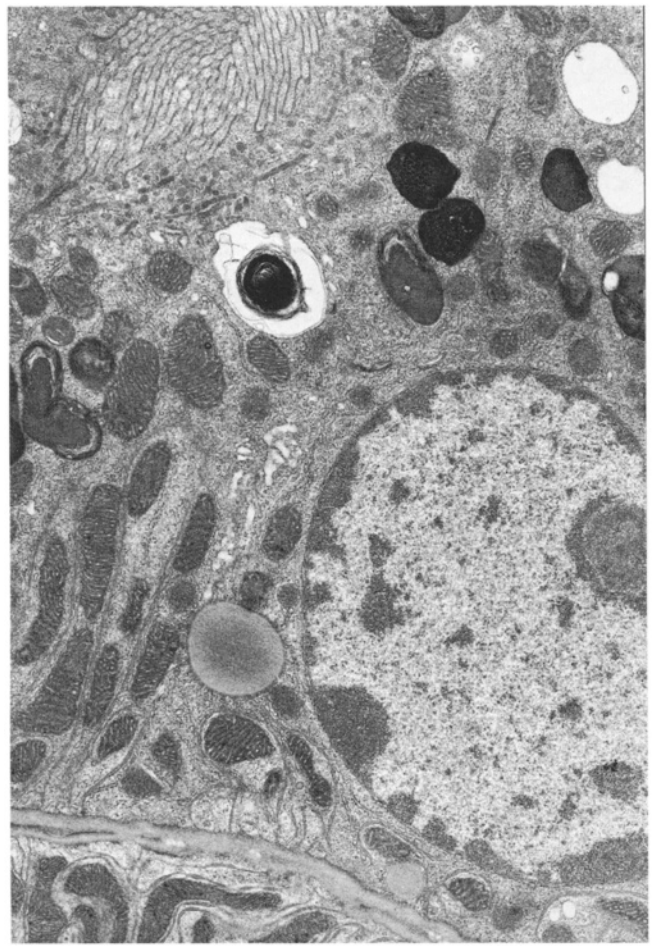

Figure 16. Mouse kidney fixed McDowell and Trump's 4F:1G in phosphate buffer, pH 7.22. Postfixed in 1% osmium in phosphate buffer (Fix #2). 10,923×.

The intestine samples (Figs. 35–44) looked well fixed except for the sample fixed with glutaraldehyde in phosphate buffer with osmium postfixation (Fig. 39), the sample treated with glutaraldehyde in cacodylate buffer with osmium postfixation (Fig. 40), the simultaneous glutaraldehyde/osmium fixation (Fig. 41), and the glutaraldehyde fixation without osmium postfixation (Fig. 42). The glutaraldehyde-fixed materials that had an osmium postfixation had mitochondrial abnormalities (swelling) in both phosphate and cacodylate buffering systems, though the defect was most noticeable with cacodylate buffer (Fig. 40). The intestine sample fixed with glutaraldehyde without osmium postfixation (Fig. 44) had empty spaces and indistinct membrane profiles, as found with the kidney and liver samples fixed in the same way.

This series of photographs is meant to illustrate that good fixation can be influenced by the type of tissue and individual sample of tissue, as well as the constituents of the fixative solution. Most of the fixations in the series resulted in usable material, but an aldehyde fixation followed by osmium postfixation seemed to offer the best preservation. The poor image quality for the intestine samples fixed in glutaraldehyde with an osmium postfixation seems to be anomalous.

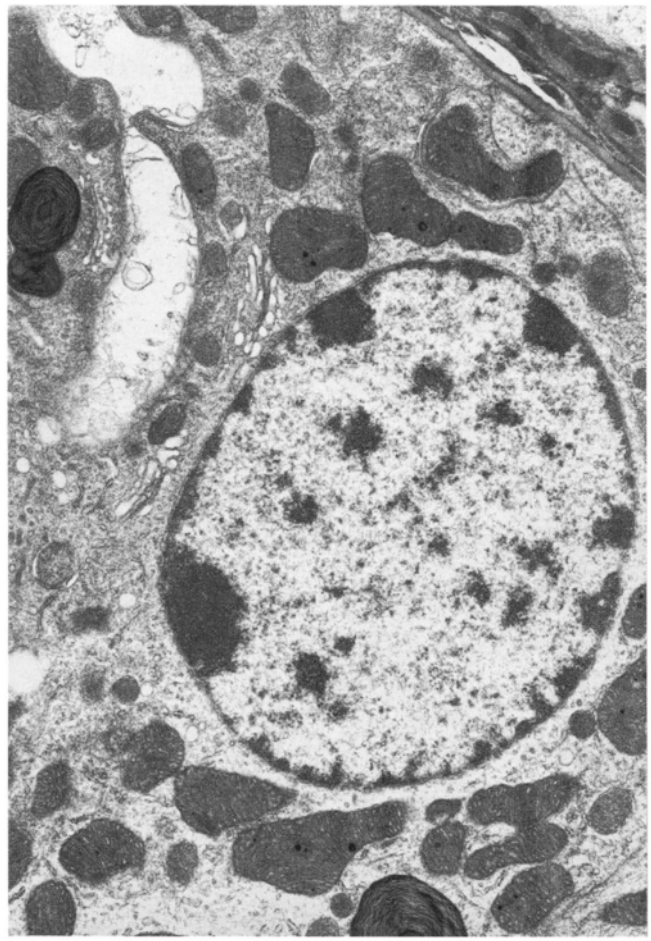

Figure 17. Mouse kidney fixed in Karnovsky's, pH 7.25. Postfixed in 1% osmium in the same buffer (Fix #3). 10,923×.

Unfortunately, it represents the fact that good fixative solutions can yield bad samples, even with rapid collection of samples thinner than 1 mm.

Evaluation of semithin sections (Figs. 45 and 46) also can deliver a wealth of information about the success of fixation techniques. Figure 45 shows a rat liver fixed in 4F:1G (McDowell and Trump, 1976), followed by osmication. The surface of the tissue block is at the lower left of the photograph. Large grayish glycogen pools are seen in the cytoplasm. As one moves deeper into the block (upper right), it becomes evident that these glycogen pools are increasingly extracted, indicating poor fixation. The nuclei also become more open as the nucleoplasm has been extracted. Figure 46 shows a mouse kidney semithin section from a block of tissue simultaneously fixed with glutaraldehyde/osmium in a phosphate buffer. The surface of the tissue (lower left) is well fixed, but only two to three kidney tubules into the block, the tissue becomes grossly understained due to poor fixation. In this case, the combined action of both fixatives working on the tissue simultaneously apparently blocked the ingress of the fixative components deeper into the sample. Similar-sized blocks fixed with sequential procedures do not show this artifact.

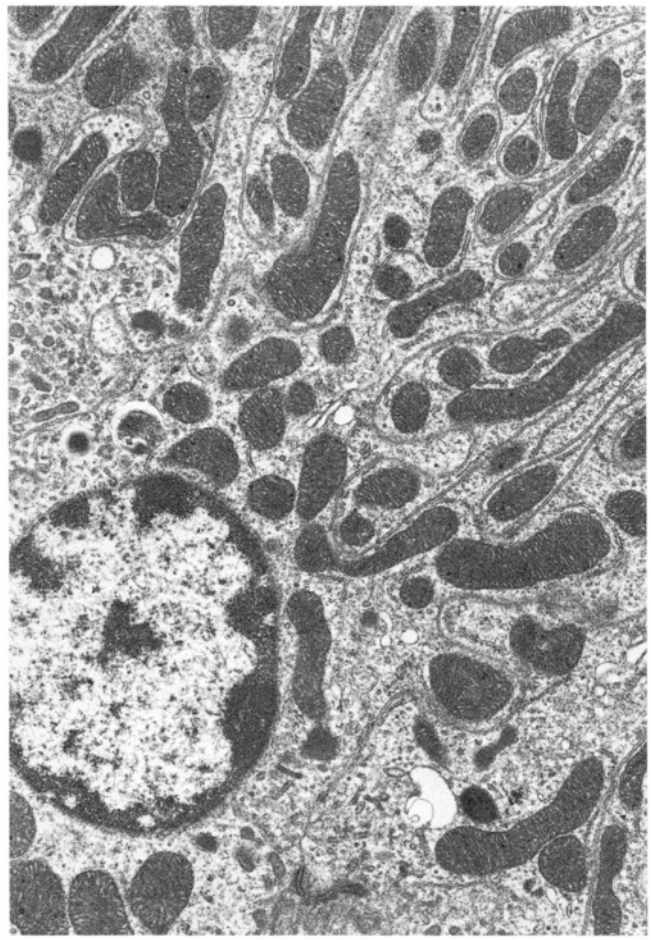

Figure 18. Mouse kidney fixed in half-strength Karnovsky's, pH 7.25. Postfixed in 1% osmium in the same buffer (Fix #4). 10,923×.

VII. A QUASI-UNIVERSAL FIXATION, DEHYDRATION, AND EMBEDMENT SCHEDULE SUCCESSFULLY USED FOR ORGANISMS FROM THE FIVE MAJOR KINGDOMS OF LIFE (SEE THE FIXATION SCHEDULE IN THE SECTION CHAPTER 1 TECHNIQUES)

Figures 11 and 12 illustrate distal convoluted tubule epithelial cells from a rat kidney that was perfused with 4F:1G in March 1985. Figure 11 is a piece of the tissue that was processed immediately after perfusion, and Fig. 12 is of the same kidney sample that was processed in 2002, after storage in 4F:1G at 4°C since 1985. Both of these figures show cells containing mitochondria that have a normal density and that have no evidence of artifactual swelling. The nuclear envelopes and the endoplasmic reticulum are not significantly dilated. Overall, cytoplasmic and

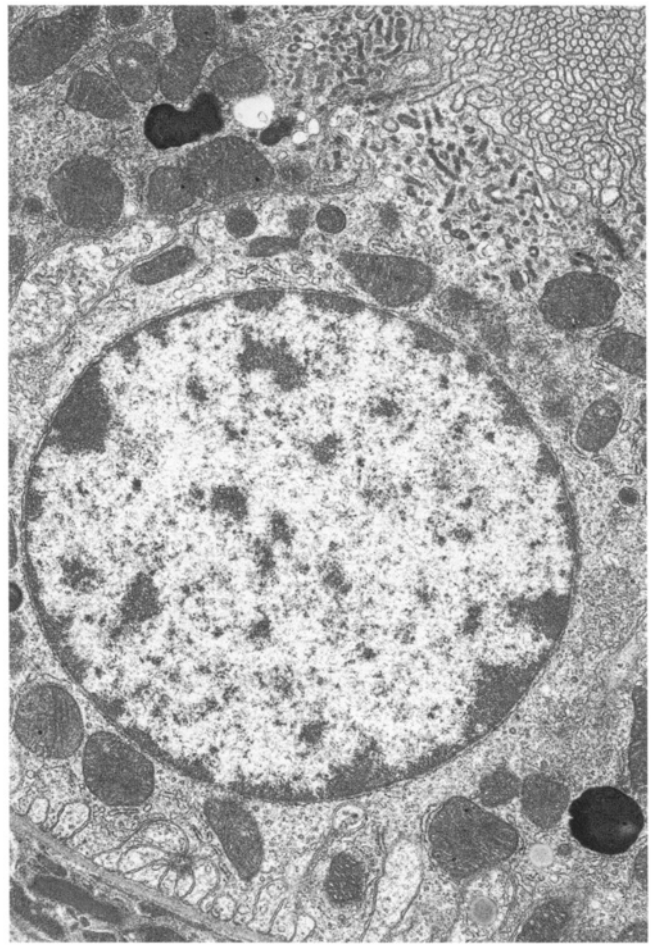

Figure 19. Mouse kidney fixed in 2% glutaraldehyde in 0.1 M phosphate buffer, pH 7.27. Postfixed in 1% osmium in the same buffer (Fix #5). 10,923×.

nucleoplasmic ground substance is well preserved, and the various cytoplasmic membranes do not show any notable discontinuities.

Figure 47 is from a small intestine of a bobwhite quail infected with *Cryptosporidium*. The enterocytes contain mitochondria, lysosomes, and nuclei, none of which show any signs of fixation damage. Part of an adjacent goblet cell also has normal ultrastructural conformation. The *Cryptosporidium* trophozoites contained nuclei and characteristic electron-dense granules, as well as a network of tubules constituting the feeding apparatus along the border of the attachment zone on host cells. There is an obvious separation of the protozoan pellicle from the cytoplasmic contents in the two more mature cells. All of these features are consistent with images published for various coccidians, including *Cryptosporidium*. The density of the nucleoplasm and cytoplasm indicates good chemical fixation.

Figure 48 shows a cell of *Giardia* that was grown in liquid artificial medium prior to fixation. A centriole and associated rootlet for a flagellum are shown, as well as the complex subpellicular microtubule array characteristic of this organism. The nuclear envelope and

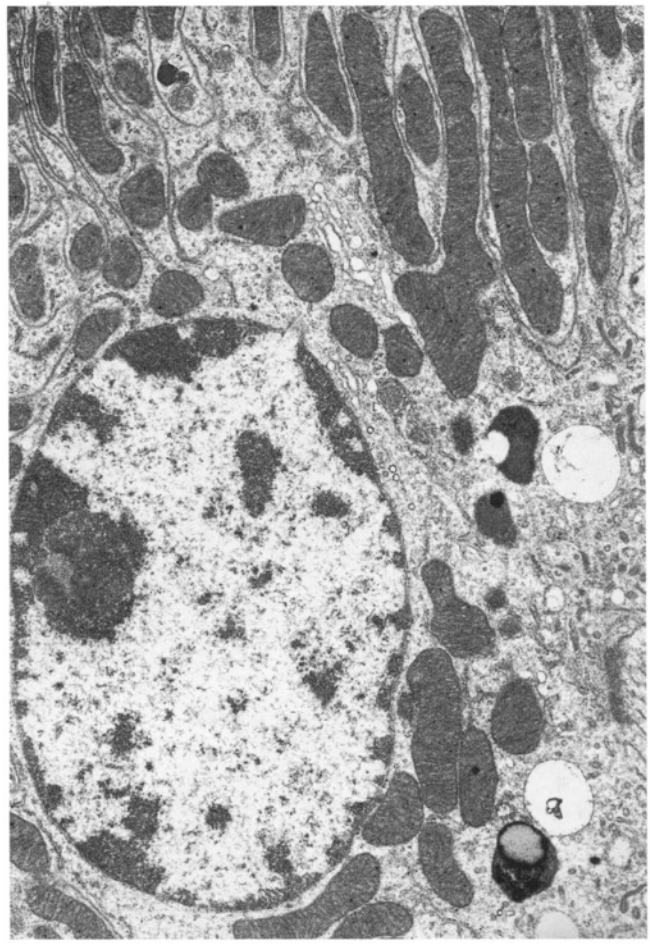

Figure 20. Mouse kidney fixed in 2% glutaraldehyde in 0.1 M cacodylate buffer, pH 7.26. Postfixed in 1% osmium in the same buffer (Fix #6). 10,923×.

endoplasmic reticulum reveal no artifactual swelling. No extraction of the cytoplasm or nucleoplasm is evident.

Mammalian cells infected with herpes virus HHV6 (Fig. 49) have slight mitochondrial abnormalities in the form of swelling and motheaten areas, which are consistent with profiles of a great number of cells grown in culture (Franks and Wilson, 1977). Otherwise, the cytoplasmic and nucleoplasmic preservation looks normal for chemical fixation.

Healthy fish skin containing both cytoplasmically dense and relatively electron-lucent epidermal cells is shown in Fig. 50. Desmosomes and their associated tonofilaments are well preserved. The nucleus and cytoplasm of the less electron-dense cell are somewhat extracted, and the nuclear envelope profiles are somewhat distended. Figure 51 is an illustration of a hypertrophied fish epidermal cell from a field-collected sample infected with the iridovirus, *Lymphocystis*. The cell surface has a network of cytoplasmic extensions, and the cytoplasm contains numerous mitochondria in apparently good condition.

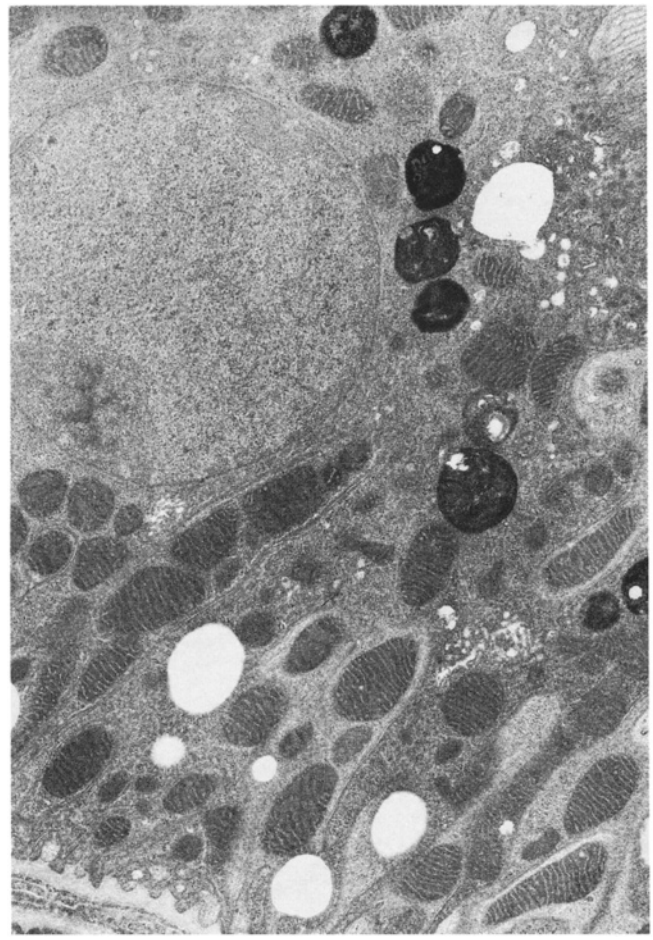

Figure 21. Mouse kidney fixed in 2% glutaraldehyde/0.5% osmium in 0.1 M phosphate buffer, pH 7.39. Simultaneous fixation with no postfixation (Fix #7). 10,923×.

The yeast, *Rhodotorula*, and the filamentous fungus, *Aspergillus*, are shown in Figs. 52 and 53, respectively. They both show well-fixed wall materials, mitochondria, and cytoplasmic ground substance. The *Aspergillus* cell contains two nuclei, which have well-preserved nuclear membranes, as well as one lipid droplet. An unevenly distributed extracellular matrix is present (Fig. 53).

Escherichia coli (Fig. 54) cells appear normal and contain the expected distribution of ribosomes and bacterial chromosomal material typical for this organism after chemical fixation. The cell membranes appear well preserved, and the cytoplasmic ground substance appears unextracted.

Root meristem cells from *Zea mays* (Fig. 55) contain well-fixed nuclei, mitochondria, vacuoles, and plasmodesmata through the cell walls. No swelling of endoplasmic reticulum, nuclear, or mitochondrial profiles is seen. Starch grains are somewhat extracted, as is typical for chemically fixed plant cells. The nucleoplasm and cytoplasm appear unextracted.

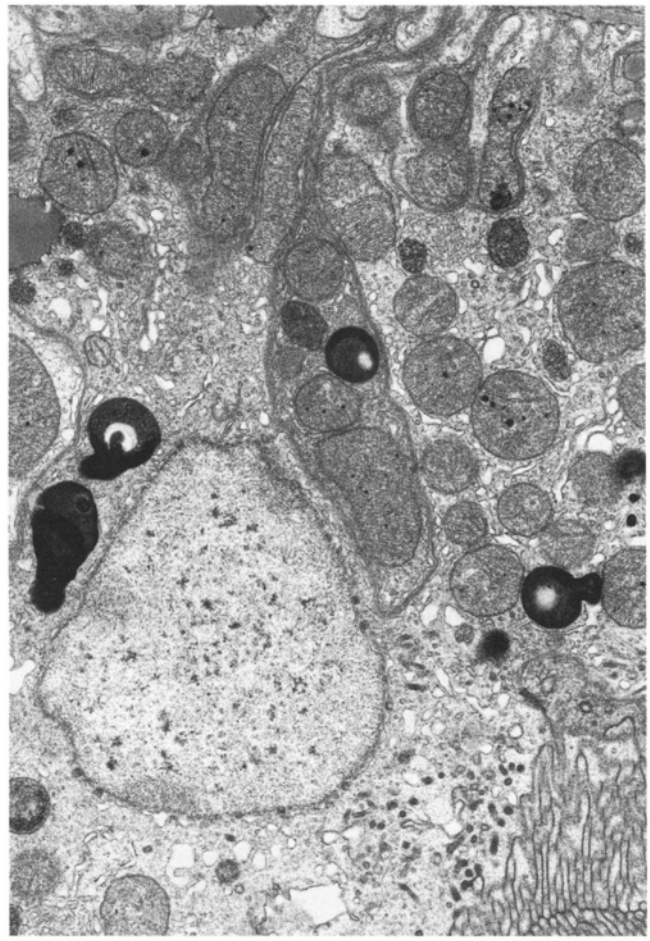

Figure 22. Mouse kidney fixed in 1% osmium in 0.1 M cacodylate buffer, pH 7.26. No postfixation (Fix #8). 10,923×.

McDowell and Trump (1976) designed their 4F:1G fixative to address a number of problems peculiar to their kidney research:

1. Kidneys need to be perfused with fixatives at physiological pressure to maintain proper structural integrity of proximal convoluted tubules.
2. Kidney researchers customarily examine materials by both light microscopy of paraffin sections and by electron microscopy of plastic sections.
3. Tissues fixed in glutaraldehyde concentrations of 2% or greater become difficult to section due to brittleness if embedded in paraffin; they also exhibit nonspecific periodic acid-Schiff staining throughout due to the free hydroxyl groups of glutaraldehyde, which are not totally bound to the fixed tissues.
4. Collection of large numbers of tissues from relatively complicated surgical procedures frequently results in sampling over long periods of time before it is possible to finish the processing run to polymerized resin blocks.

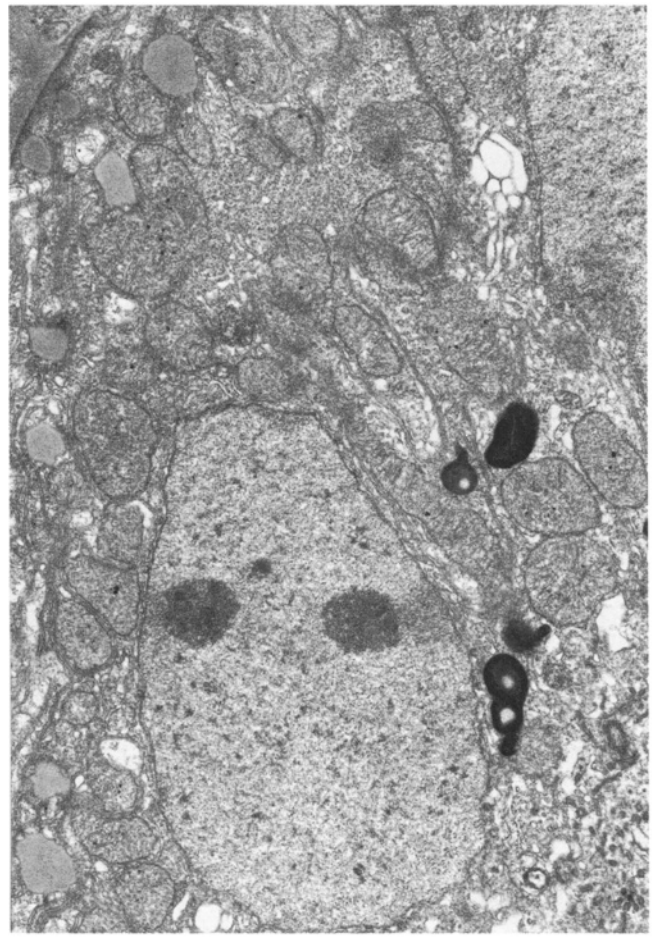

Figure 23. Mouse kidney fixed in 1% osmium in 0.1 M phosphate buffer, pH 7.39. No postfixation (Fix #9). 10,923×.

Our experience with this fixation regimen over the last 26 years has illustrated that it accomplishes the goals listed above but, fortunately, has even greater capabilities than originally described.

We have shown that good quality, publishable electron micrographs can be produced from a variety of tissues stored for greater than 5 years at 4°C in 4F:1G (Dykstra *et al.*, 2002). In addition, Figs. 11 and 12 demonstrate the comparability of images produced from the kidney tissue processed on the day it was taken, or stored for 18 years at 4°C before processing.

Probably the most significant aspect of our routine processing schedule for TEM is the potentially broad applicability to organisms from five kingdoms of life and from various environments. We have used this schedule on terrestrial plants, terrestrial metazoans, marine metazoans and protozoans, fungi, bacteria, and viruses. We have fixed free-living protozoans, parasitic protozoans, tissues, and cells in culture. There are still some cell types that do not fix well with 4F:1G, but we feel that this is always a good starting point for fixing samples that have not been approached before.

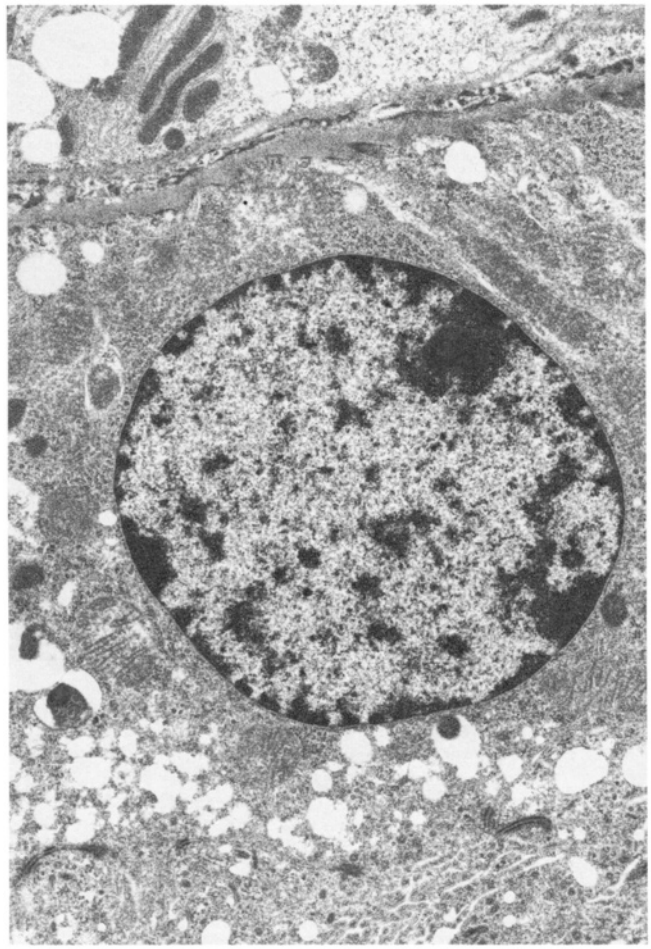

Figure 24. Mouse kidney fixed in 2% glutaraldehyde in 0.1 M phosphate buffer, pH 7.27. No postfixation (Fix #10). 10,923×.

Many fixation regimens probably will work equally well with the variety of tissues and cells from the variety of environments that we have studied. We have chosen to recommend 4F:1G because of the variety of specimens that we have personally seen respond well to the fixative. In addition, we appreciate the flexibility available to submit samples of fixed tissues for histological preparation for light microscopy concomitantly with submission for electron microscopy processing without compromising either eventual use. Finally, 4F:1G fixative can be stored for at least 3 months at 4°C before use, and once tissues are immersed in the fixative, they can be stored for years at 4°C and still be expected to provide publishable results.

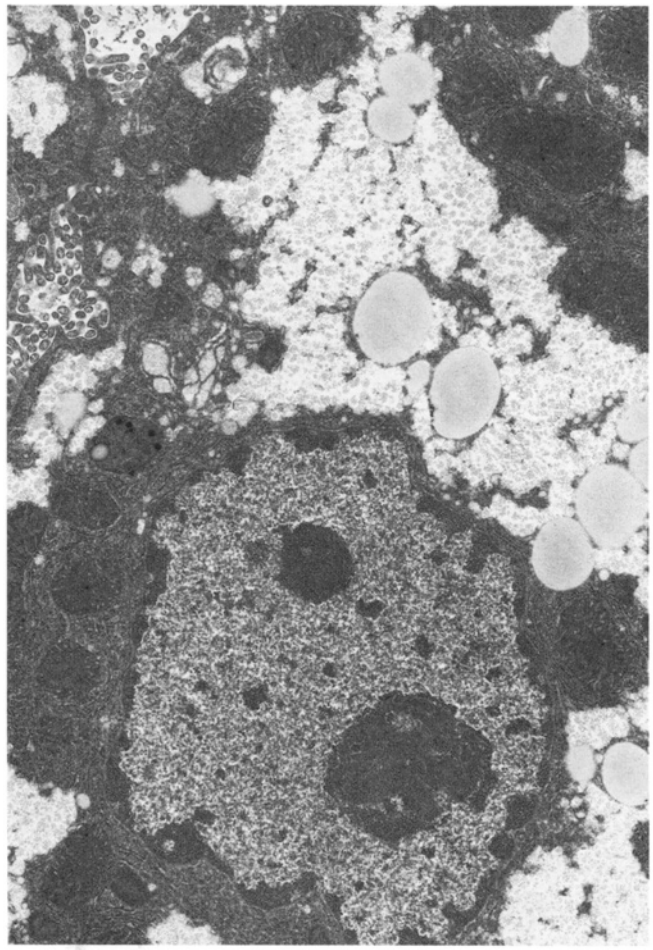

Figure 25. Mouse liver, Fix #1. 10,923×.

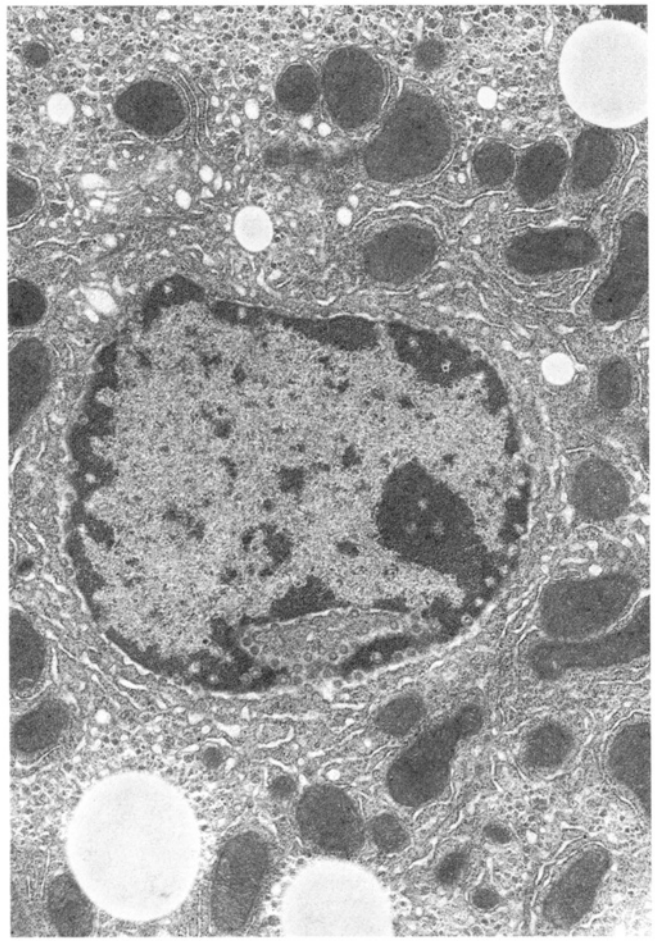

Figure 26. Mouse liver, Fix #2. 10,923×.

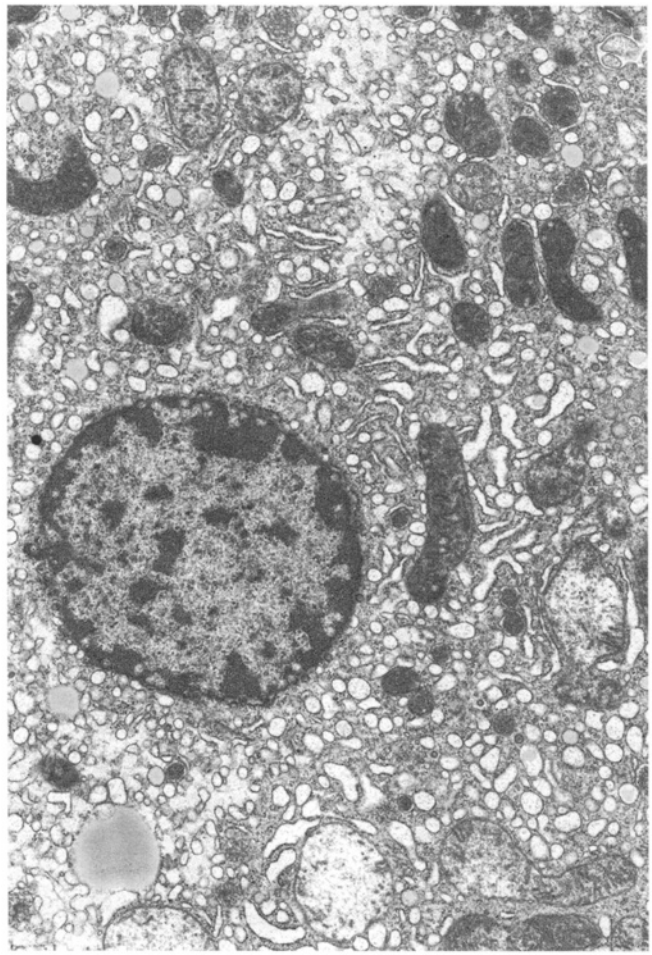

Figure 27. Mouse liver, Fix #3. 10,923×.

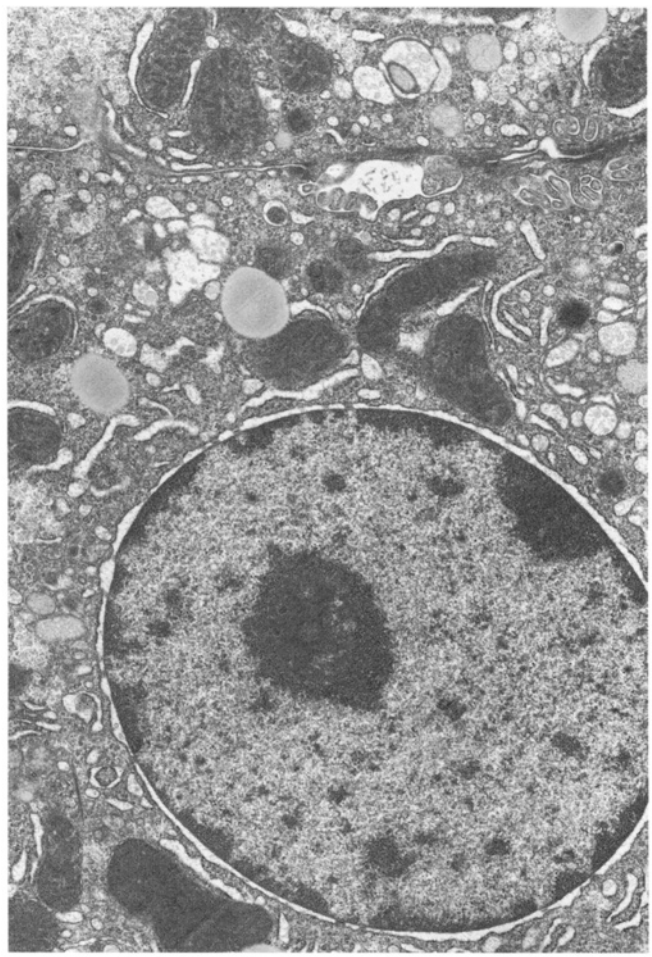

Figure 28. Mouse liver, Fix #4. 10,923×.

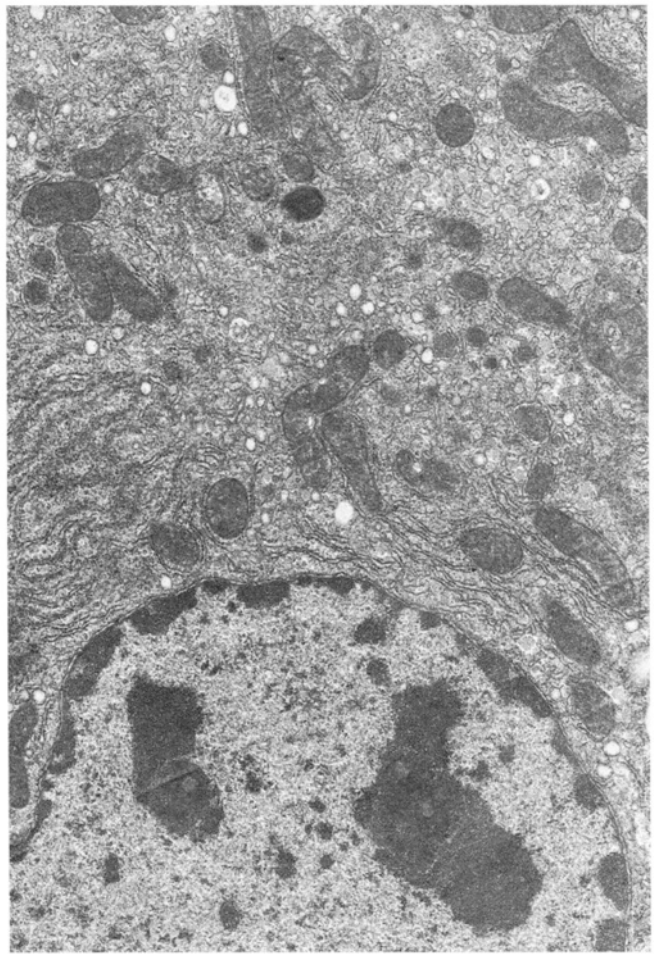

Figure 29. Mouse liver, Fix #5. 10,923×.

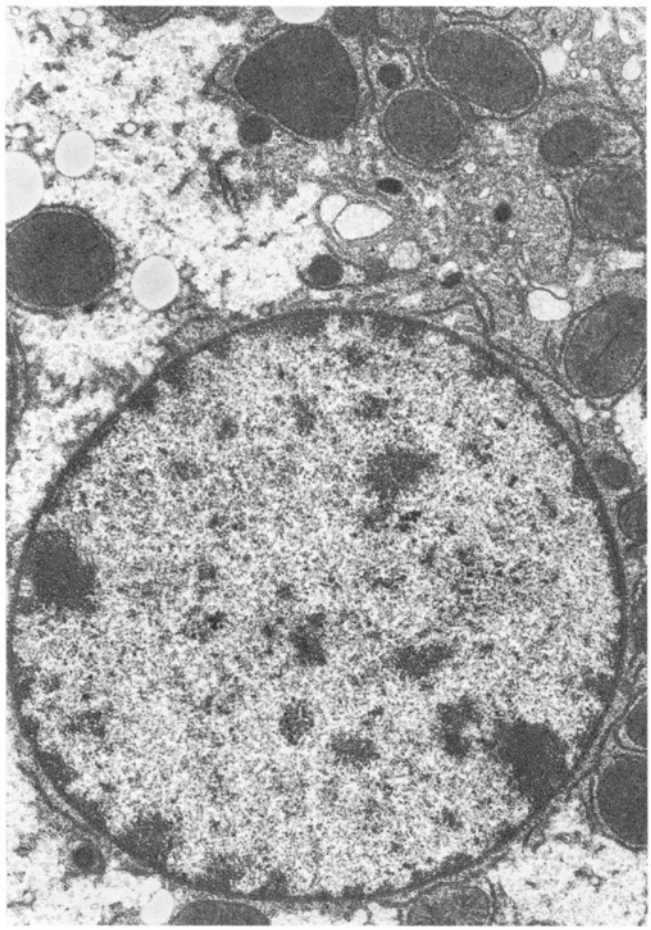

Figure 30. Mouse liver, Fix #6. 10,923×.

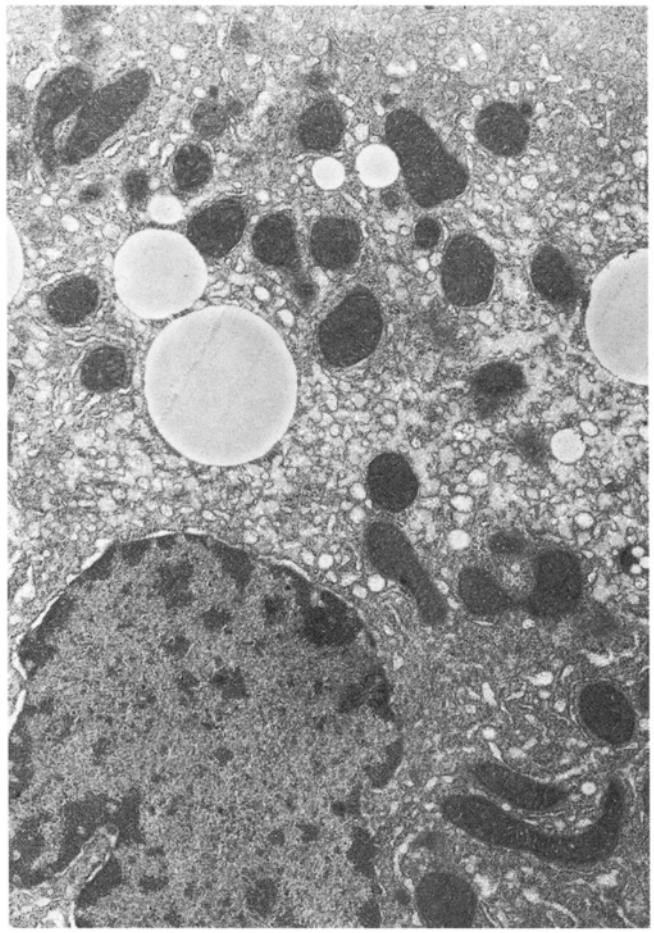

Figure 31. Mouse liver, Fix #7. 10,923×.

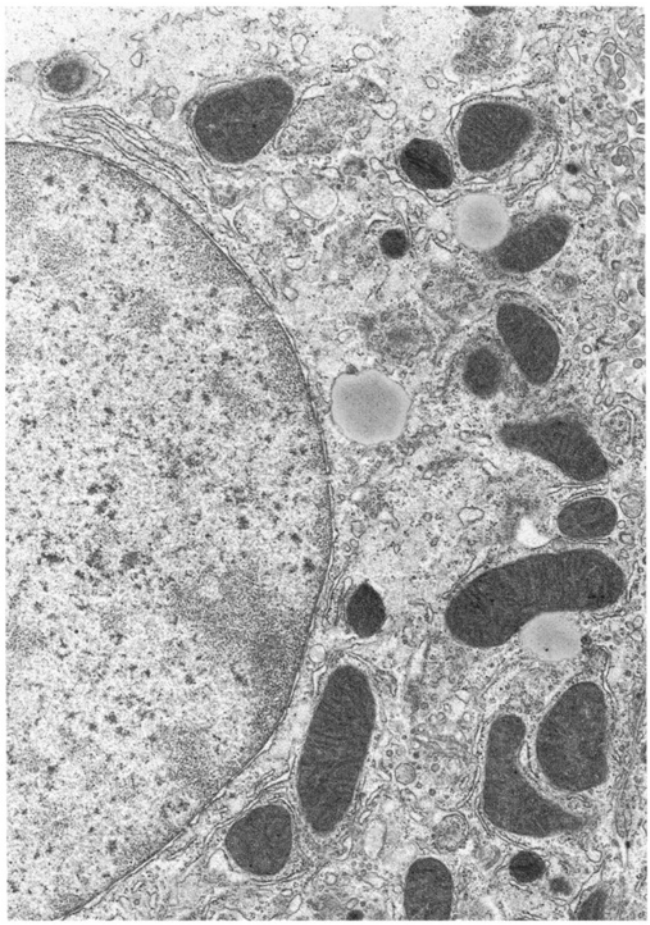

Figure 32. Mouse liver, Fix #8. 10,923×.

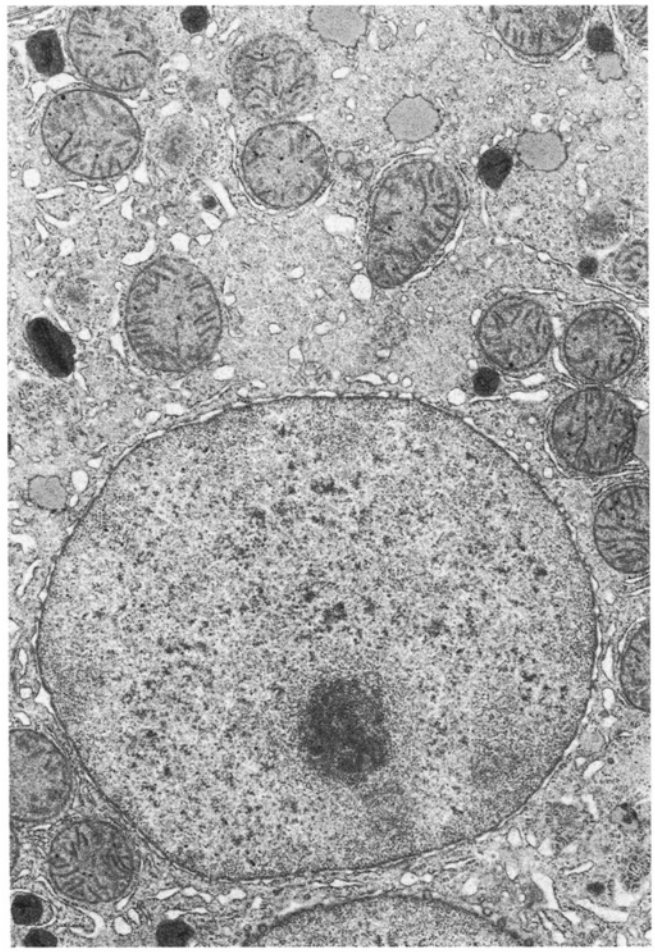

Figure 33. Mouse liver, Fix #9. 10,923×.

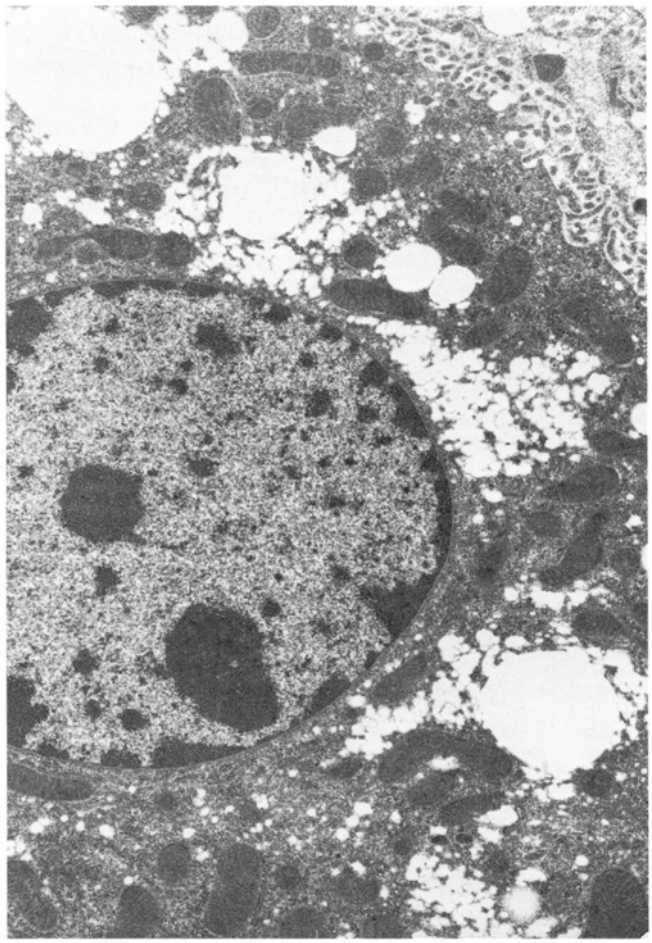

Figure 34. Mouse liver, Fix #10. 10,923×.

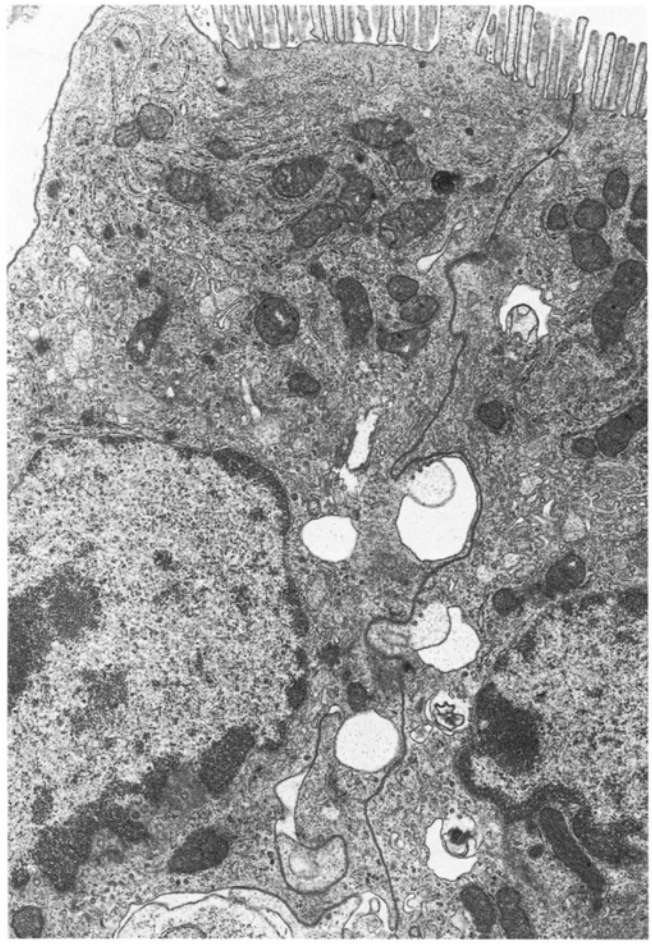

Figure 35. Mouse small intestine, Fix #1. 10,923×.

Figure 36. Mouse small intestine, Fix #2. 10,923×.

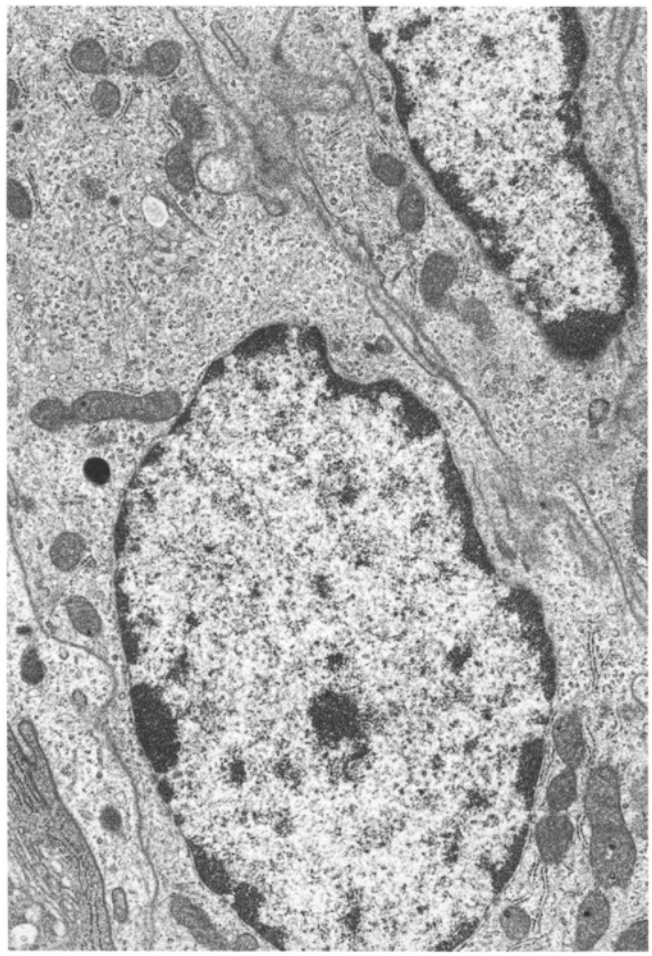

Figure 37. Mouse small intestine, Fix #3. 10,923×.

Figure 38. Mouse small intestine, Fix #4. 10,923×.

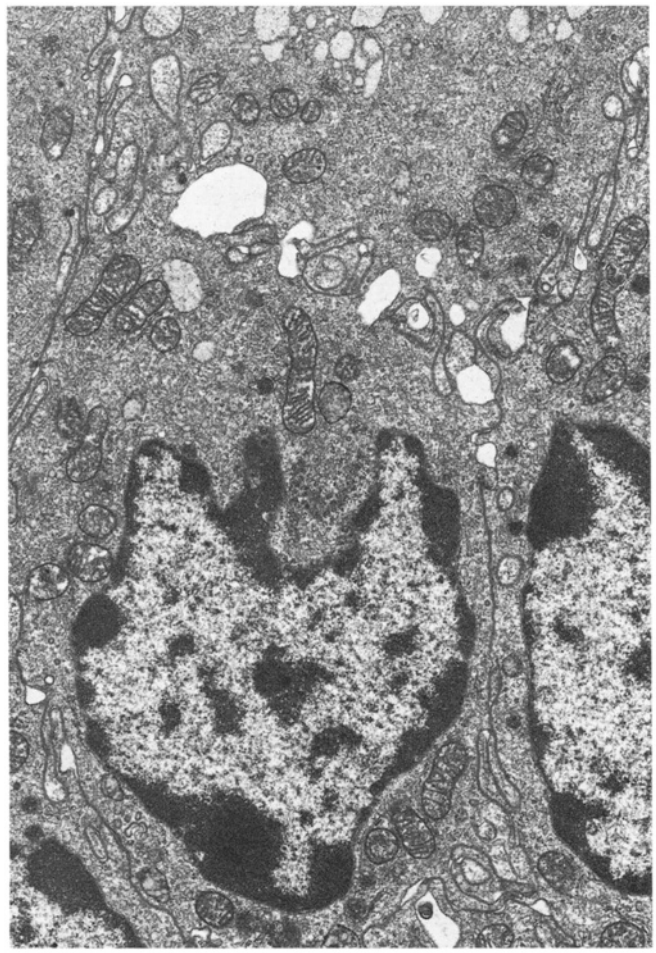

Figure 39. Mouse small intestine, Fix #5. 10,923×.

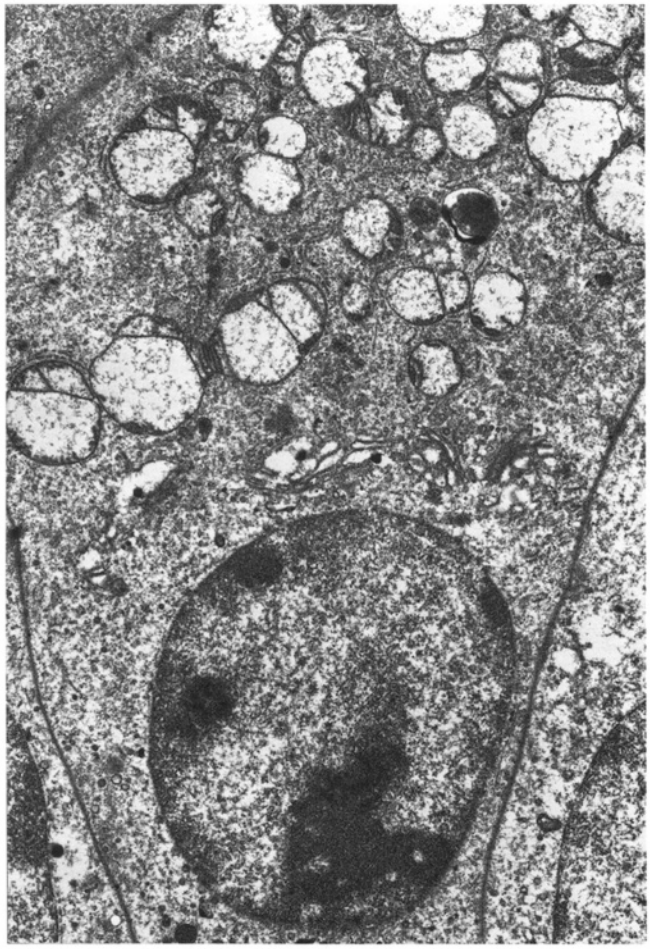

Figure 40. Mouse small intestine, Fix #6. 10,923×.

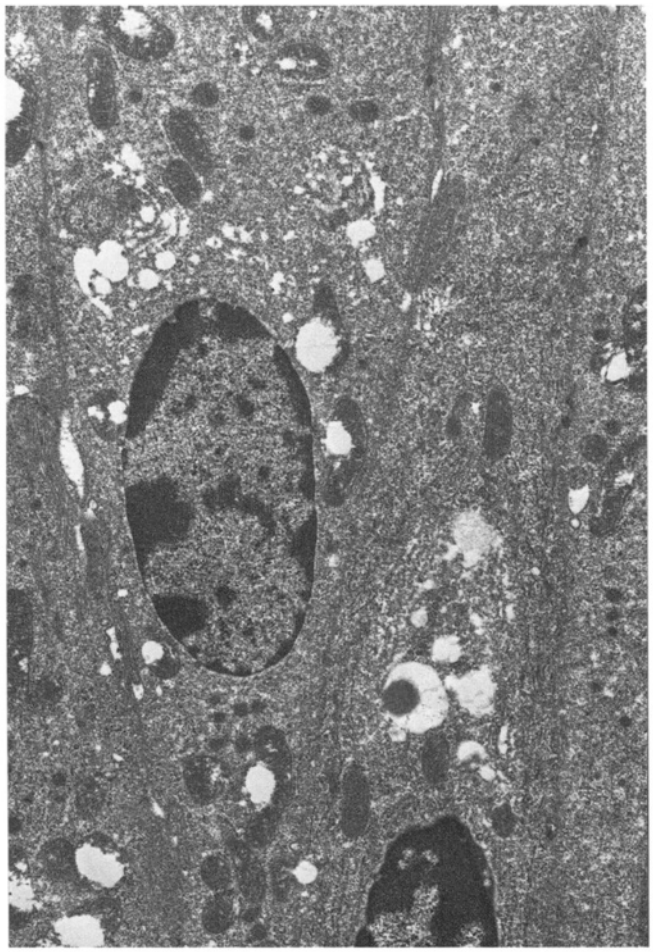

Figure 41. Mouse small intestine, Fix #7. 10,923×.

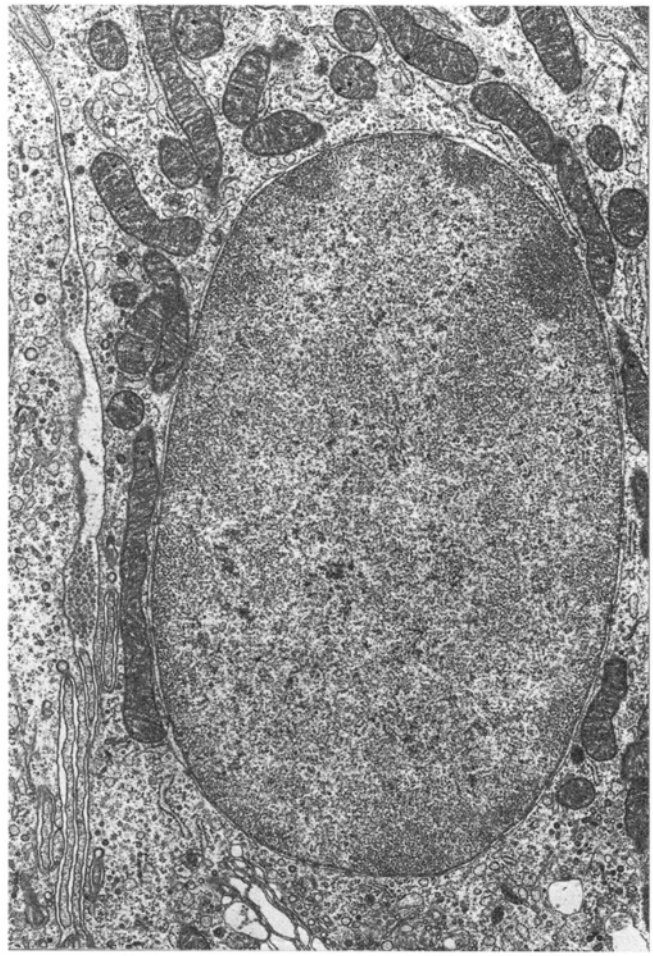

Figure 42. Mouse small intestine, Fix #8. 10,923×.

Figure 43. Mouse small intestine, Fix #9. 10,923×.

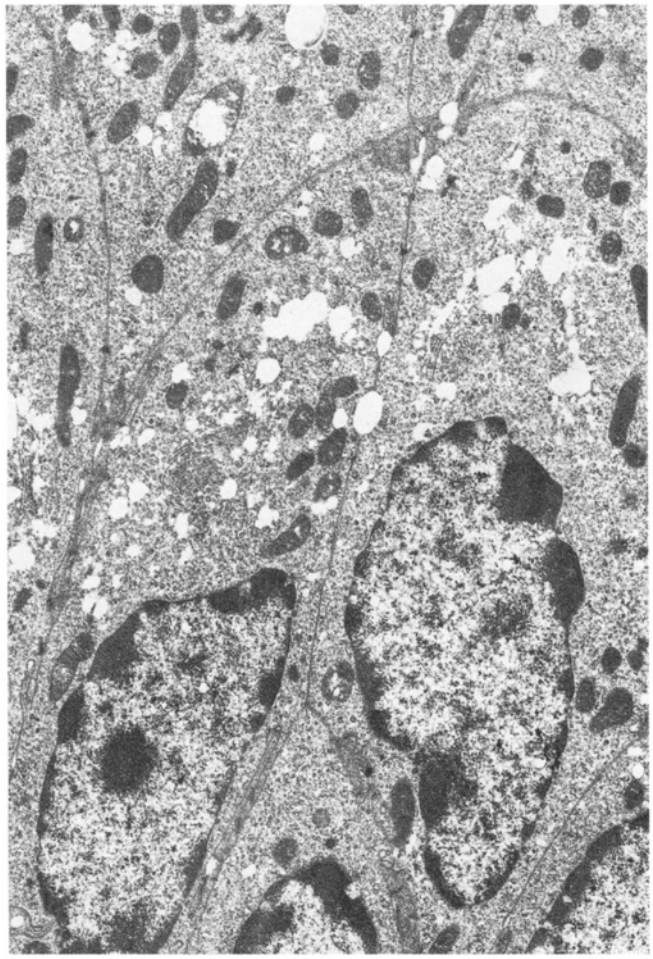

Figure 44. Mouse small intestine, Fix #10. 10,923×.

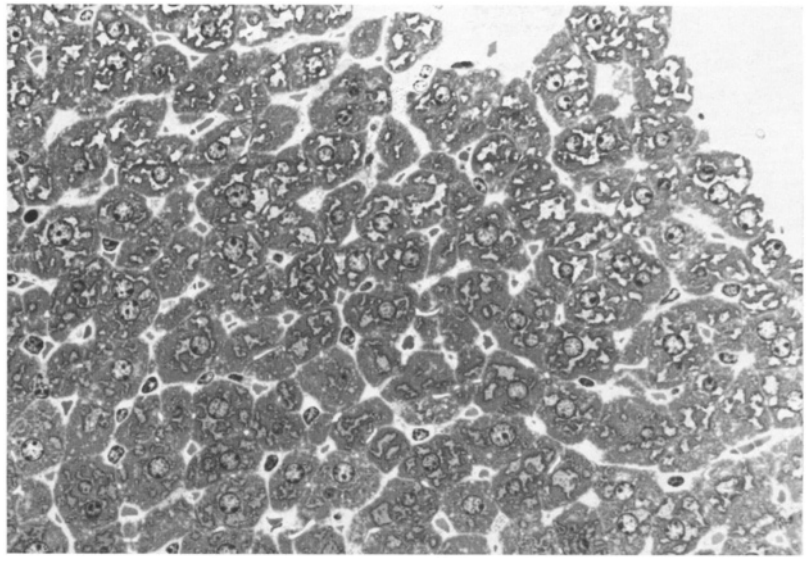

Figure 45. Rat liver, semithin section stained with toluidine blue O. 460×.

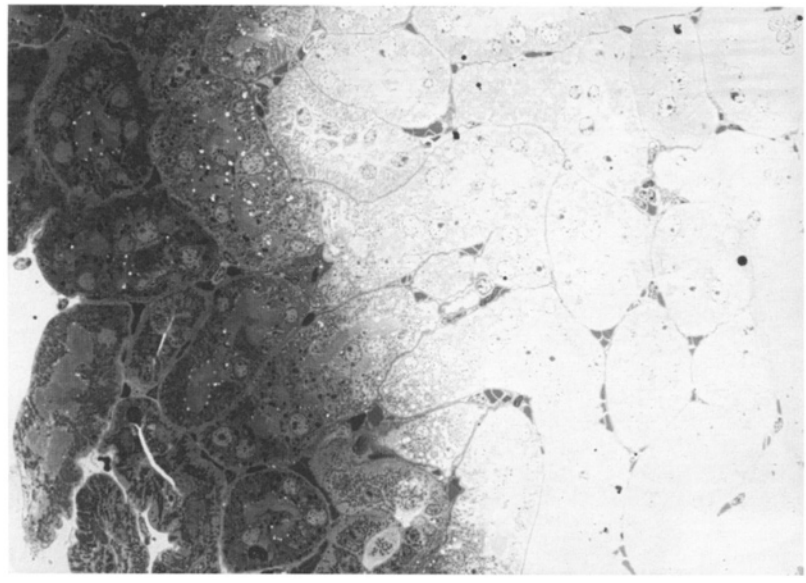

Figure 46. Mouse kidney, semithin section stained with toluidine blue O. 460×.

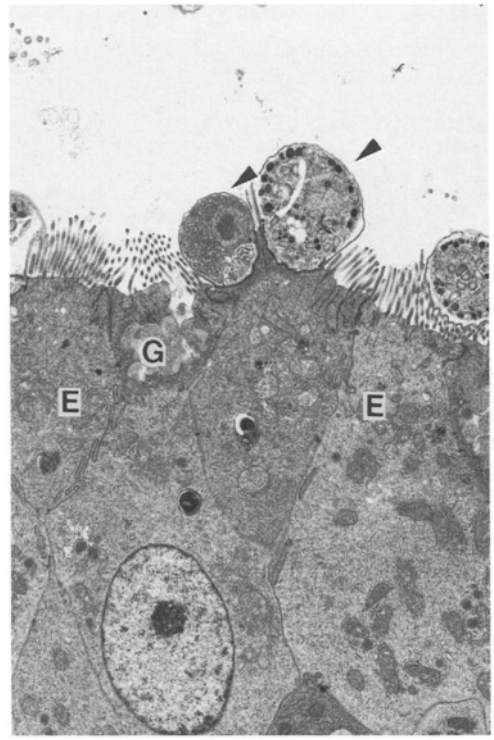

Figure 47. Bobwhite quail intestine infected with *Cryptosporidium* (arrows). Note the normal appearance of goblet cells (G) and enterocytes (E). 4,600×.

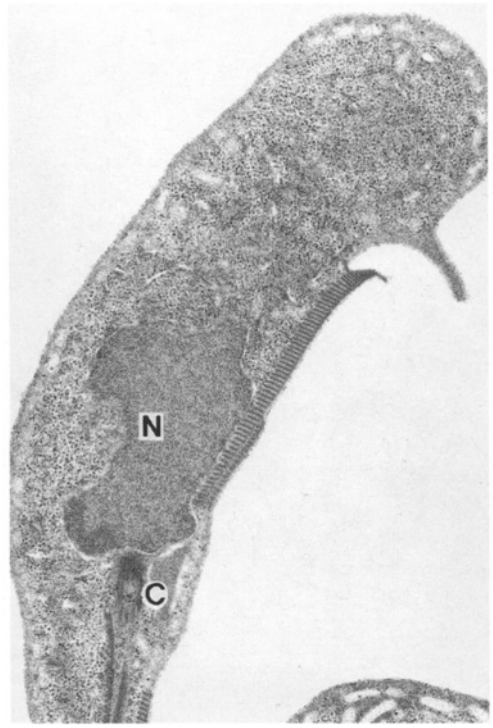

Figure 48. *Giardia* from liquid culture with centriole (C) and associated rootlet and nucleus (N) closely associated with the subpellicular microtubule array. 15,600×.

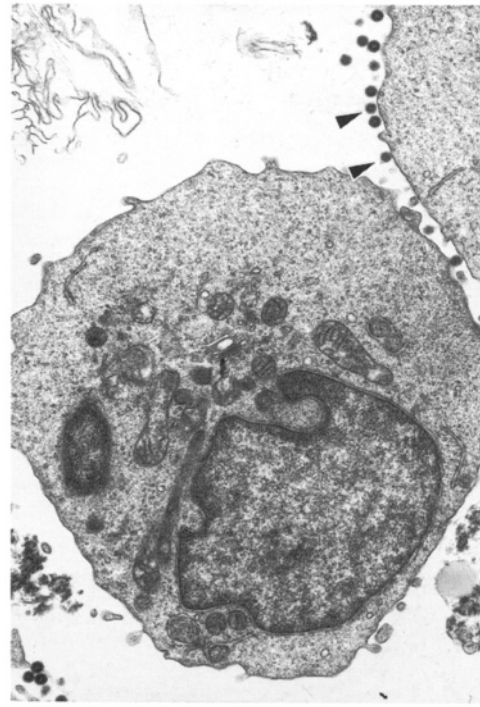

Figure 49. Human cord blood cells infected with HHV6 *Herpes* virus (arrows). 12,700×.

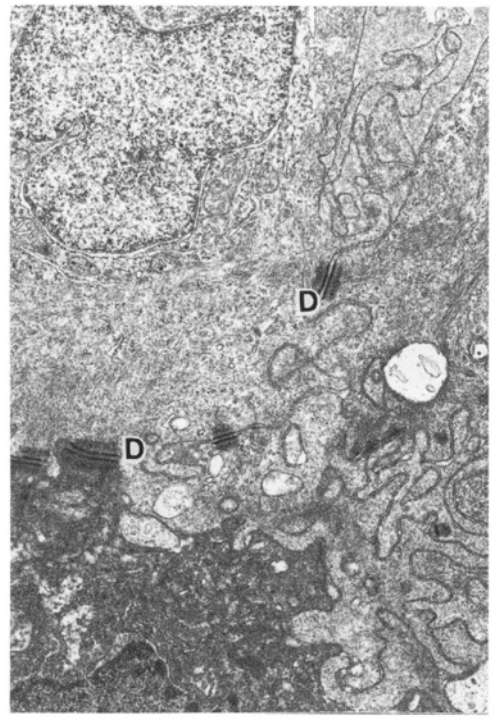

Figure 50. Healthy fish skin (*Tilapia*) showing desmosomes (D) with associated tonofilaments. 12,300×.

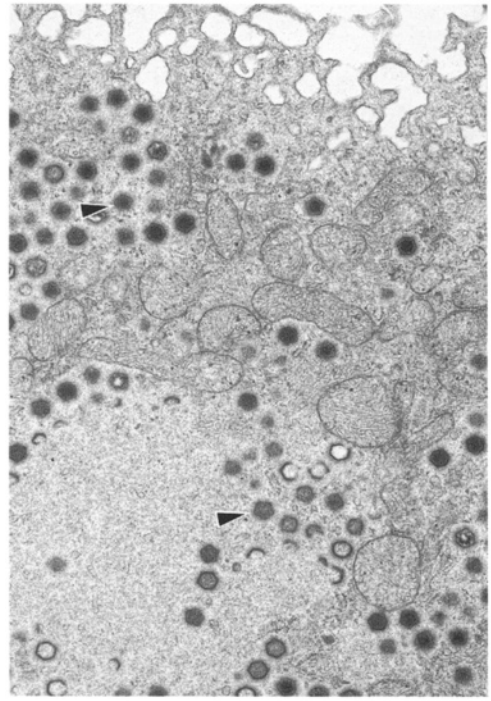

Figure 51. Field-collected fish skin cell infected with *Lymphocystis* virus (arrows). 12,000×.

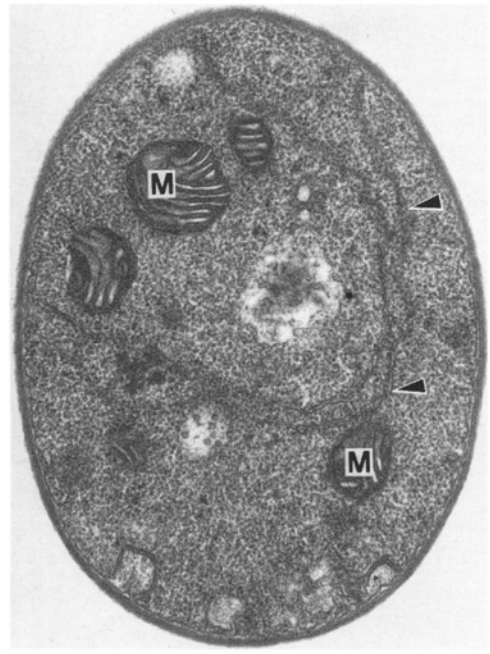

Figure 52. Yeast cell (*Rhodotorula*) with mitochondria (M) and endoplasmic reticulum (arrows). 29,400×.

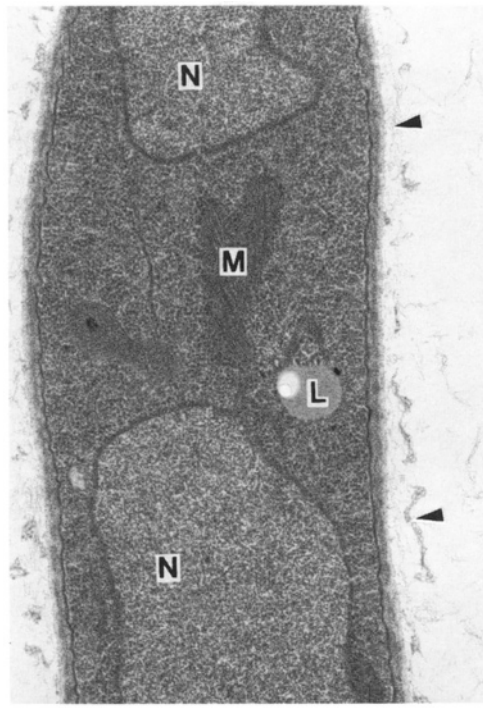

Figure 53. Filamentous fungus (*Aspergillus*) showing nuclei (N), mitochondrion (M), lipid droplet (L), and extracellular matrix (arrows). 29,100×.

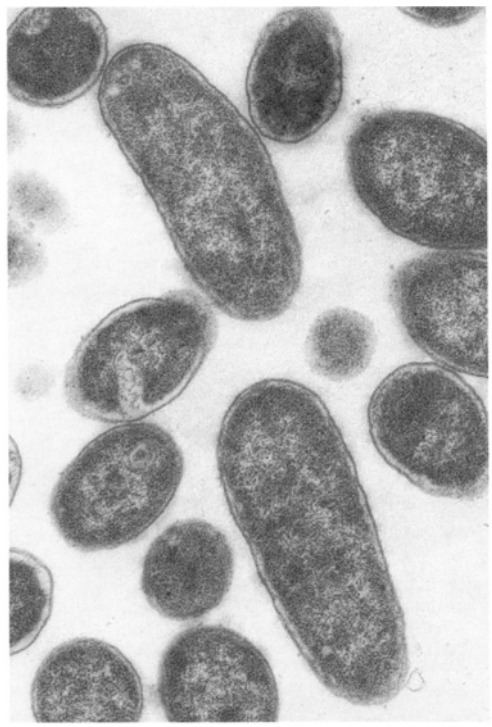

Figure 54. Bacteria (*Escherichia coli*). 23,900×.

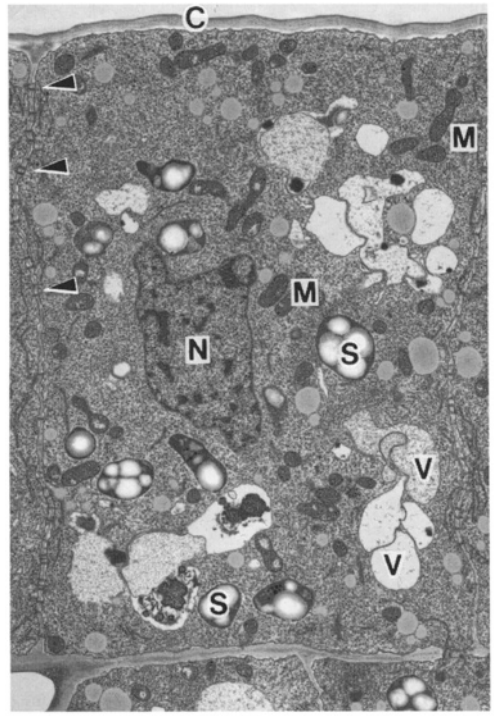

Figure 55. Corn root meristem showing nucleus (N), mitochondria (M), starch grains (S), vacuoles (V), cell wall (C), and plasmodesmata (arrowheads). 5,400×.

REFERENCES

Aldrich, H.C., Biemborn, D.B., and Schonheit, P. 1987. Creation of artifactual internal membranes during fixation of *Methanobacterium thermoautotrophicum. Can. J. Microbiol.* 33: 844.

Beckman, H.-J. and Dierichs, R. 1982. Lipid extracting properties of 2,2-dimethoxypropane as revealed by electron microscopy and thin layer chromatography. *Histochemistry* 76: 407.

Bozzola, J.J. and Russell, L.D. 1999. *Electron microscopy*, 2nd edn. Jones and Bartlett, Boston.

Carson, F., Martin, J.H., and Lynn, J.A. 1973. Formalin fixation for electron microscopy: A reevaluation. *Am. J. Clin. Pathol.* 59: 365.

Causton, B.E. 1981. Resins: toxicity, hazards, and safe handling. *Proc. R. Microsc. Soc.* 16: 265.

Coulter, H.D. 1967. Rapid and improved methods for embedding biological tissues in Epon-812 and Araldite 502.
J. Ultrastruct. Res. 20: 346.

Dykstra, M.J., Mann, P.M., Elwell, M.R., and Ching, S.V. 2002. Suggested standard operating procedures (SOPs) for the preparation of electron microscopy samples for toxicology/pathology studies in a GLP environment. *Toxicol. Pathol.* 30: 735.

Flegler, S.L., Heckman, J.W. Jr., and Klomparens, K.L. 1993. *Scanning and transmission electron microscopy*. W.H. Freeman and Co., New York.

Franks, L.M., and Wilson, P.D. 1977. Origin and ultrastructure of cells *in vitro*. In: G.H. Bourne, J.F. Danielli, and K.W. Jeon (eds.), *International review of cytology* (Vol. 48). Academic Press, New York.

Ghadially, F.N. 1985. *Diagnostic electron microscopy of tumors*, 2nd edn. Butterworths, London.

Ghadially, F.N. 1997. *Ultrastructural pathology of the cell and matrix*, 4th edn. in 2 Volumes. Butterworth-Heinemann, London.

Giberson, R.T. and Demaree, R.S., Jr. (eds.). 2001. *Microwave techniques and protocols*. Humana Press, Totowa, NJ.

Gilkey, J.C. and Staehelin, L.A. 1986. Advances in ultrarapid freezing for the preservation of cellular ultrastructure. *J. Electron Microsc. Tech.* 3: 177.

Glauert, A.M. 1975. *Fixation, dehydration and embedding of biological specimens*. Elsevier North-Holland, New York.

Glauert, A.M., Rogers, G.E., and Glauert, R.H. 1956. A new embedding medium for electron microscopy. *Nature* 178: 803.

Glauert, A.M. and Lewis, P.R. 1998. *Biological specimen preparation for transmission electron microscopy. Vol. 17.* In: A.M. Glauert (ed.), *Practical methods in electron microscopy*. Princeton University Press, Princeton, NJ.

Hanstede, J.G. and Gerrits, P.O. 1983. The effects of embedding in water-soluble plastics on the final dimensions of liver sections. *J. Microsc.* 131: 79.

Hayat, M.A. 1970. *Principles and techniques of electron microscopy: Biological applications* (Vol. 1). Van Nostrand Reinhold, New York.

Hayat, M.A. 1981. *Fixation for electron microscopy*. Academic Press, New York.

Hayat, M.A. 2000. *Electron microscopy: Biological applications*, 4th edn. Cambridge University Press, New York.

Heckman, C.A. and Barrnett, R.J. 1973. GACH: A water-miscible, lipid-retaining embedding polymer for electron microscopy. *J. Ultrastruct Res.* 42: 156.

Hopwood, D. 1967. Some aspects of fixation with glutaraldehyde: A biochemical and histochemical comparison of the effects of formaldehyde and glutaraldehyde fixation on various enzymes and glycogen with a note on penetration of glutaraldehyde into liver. *J. Anat.* 101: 83.

Hopwood, D. 1972. Theoretical and practical aspects of glutaraldehyde fixation. In: P.J. Stoward (ed.), *Fixation in histochemistry*. Chapman & Hall, London.

Karnovsky, M.J. 1965. A formaldehyde–glutaraldehyde fixative of high osmolality for use in electron microscopy. *J. Cell Biol.* 27: 137A.

Kellenberger, E., Schwab, W., and Ryter, A. 1956. L'utilisation d'un copolymere des polyesters comme materiel d'inclusion en ultramicrotomie. *Experientia* 12: 421.

Leong, A.S.-Y., Daymon, M.E., and Milios, J. 1985. Microwave irradiation as a form of fixation for light and electron microscopy. *J. Pathol.* 146: 313.

Leong, A.S.-Y. and Gove, D.W. 1990. Microwave techniques for tissue fixation, processing and staining. *Electron Microsc. Soc. Am. Bull.* 20: 61.

Login, G.R. and Dvorak, A.M. 1994. *The microwave tool book*. Beth Israel Hospital, Boston.

Login, G.R., Dwyer, B.K., and Dvorak, A.M. 1990. Rapid primary microwave-osmium fixation. I. Preservation of structure for electron microscopy in seconds. *J. Histochem. Cytochem.* 38: 755.

Luft, J.H. 1956. Permanganate—a new fixative for electron microscopy. *J. Biophys. Biochem. Cytol.* 2: 799.

Luft, J.H. 1959. The use of acrolein as a fixative for light and electron microscopy. *Anat. Record.* 133: 305.

Luft, J.H. 1961. Improvements in epoxy resin embedding methods. *J. Biophys. Biochem. Cytol.* 9: 409.

Luft, J.H. and Wood, R.L. 1963. The extraction of tissue protein during and after fixation with osmium tetroxide in various buffer systems. *J. Cell Biol.* 19: 46A.

McDowell, E.M. and Trump, B.F. 1976. Histologic fixatives suitable for diagnostic light and electron microscopy. *Arch. Pathol. Lab. Med.* 100: 405.

Millonig, G. and Marinozzi, V. 1968. Fixation and embedding in electron microscopy. In: R. Baser and V.E. Cosslett (eds.), *Advances in optical and electron microscopy* (Vol. 2). Academic Press, New York.

Mollenhauer, H.H. 1964. Plastic embedding mixtures for use in electron microscopy. *Stain Tech.* 39: 111.

Mollenhauer, H.H. 1986. Surfactants as resin modifiers and their effect on sections. *J. Electron Microsc. Tech.* 3: 217.

Newman, S.B., Borysko, E., and Swerdlo, M. 1949. New sectioning techniques for light and electron microscopy. *Science* 110: 66.

Page, S.G. and Huxley, H.E. 1963. Filament lengths in striated muscle. *J. Cell Biol.* 19: 369.

Palade, G.E. 1952. A study of fixation for electron microscopy. *J. Exp. Med.* 95: 285.

Pease, D.C. and Peterson, R.G. 1972. Polymerizable glutaraldehyde–urea mixtures as polar, water-containing embedding media. *J. Ultrastruct. Res.* 41: 133.

Robards, A.W. and Wilson, A.J. (eds.). 1993. *Procedures in electron microscopy*. Wiley, New York.

Robinson, D.G., Ehlers, U., Herken, R., Herrmann, B., Mayer, F., and Schürmann, F.-W. 1987. *Methods of preparation for electron microscopy*. Springer-Verlag, Berlin.

Sabatini, D.D., Miller, F., and Barrnett, R.J. 1963. Cytochemistry and electron microscopy, the preservation of cellular ulstrastructure and enzymatic activity by aldehyde fixation. *J. Cell Biol.* 17: 19.

Saito, Y. and Tanaka, Y. 1980. Glutaraldehyde fixation of fish tissue for electron microscopy. *J. Electron Microsc.* 29: 1.

Salema, R. and Brandao, I. 1973. The use of PIPES buffer in the fixation of plant cells for electron microscopy. *J. Submicrosc. Cytol.* 5: 79.

Smith, R.E. and Farquhar, M.G. 1966. Lysosome function in the regulation of the secretory process in the cells of the anterior pituitary gland. *J. Cell Biol.* 31: 319.

Spurr, A.R. 1969. A low-viscosity epoxy resin embedding medium for electron microscopy. *J. Ultrastruct. Res.* 26: 31.

Thorpe, J.R. and Harvey, D.M.R. 1979. Optimization and investigation of the use of 2,2-dimethoxypropane as a dehydration agent for plant tissues in transmission electron microscopy. *J. Ultrastruct. Res.* 68: 186.

Tokuyasu, K.T. 1983. Present state of immunocryoultramicrotomy. *J. Histochem. Cytochem.* 31: 164.

Wolosewick, J.J. 1980. The application of polyethylene glycol (PEG) to electron microscopy. *J. Cell Biol.* 86: 675.

CHAPTER 1 TECHNIQUES

Making Dilutions

Diluting Stock Solutions

Making dilutions from preexisting stock solutions can sometimes be confusing, but Dr. Harry Dean, who taught botanical microtechnique at the University of Iowa over 30 years ago, passed out a simple formula for such work. For example, to dilute an 80% solution of acetic acid stock to make a 28% working solution, the following formula would be used:

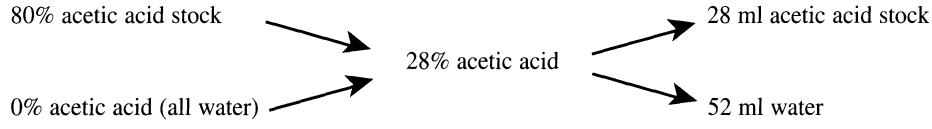

In other words, to dilute an 80% acetic acid stock to a 28% solution, subtract 28 from 80 to determine how much water (52 ml) should be added to 28 ml of the acetic acid stock.

Preparing Stock Solutions to be Mixed Together to Achieve Specific Final Concentrations in a Working Fixative Solution

Various protocols specify final concentrations of substances within them without explaining how they are prepared. It is frequently necessary to prepare stock solutions considerably more concentrated than the final working solutions so that they may be mixed together sequentially without individual components becoming overly diluted. For example, say a fixation procedure calls for a final solution containing 4% glutaraldehyde, 2% formaldehyde, and 0.1 M phosphate buffer. Most laboratories have 0.2 M phosphate buffer stocks, so these could be diluted with an equal volume of a solution containing 8% glutaraldehyde and 4% formaldehyde to produce the final solution desired. This would mean that to make 50 ml of this fixative, it would be necessary to prepare 12.5 ml of 16% glutaraldehyde from 25% biological grade glutaraldehyde stocks using the dilution formula above (16 ml glutaraldehyde added to 9 ml distilled water) and 12.5 ml of 8% formaldehyde from 37% formaldehyde (8 ml formaldehyde added to 29 ml distilled water). The resulting 25 ml of glutaraldehyde/formaldehyde mixture produced by mixing the two stocks (8% and 4%, respectively) would then be added to 25 ml of 0.2 M phosphate buffer to produce the final 4% glutaraldehyde/2% formaldehyde solution in a 0.1 M phosphate buffer.

A Routine Fixation and Embedding Schedule for Transmission Electron Microscopy Samples (Tissues or Cells)

1. Applications and Objectives

This technique can be applied to viruses, bacteria, protozoans, plants, fungi, and animal tissues or cells. Specific procedural instructions for handling microorganisms or cells in culture, monolayers *in situ* or

suspended, are provided as separate protocols later in this text. Samples can be stored in the primary fixative for several years in a refrigerator. The primary fixative is particularly useful for collecting samples in the field for further processing later in an electron microscopy laboratory. McDowell's and Trump's 4F:1G fixative (4F:1G) is equally useful for perfusion as well as immersion fixation of samples.

2. Materials Needed

- 4F:1G fixative
- 0.2 M and 0.1 M Sorenson's sodium phosphate buffer, pH 7.2–7.4
- 2% aqueous osmium
- 100% ethanol (to make the dilution series)
- 100% acetone (transitional solvent)
- Spurr resin (6.3 g DER recipe)

3. Procedure

1. Immerse samples that are no more than 1 mm thick in at least one dimension in 4F:1G fixative as quickly as possible. The fixative volume should be 5–10 times that of the sample volume. Fix for 1–2 hr at room temperature (see Cautionary Statement below about storage of fixed tissues).
2. Rinse tissue two times (15 min each) in 0.1 M Sorenson's sodium phosphate buffer at pH 7.2–7.4.
3. Postfix sample in 1% osmium/0.1 M phosphate buffer for 1 hr at room temperature (made by mixing equal volumes of 2% aqueous osmium and 0.2 M Sorenson's sodium phosphate buffer, pH 7.2–7.4).
4. Rinse tissue in distilled water two times (5 min each).
5. Dehydrate sample by passing it through the following alcohol series. Always use fluid volumes at least five to 10 times greater than the sample volume:
   - 50% ethanol 15 min
   - 75% ethanol 15 min (*If necessary, samples can be left overnight at 4°C*)
   - 95% ethanol 15 min, two times
   - 100% ethanol 30 min, two times
   - 100% acetone 10 min, two times
6. Infiltrate with Spurr resin (6.3 recipe)
   - Spurr:100% acetone (1:1): 30 min
   - 100% Spurr resin: 60 min
   - 100% Spurr resin: 60 min
   - New 100% Spurr resin; put in appropriate molds with labels
7. Polymerize in 70°C oven overnight to 3 days.

4. Results Expected

Tissues/cells will have nuclear envelopes with parallel membranes, mitochondria, and endoplasmic reticulum with no signs of swelling, and cytoplasm and nucleoplasm with no signs of excessive protein extraction (Figs. 56 and 57).

5. Cautionary Statements

The fixatives used should be handled under a fume hood because of their toxicity and should not come into contact with skin. Spurr resin is regarded as a carcinogen (Ringo *et al.*, 1982), should be formulated, handled, and polymerized under a fume hood, and should not come into contact with skin.

The primary fixative (4F:1G) is stable at 4°C for several months prior to use. Samples may be stored at the same temperature for several years without excessive extraction of cytoplasmic components.

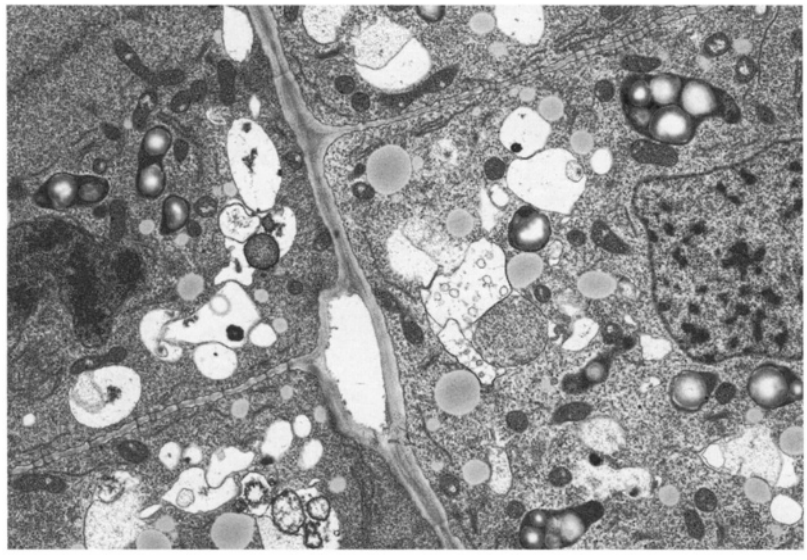

Figure 56. Corn root fixed in 4F:1G and prepared by the routine processing schedule for TEM. × 5,280.

Figure 57. Rat kidney perfused with 4F:1G and prepared by the routine processing schedule for TEM. × 5,280.

All osmium and water washes following osmium must be collected in a container designated for osmium waste.

All plastic resins and diluted plastic resins must be collected in disposable plastic beakers for polymerization before disposal. *Do not put any resins down laboratory sinks.* The resins are considered to be carcinogenic, so *do not breathe the fumes or allow skin contact* with the resin or its components.

Used Spurr resin should be removed from sample vials with 5¼ in. (13 cm) Pasteur pipets (Fig. 58) and transferred to a disposable beaker kept under the fume hood. After several weeks, any remnants of

acetone will have evaporated, and the resin will have polymerized. At that time, the beaker containing solid resin can be discarded. To add fresh resin to vials, plastic disposable pipets (Fig. 59) are used to make sure that pipets for removing waste resin are not confused with pipets containing fresh resin, leading to contamination of fresh resin.

Spurr resin is readily contaminated by water. Be careful to keep all containers of the fluid resin closed and free of water vapor. In some cases, breathing into vials containing resin or sneezing near resin in open containers has resulted in poorly polymerized, rubber-like blocks.

Labels are customarily printed with a laserjet printer (Figs. 60–63), placed in molds during the last 100% infiltration step, and then placed in a 70°C oven until needed to assure that the labels and molds are

Figure 58. Removing resin from a sample vial with a glass 5 ¼ in. (13 cm) Pasteur pipet for transfer to waste Spurr resin beaker, shown to the left in the photo.

Figure 59. Adding Spurr resin to a sample vial with a plastic transfer pipet from a polypropylene bottle containing fresh resin, located behind the tube rack.

moisture-free. See the instructions for Spurr resin formulation concerning filling molds to proper levels. If using BEEM™ capsules, remove the lids. If any of the epoxide resins contain residual amounts of the sample dehydration agents (ethanol, acetone), closing the caps of the BEEM™ capsules can result in retention of these agents, thereby preventing proper resin polymerization.

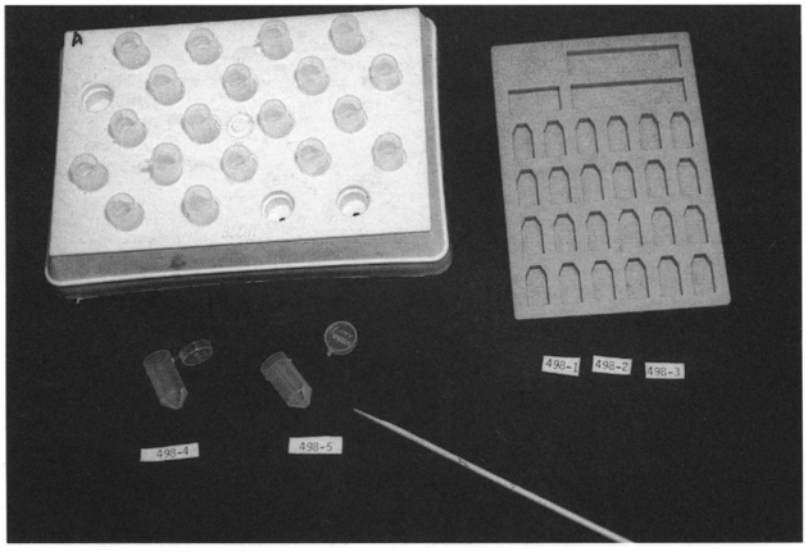

Figure 60. BEEM™ capsules (all with lids properly removed except the one on the left) and flat silicone embedding mold with prepared labels and applicator stick tapered with a razor blade, which will be used to add samples to molds after the addition of a few drops of resin.

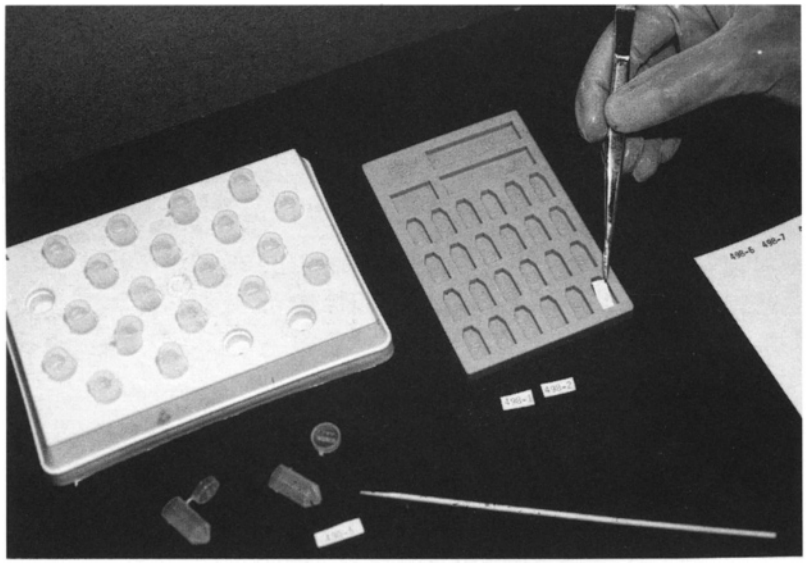

Figure 61. Putting a label in a flat embedding mold, with lettering down.

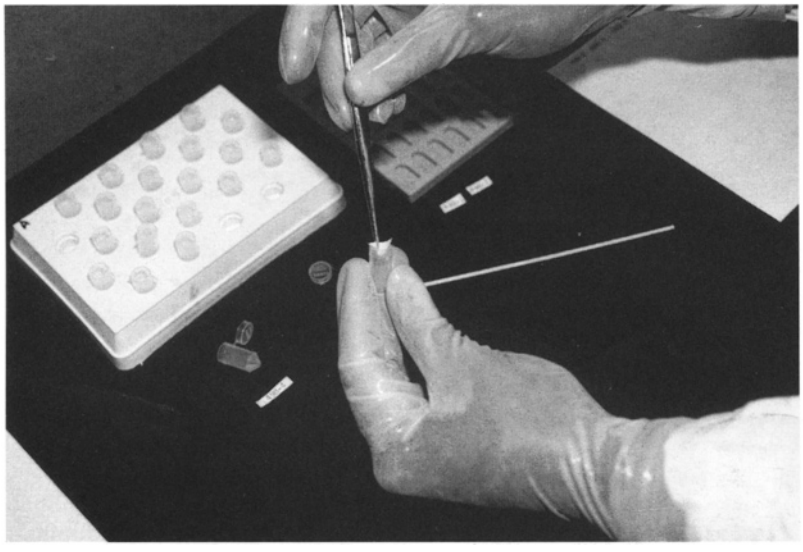

Figure 62. Putting a label into a BEEM™ capsule, with lettering facing out.

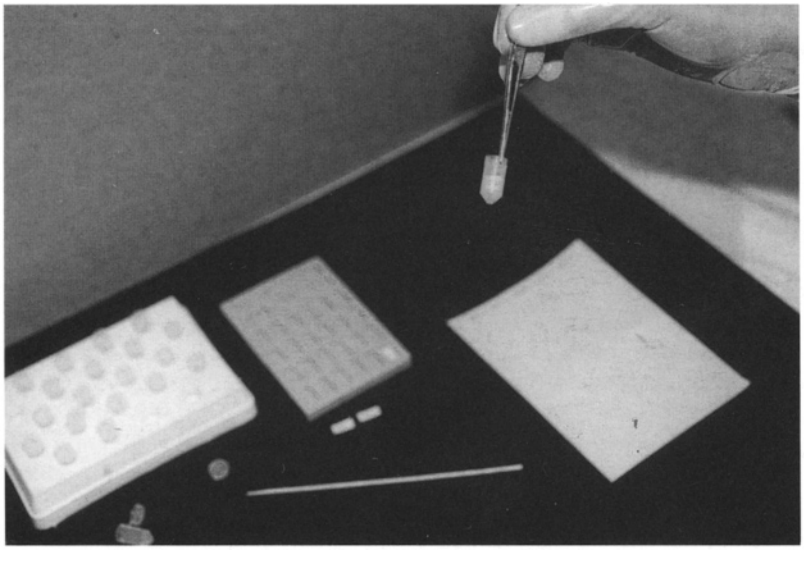

Figure 63. Label properly positioned near the tapered portion of a BEEM™ capsule tip.

References

McDowell, E.M. and Trump, B.F. 1976. Histologic fixatives suitable for diagnostic light and electronmicroscopy. *Arch. Pathol. Lab. Med.* 100: 405.

Ringo, D.L., Brennan, E.F., and Cota-Robles, E.H. 1982. Epoxy resins are mutagenic: Implications for electron microscopists. *J. Ultrastruct. Res.* 80: 280.

Spurr, A.R. 1969. A low-viscosity epoxy resin embedding medium for electron microscopy. *J. Ultrastruct. Res.* 26: 31.

Preparation of Primary (Aldehyde) Fixatives

All of the primary fixatives described are suitable for immersion fixation, while the modified Karnovsky's fixative and 4F:1G fixative are also specifically recommended as perfusates. All of the aldehyde fixatives stabilize cellular components for further dehydration (TEM and SEM preparations) and embedment in resins (TEM preparations).

1. Glutaraldehyde (2–4%) in a phosphate or cacodylate buffer is one of the most frequently used fixatives for electron microscopy. It is usually easiest to make up a double-strength fixative solution (8%) that can be diluted with equal volumes of a double-strength buffer of your choice (e.g., 0.2 M sodium phosphate buffer). This dilution produces a 4% glutaraldehyde fixative solution in a 0.1 M phosphate buffer. This concentration of glutaraldehyde (4%) is often recommended for dense, highly proteinaceous samples such as skin, since much of the glutaraldehyde in the solution will be bound to the tissue proteins as the solution diffuses to the center of the tissue block. Hence, the central portion of the tissue will receive a more diluted solution of glutaraldehyde than the surface of the tissue, so it is reasonable to start with a high concentration of aldehyde to assure that the center of the tissue receives a sufficient aldehyde concentration for good fixation. A monolayer of cells, however, will have no aldehyde penetration problem and usually fixes well in 1% glutaraldehyde within 15–30 min.
2. 4F:1G fixative (McDowell and Trump, 1976) is a mixture containing 4% formaldehyde and 1% glutaraldehyde in a monobasic phosphate buffer with a final pH of 7.2–7.4 and a final osmolality of 176 mosmol. To make 100 ml of 4F:1G, mix the following in the order listed:
   - 86 ml of distilled water
   - 10 ml of Fisher F-79 (37–40% formaldehyde)[1]
   - 4 ml of 25% biological grade glutaraldehyde
   - 1.16 g of $NaH_2PO_4 \cdot H_2O$
   - 0.27 g of NaOH (stir while adding components)
3. Modified Karnovsky's fixative (Karnovsky, 1965) is formulated at half the strength of the original recipe, which decreases the tonicity of the solution and generally provides fixation that is better than that produced by the full-strength mixture. In addition, we delete the calcium chloride called for in the original recipe and utilize a phosphate buffer rather than the original cacodylate buffer, unless we are concerned about charged materials in our fixation protocols (see recommendations about cacodylate and phosphate buffer uses in the buffer section). Our recipe produces a fixative solution containing 2% formaldehyde and 2.5% glutaraldehyde in phosphate buffer at pH 7.2–7.4.
   a. Prepare 25 ml of fresh 4% formaldehyde from paraformaldehyde (see below) in a 50-ml volumetric flask.

[1] Substitution of formaldehyde made freshly from paraformaldehyde powder is recommended for cytochemical procedures to avoid any potential problems from the stabilizers added to typical 37–40% formaldehyde stocks. *As with all procedures calling for formaldehyde made from paraformaldehyde, it is recommended that the fixative be made just before use to lessen the chance that the formaldehyde rerepolymerizes into paraformaldehyde.*

This fixative is strongly recommended for perfusions or immersion fixation of plants, animals, fungi, bacteria, viruses, and many protozoans. The fixative is stable at 4 °C for at least 3 months before use, and samples may be stored in the fixative at the same temperature for up to 5 years without any serious damage (see discussion in this chapter). In addition, the glutaraldehyde concentration is low enough that tissues embedded in paraffin still section and stain well (glutaraldehyde concentrations of 2% and above result in brittle paraffin blocks and nonspecific periodic acid–Schiff reagent staining), so this is an ideal fixative if a sample is used for both light and electron microscopy.

b. Add 5 ml of 25% biological grade glutaraldehyde.
c. Add 0.2 M Sorenson's sodium phosphate buffer pH 7.2–7.4 to bring the final volume to 50 ml. *This fixative keeps at 4°C for 1–2 weeks. After that time, it should be discarded because the formaldehyde component may have begun repolymerizing into paraformaldehyde. Most users do not recommend storing samples in Karnovksy's for extended periods of time.*
d. A 4% formaldehyde solution from paraformaldehyde powder (Karnovsky, 1965) should be prepared under a fume hood because of the toxicity of the formaldehyde fumes.
   i. Dissolve 1.0 g of paraformaldehyde in 25 ml of distilled water heated to 60–70°C (steaming) with stirring.
   ii. Add 1–3 drops of 1 N NaOH and stir until clear.
   iii. Cover and cool to room temperature.

To prepare 4% formaldehyde in a 0.1 M phosphate buffer solution from paraformaldehyde stocks, dissolve 2 g of paraformaldehyde in 25 ml of distilled water as described above, clear with NaOH, cool to room temperature, and then dilute with 25 ml of 0.2 M phosphate buffer, pH 7.2–7.4.

References

Karnovsky, M.J. 1965. A formaldehyde–glutaraldehyde fixative of high osmolarity for use in electron microscopy. *J. Cell Biol.* 27: 137A.

McDowell, E.M. and Trump, B.F. 1976. Histologic fixatives suitable for diagnostic light and electron microscopy. *Arch. Pathol. Lab. Med.* 100: 405.

Preparation of Osmium (Osmium Tetroxide, Osmium Tetraoxide)

1. Applications and Objectives

Osmium is a strong oxidizer known to interact readily with unsaturated double bonds found in various molecules. Because of the high number of double bonds found in lipids, osmium is typically thought of primarily as a lipid fixative. When osmium oxidizes double bonds, it is consequently reduced to electron-dense osmium blacks, which stop an electron beam at the site of the reduced osmium. In addition, osmium is soluble in nonpolar media, including saturated lipids, even though there will be no chemical reaction with the saturated lipids. The osmium solubilized in the saturated lipids will be reduced by ethanol during dehydration, thus resulting in an osmium black at the site of the saturated lipids.

This osmium formulation method will produce an uncontaminated 2% aqueous solution of osmium stock from crystalline osmium. For use as a postfixative, a volume of the osmium stock is mixed with an equal volume of double-strength buffer and used within a few hours. For example, mix 2 ml of 2% osmium stock with 2 ml of 0.2 M Sorenson sodium phosphate buffer pH 7.2–7.4 to produce a postfixative consisting of 1% osmium in a pH 7.2–7.4, 0.1 M sodium phosphate buffer.

2. Materials Needed

- 50 ml of distilled water
- 1.0 g of osmium crystals in a sealed glass ampule
- 100 ml plastic-clad glass bottle with a plastic screw cap
- Small triangular file
- Pasteur pipet and bulb
- Parafilm™

3. Procedure

The cleanest method for producing an uncontaminated 2% aqueous osmium stock is as follows:

1. Heat 50 ml of distilled water in a clean beaker to barely steaming on a hot plate under the fume hood.
2. Heat the glass ampule containing osmium crystals (Figs. 64 and 65) with water that is almost too hot for your hand. When the crystals have melted and run down into the bottom of the ampule (Fig. 66), allow the ampule to return to room temperature (the osmium will recrystallize).
3. Score the ampule (preferably on the painted line), or look for the factory-made score mark to rescore with a small triangular file.
4. Wrap the vial in a protective paper towel so that when the ampule is snapped, no glass fragments become embedded in your hand (Fig. 67). Snap the vial.
5. Locate the half of the vial containing the recrystallized osmium (Fig. 68).
6. Use a clean Pasteur pipet to gently pipet a small volume of the steaming distilled water into the broken ampule containing osmium crystals. Pipet the water up and down (*gently*) until the osmium crystals melt.
7. Transfer the liquid osmium to the 100-ml plastic-clad stock bottle (Fig. 69), being careful not to let the liquid osmium run down the side of the bottle. If the liquified osmium contacts the side of the room temperature bottle, it will crystallize and adhere to the side of the bottle, making it difficult to dissolve the osmium in the water if it is above the final water level. *Be extemely careful with the liquified osmium crystals, since they are heavier than water and will tend to run out of the end of the Pasteur pipet.*
8. Once all the osmium has been transferred to the plastic-clad bottle, transfer the remaining steaming distilled water to the container. A large drop of liquid osmium will be visible in the bottle. Next, cap the bottle, wrap the cap and bottle neck with Parafilm™, and then place that bottle in a larger dark bottle (or one wrapped in aluminum foil), preferably made of plastic to minimize the chance of breakage. Leave the osmium container under the fume hood for about 24 hr (for a 2% solution) or 48 hr (for a 4% solution) to allow the osmium to dissolve completely and then place it in a refrigerator designated for toxic chemical storage.

Figure 64. Osmium crystals in a sealed ampule, located both above and below the constricted and scored portion of the ampule, which will be the break line when the vial is snapped.

Figure 65. Running warm water over the ampule to melt the osmium crystals so that they will run into the bottom half of the ampule.

Figure 66. Ampule with recrystallized osmium in the bottom portion of the ampule.

4. Results Expected

After 24 hr, all of the osmium should have gone into solution, resulting in a straw-colored 2% aqueous osmium solution that is stable for months at 4°C if not contaminated by buffers or dirty pipets.

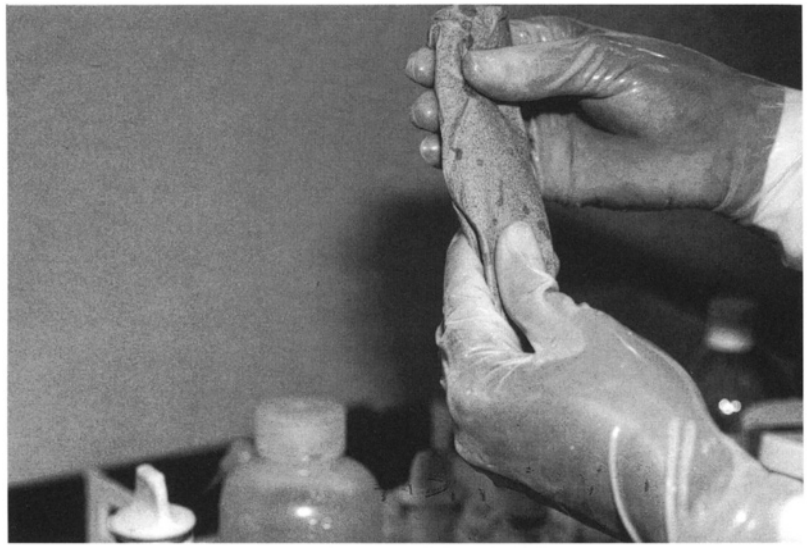

Figure 67. Ampule containing osmium wrapped in several layers of paper towels, ready to be snapped in two.

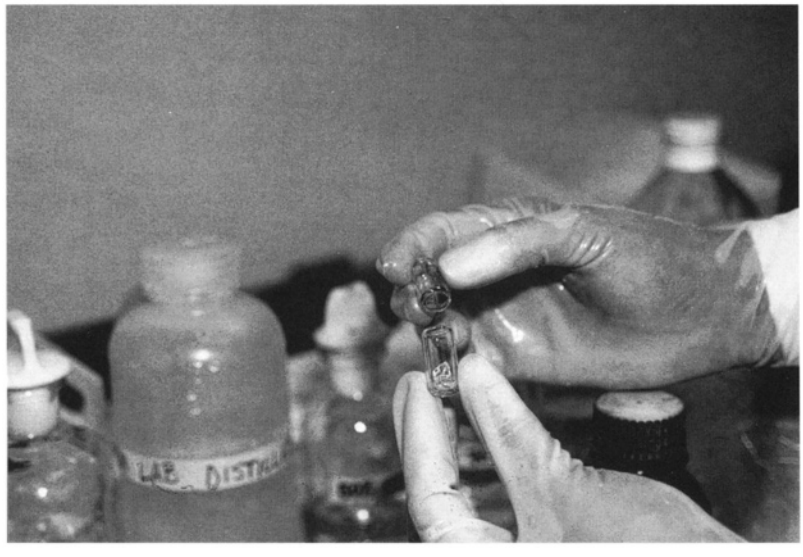

Figure 68. Ampule after breaking into two pieces, the bottom half containing osmium crystals.

5. Cautionary Statements

Osmium is a strong oxidant, has a high vapor pressure, and should not be inhaled or allowed to contact skin. Any buffers or other contaminants inadvertently introduced into the osmium solution will cause reduction and consequent contamination of the osmium, as evidenced by the solution becoming gray and finally black. If the solution is anything but straw-colored, discard it.

If the osmium is not sealed and double-bottled as described, the high vapor pressure of the osmium will allow the osmium to escape the container and contaminate the inside of the refrigerator (which will turn

Figure 69. Osmium crystals melted in steaming distilled water from beaker to the right being pipetted into the osmium stock bottle with a Pasteur pipet.

gray to black). *All osmium stocks and osmium waste that is to be disposed of should be collected by proper waste-disposal personnel after being placed in properly labeled containers.*

Buffering Systems

The most commonly formulated buffers are phosphate buffers (either sodium phosphate or a mixture of sodium and potassium phosphate) and buffers made from cacodylic acid. Both can buffer solutions in the pH range of 6.5–7.5 quite effectively and thus lend themselves to the preparation of working solutions in the physiological pH range of most tissues and cells.

Phosphate buffers are the least expensive to formulate and are regarded as nontoxic. Unfortunately, the phosphate molecule has a negative charge and thus can interact with some cytochemical reagents or salts in the medium that contains the organisms. Cacodylic acid buffers are toxic, since they contain arsenic. They are also more expensive than phosphate buffers, but they do not possess highly reactive groups and are thus the buffer system of choice when working near neutral pH with materials that contain positively charged moieties capable of reacting with the phosphate buffers.

When working with various cytochemical procedures, it is often necessary to prepare incubation media with high- or low-pH conditions, necessitating the employment of other buffering systems. These may produce images of a lower quality than those produced from phosphate or cacodylic acid buffering systems, but the pH conditions necessary for the reactions desired necessitate the use of these alternative buffering systems. Tris buffers are commonly used for high-pH conditions, while acetate buffers are used for low-pH conditions.

All buffers are intended to maintain the pH selected and to maintain the tonicity of a solution at a level that will prevent plasmolysis or swelling of cells and tissues. For typical structural studies, the buffer is intended to counteract the natural drop in pH that accompanies cell death. In addition, osmium postfixation

results in some cleavage of polypeptides into smaller peptides with a consequent increase in carboxyl groups within cells, which could cause a drop in pH leading to damage to cytoplasmic structures without buffering.

When adjusting the pH of buffers, the components in the buffers and the components contained in the fixative solutions should be considered. If a sodium phosphate buffer is being used on cells that have been previously grown in saline-containing medium, it would be appropriate to use NaOH or HCl to adjust pH, since no new ions are being introduced to the system. If, however, compounds are employed that would interact with chloride ions, the use of acetic acid to lower pH would be the best alternative. The recipes below are intended for the preparation of buffer solutions with the pH specified at room temperature. If the buffer is to be used at a temperature other than room temperature, it is necessary to check and possibly adjust the pH at the temperature specified.

Cacodylate Buffers

1. Applications and Objective

Cacodylate buffer is used at physiological pH and is normally formulated from the sodium salt of cacodylic acid with the formula $(CH_3)_2AsO_2Na \cdot 3H_2O$, which has a formula weight of 214. To make a 0.2 M stock, dissolve 4.28 g in 100 ml of distilled water and adjust the pH to 7.2–7.4 with 0.1 N HCl. This stock is used to dilute osmium stocks and to make 0.1 M cacodylate buffer for washing samples (prepared by mixing equal volumes of the stock and distilled water).

2. Materials Needed

- Sodium cacodylate
- Concentrated HCl
- pH meter
- Glassware

3. Procedure

To make 0.1 M cacodylate buffers with pHs from 6.4 to 7.4 (Robinson *et al.*, 1987), two stock solutions are prepared. Solution A is a 0.2 M sodium cacodylate stock prepared as described above. Solution B is a 0.2 N HCl stock made by adding 16.6 ml of concentrated (36–38%) HCl to 1 liter of distilled H_2O. To prepare buffer solutions, place 50 ml of solution A into a 100-ml volumetric flask, add the appropriate amount of solution B (see Table 3), and bring the final volume to 100 ml.

Table 3. Preparation of Cacodylate Buffers

pH Desired at Room Temperature	Quantity Solution B (ml)
6.4	36.8
6.6	26.8
6.8	18.8
7.0	12.8
7.2	8.4
7.4	5.6

Reference

Robinson, D.G., Ehlers, U., Herken, R., Herrmann, B., Mayer, F., and Schurmann, F.-W. 1987. *Methods of preparation for electron microscopy*. Springer-Verlag, Berlin.

Phosphate Buffers

1. Applications and Objectives

Phosphate buffers are typically used at physiological pH. They are specifically avoided in situations where the negatively charged phosphate groups could be expected to interact with positively charged ions in incubation media, causing precipitates to form. This can be a problem with cytochemical procedures such as ruthenium red staining and also if the fixation protocol involves mixing fixative and buffer with microorganisms in complex growth media or seawater without prewashing to remove the salt-containing fluids.

There are three major phosphate buffers used in most laboratories: Sorenson's phosphate buffer formulated from sodium and potassium phosphate salts, Sorenson's sodium phosphate buffer (which we use exclusively in our laboratory), and Millonig's sodium phosphate buffer.

2. Materials Needed

- Monobasic sodium phosphate ($NaH_2PO_4 \cdot H_2O$)
- Dibasic sodium phosphate (Na_2HPO_4, anhydrous)
- Monobasic potassium phosphate (KH_2PO_4, anhydrous)
- pH meter
- Glassware

3. Procedures

Sorenson's Sodium Phosphate Buffer, pH 7.3–7.4. To prepare a 0.2 M Sorenson sodium phosphate buffer at pH 7.2–7.4 for diluting osmium stocks and preparing 0.1 M phosphate buffer for washes (by diluting 1:1 with distilled H_2O):

Stock solutions:

- Stock A: 0.2 M solution of $NaH_2PO_4 \cdot H_2O$ (27.6 g/l of H_2O)
- Stock B: 0.2 M solution of Na_2HPO_4, anhydrous (28.4 g/l of H_2O)
- To make 0.2 M working buffer, pH 7.2–7.4: Mix 23 ml of stock A and 77 ml of stock B

Sorenson's Sodium Phosphate Buffer at Various pH Values (Glauert, 1975)

Stock solutions:

- Stock A: 0.2 M solution of $NaH_2PO_4 \cdot H_2O$ (27.6 g/l of H_2O)
- Stock B: 0.2 M solution of Na_2HPO_4 (28.4 g/l of H_2O)

To prepare a 0.1 M buffer solution at the desired pH, Stock A and Stock B are mixed in the amounts shown in Table 4 and then brought to a final volume of 200 ml with distilled H_2O.

Table 4. Preparation of Sorenson's Sodium Phosphate Buffer

pH Desired at Room Temperature	Stock A (ml)	Stock B (ml)
5.8	4.0	46
6.0	6.15	43.85
6.2	9.25	40.75
6.4	13.25	36.75
6.6	18.75	31.25
6.8	24.5	25.5
7.0	30.5	19.5
7.2	36.0	14.0
7.4	40.5	9.5
7.6	43.5	6.5
7.8	45.75	4.25
8.0	47.35	2.65

Reference

Glauert, A.M. 1975. *Fixation, dehydration and embedding of biological specimens*. North-Holland, New York.

Sorenson's Phosphate Buffer with Sodium and Potassium Phosphate (Robinson *et al.*, 1987)

Stock solutions:

- Stock A: 0.1 M Na_2HPO_4, anhydrous (14.2 g/l of H_2O)
- Stock B: 0.1 M KH_2PO_4, anhydrous (13.76 g/l of H_2O)

To make a 0.1 M working buffer solution at a specific pH, Stock A and Stock B are mixed in the amounts shown in Table 5.

Table 5. Preparation of Sorenson's Sodium/Potassium Phosphate Buffer

pH Desired at Room Temperature	Stock A (ml)	Stock B (ml)
6.0	87.7	12.3
6.8	50.8	49.2
7.0	39.2	60.8
7.2	28.5	71.5
7.4	19.6	80.4
7.6	13.2	86.8
7.8	8.6	91.4
8.0	5.5	94.5

Reference

Robinson, D.G., Ehlers, U., Herken, R., Herrmann, B., Mayer, F., and Schurmann, F.-W. 1987. *Methods of preparation for electron microscopy*. Springer-Verlag, Berlin.

Millonig's Phosphate Buffer (Millonig, 1964). This buffer is designed to be mixed with osmium and used to fix very hydrated tissues. The pH of the buffer is 7.4, and the osmolarity is 440 mosmol, hypertonic for most cells. It is recommended that the sodium chloride concentration be raised to 3% for fixing marine organisms.

The buffer is prepared by dissolving 1.8 g of $NaH_2PO_4 \cdot H_2O$, 23.25 g of $Na_2HPO_4 \cdot 7H_2O$, and 5.0 g of NaCl in distilled H_2O, with a final volume of 1 liter.

Reference

Millonig, G. 1964. Study on the factors which influence preservation of fine structure. In: P. Buffa (ed.), *Symposium on electron microscopy* (p. 347). Consiglio Nazionale delle Ricerche, Rome.

Tris–HCl Buffer (Chayen *et al.*, 1969)

1. Applications and Objectives

Tris buffer is not considered to be one of the better buffers for electron microscopy because it can interact with aldehydes to some extent, but it is the best choice if a pH above 7.4 is needed for cytochemical procedures, since cacodylate and phosphate buffers do not work well above pH 7.4.

2. Materials Needed

- Tris(hydroxymethyl)aminomethane (TRIS)
- HCl
- pH meter
- Glassware

3. Procedure

1. Prepare stock solutions:
   - Stock A: 0.2 M TRIS (2.4 g of Tris/100 ml of H_2O)
   - Stock B: 0.1 M HCl (1.8 ml of 36–38% HCl added to distilled H_2O and brought to 100 ml final volume)
2. To prepare a 0.05 M Tris buffer of specific pH, 25 ml of Stock A is added to the appropriate volume of Stock B (see Table 6), and the mixture is brought to a final volume of 100 ml with distilled water.

Table 6. Preparation of Tris–HCl Buffer

pH Desired at Room Temperature	Stock B (ml)
7.4	42.0
7.6	38.5
7.8	34.5
8.0	29.0
8.2	23.0
8.4	17.5
8.6	13.0
8.8	9.0
9.0	6.5
9.2	4.0

Reference

Chayen, J., Bitensky, L., Butcher, R.G., and Poulter, L.W. 1969. *A guide to practical histochemistry*. J.B. Lippincott, Philadelphia.

Sodium Acetate Buffer (Chayen *et al.*, 1969)

1. Applications and Objectives

Sodium acetate buffer is used for cytochemical procedures where a low pH is necessary for enzymatic activity (as with the acid hydrolases of lysosomes).

2. Materials Needed

- Sodium acetate ($CH_3COONa \cdot H_2O$)
- Glacial acetic acid
- Glassware
- pH meter

3. Procedure

1. Prepare stock solutions:
   - Stock A: 0.2 M sodium acetate (2.72 g/l of H_2O)
   - Stock B: 0.2 M acetic acid (1.2 g/100 ml of H_2O)
2. To prepare a 0.2 M acetate buffer of known pH, mix Stock A with Stock B, as shown in Table 7.

Table 7. Preparation of Sodium Acetate Buffers

pH Desired at Room Temperature	Stock A (ml)	Stock B (ml)
3.6	8	92
3.8	13	87
4.0	20	80
4.2	30	70
4.4	40	60
4.6	50	50
4.8	60	40
5.0	70	30
5.2	80	20
5.4	86	14
5.6	90	10

Reference

Chayen, J., Bitensky, L., Butcher, R.G., and Poulter, L.W. 1969. *A guide to practical histochemistry*. J.B. Lippincott, Philadelphia.

Dulbecco's Phosphate-Buffered Saline

1. Applications and Objectives

Dulbecco's phosphate-buffered saline (DPBS) is not customarily used for fixative preparation or washing steps during processing but is useful for washing the complex media containing salts and proteins like bovine serum from cell cultures prior to primary fixation. If the growth medium is not washed from cell cultures prior to fixation, or serum is not washed from blood samples (Fig. 70), precipitation and cross-linking of extracellular proteins present will produce a background of fibrillar material.

Dulbecco's balanced salt solution (DBSS) is often found in laboratories working with cell cultures and is used to wash cell suspensions. Since this solution is prepared by adding 100 mg/l of $CaCl_2$ and 59.2 mg/l of $MgSO_4$ to DPBS, and thus contains reactive ions not present in DPBS, it is *not* recommended for washing cells prior to primary fixation.

2. Materials Needed

- Potassium chloride (KCl)
- Monobasic potassium phosphate (KH_2PO_4)
- Sodium chloride (NaCl)
- Dibasic sodium phosphate (Na_2HPO_4)
- pH meter
- Glassware

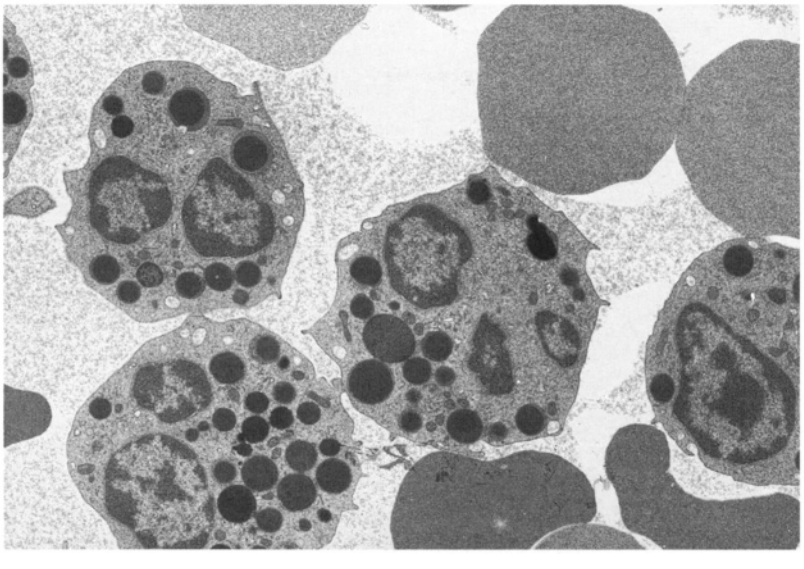

Figure 70. Canine blood sample fixed with 4F:1G without a DPBS rinse to remove serum proteins, which was subsequently processed according to the routine TEM schedule. Note the granulo-fibrillar background serum proteins stabilized by 4F:1G. ×5,000.

3. Procedure

To prepare DPBS, mix 0.2 g of KCl, 0.2 g of KH_2PO_4, 8 g of NaCl, and 1.15 g of Na_2HPO_4 in distilled H_2O, bring the final volume to 1 liter, and adjust the pH to 7.2–7.4.

Resin Formulations

The majority of ultrastructural studies undertaken today utilize one of two classes of embedding media: epoxide and acrylic resins. The former provide superior structural images and are quite stable under the electron beam but are extremely hydrophobic, while the latter exhibit somewhat diminished structural preservation, particularly since many procedures utilizing the acrylic resins do not employ osmium postfixation. Acrylic resins have diminished electron beam stability but are more hydrophilic than epoxides, which is a useful characteristic for a variety of cytochemical procedures. Epoxides are generally infiltrated at room temperature and polymerized with heat, while some of the acrylic resins can be infiltrated at low temperatures (−20 to −80°C) and polymerized with ultraviolet radiation at the same temperature. The stated characteristics of these resins explain why epoxides are employed more for structural studies, whereas the acrylics are more useful for cytochemical procedures, particularly immunocytochemical procedures.

Resin infiltration of samples with waxy or chitinous cuticles such as plants and insects, respectively, or thick cell walls and coats, as found with protozoans and seeds, may be difficult. Resin choice in terms of viscosity (cP) thus is often dictated by sample type. Some resin viscosities are given in Table 8. Resins polymerize slowly at room temperature, resulting in changes in viscosity in as little as 24 hr, but storing most epoxide resins at −20°C for 1–2 months works well as long as the resin is warmed to room temperature before being exposed to air to prevent possible condensation of atmospheric moisture onto cold resin, which would prevent proper polymerization of most epoxides.

To control the flow of viscous resin components being weighed during formulation of embedding media, applicator sticks are quite useful. They can be held across the mouth of a bottle of resin component, allowing the fluid to be dispensed into the polypropylene mixing bottle in a controlled way (Fig. 71). *Always use a new, clean applicator stick with each separate resin component to prevent cross-contamination.*

Table 8. Viscosities of Commonly Used Resins[a]

Type of Resin	Viscosity at Room temperature (cP)	Viscosity after 48 hr at 20°C (cP)
Epoxides:		
• Epon–Araldite 506	800	
• Epon 812	290	540
• Poly/Bed 812	300	330
• Spurr/Araldite 506	220	
• LX-112	190	212
• Spurr	60	
Acrylics:		
• LR White	8	

[a] After Ellis (1983).

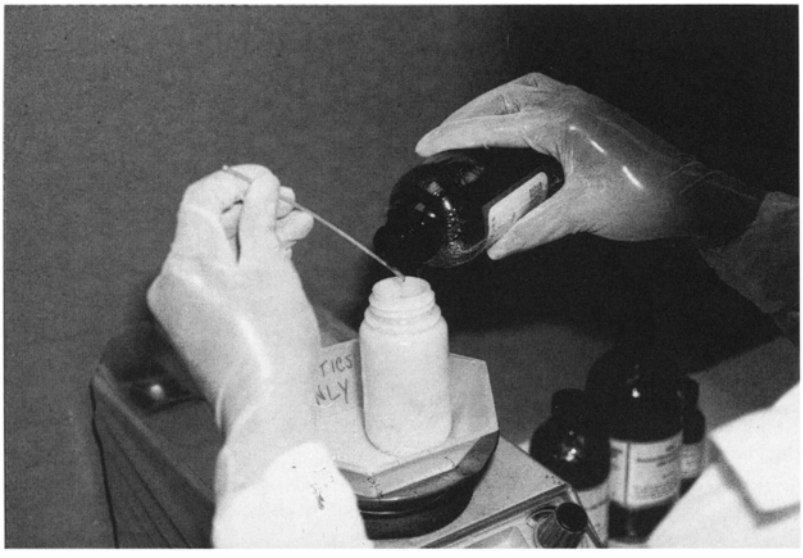

Figure 71. Measuring out one component of Spurr resin mixture on a top-loading balance protected by a weighing dish in case of spills. Note the gloves and the applicator stick used to control the flow rate into the polypropylene mixing bottle.

Reference

Ellis, E.A. 1983. Evaluation of the Epon 812 replacement resins, LX-112 and Poly/Bed 812. *Proc. Southeast Electron Microsc. Soc.* 16: 14.

Spurr Resin

1. Applications and Objectives

Spurr resin was originally designed for plants with cell walls that were hard to infiltrate with higher-viscosity epoxide resins. The resin is also ideal for other hard-to-penetrate specimens like insects and skin samples. It provides a relatively brief infiltration schedule for most materials that can shorten overall specimen processing times. The embedding resin is compatible with acetone, ethanol, and other commonly used solvents. The resin is completely miscible with ethanol, though blocks polymerized following an ethanol-only dehydration series often have a slightly tacky surface not found when acetone is used as a transitional solvent. Because of the low viscosity of Spurr resin, it is not necessary to rotate or agitate specimens in the resin during infiltration.

With proper handling, Spurr resin provides quick infiltration of difficult samples and can be readily trimmed and sectioned, yielding excellent results.

2. Materials Needed

- ERL 4206 (vinylcyclohexene dioxide): a cycloaliphatic diepoxide
- DER 736: a diglycidyl ether of polypropylene glycol, used to control hardness of the polymerized blocks
- Nonenyl succinic anhydride (NSA), a hardener that should have minimal exposure to air to lessen the chance of hydrolysis
- Dimethylaminoethanol (S-1) (DMAE), an accelerator that induces rapid curing of the resin at 70°C
- 100-ml polypropylene bottle
- Applicator sticks
- Pasteur pipet with bulb
- Top-loading balance
- Parafilm™

3. Procedure

Recipes. Several recipes are offered by the various vendors as shown in Table 9, with all components weighed out in grams:

Table 9. Possible Spurr Resin Recipes

Component	Standard Resin	Hard Resin	Soft Resin	6.3 Recipe
ERL 4206	10.0 g	10.0 g	10.0 g	10.0 g
DER 736	6.0 g	4.0 g	8.0 g	6.3 g
NSA	26.0 g	26.0 g	26.0 g	26.0 g
DMAE	0.4 g	0.4 g	0.4 g	0.4 g

In our laboratory, the resin components are added, in order, to a 100-ml polypropylene bottle with a screw cap. The bottle is capped and swirled to mix the resin. The resin initially colors a deep yellow to orange yellow but then clears to a lighter yellow. If the bottle neck and cap are wrapped in Parafilm™, the resin can be stored at −20°C for several months. *Make sure that the resin container is at room temperature before opening to prevent condensation of water on cold resin, which would prevent proper polymerization.* The resin is fully cured in all the recipes listed after 8 hr at 70°C. Leaving the resin in the oven up to 3 days (over a weekend) does not seem to change the qualities of the blocks compared with 8 hr of polymerization.

Infiltration and Polymerization. After tissues have been fixed in aldehydes, washed, postfixed in osmium, and properly dehydrated with anhydrous acetone or ethanol, room-temperature infiltration with Spurr resin can proceed.

1. Remove the solvent from vials containing samples and replace with new anhydrous solvent. Add an equal volume of 100% Spurr resin (6.3) to the vials and mix gently by pipetting the solution up and down with a fresh (and dry) Pasteur pipet. Cap the vial and let it sit 30 min.
2. Remove 1:1 mixture of Spurr resin and solvent and replace with 100% Spurr resin, cap vials and let sit for 1 hr.
3. Remove Spurr resin, replace with fresh Spurr resin, recap vials, and let sit 1 hr.
4. Prepare molds for samples.
5. Flat embedding molds or BEEM™ capsules should have *dry* labels inserted (Figs. 60–63) and should then be filled about half full with fresh Spurr resin. Insert specimens into the molds and orient them.
6. Finish filling molds. Fill BEEM™ capsules only to the line near the open end. Make sure that the label is deep enough in the capsule to be well below the plastic resin level. The BEEM™ capsule lids should be pulled off to assure that they will not be closed during polymerization, which tends to produce rubbery blocks. Flat embedding molds should have laser jet (or lead pencil-marked) labels placed information-side down in the chamber, and then the chamber should be filled about half full prior to sample introduction. After the specimen is placed into a chamber and oriented properly, resin should be added with a fresh Pasteur pipet until the resin level in the chamber is slightly convex (Fig. 72). The resin decreases in volume during polymerization, and if the resin in the chambers is concave before polymerization, the blocks will be thin and prone to breakage. If the chambers are over-filled, the resin will flow over the mold edges during polymerization. Spurr resin is the only epoxide resin that will interact with typical silicone rubber embedding molds, causing them to curl up, split, and lose pieces of silicone when blocks are removed (Fig. 73).

4. Results Expected

Polymerized blocks should be colorless to slightly yellow, not remarkably brittle when trimmed with a razor blade, and capable of being dented only slightly by a fingernail. Sections stain well with 5 min in methanolic uranyl acetate (100% methanol nearly saturated with uranyl acetate) followed by 8 min in

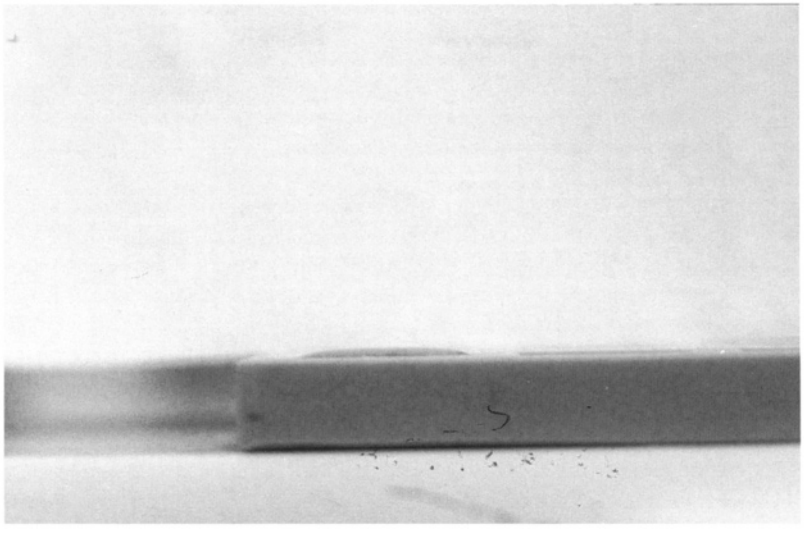

Figure 72. Side view of a silicone embedding mold with one chamber on the left end filled appropriately with Spurr resin. After polymerization, the convex aspect of the fluid will have vanished as the resin shrinks during polymerization, and the final block will have virtually parallel top and bottom sides.

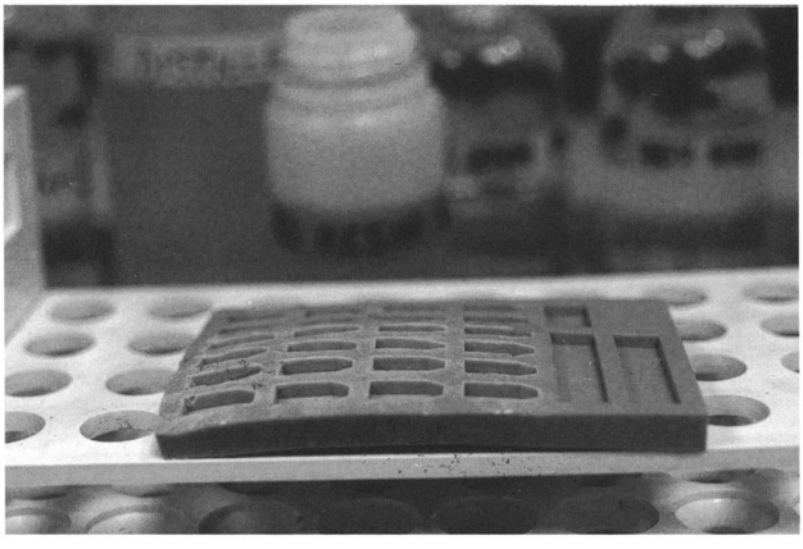

Figure 73. Silicone embedding mold used with Spurr resin. The mold has probably been used two dozen times and has interacted with the resin. The resin has caused the mold to curve. When the polymerized blocks were removed from the mold, small pieces of the silicone were pulled away, as can be seen in the corner of the chamber at the lower left.

Reynolds' lead citrate. Sections will often develop permanent folds that can intrude on virtually every grid square (on a 200 mesh grid). These folds occur during the poststaining step in methanolic uranyl acetate. Folds can be virtually eliminated by proper drying between staining steps (see the Techniques section on staining). Some investigators have left the specimens overnight in 0.5% uranyl acetate after washing out the osmium postfixative, followed by a water rinse prior to ethanolic dehydration as an alternative to uranyl acetate poststaining, which will also avoid the problem of folds.

5. Cautionary Statements

The firm formulation (6.0 g of DER 736) recommended by most vendors produces blocks that are so hard that glass knives become rapidly degraded, and diamond knives even have some difficulty with the material. When I was in Dr. R. Sjoland's laboratory at the University of Iowa, we were trained to use 6.2 g of DER 736 if we intended to cut sections with diamond knives and 6.4 g of DER if we had to cut all our sections with glass knives. For the last 23 years, my laboratories have used 6.3 g of DER 736 for materials destined for either glass or diamond knife sectioning with good results.

As has been mentioned several times, Spurr resin, specifically the DER 736 component, is purported to be carcinogenic, even after it is polymerized. For that reason, it is important to avoid contact with the complete resin or its components and to minimize exposure to dust or chips created during block trimming. We keep a vacuum cleaner at our trimming station and vacuum up the trimming debris continually as we work and always wash our hands immediately after block trimming.

Even trace amounts of water will interfere with proper resin polymerization, so moisture must not come into contact with the unpolymerized resin. The few times we have produced rubber blocks due to moisture contacting the uncured resin have been associated with excessive conversation or sneezing over exposed liquid resin.

Reference

Spurr, A.R. 1969. A low-viscosity epoxy resin embedding medium for electron microscopy. *J. Ultrastruct. Res.* 26: 31.

Poly/Bed 812 Resin

1. Applications and Objectives

Poly/Bed 812 is sold by Polysciences, Inc. as a replacement for Epon 812 resin. It has similar infiltration and polymerization qualities to Epon and sections equally well. The polymerized resin has a very fine grain and can be stained either with aqueous or methanolic uranyl acetate and lead citrate, though it does not stain as readily as the original Epon. The complete resin may be stored in the freezer in a tightly capped polypropylene bottle with the neck wrapped in Parafilm™. *Do not open the bottle of resin until it is at or above ambient temperature to avoid moisture condensation on the resin, which would compromise polymerization.* An ethanol or acetone dehydration series followed by absolute acetone as a transitional solvent and diluent for the resin works well.

The blocks produced from this resin should be hard and yellow to dark yellow in color. This material is somewhat more difficult to cut on glass knives than Spurr resin because it is harder than the 6.3 Spurr resin recipe we use.

2. Materials Needed

- Poly/Bed 812 resin
- DDSA (dodecenylsuccinic anhydride)
- NMA (nadic methyl anhydride)
- DMP-30 (2,4,6-tridimethylamino methyl phenol)
- 100-ml polypropylene bottle
- Top-loading balance
- Applicator sticks
- Parafilm™

3. Procedure

Resin Formulation. The following components should be added in the order listed to a 100-ml polypropylene bottle and then mixed vigorously by swirling the container:

- 21 ml of Poly/Bed 812
- 13 ml of DDSA
- 11 ml of NMA
- 0.7 ml of DMP-30

Sample Processing

1. Fix, wash, postfix, wash, and dehydrate specimens as specified for routine TEM sample processing.
2. Infiltration with resin (all done at room temperature):
   - Poly/Bed 812 and anhydrous acetone (1:1) for 1 hr
   - 100% Poly/Bed 812 overnight
   - 100% Poly/Bed 812 for 1 hr
   - Put fresh Poly/Bed 812 into embedding molds with labels as described for Spurr resin
   - Polymerize overnight at 60°C

4. Results Expected

The polymerized blocks are hard and clear, and section and poststain well. The sections are quite stable under the electron beam. Sections can be stained in aqueous uranyl acetate (10 min), or methanolic uranyl acetate (5 min), followed by 8 min in Reynolds' lead citrate to produce good specimen contrast.

5. Cautionary Statements

As with all organic solvents, consider this resin to be toxic or, at the very least, potentially allergenic, and avoid inhalation or skin contact. Do not allow water to come into contact with the formulated embedding mixture or any of the individual components, as it will interfere with proper polymerization.

Reference

Polysciences, Inc. product sheet 233.

SPI-Pon 812

1. Applications and Objectives

This resin is marketed by SPI Supplies as a replacement for Epon 812. It has similar infiltration characteristics, polymerization requirements, and sectioning qualities to Epon 812. The resin mixture stays usable for about 1 day at room temperature and will remain usable for several months if stored at −20°C in a Parafilm™-wrapped polypropylene bottle. The unpolymerized resin is readily soluble in acetone, so the more toxic propylene oxide transition solvent recommended by SPI Supplies is not necessary. The resin is more viscous than Spurr resin, so gentle agitation (provided by some sort of slanted rotating device) is useful for better specimen penetration. SPI Supplies suggests that the resin mixture can be combined with Araldite 6005 to produce a resin similar to Mollenhauer's Epon-Araldite formulation.

The blocks of infiltrated tissues and cells are easily trimmed, sectioned, and poststained.

2. Materials Needed

- SPI-pon 812 resin
- DDSA
- Nadic methyl anhydride (NMA)
- 2,4,6-Tridimethylamino methyl phenol (DMP-30)
- 100-ml polypropylene bottle
- Applicator sticks
- Top-loading balance
- Parafilm™

3. Procedure

Resin Formulation. Weigh out the following into a 100-ml polypropylene bottle in the order listed, with thorough mixing by swirling after all the components have been added:

- 18.5 g of SPI-Pon 812 (16.2 ml)
- 9.3 g of DDSA (10.0 ml)
- 10.0 g of NMA (8.9 ml)
- 0.6 g of DMP-30 (0.6 ml)

Sample Processing

1. Fix, wash, postfix, wash, and dehydrate specimens as recommended for routine TEM specimen preparation. All steps, including resin infiltration, are done at room temperature.
2. Infiltrate with a 1:1 mixture of complete resin mixture (hereafter referred to as "SPI-Pon")-acetone for 1 hr with gentle rotation.
3. Replace resin:acetone mixture with fresh 100% SPI-Pon and gently rotate for 1 hr.
4. Put fresh 100% SPI-Pon into molds with labels and add specimens as described for Spurr resin.
5. Polymerize resin for 24 hr at 60°C.
6. Cool blocks to room temperature, remove from molds, and section them.

4. Results Expected

The polymerized blocks trim and section easily and produce sections that poststain readily in 2% aqueous uranyl acetate (5 min) and Reynolds' lead citrate (8 min).

5. Cautionary Statements

This resin is an epoxide and thus should be handled as if toxic. It should be measured, handled, and polymerized under a fume hood.

References

Mollenhauer, H.H. 1964. Plastic embedding mixtures for use in electron microscopy. *Stain Technol.* 39: 111.
SPI Supplies. *SPI-Pon 812 kit instructions for use.*

Araldite 6005 Resin

1. Applications and Objectives

The 502 and 6005 Araldite resins most commonly used have a high initial viscosity, causing infiltration difficulties with some samples, but the polymerized blocks change volume the least of all the commonly used epoxide resins.

Araldite resins are soluble in ethanol and acetone, though acetone is recommended as a transitional solvent for the infiltration series.

This procedure will produce sample-containing blocks which, upon polymerization, have essentially the same volume as before polymerization, have excellent trimming and sectioning characteristics, stain well, have a minimal grain structure, and are stable under the electron beam.

2. Materials Needed

- Araldite 6005
- DDSA
- Benzyl dimethylamine (BDMA)
- 100-ml polypropylene bottle
- Applicator sticks
- Top-loading balance
- Parafilm™

3. Procedure

Resin Formulation. Add the following ingredients to a 100-ml polypropylene bottle in the order listed and swirl to mix:

- 29.0 g Araldite 6005
- 20.3 g DDSA
- 0.7 g BDMA

Sample Processing

1. Fix, wash, postfix, wash, and dehydrate according to the schedule for routine TEM specimen preparation.
2. Infiltrate, with continuous stirring:
   - Acetone + embedding mixture (3:1): 60 min
   - Acetone + embedding mixture (1:1): 60 min
   - Acetone + embedding mixture (1:3): 60 min
   - 100% embedding mixture 60 min

Put new 100% embedding mixture into appropriate molds, add samples, and polymerize at 45°C for 24 hr followed by 60°C incubation for another 24 hr.

4. Results Expected

According to Hayat (2000), Araldite has the finest grain structure and the greatest electron density of all the epoxides. The blocks will section and stain well.

5. Cautionary Statements

The Araldites are extremely viscous and can be difficult to handle during processing because they do not pipet well. Araldites also have difficulty penetrating some samples. The electron density of the resin can reduce the contrast in sections compared with other resins. The resin is an epoxide, and so it should be handled as if it is a toxic material (work under the hood, avoiding skin contact).

References

Hayat, M.A. 2000. *Electron microscopy: Biological applications*, 4th edn. Cambridge University Press, New York.
Polysciences, Inc. data sheet 128.

Mollenhauer's Epon/Araldite Resin (Adapted for Use with Epon Substitutes)

1. Applications and Objectives

Mollenhauer (1964) concocted a mixture of Epon 812 and Araldite 502 to provide a resin with less viscosity than Araldite alone, but with the characteristics of fine grain, minimal shrinkage during polymerization, good sectioning and staining techniques as well as good electron beam stability. Mollenhauer has reported that Epon 812 can be successfully replaced with Poly/Bed 812 in the recipe. The fixation, dehydration, and embedding protocols suitable for Epon substitutes or Araldite resins are appropriate for the Mollenhauer mixture.

The resin mixture can be applied to a variety of organisms and cell types, though it still will have some of the penetration difficulties encountered with some specimens when utilizing either Epon substitutes or Araldite alone.

2. Materials Needed

- Poly/Bed 812
- Araldite 502 or 6005
- DDSA
- BDMA
- 100-ml polypropylene bottle
- Applicator sticks
- Top-loading balance
- Parafilm™

3. Procedure

Resin Formulation. Add the following components in the order listed to a 100-ml polypropylene bottle and swirl to mix:

- 100 g of Poly/Bed 812
- 55 g of Araldite 502 or 6005
- 180 g of DDSA
- 10 g of BDMA (5 g of DMP-30 can be substituted for the BDMA)

Sample Processing. The processing schedule used for Araldite 6005 works well here.

4. Results Expected

The blocks have minimal shrinkage after polymerization. Aqueous uranyl acetate and Reynolds' lead citrate are appropriate stains for sections.

5. Cautionary Statements

The normal cautionary statements to avoid water contact with the resin and to avoid inhalation and skin contact apply, as with all the epoxides.

References

Mollenhauer, H.H. 1964. Plastic embedding mixtures for use in electron microscopy. *Stain Technol.* 39: 111.
Polysciences, Inc. data sheet 128.

London Resin Co. (LR) White Resin

1. Applications and Objectives

This resin is the resin of choice for the room-temperature preparation of samples for immunocytochemical procedures because it is an acrylic resin and thus is somewhat water-miscible.

It is easier to probe LR White-embedded tissues with immunolabels than those embedded in epoxide resins. Another advantage of LR White resin's tolerance for water is that, according to the manufacturers, samples in 70% alcohol can be passed directly into the resin. The suggestion is that the lower alcohol concentrations employed in this procedure will help prevent the antigenic site denaturation that is possible with higher alcohol concentrations.

This technique produces blocks containing samples that have not been osmicated or exposed to extensive dehydration in high concentrations of alcohols and acetone, which should leave antigenic sites less degraded than is characteristic with routine fixation, dehydration, and embedment in epoxide resins.

2. Materials Needed

LR White resin stock solution, which is marketed in 500-ml plastic squeeze bottles with a nozzle, is the working solution. This bottle is stored in the refrigerator. A catalyst is also available that can be mixed with the resin, but heat polymerization in a 55°C oven works well.

3. Procedure

1. Fix tissues in 4F:1G, or 2–4% formaldehyde prepared from paraformaldehyde, fixative for 1 hr at room temperature.
2. Rinse in 0.1 M Sorenson's sodium phosphate buffer, pH 7.2–7.4 for 5 min (three times).
3. Postfix in 1% osmium in 0.1 M Sorenson's phosphate buffer at pH 7.2–7.4 for 1 hr.
4. Rinse for 5 min (three times) in distilled water.
5. Dehydrate:
   - 50% ethanol for 15 min

- 75% ethanol for 15 min; *at this point, some workers go directly into LR White resin mixed 1:1 with 75% ethanol; if you choose to do this, make sure that the two mix well; if there is turbidity, infiltration will be compromised*
- 95% ethanol for 15 min (additional 100% ethanol rinses can be used but are not necessary) *Do not dehydrate with acetone*

6. Remove ethanol and add pure LR White resin. Leave overnight at room temperature. Change resin three times during the following day.
7. Remove tissue, put in gelatin capsules with labels, add resin to the capsules until full, cap them tightly, and then incubate them at 55°C overnight (check to see if they are completely polymerized).
8. Section as usual (they are more hydrophilic than Spurr or other epoxide resin blocks).
9. Poststain in aqueous uranyl acetate for 5 min and Reynolds' lead citrate for 8 min. Alcoholic stains may remove sections from the grids.

4. Results Expected

The omission of osmication produces samples from which almost all lipids have been extracted, leading to membranes often being indiscernible. It is always clear where all cellular compartments are and where the lipid *was* located. Low-magnification photographs look relatively normal (Fig. 74), but higher magnifications show significant membrane extraction in most cases (Fig. 75). However, immunocytochemical reactivity of sections embedded following this protocol is superior to that of conventionally fixed, osmicated, and epoxide resin-embedded samples.

5. Cautionary Statements

Acetone prevents proper polymerization of LR White resin and so must not be used in the dehydration series. *It is imperative that the tissue and resin be polymerized in tightly capped gelatin capsules*, since the resin will not polymerize properly in the presence of oxygen, and the resin may dissolve polypropylene capsules (BEEM™ capsules) during oven polymerization in some cases. The polymerized blocks may be brittle, but they still section quite well.

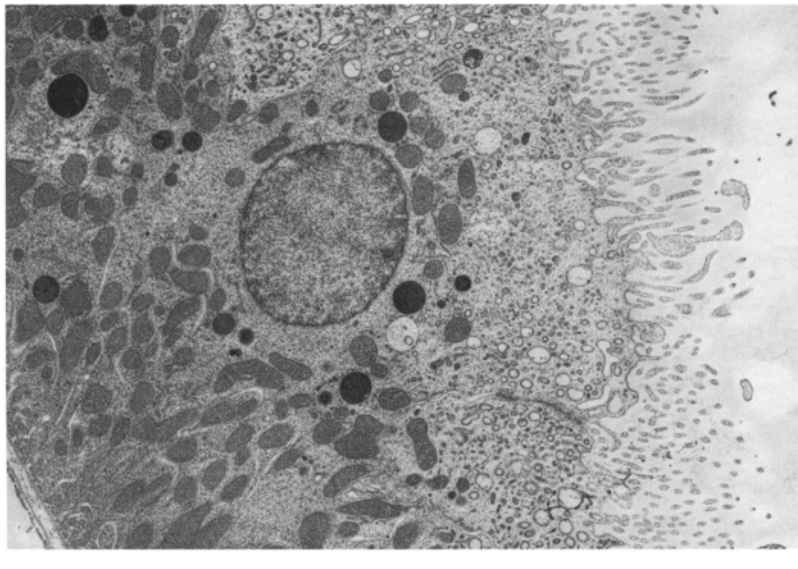

Figure 74. Rat kidney perfused with 4F:1G and embedded in LR White resin. No osmication. ×5,100.

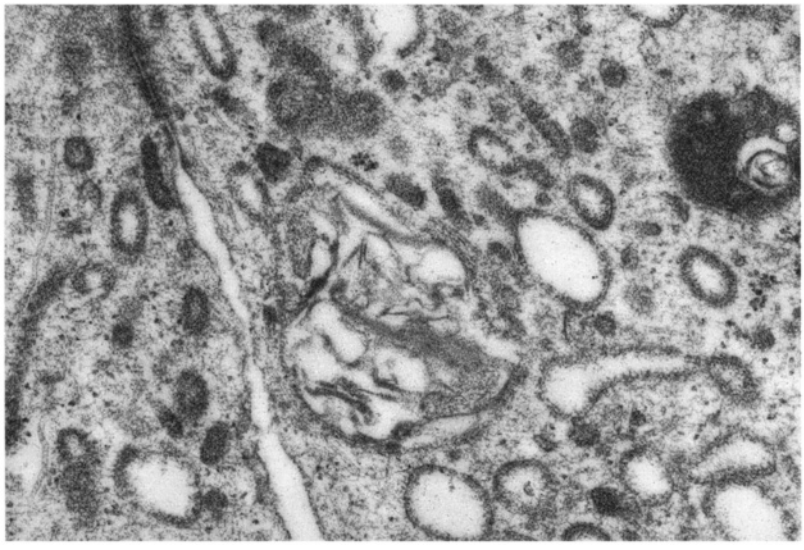

Figure 75. Rat kidney perfused with 4F:1G and embedded in LR White resin. No osmication. ×35,700.

The block faces are hydrophilic and will tend to pull water out of the knife boat unless the block is kept far away from the knife edge except just at the moment of cutting sections. At times, the block face will need to be blotted with filter paper or a Kimwipe™ before every section is cut.

The toxicity of this resin has not been thoroughly studied, so it should be treated as toxic. Resin wastes are collected in disposable beakers until full, at which time they are capped and polymerized in a 55°C oven. After polymerization, the resulting plastic block can be disposed of in normal laboratory trash bins.

Tissues can be osmicated if the resin is oven-cured at 55°C but should not be osmicated if the catalyst is used for cold curing. Samples should be immersed in a cold-water bath for catalyst curing to dissipate the heat produced by the exothermic process.

Reference

Polysciences, Inc. data sheets 305 and 305A.

Lowicryl and LR Gold Resins

1. Applications and Objectives

A number of low-temperature acrylic resins are available, some of which can be infiltrated into a specimen at temperatures as low as −80°C to reduce damage to antigenic sites. However, our laboratory does not use these resins because we find that ultrathin frozen sections can be produced more quickly and work at least as well for immunolabeling. For further information on these resins, their applications, and their formulation, consult the references listed.

References

Hayat, M.A. 2000. *Electron microscopy: Biological applications*, 4th edn. Cambridge University Press, New York.
Polysciences, Inc. Data sheets, 305 and 305A.

PEG Method for TEM Sections

1. Applications and Objectives

This method for embedding materials in polyethylene glycol (PEG) and subsequent sectioning, removal of PEG, and critical point drying (CPD) provides sections of cells and tissues without any surrounding resin materials. When viewed in the TEM without poststaining, these sections have sufficient contrast, since there is no surrounding resin embedding medium to reduce tissue contrast as with conventionally embedded materials. This helps visualization of fibrillar cytoplasmic proteins, among other cellular constituents.

2. Materials Needed

- Carbon- and Formvar-coated grids
- 5% ethanolic PEG 4000
- Pasteur pipet with heated and pulled tip (to reduce orifice diameter) to make small drops of PEG
- Container with 95% ethanol
- Containers for CPD preparation
- 0.1% poly-L-lysine solution and microscope slide
- Petri dish and filter paper
- Ceramic spot plate
- Gelatin capsules
- Liquid nitrogen

3. Procedure

PEG Embedment. Fix as usual for TEM and dehydrate to 100% ethanol, 15 min per step. Transfer to 50% PEG 4000 in 100% ethanol and leave overnight. Transfer to 70% PEG in 100% ethanol for several hours. Then put into 100% PEG at 68°C for several hours (several changes). Fill gelatin capsules with tissue and molten 100% PEG and then plunge into liquid nitrogen.

Preparation of Coated Grids

1. Take microscope slide and place one drop of 0.1% poly-L-lysine in the center.
2. Obtain previously Formvar – and carbon-coated grids. Dip each grid into poly-L-lysine solution.
3. Blot grid to dryness.
4. Repeat this three times for each grid. They are ready to use when dry.

Preparation of Block for Sectioning

1. Trim with a razor blade until a smooth surface is obtained.
2. Place block in the ultramicrotome and section at 6°C with a glass knife with no trough. Section at 0.25-μm increments.
3. Cut one section at a time. Use hair to remove and place in spot plate. Cut as many sections as needed to cover a grid. Exercise extreme caution handling sections because they easily blow away in a draft.
4. Carry spot plate carefully to dissecting microscope.
5. Focus on one spot. The sections should be obvious.
6. Use hair to pick up sections and place them onto a Formvar- and carbon-coated grid. Flatten sections.
7. Pipet a drop of 5% PEG solution onto grid.

8. Immediately blot with filter paper and put grid into CPD holder. Make sure grid is submerged in 95% ethanol, and do not let it dry out.
9. Run sections in CPD holders through two changes of 95% ethanol and two or three changes of 100% ethanol (1 min per change).
10. Critical point dry the grids.
11. Examine the grids with TEM.

4. Results Expected

The sections produced will have a good contrast when viewed with the TEM, without the need for any poststaining. The structural preservation will appear different from that found with standard plastic embedded materials poststained with uranyl acetate and lead citrate.

5. Cautionary Statements

All of the cautionary statements about fixatives and postfixatives apply to this procedure.

Reference

Wolosewick, J.J. 1980. The application of polyethylene glycol (PEG) to electron microscopy. *J. Cell Biol.* 86: 675.

JB-4™ (Glycol Methacrylate) Techniques for High-Resolution Light Microscopy

1. Applications and Objective

Cells and tissues embedded in glycol methacrylate after aldehyde fixation can be easily sectioned into 1- to 2-μm thick sections that provide excellent resolution and that, unlike epoxide-embedded samples, can be stained with the majority of standard histological techniques because of the hydrophilic nature of the resin. These materials are also appropriate for immunoprobing at the light microscopic level (Pedraza and Mason, 1984; Wordinger *et al.*, 1987).

2. Materials Needed

- JB-4™ glycol methacrylate embedding kit (Polysciences, Inc.)
- Embedding molds and chucks for JB-4 (Polysciences, Inc.)
- Rotary microtome, JB-4 microtome, or ultramicrotome
- Razor blades
- Rotary platform
- Transfer pipets for resin
- Applicator sticks for moving specimens
- Disposable beakers for mixing resin components
- Forceps
- Water bath
- Glass slides
- Coplin jars for staining solutions

- Richard–Allan Hematoxylin-1 (Richard–Allan Medical Industries, P.O. Box 351, Richland, MI 49083)
- Richard–Allan eosin-Y
- Richard–Allan bluing reagent
- Polymount™ (Polysciences, Inc.)

3. Procedure

1. Fix tissues with 4F:1G according to routine TEM procedures. Do not use osmium or Bouin's fixative because both will cause uneven or improper resin polymerization.
2. Dehydrate in ethanolic series to 100% ethanol as described for routine TEM preparation.
3. Infiltrate with JB-4™ resin:
   a. Mix the following, in the order listed to make the infiltration medium:
      - 100 ml of JB-4™ solution A
      - 0.90 g of dry catalyst C (mix until dissolved)

      The solution may be stored for several weeks at 4°C in the dark.
   b. Place the tissue (blocks no more than 2 mm^3 in size) into the infiltration medium for 5 hr at room temperature on a rotator. Change to new medium after 2–3 hr.
   c. Prepare the embedding medium by mixing the following components in the order listed:
      - 1 ml of JB-4™ solution B
      - 25 ml of freshly catalyzed solution A (see step a)

      Never use exhausted infiltration medium for embedding.
   d. Stir the mixture thoroughly and place it into an ice bath to prevent premature polymerization of the resin while arranging tissues in molds.
   e. Place tissues into the embedding molds, orient the tissues and fill the molds with embedding medium. The molds must be filled entirely with embedding medium, as air will prevent proper resin polymerization. Place tissues in molds in a desiccator overnight at room temperature.
   f. After polymerization, trim off excess plastic with a razor blade, but be sure to leave some excess around all the edges, otherwise they will curl slightly. The trimmed block face should be no more than 5 mm^2.
4. Break triangular glass knife, orient it at 6° and cut 2-μm-thick sections with a dry knife.
5. Pick up dry sections with forceps and release onto the surface of H_2O in staining dish (adding a drop of ammonium hydroxide may help the sections spread).
6. Pick up sections on glass microscope slides and heat them on a hot plate set at about 60°C for 15 min.
7. Stain the slides as described below.
   a. Hematoxylin staining: Place slide directly in Richard–Allen Hematoxylin for 15–20 min.
   b. Rinse in two changes of distilled H_2O (about 1 min each).
   c. Place slide into bluing solution for 30–60 s.
   d. Rinse in two changes of distilled H_2O (about 1 min each).
   e. Stain for 1 min in Richard–Allen Eosin.
   f. Destain in 70% ethanol (two changes) for about 1 min each.
   g. Rinse once in distilled H_2O.
   h. Dry on hotplate and add 1–2 drops of Polymount™. Place a #1.5 coverslip over the sections and examine them with a light microscope.

4. Results Expected

The sections will provide excellent resolution because they are so thin but will not be stained as darkly as paraffin-embeded sections (6–10-μm-thick sections).

5. Cautionary Statements

As mentioned above, osmium and the picric acid in Bouin's fixative should be avoided to ensure good resin polymerization. In addition, air will prevent polymerization. If using embedding molds other than those designed for JB-4™ resin, it is necessary to cover them in such a way as to exclude oxygen (BEEM™ capsules or gelatin capsules work well if filled completely and then closed). If the polymerized blocks seem slightly rubbery, refrigerating them at 4°C for 1–2 hr will make the blocks harder.

Some workers have become sensitized to JB-4™ resin, but only because customary laboratory precautions to prevent skin and respiratory exposure were neglected.

References

Pedraza, M.A. and Mason, D. 1984. Immunoperoxidase methods with plastic embedded materials. *Lab. Med.* 15: 113.

Wordinger, R., Miller, G., and Nicodemus, D. 1987. *Manual of immunoperoxidase techniques*, 6th edn. (pp. 34–35, 61–62).

Agar Embedment of Cell Suspensions or Subcellular Particulates for TEM

1. Applications and Objectives

This technique may be applied to nonadherent mammalian cell cultures and cell suspensions of various types, such as free-living protozoans, bacteria, and disaggregated tissues. In addition, the technique is useful for subcellular fractions or organelles large enough to be pelleted by clinical centrifuges or microfuges. This procedure provides a surrounding matrix to suspended cells or subcellular materials so that they can be handled similarly to tissue pieces during subsequent processing steps.

2. Materials Needed

- Specimens in primary aldehyde fixative solution
- 3–4% water agar
- Pasteur pipets
- Centrifuge tubes (preferably polypropylene microfuge tubes)
- Single-edge razor blades
- Applicator sticks

3. Procedure

1. Add 0.3–0.4 g agar to 10 ml of distilled water in a 15- to 20-ml shell vial and heat on a hot plate in a 50-ml beaker containing distilled water until the agar dissolves.
2. After the cells or particulates have been in the primary fixative for at least 1 hr at room temperature, pellet the sample with a centrifuge adjusted for an appropriate relative centrifugal force (rcf) selected from Table 10.
3. Carefully remove the fixative from the pelleted sample with a Pasteur pipet, taking care not to disturb the pellet. Replace with approximately 1 ml of an appropriate buffer. Resuspend the pellet by vortexing to avoid the potential shearing action of vigorous pipetting of particulates with Pasteur

Table 10. Sample Centrifugation

Cell Type	Fixed	Unfixed	Recommended rcf
Protozoans (4–50 μm)		X	250–300
Protozoans	X		300–2,000
Mammalian cells (10–20 μm)		X	250–300
Mammalian cells	X		2,000–2,500
Bacteria (0.5–2 μm)		X	6,000–8,000
Bacteria	X		9,000–9,500
Mitochondria, chloroplasts	X	X	6,000–9,000

pipets. Transfer the resuspended sample to a 1.5-ml microfuge tube, taking care to pipet gently. After 15 min, pellet the sample and resuspend it in fresh buffer. Incubate for an additional 15 min.

4. Pellet the sample and remove the buffer. Heat a clean Pasteur pipet by drawing up heated water several times from the beaker containing the vial of molten water agar. Then, remove approximately 1 ml of molten agar from the vial of agar with the pipet, place the pipet tip at the bottom of the pelleted sample in the microfuge tube, and expel the agar. Next, quickly place the microfuge tube into a microfuge already containing a balance tube with 1 ml of water and pellet the suspension at an appropriate rcf for 30 s.
5. Remove the microfuge tube containing the agarized sample and wait until the agar has solidified and become translucent. To speed up this step, the sample can be placed at 4°C.
6. With a single-edge razor blade, carefully slice the end off the microfuge tube just above the agarized pellet. Cut the pellet into 1-mm-thick slices. Use an applicator stick to transfer the agarized sample slices to a vial containing osmium and buffer.
7. Further processing steps can be carried out by gently pipetting fluids in and out of the processing vial as would be appropriate with slices of tissue.

4. Results Expected

This method provides slices containing agar-embedded particulates that can be subsequently handled like slices of tissues, thus avoiding centrifugation throughout the entire processing schedule.

5. Cautionary Statements

If a microfuge is not available, this technique can be performed in larger centrifuge tubes utilizing a clinical centrifuge, and the agarized pellet can be removed by using an applicator stick to remove the whole volume of agar from which the tip containing the sample can then be cut.

A sample that must be spun down with an ultracentrifuge cannot be handled in this fashion, since the molten agar would solidify long before sufficient speed was obtained. In that case, gently remove the buffer from the ultracentrifuged sample and add droplets of molten agar (two to three times the sample volume) to the sample and quickly stir with a pipet tip or applicator stick to suspend the sample in a minimum volume of the agar before it solidifies. After it has cooled, remove the droplet of agarized sample and slice it into 1-mm-thick pieces for subsequent processing. The sample will not be as concentrated as those prepared with the microfuge, but typically will be usable.

When pipetting samples (which should be done as little as possible, particularly with larger cells), remember that cells can suffer shearing artifacts if pipetting is too vigorous. In addition, cells postfixed with osmium are much more prone to damage, since they are more brittle than aldehyde-fixed cells.

It is necessary to pellet the samples in molten agar within 30–60 s to prevent shearing artifacts caused by the agar solidifying during the centrifuge run.

Preparing Adherent Tissue Culture Monolayers *in Situ* for TEM

1. Applications and Objectives

This method can be used to prepare cells grown in a variety of typical polystyrene culture vessels, such as disposable Petri dishes, T-25, and T-75 culture flasks, that are solubilized by acetone. After agar embedment, the cells are removed from the culture vessel and flat-embedded for ultramicrotomy. With this technique, cell–cell interactions and *in vitro* morphology will be accurately preserved.

2. Materials Needed

- 3–4% molten water agar
- Normal fixation and dehydration agents

3. Procedure

1. Fix in 4F:1G as described for routine TEM processing.
2. Rinse two times (10 min each) in 0.1 M Sorenson's phosphate buffer, pH 7.2–7.4.
3. Cover with 1% osmium in the same buffer for 1 hr.
4. Rinse in distilled water three times (2 min each). Drain the culture vessel and then cover monolayer with a thin layer (1–2 mm) of 4% water agar that is hot to the touch. Let the agar cool until it is hard.
5. Dehydrate the agarized monolayer within the culture vessel:
   - 50% ethanol for 15 min
   - 75% ethanol for 15 min
   - 95% ethanol for 15 min (two times)
   - 100% ethanol for 30 min (two times)
   - 100% acetone: Pour the acetone onto the surface of the agarized monolayer and watch for the polystyrene vessel to begin softening. This should start happening within 2–3 min. As it does, tease the edge of the agar from the vessel surface with a scalpel or needle until the agar layer can be completely removed from the vessel, carrying the monolayer with it. Transfer to new 100% acetone in glass vials after slicing the agarized monolayer into appropriately sized strips and let sit for 10 min.
6. Infiltrate with Spurr resin (6.3 recipe):
   - 1:1 resin and acetone mixture for 30 min
   - 100% resin for 1 hr
   - 100% resin for 1 hr
   - Put in flat molds in new 100% resin
   - Polymerize for 8 hr to 3 days at 70°C

4. Results Expected

If random sections of the monolayer are desired, the polymerized blocks can be trimmed down to the monolayer and sectioned. Alternatively, since the polymerized blocks are clear enough to be examined easily with a light microscope, areas of interest can be selected, cut out of the block, and remounted on previously prepared blank epoxide blocks with one of the 5-min epoxy cements. After the cement has polymerized at 70°C for 15 min, the selected cells can be sectioned.

5. Cautionary Statements

When the agar is poured onto the cells prior to osmium postfixation, the agar sometimes will darken. If the agarized cell layer begins lifting off of the culture vessel surface in the 100% ethanol dehydration step,

cut up the peeled agar and finish dehydration and embedment in glass vials. If peeling the agar from the culture vessel leaves most of the cells on the vessel surface, quickly drain off any residual acetone and replace with 100% ethanol, wait 10 min, and then replace with Spurr resin mixed 1:1 with 100% ethanol. Finish the infiltration procedure as above. When adding the final resin for polymerization, add enough to fill the culture vessel to a depth of 1–2 mm. Place the entire culture vessel in the polymerization oven. After polymerization, the polystyrene vessel will have a fairly opaque, milky surface beneath the cells, making it fairly difficult to see through the dish using a light microscope. Nonetheless, areas covered with cells can be removed from the culture vessel with a jeweler's saw and glued on an end to blank epoxide blocks (Figs. 76 and 77) with 5-min epoxy cement as described above. Unfortunately, when the blocks are sectioned, the Spurr resin and

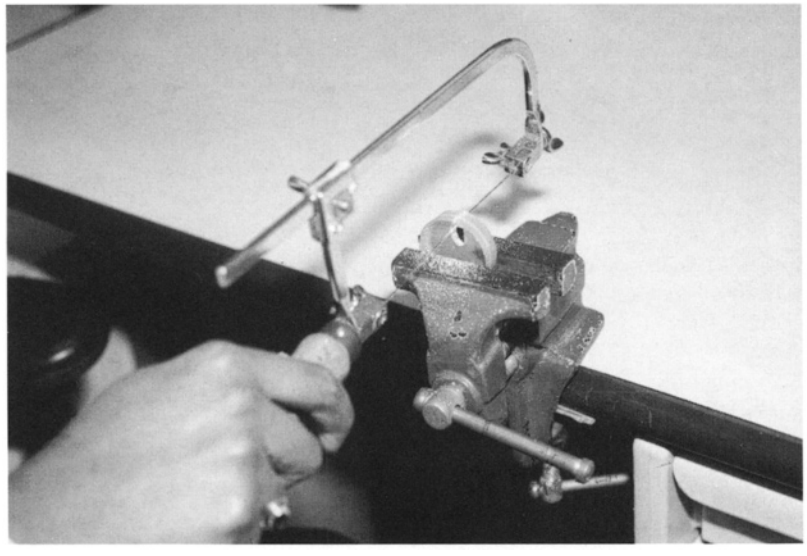

Figure 76. Plastic dish with embedded cells being cut with jeweler's saw.

Figure 77. Embedded monolayer mounted on blank epoxy block with 5-min epoxy cement.

polystyrene plastic compress and expand differently, so the sections cut should probably be placed onto Formvar-coated grids to lessen movement under the electron beam.

Flat Embedding of Cell Cultures Grown on Permanox® Tissue Culture Dishes for TEM

1. Applications and Objectives

This is an ideal technique for embedding monolayers of cells, particularly if only a small proportion of the monolayer will have a feature of interest, requiring careful selection of areas to be examined with the electron microscope (e.g., cells in anaphase of mitosis are of interest, but only represent 5% of the total cell population).

These dishes were designed for cell culture leading to physiological studies because most plastic dishes are porous to incubation chamber gases and also retain these gases within their structure. The Permanox® plastic (polymethylpentene) is porous to gases, but does not retain them.

For our purposes in electron microscopy, these dishes are particularly useful because they do not interact with ethanol, acetone, xylene, or epoxide resins (including Spurr resin).

This technique provides flat-embedded tissue culture monolayers that have not had their morphology or relationship to adjacent cells perturbed by removal from the substrate prior to fixation and embedding.

2. Materials Needed

LUX 60 × 15 mm sterile Permanox® Tissue culture dishes. These dishes are available from EMS, Thomas Scientific, PGC Scientific, and other supply houses. They are manufactured by NUNC, Inc., Naperville, IL 60566. In 2002, the cost was about $460.00 per case, or $48.00 for 40 dishes in the 60-mm-diameter size (Electron Microscopy Sciences, Ft. Washington, PA).

3. Procedure

Cells can be grown on the plates, the medium decanted, the plates rinsed briefly with buffer, and then flooded with fixative. The monolayer can then be postfixed, dehydrated, and embedded in the epoxide of choice, and finally polymerized *in situ*. After polymerization, the plate is brought to room temperature, and by gently flexing the plate, the embedding resin is popped free, taking the cells with it. These plates can also be used to flat-embed a variety of other specimens.

4. Results Expected

The polymerized resin removed from the culture dish is optically excellent and may be examined by light microscopy to select areas of interest, which are then removed with a jeweler's saw and remounted on blank epoxy blocks with 5-min epoxy cement for subsequent sectioning.

Preparation of Buffy Coats for TEM

1. Applications and Objectives

Analysis of blood samples for various types of pathology including the presence of organisms such as malarial parasites often are aided by segregating the different types of blood cells. If a subset of blood

cells, such as leukocytes, is of interest, this technique concentrates each of the three major subsets of blood cells into separate bands. Thus, analysis of these populations is quicker than if all types were mixed together at random, as occurs if whole blood is fixed without prior centrifugation.

The technique produces a pellet of cells with platelets, nucleated white blood cells, and red blood cells segregated into separate bands (Fig. 78).

2. Materials Needed

- ethylenediaminetetraacetate (EDTA) blood collection tubes
- Wintrobe tubes
- 4F:1G fixative
- Molten 3–4% water agar
- Glass microscope slide
- Glass TEM sample vial
- 2- to 3-ml plastic syringe

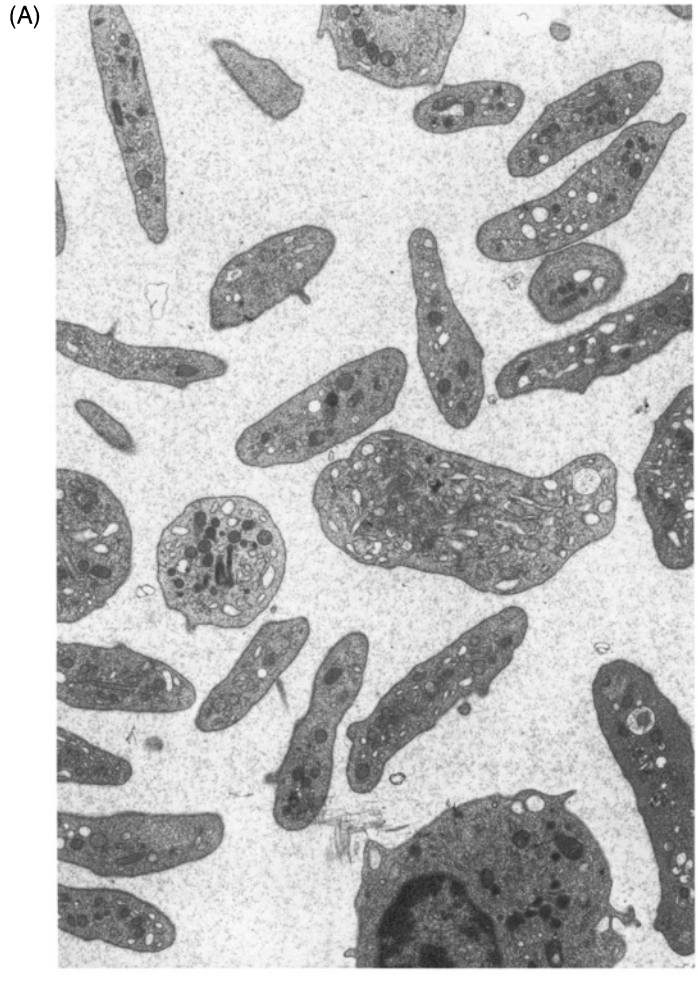

Figure 78. (A) TEM view of buffy coat preparation showing different cell populations segregated into layers. Platelets and one lymphocyte. 7,385×.

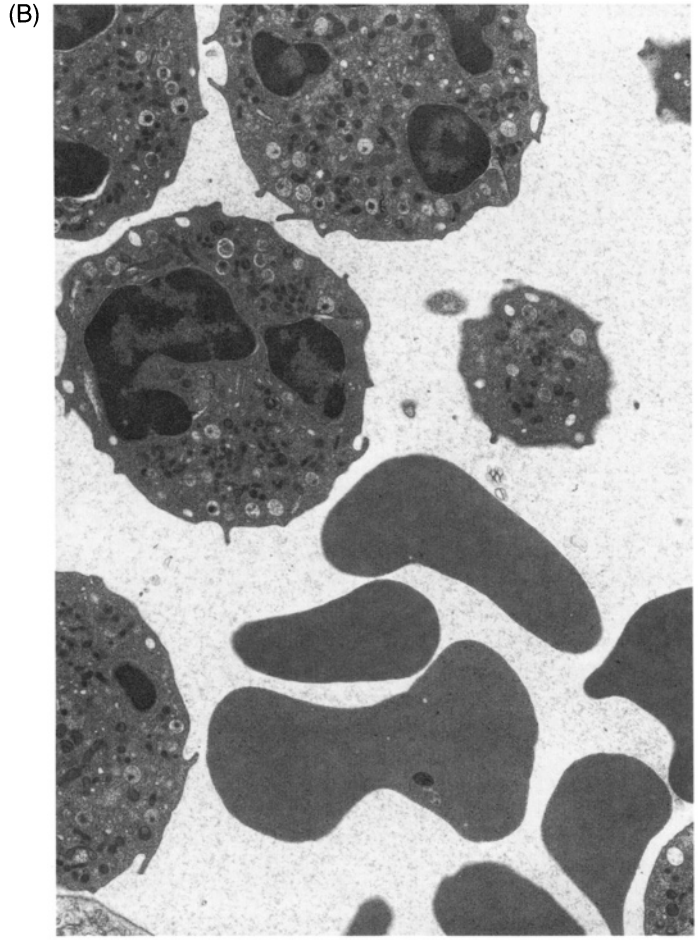

Figure 78. (B) TEM view of buffy coat preparation showing cell layer beneath (A) in the Wintrobe tube. Note polymorphonuclear neutrophils subtended by erythrocytes. 7,385×.

- Triangular file or diamond scriber
- Applicator stick
- Single-edge razor blade

3. Procedure

1. Draw 2 ml of freshly collected whole blood into a plastic syringe.
2. Immediately inject the blood into a standard EDTA blood-collection (lavender-top) tube to prevent coagulation. Invert the tube and transport to the electron microscopy laboratory.
3. Fill a Wintrobe tube with blood from EDTA tube. Centrifuge at low speed (250 rcf) for 5–10 min.
4. Gently remove plasma (transparent fluid) with a Pasteur pipet and discard.
5. Gently pipet 4F:1G fixative on top of cells in Wintrobe tube. Fill the tube to the top and refrigerate overnight (*do not stir*).
6. Remove the fixative with a Pasteur pipet, score the tube below the buffy coat (pale band at the top of the pelleted cells) with a triangular file or diamond scriber. Wash the outer surface of the

Wintrobe tube to remove glass dust, break tube, and push the buffy coat out of the tube with an applicator stick.

7. Place the buffy coat pellet onto a glass microscope slide and carefully cut the buffy coat plug lengthwise with a single-edge razor blade. Put a small pool of molten 3–4% water agar onto the glass slide and immediately add the longitudinally bisected buffy coat to the agar. Cover the buffy coat with more molten agar.
8. After the agar has solidified, trim around the buffy coat, transfer the agar-encased buffy coat plug to a sample vial containing buffer, and process as usual for any other tissue sample.
9. Flat-embed the sample so that a subsequent semithin section of the block face will contain a longitudinal section of the buffy coat from which the cell population of interest can be identified prior to block trimming for ultrathin sectioning.

4. Results Expected

Sectioning the buffy coat will reveal platelets at one end, nucleated leukocytes in the middle, and red blood cells at the other end.

5. Cautionary Statements

Be sure to collect the blood sample in an EDTA tube. If the cells coagulate, the layering of the cell populations by centrifugation will not occur. Be careful not to agitate the centrifuged blood sample during plasma removal and fixative addition to the Wintrobe tube. If agitation occurs, the layers of cells will become intermixed.

Sperm Fixation

1. Applications and Objectives

Sperm is notorious for showing fixation artifacts, primarily separation of the plasma membrane from the acrosomal region. A number of fixation techniques have been employed by different laboratories with variable results (see supplementary references below for several examples). If the procedure is successful, it will produce images of sperm with intact plasma membranes closely adherent to the acrosomal region.

2. Materials Needed

- 8% glutaraldehyde
- 4% formaldehyde
- 0.2 M cacodylate buffer, pH 7.0–7.2
- 0.1 M cacodylate buffer, pH 7.0–7.2
- Picric acid
- $CaCl_2$
- Sucrose

3. Procedure

Fixative Preparation. To prepare a final fixative containing 2% glutaraldehyde, 1% formaldehyde, 1.5 mM $CaCl_2$, 0.2 M sucrose, and 0.1% picric acid in 0.1 M cacodylate buffer at pH 7.0–7.2:

1. Add 25 ml of 8% aqueous glutaraldehyde to 25 ml of aqueous 4% formaldehyde (yields an aqueous mixture of 4% glutaraldehyde and 2% formaldehyde).

2. To 50 ml of 0.2 M cacodylate buffer, pH 7.0–7.2, add:
   - 6.84 g of sucrose
   - 0.0327 g of $CaCl_2$
   - 0.1 g of picric acid
   - Mix thoroughly
3. Mix 50 ml of the aldehyde mixture, step 1, with 50 ml of the buffer mixture, step 2.

Sample Preparation

1. Collect fresh ejaculate and add to fixative solution.
2. Leave for 1 hr to several days at 4°C.
3. Remove clumped semen from fixative solution with forceps. Centrifuge remaining fluid at 500–700 rcf for 10 min.
4. Remove fixative with a Pasteur pipet and resuspend pelleted cells in 0.1 M cacodylate buffer. After 10 min, centrifuge sample, remove buffer, and resuspend pellet in new buffer.
5. Repeat centrifugation and buffer rinse until most of the yellow color is gone and embed in 3–4% molten water agar, as previously described for handling cell suspensions.
6. Osmicate, dehydrate, and embed as described for routine processing.

4. Results Expected

Sections of this material will contain sperm with good ultrastructural preservation, with the plasma membrane closely adherent to the acrosomal region.

5. Cautionary Statements

Before working with picric acid solutions, read the Material Safety Data Sheets (MSDS) sheets describing handling of picric acid and proper disposal practices.

While this technique yields good results, it is often sufficient to fix sperm samples by the routine TEM processing technique described previously, which involves less difficult procedures.

Reference

Cran, D.G., Dott, H.M., and Wilmington, J.W. 1982. The structure and formation of rolled and crested bull spermatozoa. *Gamete Res.* 5: 263–269.

Supplementary References

Dadoune, J.P. and Alfonsi, M.F. 1986. Ultrastructural and cytochemical changes in the head components of human spermatids and spermatozoa. *Gamete Res.* 14: 33–46.

Plummer, J.M., Watson, P.F., and Allen, W.E. 1987. A spermatozoal midpiece abnormality associated with infertility in a Llasa Apso dog. *J. Small Anim. Pract.* 28: 743–751.

Vogl, A.W., Soucy, L.J., and Foo, V. 1985. Ultrastructure of sertoli cell penetrating processes found in germ cells of the golden-mantled ground squirrel. *Am. J. Anat.* 172: 75–86.

Central Nervous System Fixation (Brain, Spinal Cord)

1. Applications and Objectives

This technique, modified from Langford and Coggeshall (1980), is designed to provide good fixation of myelinated neural tissues from the central nervous system.

2. Materials Needed

- 4F:1G fixative
- 2% aqueous osmium
- 0.2 M Sorenson's sodium phosphate buffer, pH 7.2–7.4
- Potassium ferricyanide

3. Procedure

Fixative Preparation. To prepare 1% osmium and 0.5% potassium ferricyanide in 0.1 M sodium phosphate buffer:

1. Add 1 part 2% aqueous osmium to 1 part 0.2 M sodium phosphate buffer (add 1 ml of each to make 2 ml of solution).
2. Add 0.03 g of potassium ferricyanide to the solution in step 1 just before postfixing the tissue.

Sample Preparation

1. Perfuse the animal with 4F:1G fixative.
2. Remove the neural tissue and slice into 1-mm-thick slices. Put in fresh 4F:1G for 2 hr to overnight at 4°C.
3. Rinse the tissue two times (15 min each) in 0.1 M phosphate buffer.
4. Put the tissue into 1% osmium in 0.1 M phosphate buffer containing 0.5% potassium ferricyanide.
5. After 2 hr at room temperature, rinse the tissue in distilled water, dehydrate, and embed as described for routine tissue processing for TEM.

4. Results Expected

After the neural tissue is perfused with the primary fixative, it should be firm enough to slice easily into 1-mm-thick pieces for further processing. The final image should show circular profiles of myelinated neurons, with a minimal number of angular images.

5. Cautionary Statements

If the perfused neural tissue is still soft, rather than somewhat rubbery in texture, the perfusion was not totally successful. If the sample cannot be easily reproduced, cut up the tissue into 1 mm^3 pieces as best you can, put the tissue into fresh primary fixative, and continue the processing procedure outlined above.

Reference

Langford, L.A. and Coggeshall, R.E. 1980. The use of potassium ferricyanide in neural fixation. *Anat. Rec.* 197: 297–303.

Using Vacuum to Help Wet Fungal, Plant, or Insect Samples during Primary Fixation

1. Applications and Objectives

This technique is used for samples that are typically difficult to wet because of air trapped between insect hairs, plant trichomes, or filamentous structures such as fungal sporangiophores. If the specimen surfaces are not wetted, fixation will not be optimal.

2. Materials Needed

- 4F:1G fixative
- A source of vacuum (5–10 lbs/in^2, 34–69 kPa)
- A piece of Tygon™ tubing attached to a glass tube passing through a rubber stopper attached to a trapped vacuum line

3. Procedure

1. Add the specimen to 1 ml of 4F:1G contained in a 4 dram sample vial.
2. Apply a slight vacuum (5–10 lbs/in^2, 34–69 kPa) to the vial by the vacuum line attached to a glass tube passing through a hole in a rubber stopper large enough to cover the mouth of the sample vial (Fig. 79).
3. As a vacuum is applied, the fixative will become slightly turbid as minute bubbles of air are drawn from the fluid. After about 1–2 min, tap the vial firmly against the counter top several times to dislodge any of the larger air bubbles. The specimen should sink to the bottom of the vial.
4. If the specimen is still floating, the rubber stopper attached to the vacuum line can be lifted slightly from the surface of the sample vial, which will cause a large amount of turbulence right at the surface of the fixative and usually will help sink the specimen. Be careful not to suck the fixative or specimen up the vacuum line.
5. Once the specimen sinks in the sample vial, proceed with the routine fixation protocols.

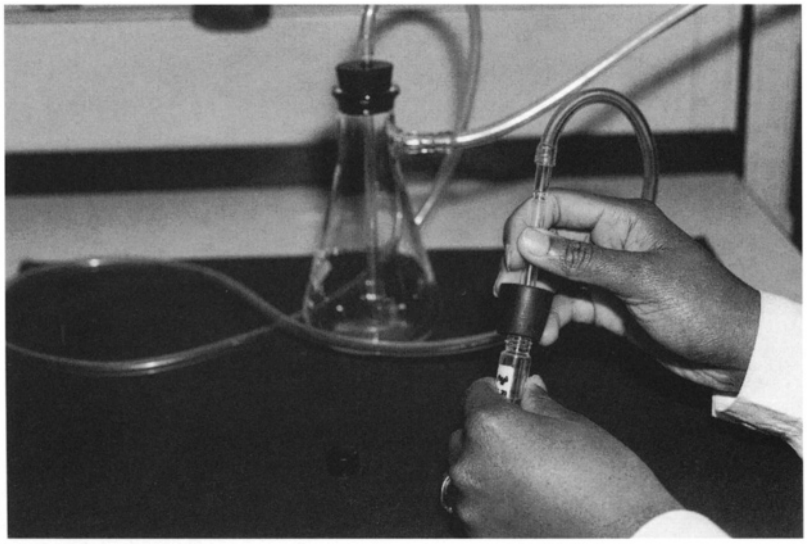

Figure 79. Rubber stopper pierced by glass tube being used to apply a vacuum to a sample vial. Note the side-arm Erlenmeyer flask used to trap the vacuum line.

4. Results Expected

The tissue will sink to the bottom of the fixative solution as the air bubbles trapped on the sample surface, which are responsible for providing specimen flotation, are removed.

5. Cautionary Statements

As mentioned above, while the stopper attached to the vacuum line is partially removed from the mouth of the sample vial, it is possible to aspirate both the fixative and sample. In particular, if the sample vial is over half full, loss of the fixative fluid or samples is very likely with this procedure. As a precaution to prevent aspirating fluids and samples into the vacuum system, it is necessary to provide a trap (Fig. 79) on the vacuum line.

Simultaneous Glutaraldehyde/Osmium Fixation for Protozoan Samples or Samples with a Large Amount of Lipid

1. Applications and Objectives

Lipids are not stabilized by aldehyde fixatives and thus may move or change configuration during primary fixation. If there is any evidence of membrane or lipid body alteration following primary aldehyde fixation, this technique may be applied to help stabilize lipids from the beginning of the fixation process. Also, some protozoans seem to exhibit a better ultrastructural preservation when fixed with this technique (Dykstra, 1976; Dykstra and Porter, 1984).

2. Materials Needed

- 4% osmium
- 8% glutaraldehyde
- 0.2 M phosphate or cacodylate buffer, pH 7.2–7.4

3. Procedure

The final solution will consist of 1% osmium and 2% glutaraldehyde in a 0.1 M buffer solution:

1. Right before adding the sample to the fixation vial, mix 1 part of the osmium stock with 1 part of the glutaraldehyde stock and 2 parts of the buffer.
2. Immerse the sample in the fixative solution, cap the vial, and place in the refrigerator for 1 hr.
3. Remove the fixative solution, which will have turned black, and rinse the sample with distilled water two to three times over 10 min, or until the wash fluid is no longer colored.
4. Dehydrate and embed the sample as described for routine processing.

4. Results Expected

The sample and fixation fluid should turn black during the 1-hr fixation in the refrigerator. The following processing steps are routine. The sample should have a superior lipid retention, compared with samples fixed by sequential aldehyde/osmium fixation.

5. Cautionary Statements

As usual, all the osmium-containing waste should be collected for proper disposal. As noted, the fixative will typically turn quite black during the 1-hr fixation process as the aldehyde reduces the osmium in the solution. Since there is an excess of fixative components when the fixative has a volume of five to 10 times that of the sample, as is customary, the chemical interaction of aldehyde and osmium with subsequent removal of both components from the fixation solution is unimportant.

This technique is not suitable for blocks of tissue of the normal 1-mm thickness. It appears that the rapid and thorough fixation of the surface layers of a tissue block impedes the further diffusion of fixative components to the center of tissues because only the outermost layers of such a specimen will be well fixed (Fig. 21).

References

Dykstra, M.J. 1976. Wall and membrane biogenesis in the unusual labyrinthulid-like organism *Sorodiplophrys stercorea. Protoplasma* 87: 329–346.

Dykstra, M.J. and Porter, D. 1984. *Diplophrys marina*, a new scale-forming marine protist with labyrinthulid affinities. *Mycologia* 76: 626–632.

Killing Cells Prior to Chemical Fixation

1. Applications and Objectives

If cell-to-cell contacts are of interest, it may be necessary to kill cells prior to immersing them in fixative solutions. In previous studies in our laboratory with amoebae of slime molds growing on an agar surface (Dykstra and Aldrich, 1978), it was noted that the cells rounded up and changed their spatial relationship with each other if fixative solutions were poured onto the culture dish surface. By exposing them to osmium vapor prior to flooding the dish with fixative, this change was prevented.

2. Materials Needed

- 2% aqueous osmium
- 4F:1G (or other suitable aldehyde) fixative

3. Procedure

1. Invert the culture dish over several drops of 2% osmium contained in a smaller dish (Fig. 80). If the cells have been grown in liquid media, decant as much fluid as possible prior to inverting the dish.
2. After 3–5 min, flood the culture dish with 4F:1G fixative.
3. Follow all the subsequent steps previously described for routine processing. The cells may be encased in agar or processed entirely and embedded *in situ* without agarizing (see the procedure using Permanox™ plates).

4. Results Expected

The cells will be fixed without having changed spatial relationships.

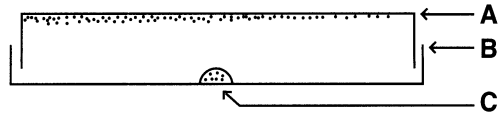

Figure 80. Monolayer of cells (A) attached to a Petri dish surface inverted over a droplet of 2% aqueous osmium (C) on the lid of the Petri dish (B).

5. Cautionary Statements

Perform this procedure under a fume hood to contain the osmium fumes.

Reference

Dykstra, M.J., and Aldrich, H.C. 1978. Successful demonstration of an elusive cell coat in amebae. *J. Protozool.* 25: 38–41.

Flat Embedding on Microscope Slides[2]

1. Applications and Objectives

Whole specimens can be embedded conveniently if they are small or flat (Reymond and Pickett-Heaps, 1983). Flat embedding can also be used to embed specimens grown on dialysis tubing (see Mims *et al.*, 1988).[3]

After processing, these specimens can be viewed easily with a light microscope, allowing areas to be selected, cut out, and reembedded.

2. Materials Needed

- Clean glass coverslips and microscope slides
- Single edge razor blades
- Cyanoacrylate glue (Crazy® glue)
- Fluoroglide® (Norton Plastics, available from EMS)[4]
- Fixed specimens in unpolymerized 100% Spurr resin
- Kimwipes™
- Spurr resin

[2] Special thanks are due to Dr. Karen Snetselaar, Department of Biology, St. Joseph's University, Philadelphia, PA, for introducing us to this technique.

[3] Dialysis tubing: Specimens can be prepared on small pieces of dialysis membrane (Mims *et al.*, 1988). This technique is especially good for subsequent plunge-freezing. Prepare the dialysis tubing by boiling it for at least 10 min in 1% sodium bicarbonate/0.1% EDTA, followed by boiling in several changes of distilled water. The membrane then can be sterilized by autoclaving prior to use. To use the membrane, touch it to a cell suspension, let it dry briefly and then plunge-freeze it. After cryosubstitution, it can be embedded with the technique above.

[4] Electron Microscopy Sciences (Ft. Washington, PA) also sells a water-soluble release agent (Liquid Release Agent) that comes as a liquid into which the slides and coverslips could be dipped instead of using the spray Fluoroglide® product.

3. Procedure

1. Glass slides and coverslips are sprayed with the Fluoroglide® and wiped well with a Kimwipe™. Repeat two times.
2. Place several specimens on the coated slide. Put a couple of *small* drops of Spurr resin on the slide. Use tape or broken bits of coverslips as spacers at the ends of the coverslip to prevent the resin from going all the way to the ends of the coverslip, otherwise the coverslip will be difficult to remove from the slide.
3. Place slides in a 60–70°C oven for resin polymerization, and make sure that they are level.
4. After the resin has polymerized (8 hr to 3 days), remove the coverslip from the polymerized resin by working a new single-edge razor blade under the edge of the coverslip. *Safety glasses are recommended, since the coverslip may shatter.*
5. Examine the plastic-embedded material remaining on the slide with the light microscope, and mark areas of interest with a diamond scribe, magic marker, or scalpel.
6. Cut out the marked area with a scalpel or razor blade and glue to the top of a blank block of polymerized resin previously cast in a BEEM™ capsule with cyanoacrylate glue or 5-min epoxide glue. When the glue is polymerized, trim block and section as usual. If possible, glue the specimen into a slot previously in the blank block (Fig. 81).

4. Results Expected

This method produces a thin wafer of polymerized resin containing the specimen, which then can be examined easily with a light microscope for selection of areas of interest to be mounted on blank blocks and sectioned.

5. Cautionary Statements

When spraying the Fluoroglide®, as with any aerosol product, work under a hood to prevent exposure to the chemical product. The coverslip should also be detached with care, utilizing safety glasses to avoid eye injury.

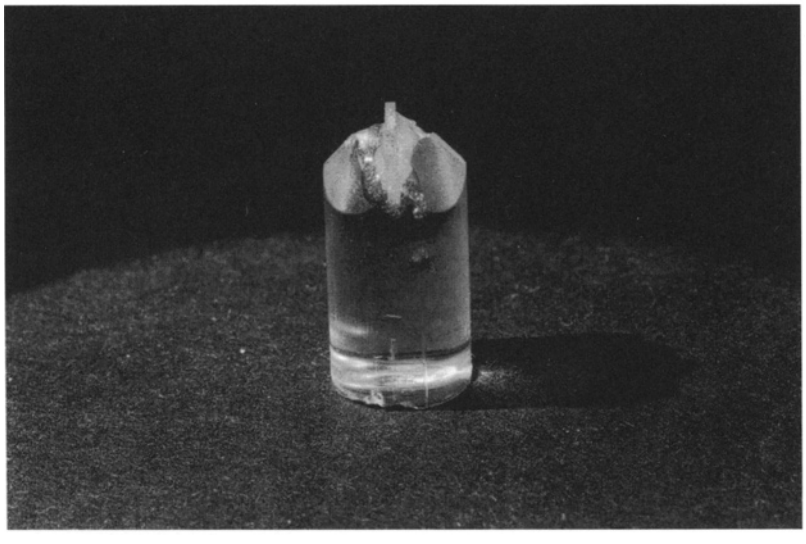

Figure 81. Slotted blank block with a flat-embedded specimen glued in place.

References

Mims, C.W., Richardson, E.A., and Taylor, J. 1988. Specimen orientation for transmission electron microscopic studies of fungal germ tubes an appressoria on artificial membranes and leaf surfaces. *Mycologia* 80: 586–590.

Reymond, O.L., and Pickett-Heaps, J.D. 1983. A routine flat embedding method for electron microscopy of microorganisms allowing selection and precisely oriented sectioning of single cells by light microscopy. *J. Microsc. (Paris)* 130: 79–84.

Procedure for Deparaffining Samples

1. Applications and Objectives

On some occasions, it is necessary to retrieve information from samples previously fixed and embedded for standard histological examination. This situation is not uncommon in a clinical setting where bioptic samples are collected, such as tumors, and all the tissue is embedded in paraffin. After light microscopic examination, the clinical staff determines that ultrastructural examination is necessary for absolute identification of the pathology present. The electron microscopy laboratory staff is then asked to supply information from a sample that may have been suboptimally aldehyde-fixed (4% formaldehyde), dehydrated, and then heated for a prolonged period during paraffin infiltration. The technique described below is modified from Weidmann *et al.* (1987).

2. Materials Needed

- Xylene
- Ethanol dehydration series
- 2% osmium
- 0.2 M Sorenson's sodium phosphate buffer, pH 7.2–7.4
- Spurr resin (6.3 recipe as described in the resin section)

3. Procedure

1. Cut a piece of tissue out of the paraffin block, removing as much excess paraffin as possible.
2. Place in 100% xylene for 1–2 hr, changing xylene several times until no evidence of paraffin remains.
3. Rehydrate tissue:
   - 100% ethanol: two changes over 60 min
   - 95% ethanol: two changes over 30 min
   - 75% ethanol for 15 min (or overnight at 4°C)
   - 50% ethanol for 15 min
   - Distilled water: two changes over 10 min
4. 1% osmium in 0.1 M phosphate buffer for 1 hr
5. Rinse in distilled water two times (5 min each). Dehydrate and embed in Spurr resin as described for routine TEM sample preparation.

4. Results Expected

Such material, usually being suboptimally fixed in 4% formalin and then washed for extended periods of time before being embedded in paraffin, will usually not look very good. Much of the cytoplasmic detail will have been leached out, and membranes will often be severely disrupted. The heating steps involved

in paraffin embedding will also have coagulated much of the cytoplasm. This procedure is a viable option if no more tissue can be obtained from important cases, because proteinaceous components such as cytoskeletal filaments, specific cellular granules, viral particles, and junctional complexes between cells can still be identified in most cases. This type of sample will not often yield publishable results, but can still provide usable diagnostic information.

5. Cautionary Statements

Handle and dispose of xylene according to MSDS information. Xylene is a toxic and potentially carcinogenic material and must be handled appropriately. Other cautions concerning routine TEM processing apply.

Reference

Weidmann, J., Freund, M., and McGeever-Rubin, B. 1987. Comparative light and electron microscopy of paraffin-embedded tissue: An assessment of three methods. *J. Histotechnol.* 10: 163–166.

Supplementary Reference

Chien, K., Van de Velde, R.L., and Heusser, R.C. 1982. A one-step method for re-embedding paraffin embedded specimens for electron microscopy. In *Proc. Electron Microsc. Soc. Am. 40th Annual Meeting* (pp. 356–357). San Francisco Press, San Francisco.

2

Cryotechniques

The first question that arises when considering cryotechniques in general is: What are the advantages to cryofixation? As we discussed in Chapter 1, fixation ideally instantaneously stops biological activity, immobilizes cellular components, and enables them to withstand any further processing procedures. In principle, biological materials can be fixed with either chemical or physical techniques (cold, heat). Good chemical fixation requires the fast diffusion of chemical agents through membranes and cytoplasmic components. Cryofixation, however, requires the rapid diffusion of heat out of the specimen. The reason cryofixation can be superior to chemical fixation is that the rate of chemical diffusion into the specimen is much slower than the rate of heat diffusion out of the specimen. However, most cryofixation techniques adequately freeze samples to a depth of no more than 10–15 μm, in contrast to chemical fixation, which consistently fixes samples to a depth of at least 0.5 mm. Cryofixation is often inferior for structural studies because of the limited sample size available but is vastly superior to chemical fixation for many microanalytical or immunocytochemical procedures because of the changes in cellular constituents caused by extraction and chemical/physical changes during the process of chemical fixation.

The second question that requires investigation concerns the freezing process itself. To understand the final product of cryofixation, it is necessary to examine the effect of freezing biological samples. When water turns to crystalline ice, the fine structure of membranes vanishes, and samples become cloudy. Improper freezing of samples can result in the growth of ice crystals by recruitment of water molecules from surrounding cytoplasmic areas, thus separating water from other nonaqueous molecules. As the crystals continue growing, they may draw extracellular water into cells. At a certain point, the attraction of water molecules to the growing ice crystals is overcome by the strength of the attraction of the remaining free water to other cellular constituents, thereby bringing a halt to further ice crystal growth. If a frozen cell is examined closely, ice crystals will be seen that have displaced normal cellular architecture and have actually penetrated structures such as membranes. The proteinaceous components of the cytoplasm and nucleoplasm become more concentrated than they were before freezing because they have been dehydrated during the growth of adjacent ice crystals. Thus, after improper freezing of cells, physical damage will have been caused by crystal formation, water will have been gathered into crystals at the expense of dehydrating the areas where the water was originally located, and various cellular structures will have been physically displaced by the growth of ice crystals.

Modern cryotechniques attempt to avoid the formation of crystalline ice by freezing the sample so rapidly that migration of water molecules followed by nucleation and crystal formation cannot occur. If frozen quickly enough, samples will have vitreous (amorphous) ice formed without a crystal lattice. Unfortunately, technical difficulties usually limit us to samples that have microcrystalline ice whose crystals are not readily visualized by electron microscopy. Careful examination with a cold stage and electron diffraction will still reveal diffraction patterns consistent with the crystalline structure of frozen water.

This chapter is devoted to exploring the history of cryotechniques, the methods for fixing cells with cryotechniques that produce minimal crystallization, and the use to which these

cryopreserved materials may be put. Three texts that are devoted to cryotechniques are those by Robards and Sleytr (1985), Roos and Morgan (1990), and Steinbrecht and Zierold (1987).

I. HISTORY

A. Organismal Period

This earliest period in cryobiology was devoted primarily to determining what organisms and life stages of organisms could withstand freezing. In the mid-1660s, Henry Power froze eel worms (nematodes) found in vinegar and discovered that they were still alive after thawing. In the late 1700s, Spalanzani froze rotifers, and embryos, eggs, and adult forms of various organisms and found that the embryos and eggs survived freezing more successfully than adults, which he attributed to the oily fluids that the embryos and eggs contained.

One of the major problems during this organismal period of cryobiology was the poor cryogens available. A saltwater and ice slush was usually the best cryogen available, causing very slow freezing and, thus, a high probability of ice crystal formation. Toward the end of the 19th century, cryotechnology had advanced to the point where −200°C temperatures were possible, and the list of organisms and tissues frozen and thawed had grown considerably. In addition, freeze-drying had been attempted on some tissues.

B. Mechanistic Period

Beginning in the 1900s, investigators began looking at the mechanisms involved in successful freezing of organisms as defined by the process producing minimal tissue damage.

In the early 1900s, the rate of freezing was determined to be a critical issue. By the 1930s, studies on the actual formation of ice crystals in protoplasm at the microscopic level demonstrated the cytoplasmic displacements that took place. By the 1940s, it was determined that it was necessary to form vitreous ice within tissue for survival. During the same period, the cryoprotectant glycerol was used during cryofixation of avian sperm and other cells and tissues to decrease the formation of crystalline ice. Later workers have subsequently demonstrated that some overwintering insects naturally contain as much as 20% glycerol in their cells (Lee and Denlinger, 1991), the percentage usually used as a cryoprotectant for freeze-fracture work.

C. Cytological Period

This period was characterized by the successful use of cryotechniques for ultrastructural studies, a period that was ushered in by the development of freeze-fracture equipment to fracture membranes and cells for subsequent replica production and TEM examination. The first device was designed by Steere (1957) and became the commercially available Denton freeze-fracture apparatus. This was followed by the production, by Moor *et al.* (1961), of a freeze-fracture apparatus, which was much easier to use and gained wide acceptance when it was marketed by Balzers (now Bal-Tec).

Sjostrand tried freeze-drying samples for electron microscopy in the 1940s with poor results but achieved reasonable preservation methods by 1958 (Sjostrand and Baker, 1958). Linner *et al.* (1986) described a highly effective method for cryofixing specimens and drying them in a molecular distillation device that was superior to previous freeze-drying equipment.

Fernandez-Moran, who was so instrumental in the development of diamond knives for ultramicrotomy, began exploring methods for freeze substitution of samples wherein cryofixed samples were subsequently dehydrated at low temperatures and embedded for sectioning at room temperature (Fernandez-Moran, 1957).

By the 1980s, a number of different specimen freezing methods had been developed that produced samples with vitreous or microcrystalline ice, and the techniques for cryoultramicrotomy pioneered by Bernhard (1965) had become routine. Tokuyasu (1973) introduced a technique for freezing tissues for cryoultramicrotomy that stimulated the development of immunolabeling of frozen ultrathin sections, which continues to be the major application for cryoultramicrotomy to biological samples.

In addition, the 1980s saw the development of low-temperature acrylic resins for embedment of specimens prepared by cryotechniques (see the section on resins in Chapter 1).

II. PURPOSE

The purpose of cryofixation is to stop biological activity, which happens in about 10 ms (Gilkey and Staehelin, 1986), prevent nucleation and crystallization of water, and preserve the spatial relationships and as much biological activity of cellular constituents as possible.

Ice crystal development begins with a nucleation point to which water from the surrounding medium migrates, resulting in the growth of an ice crystal. This causes the solute concentration in regions between the ice crystals to increase, eventually reaching a concentration sufficient to prevent further growth of the adjacent ice crystal. At this point, a solid eutectic has been formed, consisting of water and solute in a vitrified (glassy) state. In living organisms, ice crystal formation is thought to occur between -2°C and -80°C, although some workers (Linner *et al.*, 1986) maintain that some crystallization can occur even below -100°C.

The lowest temperature in the range is the recrystallization point. If a rapidly frozen specimen is allowed to warm to a temperature above -100°C, ice crystals will form (Dubochet, 1995). It is important to remember that ice crystals can form from freezing a specimen too slowly or warming a specimen too slowly.

Water that is ultrarapidly frozen with a slam-freezing device held at -196 °C with liquid nitrogen will demonstrate a structure no different from that of liquid water when studied with diffraction techniques (Linner *et al.*, 1986). This vitreous or amorphous ice goes through a transition if warmed to -135°C to -120°C and becomes microcrystalline in structure by the formation of cubic ice crystals. As the temperature increases from -120°C to -40°C, several types of ice are formed. By the time the temperature has warmed to -35°C, further crystallization results in large ice crystals, and some melting has also occurred. The size of the ice crystals is dependent on the rate of freezing or thawing and the solute concentration (cytoplasmic solutes and/or cryoprotectants added). At the high freezing rates achieved with modern cryotechniques, most of the water in a specimen crystallizes homogeneously into 20 nm^3 crystals that are difficult to resolve ultrastructurally, and the specimen is commonly described as "vitrified." If these samples are examined in the native frozen state with a cold stage-equipped TEM set up for diffraction, a crystal structure can still be demonstrated, so the sample is not truly vitrified but actually has microcrystalline structure.

The concept of cryoprotection arose out of the knowledge that certain cell types with a low water content (bacterial spores, some seeds, fungal spores) may be subjected to freezing temperatures and then thawed without any appreciable damage. Cryoprotectants have been added to other types of cells and tissues to improve their capacity to withstand the freezing process. Glycerol, ethylene glycol, dimethylsulfoxide (DMSO), and sucrose have been used extensively in this regard. A buffered solution of 20–25% glycerol is one of the most extensively used cryoprotectants and was originally developed for use with freeze-fracture methods. Cells and tissues are usually first fixed with aldehydes, since many unfixed cells will shrink in glycerol because of osmotic effects. The fixative is then rinsed out with an appropriate buffer, and the cells are immersed in the buffer/glycerol mixture for 30–60 min prior to freezing. The larger the piece of tissue, the higher the concentration of glycerol used. More than 2 hr in glycerol is considered undesirable. Some workers mix glycerol with sucrose (10% glycerol/20% sucrose) with good results. If the glycerol concentration is above 35–40%, specimen etching, if desired, becomes impossible because the water contained in the specimen cannot sublime from the surface under normal etching conditions.

Tokuyasu (1973) demonstrated that a light aldehyde fixation permeabilizes cytoplasmic membranes sufficiently to eliminate the possiblity of cryoprotectant-induced osmotic effects. Severe osmotic damage is induced in unfixed cells by 2.1 M sucrose, but no damage results from exposure to the sucrose if the cells have been lightly fixed in 2% buffered formaldehyde first.

III. CRYOGENS

Costello and Corless (1978) examined the actual temperatures and freezing rates of cryogens used for cryofixation (Table 11). Examination of this table reveals that the temperature of the cryogen is not the most important factor in determining its suitability for freezing specimens. Liquid nitrogen (−196°C) and nitrogen slush (−207°C) are the coldest cryogens in the list but have the slowest freezing rates (16,000 and 21,000°C/sec, respectively). To be effective for cryofixation, the cryogen must remain in contact with the specimen surface. Nitrogen has a low boiling point (−196°C) and quickly turns into a gas when confronted with a specimen at ambient temperature. The nitrogen gas formed is a significant thermal insulator, slowing the specimen freezing process. The most effective cryogens are those that remain liquid when cooled almost to liquid nitrogen temperature, thus allowing them to wet the specimen for quickest cooling. In addition, they have a boiling point several degrees higher, so they will remain liquid while the specimen is plunged (or sprayed) into them. Propane is the cryogen of choice for immersion, spray, or jet freezing, since it maintains a low temperature and has a fast freezing rate.

Table 11. Temperature and Freezing Rate of Cryogens Used for Cryofixation

Cryogen	Temperature at Cryogen Surface (°C)	Freezing Rate (°C/sec)
Propane	−190	98,000
Freon 13	−185	78,000
Freon 22	−155	66,000
Freon 12	−152	47,000
Isopentane	−160	45,000
Nitrogen slush	−207	21,000
Liquid nitrogen	−196	16,000

With metal mirror (slam) freezing, a polished metal surface is cooled with liquid nitrogen to −190°C to −196°C, at which time the specimen is brought into contact with the metal surface and held there until cryofixation is complete. With the specimen held in intimate contact with the nitrogen-cooled metal, the problem of nitrogen boiling is eliminated.

IV. SAFETY PRECAUTIONS

All of the cryogens must be handled carefully to avoid injury to the user. Liquid nitrogen can produce serious freezing damage if trapped inside gloves, shoes, or other articles of clothing. If liquid nitrogen is spilled onto bare skin, its rapid evaporation usually results in minimal damage. However, the other cryogens do not evaporate quickly and so can cause severe damage to exposed skin with which they come into contact. An added danger with propane is its flammability. Liquid propane, if exposed to the atmosphere, is cold enough to cause condensation of air (containing oxygen) on its surface or the surface of the vessel in which it is contained. This combination of cooled propane and oxygen is extremely flammable. For this reason, sample freezing should take place under a fume hood to avoid producing dangerous levels of gaseous propane. After specimen freezing is completed, the cryogen should be evaporated under the fume hood at a slow rate. Liquid propane and gaseous propane are both heavier than air. They will seek the lowest level in a room and can actually "run" out from under a fume hood down onto a laboratory floor if the hood is turned off. As the gaseous propane diffuses (or liquid propane vaporizes), any spark or flame in the vicinity can cause an explosion.

Finally, liquid nitrogen is generally treated as a relatively benign substance, since it rarely causes serious freezing unless trapped against body parts, but the gaseous form of nitrogen can also be extremely dangerous. If a typical 160-liter liquid nitrogen tank is stored in a small room without adequate ventilation, the very act of transferring nitrogen to another container for transport to specimen preparation areas can be dangerous, since large volumes of gaseous nitrogen can be produced. In a poorly ventilated space, this can result in air being displaced by nitrogen, leading to the real possibility of suffocation.

V. FREEZING METHODS

Four of the five basic freezing methods (immersion, metal mirror, jet, and spray freezing) will produce well-frozen cells only within 10–15 μm of the specimen surface. Below that thin layer, the thermal mass of the rest of the tissue prevents sufficient heat extraction to produce good freezing. This limits the overall mass of tissue that can be cryofixed adequately. Specimens over 0.2 mm in thickness are clearly unnecessary and counterproductive. Monolayers of cells will typically be more successful subjects for cryofixation than multicellular tissues. Various methods have been developed to try to increase this depth of cryofixation, but the only method that has succeeded is the high-pressure freezer initially introduced by Balzers and now marketed by Bal-Tec AG as the HPM 010 High Pressure Freezing Machine. In addition, Leica now markets the EM PACT High Pressure Freezer. Both units are purported to produce samples that are well-frozen to depths of approximately 200 μm, close to the normal depths for good chemical fixation (Gilkey and Staehelin, 1986; Moor, 1986).

A. High-Speed Plunging/Immersion

Cryoprotected material may be frozen by being quickly plunged by hand (held with forceps) directly into liquid nitrogen. If crystal damage to tissue is observed, the specimens can be plunged by hand into a moderate cryogen like Freon 13 or 22 cooled by liquid nitrogen with improved results.

Specimens that have not been cryoprotected have more stringent requirements for proper cryofixation. Those specimens must be immersed more quickly into a more effective cryogen like propane cooled with liquid nitrogen. Robards and Crosby (1983) studied the effect of the entry velocity of specimens into liquid nitrogen-cooled propane and found that specimen cooling increased with increasing speed of entry up to about 3 m/sec. Above that speed, cooling rates decreased, possibly because of trapped air pockets or induced turbulence insulating the specimen surface. The only exception to this velocity limitation is specimens that are prepared with the aerodynamic shape of blades or needles, which have been successfully frozen with immersion rates of 15 m/sec (Handley *et al.*, 1981). Immersion freezing devices that are laboratory-built or industrially manufactured (Fig. 82A) typically use springs or gravity to achieve desired specimen velocity. It is important to keep the cryogen surface near the top of the vessel into which the specimen is plunged. If the cryogen is at the bottom of a long tube, the air space above the cryogen can be cool enough to freeze the specimen as it passes through on its way to the cryogen but will still be too warm to freeze the specimen adequately, resulting in ice damage.

Not only are the specimen velocity, the placement of the cryogen in the freezing chamber, and the nature of the cryogen of importance, but also the shape and size of the specimen are factors that must be considered. Handley *et al.* (1981) put their specimens (blood) behind a thin titanium foil with an edged profile to improve heat transfer. Other workers have used foils of copper and gold.

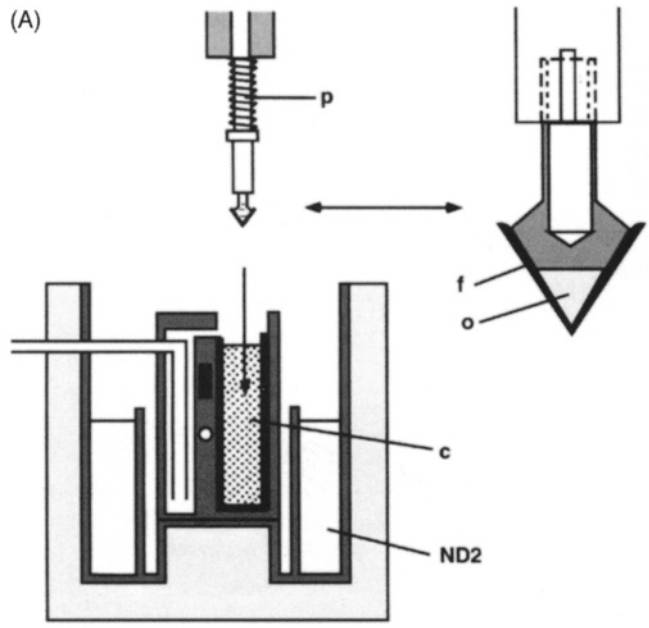

Figure 82. (A) Diagram of a Leica EM CPC high-speed immersion freezer with specimen (o) behind metal conical foil (f) driven by spring (p) into liquid propane cryogen (c) cooled with liquid nitrogen (ND2) in surrounding chamber. (Redrawn from diagram, courtesy of Leica Microsystems).

Dubochet *et al.* (1983) described a technique using a 400-mesh grid to which a droplet of subcellular particles up to the size of bacteria or mitochondria (0.5-μm diameter) had been added. The grid was wicked almost to dryness with a piece of filter paper, thus leaving a liquid film about 100-nm thick. The grid with its thin film of specimen/liquid was immersed in liquid nitrogen-cooled propane, cryotransferred to a TEM cryostage, and observed with a low-dose unit to decrease heating of the frozen specimen. The immersion speed did not have to be particularly fast, since the heat-transfer characteristics of the metal grid were excellent.

Thin slices of tissue or suspensions of cells (20-μm thick or less) have been placed between thin metal sheets (titanium or gold, typically) about 50 μm thick, resulting in excellent heat transfer upon submersion in the cryogen (Gilkey and Staehelin, 1986). Some devices, such as the Leica EM CPC (Fig. 82B), have a holder that grasps locking forceps holding the specimen. The EM CPC then plunges the specimen-holding forceps into a cylinder of nitrogen-cooled propane by spring-loaded pressure. The EM CPC can also plunge-freeze specimens situated on pins compatible with Leica Microsystems ultramicrotomes designed for cryoultramicrotomy, which then provides a sample that can be quickly transferred to the ultramicrotome cryochamber for ultrathin sectioning.

(B)

Figure 82. (B) Photograph of the Leica EM CPC unit set up for a high-speed immersion freezing. (Courtesy of Leica Microsystems).

B. Spray Freezing

This technique (Bachmann and Schmitt-Fumian, 1973) is based on the principle that cells contained in droplets of fluid, about 10–30 μm in diameter, that are sprayed into liquid nitrogen-cooled propane will be quickly frozen because of the favorable surface-to-volume ratio. The frozen droplets are then transferred to a surface held at −85°C and put under vacuum to extract the liquid propane. After the propane is removed, butylbenzene (freezing point: −95°C) is mixed with the droplets to produce a paste that can be transferred to freeze-fracture planchets and dipped into liquid nitrogen before freeze-fracturing. Gilkey and Staehelin (1986) suggest that the high freezing rates possible with this technique (>100,000°C/sec) are outweighed by the tediousness of the processing and the difficulty in obtaining good fractured surfaces because of smearing of the butylbenzene by the fracturing blade.

C. Jet Freezing

Müller *et al.* (1980) introduced the double-jet propane freezer (Fig. 83). With this technique, a thin specimen is sandwiched between two metal planchets or sheets, which protect the surface of the sample from the high-velocity propane jet and ensure rapid heat transfer. The specimen is held between the two jets through which liquid nitrogen-cooled liquid propane is propelled by high pressure toward the sample. Since the specimen is cooled from both

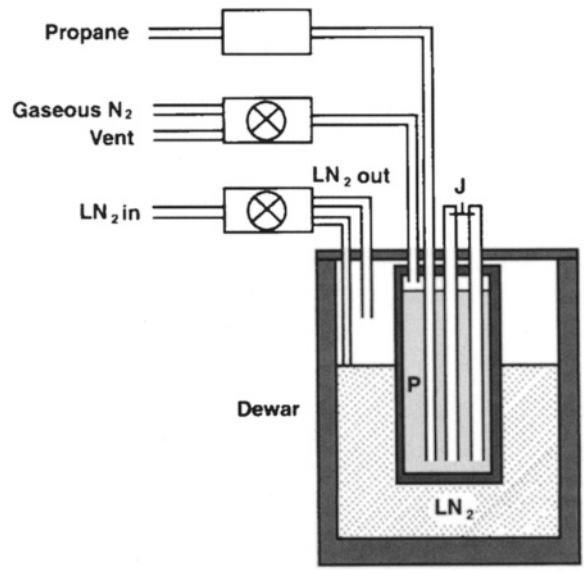

Figure 83. Propane jet-freezing device from Müller *et al.* (1980). Propane (P) cooled by liquid nitrogen (LN_2) is forced by gaseous N_2 into two tubes with small orifices (J), producing a jet of cooled propane. (Redrawn from Gilkey and Staehelin, 1986, courtesy of Wiley-Liss, Inc.)

sides at once, Gilkey and Staehelin (1986) report that the specimen is, on average, frozen to a depth of 40 μm.

D. High-Pressure Freezing

This technique was developed by Moor and his colleagues (Moor and Riehle, 1968; Moor *et al.*, 1980). A basic diagram of the functional parts of the commercially made unit produced by Bal-Tec (HPM 010) is shown in Fig. 84.

Specimens are placed between two metal planchets to help reduce the possibility of the samples being crushed. The specimen is placed within the high-pressure chamber, the chamber is pressurized, and then liquid nitrogen is forced into the chamber under pressure to freeze the sample.

As pointed out by Dubochet (1995), water increases in volume when it becomes more ordered (frozen), but by freezing water at high pressure, the increase in volume is made more difficult, thus decreasing the growth of ice crystals.

It was found that pressurizing the chamber with liquid nitrogen alone resulted in a cooling rate that was too slow. The system currently available forces a small bolus of isopropyl alcohol (2 ml) into the chamber during initial pressurization, and freezing begins when the nitrogen enters the chamber at about 210 MPa and is directed onto the specimen from jets in the chamber. The pressurization and freezing cycle, which lowers the specimen temperature to −150°C, takes about 0.5 s. The specimen temperature remains below −100°C for about 6–8 s, allowing the operator to remove the sample for storage in liquid nitrogen before it thaws.

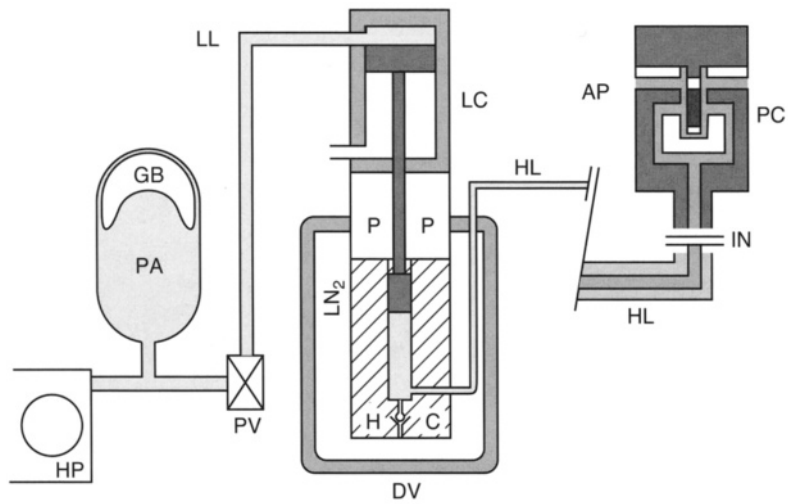

Figure 84. Diagrammatic representation of Bal-Tec AG high-pressure freezer, as designed by Moor *et al.* Abbreviations: HC: high-pressure cylinder; DV: Dewar; PP: pressure piston; HL: high-pressure line; PA: pressure accumulator; GB: gas balloon; PV: pressure valve; IN: isopropyl alcohol insertion port; PC: pressure chamber containing specimen in metal sandwich; AP: exhaust aperture; LC: low-pressure chamber; LL: low-pressure line; HP: hydraulic pump; LN_2: liquid nitrogen. (Redrawn from Gilkey and Staehelin, 1986, courtesy of Wiley-Liss, Inc.)

Moor (1986) points out several potential problems with high-pressure freezing:

1. *Euglena* exposed to 200 MPa for 0.1 sec have a 90% survival rate, while all those exposed for 4 sec die, indicating that freezing must quickly follow pressurization to ensure good results.
2. It is important to raise the chamber pressure to 210 MPa before freezing takes place, which is the purpose of the isopropyl alcohol, thus delaying the entrance of the liquid nitrogen into the chamber until it has been sufficiently pressurized (this is critical, since the liquid nitrogen is being used both to pressurize the chamber and to freeze the specimen). He reports that it takes 15 msec to pressurize the chamber sufficiently for the freezing process to work effectively.
3. The specimen should be cooled for a period following freezing so that there is no chance of the temperature rising above the crystallization point during specimen transfer to liquid nitrogen for storage.
4. Finally, as with all freezing techniques, the surface of the specimen freezes before the interior. In order to achieve the great depths of freezing (0.5–0.6 mm) produced by this technique, it is necessary to hold the pressure during freezing for at least 0.3 sec to ensure thorough freezing.

E. Metal Mirror/Slam Freezing

Van Harreveld and Crowell (1964) are credited with being the first to freeze samples for electron microscopy on cooled metal blocks. At the present time, there are a variety of commercially produced slam freezers (Fig. 85A and B) available from electron microscopy supply houses or directly from equipment manufacturers. The Leica EM CPC unit that was mentioned above in reference to high-speed plunge freezing can also be set up for metal mirror freezing utilizing three gold-plated copper targets.

All of these devices consist of a polished metal surface, usually copper, which is cooled with liquid nitrogen or liquid helium. The specimen is attached to a plunger above the metal mirror and is subsequently impinged upon the mirror surface by gravity, electromagnetic force, gas pressure, or springs. Some of the devices rely on nitrogen gas rising up from the reservoir cooling the mirror to keep air from condensing on the mirror surface, while others have the mirror within a low vacuum chamber while it is being cooled and only open the chamber milliseconds prior to slamming the specimen onto the mirror.

The copper metal mirror is polished and cleaned prior to slamming so that the specimen will be slammed onto a blemish-free surface for best thermal conductivity. The mirror is then placed into the slamming chamber and cooled with liquid nitrogen. Liquid helium can also be used, but is much more expensive and does not appear to produce a significant difference in final specimen quality. The chamber containing the target mirror is covered during the cooling process to minimize the formation of insulating frost on the mirror surface. Just as the specimen driver is being released, the chamber door is opened. After the specimen is slammed, it is held onto the cooled metal for 20–30 sec to cool areas behind the superficial well-frozen 10–15 μm. After this cooling period, the specimen is transferred quickly to liquid nitrogen for storage until subsequent processing steps.

One problem that was noted during the development of slammers was that a specimen striking the target because of gravity (a free fall device) tended to bounce after initial contact, briefly breaking thermal contact with the target. It was noted that this was sufficient to cause ice

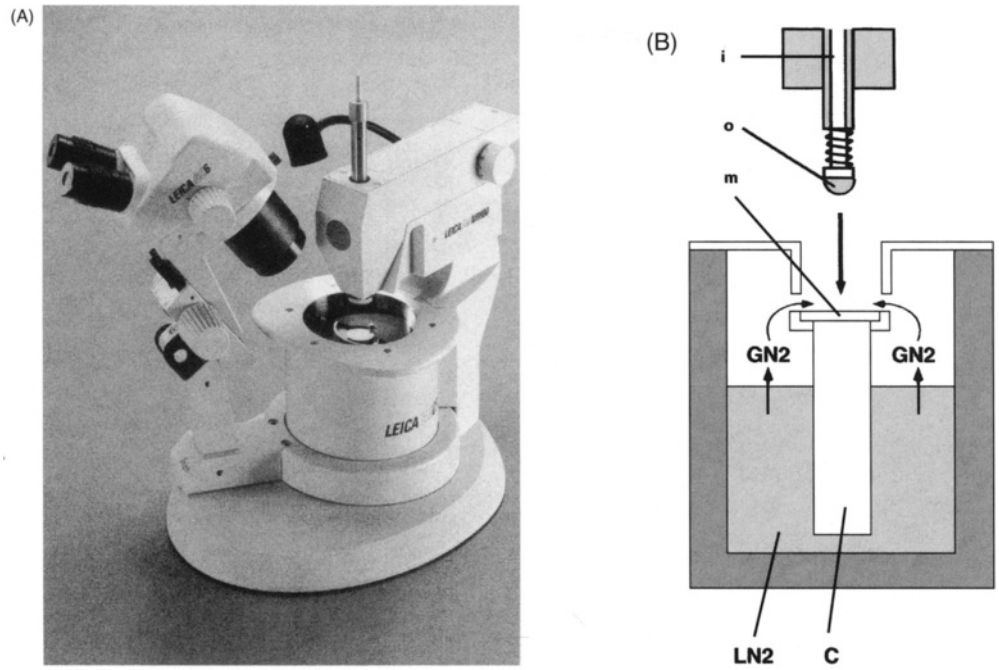

Figure 85. (A) Photograph of Leica EM CPC unit set up for metal mirror freezing. (B) Detail of chamber and specimen plunger of a slam freezer. Copper bar (C) with polished surface (m) is kept free of frost by gaseous nitrogen (GN2) produced from the liquid nitrogen reservoir (LN2) cooling copper bar. Specimen (o) is driven onto mirror by a spring wrapped around the inner shaft (i). (Both images courtesy of Leica Microsystems).

damage. To eliminate this problem, some of the devices have used shock absorbers to prevent rebound (Gentleman Jim®), and others have used gas-driven plungers or electromagnetic drivers to slam the specimen holder against the target while not allowing any recoil. Another problem concerns the target surface. All targets develop frost after removing the frozen specimen. The frost must be removed prior to the next slamming cycle by thawing the target. In the process of heating and then recooling a copper target, the surface tends to oxidize, thus providing poorer thermal contact surfaces for the specimen. It is thus necessary to remove the target and polish it between slams unless the copper target is gold-plated, which eliminates the problem of target oxidation.

VI. USES OF FROZEN SPECIMENS

Once a specimen is frozen by one of the five techniques described above, further choices must be made between different sample handling procedures determined by the eventual sample fate. Frozen samples may be prepared for freeze-fracture, cryosubstitution, freeze-drying, immunolabeling, or microanalytical approaches.

Another parameter of cryotechniques concerns the quality of the final product examined. As previously mentioned, most cryotechniques produce images that appear significantly different from conventional chemically fixed and epoxide-embedded materials (Fig. 86). Thus, when determining what techniques to employ, it is necessary to focus on the question being asked. If straight structural studies are desired, cryosubstitution or conventional chemical fixation will yield the

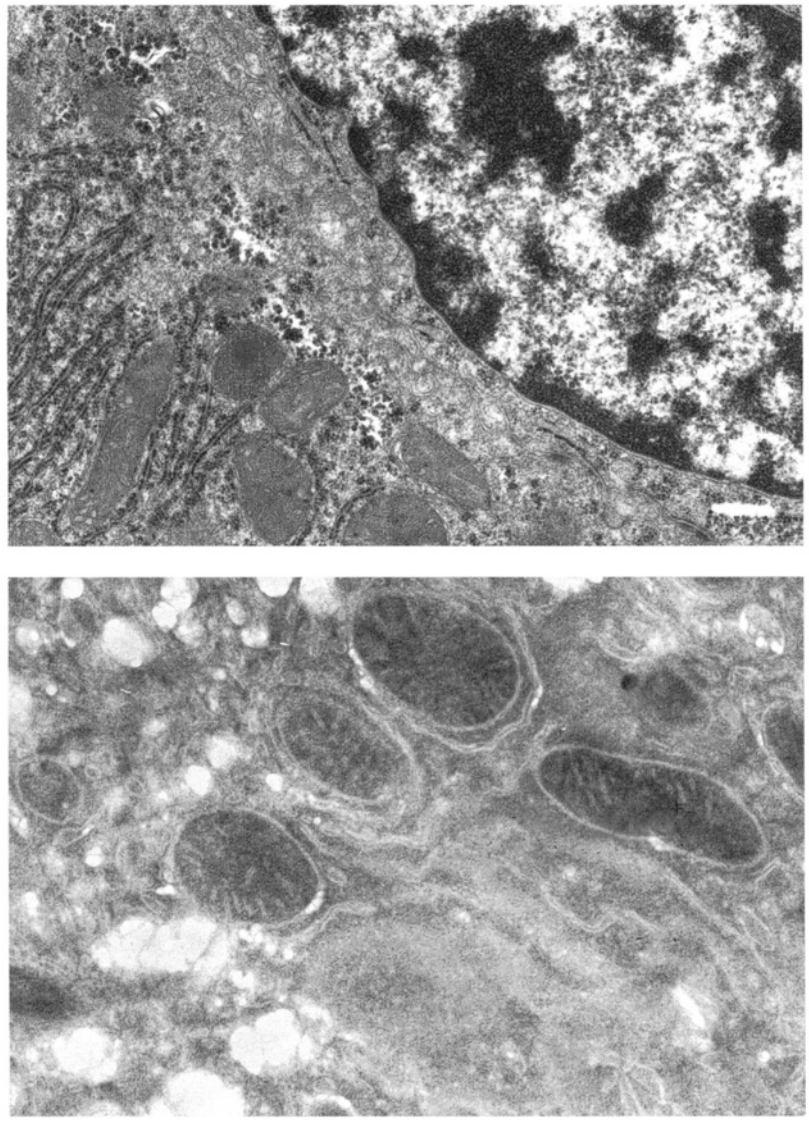

Figure 86. Top: Liver, conventional chemical fixation and embedment, poststained with uranyl acetate and lead citrate. 18,462×. Bottom: Liver, Tokuyasu (1973) technique. Light aldehyde fixation followed by cryoprotection in 2.3 M sucrose, cryofixation in Freon cooled with liquid nitrogen, cryoultramicrotomy, and staining with ammonium molybdate. 25,962×.

most cellular detail. However, if immunolabeling is the primary objective, cytological preservation is sacrificed for antigen preservation and accessibility. Some of the immunolabeling procedures sacrifice membrane preservation, but compartments can still be identified, so antibody labeling can be described as occurring inside or outside of various cellular compartments despite the poor preservation of membranes. Frozen sections or samples prepared by freeze-drying also look significantly different from conventionally prepared samples, but both techniques can minimize exposure of samples to fixatives, solvents, heat, and strongly cross-linked resins. Thus, structural detail is often sacrificed for preservation of other features being sought with cryotechniques.

A. Cryoultramicrotomy

Ultramicrotomes used for cryoultramicrotomy have had thermal advance mechanisms or mechanical advance mechanisms, though the instruments marketed today are all mechanical advance devices (Leica UCT, RMC MT-X, and Micro Star Cryoultramicrotome). Since current techniques produce ultrathin frozen sections on dry knives, eliminating the possibility of evaluating section thickness by the normal interference colors produced by sections floating on water when illuminated with diffuse light, mechanical specimen advance is preferred so that section thickness can be more accurately determined.

Cryoultramicrotomes equipped for fast arm return speeds along with adjustability to very slow cutting speeds (<0.1 mm/sec) and small cutting windows (<1.0 mm) give the most satisfying results for native frozen materials (those cryofixed without any chemical treatment) destined for microanalysis with or without cryotransfer to a cryostage in a TEM. These materials are generally sectioned at −150°C after ultrarapid freezing without cryoprotection. If the cutting speed is too fast, section melting can occur, as revealed by the presence of knife marks in sections.

Block face trimming is critical for success. The block should be reduced to 0.2–0.5-mm length, with the upper and lower edges exactly parallel, and then the face should be trimmed smooth with a glass knife. Glass knives cooled to −100°C to −120°C to produce sections by the Tokuyasu (1973) technique for immunolabeling are considerably harder than when used at room temperature and will cut many good frozen sections. Diamond knives are considered superior when cutting 10- to 50-nm sections of native frozen materials for microanalysis.

1. Immunolabeling (Tokuyasu, 1973)

Samples are typically fixed for 1 hr in 2–4% phosphate-buffered (pH 7.0) formaldehyde made up freshly from paraformaldehyde powder. After rinsing the samples in the same buffer, they are immersed in 2.3 M sucrose for 1 hr before being cryofixed. Because of the cryoprotection provided by the sucrose, they can usually be manually immersed in liquid nitrogen, producing adequate cryofixation. If excessive freezing artifacts (Fig. 87) are observed, immersion fixation in Freon cooled with liquid nitrogen may be necessary. The knife temperature (−105°C) should be slightly cooler than that of the specimen (−100°C). Sections for immunolabeling are picked up with a drop of 2.3 M sucrose just before the sucrose freezes (Fig. 88), transferred to the surface of a grid, which is then floated on distilled water in a small Petri dish to remove the sucrose. After blotting the grid dry, it can be immunolabeled and then negatively stained with 3% ammonium molybdate (see Chapter 8 Techniques).

2. Frozen Sections for Microanalysis

Native frozen sections that have had no chemical fixation or cryoprotection can be cryosectioned, cryotransferred, and examined on a cryostage-equipped TEM. Native frozen samples can yield information concerning the location of diffusible elements such as sodium and potassium as well as insoluble materials.

Since no chemical fixation or cryoprotectants are employed, native frozen sections must be frozen by the most exacting methods. Most workers use jet, slam, or high-pressure freezing to produce materials suitable for cryosectioning. Samples are usually sectioned at −120°C to −150°C. Dry sections are moved to Formvar-coated grids within the cryosectioning chamber with a precooled eyelash and then pressed down onto the grid surface with a cooled nylon-tipped rod. Static

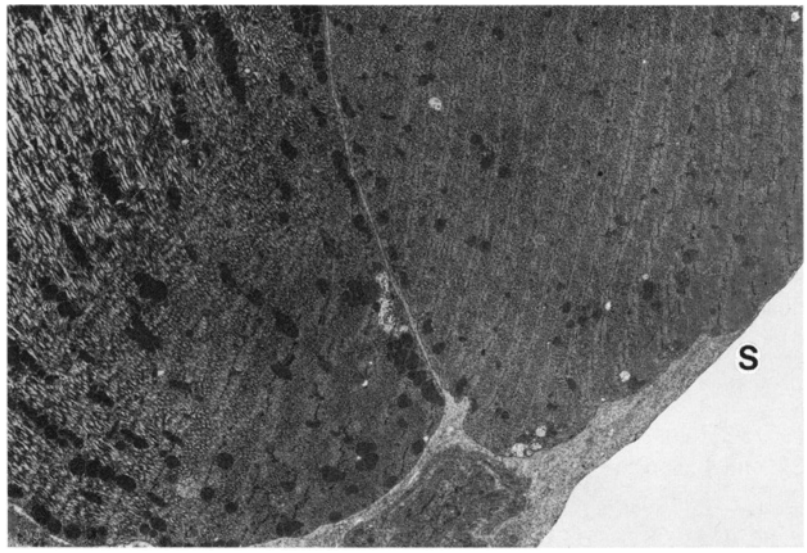

Figure 87. Sample with freezing artifacts in the form of a generalized motheaten appearance of slam-frozen and cryosubstituted sample caused by the formation of numerous small ice crystals in cytoplasmic areas away from the sample surface (S) of mouse skeletal muscle. 2,404×.

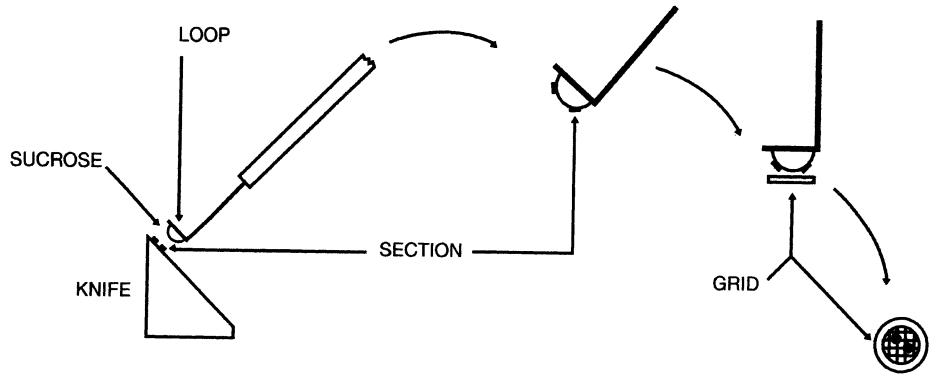

Figure 88. Tokuyasu (1973) procedure for transferring frozen sections to a grid with a loop containing a drop of sucrose.

electricity is often a problem when working at low temperatures with native frozen sections, so many workers use devices such as a Static Line II™ (Electron Microscopy Sciences, Fort Washington, PA) to decrease electrostatic charges in the ultramicrotome cryochamber.

Grids with frozen sections are then cryotransferred to a cryostage-equipped TEM for microanalysis (see Steinbrecht and Zierold, 1987, for further applications).

3. Structural Analysis

Examination of sections prepared from native frozen materials or samples prepared by Tokuyasu (1973) techniques can provide structural information about tissues exposed to minimal preparatory techniques. Native frozen sections have been exposed to no chemical treatments

whatsoever, while Tokuyasu sections have been fixed only lightly, rinsed in buffers, put into sucrose, and frozen, thereby eliminating osmium, dehydration agents, resins, and the heat used to polymerize most conventional resins.

In most cases, these frozen sections must be stained to produce contrast (e.g., with ammonium molybdate), although examining these materials with a TEM capable of electron spectroscopic imaging, which can eliminate scattered electrons from the imaging process, should produce good images even without staining.

B. Cryosubstitution

Cryosubstitution techniques have grown in popularity over the last 20 years for purely morphological investigations. Several automatic cryosubstitution units, such as the Leica EM AFS freeze-substitution system, currently marketed for under $18,000, are available.

Conventional chemical fixation and cryosubstitution produce different images (Fig. 89). Cryosubstitution often reveals materials not preserved by conventional chemical fixation, but freezing damage during initial cryofixation is a frequent artifactual element found in photographs of these materials.

Monaghan *et al.* (1998) discuss different substitution media with and without dissolved osmium, the effect of different rates of warming before embedment in epoxide resins, and alternative methods for embedment in low-temperature acrylic resins. With conventional chemical fixation, plasmalemmal profiles are often wavy, while cryosubstitution produces smooth profiles that are considered to be more representative of the living state. Studies of various fungi have shown that the populations of vesicles involved in tip growth of fungal hyphae, which appear homogeneous with conventional chemical fixation, show varied contents with cryosubstitution methods (Howard and Aist, 1979).

Cryosubstitution starts with cryofixation followed by transfer of the sample to a cryochamber containing a substitution agent that replaces water in the sample. After all the water has been replaced by the substitution agent, more of the substitution agent in which various fixatives have been dissolved is added to the chamber containing the samples. After a suitable time during which the fixative-laden substitution agent has diffused throughout the sample, the chamber temperature is raised slowly, allowing the fixatives to interact chemically with the samples.

Cryosubstitution assures rapid cessation of biological activity as a result of cryofixation followed by dehydration and then infusion of chemical fixatives at temperatures too low (usually −80°C) for chemical activity. As the chamber temperature is raised, the chemicals contained in the substitution agent simultaneously fix all areas of the sample once they reach their particular reactive temperature (e.g., −40°C for uranyl acetate and −20°C for osmium).

This is markedly different from conventional chemical fixation where the fixative diffuses from the sample surface to the interior. During the process, the fixative becomes bound to tissue constituents, thus diluting the fixative solution reaching the interior of the sample. In addition, as the sample becomes fixed from the outside in, further diffusion of the fixation solution becomes impeded by fixative cross-linking and chemical alteration of cellular constituents.

Some workers (Harvey, 1982) have used apolar substitution agents such as diethylether to preserve the original distribution of water-soluble substances for subsequent microanalysis, which presumably would have been mobilized by the use of polar substitution agents. Methods employing apolar agents take up to 14 days for cryosubstitution of the sample because of their poor miscibility with water.

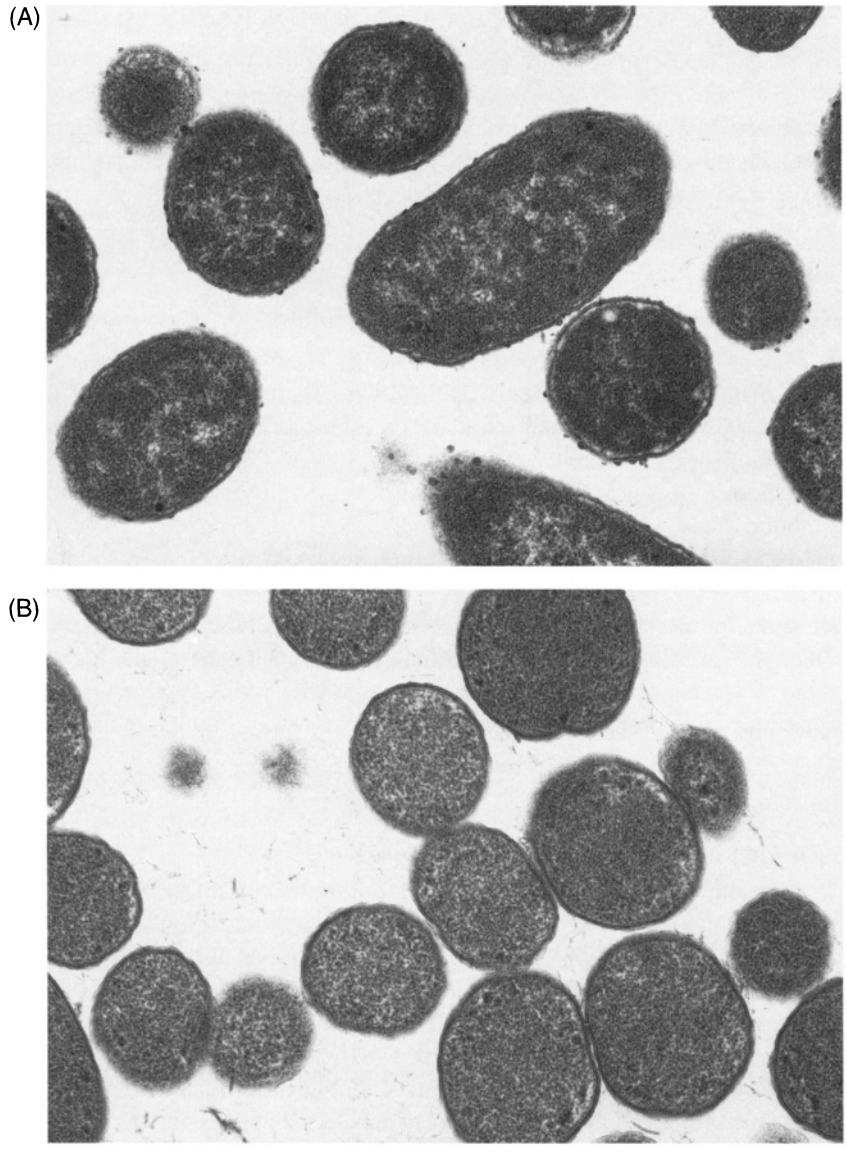

Figure 89. (A) *Escherichia coli* fixed with conventional chemical methods. 32,308×. (B) *Escherichia coli* fixed by slam-freezing, followed by cryosubstitution. 32,308×.

Most cryosubstitution is done using polar solvents (see Steinbrecht and Müller, 1987) such as acetone, which is the most widely used agent. Methanol has the advantage that it substitutes more quickly at low temperatures than acetone and is more suitable for dissolving fixatives such as glutaraldehyde.

Polar agents such as acetone or methanol placed over cryofixed samples held at −80°C typically dissolve frozen water and replace the frozen water within 6–12 hr. During this time, the substitution agent can be changed several times. The final change typically contains 2–4% osmium, although some investigators have added acrolein, glutaraldehyde, and uranyl acetate (see Steinbrecht and Müller, 1987).

Freezing artifacts may be induced in cryosubstituted samples by inadequate freezing rates, too rapid thawing rates, or by excessive sample size (depth) (Monaghan *et al.*, 1998). Evidence of freezing damage in the form of clear areas caused by nucleation of ice crystals behind the front of adequate freezing in a slam-frozen, cryosubstituted sample can be seen in Fig. 87.

C. Freeze-fracture

Steere (1957) demonstrated virus particles within cells with freeze-fracture techniques, which ushered in the first widely applied cryotechnique applied to biological materials. Most early workers felt that freeze-fracture techniques could eliminate the need for chemical fixation and would provide a more realistic picture of cellular structures than chemical fixation. Unfortunately, initial freezing of tissues and cells without cryoprotection showed freezing damage, so most laboratories resorted to light aldehyde fixation followed by treatment with 20–25% buffered glycerol for cryoprotection during subsequent manual immersion freezing in Freon 13 cooled with liquid nitrogen.

The first commercially available freeze-fracture device was designed and marketed by Balzers and Hans Moor in 1964. The current model now marketed by Bal-Tec AG (BAF 060) was introduced in 1994 and has several specimen stages capable of holding small (3 mm in diameter) gold planchets with favorable heat-transfer characteristics (Fig. 90). The cryoprotected sample is loaded into the planchets, quickly frozen, and stored under liquid nitrogen until use. After the knife arm and specimen stage have been cooled under vacuum to $-150\,^{\circ}C$ and $-100\,^{\circ}C$, respectively, the bell jar is brought to atmospheric pressure, and the specimen is quickly loaded onto the specimen stage. The bell jar is then closed and evacuated to less than 10^{-4} Pa. At that time, the knife-holding arm, which is loaded with a standard injector razor blade, is passed above the specimen and slowly lowered in 1-μm increments until the specimen surface is fractured. It is important not to make too many passes as the deeper part of the sample will generally not be frozen as well as superficial regions. After the surface of the specimen is fractured, the knife is moved out of the way, and a carbon/platinum coat is evaporated onto the specimen surface. Next, carbon is evaporated onto the specimen for added replica stability. The chamber is then brought to atmospheric pressure, the specimen is removed and thawed, and the replica is floated off the planchet onto distilled water. The replica is then transferred with a loop to successive baths of acid and

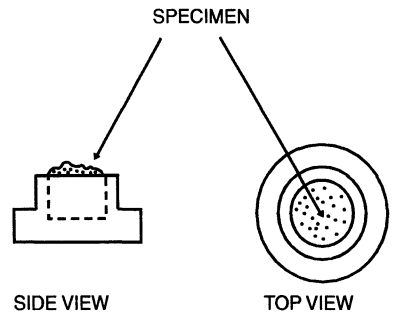

Figure 90. Gold specimen planchets used with Bal-Tec AG freeze-fracture units.

sodium hypochlorite (bleach) with intervening distilled water washes and finally rinsed several times in distilled water. The replica, which has now had all biological material corroded from its surface, is picked up with a grid, dried, and examined with the TEM. The replica will reveal cellular structures (Fig. 91) but is mostly used to examine intramembrane domains (Fig. 92) demonstrating intramembrane protein particle distribution.

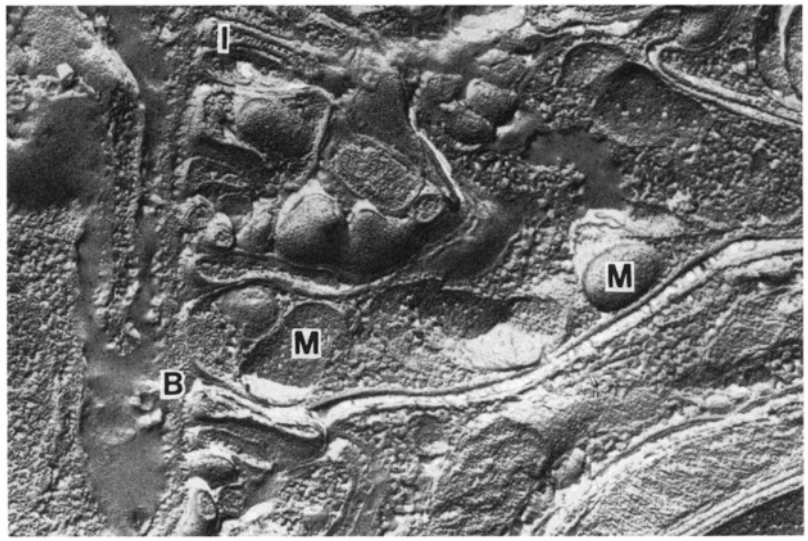

Figure 91. Freeze-fracture preparation of a rat kidney showing basement membrane (B), mitochondria (M), and basal infolding (I). 24,519×.

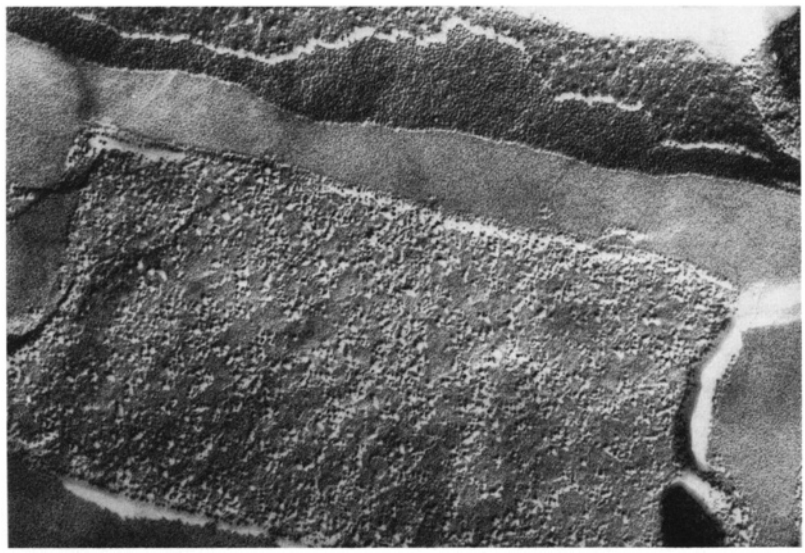

Figure 92. Freeze-fracture preparation of *Escherichia coli* cells showing intramembrane protein particles. 44,135×.

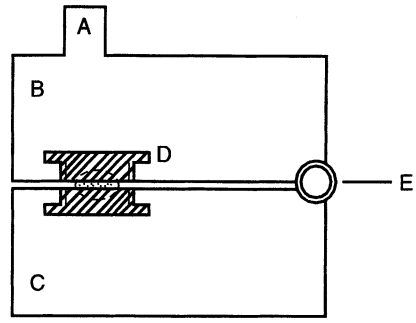

Figure 93. Freeze-fracture double-recovery device. Pin A is struck to open jaws (B, C) hinged at E. The sample (stippled) frozen between the two planchets (D) is broken in two by the process and is subsequently shadowed.

An alternative preparative procedure utilizes matched holders held in a hinged device (Fig. 93). The sample is placed between two planchets and then frozen. The frozen planchets with the sample sandwiched between them are mounted on the cooled stage of the freeze-fracture device, the bell jar is closed, and the system is evacuated. The knife-holding arm is used to open the double-recovery device, exposing two complementary fractured specimen faces that are subsequently shadowed, producing complementary replicas that are cleaned as above. The replicas can be carefully examined, and complementary faces can be located to examine the insertion of membrane proteins into the lipid bilayer.

Freeze-etch samples are prepared in the same way as for standard freeze-fracture samples, except that after the specimen is fractured, the cold knife holder is suspended over the specimen for a few minutes to allow frozen water from the sample to sublime and attach to the knife holder. After the etching period is finished, the knife is moved out of the way, and a metal replica is made as described above. The purpose of etching is to make nonaqueous domains of the cell stand up in relief against the depressed areas from which water has sublimed.

Freeze-fracture techniques are not used as much today as in the past because of the development of more sensitive techniques utilizing gold-labeled antibodies, which can not only localize the protein components within a membrane but also can identify specific proteins, which is not possible with freeze-fracture techniques. Coupling gold-labeled antibody techniques with high-resolution Field Emission Gun (FEG) scanning electron microscopy allows the identification of several specific proteins simultaneously and also can examine sample sizes much larger than possible with freeze-fracture methods. However, there is still a place for freeze-fracture techniques in conjunction with other methods such as negative staining and polyacrylamide gel electrophoresis. This combination can answer basic cell biology questions, as was done in elucidating the structure and interaction of streptolysin with the lipid component of natural and artificial membranes (Bhakdi *et al.*, 1985).

D. Freeze-Drying as Typified by Molecular Distillation

Linner *et al.* (1986) described an improved freeze-drying device called a molecular distillation device (MDD) that is, unfortunately, no longer marketed. The MDD provided a means to reproducibly dry a cryofixed specimen, which could then either be vapor-fixed with osmium prior to infiltration with room temperature Spurr resin for routine ultramicrotomy or directly infiltrated with a low-temperature acrylic resin such as Lowicryl. The former sample type proved to be good for structural studies, immunolabeling, and autoradiography, while the latter type was primarily intended for immunolabeling and microanalytical work.

The advantage of this specimen preparation technique is that a native frozen specimen could be infiltrated with resin (with or without osmium vapor fixation) without ever having been exposed to aqueous fixatives, aqueous buffers, or dehydration agents. The dried sample was directly infiltrated with resin, which was either polymerized by heat (Spurr) or polymerized with ultraviolet light at low temperatures (Lowicryl). Thus, water-soluble enzymes and ions remained as they were in life, rather than being removed or rearranged during the aqueous processing phases employed during conventional fixation schedules.

After the sample was slam-frozen, it was put into a holder that was kept under liquid nitrogen (Fig. 94). The holder was then placed in a container filled with liquid nitrogen, which was attached to the bottom of the MDD device and, in turn, was suspended in a dewar of liquid nitrogen. The chamber containing the specimens was bolted to the MDD and then connected to a mechanical pump, which pumped the liquid nitrogen out of the specimen area (which was still held at liquid nitrogen temperatures by the external dewar of liquid nitrogen in which it was immersed). Following evacuation of the liquid nitrogen, the specimen chamber was disconnected from the mechanical pump, and a turbomolecular pump backed by the mechanical pump was connected to the specimen chamber. Water sublimed from the frozen specimens over a 5- to 7-day period and was removed from the system by the turbomolecular pump. The temperature of the specimen chamber was then brought up in steps specified by the MDD processing program until the chamber reached −40°C, at which time Lowicryl resin was pulled into the chamber under slight vacuum to infiltrate the specimens. The resin was then polymerized with ultraviolet radiation before the chamber was brought to room temperature and pressure for specimen removal.

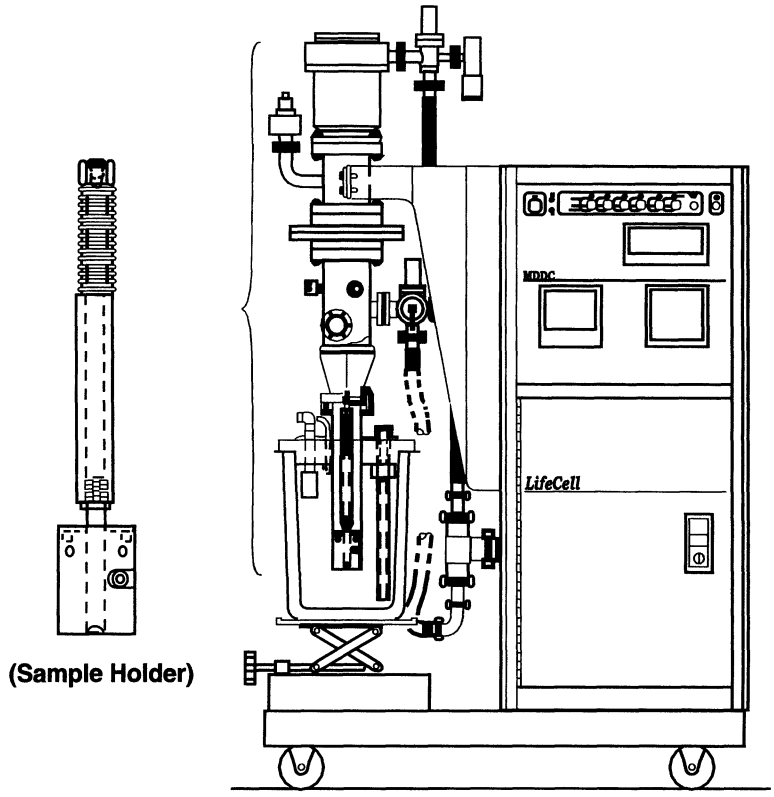

Figure 94. LifeCell MDD-C molecular distillation dryer after Linner *et al.* (1986). (Courtesy of LifeCell Corporation.)

Alternatively, the chamber containing dried specimens was brought to room temperature and low vacuum, a vial of osmium crystals was attached to a port in the chamber, and the low vacuum was used to pull osmium vapor into the chamber to vapor-fix the samples. Then, the osmium vapor was evacuated from the chamber, and Spurr resin was pulled into the chamber under low vacuum. After the specimens were infiltrated, the chamber was opened, the specimens were removed and put into molds with fresh Spurr resin, and the resin was polymerized with heat. Figure 95 shows two products from this technique.

The equipment for this technique is no longer being marketed, and even when it was readily available, it was expensive and most sample types had to have specific freezing methods

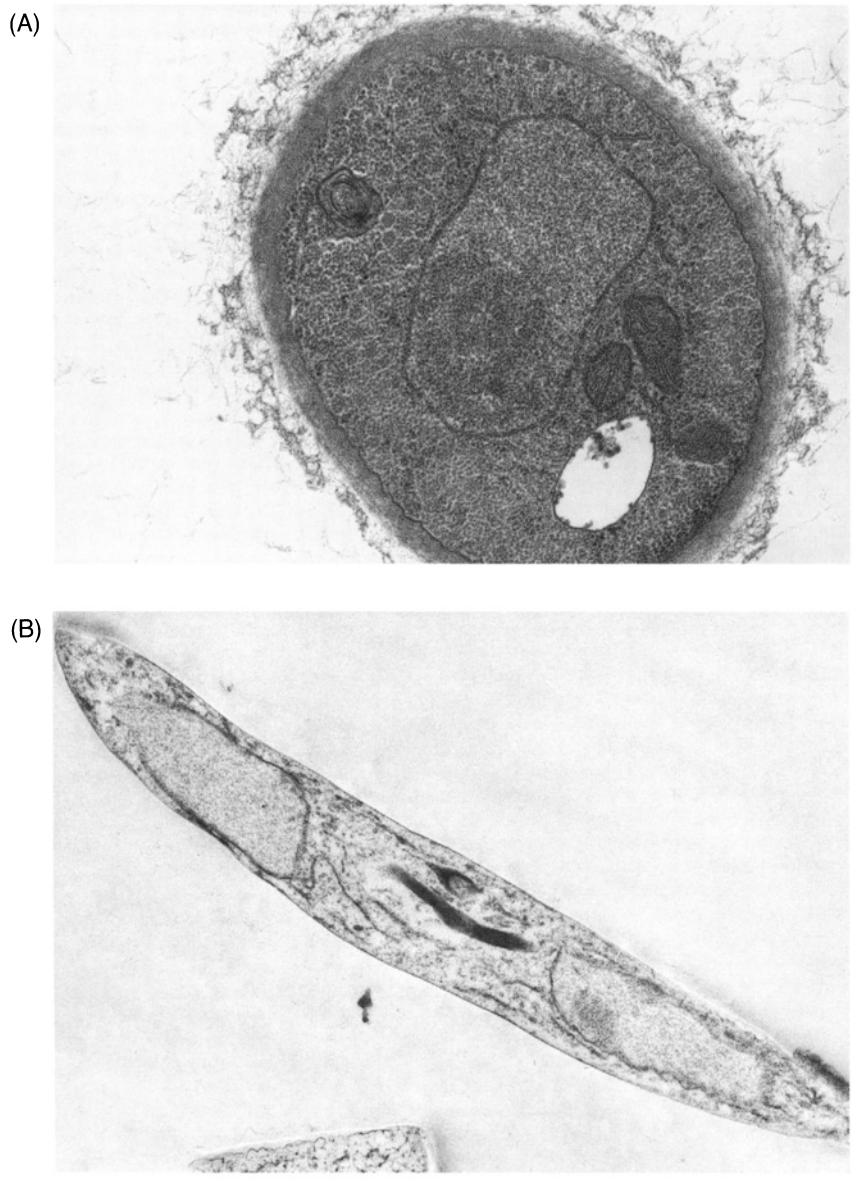

Figure 95. (A) *Aspergillus fumigatus* fixed with conventional chemical methods, embedded in Spurr resin, sectioned, and stained with uranyl acetate and lead citrate. 25,962×. (B) *Aspergillus fumigatus* slam-frozen, followed by molecular distillation, osmium vapor treatment, Spurr resin infiltration, sectioning, and uranyl acetate staining. 11,538×.

designed for them. Fortunately, there are several other techniques that are less expensive and that will answer the same questions. Unless the antigens that need to be localized are water-soluble, Tokuyasu (1973) techniques employing cryoultramicrotomy for intracellular immunolabeling will probably work well, take less time, and cost considerably less. Native frozen sections cut on a cryoultramicrotome, cryotransferred, and examined with a cryostage on a TEM will usually give the same microanalytical possibilities as a section prepared by molecular distillation.

VII. ARTIFACTS AND THEIR CORRECTION

Materials prepared for electron microscopy utilizing cryotechniques suffer from many different types of artifacts. If chemical fixation precedes freezing, as with Tokuyasu (1973) techniques for cryoultramicrotomy, chemical fixation artifacts as described in Chapter 1 can occur.

Techniques that begin with cryofixation are consistently plagued with freezing artifacts. As mentioned previously, most freezing techniques are capable of optimal sample freezing no more than 10–15 μm from the sample surface. Figure 96 clearly illustrates the tissue distortion caused by ice crystal formation and also shows that the farther from the sample surface, the larger the artifactual holes formed.

Another interesting feature associated with cryofixation is the insulating aspect of biological membranes. The freezing front passing through the tissue can be very irregular because of this aspect. Figure 97 shows cells of the bacterium *Escherichia coli* that were slam-frozen, cryosubstituted, and embedded in Spurr resin, followed by sectioning and normal poststaining with uranyl acetate and lead citrate. The cells showing dark borders with large open areas in the center were severely damaged during the freezing process. Note that relatively normal looking cells are located back from the slammed surface, interspersed with damaged cells. This demonstrates that the freezing process does not proceed in a strictly linear direction from the surface of the sample inward, but skips around some cells.

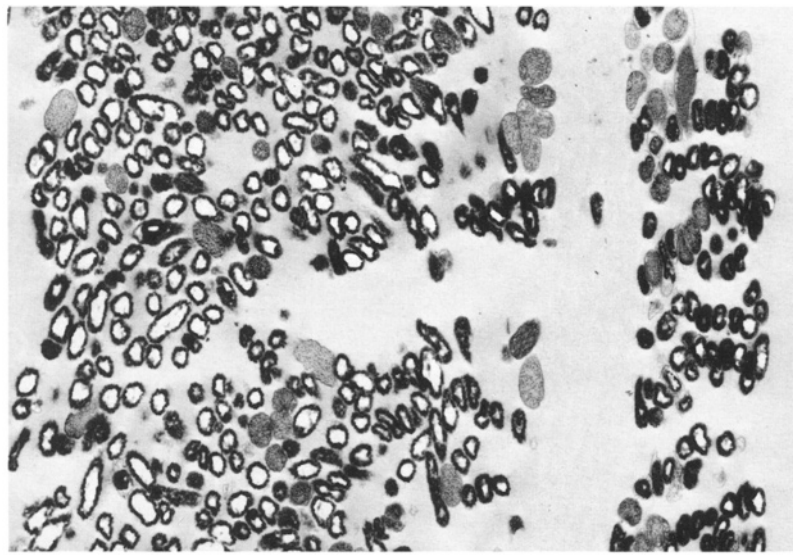

Figure 96. Slam-frozen cells of *Escherichia coli*. The surface of the specimen is to the right. The entire thickness of the slammed sample is shown. 6,731×.

Slam-freezing is one of the most successful, reproducible, and widely used methods for cryofixation, but it leads to a variety of artifacts. Numerous studies on different types of cells and tissues have made it clear that each time a new type of sample is frozen, a series of trials to determine the best type of material to put behind the specimen must be undertaken. If the backing material is inappropriate for the sample, crushing artifact may occur, even at the sample surface. Figure 98A shows cells of the fungus *Aspergillus fumigatus* that were slam-frozen, freeze-dried

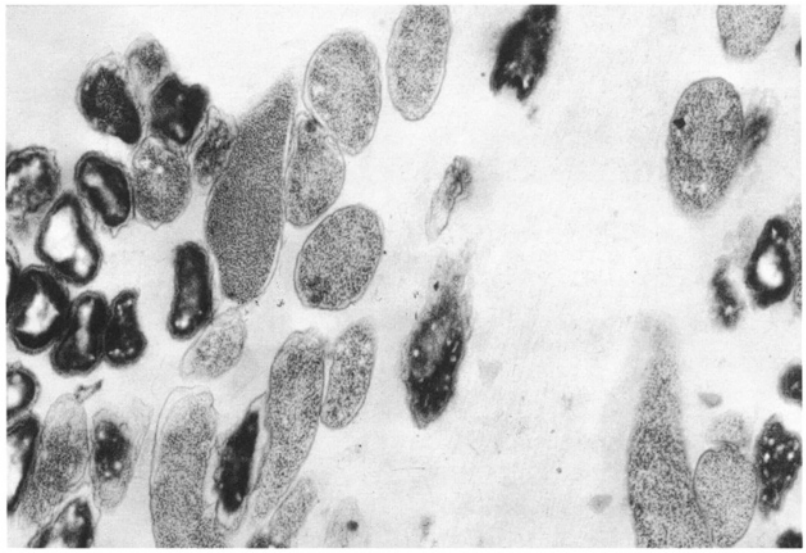

Figure 97. Slam-frozen cells of *Escherichia coli* showing cells with relatively well-preserved cytoplasmic contents intermixed with cells severely damaged by the freezing process. 21,538×.

Figure 98. (A) Slam-frozen cells of *Aspergillus fumigatus* that were subjected to molecular distillation, osmium vapor, and Spurr resin embedment before being sectioned and stained with uranyl acetate. Note that the cell on the right has a burst nuclear envelope, and nucleoplasm has spilled into the cytoplasm. The small electron-lucent areas in the cytoplasm are areas of ice nucleation during the freezing process. 23,846×.

by molecular distillation, treated with osmium vapors, embedded in Spurr resin, sectioned, and stained with uranyl acetate. The nucleus in the right-hand cell has a discontinuous nuclear envelope because the cell was crushed during the cryofixation step. Figure 98B shows a mouse liver that was slam-frozen and then cryosubstituted with acetone containing osmium, followed by embedment in Spurr resin. The nuclei, mitochondria, and rough endoplasmic reticulum are clearly visible, though their appearance is different from that seen with conventional chemical fixation.

Further discussions of cryofixation artifacts can be found in Crang and Klomparens (1988), Robards and Sleytr (1985), and Steinbrecht and Zierold (1987).

(B)

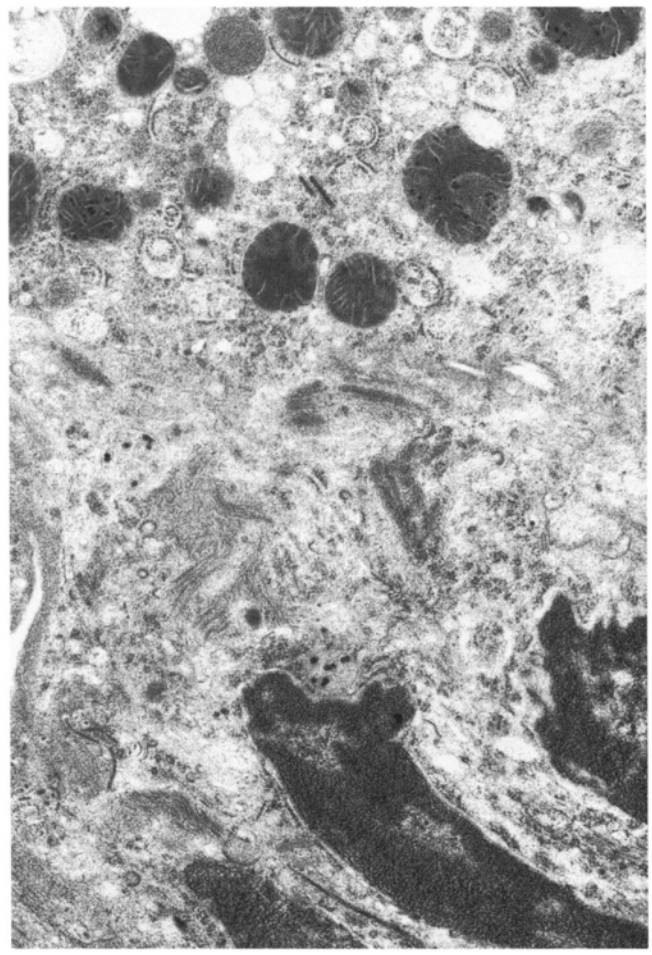

Figure 98. (B) Slam-frozen mouse liver, cryosubstituted with acetone containing osmium, followed by embedment in Spurr resin. 16,000×.

REFERENCES

Bachmann, L. and Schmitt-Fumian, W.W. 1973. Spray-freezing and freeze-etching. In E.L. Benedetti and P. Favard (eds.), *Freeze-etching, techniques and applications*. Société Française de Microscopie Électronique, Paris.

Bernhard, W. 1965. Ultramicrotomie à basse temperature. *Ann. Biol.* 4: 5.

Bhakdi, S., Tranum-Jensen, J., and Sziegoleit, A. 1985. Mechanism of membrane damage by streptolysin-O. *Infect. Immun.* 47: 52.

Costello, M.J. and Corless, J.M. 1978. The direct measurement of temperature changes within freeze-fracture specimens during rapid quenching in liquid coolants. *J. Microsc.* 112: 17.

Crang, R.F.E. and Klomparens, K.L. 1988. *Artifacts in biological electron microscopy*. Plenum Press, New York.

Dubochet, J. 1995. High-pressure freezing for cryoelectron microscopy. *Trends Cell Biol.* 5: 366.

Dubochet, J., McDowall, A.W., Menge, B., Schmid, E.N., and Lickfield, K.G. 1983. Electron microscopy of frozen-hydrated bacteria. *J. Bacteriol.* 155: 381.

Fernandez-Moran, H. 1957. Electron microscopy of nervous tissue. In D. Richter (ed.), *Metabolism of the nervous system*. Pergamon Press, Oxford.

Gilkey, J.C. and Staehelin, L.A. 1986. Advances in ultrarapid freezing for the preservation of cellular ultrastructure. *J. Electron Microsc. Tech.* 3: 177.

Handley, D.A., Alexander, J.T., and Chien, S. 1981. The design of a simple device for rapid quench freezing of biological samples. *J. Microsc.* 121: 273.

Harvey, D.M.R. 1982. Freeze-substitution. *J. Microsc. (Oxford)* 127: 209.

Howard, R.J. and Aist, J.R. 1979. Hyphal tip cell ultrastructure of the fungus *Fusarium*: Improved preservation by freeze-substitution. *J. Ultrastruct. Res.* 66: 224.

Lee, R.E., Jr. and Denlinger, D.L. (eds.). 1991. *Insects at low temperature*. Chapman & Hall, New York.

Linner, J.G., Livesey, S.A., Harrison, D.S., and Steiner, A.L. 1986. A new technique for removal of amorphous phase tissue water without ice crystal damage: A preparative method for ultrastructural analysis and immunoelectron microscopy. *J. Histochem. Cytochem.* 34: 1123.

Monaghan, P., Perusinghe, N., and Müller, M. 1998. High-pressure freezing for immunocytochemistry. *J. Microsc.* 192: 248.

Moor, H. 1986. Theory and practice of high pressure freezing. In R.A. Steinbrecht and K. Zierold (eds.), *Cryotechniques in biological electron microscopy*. Springer-Verlag, New York.

Moor, H., Bellin, G., Sandri, C., and Akert, K. 1980. The influence of high pressure freezing on mammalian nerve tissue. *Cell Tissue Res.* 209: 201.

Moor, H., Muhlethaler, K., Waldner, H., and Frey-Wyssling, A. 1961. A new freezing ultramicrotome. *J. Biophys. Biochem. Cytol.* 10: 1.

Moor, H. and Riehle, U. 1968. Snap-freezing under high pressure: A new fixation technique for freeze-etching. In D.S. Bocciarelli (ed.), *Proceedings of the Fourth European Regional Conference on Electron Microscopy, Rome.* Tipografia Poliglotta Vaticana, Rome, 2: 33.

Müller, M., Meister, N., and Moor, H. 1980. Freezing in a propane jet and its application in freeze-fracturing. *Mikroskopie (Wein)* 36: 129.

Robards, A.W. and Crosby, P. 1983. Optimisation of plunge freezing: Linear relationship between cooling rate and entry velocity into liquid propane. *Cryo-Letters* 4: 23.

Robards, A.W. and Sleytr, U.B. 1985. *Low temperature methods in biological electron microscopy*. Elsevier, New York.

Roos, N. and Morgan, A.J. 1990. *Cryopreparation of thin biological specimens for electron microscopy: Methods and applications. RMS Microscopy Handbook No. 21*. Oxford University Press, New York.

Sjostrand, F.S. and Baker, R.F. 1958. Fixation by freeze-drying for electron microscopy of tissue cells. *J. Ultrastruct. Res.* 1: 239.

Steere, R.L. 1957. Electron microscopy of structural detail in frozen biological specimens. *J. Biophys. Biochem. Cytol.* 3: 45.

Steinbrecht, R.A. and Müller, M. 1987. Freeze-substitution and freeze-drying. In R.A. Steinbrecht and K. Zierold (eds.), *Cryotechniques in biological electron microscopy* (pp. 149–172). Springer-Verlag, New York.

Steinbrecht, R.A. and Zierold, K. (eds.). 1987. *Cryotechniques in biological electron microscopy*. Springer-Verlag, New York.

Tokuyasu, K.T. 1973. A technique for ultramicrotomy of cell suspensions and tissues. *J. Cell Biol.* 57: 551.

Van Harreveld, A. and Crowell, J. 1964. Electron microscopy after rapid freezing on a metal surface and substitution fixation. *Anat. Rec.* 149: 381.

CHAPTER 2 TECHNIQUES

Cryoultramicrotomy for Structural Examinations or Consequent Immunolabeling

1. Applications and Objectives

This technique has been successfully used to prepare frozen sections for structural examination and immunolabeling for a variety of tissues and cells. The technique was pioneered by Tokuyasu (1973, 1980) and has since become a standard technique (Webster, 1998). The strength of the Tokuyasu technique is that it employs minimal fixation, very few solvents, and no resins, and avoids the heating process normally utilized to polymerize many embedding media. The procedure is quick and is one of the best ways to produce materials for consequent intracellular immunolabeling.

2. Materials Needed

- An ultramicrotome equipped with a cryostage
- Glass knives prepared without boats
- Eye brow lash on applicator stick
- Standard loop for picking up sections
- Small glass Petri dish
- Formvar- and carbon-coated grids
- Forceps
- Single-edge razor blades
- Whatman™ #1 filter paper
- Liquid nitrogen
- Freon 22™
- 2.3 M sucrose in DPBS. To prepare sucrose, put 7.378 g of sucrose into a vial and add approximately 5 ml of DPBS to bring the volume up to 10 ml. Mark the vial at the 10-ml level with a marker first.
- 2% aqueous methylcellulose (Sigma M6385) solution. Stir the powder into hot water and then leave at 4°C for 4 days to dissolve completely. After preparation, keep cool at all times.
- Glutaraldehyde (25% biological grade)
- Paraformaldehyde
- 0.1 N NaOH
- 0.2 M sodium phosphate buffer
- Single-edge razor blades
- Stainless steel cup (50 ml)
- Wide-mouth, short (soup) thermos
- 2% aqueous ammonium molybdate

3. Procedure

1. Preparation of the fixative
   a. Dissolve 2 g of paraformaldehyde in 50 ml of 70°C distilled water. Use a stir bar and work under the hood.
   b. Add 1 N NaOH with stirring until the solution clears.
   c. Cool to room temperature.
   d. Add 4 ml of 25% glutaraldehyde.
   e. Add 0.2 M phosphate buffer pH 7.2–7.4 to bring the volume to 100 ml.

2. Place small pieces less than 1-mm thick in the fixative solution.
3. After 1 hr at room temperature, use a razor blade to remove 0.5 × 1.0 mm pieces from the surface of the fixed sample.
4. Rinse for 5 min in DPBS (three changes).
5. Put tissues into 2.3 M sucrose in DPBS for 1 hr to overnight (store at 4°C).
6. Use a razor blade to prepare pieces of tissue approximately 0.5 × 0.2 mm. Mount them in a drop of the sucrose medium on the tip of an ultramicrotome sample pin suitable for the cryostage assembly available. Blot excess sucrose with filter paper.
7. Pick up the pin with attached tissue and quickly plunge it into a stainless steel cup containing Freon 22™ that is suspended in a thermos containing liquid nitrogen (Fig. 99). Hold the pin below the surface of the Freon for 30 sec and then quickly transfer it to another thermos containing liquid nitrogen. The Freon will freeze in the cup, but a small area can be thawed out by inserting a steel rod into the Freon just before the sample is introduced. *Many workers freeze the samples directly in liquid nitrogen with good results.*
8. Mount the frozen sample in the chuck of the cryostage assembly being used. Do this quickly, so the sample does not warm up. Adjust the knife temperature to −105°C and set the sample temperature to −100°C.
9. Orient the chuck so that the top and bottom sides of the sample, as it will be sectioned, are oriented vertically. Trim the vertical edges with a glass knife or carbide cutting tool in the ultramicrotome chamber so that the vertical sides are absolutely parallel.
10. Rotate the block 90° to restore the top and bottom (trimmed edges) to a horizontal position. The block should be oriented so that the longest block face is parallel to the knife edge. *Do not trim excessive amounts off of the surface of the block. Freezing artifacts will be noticed only several cells from the surface of the tissue in some cases.*
11. Cut 70- to 90-nm-thick sections with a new, dry glass knife. The ultramicrotome should be set for the maximum arm return speed and the smallest cutting window that will allow the entire block face to be cut (as close as possible to 0.2 mm if the block face is trimmed as suggested above). Set the cutting speed to 0.1 mm/sec or as close to that setting as the particular ultramicrotome will allow.

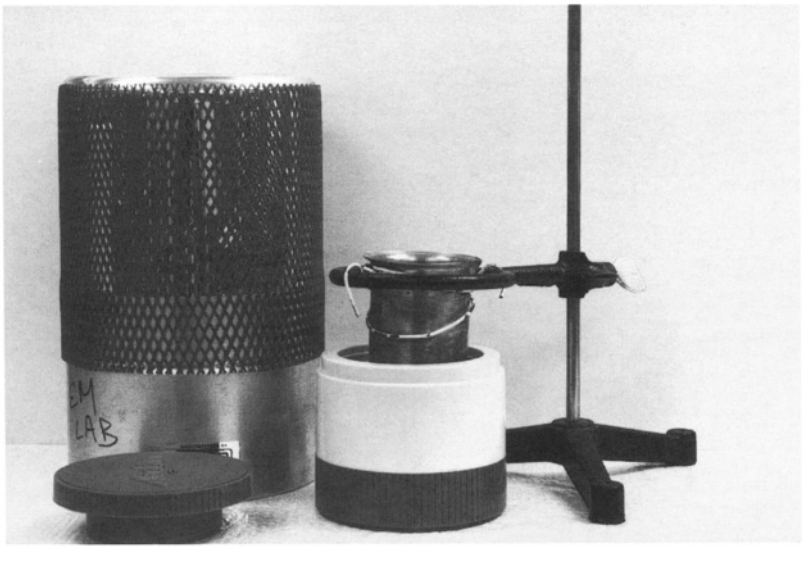

Figure 99. Apparatus for immersion-freezing samples showing stainless-steel cup suspended by wire from a ring such that the base of the cup is immersed in liquid nitrogen contained in a soup thermos. Frozen samples are subsequently dropped into the large glass Dewar at the left. Do not use the soup thermos lid when the container is filled with liquid N_2 because the thermos could explode when the liquid N_2 becomes gaseous N_2.

12. After a ribbon of three or four sections has been cut, use a standard section loop to pick up a drop of 1 part of 2.3 M sucrose and 1 part of 2% methyl cellulose (keep the solution in a small tube on ice before use). Lower the loop into the cryochamber and, just before the sucrose/methylcellulose freezes, touch it to the sections near the edge of the knife (Fig. 88).
13. Remove the loop from the chamber and allow the sucrose droplet to reach room temperature. Touch the surface of the droplet to the surface of a Formvar- and carbon-coated grid. This transfers the sections to the grid as well as most of the sucrose/methylcellulose droplet.
14. If you wish to view the sections immediately, place the grid section-side down in a small Petri dish of double-distilled water (DDW) to allow the sucrose/methylcellulose to flow off the surface of the grid.
15. Use a piece of filter paper to wick the grid dry and then stain it for 30 s with 2% ammonium molybdate before wicking it completely dry with a piece of filter paper. Alternatively, the sections can be stained in 9 parts of the methyl cellulose solution to 1 part of 3% aqueous uranyl acetate. If this mixture is to be used, mix it up just before use and keep the solution on ice at all times. Stain sections for 10 min and then dry with a piece of filter paper.
16. If the grid with sections is destined for immunolabeling, the droplet of sucrose/methylcellulose may be allowed to dry down on the grid until immunolabeling proceeds, preferably within 24 hr.

4. Results Expected

When sections are examined with a TEM, no knife marks should be evident, cellular structures should exhibit negative contrast from the uranyl acetate staining, and antigenic sites should be revealed by gold particles.

5. Cautionary Statements

When freezing the sample, plunge it quickly into the cryogen to minimize ice crystal formation. In addition, when transferring the sample to the cryostage, do so quickly to prevent thawing and consequent ice crystal formation. Trim as little as possible off the surface of the block face to avoid revealing the inevitable freezing damage found within the interior of the frozen sample. Samples left in 2.3 M sucrose overnight will be easier to cut, but times as short as 30 min may work, though uneven infiltration may occur, compromising section quality.

References

Tokuyasu, K.T. 1973. A technique for ultracryotomy of cell suspensions and tissues. *J. Cell Biol.* 57: 551.

Tokuyasu, K.T. 1980. Immunochemistry on ultrathin frozen sections. *Histochem. J.* 12: 381.

Webster, P. 1998. The production of cryosections through fixed and cryoprotected biological material and their use in immunocytochemistry. In N. Hajibagheri (ed.), *Methods in molecular biology, Vol. 117. Electron microscopy methods and protocols*. Humana Press, Totowa, NJ.

3

Ultramicrotomy

I. ULTRAMICROTOMES

A. Purpose

An ultramicrotome is designed to cut ultrathin sections (10–100 nm), semithin sections (0.25–0.5 μm), and ultrathin frozen sections if suitably equipped. These requirements have resulted in the development of two basic instruments over the years: thermal- and mechanical-advance ultramicrotomes. An excellent and concise source of information on ultramicrotomy is the booklet "Ultramicrotomy: Frequent Faults and Problems" by Sitte (1981). A more lengthy discussion of ultramicrotomy can be found in Reid's (1975) book.

B. Design

All modern ultramicrotomes have the following important features:

1. A knife-holding stage with adjustments for lateral swings of the knife, as well as the ability to tilt the knife at various angles. The former feature allows lateral swings of the knife edge to accommodate a block face trimmed to some angle other than perpendicular to its long axis, while the latter feature allows adjustment of the holder for glass knives and diamond knives that manufacturers specify for use at angles between 0 and 10°.
2. A movable specimen-holding arm, which either retracts or follows a circular arc to permit single-pass cutting. This feature, the first major modification made to the original design of histological-type microtomes, was added because the first microtomes did not have single-pass cutting, which meant that the block face touched the knife edge on the return stroke after a section had been cut. At the ultrastructural level, this contact causes damage to the block face and thus the ensuing sections.
3. A knife stage with coarse and fine advance capabilities is necessary to approach the block and to cut semithin sections.
4. A specimen-holding arm with ultrafine (nanometer range) advance capabilities, provided by thermal or mechanical advance mechanisms, with or without stepping motors is necessary to cut reproducible ultrathin sections. The thermal units accomplish this by heating a thermally expansive block attached to the specimen arm with an internal light bulb controlled by a rheostat (Reichert OM-U2 and OM-U3) or by having a set of coils wrapped around the arm connected to a rheostat that allows adjustment of the heat delivered (LKB). Some mechanical advance units have a simple threaded shaft with fine increments that allow direct nanometer-level advance adjustments (Porter-Blum MT-1, MT-2, MT-2B), while others utilize stepping motors to move the arm forward specified distances on a finely threaded shaft (Sorvall MT-6000; RMC MT-X; Reichert, Ultracut-E, Leica UCT).

5. Diffuse overhead lighting, provided by fluorescent tubes, is needed to judge section thickness by interference colors produced when sections are floated off on water. The diffuse light source reflects off the surface of the sections and also passes through the section to reflect off the surface of the water beneath. The latter reflected light has a slightly longer path back to the viewer than the former, so an interference color is developed that can be used to determine the section thickness. All ultramicrotomes designed after the 1970s also have some form of backlighting with an incandescent source to aid in approaching the block with the knife.
6. All models produced since the 1980s can be adapted for cryoultramicrotomy. Some cryostages are dedicated to their manufacturer's ultramicrotomes (Leica), while others may be fitted to a variety of instruments (RMC).
7. All ultramicrotomes have variable cutting speeds for flexibility when dealing with different types of blocks. Thus, the user can adjust the ultramicrotome for use with soft biological tissues in epoxide resins, frozen blocks of biological tissues, or resin-embedded materials such as kidney stones or battery insulator plates.
8. Most ultramicrotomes have a slow cutting stroke and a faster return speed. Some also have variable return speeds. The variable return speed is claimed to improve the quality of ultrathin frozen sections (Sitte, personal communication).
9. Currently produced ultramicrotomes have an adjustable cutting window that allows the user to position the slow cutting stroke portion of the arm movement such that it starts shortly before the block passes by the knife edge and ends immediately after the block has reached a position below the knife edge. This allows the user to work with different-sized block faces as well as with blocks oriented in various ways in the chucks used to hold them on the ultramicrotome arm.
10. Cutting force is supplied by gravity (LKB, Reichert/Leica), or the arm is driven (Sorvall, RMC). Both systems seem to work equally well.

C. History

Early attempts toward ultramicrotome design go back to 1939 when Von Ardenne modified a histological rotary microtome to cut wedges, the edges of which were thin enough to allow the electron beam to penetrate them. During the early 1950s, single-pass ultramicrotomes capable of cutting sections of uniform thickness were developed. Porter and Blum in the United States initially produced a thermally advanced unit but found that the slightly later MT-1 design that utilized mechanical advance was superior. This instrument had mechanical advance and was manually operated, with only a single fluorescent overhead light, making it the simplest of the ultramicrotomes ever produced.

During the same time period, Sitte was working in Austria to develop the Reichert OM-U1. This unit had thermal advance and cut sections automatically, but Sitte was never very satisfied with its operation. In 1957, the British Huxley MK1, which was a manual instrument with mechanical advance, was marketed.

The early 1960s saw another manufacturer enter the picture, the Swedish company LKB. They marketed the Ultrotome I, which had thermal advance in an automatic machine with a magnetically retracted arm that allowed single-pass cutting.

By 1962, Porter and Blum had developed the mechanical-advance, automatic MT-2, which quickly developed a reputation for reliability and stability. Many of these instruments can still be found in operation in various laboratories. The Reichert OM-U2 appeared on the market in 1964,

which was a thermal advance automatic unit with an adjustable cutting window, and variable cutting stroke and return speeds. LKB developed the Ultrotome III, which had a novel lighting arrangement, incorporating both an incandescent and fluorescent light in an overhead boom. The light boom could be swung over a wide arc from behind the knife to in front of the knife, depending on whether the user wanted to see the interference colors of the sections or a good reflection in the block face during the approach of the knife to the specimen. In 1970, Huxley released the MK-2, which was a mechanical advance, automatic machine. Shortly afterward, Reichert marketed the OM-U3, which had a backlight for specimen advance and various minor modifications in the knife stage controls and specimen adjustment controls when compared to the OM-U2.

The late 1970s saw the development of a new generation of ultramicrotomes with an emphasis on greater mechanical stability due to the increasing interest in cryoultramicrotomy, which introduced new design problems that had to be addressed. Along with this development, most of the manufacturers incorporated methods to have more adjustability in various operating parameters. The MT-2B from DuPont/Sorvall had an adjustable return speed for the first time. Reichert switched from their traditional thermal advance to mechanical advance with the Ultracut (OM-U4) introduced in 1978. Sitte's interest in producing an instrument more suited to cryo work was the impetus behind the development of this ultramicrotome. LKB produced the Nova, which abandoned the vacuum-tube technology of the Ultrotome III for more stable solid-state technology and also introduced the Ultrotome IV as their top-of-the-line instrument. By the late 1970s, DuPont/Sorvall produced the MT-5000, which had an adjustable cutting window for the first time as well as a stepping-motor controlled mechanical advance for the automatic cutting cycle. In addition, Huxley had bowed out of the ultramicrotome business.

During the 1980s, further refinements of ultramicrotome design devoted primarily toward the growing cryo market resulted in the development of ultramicrotomes from each manufacturer that could be adapted easily for cryoultramicrotomy.

In 1985, DuPont got out of the microtomy business and passed on most of its product line to RMC. Around 1986 and 1987, a series of corporate mergers resulted in Cambridge Instruments buying Reichert and then also buying LKB's microtomy line. In 1990, Leitz bought out Cambridge Instruments, and the various electron microscopes and specimen preparation equipment, including ultramicrotomes, are now marketed under the name Leica. At the present time, there are only three suppliers of ultramicrotomes in the United States: RMC, which offers the MT-X, Leica, which offers the UCT, and Microstar, which offers the MS1B Ultramicrotome.

II. KNIVES

A. History

Ultramicrotomy knife development began, as did ultramicrotome development, with the utilization of materials available from histological microtomy. Thus, attempts to cut ultrathin sections began with steel knives that were polished to extremely thin edges. Unfortunately, it was immediately determined that the microcrystalline structure of steel prevented the production of knife-mark-free sections. In 1950, Latta and Hartman introduced glass knives made from plate glass scored and broken into triangular pieces. These had the benefit of having extremely sharp edges that could produce sections of resin-embedded materials fairly consistently without excessive knife marks. These remain in routine use today with materials costing about 15¢ per knife. Glass knives suffer from fragility, however, and only about 10 ultrathin sections are usually cut on one area of a knife before significant knife marks begin appearing in sections. In addition, after

one semithin section is cut on a sharp area of a glass knife, that area will probably be too damaged to cut any further ultrathin sections.

The search for more durable knives was greatly aided by Dr. Umberto Fernandez-Moran (see Hawkes, 1985), who realized that diamonds would be much harder than glass and developed a process for sharpening gem-grade (flaw-free) diamonds, which ultimately had edges in the 1- to 1.5-nm thickness range. He reported on this finding in 1953 and ultimately set up a diamond-knife manufacturing group utilizing gem-grade alluvial diamonds available in his native Venezuela. Over the next 25 years, diamond knives became the tools of choice for cutting ultrathin sections due to their durability when handled properly. Fewer than a half-dozen manufacturers exist to this day, and the product is relatively expensive (approximately $2,500 for a 3-mm-long blade), but diamond knives allow workers to cut hundreds of serial sections on one part of the knife edge, and they can be resharpened a number of times for about $1,000 per sharpening.

In the late 1980s, sapphire knives became available as a compromise between inexpensive but limited-life glass knives and expensive but long-life diamond knives. Sapphire is neither as expensive as diamond nor as long-lasting. However, a sapphire knife will outlast a glass knife considerably.

When shopping for diamond knives, quite a variety are available from different vendors. There are knives produced primarily for working with soft biological tissues, knives produced primarily for materials scientists interested in sectioning extremely hard substances, knives without boats for use in cryoultramicrotomy, and knives of a lower edge quality, marketed for cutting semithin sections.

B. Glass Knife Manufacturing

Glass knife manufacturing began with, and can still be conducted using, simple tools available from the glazier's supply house. A simple glass cutter, straight edge, and glazier's pliers can be used to make glass knives. To produce two sharp knives regularly from one small square of glass usually requires the services of a knifebreaker specifically designed for the task. Several manufacturers produce these instruments that allow the user to easily cut glass strips into glass squares and then to cut the squares into two usable knives.

Glass knives for ultramicrotomy are made from plate glass, preferably "float" glass. This glass is made by floating the molten glass onto a surface rather than running the molten glass through rollers ("roller" glass) to dimension it. The latter develops many stress lines that may affect the ability to fracture the glass in the plane desired when making knives. All the glass sold by electron microscopy suppliers is float glass and will make suitable knives for sectioning.

C. Diamond Knives

Diamond knives are clearly superior to glass knives in that they can cut hundreds to thousands of sections in the same place compared with 4–10 in the case of a glass knife. Unfortunately, they are also considerably more expensive because they are made by fracturing diamonds of gem quality in the plane of the crystal and then polishing them before they are mounted in a metal boat. Diamond knives, when handled properly, are quite durable, but small mistakes can damage them instantly. The edge of a diamond knife is about 10 nm thick, so it is quite fragile. Any twisting of this edge can fracture the diamond crystal lattice. Exceptionally thick sections can also break off the edge of the knife. Diamond knives can tolerate quite a number of 0.25- to 0.5-μm-thick sections, but they will dull the knife more quickly than ultrathin sections. If epoxide sections are allowed

to dry on the knife edge, they can become molecularly bonded to the edge, necessitating knife resharpening before sections can be successfully cut on that area of the knife again. The diamond knife washers currently on the market do not seem to be able to correct this problem. Finally, it is always wise to cut semithin sections and to stain them prior to cutting ultrathin sections to look for knife-damaging materials in the block face. Various samples will be found to have some hard substances in them that can be revealed by examining glass-knife-produced semithin sections with a light microscope. If possible, it is a good policy to trim away these hard areas prior to ultrathin sectioning to help preserve the edge of the diamond knife.

Manufacturers of diamond knives specify the angle to use for cutting, though this should always be empirically checked by the user. It is imperative to check the quality of a new or newly sharpened diamond knife immediately upon receipt. Most manufacturers give a limited warranty for a month or so, during which time the knife can be sent back if it does not section adequately. New knives sometimes do not cut well. Make sure all knives are checked before the warranty expiration date.

Some manufacturers say never to clean the knife edge with balsa sticks or styrofoam blocks, while others say you should. The best procedure is probably to follow the manufacturer's included suggestions for knife care.

III. BLOCK TRIMMING

Large block faces cause more stresses on knife edges, resulting in more compression in the sections, more damage to the knife edge, and generally more artifact-laden sections. Thus, trimming blocks to the proper size is an important activity. There are three major methods commonly used to trim block faces:

1. Razor blades, and in particular single-edge razor blades, are most commonly used. *It is extremely important always to hold both edges of the razor blade.* If the thumb and forefinger of each hand are used to control the blade, the chance of any serious razor blade wounds is drastically reduced. If only one side is held, there is a good chance that the blade will slip, and the back of the other hand will be cut. Various chuck-holding assemblies are provided by ultramicrotome manufacturers to hold chucks containing blocks for trimming.
2. Milling machines are also available. Leica's EM Trim Specimen Trimmer can be provided with a diamond bit, which can mill the front and sides of a plastic block by passing the diamond bit, rotating at approximately 10,000 rpm, past the block face. The chuck holding the specimen can be moved in various directions for trimming the edges as well as the face of the block. As mentioned in the section on resins, British investigators have suggested that some polymerized epoxide resins are carcinogenic and that the fine plastic resin dust produced by milling operations may be dangerous. Leica's approach to the problem has been to provide a shield over the cutting area with a vacuum hose attached to pick up the resin dust. The main advantage of a milling machine over razor blades is that it can produce absolutely parallel top and bottom faces that have very smooth edges. This greatly improves the possibility of producing long ribbons of sections (for serial section work).
3. Block trimming can be accomplished directly on most modern ultramicrotomes, since most come with a device to hold a chuck in the same track that normally holds the knife holder assembly. The blocks can then be trimmed with razor blades on the microtome. This procedure produces a fair amount of potentially toxic epoxide debris that also gets

into the ultramicrotome body itself, and thus is not recommended. A block held in the chuck attached to the ultramicrotome specimen arm can also be trimmed with glass knives, both on the sides and on the face. Again, this produces a large amount of debris (potentially toxic) consisting of plastic sections.

IV. ULTRAMICROTOMY WORKING AREA

Ultramicrotomes should be set up in a vibration- and draft-free area (Fig. 100). In addition to the ultramicrotome, the work area should be provided with glass microscope slides, a squeeze bottle with distilled water for filling the knife boat, a tuberculin syringe with needle to adjust the water level in the boat, a loop on a stick for picking up semithin sections, an eyelash or eyebrow lash on a toothpick or applicator stick for moving sections around in the boat, fine-tipped forceps for holding specimen grids, grids (200-mesh copper grids for routine work), grid cleaning solutions, Whatman™ #1 filter paper in 10-cm disc form, and a small tape dispenser with Scotch™ tape. If using Spurr resin, which suffers from compression more than most epoxides, you will also need a small bottle of xylene or chloroform and an applicator stick that can be soaked in the xylene or chloroform and waved slowly over the ultrathin sections to stretch them out.

It is most convenient to have a hot plate adjusted to approximately 60°C nearby upon which you can place the glass slides with semithin sections in water droplets to dry. If a sink is directly adjacent to the hotplate, semithin sections can be stained and washed after they have annealed to the glass slides.

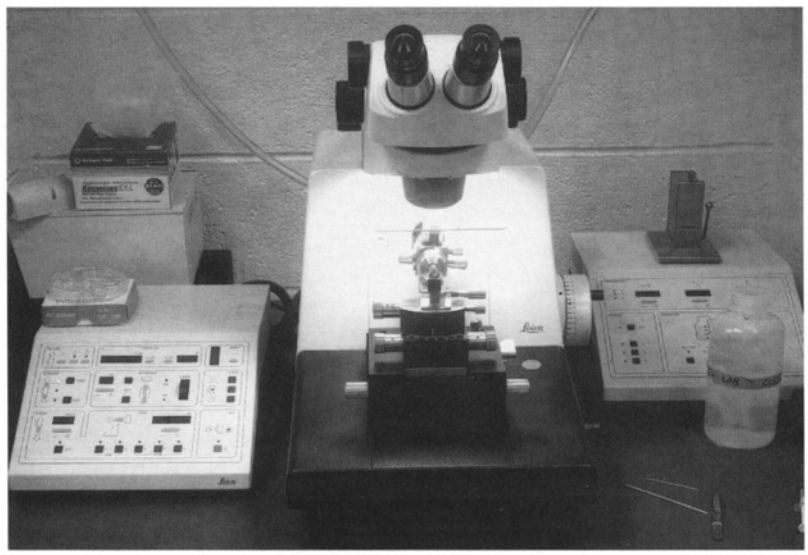

Figure 100. Leica UCT ultramicrotome station.

REFERENCES

Hawkes, P.W. (ed.). 1985. *The beginnings of electron microscopy*. Academic Press, New York.

Reid, N. 1975. Ultramicrotomy. In A.M. Glauert (ed.), *Practical methods in electron microscopy* (Vol. III, Part II, pp. 213–353). North-Holland, Oxford.

Sitte, H. 1981. *Ultramicrotomy: Frequent faults and problems*. AO/Reichert, Vienna.

CHAPTER 3 TECHNIQUES

Making a Section Retrieval Loop

To make a loop with which to pick up semithin sections to be transferred to glass microscope slides, carefully bend a 3-cm-long piece of 26-gauge or thinner nichrome wire over an applicator stick. Make the bend about 0.5 cm from the middle of the wire (Fig. 101A). Hold the two ends of the nichrome wire with needle-nose pliers and turn the applicator stick lengthwise to twist the wire ends together (Fig. 101B). This will provide a nichrome wire loop with an inside diameter of approximately 2 mm with a shank of twisted wire culminating in a single wire about 0.5 cm long. Next, prepare an applicator stick, as follows: heat a

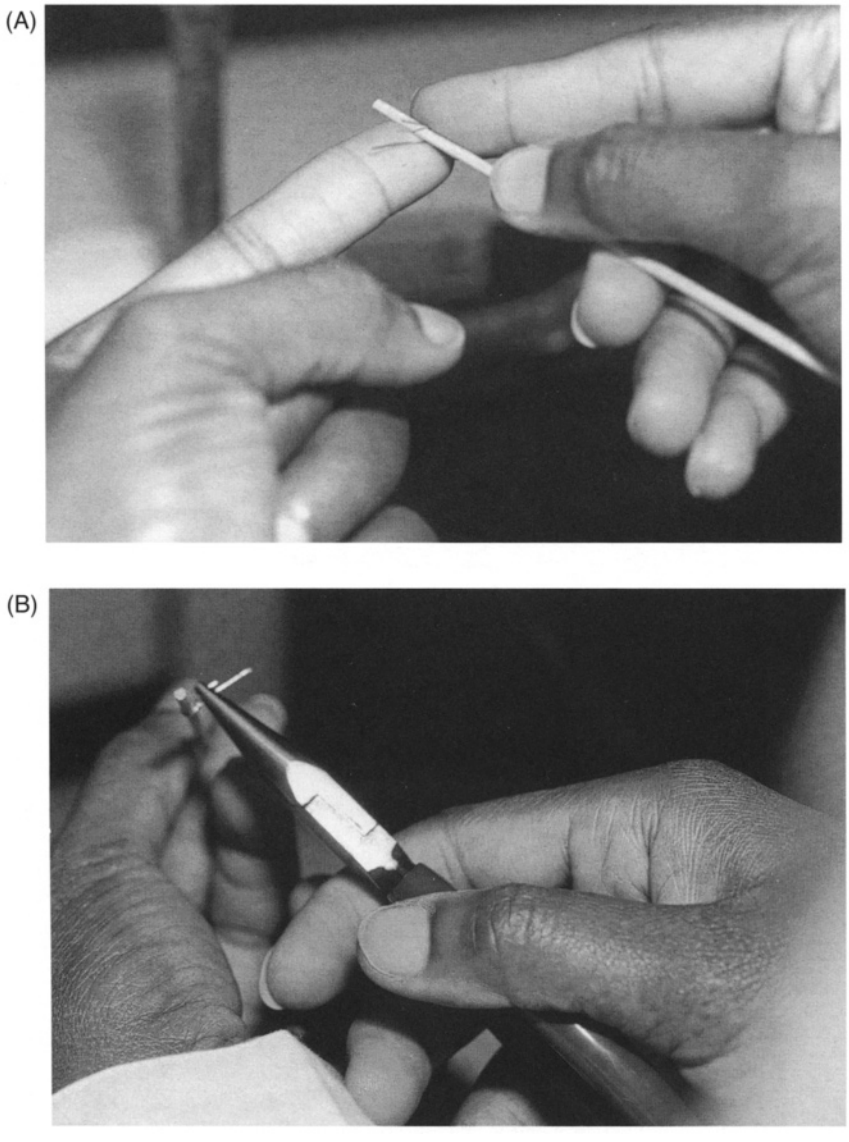

Figure 101. (A) Bending nichrome wire over an applicator stick. (B) Twisting nichrome wire around applicator stick.

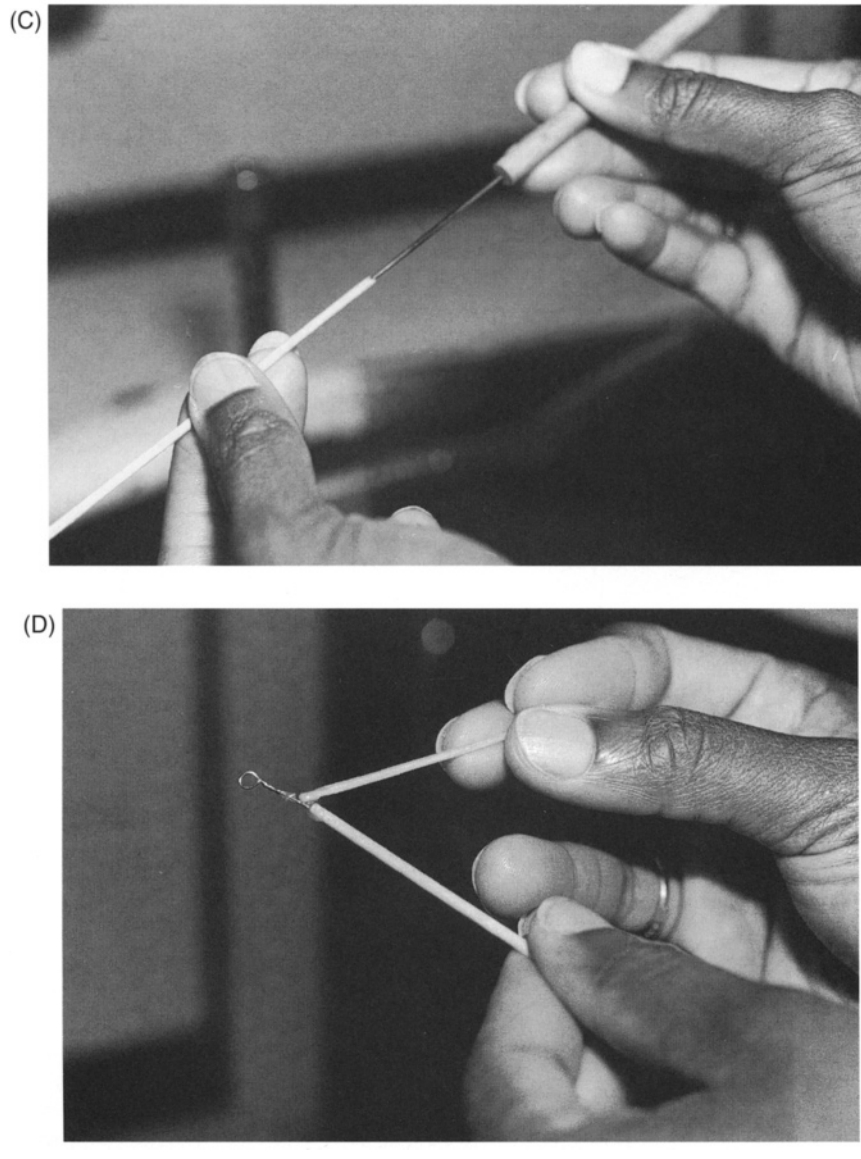

Figure 101. (C) Burning a channel into the applicator stick with a dissecting needle. (D) The final nichrome wire loop inserted into and glued to the applicator stick.

dissecting needle tip to red hot with a Bunsen burner and *very carefully* burn a small channel in the tip of the applicator stick (Fig. 101C). Next, insert the end of the nichrome wire into the burned channel and secure it by applying a small drop of 5-min epoxy to the assembly (Fig. 101D).

Making a Section Manipulation Tool

To move sections around in a knife boat, some sort of hair is attached to either a toothpick or applicator stick. The most readily available source of short, fine-tipped hairs is eyebrows. Pull a few of these

hairs out and pick the straightest one. Put one drop of 5-min epoxy on the end of the stick or toothpick and use jeweler's forceps to insert the hair root into the cement. Once the cement has hardened, the tool is ready for use (Fig. 102).

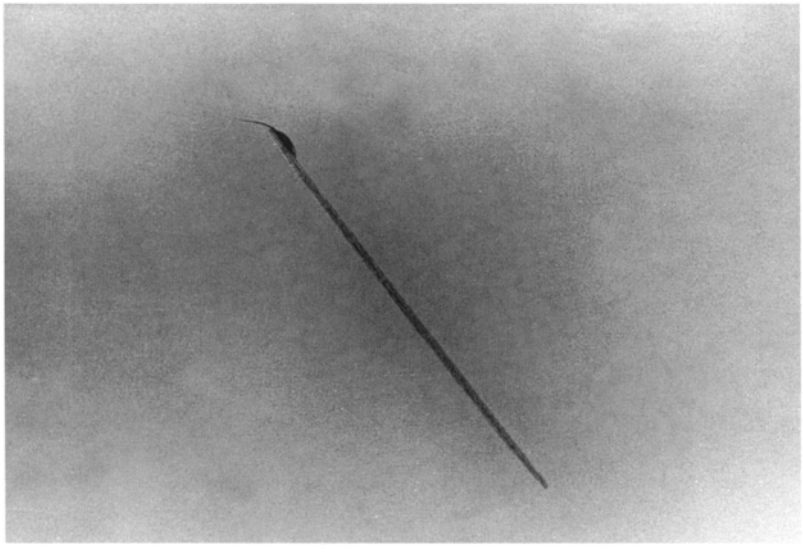

Figure 102. Eyebrow hair attached to a toothpick with epoxy cement.

Making a Locking Ring for Forceps

Since several procedures require a grid to be held in jeweler's forceps for a period of time, it is useful to have a ring that can hold the forceps blades shut. In addition, the tip guards provided with new forceps tend to get lost, so replacements are often needed to protect the forceps tips from damage. Both of these problems can be solved by cutting segments from a 1-ml plastic transfer pipet (Fig. 103A–C).

Making Glass Knives

Glass knives can be produced with various knife breakers. Glass strips suitable for glass knife making (25 mm wide, 6–6.5 mm thick, and 15–30 cm long) are available from electron microscopy supply houses.

Clean the glass strips by rubbing them with Kimwipes™. *Be careful not to cut yourself with the sharp edges of the glass strips.* If the strips do not appear clean after wiping, they can be washed with soap and water and dried before use.

Next, score and break squares from the glass strips. Adjust the knifebreaker so that the cutting wheel does not actually score completely to the edge of the glass. This allows the break along the score line to continue to the edge through the path of least resistance, thus ensuring a cleaner and sharper break. The cutting wheel should be adjusted to barely cut the surface of the glass. As the cutter head is pulled across the glass, a slight "snick" should be heard. The glass should be scored by quickly drawing the cutter across the glass. If the cutter is moved slowly across the glass strip, the glass may not be adequately scored. If

examination of the glass strip surface following scoring reveals small glass slivers or large chips of glass, the cutting pressure should be decreased. The actual breaking of the knife is affected by quickly applying pressure across a fulcrum. The resulting glass square is then cut diagonally to produce two knives. The normal adjustment of the knifebreaker will result in the cutter scoring from outside and to the left of one corner to outside and to the right of the diagonal corner opposite (Fig. 104). This results in the left knife having a sharp edge away from you and a dull edge toward you while the right knife has a sharp edge toward you and a dull edge away from you. As long as no major knife-edge flaws are noticeable to the naked eye, the knife is probably usable. A small percentage of freshly made glass knives will have poor edges, but most sectioning

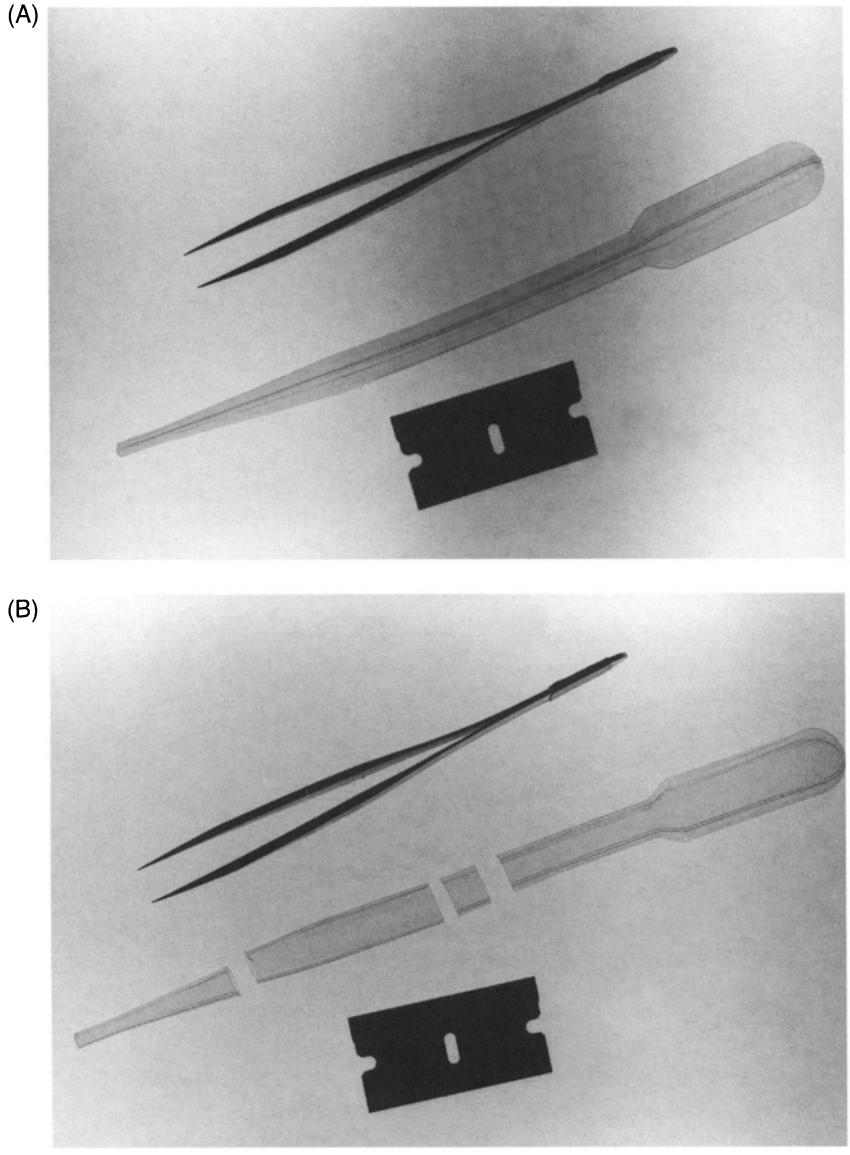

Figure 103. (A) Forceps, plastic transfer pipet, and razor blade. (B) Transfer pipet cut with the razor blade at appropriate points.

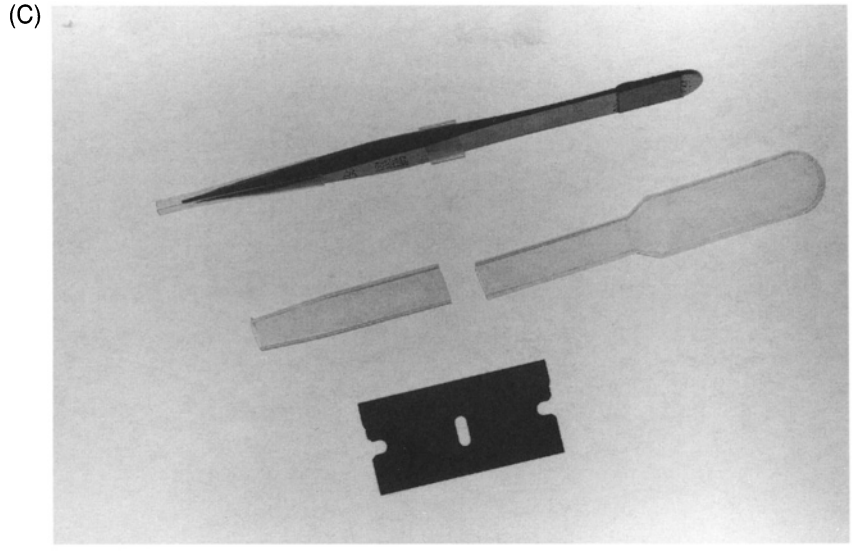

Figure 103. (C) Forceps with tip guard and closing ring in place that were made from the transfer pipet.

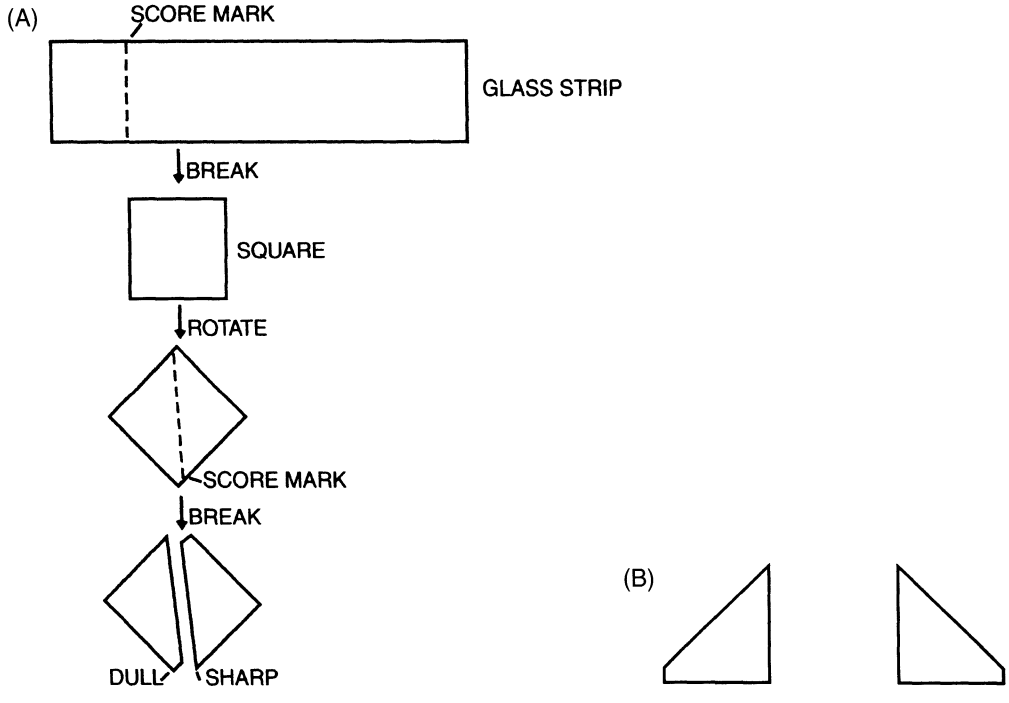

Figure 104. (A) Steps in knife-breaking. (B) The final knives.

difficulties with glass knives result from cutting too many sections in one area, cutting one or more sections that are so thick that they damage the edge, or touching the edge with some blunt object.

A face-on view of a knife edge (Fig. 105) shows the fracture plane curving to the left side of the edge. Where it intersects the knife edge, the knife is the most dull. Anywhere to the right of that area should be

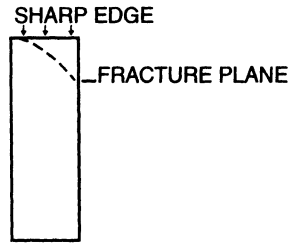

Figure 105. Face view of knife edge showing fracture plane.

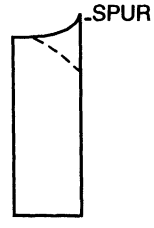

Figure 106. Face-on view of uneven knife edge, illustrating frequently encountered spur on right edge.

good for sectioning. Sitte (1981) has explained that the "whiskered" areas, which can be seen at the far right of the knife edge with back-lighting under a dissecting microscope, represent stair-stepped glass that will yield good sections after the first: However, most workers cut only semithin sections in this area.

The right side of many glass knives often visibly rises to a pointed spur (Fig. 106), but other than losing the acute portion of the blade for sectioning purposes, these spurs are of no concern.

Making Glass Knife Boats

Boats may be made by affixing manufactured plastic or metal forms to glass knives with molten dental wax or by attaching a segment of aluminized mylar™ tape to the knife and then sealing it with nail polish. If the latter technique is used, dry the nail polish for at least 15 min before use to decrease the possibility of boat leakage. Some workers apply a bead of molten dental wax some distance from the knife edge, which will hold several drops of water onto which sections can be cut. Figure 107 shows the three varieties of boats.

Glass Knife Storage

Glass knives can be stored for months before use, provided they are kept in dust-free conditions. Applying double-stick tape to the bottom of a cardboard box allows the knives to be attached by their bases

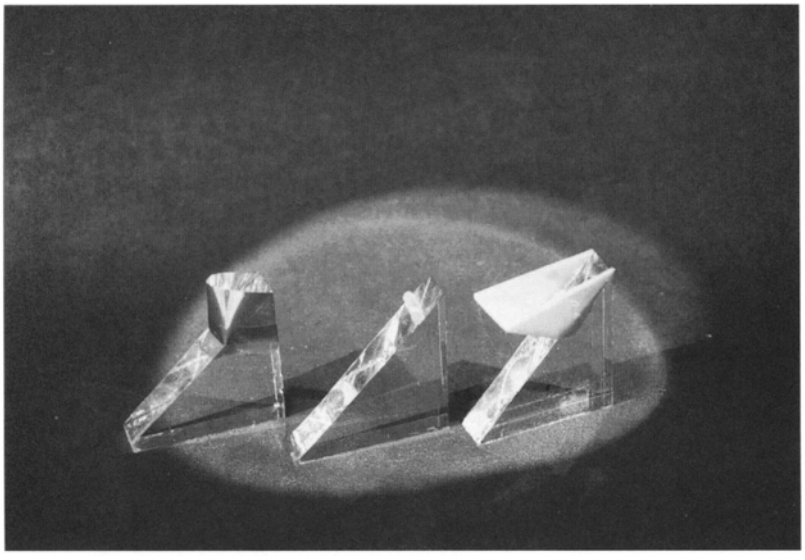

Figure 107. Three types of glass knife "boats."

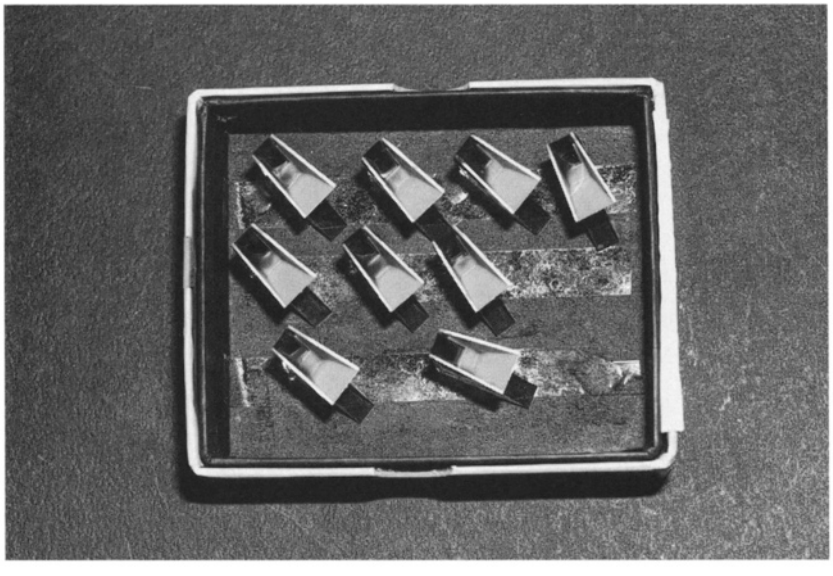

Figure 108. Glass knives affixed to the bottom of a box with double-stick tape.

to the tape to prevent their sharp edges from being degraded by contact with other surfaces (Fig. 108). Plastic boxes with slots for glass knives also may be purchased from electron microscopy supply houses.

Block Trimming

Proper trimming of block faces will decrease section compression, damage to knife edges, and staining artifacts. In most cases, blocks are trimmed so that the entire block face is resin-embedded tissue

(Fig. 109). If the sample has surfaces of interest, trim the block so that the block face contains empty plastic beyond the surface (Fig. 110). In such cases, section the specimen at right angles to the potential direction of separation between the sample-containing and sample-free areas.

Place the block in an ultramicrotome chuck held in a block-trimming holder. A dissecting microscope makes it possible to observe the thin slices of resin removed with a single-edged razor blade. It should be easy to see black material, indicating that you have trimmed down to the specimen.

The sides of the block should be cut down fairly obliquely (Fig. 111). If the sides are perpendicular to the face, the tip of the block will be more likely to flex under the great forces generated during sectioning. Cutting the sides at an oblique angle will provide more support at right angles to the cutting stroke.

Always control the razor blade by holding both edges of the razor blade while trimming (Fig. 112). If the thumb and forefinger of each hand are used to control the blade, the chance of any serious razor blade

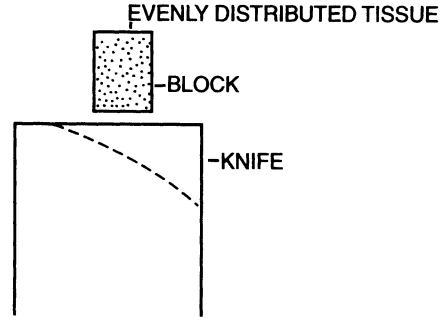

Figure 109. A properly trimmed block face containing a homogeneous sample with no surfaces of interest.

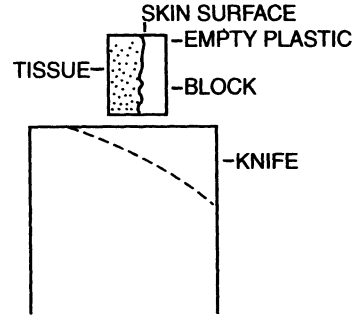

Figure 110. A properly trimmed block face containing skin, the surface of which is of interest and which may tend to separate from the empty plastic during sectioning.

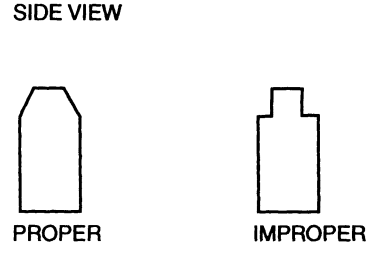

Figure 111. A comparison of properly and improperly trimmed blocks.

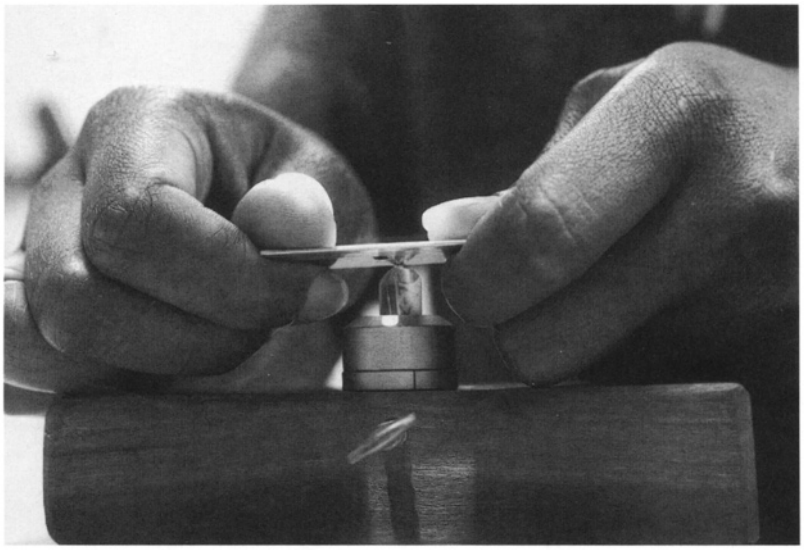

Figure 112. The safest method for holding a razor blade during block trimming. *Note: Both hands are holding the razor blade to totally control the cut.*

wounds is drastically reduced. If only one side is held, there is a good chance that the blade will slip, and the back of the other hand may be cut.

Sectioning Procedures

1. Put a trimmed block into an ultramicrotome chuck and clamp securely. If working with flat blocks, make sure that all four corners are contacting the chuck.
2. Clamp the block chuck securely in the specimen arm of the ultramicrotome.
3. Turn on the overhead (diffuse fluorescent) light source on the ultramicrotome.
4. Put a glass knife into the knife holder and securely tighten the knife securing screw.
5. Adjust the knife angle to 5–6° and tighten the knife angle screw securely.
6. Bring the knife holder stage to within several millimeters of the block held in the specimen arm by looking from the side of the ultramicrotome.
7. Look through the ultramicrotome microscope and inject water into the knife boat with a water bottle or a tuberculin syringe until the water level is convex and the knife edge is completely wetted.
8. Remove water from the knife boat with the syringe until a mirror-like area on the water surface can be seen behind the knife edge while the knife edge remains wetted. If the water level is not properly adjusted, the reflection of the knife edge will not be visible, which is critical for bringing the knife and block together. In addition, the interference colors of the sections floating in the knife boat will not be visible, which is critical for calculating section thickness visually and assessing section quality.
9. Looking through the microscope, use the specimen arm control wheel to bring the specimen arm through its cutting stroke to the point in its travel where the block is opposite the knife edge.
10. Carefully move the knife stage forward until it is within about 1 mm of the specimen block and lock the knife holder stage securely in place.
11. Turn on the ultramicrotome backlight, if so equipped, and look through the microscope, while advancing the knife stage toward the block with the coarse advance control.

12. Depending on the type of ultramicrotome lighting, either a bright reflection or a dark shadow is cast by the knife edge onto the block face when the two are close together. If this reflection cannot be seen easily in the block face, the delicate approach of the knife to the block face will be extremely difficult.
13. Once the block face and knife edge are close enough to each other to produce a reflection or shadow, switch to the fine advance control for the knife stage.
14. Rotate the specimen in the specimen arm as necessary until the top and bottom of the block are parallel to the knife edge (Fig. 113).
15. Sweep the specimen arm slowly through its stroke while observing the reflection of the knife edge in the block face. The reflection should appear as a band across the block face that becomes increasingly narrow as the knife gets closer to the block. The specimen should be swept through its cutting stroke after each forward adjustment to observe any reflection present, and to note how wide the reflection is. A wider reflection indicates a greater distance between the block edge and block face. If the reflection is the same width from right to left, the knife is parallel to the block in a right-to-left direction. If it is wider on one side of the block than on the other, it means that the knife stage should be swung toward the block on the wide side (Figs. 114 and 115). If the reflection is wider as the bottom of the block passes the knife edge and then becomes narrower as the top of the block passes the knife edge (Fig. 116), this means that the top of the block is tilted toward the knife compared with the bottom of the block. This is particularly dangerous if you do not approach slowly, making a pass with each minor adjustment. If the reflection is wider at the bottom of the block than at the top, and the clearance is taken up at the bottom of the block travel without going

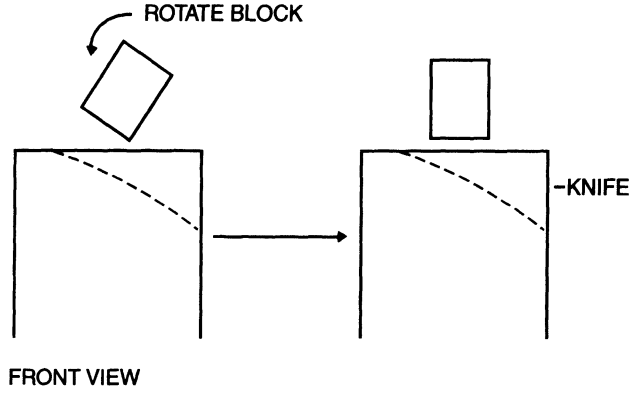

Figure 113. Block rotation to orient the specimen edge parallel to the knife edge.

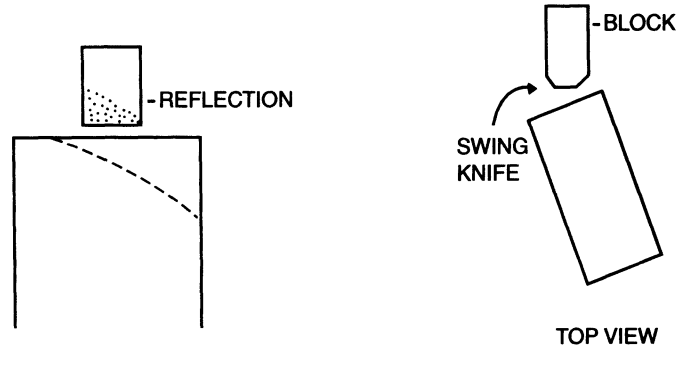

Figure 114. To correct the wide reflection seen on the right side of the block face, swing the knife clockwise.

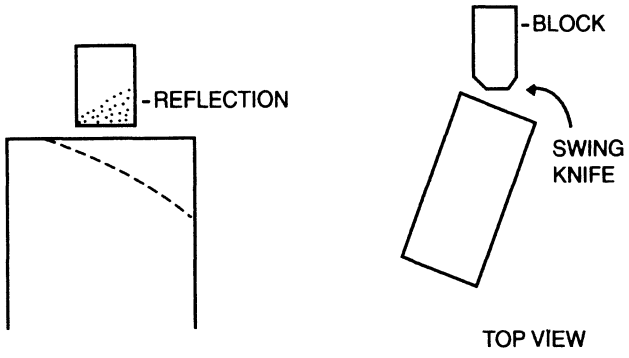

Figure 115. To correct the wide reflection seen on the left side of the block face, swing the knife counterclockwise.

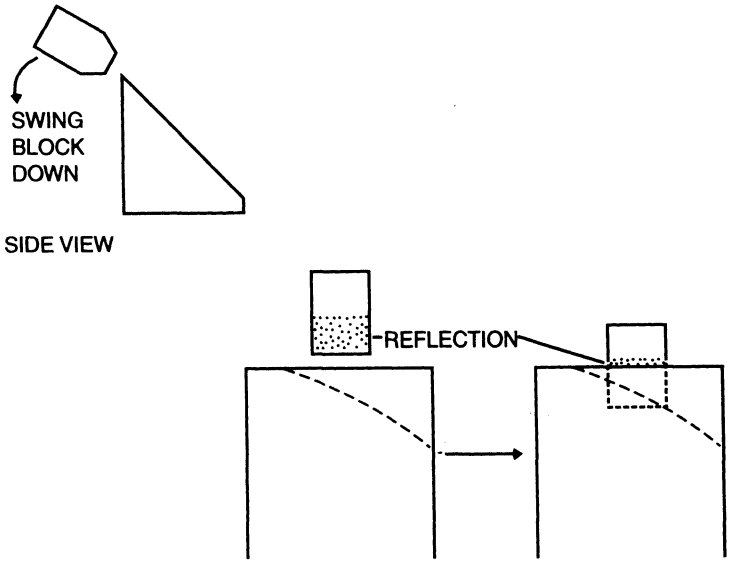

Figure 116. To correct the tilt of the block resulting in a reflective band that is wider at the bottom of the block than at the top, swing the block in the direction shown.

completely through the cutting pass, the knife will be damaged during the next pass. Monitor the distance between the knife and the rest of the block through the cutting cycle while the block is some distance from the knife edge to avoid this problem.

16. After all the adjustments are made so that the reflection is now even side-to-side and stays the same width as the block is passed by the knife edge, slowly advance the fine stage control until the reflection is no longer visible.
17. Now, continue to use the fine stage control to advance the knife about 0.5 μm per cutting pass. When the first semithin section is cut, continue to advance the stage 0.5 μm with each pass until three or four sections have been cut.
18. Pick up the sections with a loop and transfer them onto the drop of water on a microscope slide by touching the section-containing side of the water drop in the loop to a large drop of distilled water placed in the center of the microscope slide shortly before adding sections. Put the slide with semithin sections floating on the water droplet onto a hot plate at approximately 60°C immediately. If the water droplet spreads out before the slide is put on the hot plate, the sections will wrinkle as they dry down because there is not enough surface tension exerted by the water to flatten the sections.
19. Continue cutting semithin sections until no surface imperfections left over from razor blade trimming are visible in the sections floating in the knife boat.

20. To begin cutting ultrathin sections, retract the knife stage somewhat so that the block is nowhere near the knife edge. Then, move the knife stage laterally to a fresh knife edge and reapproach as above. Note that the tilt of the specimen will not have to be readjusted, but the lateral swing adjustments of the knife will have to be redone. After the lateral swing adjustments are made, slowly bring the knife toward the block with the fine advance as before. Once the reflection is no longer visible, adjust the cutting window, if the feature is available on the ultramicrotome, so that the cutting stroke ends when the block is just below the edge of the knife. Then set the cutting speed to 0.5–1.0 mm/sec, and set the cutting thickness to 75–85 nm. Switch the ultramicrotome to the automatic mode and continually observe the cutting process. All ultramicrotomes will require minor adjustments to section thickness during sectioning.
21. When four to 10 ultrathin sections with a silver–gold interference color have been cut, turn off the automatic cycle control and put the arm in its standby position safely away from the knife edge. Remove the last section from the knife edge with an eyelash tool. This is especially important if using a diamond knife, to prevent sections from drying on the knife edge. Once dried to the knife edge, the sections can become permanently bonded to the edge of the diamond knife and will have to be removed by resharpening the knife.

Semithin Sections

Semithin sections are usually cut about 0.25–0.5 μm thick (green to red in color in the boat under diffuse light). They are used mostly to give us an idea of what is contained in the block face. Thus, it is useful to include as much as is practical of the block face. Semithin sections are removed from the boat by submerging a nichrome wire loop tool in the boat water and then bringing it up from beneath the sections. The captured drop of water containing the sections is inverted onto a drop of water previously placed on a glass slide. The droplet is then heated on a hot plate at approximately 60°C so that the sections can adhere to the glass, allowing them to be stained without loss from the slide. *Put the water droplet on the slide just before adding the semithin sections to minimize the spreading of the water droplet, along with consequent spreading out of the semithin sections on the slide.* Twenty to 30 semithin sections can be cut at a given point on a knife edge in most cases. With both semithin and ultrathin sections, the larger the block face, the fewer sections that can be cut before the knife edge becomes degraded. It is generally safe to continue cutting semithin sections until the sections begin to show lines in the direction being cut as they come off into the boat from the knife edge. Many of these microscopic tears caused by degradation of the knife edge will become invisible once the sections are covered with mounting medium and a coverslip is applied.

Block trimming that produces an asymmetrical block face makes it easier to trim down to specific features for subsequent ultrathin sectioning. When semithin sections are picked up and placed on a microscope slide, the sections will be upside down. When they are finally viewed with a compound light microscope, which projects an image of the specimen reversed right to left, the image will be properly oriented in relationship to the block face viewed with a nonimage-reversing dissecting microscope. Thus, if a corner of the block has been removed, or the block face is trimmed into an irregular trapezoid shape, it will be possible to locate specific features noted during the microscopic evaluation of the semithin sections when the block is once again viewed with a dissecting microscope. This will assure that further trimming of the block face to make it small enough for ultrathin sectioning will not remove important features in the specimen.

Larger sections do not spread out and adhere well to glass slides when heated in the drop of water on a hot plate. If wrinkling is encountered, increasing the size of the water droplet into which the sections are placed or increasing the hot plate temperature slightly may help. However, it may be necessary to reduce the overall size of the block face.

Scotch™ tape can be used to remove excess sections from water-filled glass knife boats by touching the tape briefly to the surface of the water. The tape with adherent sections then can be discarded.

Grid Selection

Grids come in a variety of styles illustrated in Fig. 117 (square mesh, octagonal mesh, rectangular mesh, holes, slots, bars), mesh sizes (50–1,000 mesh), and materials (copper, gold, nickel, stainless steel, beryllium, nylon/carbon, gold). For routine work, 200 mesh copper grids are generally used because they have a good electrical conductivity, which allows excess electrical charge from the electron beam to be grounded to the microscope column. In addition, they offer good specimen support and a reasonable amount of open (viewing) area, and are inexpensive. For special applications like cytochemical or immunocytochemical procedures, stainless steel, nickel, or gold grids may be necessary, since they are inert and will not interfere with biochemical reactions. Microanalytical specimens may be picked up on beryllium grids, which are preferred by some workers because of their electron transparency, thus reducing the amount of X-rays generated from the specimen support grid under the electron beam.

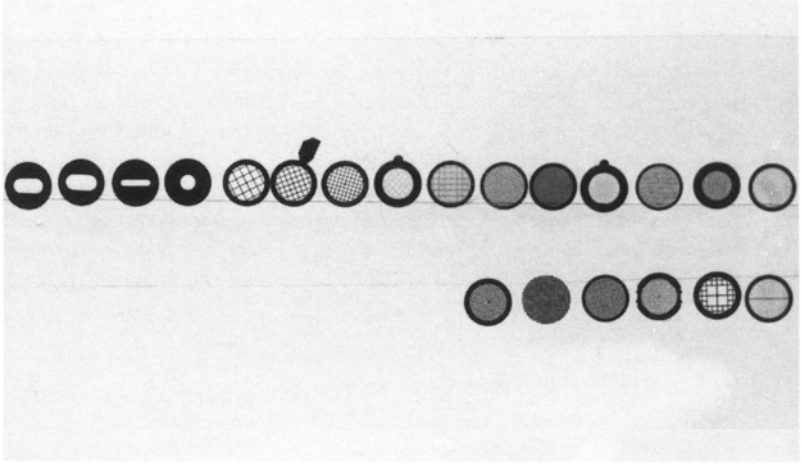

Figure 117. Various types of grids.

Grid Cleaning

Before picking up sections on copper grids, it is necessary to clean oxidation and manufacturing oils from the grids so that the sections will adhere properly. The cleaning process should be done just before using the grids, since the copper will oxidize again overnight.

The easiest method for cleaning the grids makes use of three scintillation vial-sized containers, the first containing 0.1 N HCl, the second 95% ethanol, and the third 100% acetone:

1. Pick up a grid by the edge with forceps and dip it into the acid for about 10 sec.
2. Dip quickly three times in 95% ethanol.
3. Dip quickly three times in 100% acetone.
4. Take a piece of Whatman™ #1 filter paper and slip it between the jaws of the forceps holding the grid to absorb any liquid held there.
5. Place the grid on a clean piece of filter paper while simultaneously pushing it out of the forceps jaws with a clean piece of filter paper. The grid is then ready to pick up sections.

Ultrathin Sections

Ultrathin sections of 50–90-nm thickness, with gray to gold interference colors, respectively, are picked up from below with a freshly cleaned grid. Sections picked up from below usually exhibit less wrinkling than those obtained by pushing the grid down upon the sections from above. Sections from block faces larger than than 0.5 mm^2 tend to have more chatter, wrinkles, and stain dirt. *After the sections have been picked up, blot the bottom (nonsection) side of the grid with a piece of filter paper to pull the drop of water* through *the grid holes, thus pulling the sections tightly down on the grid surface.* Use the manufactured edge of a piece of filter paper to go between the forceps jaws to absorb water that has crept in between the forceps jaws due to capillary action. Push the grid off onto a clean piece of filter paper in a Petri dish with the filter paper piece.

Different workers insist that sections should be picked up on either the shiny side or the dull side of copper grids that have sidedness. The argument is that the dull side is not as flat as the shiny side (it is rougher). It makes no practical difference which side is used, but we pick up sections on the shiny side of grids routinely, which allows any worker in the laboratory to know on which side of the grids the sections are located for subsequent handling.

To be safe, no more than four ultrathin sections should be cut at a given point on a glass knife edge. If each group of four sections is picked up on a grid immediately following cutting, the sections can be examined with an electron microscope with the knowledge that one will probably be excellent, and the other three will show increasing evidence of knife defects. If, however, numerous sections are cut from various areas of the knife before any are put on grids, there is a great chance that a series of later sections from various areas on the knife could be picked up on one grid, none of which will be of adequate quality to be worthy of photography.

The unsupported edges of sections will curl slightly under the electron beam and will move as they become heated by the beam, so sample areas right at the edge of a section often cannot be photographed. In addition, the junction between the specimen surface and empty resin can sometimes come apart during sectioning, so it is advisable to orient this junction vertically for sectioning, if possible.

Common Sectioning Problems

1. If sections stick to the hair used for manipulating them, run the hair between your thumb and forefinger to apply a slight coat of body oil. The oil should keep sections from sticking to the hair.
2. If the forming ribbon of sections curves excessively to one side or the other, rotate the block so that the bottom edge is truly parallel to the knife edge. If this does not work, try to trim the block to make the top and bottom edge parallel.
3. If an individual section has uneven bands of interference colors, something is probably loose on the ultramicrotome. Check all locking knobs to make sure that they are tight. If you are using a Leica-type chuck with stepped ledges to hold a flat block, make sure that all four corners of the block are in contact with some chuck surface. Finally, make sure that there is no external source of vibration in the room caused by large equipment or construction activity nearby. A section exhibiting uneven thickness can also be indicative of poor resin quality (inadequately polymerized or unevenly polymerized) or poor specimen infiltration. There will always be a slight difference in resin quality between areas with specimens and those that consist of resin alone.
4. If section thickness varies between consecutive sections, it usually suggests that ultramicrotome knobs are not secured or that there are strong air currents resulting in local temperature changes over short time intervals. If all else fails, increase the section thickness for the stroke that cuts the thinner of the two sections. In other words, thicken the thinnest section. This remedy does not work as well when the thicker section is thinned.
5. If sections show chatter, which is regularly spaced lines visible under the electron microscope beam at a right angle to the direction of sectioning as shown in Fig. 118, or the more severe problem of

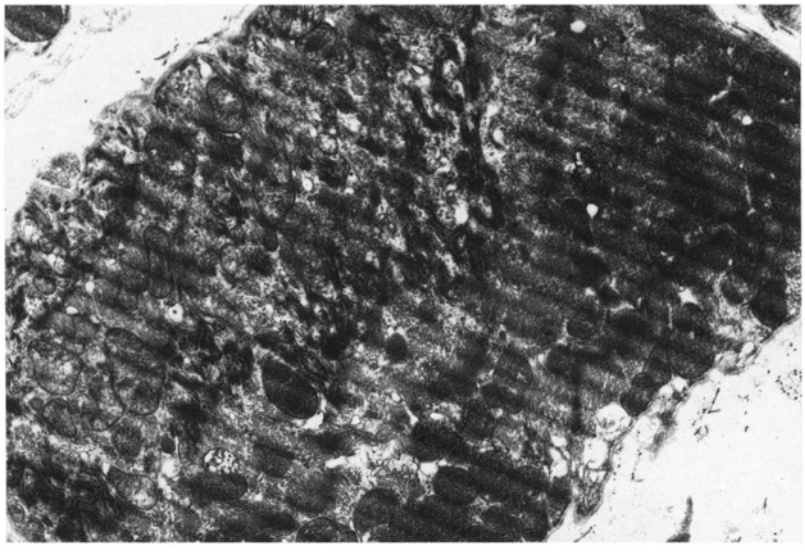

Figure 118. A section exhibiting chatter, consisting of evenly spaced lines at a right angle to the cutting direction. This resulted from an incorrectly set knife angle but could also be caused by poor infiltration, soft resin, or a block or knife inadequately secured during microtomy.

compression, which can usually be seen while sectioning, it usually indicates that the knife angle is wrong, the knife or specimen is not secured, or the plastic blocks are too soft. To determine if the knife angle and sharpness are adequate, cut sections from a block with known sectioning qualities and examine them. If they show chatter as well, increase the knife angle 1° and cut more sections from the test block. If chatter remains, increase the angle 1° more. If chatter remains, the knife is probably dull. If the test block cuts well at the normal knife angle, check that the new block is properly secured in the chuck. If it is, the resin is probably too soft. A day or two in the polymerizing oven may salvage the block (it may be necessary to put it at 80°C).

6. Knife marks in the form of streaks or tears showing uneven spacing and width in the direction of sectioning (Fig. 119) indicate either a dull knife or hard substances in the block face. The former is cured by using a new knife, while the latter is best solved by removing the hard materials revealed during semithin sectioning prior to cutting ultrathin sections.
7. If the block face wets as the block passes the knife edge, it indicates that the water level is too high or that the knife angle is too shallow. Acrylic resin blocks are notorious for picking up water. To solve the problem, it is often necessary to blot the block face with filter paper following each cutting pass.
8. When sections are dragged out of the knife boat and down the back side of the knife with the next cutting stroke, it is a clear indication that the boat water level is too high, or the knife angle is too shallow.

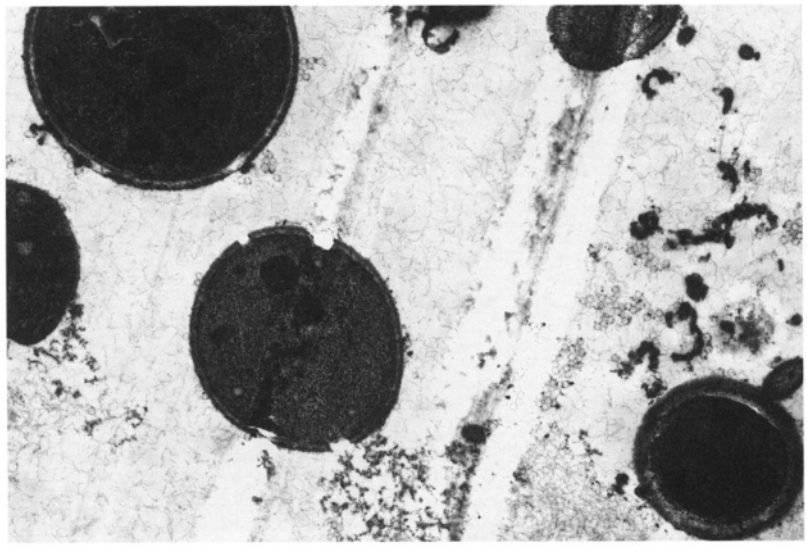

Figure 119. Knife marks, probably caused by hard materials in the block face.

References

Sitte, H. 1981. *Ultramicrotomy: Frequent faults and problems*. AO/Reichert, Vienna.

4

Staining Methods for Semithins and Ultrathins

I. SEMITHIN SECTION STAINING

When we speak of staining semithins, we are generally referring to 0.25- to 0.5-μm-thick sections cut from blocks of epoxide-embedded tissues. There are other resins such as the acrylic resins (Lowicryls, LR White and LR Gold) in common use that will have different staining responses from epoxides because of their partial miscibility with water. In addition, semithin frozen sections have still other staining characteristics resulting from their significant hydrophilicity. For the purposes of this chapter, however, we will limit our discussion almost exclusively to the epoxide sections, since these are the most commonly used resins for biological work. Any of the stains for these resins will work with much reduced staining time on more water-miscible sections.

Ideally, staining will produce sections with enough contrast for easy visualization and, better yet, some sort of differential contrast for various cellular components. Histological sections that have been deparaffinized so that only naked tissue remains on the slide accept a variety of polychrome stains, which accomplish both these tasks admirably. Unfortunately, because of the presence of osmium, the heavily cross-linked nature of the epoxide resins, and the hydrophobicity of the resins, it is usually extremely difficult to obtain reproducible results from the numerous staining regimens used for paraffin sections if applied to epoxide-embedded materials. Lists of various stains with references to the original works may be found in Hayat (1975) and Lewis and Knight (1977). Microwave staining has been used to achieve shorter staining times but generally does not increase the list of stains that work well on epoxide sections.

Various solvents for epoxides have been used to partially dissolve the resins so that stains could access the tissues more easily, but on a day-to-day basis, this procedure generally is more trouble than it is worth. Semithin sections are typically just a step along the path to the finished product, which are photographs of ultrathin sections. Most of these sections are used to determine where to trim block faces so that ultrathin sections will contain materials of interest, so spending a great deal of time producing semithins of publishable quality is usually counterproductive.

A. Toluidine Blue-O

Mixing 0.25 g of toluidine blue-O in a 1% solution of sodium borate will produce a staining solution capable of staining tissues embedded in epoxide resins. This is probably the most commonly used semithin section stain. Various elements of tissues and cells will stain differentially, yielding sections with a variety of shades of blue. Occasionally, lipids may take on a slightly greenish hue, and other areas may exhibit a little metachromasia, appearing reddish. These effects

can be very pleasing and can help to differentiate between cellular structures, but colors other than basic blue are generally not consistently reproducible.

The standard procedure is to cut semithin sections and to transfer three or four of them with a nichrome wire loop attached to an applicator stick to a 1-cm-diameter drop of distilled water on a glass microscope slide. This slide is placed on a hot plate adjusted to approximately 60 °C and left until the drop of water has dried completely, allowing the sections to anneal to the glass slide. Next, a drop of stain is applied to the sections, and the stain drop is observed until the edges become gold in color, about 15–30 s on the hot plate. Then, it is important to rinse the stain droplet off into a waste container with a stream of distilled water from a squeeze bottle quickly and completely. It is usually best to direct the stream of water to an area on the slide just above the sections rather than right at them to diminish the chance of washing them off of the slide. If the stain dries on the sections, it will produce masses of crystallized stain, rendering the slide unusable (Fig. 120). Once the stain has been washed from the sections, the slide can be reheated for drying, and then it should be removed from the hot plate.

The dried sections may now be observed with the light microscope. Unless a coverslip is used, however, good resolution is not possible since most light microscope lenses are designed to be used with #1.5 coverslips (0.17 μm thick, as marked on most objectives). In addition, any minor section defects such as small wrinkles and small knife marks, will be clearly visible, which is not the case after a mounting medium and coverslip are added.

It is important to remove all the water if you intend to use a coverslip on the sections, since the common permanent mounting media are immiscible with water. A satisfactory temporary mounting medium for observing semithin sections is either a drop of water or a drop of oil used for oil immersion lenses.

If the permanent medium Permount® is used, make sure that the area containing the sections is circled with a marking pen on the bottom of the slide because the stain usually fades over time as the mounting medium yellows. By marking the slides, the sections can be located again fairly easily with a phase contrast microscope if the stain does fade. An alternative is to use

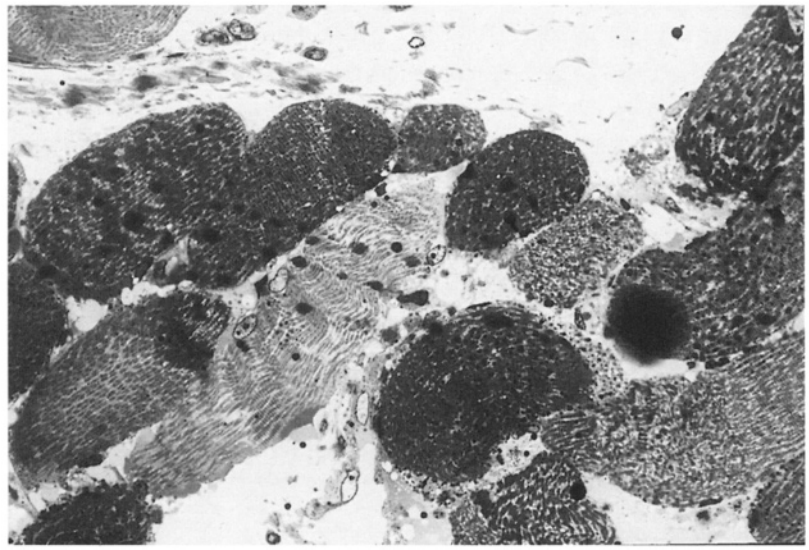

Figure 120. Stain dirt on a toluidine blue-O stained section of muscle tissue. 346×.

Polysciences Polymount®, which handles just like Permount®, except that it does not cause the stain to fade, and it does not yellow with time. Polymount® has been used in our laboratory for 18 years, and few of our archived semithin section slides have faded, and none have yellowed. If either of these media becomes too viscous, it may be diluted with xylene.

If numerous tiny wrinkles (Fig. 121) appear, increasing the hot plate temperature seems to help. If the section dimensions are significantly larger than 1.5 mm^2, large wrinkles are likely to be a problem, and the stain tends to pool underneath the wrinkles, resisting removal by rinsing and making these preparations unattractive. If sections are thicker than recommended or are overly large, they are extremely likely to be washed off the slides during rinsing.

If sections refuse to stick to slides, try washing the slides before use, but this is now an uncommon problem. Years ago, the slides had more oils on their surfaces from manufacturing, necessitating washing. Slides may be subbed to help section adherence, as described in the Techniques section of this chapter, or special coated slides may be purchased from various scientific suppliers. Fisher Scientific markets their coated slides under the name Colorfrost®-Plus.

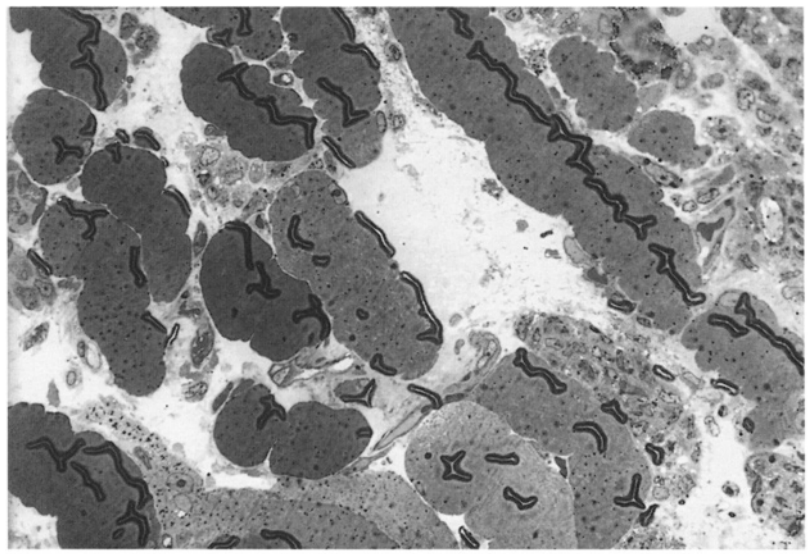

Figure 121. Small wrinkles on a toluidine blue-O stained section resulting from insufficient heat when sections were dried onto the slide. 346×.

B. Toluidine Blue-O and Acid Fuchsin

Utilization of these two stains can result in polychromasia (Hayat, 1975; Hoffman *et al.*, 1983). Nuclei stain dark purple–blue, keratinized tissues stain red, collagen stains red, and other tissue components stain bluish. Three stocks are necessary: (1) 1% toluidine blue-O in 1% sodium borate (1 g of each in 100 ml of distilled water), (2) 1% sodium borate solution in distilled water, and (3) 0.10 g of basic fuchsin dissolved in 100 ml of distilled water. Heat the water to 100 °C, add the basic fuchsin, and then filter. This solution keeps for about 1 year at room temperature.

Heat-fixed sections are stained with the toluidine blue as described above and then quickly rinsed. Just prior to use, mix equal parts of basic fuchsin stock and sodium borate stock in a test

tube. Put a drop of the mixture on the sections and heat them briefly, then rinse with a jet of distilled water and dry.

As with so many of the polychrome section stains designed for epoxide sections, the results are not consistent, at least in our laboratory, and so this technique is recommended only when a photographable section is needed, and time is available to repeat the procedure until the stain produces the desired result. When staining produces poor results, the sections look very much like toluidine blue-O-stained sections.

C. Basic Fuchsin/Methylene Blue

This technique, as described by Sato and Shamoto (1973), should produce polychromatic sections, but unfortunately, the results are often erratic. Sections are stained on a heated slide for about 4–5 s. The staining procedure is essentially the same as for toluidine blue-O. The staining solution contains the following ingredients:

- 0.5 g of monobasic sodium phosphate
- 0.25 g of basic fuchsin
- 0.2 g of methylene blue
- 15.0 ml of 0.5% boric acid
- 70 ml of distilled water
- 10 ml of 0.72% NaOH

The pH should be adjusted to 6.8–7.5. If the pH is above 8.0, sections become excessively blue. Once made up, the solution is stable for several months, though it should be shaken before use. When the stain works properly, it colors mitochondria red, erythrocytes, glomeruli, and kidney tubules pink, collagen brilliant pink, elastic lamina and zymogen granules reddish purple, and nuclei bluish purple.

D. Methylene Blue

Some workers prefer a solution of 0.5–1.0% methylene blue in 1% sodium borate to the toluidine blue-O stain described above. The procedures for use are identical, but the stained sections have a more delicate blue than found with toluidine blue.

E. Periodic Acid/Schiff's Reagent

The staining procedure that has been described by Pool (1973) is good at differentiating polysaccharide-rich areas in epoxide sections. However, this stain cannot be used to definitively locate polysaccharides because it can also stain glutaraldehyde molecules and often stains the same areas whether or not periodic acid is used to open up hydroxyl groups. This stain often produces somewhat inconsistent results, but it can give outstanding results when it works properly.

II. ULTRATHIN SECTION STAINING

A. Purpose

The objective in staining ultrathin sections is to render materials with little inherent contrast visible by causing the materials to scatter the electron beam. It is also useful to be able to selectively stain various cellular components. Unfortunately, the commonly used poststains (lead and uranyl stains) are only semiselective. Even this partial selectivity depends on a number of factors such as pH, length of staining time, vehicle, previous chemical exposures during fixation, and specific formulation used. Typically, the longer the staining time with a given stain, the more elements within the tissue that become stained.

Various cytochemical procedures (see Chapter 5) have been developed to specifically identify specific cellular components, but this section will be devoted primarily to the process of poststaining to develop general contrast.

Embedding media and biological materials are chemically similar, containing large amounts of carbon, hydrogen, oxygen, and other fairly electron-transparent atoms, and few atoms of large atomic weight. Since major contrast differences between the specimen and the embedding medium do not exist, other materials must be introduced to help develop contrast. The most effective stains are those containing heavy metals such as lead, uranium, and osmium, which have sufficient mass to block or scatter electrons that strike the specimen. The larger the mass of the stain molecules, the better they will block the beam, but the size of the heavy metal ions deposited during staining can also affect resolution in certain instances. Some workers also suggest that staining helps to stabilize certain specimen components during bombardment by the electron beam.

The effects of stain interactions within sections have been studied, and it has been noted that dye-stacking effects can actually interfere with resolution, in some cases increasing the size of specific biological structures (see Hayat, 2000 for a discussion of this issue). It has been reported that poliovirus combines with approximately its own weight of stain before adequate staining is achieved.

B. *En Bloc* versus Poststaining

An *en bloc* stain is used on wet tissue, whereas poststaining is done on sections of tissue after embedding is completed. Even though osmium tetroxide is usually considered a lipid fixative (postfixative), it can also be thought of as an *en bloc* stain, since wherever it becomes reduced and fixed into the sample, it confers an electron density because of the high atomic weight (190) of osmium atoms (atomic number 76).

A commonly used *en bloc* stain is uranyl acetate (Fig. 122). The typical procedure is to rinse samples thoroughly with distilled water after osmication, since the phosphate and cacodylate buffers usually used with osmium react strongly with uranyl acetate, and to place them in 0.5% aqueous uranyl acetate at 4 °C overnight. They are then rinsed with distilled water, dehydrated and embedded. The disadvantages to this technique are that the fixation schedule becomes lengthened, and the effect of the staining is less than that seen when it is used as a post-stain. Hayat (2000) recommends using 2% uranyl acetate in the first alcohol or acetone step in the dehydration series for approximately 15 min, which eliminates one of the objections to *en bloc* staining with uranyl acetate.

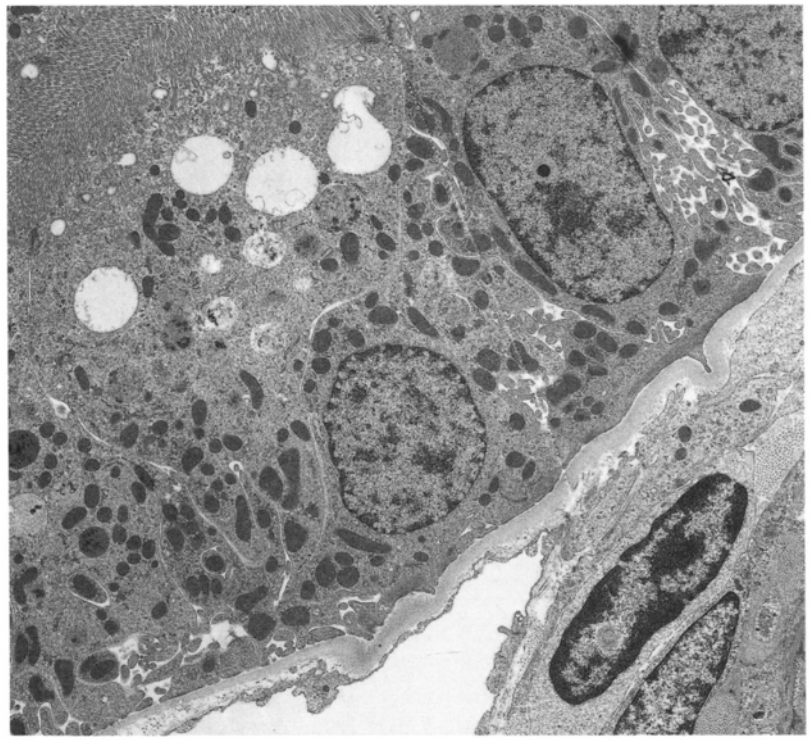

Figure 122. Horse kidney stained *en bloc* with 0.5% uranyl acetate. Poststained with Reynold's lead citrate for 8 min. 5,077×.

Poststaining of ultrathin sections has several features to recommend it: (1) it is a simple procedure; (2) staining is more uniform than with *en bloc* procedures because access to the sample is easier; (3) there is less chance of tissue damage than with *en bloc* procedures because structures are stabilized with the resin matrix; (4) stains will not be extracted during subsequent procession steps, when the *en bloc* stains are subsequently subjected to dehydration agents and the extractive capabilities of the liquid resins themselves; (5) contrast builds faster and generally exceeds that produced by *en bloc* staining; and 6) the effect of different staining procedures can be quickly evaluated on serial sections from the same block, rather than having to process several samples separately.

C. Commonly Used Post-Stains

1. Uranyl Stains

Uranium atoms with an atomic number of 92 (atomic weight = 238) are the heaviest stain molecules used. As mentioned above, uranyl stains may be used *en bloc*, where they can also be considered to have a fixative effect. They can also be used as poststains or as negative stains (see Chapter 8). Uranyl stains interact with anionic compounds and are known to bind strongly to phosphate groups associated with nucleic acids and phospholipids. They also react with carboxyl

groups so that various amino acids of proteins can become stained. Uranyl stains are usually used at pH 3.5–4 and strongly stain proteins. If the pH is adjusted to higher levels, DNA becomes more strongly stained.

One of the most important features of uranyl stains is that they serve as mordants for lead stains. This means that subsequent staining procedures involving lead will interact much more strongly with tissues that have had uranyl exposure. Thus, it is important to perform uranyl and lead staining procedures in the proper sequence to achieve maximum staining.

Uranyl stains used *en bloc* must be handled carefully because they will interact with phosphate and cacodylate buffers, coprecipitating with the buffer compounds and resulting in ineffective staining. When used as poststains, uranyl solutions are made up in alcohol or water, so this problem does not arise. Uranium is both a heavy metal and radioactive, though the product marketed by electron microscopy supply houses is significantly depleted of its radioactivity. The toxicity of this element mandates that it should be handled carefully, with all of the waste generated viewed as toxic. The staining solutions are photolabile and should be stored in the dark between uses.

The mechanism of staining appears to be ionic, though it is not clearly defined in all cases. Binding of uranyl ions can be reduced as much as 75% in phosphate-depleted cells (Van Stevenick and Booij, 1964).

Uranyl ions form simple salts with phosphate groups of DNA and thus reduce the net charge of DNA molecules, thereby allowing them to clump together to some extent. Bacterial DNA is stabilized, and extraction of eukaryotic DNA from its histone shell is prevented by uranyl acetate treatment (Stoeckenius, 1960). However, RNA is more reactive with lead stains. Huxley and Zubay (1961) reported that sufficient uranyl ions complex with DNA to almost double its weight.

Uranyl stains are known to reduce the solubility of phospholipids when used *en bloc*. Uranyl ions have also been shown to interact with phosphate groups in lecithin monolayers and to react with phosphate groups in both saturated and unsaturated lecithins, but not with the fatty-acid side chains (Shah, 1969).

Proteins such as histones, ribonucleoproteins, and phosphoproteins stain, with the stain density apparently related to the amount of charge on the protein molecule. The collagen protein stains strongly, and the protein moieties in membranes seem to be largely responsible for cytomembrane staining.

As with all staining regimens, prior treatment of the tissue with other chemical agents can affect staining. In particular, if long osmium treatment is used, uranyl acetate staining is reduced.

There are a variety of uranyl stains utilized for poststaining such as uranyl acetate, uranyl formate, uranyl magnesium acetate, and uranyl nitrate (see Hayat, 2000, for further discussion). The most commonly used formulations are either aqueous or alcoholic uranyl acetate. Powdered uranyl acetate can be purchased from all the electron microscopy supply houses. All resins except Spurr resin and a few of the Epon 812 substitutes stain readily with a 3–4% aqueous solution produced by adding the powdered uranyl acetate to distilled water in a lightproof container, sonicating it briefly, and letting it sit overnight before use. If Spurr resin is used, either methanolic or ethanolic uranyl acetate must be used to yield effective staining. A 4–5% solution is made up with 50–100% methanol. With all three of the solvents used, a saturated solution is generally the objective, and solubility increases through the series from water to ethanol to methanol. Since the solution is saturated, it is important not to pick up drops of the stain from the bottom of the container, or masses of large, elongate crystals characteristic of uranyl acetate will be deposited on the sections being stained (Fig. 123). Any time elongate crystals are seen on sections, the uranyl acetate staining step should be evaluated.

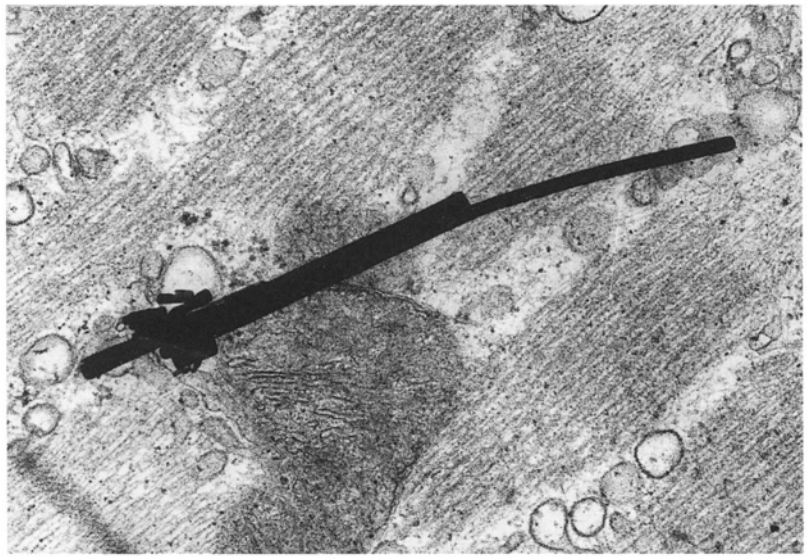

Figure 123. Needle-like crystals of uranyl acetate on muscle tissue section. 45,500×.

Since uranyl acetate solutions are photosensitive, some workers stain materials in the dark, but this is not necessary. It is important to remove all the uranyl acetate stain because the solution is acidic and will coprecipitate with the basic lead secondary poststains. Uranyl acetate solutions stored in the dark will keep for approximately one month at room temperature. If large amounts of precipitate are observed on the sides or bottom of the vessel containing the solution, discard it. If such solutions are used to stain sections, it will become evident because the chromatin in nuclei will be largely unstained, and mitochondrial membranes do not stain normally.

2. Lead Stains

Lead has an atomic number of 82 (atomic weight = 207) and is used as a poststain because it scatters electrons very effectively. It has also occasionally been used *en bloc* (Pisam *et al.*, 1987). Lead salts produced in poststained sections increase contrast more intensely in the presence of reduced osmium bound to tissue than do uranyl salts. As mentioned in the previous section, uranyl acetate poststaining serves as a mordant for lead stains, resulting in much more intense staining. Figure 124 compares sections block of rat kidney that have received no poststaining (Fig. 124A), have been poststained only with methanolic uranyl acetate (Fig. 124B), or have been stained with methanolic uranyl acetate, followed by lead citrate (Fig. 124C).

Lead precipitates form quite readily because of the high reactivity of lead with carbon dioxide and oxygen in the air to form lead carbonate ($PbCO_3$), which may appear as finely granular "pepper" precipitates. It may also present as larger granular aggregates (Fig. 125) or, in some cases, as large globose deposits (Fig. 126). Many workers go to great lengths to exclude air from staining dishes or to surround stain drops with carbon dioxide scavengers such as KOH. Lead forms crystals with most anions, and these crystals are highly insoluble because they are hydrophobic. Any lead solution with evidence of precipitate should be discarded because of the likelihood of producing large amounts of stain dirt on sections. Lead staining solutions and waste should be handled carefully because of their well-known toxicity.

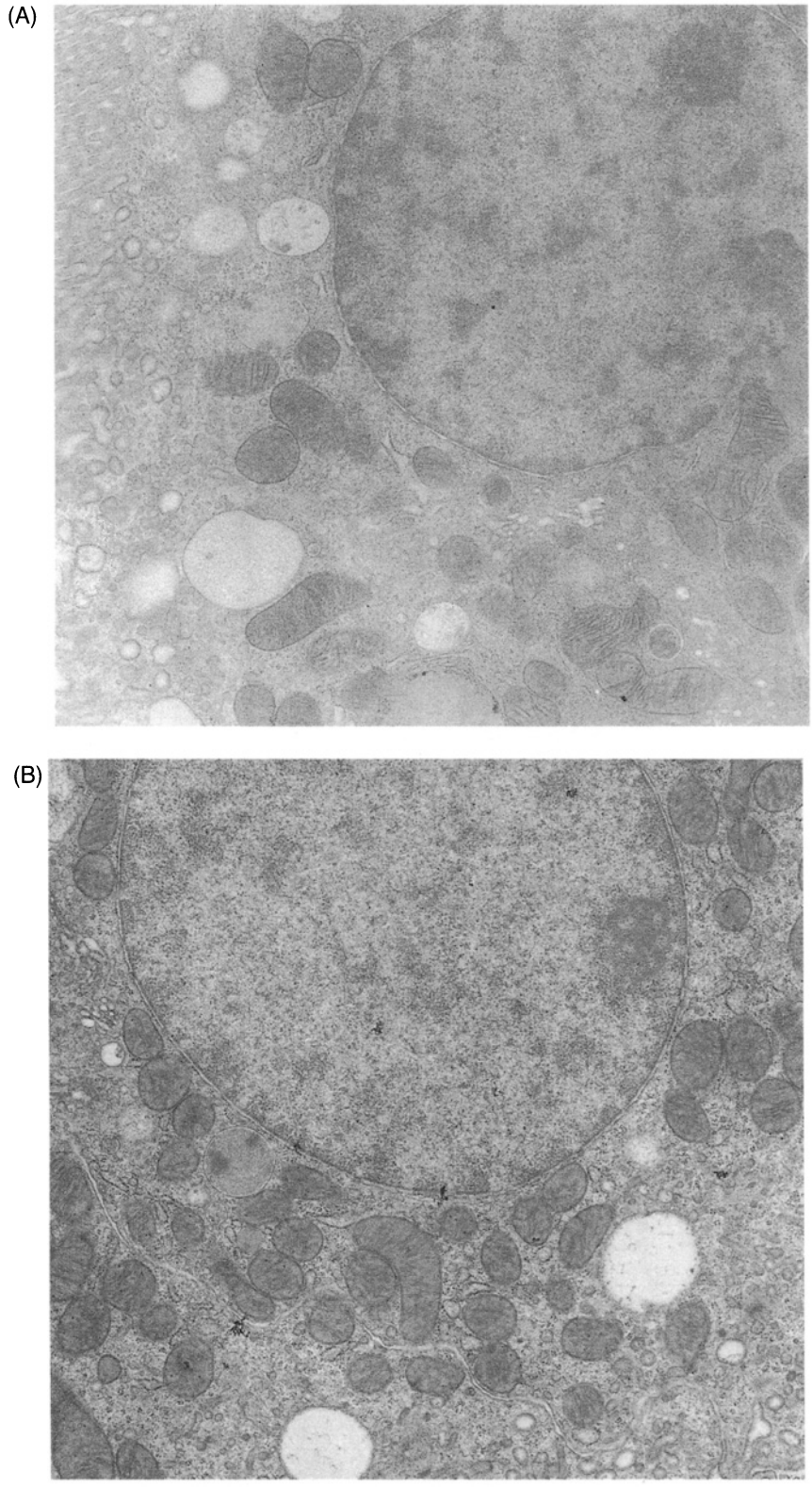

Figure 124. Gold sections of rat kidney in Spurr resin. (A) No poststain. Minor electron density primarily due to osmium incorporated during postfixation. 13,327×. (B) Poststained only with methanolic uranyl acetate for 5 min. Overall increase in contrast is obvious, particularly with membranes. Ribosomes are clearly visible in the cytoplasm, which was not the case with (A) above. 13,327×.

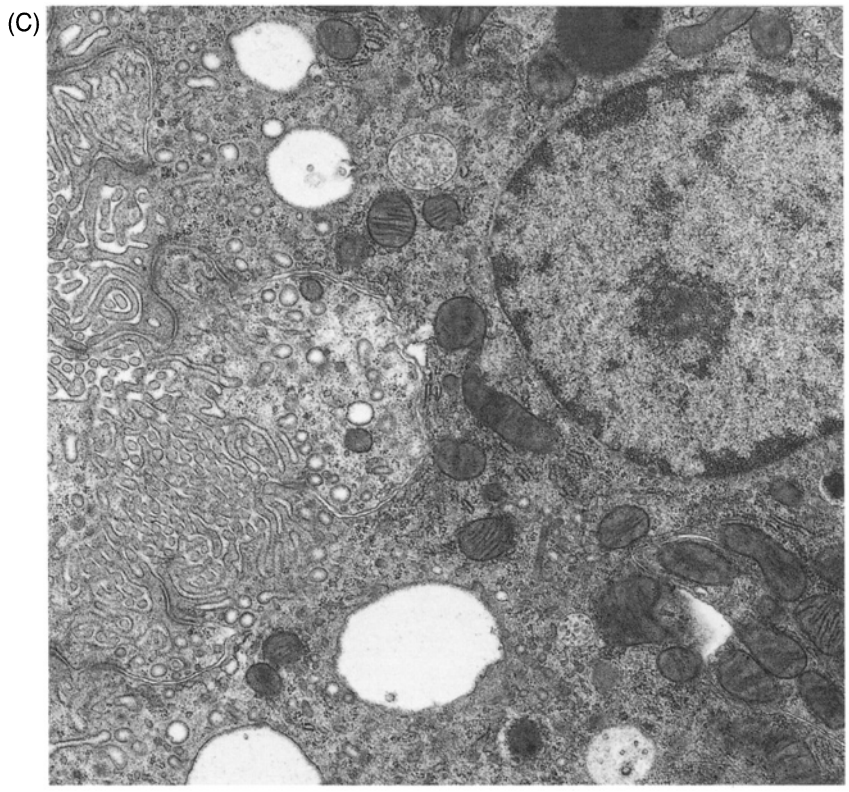

Figure 124. (C) Poststained for 5 min with methanolic uranyl acetate, followed by 8 min with Reynold's lead citrate. All cellular components are well defined. Membranes are dark, ribosomes are clearly obvious, and heterochromatin is well stained. 13,327×.

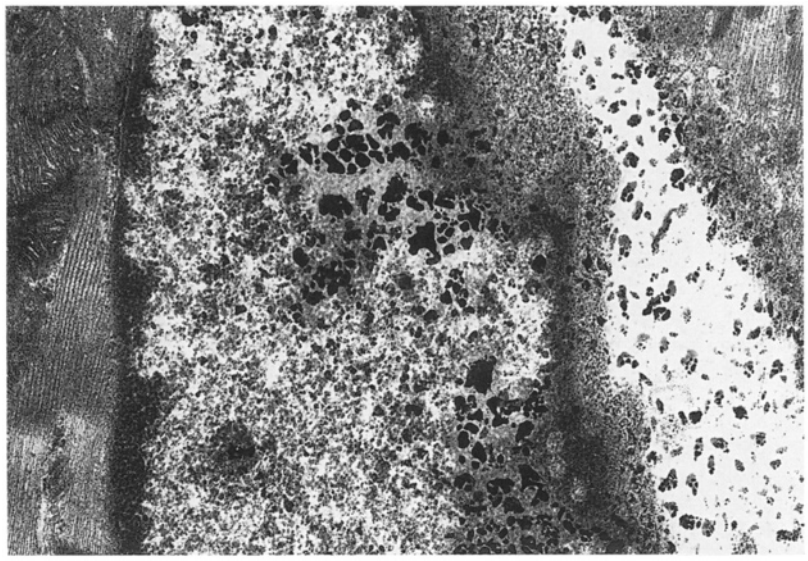

Figure 125. Granular lead deposits on sections of muscle resulting from contaminated lead poststaining solution. 21,923×.

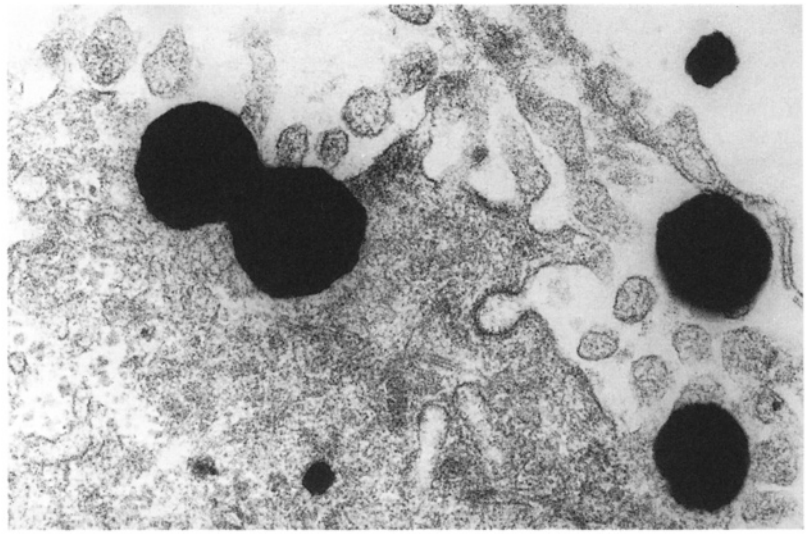

Figure 126. Globose lead stain deposits on tissue section. 38,127×.

Lead staining is influenced by the fixatives used in tissue preparation and the individual cellular constituents being examined. Nucleoli and ribosomes are stained more by lead in formalin-fixed tissue than in tissues fixed with osmium alone, while glycogen stains about the same in both instances.

Lead stains are most effective and stable at high pH. The widely used formulation of lead citrate introduced by Reynolds (1963) has a pH of 12–13. As with most poststains, prolonged staining results in less specific staining. All of the alkaline lead stains react with similar cellular components, differing only in speed of staining, ease of formulation, and storage characteristics.

The detailed mechanisms of staining particular cellular components are not clearly understood. Membrane staining is thought to result from lead interacting with the previously bound acidic osmium molecules, which have an affinity for positive dye ions such as lead. Glycogen is stained by the attachment of lead to the hydroxyl groups of carbohydrates by chelation, and then additional lead accumulates around the primarily attached lead. Proteins with large numbers of sulfhydryl groups stain readily, as do other proteins containing amino acids with negative charges. Nucleic acids are stained when lead complexes with negatively charged phosphate groups. RNA, in particular, has a high affinity for lead.

A number of lead formulations have been tried over the years. Watson (1958) worked with lead hydroxide, which is probably the best stain, but it is tedious to formulate and forms lead carbonate upon reacting with air extremely readily. It also seems to produce higher levels of precipitate, probably because of the highly saturated nature of the solution. Lead acetate was introduced by Dalton and Ziegel (1960) with the intention of reducing lead carbonate formation. Lead tartrate (Millonig, 1961) was suggested as less likely to produce lead carbonate deposits because of the chelation of lead by tartrate. Reynolds (1963) introduced the most widely used lead stain, lead citrate. In his formulation, lead is strongly chelated with citrate, reducing its tendency to form lead carbonate upon interaction with air while still producing better staining than the lead tartrate formulation introduced earlier. The basic mechanism of action for this formulation is that anionic staining sites have a greater affinity for lead cations than does the citrate portion of the solution, while, at the same time, CO_2 and oxygen have less affinity for the lead.

Dispose of all lead waste in dedicated containers that can be picked up by toxic waste disposal personnel. Remember that the solutions are toxic, dried droplets of stain are toxic if inhaled, and lead should not be discarded down drains.

As mentioned previously, uranyl acetate serves as a mordant for lead, so lead poststaining should always follow uranyl acetate treatment (*en bloc* or as a poststain). Mollenhauer and Morré (1978) suggested that grids floated on a droplet of lead stain will become more contaminated from interactions with CO_2 in the air than those buried beneath the drop.

In recent years, we discovered that the pH of city water as well as deionized and distilled water made from city water can have a disturbingly low pH on some occasions. If grids stained with the typical combination of uranyl acetate followed by lead citrate have a final rinse in low pH water (we have recorded tap water with a pH of less than 3.5 on occasion), the stain will be seriously compromised (Fig. 127).

It is imperative that grids be carefully dried before going from uranyl acetate solutions to lead solutions, to prevent coprecipitation of the stains. In addition, proper drying of grids will prevent folds in sections, particularly with Spurr resin sections (Fig. 128). The method is described in the section Chapter 4 Techniques.

Double lead staining has been recommended for tissues that do not stain well with conventional procedures (Daddow, 1986). The procedure is to stain sections in Reynolds' lead citrate for 30 s, rinse in distilled water, stain with uranyl acetate for 1 min, rinse again, and restain with Reynolds' lead citrate.

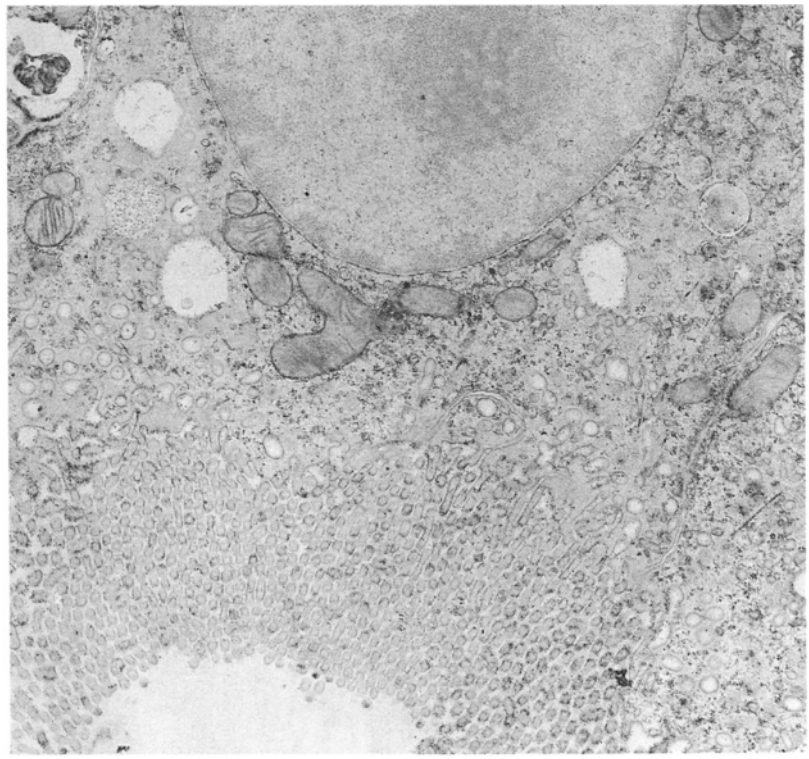

Figure 127. Section of rat kidney stained with uranyl acetate and lead citrate, inadvertently rinsed in distilled water at approximately pH 3.5. 13,327×.

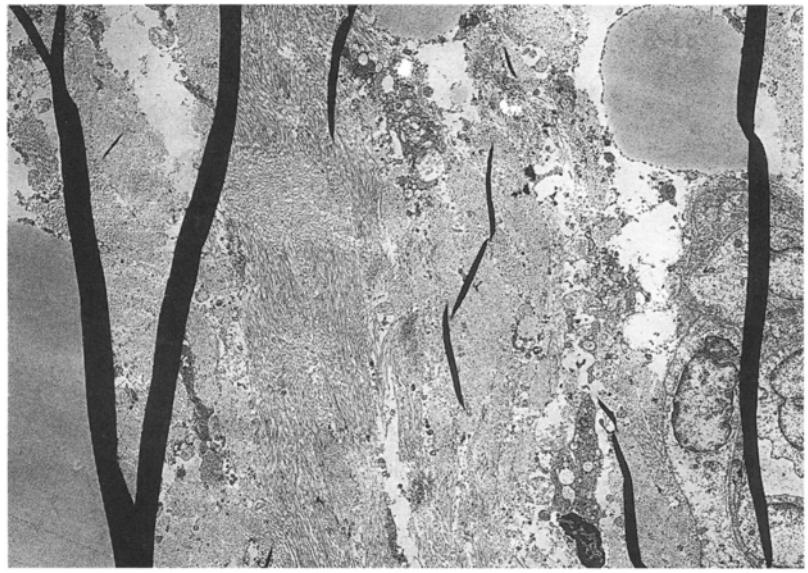

Figure 128. Folds in an ultrathin section of a Spurr resin block, induced by improper drying of the sections. 2,720×.

3. Phosphotungstic Acid

Phosphotungstic acid (PTA) was first used to impart electron density to tissues by Hall *et al.* (1945). It has been used as an *en bloc* stain but is most commonly employed as a negative stain for bacteria, viruses, and subcellular particle suspensions (see Chapter 8 on Negative Staining). Negatively charged molecules are the principal sites of PTA binding. Complex polysaccharides with negative charges are stained well. The mechanisms of staining for various cellular components are still uncertain. *En bloc* staining with PTA has been said to result in blocks that are more difficult to section, and much of the bound PTA can be removed by the solvent activity of epoxide resins. Since most conventional fixation methods involve epoxide embedment, the use of PTA as a general *en bloc* stain is not commonly seen. Hayat (2000) provides an extensive discussion of PTA staining of tissues for the interested reader.

4. PTA/Chromic Acid

Roland *et al.* (1972) introduced a novel poststain composed of PTA and chromic acid that preferentially stained the plasma membranes of plant cells while leaving the other cytomembranes unstained. They did not know the mechanism or why it worked with tissues embedded in most epoxide resins, but not Spurr resin. It has been used successfully to analyze populations of isolated cytomembranes to determine the percentage of plasma membranes in the samples.

5. Barium Permanganate

Permanganates have been used as general poststains in the past, but because of frequent precipitate formation on sections, they are not currently used much. Hohl *et al.* (1968) used

barium permanganate as a specific stain for cellulose fibrils in the cellular slime mold, *Acytostelium*. A solution of 0.5–1% in distilled water effectively increases the electron density of cellulose if sections are stained for 1–2 min after lead staining (rinse with distilled water between the stains). Stain precipitation can still be a problem, so excessive staining is to be avoided, and careful washing is mandatory.

D. Microwave Staining

During the last 15–20 years, microwaves have come into common use for staining histological sections for light microscopy, particularly with those stains involving silver compounds (Brinn, 1983). Various workers have also utilized microwave staining for ultrathin sections of epoxide-embedded materials, particularly in the setting of human pathology laboratories where diagnostic materials need to be processed quickly. Estrada *et al.* (1985) described a procedure utilizing a 400 W, 2,450 MHz microwave with a rotating platform to accelerate both uranyl acetate and lead staining. They illustrated their work with photographs of human heart biopsy material fixed with glutaraldehyde and osmium, dehydrated and embedded in Epon. They cut ultrathin sections, placed them on grids, and then immersed the grids in 3–4 ml of the staining solutions for the microwave step. The two stains used were 4% aqueous uranyl acetate and Reynolds' (1963) lead citrate. If they microwaved the grids for 15 sec in each stain, they achieved excellent results. The normal procedure they had previously used was 30 min in the uranyl acetate solution followed by 10 min in lead citrate. The materials so stained actually appeared slightly overstained in their illustrations, but their main point was that they could cut about 39 min from their procedures for preparing sections to make diagnoses. They also mentioned that they used the technique successfully on kidney, liver, nasal brushings, skin biopsies, and tumors.

E. Dark-Field Imaging without Staining

Dark-field imaging is a method that can provide added contrast for low-contrast specimens, though with a decrease in overall image intensity. Rather than utilizing the axial and only slightly scattered part of the beam in imaging as is done with conventional TEM (bright-field) observation, the widely scattered part of the beam is used for imaging. Since the scattered part of the beam is being used, the electrons have more varied energy levels than with bright-field viewing, leading to greater levels of chromatic aberration and, hence, lower resolution.

There are two ways to produce dark-field images in a TEM. The first and simplest is to manually displace the objective aperture so that its edge blocks part of the electron beam. The second requires a microscope with circuitry designed to perform dark-field imaging. In such a system, the beam is deflected off-axis to produce the dark-field image.

Dark-field imaging in TEM can produce increased contrast levels in unstained materials with very little contrast and is particularly well suited to the examination of biological crystals (paracrystalline arrays of proteins) whose lattices will show up more clearly with dark field. Another advantage of the technique is that the crystals do not need to be stained before viewing, thus avoiding the potential of obscuring structural detail by dye stacking.

In reality, dark-field imaging is of more use to crystallographers, but we occasionally use the technique with selected biological specimens.

REFERENCES

Brinn, N.T. 1983. Rapid metallic histological staining using the microwave oven. *J. Histotechnol.* 6: 125.

Daddow, L.Y.M. 1986. An abbreviated method of the double lead stain technique. *J. Submicrosc. Cytol.* 18: 221.

Dalton, A.J. and Ziegel, R.F. 1960. A simple method of staining thin sections of biological material with lead hydroxide for electron microscopy. *J. Biophys. Biochem. Cytol.* 1: 409.

Estrada, J.C., Brinn, N.T., and Bossen, E.H. 1985. A rapid method of staining ultra-thin sections for surgical pathology TEM with the use of the microwave oven. *Am. J. Clin. Pathol.* 83: 639.

Hall, C.E., Jakus, M.A., and Schmitt, F.O. 1945. The structure of certain muscle fibrils as revealed by the use of electron stains. *J. Appl. Phys.* 16: 459.

Hayat, M.A. 1975. *Positive staining for electron microscopy*. Van Nostrand Reinhold, New York.

Hayat, M.A. 2000. *Electron microscopy: Biological applications*, 4th edn. Cambridge University Press, New York.

Hoffman, E.O., Flores, T.R., Coover, J., and Garrett, H.B. II. 1983. Polychrome stains for high resolution light microscopy. *Lab. Med.* 14: 779.

Hohl, H.R., Hamamoto, S.T., and Hemmes, D.E. 1968. Ultrastructural aspects of cell elongation, cellulose synthesis, and spore differentiation in *Acytostelium leptosomum*, a cellular slime mold. *Am. J. Bot.* 55: 783.

Huxley, H.E. and Zubay, G. 1961. Preferential staining of nucleic acid containing structures for electron microscopy. *J. Biophys. Biochem. Cytol.* 11: 273.

Lewis, P.R. and Knight, D.P. 1977. *Staining methods for sectioned material*. North Holland, New York.

Millonig, G. 1961. A modified procedure for lead staining of thin sections. *J. Biophys. Biochem. Cytol.* 11: 736.

Mollenhauer, H.H. and Morré, D.J. 1978. Contamination of thin sections, cause and elimination. In *Proc. 9th Int. Cong. Electron Microsc.* (Vol. II, p. 78). Microscopical Society of Canada, Toronto.

Pisam, M., Caroff, A., and Rambourg, A. 1987. Two types of chloride cells in the gill epithelium of a freshwater-adapted euryhaline fish: *Lebistes reticulatus*; their modifications during adaptation to saltwater. *Am. J. Anat.* 179: 40.

Pool, C.R., 1973. Prestaining oxidation by acidified H_2O_2 for revealing Schiff-positive sites in epon-embedded sections. *Stain Tech.* 48: 123.

Reynolds, E.S. 1963. The use of lead citrate at high pH as an electron-opaque stain in electron microscopy. *J. Cell Biol.* 17: 208.

Roland, J.C., Lembi, C.A., and Morré, D.J. 1972. Phosphotungstic acid-chromic acid as a selective electron-dense stain for plasma membranes of plant cells. *Stain Tech.* 47: 195.

Sato, T. and Shamoto, M. 1973. A simple rapid polychrome stain for epoxy-embedded tissue. *Stain Tech.* 48: 223.

Shah, D.O. 1969. Interaction of uranyl ions with phopholipid and cholesterol monolayers. *J. Colloid Interf. Sci.* 29: 210.

Stoeckenius, W. 1960. Osmium tetroxide fixation of lipids. In: *Proceedings of the European Conference on Electron Microscopy* (Vol. 2). Nederlandse Vereniging voor Electronmicroscopie, Delft.

Van Stevenick, J. and Booij, H.L. 1964. The role of polyphosphates in the transport mechanism of glucose in yeast cells. *J. Gen. Physiol.* 48: 43.

Watson, M.L. 1958. Staining of tissue sections for electron microscopy with heavy metals. II. Application of solutions containing lead and barium. *J. Biophys. Biochem. Ctyol.* 4: 727.

CHAPTER 4 TECHNIQUES

Semithin Section Staining with Toluidine Blue O

1. Applications and Objectives

This procedure is used to stain 0.25- to 0.5-μm epoxide or acrylic resin sections for light microscopy and to impart contrast to the originally low-contrast semithin sections of these resin-embedded materials.

2. Materials Needed

- 1% aqueous sodium borate
- Toluidine blue O
- Storage bottle for stain solution
- 10-ml plastic syringe with 0.45-mm-pore-size filter attached
- Hot plate
- Poly-mount™ (Polysciences, Inc.)
- Glass microscope slides
- Glass coverslips
- Plastic squeeze bottle containing distilled water
- Transfer loop

3. Procedure

Stain Preparation. Put 0.25 g of sodium borate into 25 ml of distilled water. Stir until dissolved. Add 0.25 g of toluidine blue O and stir. Put the solution into a storage bottle. Fill a 10-ml syringe with some of the stain and affix a 0.45-μm filter to the syringe.

Section Staining

1. Pick up semithin sections with a loop and transfer to a drop of distilled water on a glass microscope slide. The droplet should be approximately 1–1.5 cm in diameter and should be applied just before the sections are added.
2. Immediately place the slide on a hot plate at approximately 60°C and wait until the drop of water has totally evaporated.
3. Add just enough of the toluidine blue O staining solution to cover sections.
4. When the edge of the stain drop just begins to turn to a metallic gold color (15–30 s), quickly remove the slide from the hot plate and direct a stream of distilled water from the squeeze bottle just above the stain drop so that the stain is quickly and completely washed from the slide into a waste dish.
5. Wipe any water from the bottom of the slide, circle the area containing sections (on the bottom of the slide) with a Sharpie®, and put the slide back onto the hot plate until totally dry.
6. Place 1–2 drops of Poly-mount™ onto the sections and carefully place a coverslip onto the slide to minimize any bubbles in the Poly-mount™. Examine with a light microscope.

4. Results Expected

Sections should be wrinkle- and dirt-free, with different components of the sample exhibiting different shades of blue.

5. Cautionary Statements

If the sections are too large (more than 1 mm^2) or too thick (over 0.5 μm), wrinkles will be likely. If sections are of appropriate size but still have excessive wrinkles, make sure that the drop of water is large

enough for the sections to stretch in the heated water before they anneal to the glass slide. Do not add the drop of water to the slide until just before the sections, and promptly put the slide onto the hot plate. If wrinkles persist, increase the hot plate temperature slightly.

Thicker sections tend to wash off the microscope slide as the stain is being removed. Stain dirt also tends to increase with the size of the sections. If the stain solution is filtered as described, dirt does not appear to be a problem, even if the stain dries completely on the slide before it is washed off.

The toxicity of toluidine blue O is not well documented, but it should not be inhaled, ingested, or allowed to come into contact with skin.

Polychrome Stain for Semithin Sections

1. Applications and Objectives

This method serves the same purpose as the toluidine blue O procedure for staining semithin sections but provides semithin sections with red and blue colors.

2. Materials Needed

- 1% sodium borate stock (1 g in 100 ml of distilled water)
- 1% toluidine blue O in 1% sodium borate (1 g of each in 100 ml of distilled water)
- 0.1% basic fuchsin (0.10 g of basic fuchsin in 100 ml of distilled water); dissolve by heating to 100°C and then filter; this solution keeps for about 1 year at room temperature
- Hot plate
- Microscope slides and coverslips
- Squirt bottle containing distilled water
- Small glass test tubes
- Poly-mount™

3. Procedure

1. Collect semithin sections in a drop of distilled water on a slide. Dry on a hotplate. Circle sections on the bottom of the slide with a Sharpie®.
2. Place a drop of toluidine blue O solution on the sections; put on hot plate and heat until the edge of the stain drop turns slightly golden.
3. Rinse with a jet of distilled water and dry on the hot plate.
4. Mix equal parts of basic fuchsin stock and sodium borate stock in a test tube. Put a drop of the mixture on sections and heat briefly, then rinse with a jet of distilled water and dry on the hot plate.
5. Add 1–2 drops of Poly-mount™ and coverslip.

4. Results Expected

The semithin sections should be stain- and wrinkle-free, with both red and blue areas.

5. Cautionary Statements

Refer to the toluidine blue O procedures for semithin sections.

Reference

Hoffman, E.O., Flores, T.R., Coover, J., and Garrett, H.B., II. 1983. Polychrome stains for high resolution light microscopy. *Lab. Med.* 14: 779.

Staining Ultrathin Sections

1. Applications and Objectives

This procedure is meant to impart contrast to resin-embedded ultrathin sections. The stained ultrathin sections should have sufficient contrast to be easy to visualize on a TEM viewing screen.

2. Materials Needed

- Uranyl acetate
- Lead nitrate
- Sodium citrate
- Squirt bottle of distilled water
- 100% methanol
- Parafilm™
- Petri dishes
- Forceps
- Ultrathin (60–90 nm thick) sections on grids
- Whatman™ #1 filter paper (9-cm disks)
- 1 N NaOH
- 50-ml volumetric flask with a plastic snap-cap
- 20- to 50-ml brown glass storage container (or foil-wrapped glass container)
- 50-ml disposable beakers

3. Procedure

Stain Preparation

1. *Methanolic uranyl acetate*: Add 1.25 g uranyl acetate to 25 ml of absolute or 50% methanol in a brown glass bottle or a storage container wrapped in aluminum foil. Sonicate the solution until little precipitate is visible. Store the solution at room temperature. It is ready to use after standing overnight. A small amount of precipitate in the bottom of the container is acceptable, since the solution is essentially saturated. The solution may be stored for about 1 month and used until it has evidence of precipitate or stained grids have noticeable uranyl acetate crystals (needle-like dirt) when viewed with the TEM.
2. *Reynolds' (1963) lead citrate*: To a 50-ml volumetric flask with a plastic snap cap, add the following, in the order listed:
   - 30 ml of distilled water
   - 1.33 g of $Pb(NO_3)_2$ (lead nitrate)
   - 1.76 g of $Na_3(C_6H_3O_7)H_2O$ (sodium citrate)

   Mix in the 50-ml volumetric flask by shaking continuously for 1 min and then allow to stand with intermittent shaking for an additional 30 min. Next, add 0.32 g of NaOH pellets. The previously milky solution should change quickly to an absolutely clear solution with no evidence of precipitate. Dilute to a final volume of 50 ml with distilled water. The final pH is about 12. The stain can be stored at 4°C for 1–3 months. If it becomes cloudy, or any precipitate is visible, discard the solution.

Staining Spurr Resin Sections (see Cautionary Statements for other types of resins)

1. Prepare a square of Parafilm™ slightly smaller than a plastic Petri dish and attach it to the bottom of the dish by applying pressure to the four corners of the Parafilm™ square with the blunt end of a pair of forceps (Fig. 129).
2. Put 1 drop of methanolic uranyl acetate on Parafilm™, touch the section-side (shiny side) of a grid to the drop, turn grid over, and leave the grid section-side up at the bottom of the drop (Fig. 130). Cover the Petri dish staining chamber and leave for 5 min.

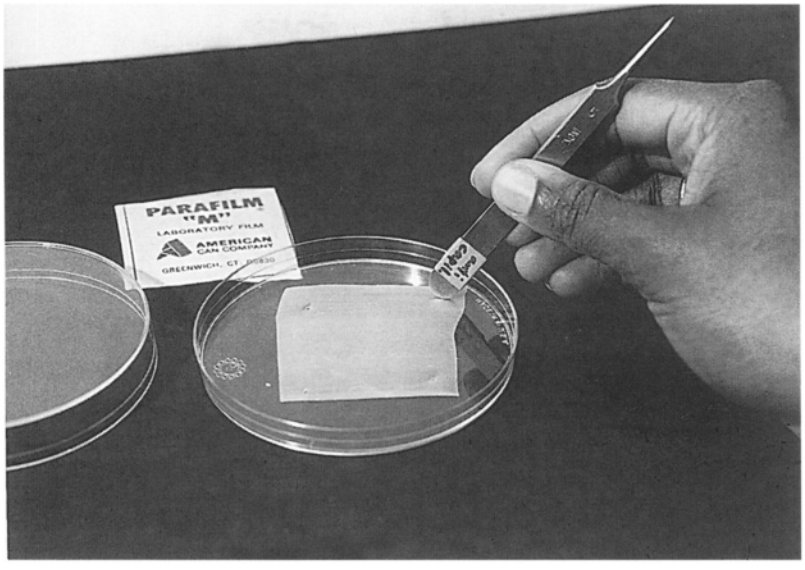

Figure 129. Parafilm™ attached to the bottom of a Petri dish. Note the pressure-tack marks at the corners of the Parafilm™ where forceps were used to attach the Parafilm™ to the dish.

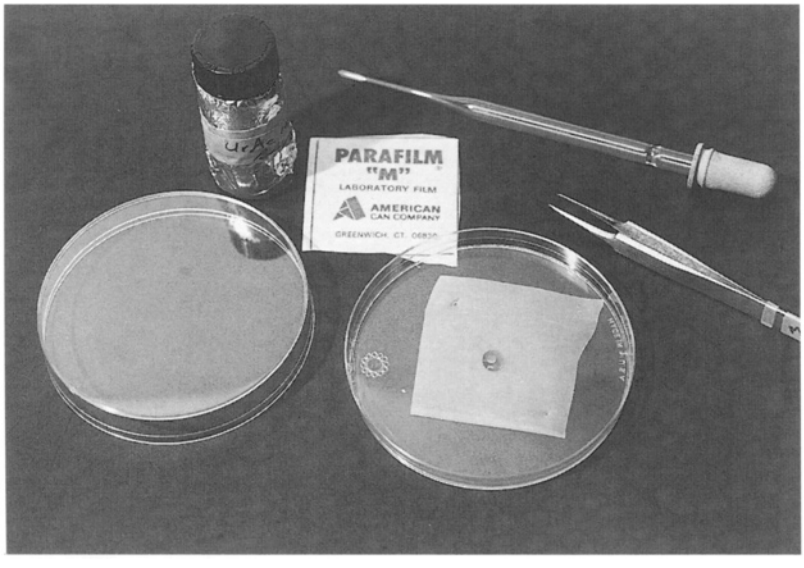

Figure 130. Staining chamber (Petri dish) containing a grid with sections facing up at the bottom of a drop of methanolic uranyl acetate sitting on a sheet of Parafilm™.

3. Retrieve the grid from the drop of uranyl acetate with forceps and quickly dip it three times in each of a series of three 50-ml disposable beakers containing distilled or deionized water, pH 6.0–7.5 (Fig. 131). Enter the first rinse beaker gently and do not agitate excessively as this may wrinkle or dislodge the sections.
4. Blot the grid dry by touching a piece of filter paper to the edge of the grid where it is held by the forceps (Fig. 132). Repeat on the opposite side of the forceps. Blot the grid on clean filter paper in

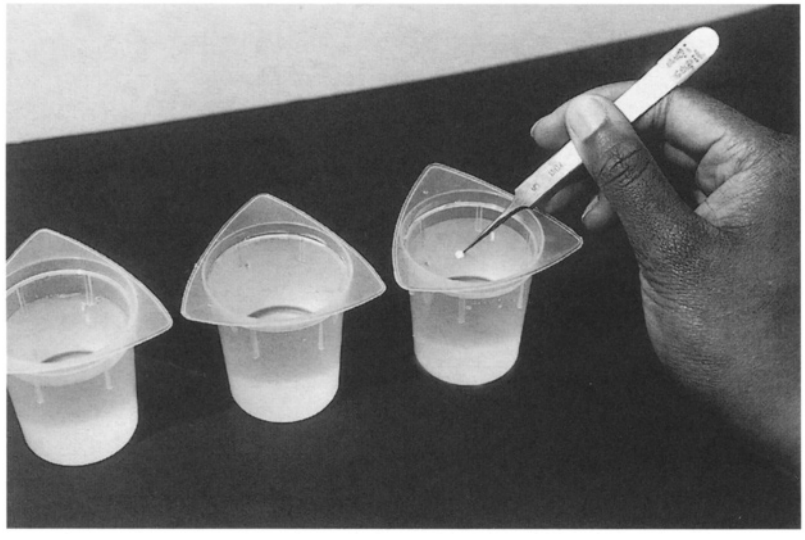

Figure 131. Dipping a stained grid in first of three beakers of distilled water for rinsing.

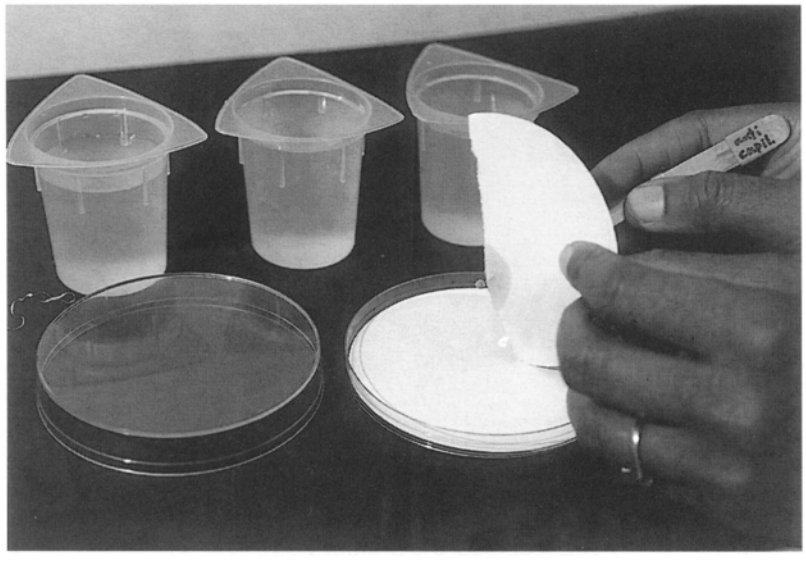

Figure 132. Drying a grid with a piece of filter paper applied to the edge of the grid held with forceps.

a Petri dish *on both sides*, and then slide a fresh part of the filter paper between the forceps blades and use it to push the grid out of the forceps and onto a clean and dry piece of the filter paper in the Petri dish (Fig. 133).

5. Using the same chamber, put one drop of Reynolds' lead citrate on the Parafilm™ and insert grid as above. Quickly cover the dish and leave for 8 min.
6. While the grid is staining, empty the rinse beakers and wash them thoroughly with deionized water. Refill with distilled or deionized water, pH 6.0–7.5. After the grids have been stained for 8 min, rinse and blot dry as above. They are now ready for examination with the TEM.

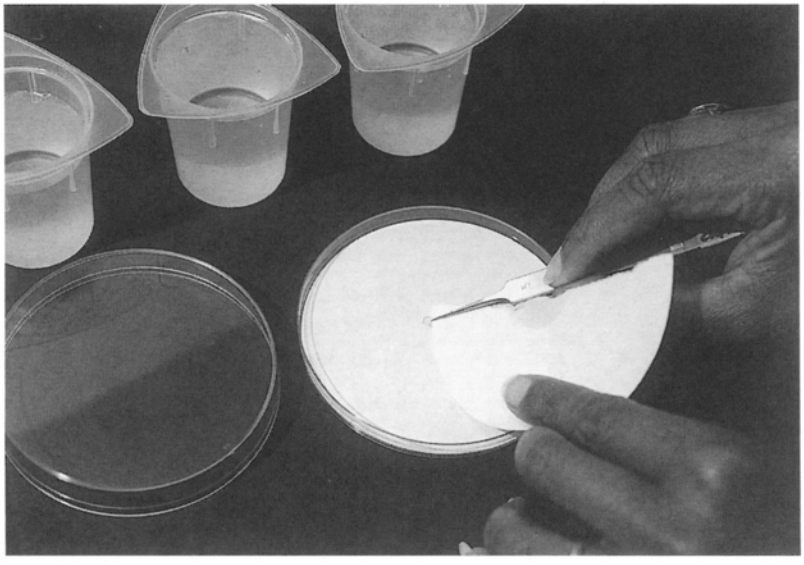

Figure 133. Pushing the dried grid out of the forceps jaws onto a clean piece of filter paper in a Petri dish with a dry portion of a piece of filter paper.

4. Results Expected

The grids should have sufficient contrast to be seen easily on the TEM screen, with membranes, ribosomes, DNA in the nucleus, glycogen, and proteinaceous elements clearly defined.

5. Cautionary Statements

Both the uranyl acetate and lead citrate solutions are heavy metals and are thus toxic compounds. The waste generated should be collected in separate containers, and disposal should be done by hazardous waste personnel. These compounds should not come into contact with the skin or be inhaled or ingested. The radioactivity of uranyl acetate is not a major concern when these handling cautions are observed.

Methanolic uranyl acetate must be used to allow sufficient staining of Spurr-embedded materials. Most other epoxide resins will stain sufficiently in 3% aqueous uranyl acetate (for 5 min) followed by 8 min in Reynolds' lead citrate. Acrylic resins may be stained like non-Spurr epoxides.

The folds encountered at times in Spurr sections with this staining procedure are specifically caused by the methanolic staining and because sections are not quickly and fully dried. Less aggressive dipping in the first rinse (when the methanol-treated sections first contact the deionized water) sometimes will reduce this artifact, but the main cure for the problem is to follow the drying instructions between fluids precisely.

It is imperative that the lead citrate have minimal contact with air because such contact leads to the formation of lead carbonate precipitate, which will be seen as granules of lead "dirt" on the sections when viewed with the TEM. Lead citrate should be quickly transferred from the volumetric storage flask onto the Parafilm™ within a Petri dish and the dish immediately covered. Grids should be quickly added to the lead citrate droplet by lifting the edge of the Petri dish lid. As soon as the grids are within the droplets, the dish should be closed again. If more than one grid is being stained at a time (it is difficult for most workers to stain more than five or so at a time without getting excessive stain dirt), the dish lid should be lifted slightly, a grid removed, and the lid immediately closed again. The grid should be plunged into the first beaker of deionized or distilled water as quickly as possible to prevent interaction with air and the formation of lead carbonate crystals.

After each staining step, it is necessary to make sure that the grid is dried quickly and completely and put down on a clean, dry area of filter paper. If a grid is put down on the filter paper and a slight damp spot is seen, there is a strong possibility that there will be excessive stain dirt on the grid, as well as excessive folds and wrinkles.

Reference

Reynolds, E.S. 1963. The use of lead citrate at high pH as an electron opaque stain in electron microscopy. *J. Cell Biol.* 17: 208.

Subbing Slides

1. Applications and Objectives

This procedure provides slides with a more sticky surface, suitable for attaching extra-thick semithin sections, frozen sections, or semithin sections intended for autoradiography methods.

2. Materials Needed

- Gelatin
- 300-ml clean glass vessel
- Distilled water
- 10% chromium potassium sulfate solution
- Glass slides
- Rectangular slide-dipping chamber with glass rack

3. Procedure

1. Wash glass slides in Alconox® or other laboratory detergent, rinse thoroughly with deionized or distilled water and let dry.
2. Dissolve 5 g of gelatin in 250 ml of 100°C distilled water.
3. Cool the gelatin water to room temperature.
4. Add 0.5 ml of the 10% solution of chromium potassium sulfate.
5. Put enough of solution into slide-dipping chamber to cover slides in rack.
6. Load slide rack, dip in solution, remove from slide-dipping chamber, and set aside to dry.

4. Results Expected

The slides will be coated with a virtually invisible coating that will make any sections put on the slides stick better.

5. Cautionary Statements

The dipping solution does not keep, and the slides must be thoroughly dried before use. The disadvantage of this technique is that the gelatin will become stained along with the tissue with toluidine blue-O staining procedures.

5

Cytochemistry

Cytochemistry at the ultrastructural level is a broad subject, encompassing considerations of fixation and its effect on enzyme activity, problems with reagent and label penetration of tissues and cells, and problems distinguishing reaction products from other cellular constituents. The aim of this chapter is to introduce some of the different general types of staining procedures frequently employed to demonstrate specific chemical entities associated with cellular surfaces and cytoplasmic contents.

As with many of the specialized techniques in electron microscopy, it is always advisable to examine the current literature concerning the group of organisms being studied and the particular cytochemical procedures that are of interest. There are also various routinely used techniques, which are described in Hayat (1981, 2000). Even though now seriously dated, some of the classical cytochemical procedures (many of them still widely used) as well as in-depth discussions of their mechanisms are provided in the five-volume series entitled *Electron Microscopy of Enzymes* edited by Hayat (1973–1977). Immunocytochemistry has evolved into a major specialized area of cytochemistry that warrants the separate treatment provided in Chapter 6.

I. PROBLEMS

As was mentioned in Chapter 1, the goal of fixation is to stabilize the colloidal suspension of cellular constituents so that the individual components are immobilized and made resistant to the further steps of dehydration, embedment, and polymerization that are employed with standard processing procedures. We have seen that cryotechniques avoid some of the stresses associated with the processing steps but introduce other problems, primarily shallow depth of fixation. If a cytochemical procedure yields positive results after chemical fixation, that approach is recommended because the sample size is generally larger than is possible with cryotechniques, and the photographic image that results is generally more pleasing. However, if a procedure does not work with conventional chemical fixation, cryotechniques offer a potential solution.

For enzyme cytochemistry, we have the twin problems of not only needing to stabilize cellular components in an attempt to prevent their extraction during processing, but also needing to maintain an active three-dimensional protein. Since enzyme specificity is determined by reactive sites defined by the complex tertiary folding of the protein molecules comprising enzymes, the cross-linking fixatives used in electron microscopy have the capacity to inactivate enzymes. This result may occur because the cross-linking process changes the spatial relationship between different areas within an enzyme's active site, or it may occur because the act of cross-linking the enzyme to another adjacent protein makes the enzyme's active site inaccessible for enzymatic activity. This is probably the mechanism accounting for significantly reduced activity of enzymes following glutaraldehyde fixation, since attaching this large five-carbon molecule can produce steric hindrance by bridging reactive sites.

Each aldehyde fixative inactivates various enzymes to a different extent. Aldehydes such as glutaraldehyde and acrolein that cross-link more strongly are usually less desirable for enzyme

cytochemistry than formaldehyde, which is a smaller molecule and cross-links weakly. Since each aldehyde can inactivate a spectrum of enzymes, it is generally a poor idea to use a primary fixative containing a mixture of aldehydes such as formaldehyde and glutaraldehyde (Karnovsky's, McDowell's and Trump's 4F:1G), because more enzymes will become inactivated than if only one aldehyde is used. At the same time, all aldehydes produce membrane leakage, and thus increase the permeability of cells and organelles to reagents, which can be helpful. Unfortunately, the process also allows enzymes and other materials originally contained within organelles, such as lysosomes, to leak into the cytoplasm. This latter phenomenon presumably accounts for some of the leaching of cytoplasmic contents encountered with long-term storage of tissues in aldehyde solutions. As the cells become fixed, their membranes become permeable, and their lysosomes leak some of their hydrolytic enzymes into the cytoplasm where the enzymes then degrade cytoplasmic materials, which are subsequently washed out during further processing steps.

Most of the literature on cytochemical procedures for electron microscopy suggests that biological-grade 37–40% formaldehyde should not be used to formulate fixatives because of the small amounts of methanol added during manufacture to prevent polymerization. Various procedure manuals and textbooks for electron microscopy even state that structural work will be compromised unless formaldehyde is made from freshly depolymerized paraformaldehyde containing no additives. However, it is clear from all the papers published using 4F:1G fixative (see Chapter 1) that biological grade formaldehyde is adequate for preparing fixatives for straightforward structural work.

A number of enzyme cytochemical procedures have been modified from techniques originally developed for light microscopy utilizing tissues fixed in 4% BNF formulated from biological-grade formaldehyde. This indicates that it is not absolutely necessary to go to the trouble of making up solutions of formaldehyde from paraformaldehyde, which have a relatively short shelf life. Nonetheless, most recipes in the literature that use formaldehyde still specify making it up fresh, and so it is customary to follow that procedure.

Other aspects of fixation procedures may cause problems. Osmium is a strong oxidant and will damage the reactivity of most enzymatically active sites in cells. The fact that osmium is a heavy metal may also interfere with enzymatic activity.

Even with nonenzymatic cytochemistry used to localize carbohydrates or various types of charged sites associated with cells, processing chemicals may introduce problems. If a procedure for demonstrating negatively charged groups is employed, phosphate buffers will usually decrease or eliminate the stain's effectiveness. The negative charges of phosphate buffers will exhibit reactivity with some stains, possibly resulting in coprecipitation of the stain and the buffer, preventing the desired interaction of the stain with cellular components.

Cytochemical procedures are designed to leave a recognizable product at the site of a specific cellular component that is being identified. The reaction product ideally should be electron-dense and hard to confuse with other normally encountered cellular components. It also needs to be large enough to be easily visualized with an electron microscope. Producing a reaction product of sufficient size to be visualized proves to be one of the most significant problems encountered in designing cytochemical protocols. Many reaction products that are large enough to be visualized easily will not cross membranes even after aldehyde fixation. One of the reasons for the popularity of peroxidase procedures is that the reagents have the capability of penetrating aldehyde-fixed membranes. However, the typical product of these reactions is an osmicated area within a cell, which can be confused with other normally osmicated materials within the cell.

Various procedures have been employed to improve reagent accessibility to cells and tissues. Conventional samples 1 mm thick can be exposed to cytochemical reagents, embedded, and sectioned, and then only the surface cells that have been easily penetrated examined. This procedure is fairly inefficient and produces limited usable sample size, but will often work.

Another method frequently used involves aldehyde fixation followed by chopping or slicing of the tissue into 40- to 50-μm-thick slices, utilizing a Smith–Farquahar™ or MacIlwaine™ tissue chopper in the former case or a Vibratome® in the latter case, prior to cytochemical staining. The thin slices of tissue produced provide superior reagent accessibility. Some tissues are sliced or chopped in the living state, exposed to cytochemical procedures, and then fixed and embedded. After the tissue slices have been fixed and the cytochemical procedures have been completed, the slices may be put into molten (45–50 °C) agar and centrifuged gently before the agar solidifies to produce a concentrated sample that is easier to handle in subsequent processing steps.

II. SPECIFIC REACTION PRODUCTS

To be an effective stain for electron microscopy, a material incorporated into tissues must be capable of scattering the electron beam, thus producing dark areas in the viewed image because of subtractive contrast. Some of the stain products are also visible at the light microscopic level, which can be helpful for the analysis of staining success. If possible, it is useful to ascertain that some staining is occurring and to examine a comparatively large amount of sample at the light level before embarking on the lengthy procedures usually required for the preparation of samples for electron microscopy. Since conventional chemical fixation and embedment procedures profoundly inactivate most enzymes, most cytochemistry is done *en bloc*.

A. Peroxidase Methods

The enzyme peroxidase is easily demonstrated at the light microscopic level by exposing it to hydrogen peroxide, which is reduced to water. To produce an electron-dense stain for electron microscopy, 3,3′-diaminobenzidine • HCl (DAB) is provided as an electron donor.

It should be noted that DAB is a confirmed carcinogen and must be handled with great care. If used in powdered form, it is scattered easily by electrostatic forces during weighing, so it is usually better to use sealed vials into which diluent is injected prior to removal of the solution.

The highly reactive DAB molecule becomes localized at the site of the peroxidase and can, in turn, reduce osmium applied as a postfixative, thereby amplifying the peroxidase and producing an osmium black. The product is seen as an amorphous electron-dense area within the tissue that has no other characteristics, so it must be interpreted with care to prevent confusion with naturally osmicated regions. Other reactive chemical entities such as Hatchett's brown (described below) can be localized within cells by amplification with DAB and osmium.

B. Lead Capture

Another commonly employed reaction product borrowed from enzyme histochemical techniques is lead. Various lead-capture techniques developed for the demonstration of enzymes at the light microscopic level are easily transformed into electron microscopy procedures because of the electron density of the product. These techniques may confuse naturally occurring lead products with products found in tissues poststained with lead. If lead-capture procedures are used, it is advisable to prepare two grids for examination, one with poststaining and one without. If the

grid that was not poststained is examined first, the lead products will stand out clearly, allowing easier interpretation of the poststained grid, which will have additional lead deposits produced by the poststaining.

C. Ferritin

The iron-containing protein, ferritin, was used extensively in the early days of immunocytochemistry and to demonstrate ionic sites on cell surfaces (Danon *et al.*, 1972) because of the electron density of the ferritin molecule. Since ferritin occurs naturally in some tissues, it must be used with care. In addition, it is not so dense as lead or so discrete as gold, so it is rarely used in contemporary procedures.

D. Colloidal Gold

Colloidal gold, which will be discussed more extensively in Chapter 6, has been conjugated to antibodies for immunocytochemical procedures and to lectins to localize saccharides during the last 10 years. It also can be conjugated to enzymes such as phospholipase A_2 (Coulombe *et al.*, 1988) and used to probe cells for the location of specific reactive sites. Despite its size (1 nm or larger), which prevents passage across membranes, colloidal gold is a clearly nonbiological entity that cannot be confused with any other stain products, a characteristic that enhances its usefulness.

E. Ruthenium Red, Alcian Blue, Pyroantimonate

There are also a variety of naturally electron-dense chemicals such as ruthenium red, alcian blue, and pyroantimonate that can be visualized easily with electron microscopy following binding to specific cellular constituents. Again, these chemicals produce amorphous electron-dense areas within cells, so these areas must be interpreted with care.

III. EXAMPLES OF ENZYME CYTOCHEMISTRY (SEE POWELL, 1986)

A. Peroxidase Methods

Naturally occurring endogenous peroxidases (Novikoff and Goldfischer, 1969) located in microbodies are easily demonstrated by briefly fixing tissues or cells with formaldehyde freshly prepared from paraformaldehyde. After quickly washing with buffer, samples are exposed to hydrogen peroxide and DAB, rinsed, then postfixed in osmium, dehydrated, and embedded. As stated above, the product is an amorphous, electron-dense osmium black (Fig. 134). To interpret the results, various controls should be employed such as eliminating the initial substrate (H_2O_2) or briefly boiling the tissue for 5 min following the rinse after initial aldehyde fixation.

Exogenously applied peroxidase techniques introduced by Graham and Karnovsky (1966) have also been utilized to demonstrate leakage between normally tightly bound cell populations, such as endothelial cells of vascular tissues or epithelial cells lining various organ systems. In this application, horseradish peroxidase is injected into a living animal as a tracer, tissues are removed and fixed, and then amplification of the peroxidase is produced by interaction with DAB and osmium.

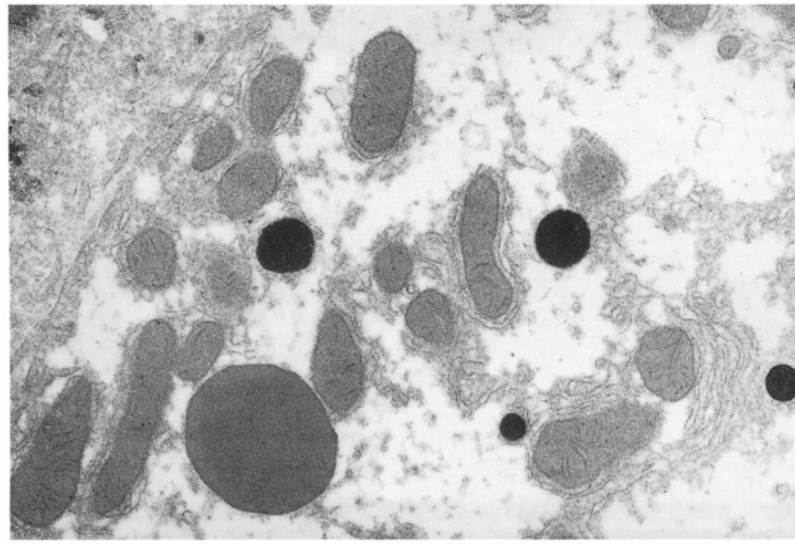

Figure 134. Demonstration of peroxisomes (microbodies) in rat liver with the DAB/osmium technique of Novikoff and Goldfischer (1969). The round, extremely electron-dense structures in the cytoplasm are microbodies. 17,692×. Micrograph courtesy of Philip L. Sannes.

Finally, peroxidases have been conjugated to other products that are bound by enzymes (see Sternberger, 1973), which are then localized by the interaction of the peroxidase with reaction mixtures of hydrogen peroxide, DAB, and osmium.

B. Hatchett's Brown Methods

Several methods have been developed that utilize a reaction originally developed for light microscopy, which yields cupric ferrocyanide at the site of enzyme activity. This product is visible as a brown deposit with light microscopy, and it can be further amplified by DAB with subsequent osmication to produce an osmium black visible with electron microscopy.

This technique has been used to demonstrate the activity of aryl sulfatase on the substrate 4-nitro-1,2-benzenediol mono(hydrogen sulfate) as originally described by Hanker *et al.* (1975). Another application of this procedure is used to localize the enzyme involved in membrane turnover, acyl transferase, as shown in Fig. 135 (Dykstra, 1976).

C. Lead-Capture Methods

Lead-capture methods appropriated from light microscopy techniques were some of the first methods used to demonstrate hydrolytic enzymes associated with lysosomes such as acid phosphatase, alkaline phosphatase, and aryl sulfatase (see Essner, 1973).

Barka and Anderson (1962) introduced a still widely used modification of previous lead-capture methods for the demonstration of acid phosphatase. It was formulated with less lead than used with previous procedures and employed a maleate buffer, which was said to keep lead ions in solution, thus decreasing random deposition of lead in tissues and cells. As with the previous

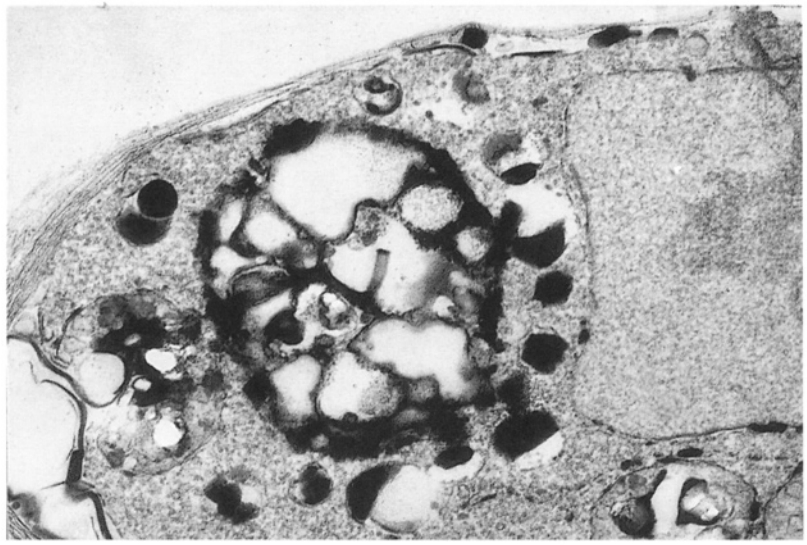

Figure 135. Acyl transferase demonstrated by a copper capture method (Hatchett's brown) associated with membranes of *Sorodiplophrys stercorea*, a terrestrial protozoan. The product appears as an electron dense deposit within the cell, which was not poststained. 31,154×.

procedures, Na-β-glycerophosphate is the substrate for the enzyme, Tris-maleate buffer is used to maintain a pH of 5.0 for best enzymatic activity, and lead nitrate is the lead source. Acid phosphatase causes the release of phosphate ions from the substrate, which replace the nitrate molecules attached to lead nitrate, resulting in the formation of insoluble lead phosphate at the site of enzymatic activity (Fig. 136).

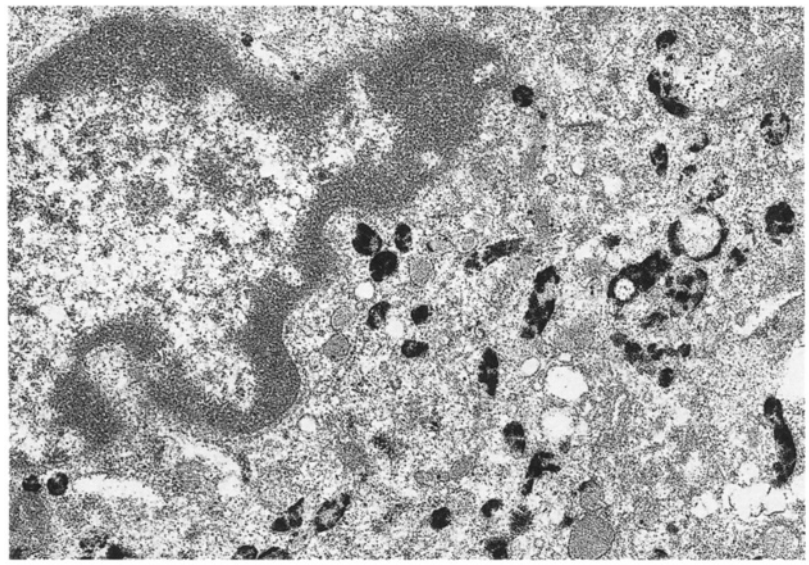

Figure 136. Demonstration of acid phosphatase located in lysosomes of rat alveolar macrophages with the lead capture method of Barka and Anderson (1962). The lead phosphate product is visualized as the extremely electron-dense areas within the cell. 21,538×. Micrograph courtesy of Philip L. Sannes.

IV. EXAMPLES OF NONENZYMATIC CYTOCHEMISTRY

A. Cationic Dyes

Three major cationic materials have been used extensively for the demonstration of the glycocalyx associated with most cell surfaces. Initially, only plants, fungi, and many bacteria were known to have walls composed of complex assemblages of carbohydrate moieties and other chemical entities, but during the 1970s, closer examination demonstrated the presence of a polysaccharide cell coat on the surface of virtually all cell types. It became evident that these carbohydrate-loaded, typically negatively-charged coats were frequently involved in cellular recognition, so cell biologists became more interested in being able to delineate them clearly. This was achieved by applying cationic ferritin, alcian blue, or ruthenium red. In some cases (Dykstra and Aldrich, 1978), it was necessary to use both alcian blue (0.5% in the primary fixative) and ruthenium red (0.05% in the osmium postfixative) to demonstrate evanescent glycocalyx materials (Fig. 137). When using these dyes, it is imperative that cacodylate buffers be used rather than phosphate buffers, since the latter will coprecipitate with the dyes, rendering them useless. None of these dyes reveals the exact chemical nature of glycocalyx materials, only that they are present and possess some negative charges.

B. Polysaccharide Stains

Several widely used semispecific polysaccharide stains have been developed (see Erdos, 1986), which primarily reveal hydroxyl groups of polysaccharides opened by oxidation with periodic acid. These techniques are essentially equivalent to periodic acid–Schiff's reagent reactions employed in light microscopy. The three most commonly employed stains are silver methenamine (Edgar and Pickett-Heaps, 1982; Pickett-Heaps, 1967), which is equivalent to Gomori methenamine–silver staining used for light microscopy (Fig. 138), thiocarbohydrazide (Thiery and Rambourg, 1975), and silver protein (Thiery, 1967). All three are used to stain carbohydrate molecules associated with cells and tissues that have been fixed, embedded in commonly used resins, and then sectioned before staining. Osmium will often react with these stains, so it must either be removed from the sections by fairly strong oxidants prior to the polysaccharide reactions or be deleted from the initial fixation steps. If osmium is not used as a postfixative, cell structure is somewhat compromised. Nonetheless, if optimal polysaccharide localization is desired with minimal interpretational difficulties, osmium should be eliminated.

All three techniques stain similar molecules, and all three should be used on sections picked up on inert grids made of stainless steel or nickel. Copper grids are chemically reactive and can interfere with the stains. The grids can be inserted into small segments of Tygon™ tubing with small slits in the surface (Fig. 139) to allow easy transfer from one staining solution to another.

C. Monosaccharide and Disaccharide Stains

The polysaccharide stains described above are still fairly nonspecific, staining charged entities such as osmium in addition to polysaccharides. In addition, even when sufficient controls

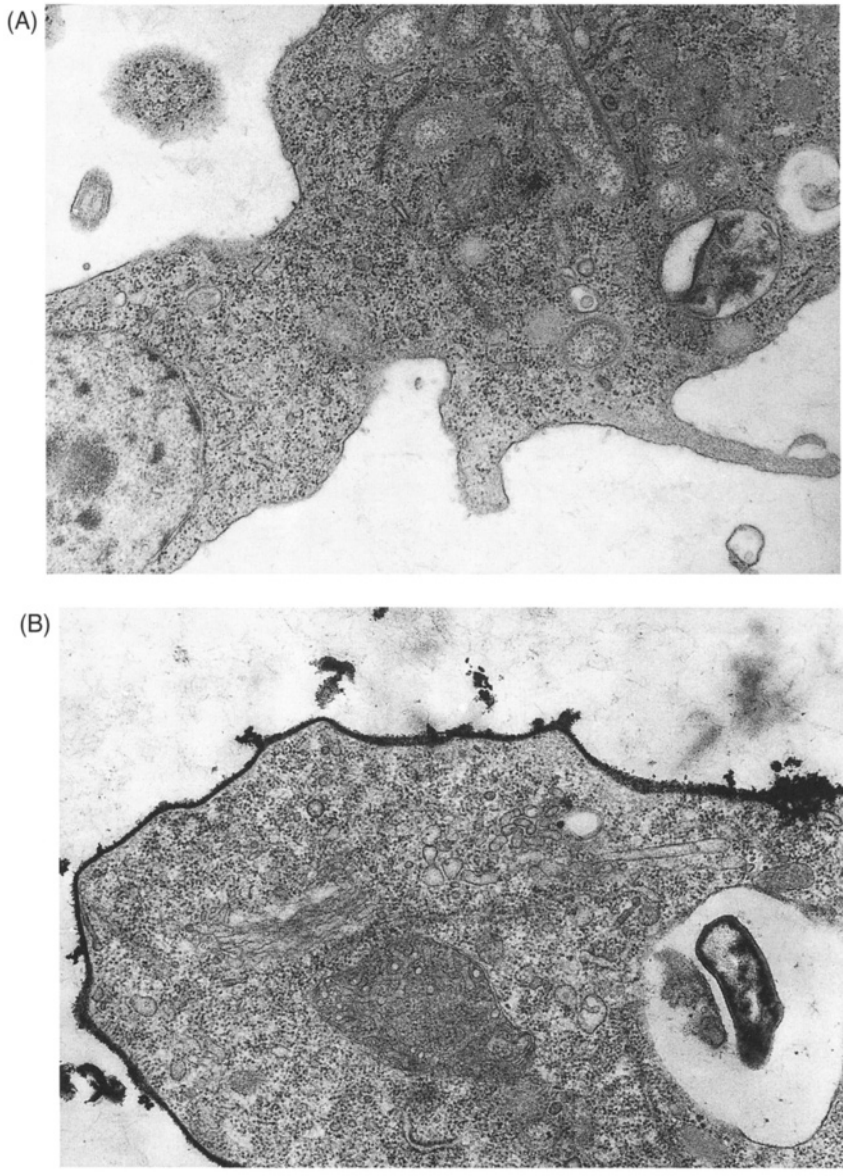

Figure 137. Amoebae of the slime mold, *Fuligo septica*. (A) A cell with no cytochemical staining or poststaining. 19,712×. (B) A cell stained with 0.5% alcian blue in the glutaraldehyde primary fixative and 0.05% ruthenium red in the osmium postfixation step. The glycocalyx can be seen as an electron-dense, granular deposit on the surface of the plasma membrane. No poststain. 25,192×.

have been employed to unequivocally demonstrate polysaccharides, the specific sugars involved are not identified. Various workers (see Erdos, 1986; Sharon and Lis, 1989) have found, however, that a number of plant proteins, called lectins, are capable of binding to specific sugar residues in or on cells. Initially, lectins were conjugated with fluorochromes such as fluoroisothiocyanate (FITC) or peroxidase. They were attached to sugars associated with cells, and demonstrated with

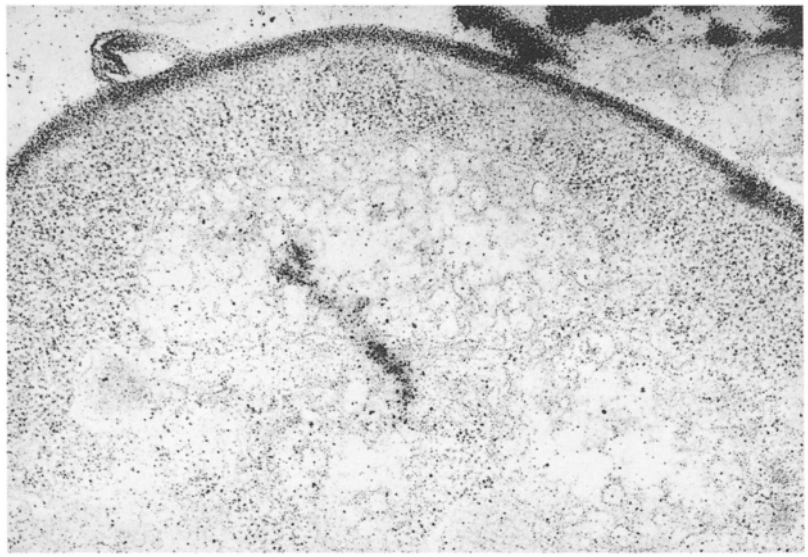

Figure 138. Demonstration of polysaccharide scales comprising the cell wall of the terrestrial protozoan *Sorodiplophrys stercorea* with silver methenamine staining. Large quantities of silver grains are deposited on the polysaccharide cell wall. Nonspecific deposits are located throughout the cell, presumably because of interaction with osmium, which was used as a postfixative. 33,173×.

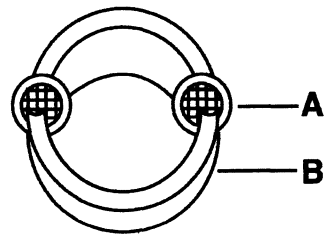

Figure 139. Tygon™ tubing with slits holding grids for cytochemical procedures.

fluorescence or bright-field microscopy, respectively. Cell biologists then used lectins conjugated with compounds such as ferritin or peroxidase so that the lectins could be identified with the electron microscope. When colloidal gold became widely used as an electron-dense marker, investigators conjugated it with lectins to produce a superior marker for the presence of specific sugars in tissues and cells. Lectin binding of surface sugars is most easily done *en bloc*. If sugars inside cells are to be demonstrated, cryoultramicrotomy is indicated, since the lectin molecule with its associated label is too large to pass through a plasma membrane.

Lectin binding is particularly useful because of its specificity. A variety of sugars can be identified with the various lectins available (Table 12).

Table 12. A Selection of Lectins and the Sugar Residues with which they React

Lectin	Source	Sugar Specificity
Abrin	*Abrus precatorius* (Jequirity bean)	D-Galactose
Concanavalin A (Con A)	*Canavalia ensiformis* (Jack bean)	α-D-Mannose, α-D-glucose
Limulus (LPA)	*Limulus polyphemus* (Horseshoe crab)	*N*-Acetylneuraminic acid (sialic acid), glucuronic acid, phosphorylcholine analogs
Ricin	*Ricinus communis* (Castor bean)	*N*-Acetyl-D-galactosamine, β-D-galactosyl residues
Ulex	*Ulex europaeus* (Gorse or Furze)	α-L-Fucose, *N,N'*-diacetylchitobiose
Wheat-germ agglutinin	*Triticum vulgaris* (Wheat)	*N*-Acetyl-β-D-glucosaminyl residues, *N*-acetyl-β-D-glucosamine oligomers

D. Calcium Staining

Calcium localization is of great interest to muscle researchers, membrane biologists, and others, since it is critically involved in numerous cellular functions. Potassium pyroantimonate or sodium pyroantimonate has been used extensively (see review by Wick and Hepler, 1982) to demonstrate calcium. Pyroantimonate is not strictly calcium-specific because it also binds to sodium, potassium, and magnesium. With proper controls, however, pyroantimonate staining has been recognized as a relatively reliable and simple procedure to localize calcium. Pyroantimonate staining during postfixation with osmium (Dykstra and Hackett, 1979), as shown in Fig. 140, will reveal calcium deposits as electron-dense material. Any soluble calcium in the tissue will have

Figure 140. Proximal convoluted tubule of a rat kidney showing a large crystalline array of calcium oxalate stained with potassium pyroantimonate within the tubule lumen. Finely granular, black deposits of pyroantimonate-stained calcium are also located in apical vesicles of tubule epithelial cells. 2,067×.

been washed out during fixation and processing up to the postfixation step, however. To demonstrate soluble calcium, pyroantimonate must be applied to tissue during primary fixation. The technique described by Oberc and Engel (1977) demonstrates such soluble calcium entities (Fig. 141) but does not work well with tissues other than muscle. Muscle tissue is relatively stable compared with other tissues. Even if muscle tissue is stored at 4°C on saline-dampened gauze for a number of hours, it will still look normal when fixed. The pyroantimonate method developed by Oberc and Engel uses a solution of pyroantimonate to stabilize calcium in the tissues prior to aldehyde fixation. Again, this method works for muscles, which are relatively stable, but works poorly for tissues, such as kidney, that suffer severe fixation damage during the procedure.

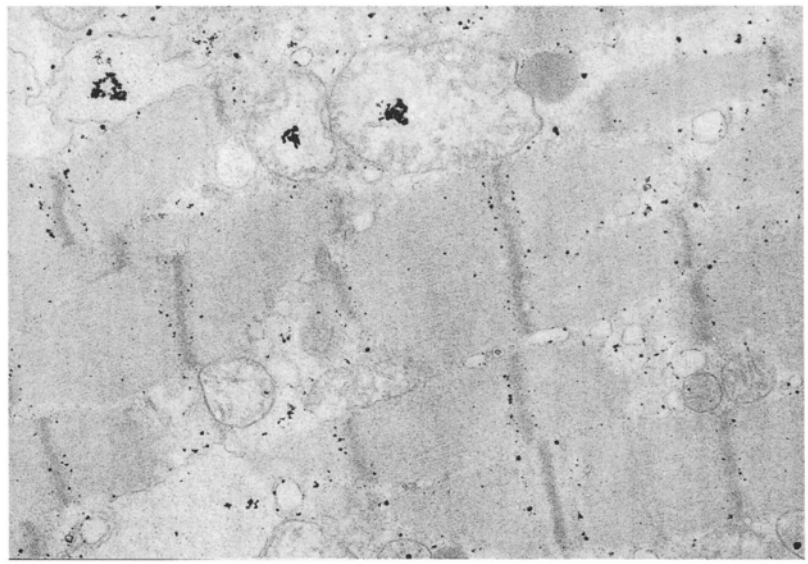

Figure 141. Demonstration of soluble calcium in canine skeletal muscle. Note that calcium is preferentially associated with the Z-bands of sarcomeres. Larger granular deposits of calcium stained with pyroantimonate are located in the matrix area of mitochondria. If pyroantimonate staining is done during postfixation in osmium rather than prior to aldehyde fixation, none of these deposits remain. 13,462×.

REFERENCES

Barka, T. and Anderson, P.J. 1962. Histochemical methods for acid phosphatase using hexazonium pararosanilin as a coupler. *J. Histochem. Cytochem.* 10: 741.

Coulombe, P.A., Kan, F.W.K., and Bendayan, M. 1988. Introduction of a high-resolution cytochemical method for studying the distribution of phospholipids in biological tissues. *Eur. J. Cell Biol.* 46: 564.

Danon, D., Goldstein, L., Marikovsky, Y., and Skutelsky, E. 1972. Use of cationized ferritin as a label of negative charges on cell surfaces. *J. Ultrastruct. Res.* 38: 500.

Dykstra, M.J. 1976. Wall and membrane biogenesis in the unusual labyrinthulid-like organism *Sorodiplophrys stercorea. Protoplasma* 87: 329.

Dykstra, M.J. and Aldrich, H.C. 1978. Successful demonstration of an elusive cell coat in amoebae. *J. Protozool.* 25: 38.

Dykstra, M.J. and Hackett, R.L. 1979. Ultrastructural events in early calcium oxalate crystal formation in rats. *Kidney Int.* 15: 640.

Edgar, L.A. and Pickett-Heaps, J.D. 1982. Ultrastructural localization of polysaccharides in the motile diatom *Navicula cuspidata. Protoplasma* 113: 10.

Erdos, G.W. 1986. Localization of carbohydrate-containing molecules. In: H.C. Aldrich and W.J. Todd (eds.), *Ultrastructure techniques for microorganisms*. Plenum Press, New York.

Essner, E. 1973. Phosphatases. In: M.A. Hayat (ed.), *Electron microscopy of enzymes: Principles and methods* (Vol. 1). Van Nostrand Reinhold, New York.

Graham, R.C., Jr. and Karnovsky, M.J. 1966. The early stages of absorption of injected horseradish peroxidase in the proximal convoluted tubules of mouse kidney: Ultrastructural cytochemistry by a new technique. *J. Histochem. Cytochem.* 14: 291.

Hanker, J.S., Thornburg, L.P., Yates, P.E., and Romanovicz, D.K. 1975. The demonstration of aryl sulfatases with 4-nitro-1,2-benzenediol mono (hydrogen sulfate) by the formation of osmium blacks at the sites of copper capture. *Histochemistry* 41: 207.

Hayat, M.A. (ed.). 1973–1977. *Electron microscopy of enzymes: Principles and methods* (Vols. 1–5). Van Nostrand Reinhold, New York.

Hayat, M.A. 1981. *Fixation for electron microscopy*. Academic Press, New York.

Hayat, M.A. 2000. *Electron microscopy: Biological applications*, 4th edn. Cambridge University Press, New York.

Novikoff, A.B. and Goldfischer, S. 1969. Visualization of peroxisomes (microbodies) and mitochondria with diaminobenzidine. *J. Histochem. Cytochem.* 17: 675.

Oberc, M.A. and Engel, W.K. 1977. Ultrastructural localization of calcium in normal and abnormal skeletal muscle. *Lab. Invest.* 36: 566.

Pickett-Heaps, J.D. 1967. Preliminary attempts at ultrastructural polysaccharide localization in root tip cells. *J. Histochem. Cytochem.* 15: 442.

Powell, M.J. 1986. Cytochemical techniques for the subcellular localization of enzymes in microorganisms. In: H.C. Aldrich and W.C. Todd (eds.), *Ultrastructure techniques for microorganisms*. Plenum Press, New York.

Sharon, N. and Lis, H. 1989. Lectins as cell recognition molecules. *Science* 246: 227.

Sternberger, L.A. 1973. Enzyme immunocytochemistry. In: M.A. Hayat (ed.), *Electron microscopy of enzymes. Principles and methods* (Vol. 1). Van Nostrand Reinhold, New York.

Thiery, J.P. 1967. Mise en évidence des polysaccharides sur coupes fines en microscopie électronique. *J. Microsc.* 6: 987.

Thiery, J.P. and Rambourg, A. 1975. Polysaccharides cytochemistry. *J. Microsc.* 21: 225.

Wick, S.M. and Hepler, P.K. 1982. Selective localization of intracellular Ca^{2+} with potassium antimonate. *J. Histochem. Cytochem.* 11: 1190.

SUPPLEMENTARY GENERAL REFERENCES

Pearse, A.G.E. 1980. *Histochemistry. Theoretical and applied* (Vol. 1), 4th edn. Churchill Livingstone, New York.

Pearse, A.G.E. 1985. *Histochemistry. Theoretical and applied* (Vol. 2), 4th edn. Churchill Livingstone, New York.

Stoward, P.J., Everson, A.G., and Pearse, A.G.E. (eds.). 1985. *Histochemistry. Theoretical and applied* (Vol. 3), 4th edn. Churchill Livingstone, New York.

CHAPTER 5 TECHNIQUES

Polysaccharide Stains

Negatively charged glycocalyx materials (polysaccharides, mucopolysaccharides) are associated with the surfaces of all cells. Some of these materials are not easily demonstrated by conventional chemical fixation techniques. It is thought that many of these substances are not sufficiently stabilized during primary fixation and are consequently leached from the sample during passage through the various processing fluids. Some of the techniques use cationic dyes that bind to negatively charged materials and thus help stabilize them. These dyes give little information about the stabilized material except for the molecular charge present. Other cytochemical procedures (silver stains) are used with proper controls to demonstrate polysaccharide materials through a Schiff reaction with polysaccharide hydroxyl groups exposed by periodic acid oxidation.

Ruthenium Red Staining

1. Applications and Objectives

Ruthenium red is a cationic dye that stains any anionic sites with which it comes into contact. When bound, the dye is detectable as a granular electron-dense deposit. Ruthenium red also reacts with anionic buffers (phosphate), so it is necessary to use uncharged cacodylate buffering systems during staining. Some workers use alcian blue to achieve the same effect or even a combination of alcian blue and ruthenium red as a stain. See Dykstra and Aldrich (1978) for a discussion of potential variations.

2. Materials Needed

- Aldehyde primary fixatives such as 4F:1G
- 0.1 M and 0.2 M sodium cacodylate buffer, pH 7.2–7.4
- Ruthenium red
- 2% aqueous osmium
- Ethanolic dehydration series
- Acetone
- Spurr's resin (6.3 recipe)
- Sonicator

3. Procedure

Preparation of the Staining Solution. Add 0.75 mg of ruthenium red to 1 ml of 0.2 M sodium cacodylate buffer and sonicate until dissolved. Add to an equal volume of 2% aqueous osmium *just before adding tissues/cells.*

Sample Preparation

1. Fix cells in conventional fixative (e.g., 4F:1G) as specified for routine TEM sample processing.
2. Rinse sample thoroughly with 0.1 M sodium cacodylate buffer to remove any phosphate groups which will coprecipitate with ruthenium red.
3. Place tissue/cells into staining solution at room temperature.
4. After 1 hr in the staining solution, rinse tissue/cells with distilled water (three times, 5 min each). If working with cell suspensions, embed them in molten 3–4% water agar (as previously described) after the water rinses.
5. Dehydrate and embed as for routine TEM sample preparation.

4. Results Expected

Negatively charged glycocalyx materials will be demonstrated by the presence of finely granular electron-dense material (ruthenium red). The stain should be excluded from cells by intact cell membranes.

5. Cautionary Statements

As stated above, it is extremely important to keep negatively charged molecules (like phosphate buffers) from coming into contact with ruthenium red to prevent their coprecipitation, resulting in the inactivation of the staining capability of ruthenium red molecules. In addition, once the osmium is mixed with ruthenium red, the two compounds begin interacting, resulting in a dark blackish-red, turbid solution within 1 hr at room temperature. Ruthenium red can be mixed with buffer and sonicated to dissolve it and then stored for days in the refrigerator before adding osmium. Ruthenium red and osmium should be considered to be highly toxic and handled carefully under a fume hood at all times.

As a control, some of the tissue/cells should be processed simultaneously with routine procedures to record the appearance of nonstained glycocalyx materials for comparison.

If this procedure does not reveal the expected glycocalyx material, it may be necessary to stain with alcian blue during primary fixation (see Dykstra and Aldrich, 1978).

Reference

Dykstra, M.J. and Aldrich, H.C. 1978. Successful demonstration of an elusive cell coat in amoebae. *J. Protozool.* 25: 38.

Silver Methenamine Staining for Polysaccharides

1. Applications and Objectives

Silver methenamine staining, with proper controls, can be used to demonstrate the presence of polysaccharides (Edgar and Pickett-Heaps, 1982; Lehnen and Powell, 1988; Pickett-Heaps, 1967). The hydroxyl groups of polysaccharides are oxidized with periodic acid, allowing their subsequent interaction with silver methenamine. The electron density of the silver deposits on sections ensures that reaction sites can be visualized easily.

2. Materials Needed

Stain Components (see Cautionary Statements before formulating)

- 0.05 M borate buffer: 0.31 g of H_3BO_3 (boric acid) in 90 ml of distilled H_2O. Adjust the pH with 1 N NaOH to 9.0 and bring the final volume to 100 ml
- 5% sodium thiosulfate clearing solution: 0.5 g of sodium thiosulfate in 10 ml of distilled H_2O
- 3% methenamine: 0.3 g of hexamethylenetetraamine in 10 ml of distilled H_2O
- 1% silver nitrate: 0.1 g of $AgNO_3$ in 10 ml of distilled H_2O
- 1% periodic acid: 0.1 g of periodic acid in 10 ml of distilled H_2O

Blockers

- 2% sodium bisulfite: 0.2 g of sodium bisulfite in 10 ml of distilled H_2O
- 1.0 M iodoacetic acid, pH 8.0: 1.86 g in 10 ml of distilled H_2O, adjust pH with 0.1 N NaOH
- 15% H_2O_2 in 0.6 N HCl: 3.7 ml of 30% H_2O_2 + 3.7 ml of 1.2 N HCl (0.44 ml concentrated [37%] HCl + 3.26 ml of H_2O)

Miscellaneous supplies

- Shell vials for oxidizer, stain, and blockers
- Whatman™ #1 filter paper
- $^1/_4$-in. (6-mm) i.d. Tygon™ tubing
- Single-edge razor blades
- Stainless steel or nickel 200-mesh grids
- Forceps
- Aluminum foil

3. Procedure

Preparation of Staining Solution. To prepare the staining solution, which will keep less than 24 hr, mix the following in a shell vial in the order listed:

- 15 ml of 3% methenamine
- 25 ml of 0.05 M borate buffer
- 5 ml of 1% aqueous $AgNO_3$ (add dropwise with constant stirring)
- 5 ml of distilled H_2O

Preparation of Sections and Staining Rings

1. Cut epoxide sections and place them on inert grids made of stainless steel or nickel.
2. Use a razor blade to cut short (3 mm) segments of Tygon™ tubing, then make shallow cuts in the tubing wall into which grids with sections are inserted (Fig. 139).

Staining Procedure

1. Put the ring holding grids with sections into 1% periodic acid for 25 min at room temperature to oxidize polysaccharides.
2. Rinse three times (5 min each) in distilled H_2O.
3. Place the ring in staining solution for 60 min at 60 °C in the dark.
4. Rinse in distilled H_2O for 5 min.
5. Place ring into 5% sodium thiosulfate for 15 min to overnight in the dark at room temperature.
6. Rinse in distilled H_2O, blot dry with filter paper, and examine with a TEM.

Controls

1. To block reactions with aldehydes: 2% sodium bisulfite for 30–60 min at 60 °C; rinse thoroughly with distilled H_2O before staining.
2. To block reactions with sulfhydryls: 1.0 M iodoacetate for 1 hr at 60 °C; rinse thoroughly with distilled H_2O and then stain.
3. To oxidize osmium in sections, preventing argentophilic reaction of osmium with staining solution: 15% acidified H_2O_2 for 30 min at room temperature; rinse thoroughly with distilled H_2O before staining procedure.
4. Eliminate the periodic acid step used to oxidize hydroxyl groups of polysaccharides.

4. Results Expected

Polysaccharides in the plastic sections will be revealed by the presence of coarsely granular silver deposits that totally block the electron beam (Fig. 142).

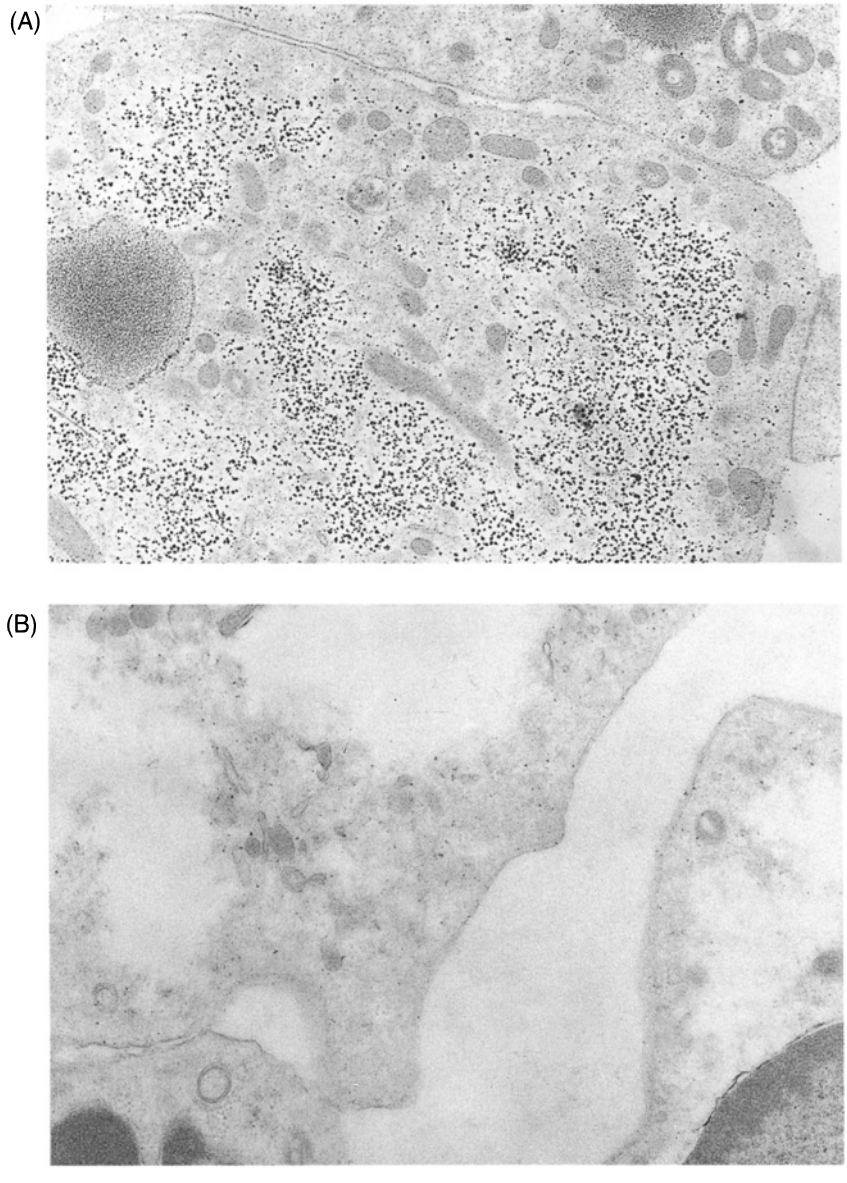

Figure 142. Glycogen staining with silver methenamine. (A) Cultured canine leukocytes with silver-stained glycogen (dark granules). (B) A section of the canine leukocytes from the same block shown above but not stained with silver methenamine. No silver is visible. Both 24,231×.

5. Cautionary Statements

The staining reaction is pH-dependent, with less staining at pH 8.2 and increased staining up to pH 9.2. All glassware must be scrupulously clean. The photosensitivity of the staining solution is fairly low, so mixing the staining solution as well as adding grids and removing grids from the staining solution can be done under laboratory lighting conditions. During staining and clearing (thiosulfate), the reaction vials should be kept in the dark (wrapped in aluminum foil).

If possible, tissues should be fixed only with aldehydes, without osmication. This prevents osmium in the tissue from interacting with the silver in the staining solution. The acidified peroxide solution will

decrease nonspecific staining from interactions with bound osmium if previously prepared postfixed blocks are sectioned and stained.

Hydrogen peroxide solutions, hydrochloric acid, and the silver solutions should be handled with care and disposed of properly.

All pH measurements should be done with pH paper, since silver can damage pH electrodes.

References

Edgar, L.A. and Pickett-Heaps, J.D. 1982. Ultrastructural localization of polysaccharides in the motile diatom *Navicula cuspidata. Protoplasma* 113: 10.

Lehnen, L.P., Jr. and Powell, M.J. 1988. Cytochemical localization of carbohydrates in zoospores of *Saprolegnia ferax. Mycologia* 80: 423.

Pickett-Heaps, J.D. 1967. Preliminary attempts at ultrastructural polysaccharide localization in root tip cells. *J. Histochem. Cytochem.* 15: 442.

Calcium Staining

Calcium in tissues and cells may be found as relatively insoluble products (calcium oxalate crystals in kidneys, hydroxyapatite crystals in bone) or may be extremely soluble. In the former case, calcium can be demonstrated by primary fixation followed by postfixation in osmium containing 2–4% potassium pyroantimonate with good results. In the latter case, the calcium is solubilized during primary fixation and subsequent washing so that an osmium–pyroantimonate staining solution will no longer reveal calcium in the cells or tissue.

Pyroantimonate staining has the potential to localize sodium, potassium, calcium, and magnesium, but the general consensus (Wick and Hepler, 1982) is that the specificity of the pyroantimonate staining methods utilized today is sufficient to conclude that a positive staining reaction demonstrates the presence of calcium. If any doubt remains, electron dispersive spectroscopy, electron energy loss spectroscopy, or electron spectroscopic imaging systems can be used to confirm the presence of calcium. Wick and Hepler (1982) suggest, however, that the pyroantimonate is actually more sensitive to the presence of calcium than typical microanalytical techniques.

Reference

Wick, S.M. and Hepler, P.K. 1982. Selective localization of intracellular Ca^{2+} with potassium antimonate. *J. Cytochem. Histochem.* 30: 1190.

Prefixation Calcium Staining for Muscle Tissue

1. Applications and Objectives

This technique is utilized to demonstrate soluble calcium in muscle (Oberc and Engel, 1977). Tissues are initially placed into the staining solution containing potassium pyroantimonate, which interacts with and stabilizes calcium. Unfortunately, it is not actually a fixative for any other cellular constituents, and few tissues and cells other than muscle can be expected to be well preserved following the procedure. Muscle is highly proteinaceous and highly resistant to autolysis. For this reason, it is possible to incubate muscle in the pyroantimonate solution for hours before aldehyde fixation and still have good ultrastructural preservation (as well as excellent calcium staining). Unfortunately, the stabilizing mixture of formaldehyde and pyroantimonate used after the primary pyroantimonate incubation does not appear to produce adequate calcium stabilization and localization if utilized as the first incubation medium.

2. Materials Needed

- 2% potassium pyroantimonate (KPA): Add 2 g of KPA to distilled H_2O (previously heated until steaming) while stirring; cool and adjust the pH to 9.4 with 0.1 N KOH
- KPA/formaldehyde: Add 7 parts of KPA mixture above to 1 part of 37–40% formaldehyde; adjust the pH to 9.4 if needed
- 10 mM ethyleneglycotetraacetic acid (EGTA): 0.038 g of EGTA/10 ml of distilled H_2O, adjust pH to 9.4 with 0.1 N KOH (the EGTA will not go into solution until the pH is raised; do this slowly so as not to overshoot the pH desired)
- 2% aqueous osmium

3. Procedure

Staining Procedure

1. Gently stretch the muscle and make an incision sufficient to insert a sterilized hairclip. After the hairclip is attached to the muscle at a right angle to the fiber orientation, use a scalpel to cut the muscle just outside the hairclip jaws. Place the clamped muscle (Fig. 143) into the KPA staining solution at room temperature.
2. After 24–48 hr at room temperature, place the tissue into a KPA–formaldehyde mixture and leave at room temperature for an additional 24–48 hr.
3. Rinse the tissue in distilled H_2O and postfix in aqueous 2% osmium for 1 hr at room temperature.
4. Remove the tissue from the hairclip and cut it into millimeter-thick strips so that the longitudinal orientation can still be seen.
5. Dehydrate, embed, and polymerize the tissue samples as described for routine TEM sample processing.
6. Poststain sections only with uranyl acetate to provide contrast.

Control. Incubate the tissue for 4–16 hr in 10 mM EGTA and then rinse thoroughly in distilled H_2O prior to KPA incubation. This should remove calcium from the tissue and result in a negative result for KPA staining.

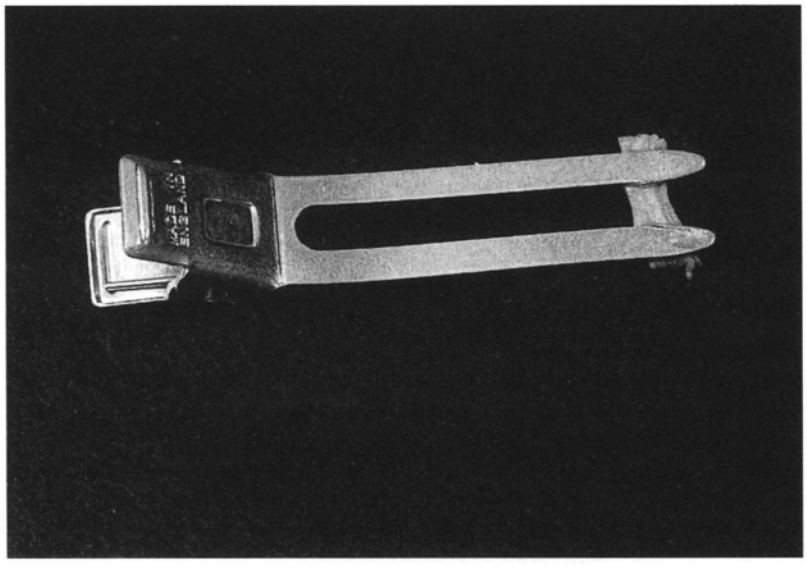

Figure 143. Muscle clamped in hairclip for pyroantimonate.

4. Results Expected

Calcium should be demonstrated by the presence of electron-dense granular deposits in sarcoplasmic reticulum, mitochondrial matrices, and cytoplasmic domains.

5. Cautionary Statements

Do not poststain sections with both uranyl acetate and lead citrate, because the stain product will be more difficult to see against the overall electron density of the cellular components. Uranyl acetate alone produces sufficient contrast in the sections to focus and produce good photographs.

The EGTA control does not seem to work consistently. Since the purpose of the control is to demonstrate that the material stained with KPA can be chelated and removed from the tissue by EGTA (thus suggesting its calcium identity), a more conclusive method would be to utilize microanalytical techniques alluded to above on a subsample to characterize the deposits.

The 4% KPA solution is supersaturated, so there may be some residual precipitate that refuses to go into solution. If the pH is allowed to drop below 7.6, the pyroantimonate will precipitate from the solution. When making pH adjustments, add reagents slowly with stirring to prevent precipitation. If visible precipitation occurs, discard the mixture and start again. To raise the pH, use KOH, and to lower the pH, use acetic acid. Do not use HCl, which could complex with calcium to produce calcium chloride.

Reference

Oberc, M.A. and Engel, W.K. 1977. Ultrastructural localization of calcium in normal and abnormal skeletal muscle. *Lab. Invest.* 36: 566.

Postfixation Calcium Staining with Pyroantimonate

1. Applications and Objectives

Pyroantimonate may be used to demonstrate largely insoluble or partially insoluble calcium in a variety of tissues and cells. Potassium pyroantimonate is mixed with osmium so that poststaining and calcium staining take place simultaneously. Calcium not solubilized during primary fixation and subsequent washing with buffers will be revealed.

2. Materials Needed

- 4% potassium pyroantimonate: Add 4 g of potassium pyroantimonate to 100 ml of steaming distilled H_2O with stirring; adjust the pH to 7.6 with 0.1 N KOH
- 4% aqueous osmium

3. Procedure

1. Fix the samples as per routine TEM processing instructions.
2. Rinse in distilled H_2O (three times, 10 min each).
3. Incubate in a pyroantimonate–osmium mixture for 1 hr at room temperature. Prepare an incubation solution by mixing equal volumes of the 4% pyroantimonate solution and 4% osmium solution just before adding tissues/cells.
4. Rinse in distilled water three times (5 min each).
5. Dehydrate and embed as per routine TEM procedures.

4. Results Expected

As with the technique for soluble calcium staining, calcium deposits will be demonstrated as electron-dense, granular deposits. Large insoluble crystals containing calcium such as those of calcium oxalate are typically difficult to section because they damage glass and diamond knife edges, and the crystals are often ripped from the plastic during sectioning, leaving large holes (Fig. 144). After staining with pyroantimonate, the electron-dense product is much easier to section, leaving far fewer holes in the sections (Fig. 145).

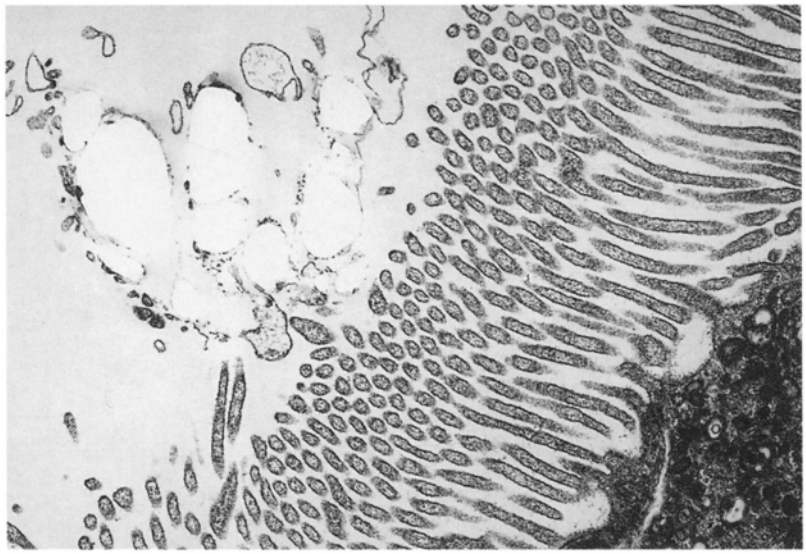

Figure 144. Calcium oxalate crystals in proximal convoluted tubule of a rat kidney. After sectioning, large holes represent areas where crystals have been torn from the section by the knife. 18,678×.

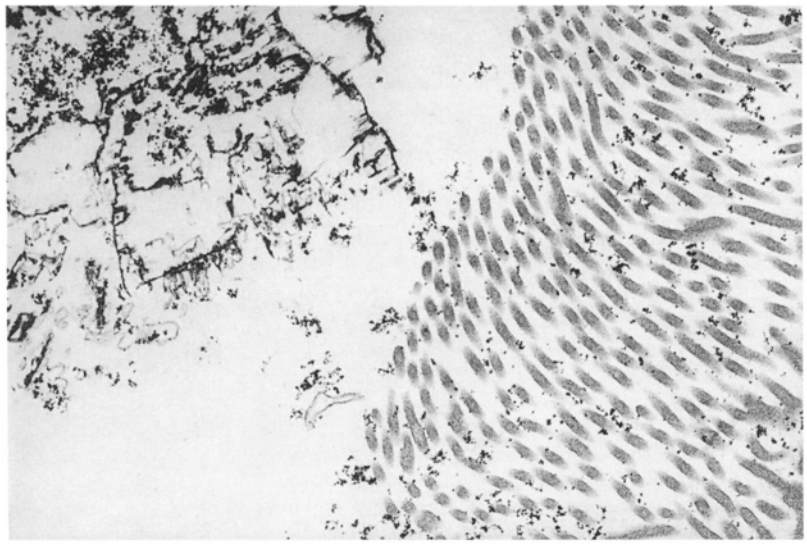

Figure 145. Calcium oxalate crystals in proximal convoluted tubules of rat kidney after staining with potassium pyroantimonate. Note that the black crystalline arrays stained with pyroantimonate have not been torn from the plastic during sectioning. 18,678×.

5. Cautionary Statements

As a control, incubation in EGTA prepared as explained for calcium staining in muscle is recommended. When mixing the supersaturated solution of potassium pyroantimonate with osmium, mix gradually to avoid precipitation of the pyroantimonate. Maintain the pH at 7.6 or above to prevent precipitation, and discard the mixture if any precipitate forms.

Reference

Dykstra, M.J. and Hackett, R.L. 1979. Ultrastructural events in early calcium oxalate crystal formation in rats. *Kidney Int.* 15: 640.

6

Immunocytochemistry

I. PURPOSE

A good historical account of the beginnings of immunolabeling is found in a chapter by Romano and Romano (1984). This history includes the work of Coons *et al.* (1941), who introduced fluorescent-labeled antibodies to light microscopy, followed by the introduction of antibodies conjugated to ferritin (Singer, 1959), peroxidase (Nakane and Pierce, 1966), and gold (Faulk and Taylor, 1971; Romano *et al.*, 1974). The ability to detect antibodies easily at both the light and electron microscopic level has made it possible to localize a variety of antigenic substances associated with the surfaces and interiors of cells. Modifications of these techniques have been used to demonstrate the presence of nucleic acids (Beesley, 2001; Raap *et al.*, 1989; Silva *et al.*, 1989), carbohydrates (Horisberger, 1985), and enzymes (Bendayan, 1985; Bendayan and Zollinger, 1983) as well. There are a number of excellent books dealing with immunolabeling at the light microscopic and ultrastructural level (Beesley, 1989a, 1993; Bullock and Petrusz, 1982, 1983, 1985, 1989; Hayat, 1989, 1990; Polak and Van Noorden, 1983; Polak and Varndell, 1984; Shi *et al.*, 2000; Sternberger, 1986; Williams, 1977). Ritter and Ladyman (1995) assembled a book providing detailed techniques for producing monoclonal antibodies.

As with the techniques developed for ultrastructural localization of enzymes, fixation and embedment procedures must be critically evaluated prior to embarking on new immunocytochemical procedures. Willingham (1980) has described intracellular antigen localization with ferritin-labeled antibodies using a technique to make membranes permeable to large molecules with saponin. The technique has been supplanted by cryosectioning procedures, but the stepwise approach to determination of ideal fixation concentration and the design of labeling protocols may be applied to other systems, providing an excellent example of experimental design. Shi *et al.* (1996) wrote a seminal paper for systematic approaches for achieving the best staining results, utilizing the antigen retrieval technique.

Ideally, the preparative procedures chosen will maintain good ultrastructural morphology without denaturing the antigenic determinants associated with cells and tissues that are to be demonstrated immunocytochemically. These two goals tend to be mutually exclusive, however. Typical chemical fixation, dehydration, and embedment procedures utilizing epoxide resins have a strong tendency to either change protein structure or make the active regions of proteins such as enzymes and antibodies inaccessible, as discussed in Chapter 5. Antigen–antibody interactions take place over short distances (0.1 nm or less) and are reversible (Garsha, 2001). Thus, anything that interferes with this close fit can prevent antigen–antibody binding. The number of noncovalent interactions between the antibody and antigen determines the strength of binding, which accounts for the fact that different monoclonal antibodies can exhibit different affinities for a given antigen. In addition, cross-reactivity can occur if two antigens share an identical epitope, or an antibody can bind to an epitope unrelated to the antigen to which it was raised if both antigens have similar chemical characteristics.

Techniques developed in the 1980s have applied approaches such as cryofixation, cryosubstitution, cryoultramicrotomy, freeze-drying, and acrylic resin embedding to solve some of the traditional problems associated with immunocytochemistry.

Some techniques use the Fab region of an antibody to recognize an antigen, while other techniques use another molecule (Protein A or G) to recognize the Fc portion of an antibody molecule present in cells or tissues (Fig. 146). Direct and indirect labeling techniques (Falini and Taylor, 1983) have been developed, the latter primarily to amplify the resulting product for easier visualization.

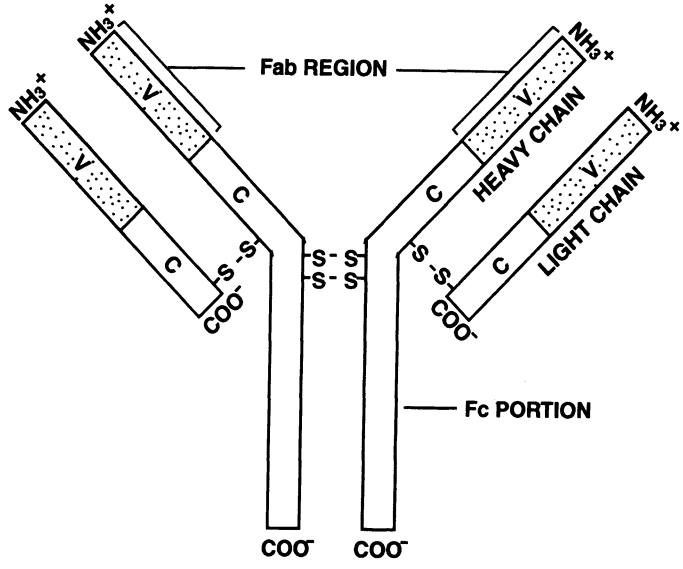

Figure 146. Diagram of an antibody molecule, showing the two potentially reactive sites, the Fab region, usually employed to react with specific antigens, and the Fc portion, to which protein A or G binds to demonstrate the presence of any immunoglobulin. V: variable region; C: constant region.

II. PREPARATIVE TECHNIQUES

A. Preembedding Labeling

If the antigen to be identified is associated with the surface of cells grown in culture, unfixed, unembedded samples can be labeled and subsequently negatively stained. Alternatively, living cells can be labeled, fixed, embedded, and then sectioned for transmission electron microscopy or prepared for scanning electron microscopy (Priestley, 1984). Since the cells are labeled prior to fixation, antigenicity is not diminished or destroyed, as often happens during fixation procedures. In addition, once the labeling procedures are completed, fixation by typical chemical procedures provides excellent ultrastructural morphology.

As mentioned in the previous chapter on cytochemical techniques, tissue choppers or slicers may yield thin samples of tissues that will be penetrated more easily by immunolabeling reagents, which otherwise would react only with the most superficial layers of cells within a sample. However, during the last 20 years, cryosectioning techniques have become routine in laboratories performing ultrastructural immunolabeling and have tended to supplant tissue-chopping and -slicing techniques.

B. Postembedding Procedures

As previously stated, it is preferable to expose antigens to antibodies before the antigens are denatured or possibly eluted by processing and embedding, but it is difficult to guarantee adequate antibody penetration into fresh or fixed tissues. However, fixation before immunolabeling allows sample storage before further processing, and proper fixation has been shown to inhibit binding of antibodies to Fc receptors on the surface of certain types of white blood cells (Leenen *et al.*, 1985).

Tissues can be dehydrated and rehydrated, freeze–thawed, treated with DMSO, detergents such as saponin (Willingham, 1980), or Triton X-100 to disrupt membranes sufficiently to allow antibodies to pass into cells. Most of these techniques compromise good ultrastructural preservation.

The study by Leenen *et al.* (1985) evaluated the effect of fixatives made from four different types of chemical stocks on the subsequent immunolabeling of 11 different antigens associated with surfaces of white blood cells. Glutaraldehyde fixatives were made from distilled stocks (8%), with a single UV absorbance peak of 235 nm (indicating a solution containing only monomeric glutaraldehyde) or 25% biological grade glutaraldehyde, which contained monomeric and dimeric glutaraldehyde as well as glutaric acid. Pure formaldehyde prepared from paraformaldehyde powder was compared with biological-grade formaldehyde (37–40%) containing methanol as a stabilizer. All fixations were for 30 min at 4°C. The cells were then washed with DPBS at pH 7.2 and then with DPBS supplemented with 0.02% gelatin prior to antibody labeling.

Beesley (1989b) explained the common use of gelatin or bovine serum albumin to reduce nonspecific antibody binding in immunolabeling procedures:

> Bovine serum albumin in the buffer competes with the antibody proteins for non-specific "sticky" sites on the preparation, thereby reducing non-specific background labeling. A short incubation of the tissue in 1% gelatin in phosphate buffered saline will also reduce the number of non-specific sticky sites. If the tissue has been fixed with an aldehyde it is useful to pre-treat the sample with 0.02 M glycine in phosphate-buffered saline in order to quench any free aldehyde groups which may promote "non-immunological" protein sticking to the tissue.

Antibody binding was evaluated by enzyme-linked immunosorbent assay (ELISA) techniques in the study by Leenen *et al.* (1985). In some cases, fixation decreased antibody binding, in some cases, it increased binding, and in some cases, it had no effect on antibody binding. This demonstrates the difficulties experienced in predicting the outcome for antibody labeling procedures used for the first time on new systems.

Formaldehyde fixation, whether from biological-grade stocks or prepared from paraformaldehyde powder, had similar effects on antigen binding in most cases. Leenen *et al.* (1985) found that two of their antibodies (out of 11) were unaffected by formaldehyde made from paraformaldehyde or had increased binding compared with unfixed controls. Biological-grade formaldehyde resulted in a maximum loss of antibody binding of 25–30%. It was suggested that this latter effect might be due to the presence of methanol in the formaldehyde stock.

Both types of glutaraldehyde stocks examined by Leenen *et al.* (1985) diminished antibody binding to a greater extent than formaldehyde. High concentrations of glutaraldehyde left only 55–70% of certain antigenic determinants intact. One antibody was hardly affected by distilled glutaraldehyde but had seriously diminished binding if fixation was performed with biological-grade glutaraldehyde. In some instances, crude glutaraldehyde had a denaturing effect at lower concentrations than distilled glutaraldehyde.

Leenen *et al.* (1985) further state that aldehyde groups are known to react mostly with free amino groups, present mainly on lysine residues. Formaldehyde is also known to react with arginine and asparagine side-chains. Both of these aldehydes form intermolecular and intramolecular

cross-links, but glutaraldehyde is more effective in this regard because of the two aldehyde groups per molecule. Primary and tertiary structures of antigens thus can be changed by aldehyde fixation. However, fixation has a minimal effect on antibody binding when the antigenic determinant has a primary structure without lysine residues. Antibody binding may also be inhibited because of steric hindrance from neighboring groups.

Leenen *et al.* (1985) also suggest that if glutaraldehyde is used for fixation, pretreatment with sodium borohydride prior to immunolabeling, might restore some of the decreased immunoreactivity, since borohydride reduces free aldehyde groups and/or double chemical bonds induced by the fixation procedure.

Bendayan and Zollinger (1983) clearly demonstrated that some antigens retain antigenicity even after conventional fixation with aldehydes and osmium, dehydration, infiltration with epoxide resins, and heat polymerization. They also showed that the problem of penetrating the surface of strongly cross-linked, hydrophobic epoxide resins with immunoprobes can be overcome by etching sections with sodium meta-periodate. Unfortunately, many antigens are completely or partially inactivated by conventional processing methods.

Various workers have realized the efficacy of developing techniques by which samples can be fixed and embedded in resins, and then repeatedly sectioned. If numerous grids of sections can be prepared, it is easy to test various controls or to examine a variety of antibody concentrations (Newman and Jasani, 1984).

Resin components not only react with each other during polymerization, but also react with substituents and end groups on the biological material (Carlemalm and Villiger, 1989). This may make sectioning easier, since the tissue becomes integrated with the resin matrix. However, it may interfere with postembedding labelling, since reactive sites may be modified or occupied by the resin. Epoxides such as Araldite, Spurr, and Epon substitutes are reactive to a number of groups (carboxyl, amino, indol, amide). To minimize reductions in antigenicity, low-temperature acrylic embedding media such as the LR Gold and Lowicryl resins were developed (Carlemalm and Villiger, 1989). These resins are much more selective in their reactivity than epoxides, resulting in poorer retention of cellular materials in general but in less antigen modification. Acrylics are also more water-miscible, allowing processing schedules with transitions from lower alcohol concentrations (70%) directly into the resins. The higher hydrophilicity of these resins when compared with most epoxides also allows easier access to antigens within sectioned cells and tissues. Acrylic resin-embedded material prepared for immunolabeling frequently is not osmicated to avoid the potential for antigen oxidation or heavy-metal denaturation resulting from osmium treatment. The dehydration process and the lipid-extractive capabilities of the acrylic resins themselves result in images of cells that have indistinct membrane domains, since most of the lipids are extracted. Other cellular features are not as crisp and distinct as with conventionally fixed and epoxide-embedded tissues, but all the cellular compartments (nuclei, mitochondria, endoplasmic reticulum, lysosomes, etc.) are still identifiable. Thus, determinations about the location of antigens within or outside of these compartments can be made effectively with these techniques.

C. Cryoultramicrotomy Techniques

An alternative procedure for immunolabeling that involves no resin embedment was developed by Tokuyasu (1973, 1984) and employs brief fixation of cells and tissues in relatively weak aldehyde solutions, usually 2–4% phosphate-buffered formaldehyde prepared from paraformaldehyde with or without a trace (0.01–0.1%) of glutaraldehyde, followed by infiltration with 2.3 M

sucrose, freezing in liquid nitrogen or liquid nitrogen-cooled cryogen, and subsequent ultracryomicrotomy. Detailed procedures are outlined in Chapter 2.

The advantage of Tokuyasu's technique is that antigens that are normally difficult to label within intact cells become accessible to antibodies and labels too large to pass through membranes because the cells have been physically cut open during cryoultramicrotomy. This technique is also useful for improving surface labeling of cells within dense tissues. In the intact specimen, cells are so densely packed or actually interconnected by junctional complexes that access to nonsuperficial cells by large stain molecules is blocked.

D. Negative Staining Procedures

If viruses, bacterial flagella and pili, or the surfaces of isolated membranes or subcellular components are to be probed by antibodies, visualization of products is quite simple. The sample is usually attached to a film-coated grid as with normal negative-staining procedures (see Chapter 7). The grid then can be floated on drops of the various reagents used for immunolabeling, preferably in a moist chamber on a gently rocking platform. Inert grids made of nickel or stainless steel are usually used to avoid the possibility of copper interacting with the antibodies. Gold-labeled antibodies are the label of choice, since the gold particles are so discrete and have such great electron density. After the final immunolabeling step, the grid is rinsed and then negatively stained with routine procedures to produce specimen contrast (see Chapter 8). Since no fixation is employed prior to negative staining, the antigens are unperturbed by chemicals, and reactivity remains high (Fig. 147).

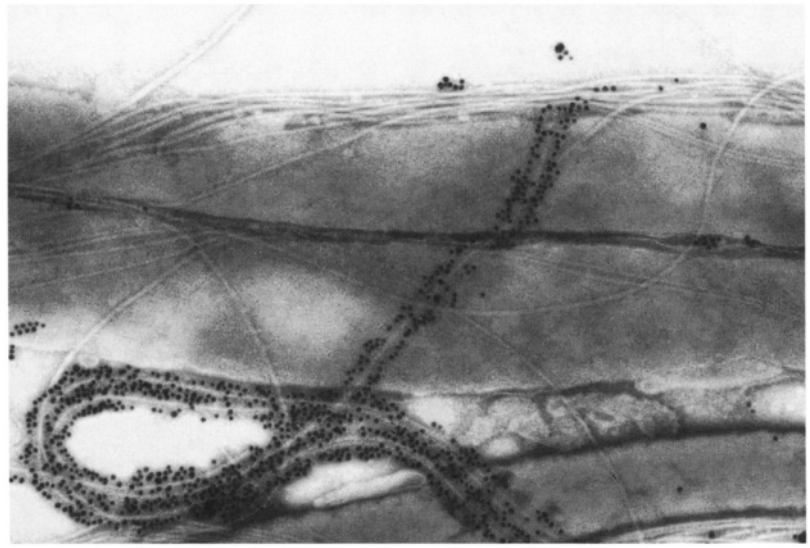

Figure 147. Transmission electron micrograph of *Borrelia burgdorferi*, the Lyme disease spirochete, reacted with a monoclonal antibody to a flagellar protein, followed by a gold-labeled (5-nm) antibody to the primary antibody. Negatively stained with 2% phosphotungstic acid. 59,615×.

III. IMMUNOGLOBULINS

A. Protein A and Protein G Techniques

Antibodies can be localized by immunocytochemical techniques. Evaluation of autoimmune disease problems often involves probing tissues for the presence of immune deposits, typically IgG, in inappropriate locations. In this case, the precise identification of the antigen is not necessary, and a technique such as the protein A technique would be applicable.

Protein A has a molecular weight of 42,000 and is obtained from the bacterium *Staphylococcus aureus*. It binds to the Fc portion of IgG of many animal species without interacting at the antigen binding site. It binds strongly to IgG of humans, rabbits, guinea pigs, swine, and dogs. Binding to IgG of cattle, horses, and mice is weaker, and binding to IgG of chickens, goats, rats, and sheep is very weak.

Protein G produced from the walls of Group C *Streptococcus* sp. binds more efficiently to the Fc region of cattle, goats, sheep, and certain human and mouse immunoglobulins than Protein A (Polak and Van Noorden, 1997).

B. Polyclonal and Monoclonal Antibodies

Antibodies are circulating immunoglobulins produced by B-cells of the immune system. Most antigens possess multiple antigenic determinants (epitopes) that can be recognized by antibodies. Each B-cell stimulated to produce antibodies produces a single monoclonal antibody. The collective response of the B-cell population to a specific antigen consists of a variety of B-cells, each producing their unique monoclonal antibody. The collection of circulating antibodies produced against a given antigen, which typically are raised against more than one epitope of the antigen, are collectively known as polyclonal antibodies.

In most immunological studies, the goal is to precisely identify a specific antigen, usually against a background of other specific antigens. This requires the use of a polyclonal or monoclonal antibody developed against the specific antigen. Polyclonal antibodies are more cross-reactive than monoclonals. Beesley (1989b) points out that monoclonal antibodies are more specific than polyclonal antibodies because they react with only a single antigenic determinant consisting of a few amino acids. He suggests that light fixation is required to prevent damage to these critical amino acids. A fixative containing 4% formaldehyde with 0.05% glutaraldehyde in either phosphate or cacodylate buffer is suggested. If antigenicity is not optimal, he suggests deleting the glutaraldehyde. Beesley further states that since polyclonal antibodies are reactive with a number of different epitopes, fixation with 1% glutaraldehyde is usually permissible.

C. Antigen Retrieval Techniques

Since the introduction of immunocytochemical and immunohistochemical techniques, it has been recognized that chemical fixatives, dehydration agents, pH, temperature, and properties of various embedding media all have the potential for impacting the eventual capability of seeing immunolabels in cells and tissues. For electron microscopy preparations, glutaraldehyde and

osmium exposure, as well as epoxide resin embedding and resin polymerization at 60–70 °C were often seen to diminish or eliminate immunological reactivity.

There are two major classes of fixatives used for cytological preparations, cross-linking fixatives (aldehydes) and precipitant fixatives (ethanol and acetone). Formaldehyde and glutaraldehyde form hydroxyl-methylene bridges between the reactive end-groups of adjacent protein chains (Polak and Van Noorden, 1997). The advantage of this is that small peptides typically lost during fixation with precipitant fixatives are preserved. The potential disadvantage of this is that longer fixation times cause more cross-linking and thus can diminish immunoreactivity or accessibility to immunoreactive sites.

Precipitant fixatives precipitate proteins but also denature their tertiary structure by destroying hydrophobic bonds. Amino acid sequences defining antigenic sites are typically still available, since primary and secondary protein structures are not affected.

Antigen retrieval methods have been developed over the last dozen years that reverse some of the masking effects of chemical fixation techniques on a variety of antigens. The majority of the techniques were developed for paraffin-embedded samples for light microscopy analysis.

One simple technique for potentially increasing the immunoreactivity of formaldehyde-fixed samples is to wash them thoroughly in buffer solutions for extended periods of time. Since formaldehyde linkages are reversible, the cross-linking that can interfere with immunolabeling can be undone to some extent. In addition, Polak and Van Noorden (1997) recommend no more than 30- to 120-min fixation times in a mixture of 2% formaldehyde (made freshly from paraformaldehyde) and 0.05% glutaraldehyde. They also recommend that osmication be avoided, despite some of the successful methods described for labeling osmicated tissues by Bendayan and Zollinger (1983).

Another technique pioneered for paraffin-embedded samples, which is still primarily limited to light microscopy samples, involves the exposure of samples to proteases such as trypsin and pronase. Protease treatments are thought to break the cross-links between proteins and aldehydes, revealing antigenic sites otherwise masked (Polak and Van Noorden, 1997). Unfortunately, some antigens may be adversely affected by the action of proteases in that the antigenic protein of interest may be cleaved into smaller, nonreactive peptides. In addition, some larger nonreactive proteins that are precursors to a given antigen may be subject to cleavage by the proteases, yielding the bioactive antigen. Thus, an antigenic site may be revealed that was not originally accessible, creating a false positive reaction. Finally, the proteases may adversely affect overall ultrastructural preservation due to generalized protein degradation. Polak and Van Noorden (1997) discuss several different techniques in detail and note that different antigens located in different tissues may need different digestion times for effective antigen retrieval. For example, immunoglobulin deposits in skin and glomerular basement membranes needed 1.5 hr of trypsin treatment for immunolabeling, while plasma cells needed only 10 min of treatment.

Heat-mediated methods are the other main antigen retrieval technique. Heat from microwaving, autoclaving, or boiling sections in a buffer solution has successfully increased immunoreactivity in both paraffin-embedded and plastic resin-embedded sections of cells and tissues. Morgan *et al.* (1994) suggested that heating breaks the hydroxyl bonds between aldehydes and antigens, as well as other proteins in the samples. Heating also releases calcium ions that help provide tighter bonds between the antigen and aldehyde molecules. Antigens seem to be more tolerant of heat-mediated retrieval than they are for protease-mediated methods. Morgan *et al.* (1994) reported that the technique is so successful that it is often necessary to use more diluted antibody solutions than would be used for conventional nonretrieval immunological staining methods. There is no universal method for all antigens, so doing a test battery as outlined by Shi *et al.* (1996) is recommended.

As is so often the case, postembedding immunocytochemistry on resin-embedded samples for transmission electron microscopy does not lend itself as readily to antigen retrieval techniques as do paraffin-embedded samples. Heat-mediated antigen retrieval methods seem to be the most successful (Beesley, 2001; Brorson, 2001; Morgan *et al.*, 1994; Polak and Van Noorden, 1997; Shi *et al.*, 2000), in general, though Brorson and his coworkers (Brorson, 1998, 1999, 2001; Brorson *et al.*, 1999a, 1999b, 2001) have written a series of reports on the application of chemically mediated retrieval methods, with and without additional heat-mediated methods, on resin-embedded sections. Brorson (1998) reported that acrylic-embedded samples were generally more easily immunolabeled than epoxide-embedded samples, and that sodium ethoxide or sodium metaperiodate treatments enhanced immunolabeling, as originally described by Bendayan and Zollinger for enzyme cytochemical methods (1983). He also found that an eightfold improvement in immunolabeling of epoxide-embedded samples was achieved by increasing the accelerator concentration of the resin mixture. Brorson *et al.* (1999a) reported that antigen retrieval mediated by changes in accelerator concentrations in epoxide resin, coupled with heat-mediated methods, could yield labeling up to 70% of that found for comparable samples in acrylic resins. They believed that the basis for this improvement is the dissolution of bonds between the epoxide resin and embedded tissue. In all cases, osmication reduced the ability to achieve immunolabeling. Brorson (1999) further hypothesized that high accelerator concentrations reduce the tendency of proteins to be cleaved by a knife during sectioning, thus yielding greater labeling. A comparison of H_2O_2-treated sections, heat-treated sections, and sections treated with both heat and H_2O_2 (Brorson *et al.*, 2001) showed that heated sections were labeled twice as strongly as H_2O_2-treated sections and that the combination of the two methods did not improve labeling over sections both treated with H_2O_2 and heat. In the same study, sections receiving neither treatment labeled very weakly. They suggested that heating in citrate buffer breaks more bonds than H_2O_2 treatment.

IV. COMMON IMMUNOLABELING TECHNIQUES FOR ELECTRON MICROSCOPY

A. Immunoferritin

Ferritin is a naturally occurring biological protein with a molecular weight of 750,000, an electron-dense iron core, and a diameter of 7.0 nm. Its apoprotein coat permits conjugation to other proteins such as antibodies by means of bivalent reagents, typically glutaraldehyde. When antibodies are coupled to ferritin by reaction with glutaraldehyde, there may be a diminution of antibody activity, primarily resulting from the bound glutaraldehyde decreasing access to the characteristically reactive regions of antibodies. Other problems include the heterogeneity of products produced during the coupling procedures, which necessitates the isolation of active ferritin/antibody conjugates from other moieties in the reaction mixture. The general inefficiency of the coupling procedure also causes problems. Not only will many of the antibody molecules remain unlabeled and thus unviewable because of insufficient inherent electron density, but unlabeled antibody in the reaction mixtures can compete with the labeled antibody for antigens within cells and tissues, denying access to the labeled antibody molecules. This, of course, is one of the standard controls to demonstrate the specificity of labeling procedures. A pretreatment of cells or tissues with unlabeled antibody, followed by incubation with labeled antibody to the same antigen, should prevent all labeling. The use of ferritin as a cationic stain as described in the section on

cytochemistry explains why ferritin can bind nonspecifically to some charged sites. It even binds nonspecifically to some epoxide resins during postembedding immunolabeling techniques.

Since ferritin is a naturally occurring molecule in certain tissues, a careful evaluation of the system to which it is to be applied must be undertaken. The size of the molecule prevents passage through intact membranes, so it is usually appropriate only for preembedment labeling of cellular surfaces (Fig. 148) or postembedding labeling of sectioned materials. If ferritin is to be used in postembedding procedures, acrylic resins should be used for sample embedment because of the potential reactivity of ferritin with epoxide resins.

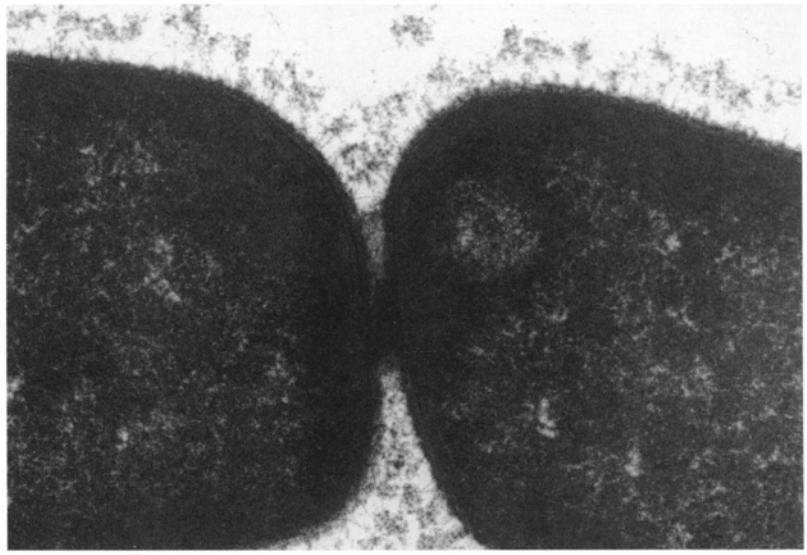

Figure 148. Transmission electron micrograph of preembedding labeling of pili on the surface of the causative agent for bovine pinkeye, *Moraxella bovis*. A ferritin-labeled antibody was used to demonstrate the primary antibody raised against the pili. 31,154×.

B. Immunoperoxidase Techniques

All of the commonly used immunoperoxidase techniques are described in the review article by Falini and Taylor (1983). The peroxidase molecule is one tenth smaller than ferritin, with a molecular weight of 40,000. It is easily conjugated to antibodies with glutaraldehyde. Because of its relatively small size, it can penetrate membranes of cells fixed with aldehydes. It was first utilized for light-microscopy techniques, and its easy visualization at the light-microscope level allows a relatively quick assessment of the efficacy of localization techniques to be utilized for electron microscopy (Fig. 149).

The immunoperoxidase technique has the disadvantage of all enzymatic procedures in that the catalytic activity of enzymes can result in the accumulation of products capable of diffusion away from the site of the enzymatic activity and, in this case, the site of the antigen being localized. Another potential problem that must be considered is the presence of endogenous peroxidase activity within cells. The endogenous peroxidases may make interpretation of immunoperoxidase techniques difficult.

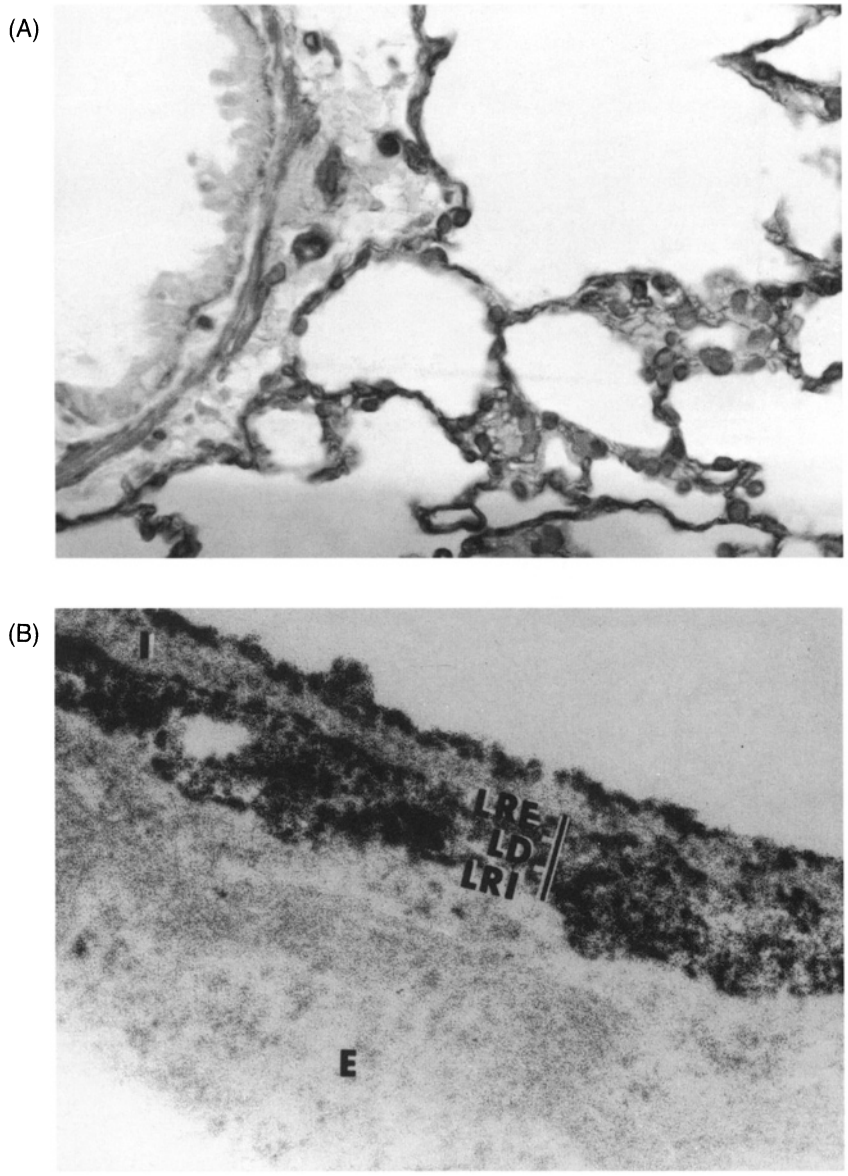

Figure 149. Light-and electron-microscopic demonstration of peroxidase/avidin/biotin immunolabeling. (Courtesy of Philip L. Sannes.) (A) Light micrograph of an adult rat lung immunolabeled with an avidin–biotin complex/peroxidase procedure for the localization of chondroitin sulfate proteoglycan. Alveolar basement membranes, capillary basement membranes, and external laminae of smooth muscle are stained. 635×. (B) Electron micrograph of an adult rat lung immunolabeled with an avidin–biotin complex/peroxidase procedure for the localization of heparin sulfate proteoglycan. The alveolar basement membrane profile is divided into the lamina rara externa (LRE) adjacent to a type I epithelial cell (vertical line), the lamina rara interna (LRI) adjacent to a capillary endothelial cell (E), and the lamina densa (LD). The reaction product, indicating the heparin sulfate proteoglycan, is darkly stained. 153,846×.

Another problem with immunoperoxidase techniques is that if a single antibody molecule with peroxidase bound to it attaches to an antigen, and then the peroxidase activity with the hydrogen peroxide substrate is amplified with DAB and osmium, the product may not be discernible. As a result, different amplification techniques have been developed. Falini and Taylor (1983)

provide illustrations of direct and indirect conjugate procedures, labeled antigen methods, enzyme bridge methods, and the most commonly used peroxidase procedure, the peroxidase–antiperoxidase procedure (PAP) illustrated in Fig. 150.

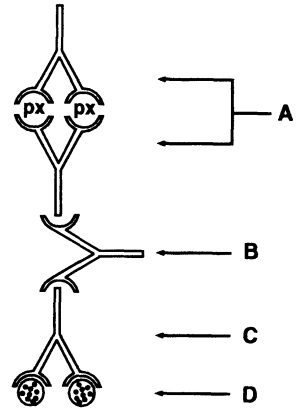

Figure 150. PAP procedure (after Falini and Taylor, 1983). A: mouse anti-px (peroxidase); B: goat anti-mouse; C: mouse antibody to D; D: antigen.

C. Immunogold Techniques

The strength of immunogold techniques is that the gold particles that are bound to antibodies are totally opaque and discrete. They are not diffuse products like the osmium blacks produced by immunoperoxidase procedures and, unlike peroxidase and ferritin that occur naturally in some tissues, gold is a nonbiological entity. In addition, gold cannot diffuse from the site of binding, as can happen with enzymatic procedures. Colloidal gold can be bound to immunoglobulins (De Mey and Moeremans, 1986), to protein A and protein G (Bendayan and Zollinger, 1983), to lectins (Horisberger, 1985), and to enzymes (Bendayan, 1985). The process by which colloidal gold is bound to these molecules is poorly understood, but is a simple adsorptive process that involves no chemical conjugation. Binding only requires proper pH, reagent concentration, and ionic strength of the reaction mixture. Colloidal gold itself has a relatively low nonspecific adsorption to specimen surfaces (unlike ferritin, which binds readily to many epoxides). Colloidal gold probes may be prepared in a variety of sizes (from 1 to 150 nm), determined by buffer and pH (see De Mey and Moeremans, 1986, for specific recipes). For electron microscopy, gold probes over 20 nm are rarely employed, since larger particles are thought to produce steric hindrance for immunolabeling procedures. In addition, the density of labeling generally increases with decreasing gold particle diameter. Ten-nanometer probes are usually the smallest used directly. When using gold particles of smaller size, some amplification technique, typically with silver, is employed (Polak and Van Noorden, 1997). The introduction of high-resolution, low-voltage scanning electron microscopes (see Chapter 13) recently has made it possible to visualize all gold labels easily with scanning as well as TEM techniques.

After macromolecules are adsorbed to colloidal gold particles, most still have their full biological activity (tertiary structures are preserved). During preparation of colloidal gold probes, it is usually necessary to coat them with the active macromolecules desired (antibodies, lectins, protein A) fairly quickly, since uncoated gold particles often self-assemble into aggregates.

Nanoprobes, Inc. (Stony Brook, NY) has pioneered the use of 1.4-nm Nanogold® particles, which covalently react with reactive groups on a variety of molecules. These molecules include enzyme inhibitors, lipids, oligonucleotides, peptides, proteins, and other small molecules. This allows a broader array of conjugates to be produced than can be made with colloidal gold, which adsorbs only to peptides, proteins, and antibodies. Because the conjugates are considerably smaller than those formed with colloidal gold, the conjugates can penetrate more deeply into tissues, permeabilized cells, and nuclei, according to the manufacturer. In addition, a higher density of immunolabeling can be achieved than with larger probes, because of less steric hindrance. Finally, the covalent nature of the bonds holding the conjugates together ensures that they may be stored for at least a year without degradation.

Detection of the Nanogold® particles directly with the electron microscope is possible, though most reaction products are intensified by complexing the gold with silver for easier visualization with electron microscopy, confocal microscopy or standard light microscopy (Powell *et al.*, 1997; Robinson and Vandré, 1997; Sun *et al.*, 1995).

REFERENCES

Beesley, J.E. 1989a. *Colloidal gold: A new perspective for cytochemical marking*. Oxford University Press, New York.

Beesley, J.E. 1989b. Immunocytochemistry of microbiological organisms: A survey of techniques and applications. In: G.R. Bullock and P. Petrusz (eds.), *Techniques in immunocytochemistry* (Vol. 4, pp. 67–93). Academic Press, New York.

Beesley, J.E. (ed.). 1993. *Immunocytochemistry, a practical approach*. Oxford University Press, Oxford.

Beesley, J.E. (ed.). 2001. *Immunocytochemistry and* in situ *hybridization in the biomedical sciences*. Birkhäuser, Boston.

Bendayan, M. 1985. The enzyme-gold technique: A new cytochemical approach for the ultrastructural localization of macromolecules. In: G.R. Bullock and P. Petrusz (eds.), *Techniques in immunocytochemistry* (Vol. 3, pp. 179–201). Academic Press, New York.

Bendayan, M., and Zollinger, M. 1983. Ultrastructural localization of antigenic sites on osmium-fixed tissues applying the protein A-gold technique. *J. Histochem. Cytochem.* 31: 101.

Brorson, S.H. 1998. Antigen detection on resin sections and methods for improving the immunogold labeling by manipulating the resin. *Histol. Histopathol.* 13: 275.

Brorson, S.H. 1999. Comparison of the immunolabeling of heated and deplasticized epoxy sections on the electron microscopical level. *Micron* 30: 319.

Brorson, S.H. 2001. Heat-induced antigen retrieval of epoxy sections for electron microscopy. *Histol. Histopathol.* 16: 923.

Brorson, S.H., Andersen, T., Haug, S., Kristiansen, I., Risstubben, A., Tchou, H., and Ulstein, J. 1999a. Antigen retrieval on epoxy sections based on tissue infiltration with a moderately increased amount of accelerator to detect immune complex deposits in glomerular tissue. *Histol. Histopathol.* 14: 151.

Brorson, S.H., Halvorsen, I., Lonning, L.C., Slaattun, G., Sletten, M., and Rashid, S. 1999b. Increased yield of immunogold labeling of epoxide sections by adding para-phenylenediamine in the tissue processing. *Micron* 30: 561.

Brorson, S.H., Hansen, A.R., Nielsen, H.Z., and Woxen, I.K. 2001. A comparative study of the immunogold labeling on H_2O_2-treated and heated epoxy sections. *Micron* 32: 147.

Bullock, G.R., and Petrusz, P. (eds.). 1982, 1983, 1985, 1989. *Techniques in immunocytochemistry* (Vols. 1–4). Academic Press, New York.

Carlemalm, E., and Villiger, W. 1989. Low temperature embedding. In: G.R. Bullock and P. Petrusz (eds.), *Techniques in immunocytochemistry* (Vol. 4, pp. 29–45). Academic Press, New York.

Coons, A.H., Creech, H.J., and Jones, R.N. 1941. Immunological properties of an antibody containing a fluorescent group. *Proc. Soc. Exp. Biol.* 47: 200.

De Mey, J., and Moeremans, M. 1986. The preparation of colloidal gold probes and their use as a marker in electron microscopy. In: J.K. Koehler (ed.), *Advanced techniques in biological electron microscopy III* (pp. 229–271). Springer-Verlag, New York.

Falini, B., and Taylor, C.R. 1983. New developments in immunoperoxidase techniques and their application. *Arch. Pathol. Lab. Med.* 107: 105.

Faulk, W.P., and Taylor, G.M. 1971. An immunocolloid method for the electron microscope. *Immunochemistry* 8: 1081.

Garsha, K. 2001. Concepts, considerations and control experiments for immunolabeling. *Microsc. Today* 01–1: 16.

Hayat, M.A. (ed.). 1989, 1990. *Colloidal gold: Principles, methods and applications* (Vols. 1–3). Academic Press, New York.

Horisberger, M. 1985. The gold method as applied to lectin cytochemistry in transmission and scanning electron microscopy. In: G.R. Bullock and P. Petrusz (eds.), *Techniques in immunocytochemistry* (Vol. 3, pp. 155–178). Academic Press, New York.

Leenen, P.J.M., Jansen, A.M.A.C., and Ewijk, W.V. 1985. Fixation parameters for immunocytochemistry: The effect of glutaraldehyde or paraformaldehyde fixation on the preservation of mononuclear phagocyte differentiation antigens. In: G.R. Bullock and P. Petrusz (eds.), *Techniques in immunocytochemistry* (Vol. 3, pp. 1–24). Academic Press, New York.

Morgan, J.M., Navabi, H., Schmid, K.W., and Jasani, B. 1994. Possible role of tissue-bound calcium ions in citrate-mediated high-temperature antigen retrieval. *J. Pathol.* 174: 301.

Nakane, P.K., and Pierce, G.B. 1966. Enzyme-labeled antibodies: Preparation and application for the localization of antigens. *J. Histochem. Cytochem.* 14: 929.

Newman, G.R., and Jasani, B. 1984. Post-embedding immunoenzyme techniques. In: J.M. Polak and I.M. Varndell (eds.), *Immunolabeling for electron microscopy*. Elsevier, New York.

Polak, J.M., and Van Noorden, S. (eds.). 1983. *Immunocytochemistry. Practical applications in pathology and biology*. Wright PSG, London.

Polak, J.M., and Van Noorden, S. 1997. *Introduction to immunocytochemistry*, 2nd edn. BIOS Scientific, Oxford.

Polak, J.M., and Varndell, I.M. 1984. *Immunolabeling for electron microscopy*. Elsevier, New York.

Powell, R.D., Halsey, C.M.R., Spector, D.L., Kaurin, S.L., McCann, J., and Hainfeld, J.F. 1997. A covalent fluorescent-gold immunoprobe: Simultaneous detection of a pre-mRNA splicing factor by light and electron microscopy. *J. Histochem. Cytochem.* 45: 947.

Priestley, J.V. 1984. Pre-embedding ultrastructural immunocytochemistry: Immunoenzyme techniques. In: J.M. Polak and I.M. Varndell (eds.), *Immunolabeling for electron microscopy*. Elsevier, New York.

Raap, A.K., Hopman, A.H.N., and Van Der Ploeg, M. 1989. Hapten lableing of nucleic acid probes for DNA *in situ* hybridization. In: G.R. Bullock and P. Petrusz (eds.), *Techniques in immunocytochemistry* (Vol. 4, pp. 167–197). Academic Press, New York.

Ritter, M.A., and Ladyman, H. (eds.). 1995. *Monoclonal antibodies, production, engineering and clinical application*. Cambridge University Press, Cambridge.

Robinson, J.M., and Vandré, D.D. 1997. Efficient immunocytochemical labeling of leukocyte microtubules with FluoroNanogold: A important tool for correlative microscopy. *J. Histochem. Cytochem.* 45: 631.

Romano, E.L., and Romano, M. 1984. Historical aspects. In: J.M. Polak and I.M. Varndell (eds.), *Immunolabeling for electron microscopy*. Elsevier, New York.

Romano, E.L., Stolinski, C., and Hughes-Jones, N.C. 1974. An antiglobulin reagent labelled with colloidal gold for use in electron microscopy. *Immunochemistry* 11: 521.

Shi, S.-R., Cote, R.J., Yang, C., Chen, C., Xu, H.-J., Benedict, W.F., and Taylor, C.R. 1996. Development of an optimal protocol for antigen retrieval: A 'test battery' approach exemplified with reference to the staining of retinoblastoma protein (pRB) in formalin-fixed paraffin sections. *J. Pathol.* 179: 347.

Shi, S.-R., Gu, J., and Taylor, R (eds.). 2000. *Antigen retrieval techniques: Immunohistochemistry and molecular morphology*. Eaton, Natick, MA.

Silva, F.G., Lawrence, J.B., and Singer, R.H. 1989. Progress toward ultrastructural identification of individual mRNAs in thin sections: Myosin heavy-chain mRNA in developing myotubes. In: G.R. Bullock and P. Petrusz (eds.), *Techniques in immunocytochemistry* (Vol. 4, pp. 147–165). Academic Press, New York.

Singer, S.J. 1959. Preparation of an electron dense antibody conjugate. *Nature* 183: 1523.

Sternberger, L.A. 1986. *Immunocytochemistry*. John Wiley, New York.

Sun, X.J., Tolbert, L.P., and J.G. Hildebrand. 1995. Using laser scanning confocal microscopy as a guide for electron microscopic study: A simple method for correlation of light and electron microscopy. *J. Histochem. Cytochem.* 43: 329.

Tokuyasu, K.T. 1973. A technique for ultracryotomy of cell suspensions and tissues. *J. Cell Biol.* 57: 551.

Tokuyasu. K.T. 1984. Immuno-cryoultramicrotomy. In: J.M. Polak and I.M. Varndell (eds.), *Immunolabeling for electron microscopy*. Elsevier, New York.

Williams, M.A. 1977. *Autoradiography and immunocytochemistry*. Elsevier, New York.

Willingham, M.C. 1980. Electron microscopic immunocytochemical localization of intracellular antigens in cultured cells: The EGS and ferritin bridge procedures. *Histochem. J.* 12: 419.

CHAPTER 6 TECHNIQUES

Colloidal Gold Techniques

Colloidal gold techniques provide cellular markers (gold particles) that are spherical and extremely electron-dense (Fig. 151). One of the chief advantages of colloidal gold techniques is that the gold particles cannot be confused with any other cellular constituents, unlike the products of previously discussed ferritin and peroxidase/DAB/osmium staining procedures.

When properly prepared, colloidal gold consists of a permanent suspension of tiny gold particles. In the mid-1800s, Michael Faraday explained the colloidal nature of these suspensions and noted that they were subject to flocculation in the presence of electrolytes. The suspensions could be stabilized against flocculation by adding fats, glycols, or proteins to the solutions.

By manipulating buffer and pH conditions during the production of colloidal gold, probes of several sizes can be produced (De Mey and Moeremans, 1986; Horisberger, 1985). Colloidal gold can be conjugated with antibodies for immunolabeling, enzymes for determining the location of enzyme substrates, and lectins for the demonstration of mono- and disaccharides in cells and tissues.

The manufacture of colloidal gold requires the reduction of gold chloride. See Frens (1973) and Slot and Geuze (1981) for discussions of the production of colloidal gold particles of specific size through controlled nucleation. Once the colloidal gold suspension is manufactured, surface charges keep the particles apart (gold particles are positively charged by nature). Conjugation of the gold to proteins requires that the ligand be slightly negatively charged. Before the protein is conjugated, the pH of the colloidal gold suspension should be adjusted to about 0.1–0.2 pH points to the negative side of the protein's isoelectric point. PEG (20,000 MW) is then added to the conjugated gold/protein solution to neutralize any remaining surface charges on the complexes.

The procedures for the preparation of colloidal gold and its conjugation with the respective proteins are identical for antibody, enzyme, and lectin work. Preparation of the specimens to be labeled, however, is not. Enzymes and lectins bound to colloidal gold can usually be used to probe epoxide-embedded materials, while antibodies often tend to be hard to demonstrate after epoxide embedment due to the rigors of fixation,

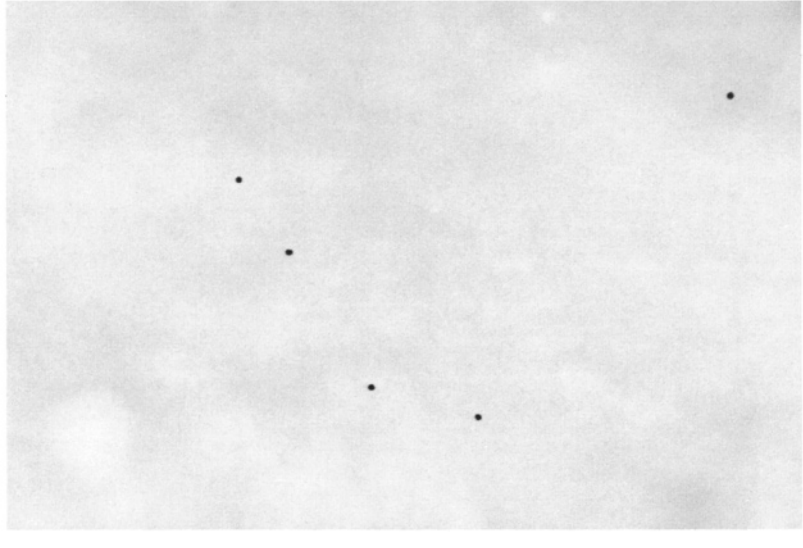

Figure 151. Unconjugated colloidal gold particles prepared by the Frens (1973) isocitrate technique, resulting in 13-nm particles. This sample was stored for 3 months at 4°C before being put on a coated grid for photography. 56,038×.

dehydration, and heat polymerization. In addition, monoclonal antibodies generally demonstrate antigens with more difficulty than polyclonal antibodies because the former only recognize one epitope, while the latter recognize several. Thus, colloidal gold-labeled enzymes and lectins can usually be used to probe epoxide embedded (as well as glutaraldehyde/osmium fixed) materials with great success, while gold-labeled antibodies are usually used to probe the more accessible acrylic resins after minimal fixation (formaldehyde with or without trace amounts of glutaraldehyde), minimally fixed ultrathin frozen sections, or unfixed cells or tissues prior to embedment (if the antigen is located on cell surfaces).

Beesley (1989), Bullock and Petrusz (1982, 1983, 1985, 1989), Hayat (1989, 1991), and Polak and Varndell (1984) provide in-depth discussions of all aspects of immunolabeling.

References

Beesley, J.E. 1989. *Colloidal gold: A new perspective for cytochemical marking. Royal Microscopical Society Microscopy Handbook #17.* Oxford Science Publications, Oxford.

Bullock, G.R., and Petrusz, P. (eds.). 1982, 1983, 1985, 1989. *Techniques in immunocytochemistry* (Vols. 1–4). Academic Press, New York.

De Mey, J., and Moeremans, M. 1986. The preparation of colloidal gold probes and their use as marker in electron microscopy. In: J.K. Koehler (ed.), *Advanced techniques in biological electron microscopy III*, pp. 229–271. Springer-Verlag, New York.

Frens, G. 1973. Controlled nucleation for the regulation of the particle size in monodisperse gold solutions. *Nature (London) Phys. Sci.* 241: 20.

Hayat, M.A. 1989 and 1991. *Colloidal gold: Principles, methods and application.* Academic Press, New York.

Horisberger, M. 1985. The gold method as applied to lectin cytochemistry in transmission and scanning electron microscopy. In: G.R. Bullock and P. Petrusz (eds.), *Techniques in immunocytochemistry* (Vol. 3, pp. 155–178). Academic Press, London.

Polak, J.M., and Varndell, I.M. 1984. *Immunolabeling for electron microscopy.* Elsevier, New York.

Slot, J., and Geuze, H. 1981. Sizing of protein A-colloidal gold probes for immunoelectron microscopy. *J. Cell Biol.* 90: 533.

Preparation of 13-nm Colloidal Gold

1. Applications and Objectives

This technique will reproducibly produce 13-nm colloidal gold particles suitable for conjugation to enzymes, lectins, and antibodies. By altering the conditions of this procedure, gold particles of different diameters can be produced (see Table 13).

Table 13. Methods for Producing Gold Particles of Various Sizes[a]

Reducing Agent	pH	Particle Diameter (nm)	Particles/ml	Color	Absorbance (nm)
Phosphorus	7.4	5.3	3,466	Red	518
Sodium ascorbate	7.9	13.3	157	Orange–red	523
1% sodium citrate					
2 ml/100 ml	4.8	23.7	33.1	Red	526
1.6 ml/100 ml	4.4	30.3	14.1	Red	527
0.8 ml/100 ml	3.3	46.6	3.76	Dark red	539
0.6 ml/ 100 ml	3.3	63.3	1.47	Red–violet	542

[a] From Hayat (1989).

2. Materials Needed

- pH meter
- 10-ml pipets
- 250-ml Erlenmeyer flasks
- Aluminum foil
- Double-distilled (glass) water (DDW)
- Sigmacote™ (Sigma Co., St. Louis, MO)
- 1% aqueous gold chloride: 1 g of gold chloride in 100 ml of DDW (this solution will be kept at 4°C in a light-tight container for 1 year)
- 1% aqueous sodium citrate: 1 g sodium citrate in 100 ml of DDW

3. Procedure

1. Glassware should be acid-washed or siliconized to make it thoroughly hydrophobic. If acid-washed, rinse glassware with tap water, then deionized water, culminating in DDW. The dried glassware should allow water to sheet off when inverted, with no droplets forming on the glass.
2. To siliconize glassware, pour a small volume of Sigmacote in the vessel, and then pour back into the original container for later use. Drain the vessel thoroughly and place in a 47 °C oven overnight. The vessel will appear to be coated with a colored oily film. After the vessel is siliconized and dried, it can be washed with Alconox™ and scrubbed, followed by the water rinses described above.
3. Put 100 ml of DDW into a siliconized 250-ml Erlenmeyer flask.
4. Add 1 ml of the 1% gold chloride solution to DDW and bring it to boil to increase the rate of reaction.
5. Add 4 ml of the 1% sodium citrate solution, the reductant, as fast as possible (squirt it into the flask containing the boiling gold chloride with a pipet while swirling the flask). The molecules of sodium citrate serve as nucleation sites for the gold. It is desirable for all the nucleating sites to appear at the same time and to begin nucleating at the same rate to ensure a uniform final particle size. The final colloidal gold is a reddish solution because of the refractive index of the 13-nm particles formed. When the sodium citrate is first added, the slightly yellowish gold chloride solution becomes totally clear. As the solution continues to boil, it then becomes lavender and finally burgundy–orange. Keep the vessel covered with aluminum foil as the heating/nucleation process continues. (The initial decolorizing of the solution should be followed by the development of a lavender tint in about 90 sec, which then turns into a deep violet after another 5 min, followed by the final burgundy–orange at about 11 min.) When the solution achieves the final color, take it off the burner and cool it to room temperature with ice. If the color does not turn to burgundy–orange, the solution has either too little gold or too much reductant. If the color shifts back to purple, the gold particles will be much too large.

4. Results Expected

The burgundy–orange heated gold solution will remain the same color after it has been cooled to room temperature. An aliquot placed upon a Formvar- and carbon-coated grid and wicked to dryness a few minutes later can be examined with a TEM, revealing gold particles about 13 nm in diameter that are not aggregated into large clusters (Fig. 151). The gold solution is stable at 4 °C for at least 6 months (DeMey, 1984).

5. Cautionary Statements

Use double-distilled (glass) water for all solutions and rinse to make sure that no extraneous nucleation sites are introduced. The silicon coating of glassware is essentially permanent however many times the

vessels are washed. Both acid-washing and siliconizing are meant to prevent the positively charged gold from interacting with the glass surface and to prevent any extraneous dirt from serving as a nucleating site for gold.

The absorption spectrum of the gold solution should be around 520 nm (DeMey, 1984). The larger the size of gold particles, the longer is the wavelength of the absorption peak. If the color shifts from the burgundy–red described into the dark purplish or even brownish range, the solution is suspect and should be checked by electron microscopy.

References

DeMey, J. 1984. Colloidal gold as marker and tracer in light and electron microscopy. *Bull. Electron. Microsc. Soc. Am.* 14: 54.

Frens, G. 1973. Controlled nucleation for the regulation of the particle size in monodisperse gold solutions. *Nature Phys. Sci.* 241: 20.

Hayat, M.A. 1989. *Principles and techniques of electron microscopy. Biological applications*, 3rd edn. CRC Press, Boca Raton, FL.

Conjugation of Gold to Proteins[1]

1. Applications and Objectives

This technique allows conjugation of the gold particles produced in the previous procedure to various types of proteins (antibodies, enzymes, and lectins). After conjugation is effected, the colloidal gold–protein complexes are stabilized with polyethylene glycol.

2. Materials Needed

- 0.1 M acetate buffer, pH 5.0–5.5
- Microfuge and microfuge tubes
- An ultracentrifuge with a fixed-angle rotor and tubes suitable for 48,000 rcf centrifugation
- pH meter
- 0.1 N potassium carbonate solution (1.38 g of K_2CO_3 in 100 ml of DDW)
- 0.1 N HCl
- 1% aqueous solution of 20,000 MW PEG (Fluka Chemicals)
- Shell vials large enough to accept a pH electrode (scintillation vials are ideal)
- 10 ml of a 13-nm colloidal gold suspension prepared in previous procedural instructions
- Pasteur pipets
- Buffer appropriate for the activity of the antibody, enzyme, or lectin
- Parafilm™

3. Procedure

1. Put 3 drops of 1% PEG into each of about six to eight vials. The vials should be filled about half full with the cooled gold solution and then swirled. After about 5 min at room temperature, all of the gold particles should be coated with PEG. The shell vials do not need to be siliconized, as they will be discarded. If the pH meter probe is put into the gold solution before the PEG is added, the probe will eventually be plugged by gold particles.

[1] Special thanks are due to Ron Clay, Botany Department, University of Georgia, for introducing us to this technique.

2. Calibrate the pH meter and adjust the pH of the gold solution (try not to overshoot) to 0.1–0.2 pH points above the isoelectric point of the antibody, enzyme, or lectin being conjugated. Use 0.1 N HCl to lower the pH and potassium carbonate to raise the pH. The colloidal gold in sodium citrate has a pH of 5.3–5.4.
3. Conjugate the gold with the protein (Worthington CEL cellulase in this example):
   a. Adjust the pH to 0.1–0.2 pH points above the isoelectric point of the protein first (see Table 14 for some examples). Cellulase has an isoelectric point of 4.3–4.4, so adjust the pH of the gold solution to 4.5–4.6 with 0.1 N HCl.
   b. Put one drop of DDW into a 10- to 15-ml siliconized centrifuge tube. Add 100 μg of the enzyme powder. Sonicate the protein suspension for about 3–4 min to get it thoroughly into solution.
   c. In general, add about 100–500 μg of protein to 10 ml of the prepared colloidal gold. An excess of protein is desired. Add the gold to the drop of protein molecules in the tube, never the other way around. Add about 10 ml of the gold solution to the centrifuge tube containing the drop of sonicated protein molecules, and then cover the top of the tube with Parafilm™ and invert the tube several times to mix the solutions.
   d. Add 5–10 drops of PEG, cover the tube mouth with Parafilm™, and invert the tube several times to mix the materials.
   e. Centrifuge the tube in a fixed angle rotor at 48,000 rcf for 30 min at 5 °C. This concentrates the conjugated gold/protein particles and produces a "mobile pellet," which is on the side of the tube but will run down slowly to the bottom if held in a vertical position in a tube rack. The supernate in the tube contains unconjugated protein and must be totally removed, or the proteins can occupy reactive sites during staining and prevent the conjugated proteins from binding and being detected. A small, nonmobile black pellet may remain in the tube. This consists of unconjugated gold and should not be collected.
   f. Discard the supernate and resuspend the mobile pellet in 1 ml of 0.1 M acetate buffer, pH 5.0–5.5, which is appropriate for the activity of cellulase. Put the buffered gold conjugate into a microfuge tube and then centrifuge for a few seconds at full speed to dislodge only large aggregates of gold.

4. Results Expected

The conjugated gold/protein should be a monodisperse suspension with a good chemical reactivity.

5. Cautionary Statements

Some of the gold/protein conjugates are stable at 4 °C for months, while others like Protein A-gold complexes need to be stabilized by the addition of 20% glycerol and then frozen in small aliquots at − 70°C to avoid dissociation of the complexes. It is advisable to use conjugates shortly after they are prepared to ensure maximum chemical reactivity.

To standardize reaction conditions, it is possible to determine the relative content of colloidal gold in a given suspension by using a spectrophotometer to measure the optical density of the solution at 520 nm (Hayat, 1989).

Table 14. Some Examples of Isoelectric Points for Proteins to Be Conjugated with Colloidal Gold

Compound	Isoelectric Point	Specificity
Cellulase	4.3–4.4	Cellulose
Chitinase	4.5–5.5	Chitin
Protein A	5.0	Fc portion of IgG
IgG	7.0	Specific antigens
Bauhinia purpureas (camel's foot tree) lectin	5.4–7.1	β-D-Gal-(1→3)-D-GalNac

To determine proper protein/gold concentrations (Hayat, 1989), place 20 μl of DDW in each well in the first two rows of a 96-well microtiter plate. Add 20 μl of a 500–1000 μg/ml protein solution to the first well in each row, mix, and then transfer 20 μl to the next well in the row. Repeat the dilution process down the row of wells. This leaves 20 μl of protein solution in each well except the last one, which will contain 40 μl. Add 100 μl of buffered colloidal gold solution that has had its pH adjusted to 0.1–0.2 points above the isoelectric point of protein being tested to each well except the last ones in each row. Tap the plate and let it sit for 15 min at room temperature. Add 20 μl of 10% NaCl in DDW to all the wells except the last two in each row. The last well in the series of dilutions that retains a red color represents the endpoint at which the protein stabilizes 100 μl of the colloidal gold suspension. In other words, an endpoint in well #5 would indicate that 20 μl of protein diluted 1:32 stabilizes 100 μl of the colloidal gold suspension. If further examination of the endpoint well contents reveals aggregates containing five or fewer gold particles, the preparation should be good for probing.

Reference

Hayat, M.A. 1989. *Principles and techniques of electron microscopy. Biological applications*, 3rd edn. CRC Press, Boca Raton, FL.

Indirect Immunolabeling Procedure for Sections of Materials Embedded in LR White or Lowicryl K4M Resin (Acrylic Resins)

1. Applications and Objectives

Acrylic-resin-embedded materials can be sectioned to provide access to intracellular antigens, which can be subsequently probed with antibodies conjugated with gold because of the hydrophilic nature of acrylic resins. Materials prepared for immunoprobing are typically not osmicated so that the antigens remain more reactive.

2. Materials Needed

1. Quenching solution (any one of the following in DPBS will work):
   - 0.1 M ammonium chloride
   - 0.1 M glycine
   - 0.1% sodium borohydride
2. Blocking agents (any one of the following in DPBS):
   - 1% bovine serum albumin
   - 1% fish gelatin
   - 5% normal goat serum
   - 1% nonfat dried milk
   - 0.2% ovalbumin
3. Moist chamber (a Petri dish containing filter paper moistened with distilled water). A piece of Parafilm™ is placed upon the moistened filter paper. The incubation media consist of drops of fluid put onto the Parafilm™ surface.
4. DPBS.
5. Sections of acrylic-resin-embedded tissues or cells on inert grids made of nickel or stainless steel.
6. Rotating platform such as an Adams Nutator.

3. Procedure

1. If the sample was fixed in glutaraldehyde prior to embedment, quench by floating the grid with sections for 15 min at room temperature on a droplet of one of the quenching agents listed to neutralize any reactive glutaraldehyde in the sections.

2. Rinse in DPBS briefly by floating the grid with sections for a few seconds on two different drops of DPBS.
3. Float the grid for 15 min at room temperature on a drop of one of the blocking agents to reduce non-specific antibody binding.
4. Rinse in DPBS as described above.
5. Float the grid on a droplet of primary antibody (5–20 μg/ml) for 60 min at room temperature. A dilution series will determine the best antibody concentration. Monoclonal antibodies (MAbs) should be somewhat more concentrated than polyclonals. A good dilution series for Mabs would be 1:10, 1:20, 1:40, and 1:80, while polyclonals could be diluted 1:50, 1:100, 1:200, and 1:400.
6. Rinse in DPBS three times (5 min each).
7. Float the grid on a droplet of gold conjugated to anti-primary antibody or Protein A (or G) for 60 min at room temperature.
8. Rinse in DPBS three times (5 min each) and then wick the grid dry with filter paper.
9. Poststain grids with normal procedures for acrylic resins.

4. Results Expected

Gold particles will be evident where the primary antibody has bound to the cellular antigen and has, in turn, bound the secondary antibody conjugated to colloidal gold.

5. Cautionary Statements

It is recommended that the drops of incubation media on which sections are floating be put onto a gently rotating platform such as an Adams Nutator. *The grid should never be allowed to dry out at any stage in the process, or it will become coated with proteinaceous materials that will make it largely electron-opaque.*

Epoxide sections can sometimes be successfully immunolabeled, even if the cells/tissues have been osmicated during processing (Bendayen and Zollinger, 1983), but many antigens are profoundly altered by the processes involved in fixation, dehydration, and embedment in epoxide resins. The acrylic resins do not produce images as pleasing as conventional epoxide methods, but the cellular compartments and structures are still quite clear. The increased possibility of successful immunolabeling with acrylic embedded materials compared with epoxide-embedded samples argues strongly for this technique. If intracellular labeling is expected, thus necessitating sectioned material, but is not successful, labeling of ultrathin frozen sections would be another valuable technique to try.

Antigen retrieval techniques cited in the body of this chapter may allow successful antibody labeling in situations where primary fixation with aldehydes seems to be interfering with antibody labeling.

References

Bendayan, M., and Zollinger, M. 1983. Ultrastructural localization of antigenic sites on osmium-fixed tissues applying the protein A-gold technique. *J. Histochem. Cytochem.* 31: 101.

Hayat, M.A. 1989. *Principles and techniques of electron microscopy. Biological applications*, 3rd edn. CRC Press, Boca Raton, FL.

Procedure for Immunolabeling Intact Cells (Preembedment Labeling of Cell Surfaces)

1. Applications and Objectives

This technique is designed to indirectly label antigens on the surfaces of isolated bacteria, cultured eukaryotic cells, or viruses.

2. Materials Needed

The same materials as those used for the acrylic resin immunolabeling method are used.

3. Procedure

1. Rinse cells or virus free of growth medium with a noninjurious buffer solution such as DPBS.
2. Incubate cells in primary antibody to antigen (e.g., rabbit antibody in the same buffer at neutral pH for 1 hr at room temperature at various dilutions [1:32, 1:64, 1:128]). All incubations in this procedure can be done in some sort of plate (Costar tissue culture Cluster^{24} plate) with wells lined by Parafilm™. The plate should be on some sort of gentle rocking platform such as an Adams Nutator. A microfuge tube would also be a good reaction vessel.
3. Rinse the labeled cells in DPBS containing 0.5% bovine serum albumin (BSA) and 0.1% gelatin, pH 7.0 (washing buffer).
4. Incubate for 1 hr at room temperature in secondary antibody conjugated to gold label (e.g., goat anti-rabbit conjugated with 13 nm gold) diluted 1:32, 1:64, 1:128 with DPBS containing 0.1% BSA, and 5% fetal bovine serum, pH 7.0.
5. Rinse the cells in DPBS without added BSA or gelatin.
6. The bound antibodies can be stabilized by adding 4F:1G fixative to cells. Add about 5 to 10 times the cell volume. Resuspend the cells and store at 4 °C until they can be negatively stained and examined with the TEM or dehydrated, embedded, and sectioned for TEM examination.

4. Results Expected

Gold particles will be located on the surface of the cell membranes or surface extensions such as pili or flagella, depending on the location of the antigen for which the cells are being probed. Excessive clustering of gold particles should not be evident. Negative staining of cells diluted appropriately and put onto coated grids as described in the chapter on negative staining will allow a quick assessment of labeling success.

5. Cautionary Statements

If the cells are kept in gentle motion during labeling, surface labeling should take place uniformly over the population. The antigen should not be clustered on certain members of the population while being absent from others. If uneven labeling is observed, agitate the sample more thoroughly.

7

Support Films

I. PURPOSE

Support films attached to the surface of grids can be used for negative staining or shadowing of particulate samples (mitochondria, microsomes, bacteria, viruses). The films serve as electron-transparent substrates for these samples. In addition, grids with large amounts of open space (bar, hole, or slot grids) that otherwise would provide inadequate support for plastic sections can be coated with films so that large areas of sections, or the entire section in the case of slot and hole grids, may be viewed without grid bars obscuring section detail. Support films are usually made from Formvar, Butvar, collodion, or carbon.

Carbon is often used to help stabilize films made from the first three materials. General instructions for producing a carbon coat are given in the section on Shadow Casting in Chapter 8. Only a light carbon coat is necessary to stabilize polymer films, though the actual amount of carbon is not usually critical because carbon films are so electron transparent.

A coated grid will provide a stable support for particulates or sections with minimal evidence of thermal drift or destruction by the electron beam of the TEM. Even though the film decreases contrast a slight amount, this factor should not be significant if the film is of proper thickness. Finally, holey films can be prepared that are used for minimizing astigmatism in objective lenses and apertures and to judge image stability.

Various film types, their preparation, and avoidance of typical difficulties are discussed by Hayat and Miller (1990) and Faberge (1984).

II. TYPES

A. Nitrocellulose

Nitrocellulose comes as strips of material, under the name Parlodion, that must be dissolved before use in a solvent such as amyl acetate. Alternatively, 1–2% solutions of nitrocellulose in amyl acetate may be purchased under the name collodion.

B. Formvar

Formvar (polyvinyl formaldehyde) may be obtained as a 0.25–0.5% solution in either chloroform or ethylene dichloride (2,2-dichloroethane), or may be purchased as a powder. This resin is purported to produce films that are more beam-stable than those made from nitrocellulose.

Another polymer, Butvar (polyvinyl butyraldehyde), is available from some suppliers and is used in a similar fashion to Formvar and is thought to be even more resistant to beam damage than Formvar.

Carbon may be evaporated onto plastic-coated (collodion, Formvar, Butvar) grids to increase their conductivity and, thus, to increase their stability under the electron beam. This is usually accomplished by placing air-dried, filmed grids into a vacuum evaporator, producing a vacuum of about 1.33×10^{-2} Pa, and then evaporating about 10–20 nm of carbon onto the surface of the filmed grids at 45–90°. The carbon should make the substrate bearing the grid light to dark gray (see the section on vacuum evaporators for methods of judging carbon film thickness).

III. METHODS

When support films are made from any of the substrates mentioned above, it is imperative that the grids be clean so that the materials will adhere readily to the grid surface. The grid-cleaning procedure described in the chapter on ultramicrotomy is modified in this case to clean as many as 100 grids at a time. Rather than dipping the grids one at a time into the three cleaning solutions (acid, ethanol, and acetone), it is more efficient to put the contents of a vial of grids into a BEEM™ capsule, add 0.1 N HCl, cap the capsule, and shake for 10 sec. Next, pipet out the acid and replace it with 95% ethanol, shake for a few seconds, and remove the ethanol. Finally, introduce 100% acetone with a fresh pipet, shake vigorously, remove the acetone with a pipet, and shake the grids onto a piece of clean filter paper in a Petri dish. Once the acetone has evaporated, separate the grids with forceps and line them up face down (shiny side down) on the filter paper in preparation for placing them on a coating film. Clean the grids immediately before placing them onto the films, as they may oxidize again within a few hours.

All film-casting procedures need to be done in a clean glass vessel such as a rectangular histological staining dish for racks containing 10 slides. This dish is filled with deionized or distilled water and placed over a black surface, such as a bag from a box of photographic paper, in an area with diffuse overhead lighting (fluorescent) so that interference colors can be adequately judged to determine the film thickness after casting. A gold film is very sturdy and easily used for most particulates, but a gray–silver film is more appropriate for work with sections. If the thickess of a film supporting sections is too great, it will impede penetration of the electron beam, resulting in more scattering and a reduction in specimen contrast.

A. Droplet

The droplet method is generally used with collodion because nitrocellulose in amyl acetate spreads readily on the surface of water, unlike the other plastic materials dissolved in ethylene dichloride or chloroform, which tend to sink to the bottom without spreading completely. A Pasteur pipet is used to drop 1–3 droplets of a 2% collodion solution onto the surface of the water in the film-casting dish. As the solvent begins evaporating, the plastic film will be seen to cover the entire surface of the dish. The film will have areas of differing thickness, as judged by the interference colors. It will also have many evident wrinkles. After the solvent has completely evaporated (1–2 min), the film will cease to change color and can be evaluated. Pick areas on the film of the appropriate color and begin placing freshly cleaned grids face down on the surface. The grids are then picked up by placing a stainless steel screen, pieces of 3×5 in. (7.6×12.7 cm) card stock, or a previously plastic-coated glass slide (as prepared for slide stripping, as described below) on top of the grids. After contacting the grids and the subtending plastic film, push the support matrix (screen, paper, or slide) beneath the surface of the water, turn it over, and bring it out of the water. Thus, the film

emerges first, with the grids trapped beneath the film and above the support matrix. The matrix is then blotted dry from beneath and placed into a Petri dish with the cover propped up slightly with a piece of crumpled filter paper to allow the moisture to evaporate. If the grids are to be carbon-coated, wait at least overnight so that the film will be completely dry. Otherwise, the vacuum evaporator will have difficulty developing adequate vacuum.

B. Slide Stripping

Slide stripping is the method generally employed for producing films of Formvar or Butvar (Faberge, 1984). In this procedure, the greatest difficulty lies in preparing the glass slide to be coated with dissolved resin. If the glass slide is too clean, the plastic film cannot be forced to separate from the glass; if it is too dirty, the film will have numerous imperfections (streaks, holes) visible under the electron beam. Many labs have found that certain types of glass slides are easier to strip than others. Unfortunately, the manufacturers change their methods periodically, so what was once a very suitable slide for stripping may no longer work well. Various methods are suggested by electron microscopists such as buying only one brand of glass slides, rubbing the slides with nose grease prior to dipping in the resin, washing the slides with various solvents before dipping, or coating them with various detergents in order to ensure good film release. A method that seems to work for slides of any origin is to spray them with 409™ detergent and then wipe them dry with Kimwipes™. Examine the slides closely to make sure that no streaks or imperfections are grossly visible.

After the cleaned slides are prepared, they must be dipped in the plastic resin. Electron microscopy supply houses market side-arm flasks with elongated thistle tubes attached to the top that cost over $100.00 and allow the user to pump resin into the covered thistle tube containing a glass slide and then to let it drain back into the flask again. A 30-ml beaker achieves the same end at a greatly reduced price. The beaker should be dedicated to slide dipping and kept clean by always rinsing it before and after use with the solvent used with the resin.

Freshly filmed grids tend to be fairly hydrophilic and wetable, but grids become hydrophobic upon sitting. Carbon coating gives variable results in relation to hydrophilicity. Sometimes, the grids become harder to wet, and in other situations, easier. Hayat and Miller (1990) recommend exposing filmed grids to ultraviolet light for 40 min to increase their wettability. Another method recommended by some workers to make filmed grids more hydrophilic is to glow-discharge filmed grids. Unfortunately, this requires a vacuum evaporator specifically equipped to do the task. Such a device is capable of producing a 5–10 kV potential between the coated grids, which are sitting on a grounded platform, and a wire loop (typically) suspended above them at a positive potential. The grids are introduced into the vacuum evaporator, which is then pumped to a minimal vacuum (1.3×10^{-1} Pa is adequate), at which time the glow-discharge unit is turned on. The high voltage developed between the grid-bearing platform and the positive pole in the presence of a slight amount of atmosphere results in minor etching of the plastic film, producing a slightly hydrophilic surface. It is recommended that glow-discharged grids be used within hours of manufacture.

C. Holey Films

Holey films for microscope alignment can be prepared by adding 1–5% water to a 0.5–1.0% Formvar solution. Shake the solution well, or sonicate it for a few minutes and then immediately dip precleaned slides. The water should result in numerous miniscule holes in the plastic film. Another method is to dip slides in a normal Formvar mixture but to breathe heavily

upon them just after dipping to introduce moisture into the film. In either case, strip the slides as usual, put grids upon them, and retrieve them as above. It is also important to carbon-coat them to give them added stability.

D. Carbon Films

Carbon films can be used as the sole support film on grids. Carbon-filmed grids are utilized chiefly for the purpose of supporting materials for microanalytical purposes where the impurities in plastic films would result in spurious readings. These grids are more fragile than plastic-coated grids and are considerably more difficult to produce consistently. The most common method is to purchase mica sheets, which are split just before use by inserting a razor blade between the crystal layers and prizing them apart. The freshly revealed mica surface is then placed in a vacuum evaporator, and a film of about 20 nm is evaporated onto the mica. The mica is then introduced into a vessel of clean water (as in slide stripping) at an angle of about 30°. The carbon film will float off onto the surface of the water. Allow the mica to fall to the bottom of the vessel.

Most workers utilize a device with a stainless steel screen platform on which cleaned grids are held down by an overlying stainless steel plate with holes. This support with the grids and restraining plate above them is slowly lowered until the grids and plate are submerged in the water. The plate restraining the grids is gently removed, leaving the grids beneath the water surface, supported by the stainless steel screen support. A carbon film is stripped off of a mica support onto the water surface. The stainless steel support with grids is then raised slowly until it contacts the carbon film floating on the water. As the support emerges from the water, the grids become coated with the overlying carbon film. The support with the carbon-coated grids is placed into a dust-free chamber until the grids are dry and ready for use.

REFERENCES

Faberge, A.C. 1984. Formvar and butvar support films; some general considerations. *Bull. Electron Microsc. Soc. Am.* 14: 102.
Hayat, M.A., and Miller, S.E. 1990. *Negative staining*. McGraw-Hill, New York.

CHAPTER 7 TECHNIQUES

Preparation of Formvar-Coated Grids

1. Applications and Objectives

Polyvinyl formaldehyde resin (Formvar) is the most widely used support film material for coating grids because of its stability under the electron beam and the consistency of the films produced.

2. Materials Needed

- Windex™ or 409™ cleaner
- Glass microscope slides
- Deep glass staining dish
- 30-ml beaker
- Formvar powder (or 0.25–0.5% solution in ethylene dichloride purchased from an EM supply house)
- Ethylene dichloride
- 100-ml stock bottle
- Teflon™ tape
- Paper towels
- Razor blades
- Diffuse overhead light (fluorescent light source)
- Grids
- Pasteur pipets
- Grid cleaning solutions (0.1 N HCl, 95% ethanol, 100% acetone)
- Whatman™ #1 filter paper (9-cm disks)
- Disposable Petri dishes (10 cm)
- Kimwipes™
- BEEM™ capsules

3. Procedure

Preparation of Formvar Solution. Add 0.125 g of Formvar powder to 50 ml of ethylene dichloride in the stock bottle. Wrap the ground-glass stopper with Teflon™ tape to prevent the Formvar solution from gluing the stopper to the neck of the stock bottle. Swirl the solution, and allow it to sit at room temperature. After 8 hr, the Formvar powder should be completely dissolved, yielding a clear solution.

Preparation of Clean Grids. Grids are cleaned in batches by putting 25–100 grids into a BEEM™ capsule, which is then filled with 0.1 N HCl, capped, and shaken vigorously for 10 sec. Use a Pasteur pipet to remove the HCl, which is replaced immediately with 95% ethanol and shaken. Next, remove the ethanol, replace it with acetone, and shake the capsule for another 10 sec. Remove the acetone with a pipet and then shake the grids onto the surface of Whatman™ #1 filter paper in a Petri dish. Separate all the grids, and place them shiny-side down in the Petri dish.

Microscope Slide Cleaning. Shortly before use, spray new microscope slides with Windex™ or 409™ cleaner and wipe them dry with Kimwipes™. This removes any manufacturing oils or dirt and leaves a thin film of detergent, which makes the applied Formvar coat easier to strip off the slide.

Making the Formvar Film

1. Rinse a 30-ml beaker by filling it with ethylene dichloride, and then pour the ethylene dichloride, back into the rinse storage bottle. It is not necessary to use fresh ethylene dichloride for this purpose.
2. Pour 0.25% Formvar solution into the rinsed beaker to a depth of 3–5 cm. Do this immediately before dipping the slides.
3. Dip detergent-cleaned slides to the bottom of the beaker of Formvar solution. Touch the bottom corner of the slide on the side of the beaker, then blot the bottom edge of the slide on a paper towel. Always dip at least two slides, one for stripping and one for picking up filmed grids from the water surface. Stand dipped slides up on end on a paper towel, and lean them against a vertical surface in a dust-free area to dry (Fig. 152).
4. After the slides have air-dried (3–5 min), select one and score the sides and bottom of the microscope slide with a razor blade about 2 mm in from the edges (Fig. 153).
5. Breathe on the end of the slide until the Formvar fogs.
6. Take the fogged, scored slide and quickly hold it perpendicular to the surface of distilled water in the slide-staining dish. Touch the slide to the surface of the water (Fig. 154A). Slowly submerge the edge of the slide until one or two 1 × 1-in. (2.5 × 2.5-cm) pieces of Formvar have floated off (one per side), as shown in Figure 154B. If neither comes off, remove the slide, breathe on it from the coated end until it is slightly fogged, and try again. Scraping more of the film from the end of the microscope slide with a razor blade may help.
7. Place precleaned grids shiny-side down on floating Formvar film (Fig. 154C).
8. Pick up another Formvar-coated slide, and push down on the floating film of Formvar and grids at an angle until the Formvar film with attached grids is annealed to the slide (Fig. 154D). Quickly pull the slide straight up and out of water (Fig. 154E). The slide with coated grids (Fig. 154F) should be stored in a closed Petri dish until use to keep the surfaces dust-free.

Figure 152. Formvar-coated microscope slides drying on a paper towel.

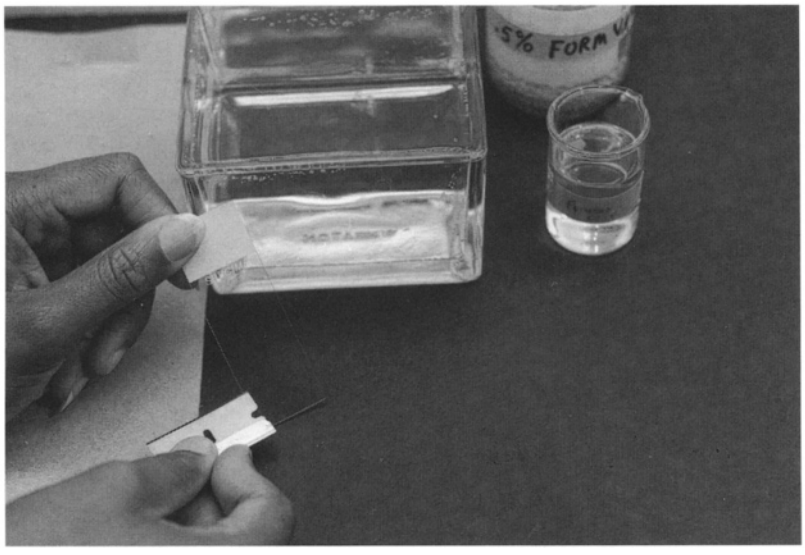

Figure 153. Scoring Formvar film with a razor blade.

(A)

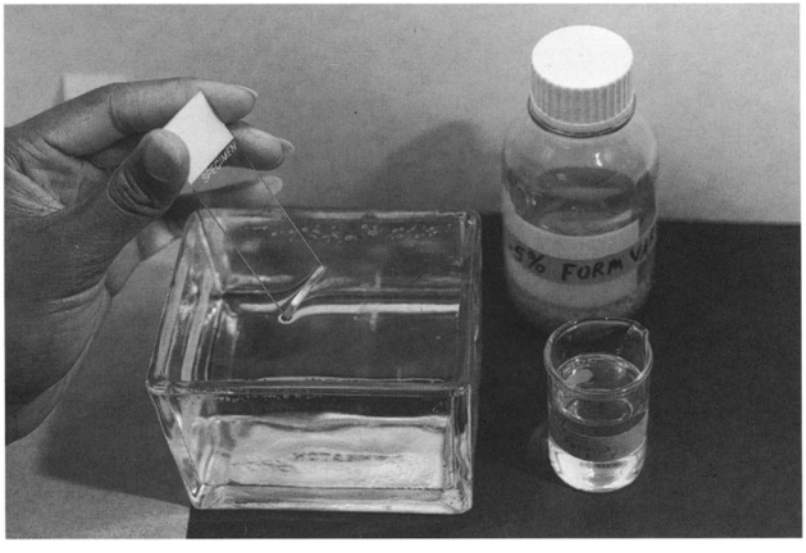

Figure 154. Stripping Formvar from a microscope slide. (A) Touching the slide to the water surface.

9. For greater film stability, carbon-coat the Formvar-coated grids (see the instructions for vacuum evaporation). Carbon coating will make the film more stable under the electron beam, though potentially more hydrophobic.
10. Always place specimens on the Formvar-coated side of a grid (the shiny side of the grid).

4. Results Expected

Grids will be coated with an electron-transparent plastic film with minimal holes, pseudo-holes (thin places in the plastic film), or dirt.

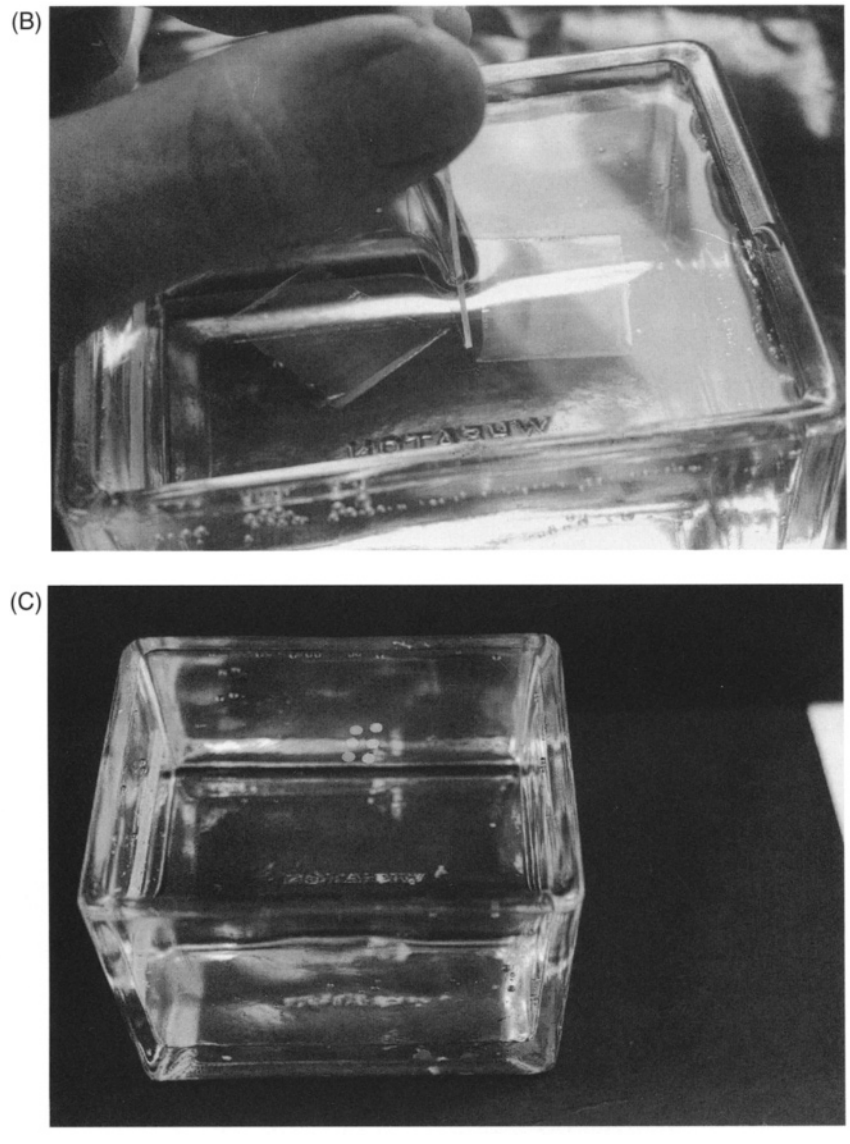

Figure 154. (B) Formvar film lifting off the surface of the microscope slide and floating onto the water surface. (C) Grids floating on Formvar film.

5. Cautionary Statements

Avoid inhalation or skin contact with ethylene dichloride. The Formvar solution can be used for months to make coated grids for negative staining purposes but will produce films with more holes and pseudo-holes as time goes on. With negative staining of particulates, the increasing level of imperfections seen because of aging Formvar solutions is usually not objectionable. When coated slot grids are prepared by the aluminum bridge technique for examining sections of tissue, it is recommended that fresh, commercially prepared Formvar be used to avoid films with imperfections. Films made from Formvar solutions

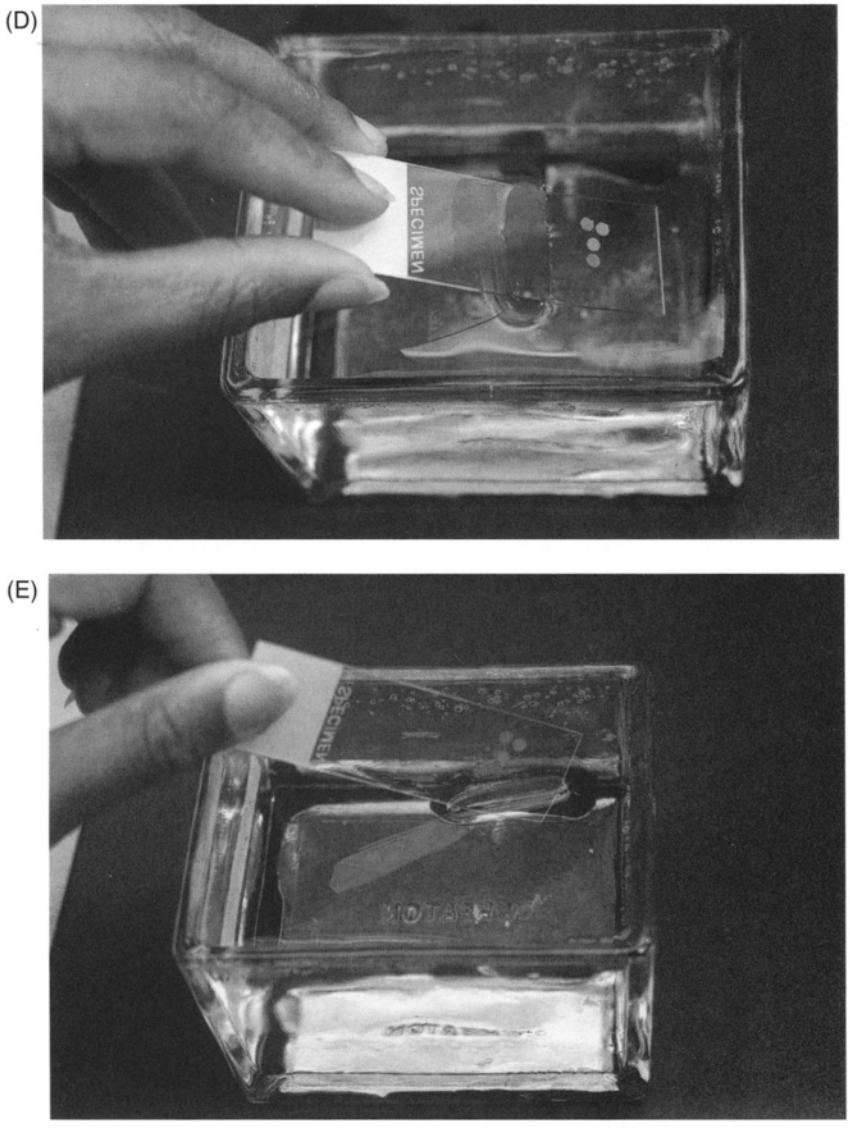

Figure 154. (D) Formvar-coated slide pushing Formvar-coated grids beneath the water surface. (E) Removing Formvar-coated slide with attached Formvar-coated grids from the water bath.

prepared in our laboratory during the summer (when the humidity is over 60%) have more holes and pseudo-holes than are acceptable for coating slot grids. Fresh commercial stocks do not show these defects. Rows of pseudo-holes along the longitudinal axis of the microscope slide usually are *not* caused by the slide cleaning process. They are caused by moisture in the dipping solution. See the comments on dryness of films by Faberge (1984).

Formvar-coated grids may be stored in covered Petri dishes or grid boxes for up to a year before use, though they become more hydrophobic with time.

(F)

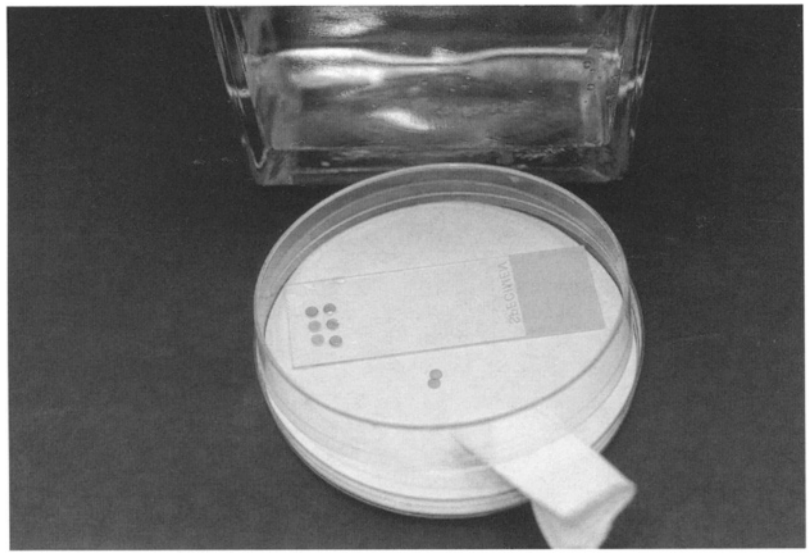

Figure 154. (F) Formvar-coated grids ready for use.

Reference

Faberge, A.C. 1984. Formvar and butvar support films; Some general considerations. *Bull. Electron Microsc. Soc. Am.* 14: 102.

Formvar-Coated Aluminum Bridges for Slot Grids

1. Applications and Objectives

This technique is used to prepare 1 × 2-mm slot grids coated with Formvar (or Butvar) upon which ultrathin sections are supported such that photographs of entire sections can be taken without intruding grid bars. This technique is ideal for situations where an entire plastic section must be photographed or where an important feature rarely encountered within a given section should not be missed because of grid bars. The objective is to produce virtually blemish-free, unwrinkled ultrathin sections borne on an electron-transparent substrate with good beam stability.

2. Materials Needed

- 0.25% Formvar in ethylene dichloride (or 0.25% Butvar in chloroform)
- 1 × 3-in. (2.5 × 7.6-cm) aluminum bridges with 5-mm holes bored in them
- Clean microscope slides prepared as described for Formvar procedures
- 1 × 2-mm copper slot grids
- Petri dishes to contain bridges while drying
- Film-casting chamber (slide-staining or crystallizing dish) with distilled water
- 30-ml beaker

- Ethylene dichloride (or chloroform if using Butvar)
- Whatman™ #1 filter paper (9 cm)
- Anticapillary forceps

3. Procedure

1. Dip a cleaned glass slide in Formvar (Butvar) solution and strip the slide, as described for Formvar films.
2. Prepare an aluminum bridge by wiping thoroughly with Kimwipe™.
3. Touch the polished surface of the aluminum bridge to the surface of film (Fig. 155). After the film has adhered, remove the bridge and place in a covered chamber to dry (about 3 hr).
4. Clean the slot grids by sonicating in ethylene dichloride. Then, dip into Formvar (Butvar) solution and place onto clean Whatman™ #1 filter paper to dry. Keep in closed Petri dishes until needed.
5. Pick up the sections in the slot grid hole. Use anti-capillary forceps to hold the slot grid, come up beneath the sections, and make sure that the sections remain in the drop of water suspended in the hole of the slot grid.
6. Place the slot grid on Formvar (Butvar) film over the hole in the aluminum bridge with sections on top of the drop. Allow the sections to dry on the film surface in a dust-free chamber for several hours (Fig. 156). Remove the grids from the bridge by gently perforating the film around the edge of the hole in the bridge. When there is only a small strand of the film remaining, pull the grid from the bridge hole.
7. Stain as usual with normal poststains.
8. The grid then can be shadowed with carbon to confer a greater beam stability if needed.

4. Results Expected

Film-coated slot grids should bear wrinkle-free, poststained sections with good contrast and minimal stain artifacts.

Figure 155. Aluminum bridge being touched to a Formvar film floating on water in a staining dish.

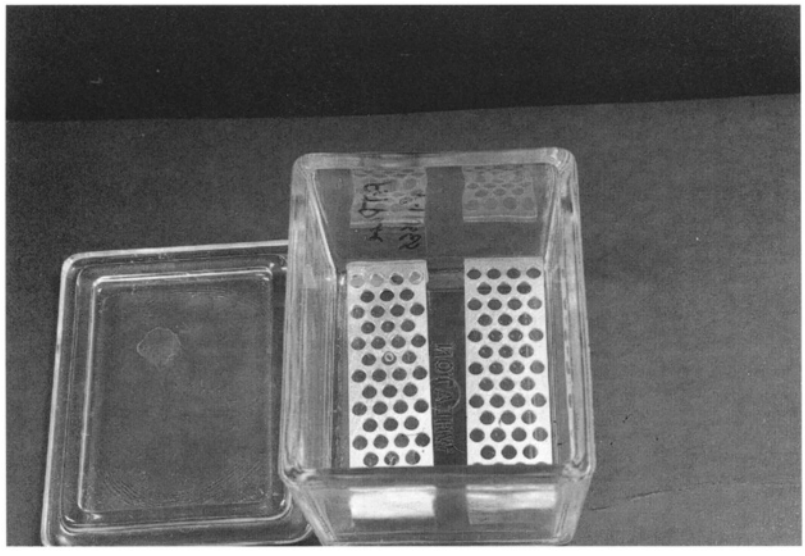

Figure 156. Aluminum bridge with Formvar film supporting a slot grid (the bridge on the left side).

5. Cautionary Statements

The toxicity and volatility of the solvents, as described for Formvar procedures, should be noted. Excessive humidity or other sources of water should be avoided because of the danger of inducing excessive holes or pseudo-holes in the plastic film. Coated slot grids are extremely fragile and must be handled carefully to avoid ripping the film bearing the sections. The process of removing these grids from a microscope vacuum system may cause the film to break, so it is good practice to photograph all materials of interest the first time that the grid is put into the TEM.

Reference

Rowley, J.C., and Moran, D.T. 1975. A simple procedure for mounting wrinkle-free sections on Formvar-coated slot grids. *Ultramicroscopy* 1: 151.

Coating Grids with Butvar B-98

1. Applications and Objectives

According to Crowley (1991), Butvar support films are more mechanically stable, are more translucent, and have less inherent structure than Formvar films. She also notes that they are more hydrophilic, which is a useful feature for negative staining purposes.

Slide-stripping procedures like those described for Formvar should produce Butvar films well suited for coating grids for negative staining and observation of plastic sections on large mesh, hole or slot grids. The coated grids should be good for at least 9 months (Crowley, 1991).

2. Materials Needed

- Cleaned grids
- 0.15% Butvar B-98 in chloroform
- 0.25% Butvar B-98 in chloroform (Dipping mixture)

- Pasteur pipets
- Whatman™ #1 filter paper (9 cm)
- Petri dishes
- 100-ml stock bottle with Teflon™ tape-wrapped stopper
- Clean stir bar
- Stir plate
- 50°C water bath
- Thermometer
- 30-ml beaker
- Slide-staining dish
- Distilled water

3. Procedure

1. Spread clean grids (clean as described under Formvar methods) on filter paper in a Petri dish. Use a Pasteur pipet to put one drop of 0.15% Butvar onto each grid. This allows the grids to stick more efficiently to the film to be cast.
2. Prepare a Butvar–chloroform dipping mixture (0.25%) by putting 0.125 g of Butvar powder into the stock bottle, adding 50 ml of chloroform and a clean stir bar, and then stirring the mixture on a stir plate for 15 min at room temperature.
3. Place the beaker into the water bath and monitor the temperature. When the solution has reached 50°C, place the stock bottle back on the stirring plate, and stir for an additional 10 min at room temperature. The solution should then be allowed to sit without stirring for 2 hr at room temperature before use.
4. Slides are dipped into the Butvar solution and stripped on the water surface. Grids are then added to the floating film, and the film with its attached grids is picked up with a previously Butvar-coated glass slide as described under the Formvar techniques.

4. Results Expected

The Butvar film stripped from a microscope slide and floating on a water surface will be dark silver when viewed with diffuse (fluorescent) light. The coated grids will be somewhat more hydrophilic than Formvar-coated grids, and the visible structure, transparency, and resistance to beam damage will be superior to Formvar films.

5. Cautionary Statements

All work with chloroform should be done under a fume hood. Crowley (1991) suggests that the stirring Butvar solution should be watched carefully to avoid explosions, presumably caused by sparks near the heated solvent. If the procedure is performed under an operating fume hood, this should not be a risk. Cleanliness of all glassware is critical, and the chloroform and Butvar solutions must be water-free to avoid any film imperfections. Crowley (1991) states that the dipping solution should not be saved.

Reference

Crowley, H.H. 1991. Butvar B-98 support film. *Bull. Electron Microsc. Soc.* 21: 99.

Coating Grids with Collodion Films

1. Applications and Objectives

Collodion (nitrocellulose) films are cast directly on the surface of water, as opposed to being stripped off of glass slides, so some workers feel that the films are cleaner and that the technique is easier than

Formvar slide-stripping. The films are suitable for supporting particulates or for coating large mesh or slot grids to be used for plastic sections. The films are relatively stable under the electron beam and of high electron transparency.

2. Materials Needed

- 2% collodion (nitrocellulose) in amyl acetate purchased from an EM supply house
- 30-ml beaker
- Staining dish containing distilled water
- Glass microscope slides
- Clean grids (see Formvar instructions for cleaning procedure)
- Pasteur pipets

3. Procedure

1. Fill a 30-ml beaker to a depth of 3–4 cm with 1% collodion solution.
2. Dip several clean microscope slides into collodion solution, drain the slides, and stand on end to air-dry.
3. Use a Pasteur pipet to drop two or three droplets of the collodion solution onto the distilled water surface in the staining dish.
4. After 2–5 min, the amyl acetate will have evaporated, leaving a silver to gold film of collodion covering the entire surface of the staining dish. The color can be seen clearly only under diffuse (fluorescent) light.
5. Pick minimally wrinkled areas of the film that exhibit the color representing the thickness desired and place clean grids shiny-side down on these areas (Fig. 157A).
6. Push a piece of card stock or one of the slides previously coated with collodion down onto the surface of the grids, submerging the film and grids beneath the water surface (Fig. 157B and C). While holding the slide that is keeping the film and grids under the surface of the water with one

Figure 157. Film casting and grid retrieval as used with the droplet method (Parlodion). (A) The film created by dropping Parlodion solution on the surface of water in a slide-staining dish is wrinkled and variable in interference color. Note the grids placed on a relatively wrinkle-free area.

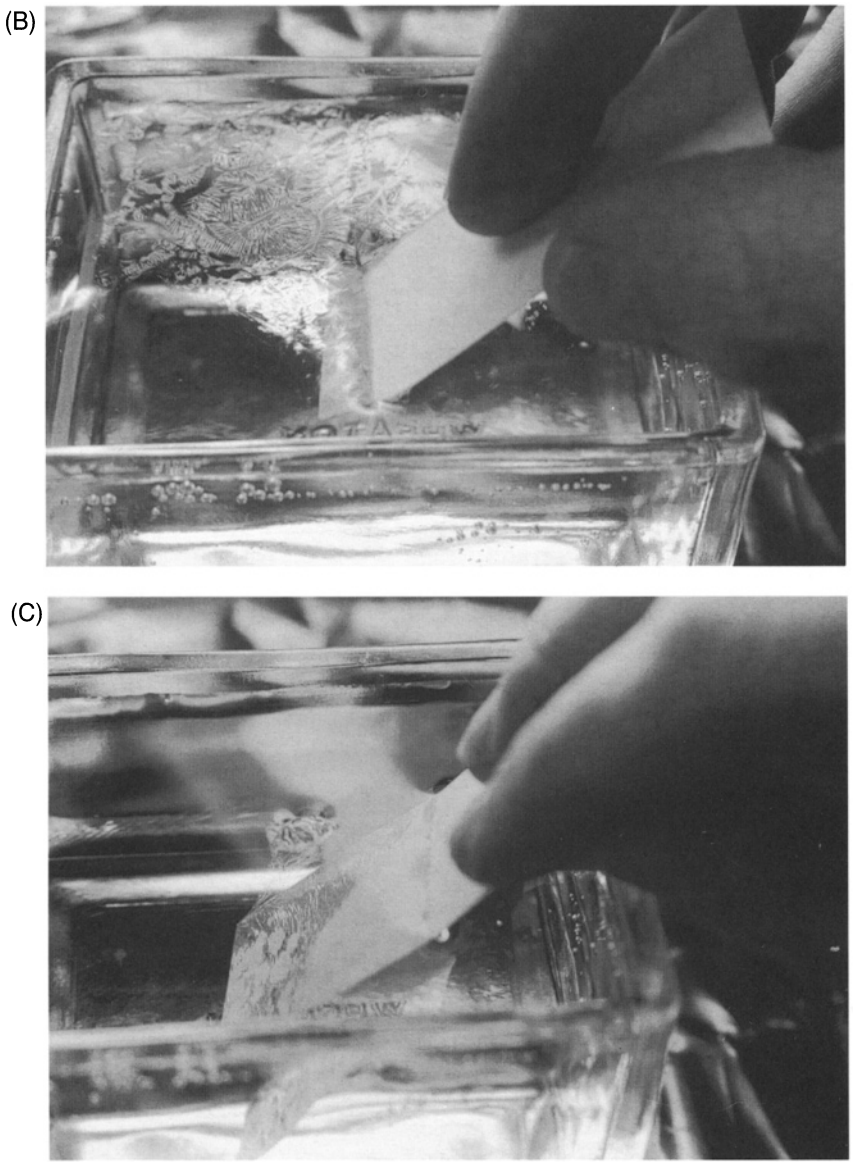

Figure 157. (B) A piece of card stock is being pushed down into the film over the grids seen in the previous figure. (C) The card stock with grids held down by the Parlodion film has been turned over in the water bath.

hand, take some forceps with the other hand and carefully tease most of the rest of the collodion film away from the microscope slide. Then, when the slide is removed from the water bath, it does not become coated with the excess film.

7. Quickly sweep the slide out of the water bath while turning it over such that the side of the slide or card with the coated grids emerges from the water first.
8. Blot the slide or card edges with a paper towel to remove the bulk of the adherent water.
9. Store the slide grid-side up in a Petri dish with the lid propped slightly open with a piece of filter paper until the slide is dry, usually overnight.
10. Coat the grids with carbon if extra beam stability is desired.

4. Results Expected

The collodion-coated grids should have the same characteristics as Formvar-coated grids, though some workers feel that they are not quite as beam stable. The coated grids can be stored for months before use, if kept in a dust-free chamber (a Petri dish).

5. Cautionary Statements

Most of the cautionary statements for the Formvar procedure apply here. Amyl acetate has a high vapor pressure and should be handled under a fume hood. The thickness of the film can be varied depending on the number of drops of the 2% collodion solution added to the water surface in the staining dish. After the proper number of drops for the film thickness desired has been decided on, make sure that they are added quickly to the water surface.

Making Carbon Support Films

1. Applications and Objectives

Support films made solely from carbon, as opposed to carbon-coated plastic films, are generally prepared for microanalytical purposes, since plastic films usually contain various impurities that can deliver spurious signals during energy dispersive spectroscopy. They are also indicated for high-resolution electron microscopy using support films, because they compromise image quality less than polymer films. Hayat and Miller (1990) discuss several different methods for producing carbon films.

Carbon films are highly thermally stable, highly conductive, electron-transparent, and capable of supporting particulates or sections borne on large mesh, hole, or slot grids.

2. Materials Needed

- Vacuum evaporator
- Carbon rods
- Mica sheets
- Clean copper grids
- Staining dish with distilled water
- Movable stainless steel support grid for grids
- Whatman™ #1 filter paper disks
- Dried 3 × 5 in. (7.6 × 12.7 cm) card stock
- Single-edge razor blades

3. Procedure

1. Split a piece of mica to produce a fresh, clean surface.
2. Load the mica into a vacuum evaporator along with a small piece of predried card stock used to monitor carbon coat thickness (see instructions for carbon evaporation).
3. Prepare a grid-coating device (Fig. 158) by filling a staining dish with distilled water, placing a piece of filter paper on the stainless steel support grid, and slowly lowering it into the distilled water until the filter paper is wetted. Alternatively, the grids can be placed directly on the support grid.
4. Bring the filter paper back up to the surface of the water in the staining dish, and carefully load the precleaned grids (see Formvar film-coating section for grid cleaning procedure) shiny-side up onto the filter paper. Touch the shiny side of the grid to the water surface, then turn the grid over, and place it on the slightly submerged filter paper.

5. Slowly lower the grid support assembly so that the grids are at the bottom of the staining dish. If the filter paper or grids start to float, use a pair of clean forceps to push them down on the stainless steel support grid.
6. Gently introduce carbon-coated mica into the staining dish at an angle of approximately 45° so that the carbon film floats off of the mica.
7. Once the carbon film is detached from the mica, remove the mica from the staining dish.
8. Slowly raise the grid support assembly until the grids contact the floating carbon film. If necessary, align the carbon film with the grids by gently touching it with clean forcep tips and moving it into the desired position.
9. After the grids have contacted the carbon film, very slowly raise the support assembly with grids and carbon film from the surface of the water.
10. Allow to air-dry for 15 min. Then, transfer the filter paper supporting the grids coated with carbon to a Petri dish containing two dry pieces of filter paper. Prop the Petri dish lid open slightly with a folded piece of filter paper.
11. After 1 hr, remove the single filter paper supporting the grids and carbon film to an empty Petri dish, prop the lid open slightly with the folded piece of filter paper, and leave at room temperature. The grids should be dry and ready to use the next day.

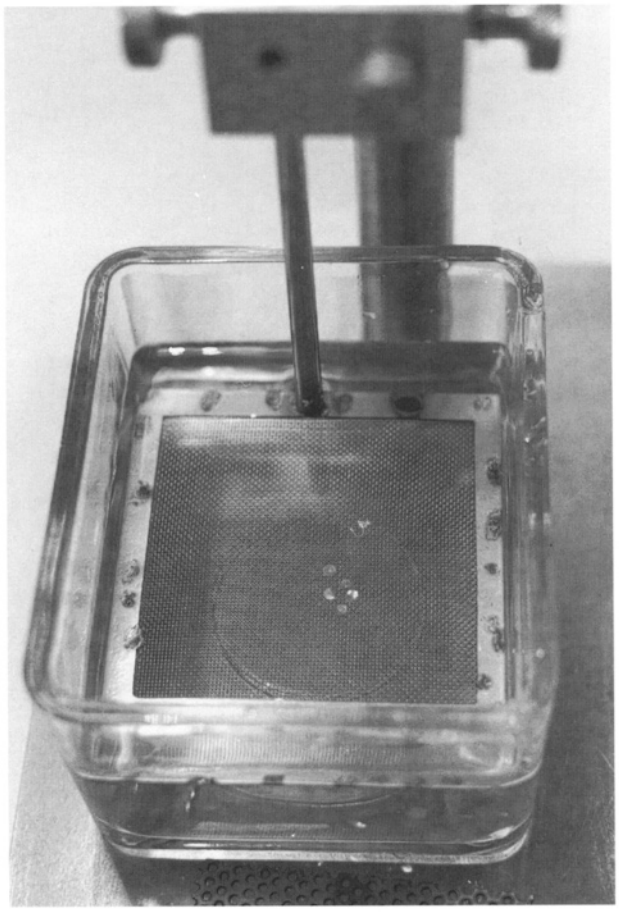

Figure 158. Grid-coating device for carbon-coating grids.

4. Results Expected

The carbon-coated grids should be essentially contaminant-free, stable under the electron beam, and very electron-transparent.

5. Cautionary Statements

Carbon films are much more brittle than those made from plastic resins. Grids should be handled carefully, since bending them will readily fracture the carbon coating. Some workers precoat the grids with dilute adhesive to bind the carbon film more securely to the grids (see Hayat and Miller, 1990).

Reference

Hayat, M.A., and Miller, S.E. 1990. *Negative staining*. McGraw-Hill, New York.

8

Replicas, Shadowing, and Negative Staining

Contrast in transmission electron microscopic (TEM) specimens occurs when there are specimen areas that stop (scatter) electrons and also areas that let most of the electrons pass through. Thus, the image results from subtractive contrast. We impregnate tissues and sections with a variety of heavy metals to scatter electrons as discussed in Chapter 4, but we can also surround particulates with heavy metals (negative staining) or cover particulates, cells, and tissues with thin metal films that have areas of differential beam-stopping capability (replicas produced by shadowing). This chapter will discuss these two added techniques for building subtractive contrast, pointing out the commonly used techniques and a few remedies to specific problems that may be encountered.

I. SHADOW CASTING

Shadowing casting (shadowing) and making replicas both involve coating a specimen surface with metals. A shadowed preparation is one in which metals are evaporated at an angle to the specimen so that the metal is preferentially condensed on the high points of the sample surface toward the evaporated metal source (Fig. 159). If the specimen consists of a thin layer of particulates such as bacterial flagella, the specimen with its overlying shadow of metal may be viewed *in toto*. However, if the specimen is a relatively thick sample (e.g., a layer of mammalian cells), a conventional electron microscope beam would have difficulty penetrating both the thin film of evaporated metal and the biological material beneath. In this case, after the tissue is shadowed, all

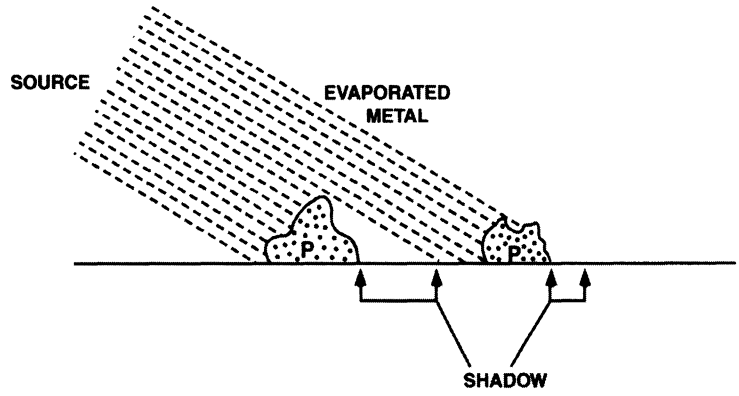

Figure 159. Diagram of a sample of particulates (P), showing the deposition of metal on the electrode side of raised portions of the sample, producing a shadow.

biological materials are removed by digestion with acids (concentrated HCl or H_2SO_4) and/or bases (sodium hypochlorite such as Clorox®). The remaining film is then rinsed thoroughly, picked up on a grid, and dried. The metal film is a replica of the original sample surface that can be penetrated by the electron beam and viewed with the TEM.

Shadowing may be used to develop contrast in specimens of low topography (DNA, RNA, flagella, bacterial pili) or specimens of relatively high topography (freeze-fracture preparations or cellular organelles such as whole Golgi bodies). The ultimate resolution is typically limited by the grain structure characteristic of the metal(s) employed in the shadowing process, even though other factors are capable of decreasing resolution, as discussed below.

A. Mechanism

The principle behind shadowing is that if a metal is heated to its boiling point in a chamber held at 1.3×10^{-2} Pa (10^{-5} Torr) or less, the individual evaporated atoms of metal will have a fairly unimpeded path through the chamber until they encounter the specimen and other surfaces such as the bell jar surface and electrode assemblies. When the metal atoms strike the specimen surface, they will condense, since the specimen temperature is lower than that of the recently evaporated atoms. At a vacuum of 1.3×10^{-3} Pa, the mean free path of an evaporated metal atom is about 6.8 cm (Stuart, 1983). In basic terms, this means that an atom of metal leaving the heated electrode surface will, on average, travel 6.8 cm before colliding with any residual gas molecules. Stuart states that "our calculations have included mere elbow brushes and bumps between molecules as collisions" meaning that the mean free path is actually considerably greater than that stated above. Electrodes are usually placed within 8–10 cm of the specimen being shadowed. Hence, the evaporated metal atoms that leave the filament in a trajectory toward the specimen (since metal atoms evaporate from all around the filament, and many are not aimed in the direction of the specimen) should arrive and condense onto the specimen surface without any serious deflection from their path caused by gas molecules within the chamber.

B. Metals Used

A number of different metals are used to shadow specimens and to make replicas. The metals are chosen on the basis of ease of evaporation, fineness of grains produced on the specimen, and alloying properties with each other as they condense on specimen surfaces. Some of the characteristics of the metals most commonly employed are listed in Table 15.

Table 15. Metals Commonly Used for Shadowing

Element	Atomic Number	Atomic Weight	Melting Point (°C)	Boiling Point (°C)
Chromium (Cr)	24	52	1,857	2,672
Gold (Au)	79	197	1,065	2,700
Palladium (Pd)	46	106	1,555	3,167
Platinum (Pt)	78	195	1,774	3,827
Tantalum (Ta)	73	181	2,996	5,429
Tungsten (W)	74	184	3,410	5,900

C. Vacuum Evaporators

Shadowing is performed with vacuum evaporators, which provide the high vacuum (1.3×10^{-2} to 1.3×10^{-3} Pa) necessary to ensure a largely unimpeded path between the metal source and the specimen surface. The typical apparatus consists of a bell jar, which is ultimately evacuated by a diffusion pump (with or without a cold trap), backed by a rotary pump. Thermocouple or Pirani gauges monitor low vacuum, while a discharge gauge is used once high vacuum is reached. The vacuum chamber contains a number of terminals to which electrodes can be attached, as well as low-voltage terminals to which devices for rotating and tilting specimens can be connected. Some vacuum evaporators are also equipped with a glow-discharge unit, which is used to increase the hydrophilicity of film-coated grids. See Hayat and Miller (1990) for construction details for a simple bench-top glow-discharge unit.

Evaporators may contain three types of evaporative sources. The simplest consists of two electrically isolated terminal posts between which metal wire or metal foil boats can be connected and heated (Fig. 160). A second type of source has terminals that hold carbon rods. One of the carbon rods is driven by spring pressure toward the other to keep the two carbon rods in intimate contact as they evaporate (Fig. 161). Metal wire can be wrapped around the reduced-diameter carbon rod for evaporation (Fig. 162). The final source type (electron beam gun) contains a coil of tungsten in close proximity to a carbon rod with a hollowed-out tip within which is fused a metal pellet (Fig. 163).

Some evaporators are equipped with crystal film monitors used to determine the precise thickness of metal and/or carbon films evaporated onto specimens. These devices consist of a quartz crystal, which oscillates at a specific frequency when supplied with electrical current. As films are deposited on its surface, the frequency of the crystal vibration changes. The frequency of vibration is monitored with an electronic sensing circuit so that evaporation can be halted when the film being deposited is thick enough.

If a crystal film monitor is not available, a small piece of predried $3 \times 5''$ card stock can be put into the vacuum chamber along with the specimen. After a typical evaporation run, the card should appear light brown from the evaporated material. After the actual specimen is examined, future evaporation runs can be matched to the previously successful conditions that produced the card color.

Caution should be exercised with all vacuum equipment to avoid backstreaming. If excessive roughing of a bell jar takes place, there is some danger that oil from the rotary pump will backstream into the chamber, potentially coating the specimen surface and preventing the evaporated metal from adhering to the specimen. The diffusion pump can also produce an oil film on a specimen surface if not backed adequately or cooled properly.

An oil film is used to monitor film deposition in some laboratories. A droplet of diffusion oil is placed on a small cleaned porcelain crucible top near the specimen to be shadowed. As the metal and/or carbon is evaporated, the cap surface becomes darkened, except where the droplet of oil is located. Some vacuum evaporator manufacturers do not recommend this practice because of the chance that the oil may become vaporized by the vacuum developed in the system, thereby contaminating specimen and bell jar surfaces.

D. Electrodes

Electrothermal heating is produced when a current is passed through electrodes composed of a resistant material (carbon rods, tungsten wire, molybdenum boats). If the current is sufficiently high (20–50 A), the resistant material will become hot enough to evaporate.

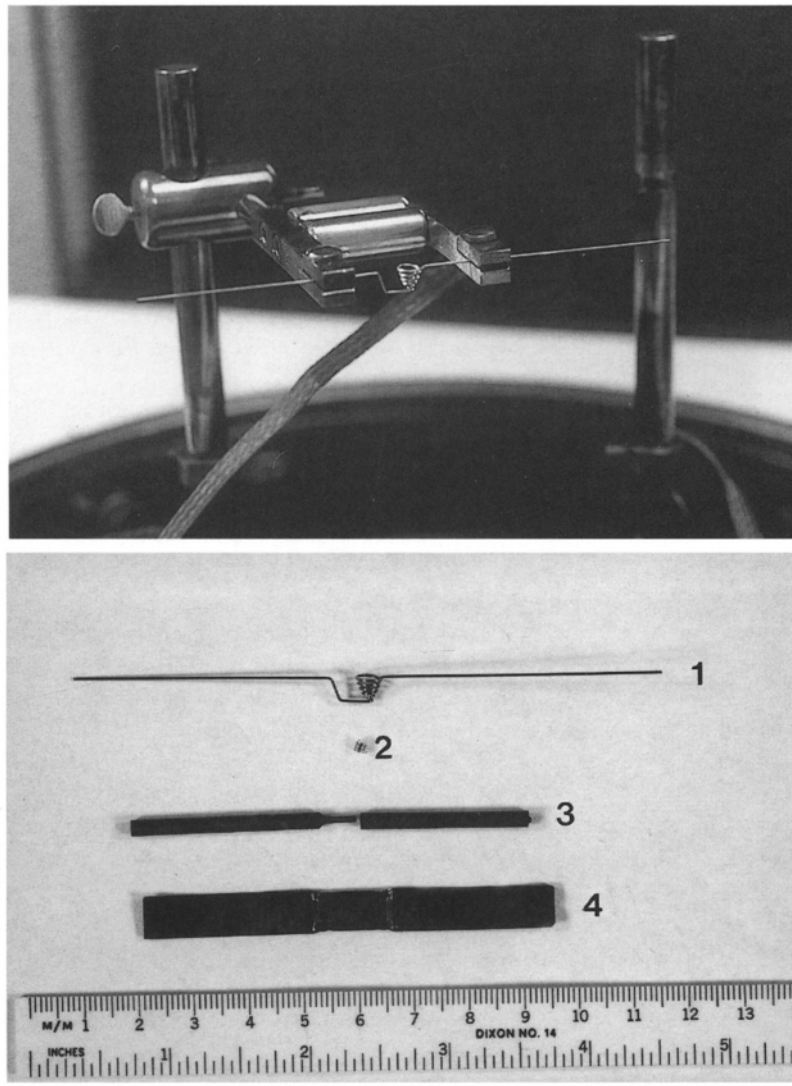

Figure 160. Types of electrodes. Top: Wire/boat-holding electrodes. Bottom: Examples of evaporator supplies: 1: tungsten wire basket; 2: coil of platinum wire to be evaporated; 3: carbon rods prepared for evaporation; 4: molybdenum boat for cleaning apertures.

For carbon evaporation, one of the rods (the nondriven rod) is left flat, but polished with 400–600 grit emery paper followed by further polishing on a piece of card stock until it has a mirror-like surface. The driven rod is polished in the same way and then sharpened to a point or the tip is reduced to a smaller diameter (Fig. 161). The decreased diameter produces increased resistance to current flow, yielding increased heating and evaporation in the tip area. The length of the reduced diameter tip can be adjusted to determine the amount of carbon to be evaporated. If metal wires such as platinum are to be evaporated simultaneously with the carbon, they are wound tightly around the tip of the driven rod (Fig. 162), heated gently once a good vacuum has been achieved so that they fuse with the carbon rod, and then heated more vigorously to evaporate them. If they are heated too rapidly, the wire will suddenly melt and drop off the rod before it evaporates significantly.

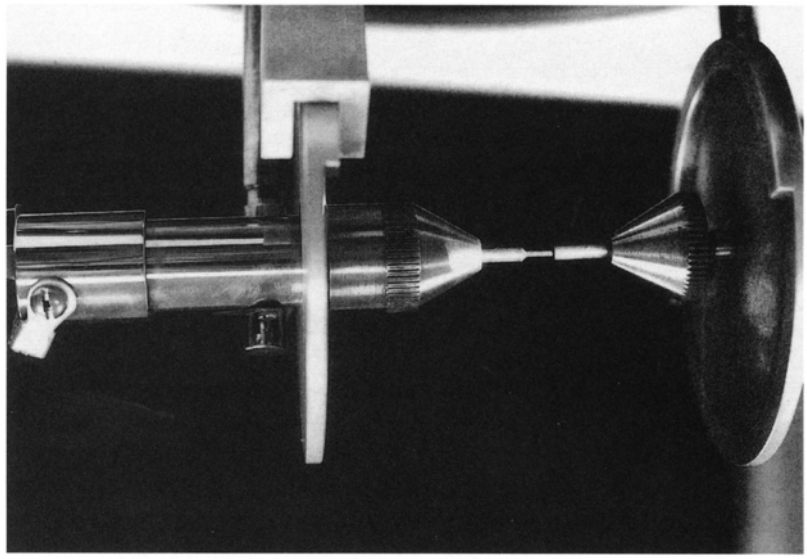

Figure 161. Carbon rods prepared for evaporation.

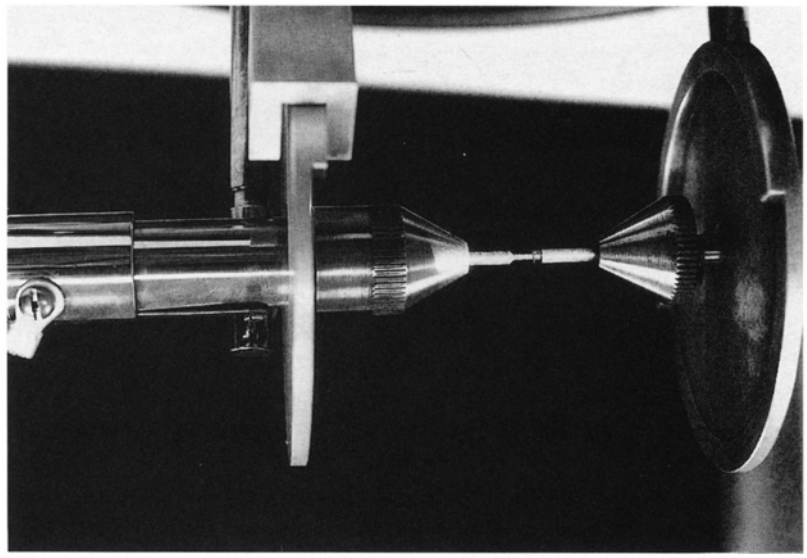

Figure 162. Carbon rod electrodes. The attachment of the platinum wire coil for evaporation is shown.

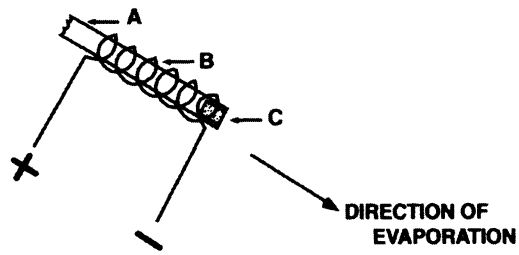

Figure 163. Electron beam gun minus shields, aperture, and power supply. The carbon rod (A) has a hole drilled into its end into which a platinum pellet (C) is fused. The rod is surrounded by a tungsten coil (B) that is heated by an electrical current to produce simultaneous evaporation of the tip of the carbon rod and platinum pellet.

Wire electrodes are typically made from tungsten, which is either coiled into baskets (Fig. 160) or bent in the middle. The coiled area or the bend in the wire is the point of highest resistance. Metals with boiling points below that of tungsten are placed in the basket (wires should be balled up first) or wrapped around the bend in the filament. When a high vacuum has been reached, the filament current is increased slowly until the noble metal alloys with the filament. Then, the filament temperature is gradually increased until evidence of evaporation is noted as darkening of the card stock or activity of the crystal film monitor. When all the noble metal is evaporated, the current is turned off to the electrode. Unless the original source was a carbon/platinum mixture, it is customary to follow the metal evaporation with a coat of evaporated carbon to give greater stability to the metal film.

Metal boats are usually used to clean apertures from the electron microscope. The apertures are placed within the molybdenum boat, a high vacuum is achieved, and then a current is applied to the electrodes holding the boat until the apertures glow red. After about 1 min, the current to the electrodes is shut off, the apertures are allowed to cool, and then they are removed from the vacuum evaporator. Do not vent the bell jar when the apertures are still glowing, because there will be a risk of oxidation and contamination.

Electron beam heating employs a source where the metal to be evaporated (usually platinum) comes in the form of a small pellet, which is placed in the hollowed-out tip of a carbon rod. The rod is heated under vacuum until the pellet fuses with the carbon. To evaporate both carbon and platinum onto the specimen surface, a heated coil of tungsten (the cathode) emits electrons, which bombard the anode (the carbon rod containing the metal pellet). The kinetic energy of the electrons elevates the anode temperature, causing evaporation of the rod tip (carbon and metal). The rod itself is not subject to current flow as is found with electrothermal heating of filaments described above. The advantage of electron beam guns is that 10–15 evaporative runs can be made without having to replace the carbon rod/pellet source, while the typical tungsten basket containing metal to be evaporated or the carbon rods driven into each other have to be replaced after every run.

E. Factors Leading to Fine Grains of Shadowed Metal

The evaporative process results in metal deposition (condensation on any relatively cooler surface) followed by nucleation (accumulation of metal atoms around previously deposited metal atoms). There are several factors that must be considered to maintain the finest grain size and, thus, the highest resolution.

Low total metal deposition will produce a finer grain because the nucleation process will be minimized. Thus, only the minimal amount of metal necessary to produce the image quality desired should be evaporated.

If the current is raised quickly, larger groups of metal atoms can be released from the filament at a time. However, if the current is increased too quickly, the metal to be evaporated will fall off the electrode filament without actually evaporating. Thus, more gradual deposition is achieved by raising the current slowly to just above the point where evaporation begins, and a finer grain size will result.

A cooler substrate (specimen) temperature will result in quicker condensation of the evaporated metal. In some instances, the stage surface upon which the specimen is placed may be cooled with water to increase the rate of condensation.

Metals evaporated at a steep angle (normal to the specimen surface) will produce finer grains than those evaporated at a shallow angle. Of course, a steep angle would also produce negligible shadow, the point of the exercise. Shadowing at a more oblique angle will cause greater nucleation.

Finally, simultaneous evaporation of two metals (or carbon and a metal) will reduce the metal aggregate size by increasing the distance over which an atom must move in order to find a place within the crystal lattice formed.

F. Shadowing Techniques

Shadowing may be directional or rotary, high angle or low angle. If the specimen has a relatively high topography, as with a fractured surface or whole cells, it is customary to use a relatively steep angle (45°) with a stationary specimen. This results in a reasonable amount of metal deposited on surfaces projecting above the specimen support and facing the electrodes. If, however, the specimen has little height or topography, as is typical for DNA or protein molecules, and shadowing is used to produce more specimen bulk for visualization, rotary shadowing at a low angle (10°) is employed. With DNA preparations, the relaxed and spread DNA is put onto grids, which are then attached to a platform turned rapidly by an electric motor while metal is evaporated onto the surface at a low angle.

G. Sputter Coating

The most widely used sputter coaters utilize a mechanical pump to achieve relatively low vacuum (1.3 Pa). These units produce metal films of a greater grain size than those produced by evaporative coaters but do not produce objectionable coating grain at magnifications below 50,000×. With the development of high-resolution SEMs, chromium sputter coaters utilizing turbomolecular-pumped vacuum systems capable of higher vacuum (10^{-2} Pa) came into use. These typically utilize fine-grain chromium and produce a grain size that does not interfere with the resolving capabilities of the high-resolution SEMs. Since chromium can oxidize, unlike the noble metals used for conventional sputter coating, coated samples suffer from a reduced shelf life.

Conventional sputter coaters were developed primarily to coat specimens for relatively low-resolution SEM work. They do not need a high vacuum to operate (a rotary pump producing 1.3 Pa is adequate) because they do not need to provide a long mean free path for metal atoms as is necessary for vacuum evaporation. A sputter coater (Fig. 164) consists of a vacuum chamber containing a noble metal-plated cathode and an anode upon which the specimens are placed. A permanent magnet is situated in the center of the cathode to deflect electrons from the specimen surface (to avoid heating the specimen). After vacuum is achieved, a high voltage field is produced between the cathode and anode surfaces. Then, an inert gas (argon) is admitted to the chamber, allowing current flow between the cathode and anode. The electron flow ionizes the argon gas. Argon ions are accelerated by the electrical field toward the cathode. As they strike the cathode at high speed, the argon ions dislodge metal atoms (e.g., gold/palladium), which then condense on surfaces inside the vacuum chamber, including the specimens. All of this activity takes place below the boiling point of the metals used. Thus, unlike vacuum evaporators, the metal being deposited has little heat to transfer to the specimen surface, since the metal has not been heated to

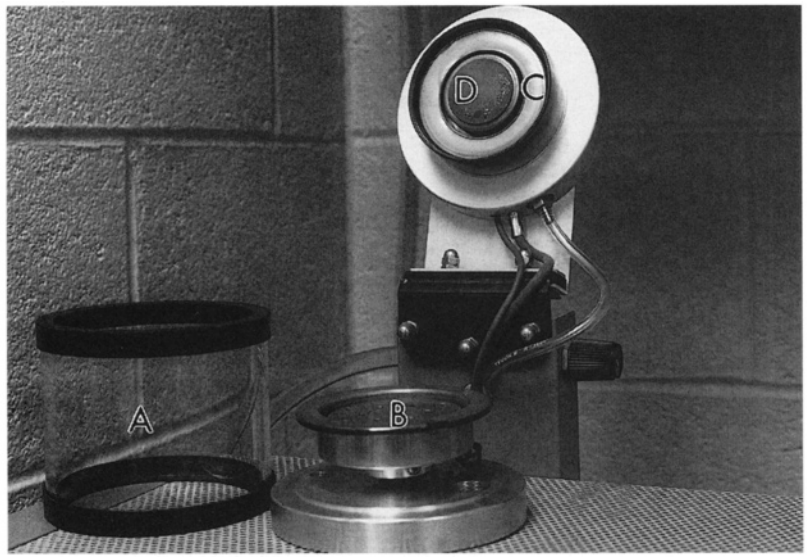

Figure 164. Sputter coater (Hummer VI from Anatech) showing the bell jar (A); specimen stage (B), which is the anode; the gold–palladium ring (target) serving as the cathode (C); and the permanent magnet (D) in the center of the cathode.

its boiling point, so there is little chance of thermal damage to the specimen. Sputter coating at a relatively low vacuum also results in numerous collisions between metal atoms, argon ions, and electrons, so a visible discharge cloud arises. All of these collisions result in a nondirectional metal coating that will evenly coat very irregular surfaces, resulting in no shadows as produced with vacuum evaporators, even though the specimen is neither rotated nor tilted during the coating process.

To further reduce the possibility of charging in sputter-coated biological samples, the samples can be put in racks tilting them 45° while sputtered for $^1/_2$ the normal time. They are then tilted in the opposite direction for a second sputter-coating for $^1/_2$ the normal time. This produces a more even, complete metal coating (Dr. John Mackenzie, personal communication).

II. NEGATIVE STAINING

Farrant (1954) introduced negative staining as a method to visualize ferritin particles. Since then, it has been utilized to visualize macromolecules (milk proteins, enzymes, hemoglobin), surface components of cells (bacterial pili, flagella, protozoan scales), internal cellular organelles (Golgi bodies, nuclear pores, mitochondrial membranes, microtubules, microfilaments), and viruses.

A. Mechanism

Suspensions of the structures to be visualized are supported on a film-coated grid and surrounded by a solution of heavy metal stain that covers the grid surface and is mostly excluded by the biological material because of surface-tension interactions. Thus, the bulk of the grid surface is covered with heavy metal that blocks some of the electron beam. The specimen, which has excluded most of the stain but has had stain penetration of open irregularities in the particle surface, allows more of the beam to pass through. This procedure produces contrast between the specimen and the background, and also dehydrates the specimen. After a specimen is negatively

stained, it should be examined within a day or so because the preparations do not keep indefinitely. Viral capsomeres that are clearly defined shortly after negative staining with phosphotungstic acid (PTA) will usually be indecipherable 1–2 days later.

The negative staining process is inexact and not reproducible in the normal sense of the word. Two grids prepared at exactly the same time in the same fashion often have dissimilar stain distributions. Adjacent grid squares on the same grid will often have different stain-spreading characteristics. With a typical viral preparation, some of the particles will exclude the stain, which will form a slightly gray background right up to the edge of the viral particle. Other particles will exclude the stain but will have large amounts of stain pooled next to the particle, resulting in a completely electron-opaque zone around the particle. Some of the particles, usually described as defective, will exhibit leakage, with stain inside the particles making them electron dense. Some areas of the grid may appear to be unstained, with no gray or black stain background and no visible particles, while an occasional grid square will contain such a deep layer of negative stain that the grid square is impenetrable to the electron beam. All of these situations can be encountered on one grid, which is why workers attempting to do quantitative virology or any study involving counting structures per unit area would be best advised to use another technique for their studies, although the technique does have some supporters (Miller, 1982).

Some staining solutions cause shrinkage, some structures are best fixed first, and some specimens are fragile at certain pH ranges. Hayat and Miller (1990) provide lengthy discussions of artifacts produced during negative staining along with information about other aspects of negative staining.

B. Methods

1. Nebulizers

Horne (1965) introduced a technique using a nebulizer to spray a mist of suspended viral particles onto film-coated grids that were subsequently negatively stained. This procedure has always been discouraged in our laboratory because an aerosol of viruses could have serious repercussions. Many viruses remain viable after drying, exposure to negative stains, and, in some cases, fixation with aldehydes. Even viruses that have no demonstrated human pathogenicity should be handled carefully, since they may cause respiratory problems or replicate in humans without necessarily producing overt disease (Hayat and Miller, 1990).

2. Droplet Method

A droplet of the suspension to be examined is placed on a film-coated grid held in forceps lying on a Petri dish lid under an appropriate hood. After 4–5 min, during which the particulates attach to the film (primarily by electrostatic forces), the grid is wicked almost to dryness with a fresh sheet of Whatman™ #1 filter paper, which should be disposed of in the autoclave waste container (as are all waste materials generated by this procedure). Do not let the grid completely dry, or crystals of precipitated media or buffer salts may form on the grid surface. Immediately add one drop of the negative stain solution to the surface of the grid. Any remaining salts from the media or buffer will be sufficiently diluted by the negative stain that they will not precipitate when the grid is subsequently dried. After 30 sec, wick the grid completely dry with a fresh piece of filter paper. Gently blot the surface of the grid with the filter paper, and place the grid on a dry piece of filter paper in a Petri dish until it can be examined.

If a brief distilled water rinse is utilized after negative staining, very light staining with excellent resolution can be achieved in some cases. However, this procedure may produce grids with too little contrast to be of any use.

Rather than placing particle suspensions onto grids held in forceps, some workers place the suspensions and the negative stain drops on Parafilm™ and then float grids with coated surfaces down on the droplets. Some workers leave suspensions on grids for 30 min, but this does not appear to increase particulate attachment to the grid surface appreciably. In some instances, particulate suspensions and negative stain are mixed together and brought into contact with a film-coated grid for several minutes, and then the grids are blotted dry. Hayat and Miller (1990) suggest that a grid with adsorbed viral particles that could be pathogenic should be placed onto a drop of glutaraldehyde for 10 min to kill the viruses and reduce the danger of accidental infection. A thorough review of various methods for staining particulates with negative stains may be found in Hayat and Miller (1990).

3. Types of Negative Stains

Solutions of various heavy metals at different pHs have been used effectively to stain biological materials, but the four most commonly used are uranyl acetate, phosphotungstic acid, ammonium molybdate, and methylamine tungstate. Nermut (1982) discussed the advantages of various stains and the appropriate pH at which they should be used to accentuate features of enveloped versus nonenveloped viruses. He reported that acidic pH is best for membrane structures (like glycoprotein knobs or spikes associated with enveloped viruses such as coronaviruses), and an alkaline pH works well to demonstrate proteinaceous components (nucleocapsids). He also suggested that the grain size of the final dried stain should be considered, with phosphotungstic acid and ammonium molybdate having a fine grain size. Unfortunately, they also have less contrast than the more coarsely-grained uranyl acetate.

a. Uranyl Acetate

Uranyl acetate is used as a 0.2–4% aqueous solution with a pH of 4–5. Since a 4% solution is saturated, the stain should not be taken from the bottom of the container to avoid picking up crystals of uranyl acetate. The solution will keep for weeks at room temperature in a dark bottle. The stain is unstable above pH 6.0. Both negative and positive staining can be observed in the same material. Hayat and Miller (1990) suggest that 2% aqueous uranyl acetate is good for viral staining (30 sec to 2 min) because viral structure is stabilized, and grids can be observed months after preparation. They also suggest that a 1% aqueous solution is the preferred stain for visualizing macromolecules.

b. Phosphotungstic Acid (PTA)

PTA is customarily made by dissolving sodium phosphotungstate in distilled water and adjusting the pH to 7.0–7.2 with NaOH. The solution is stable for several years if stored at 4°C. At this pH, viral nucleocapsids are well defined. Hayat and Miller (1990) state that staining time over 30 sec will result in overstaining, but our laboratory has not noted any major differences in materials stained from 30 sec to 5 min. This is probably the most commonly used negative stain solution in the literature.

c. Ammonium Molybdate

A 3% solution of ammonium molybdate in distilled water will have an unadjusted pH of about 6.5. Ultrathin frozen sections stain well in about 30–60 sec (H. Sitte, personal communication). Large crystals can sometimes form through recrystallization caused by heating from the electron beam.

d. Methylamine Tungstate

Methylamine tungstate was first used by Faberge and Oliver (1974) as a negative stain. Stoops *et al.* (1991) employed this stain to visualize human α_2-macroglobulin. It is complicated to formulate (see Hayat and Miller, 1990) but can be used over a broad pH range and can be mixed with PTA. It is customarily prepared as a 2% aqueous solution at pH 6.5–8.

4. Wetting Agents

As mentioned previously, an unfortunate aspect of negative staining is that the stain does not spread evenly or even predictably in almost all cases. This is caused primarily by the hydrophobicity of the plastic film (Formvar, collodion) that serves as a specimen substrate. Some workers insist that grids should be used immediately after preparation; some say that they will only work well for a few weeks; some say carbon coating improves them; some say carbon coating makes them more hydrophobic; and some say they should be glow-discharged and used immediately to make them more hydrophilic or exposed to strong ultraviolet radiation (see Hayat and Miller, 1990 for further discussion). Our laboratory has not been able to demonstrate that carbon-coating improves specimen and stain spreading. Fresh films tend to wet better than films over a week old, but the difference between week-old and year-old coated grids seems negligible. The only guaranteed method for spreading the specimen and subsequent stain is to utilize a wetting agent such as the antibiotic bacitracin (500 μg/ml) or bovine serum albumin (0.01–0.02%). Bacitracin is a smaller molecule than BSA, so it usually gives less background.

Bacitracin (Gregory and Pirie, 1973) dissolved in distilled water (1,000 μg/ml) not only allows the stain to spread evenly on the film-coated grid surface, but also can reduce surface tension features associated with the specimen. Dykstra (1976) studied a protozoan with scales 4.0 nm × 4.0 μm, which coated the cell surface. When isolated, the scales rolled up tightly into tubes, and normal negative staining procedures did not relax the scales. If the scale suspension was mixed 1:1 with the bacitracin solution, and a film-coated grid was then suspended on the resulting droplet for 2 min and subsequently stained with 1% aqueous uranyl acetate, the scales flattened out and were easy to visualize.

REFERENCES

Dykstra, M.J. 1976. Wall and membrane biogenesis in the unusual labyrinthulid-like organism *Sorodiplophrys stercorea. Protoplasma* 87: 329.

Faberge, A.C., and Oliver, R.M. 1974. Methylamine tungstate, a new negative stain. *J. Microsc.* 20: 241.

Farrant, J.L. 1954. An electron microscopic study of ferritin. *Biochim. Biophys. Acta* 13: 569.

Gregory, D.W., and Pirie, J.S. 1973. Wetting agents for biological electron microscopy: I. General considerations and negative staining. *J. Microsc.* 99: 261.

Hayat, M.A., and Miller, S.E. 1990. *Negative staining*. McGraw-Hill, New York.

Horne, R.W. 1965. Negative staining methods. In: R.W. Kay (ed.), *Techniques for electron microscopy*, 2nd ed. Blackwell, Oxford.

Miller, M.F. 1982. Virus particle counting by electron microscopy. In: J.D. Griffith (ed.), *Electron microscopy in biology* (Vol. 2). John Wiley and Sons, New York.

Nermut, M.V. 1982. Advanced methods in electron microscopy of viruses. In: C.R. Howard (ed.), *New developments in practical virology*. Alan R. Liss, New York.

Stoops, J.K., Schroeter, J.P., Bretaudiere, J.-P., Olson, N.H., Baker, T.S., and Strickland, D.K. 1991. Structural studies of human α_2-macroblobulin: Concordance between projected views obtained by negative-stain and cryoelectron microscopy. *J. Struct. Biol.* 106: 172.

Stuart, R.V. 1983. *Vacuum technology, thin films, and sputtering. An introduction*. Academic Press, New York.

CHAPTER 8 TECHNIQUES

Vacuum Evaporation

Vacuum evaporators are used to coat substrates or specimens with carbon and/or metals and to produce pure carbon substrates for specimen support. The duration of evaporation, temperature of electrodes during evaporation (amperage used), angle of evaporation, vacuum at the time of evaporation, material being evaporated, and the temperature of the stage holding the specimen or support being coated are all factors for the end-product desired. As stated earlier, the shortest duration that delivers a usable coat, the lowest source (electrode) temperature that will cause evaporation, the largest angle between the source and substrate, the highest vacuum, the metal with the smallest grain structure, and a cooled stage will work together to produce the finest grain structure on the coated substrate.

However, since other factors must be considered, all of these conditions cannot always be met. When shadowing a substrate with topography (e.g., a freeze-fracture specimen), contrast is developed by the deposition of metal/carbon on one side of a particulate specimen, with a clear area behind the specimen that is not coated. This area is known as the shadow.

Taller objects (like protozoan cells) are typically shadowed from one direction with metal at an angle of 45°, followed by a stabilizing carbon coat from sources directly overhead. Alternatively, carbon and metal are deposited simultaneously at a 45° angle.

Specimens with little relief (nucleic acids, bacterial pili, viruses) are shadowed at a lower (10°) angle (Fig. 165A). If specimens are supported on a stage that is rotated rapidly during evaporation, the specimen is coated from all sides, producing very little shadow, but giving overall bulk to the sample (Fig. 165B).

Carbon is evaporated onto most metal coatings to provide further mechanical stability to the coat. It is also evaporated onto plastic film-coated grids to provide mechanical stability and electrical conductivity to decrease thermal drift when the electron beam interacts with the coated grid. The barest perceptible carbon coat is usually adequate for this purpose.

Finally, as already described in the section on film-coating grids, thicker carbon coats can be evaporated onto mica, which are then stripped from the mica substrate. The carbon film is then used to coat grids, ultimately serving as a support film for specimens.

A variety of metals requiring different evaporative temperatures can be used in shadowing. Those requiring higher evaporative temperatures have a finer grain structure. Using metal alloys or evaporating a metal and carbon at the same time produces finer-grain coatings, because nucleation of single metals takes place more rapidly than mixtures, resulting in larger deposited grains.

For freeze-fracturing and similar applications, the objective is to produce an electron-transparent replica of the specimen surface. The specimen is digested with acids or bases so that only the replicated surface of the specimen is examined with the electron microscope.

In the past, vacuum evaporators were used to coat SEM samples by attaching the samples to rotating, tilting stages during the coating process in an attempt to coat all the hills and valleys in typical SEM specimens with lots of topographic detail. With the advent of sputter coaters that have nondirectional metal deposition on sample surfaces, the vacuum evaporator has been retired from most SEM specimen preparations.

Shadow Casting

1. Applications and Objectives

Shadow casting metals onto specimens at high or low angles from a fixed direction is used to develop contrast in a specimen (tall or short, respectively) as a result of topographic differences in specimen details. Shadow casting of specimens on a rotating stage confers bulk to a sample with little topography. It is also possible to calculate the height of specimen structures by measuring shadow length and relating it to the angle of shadow.

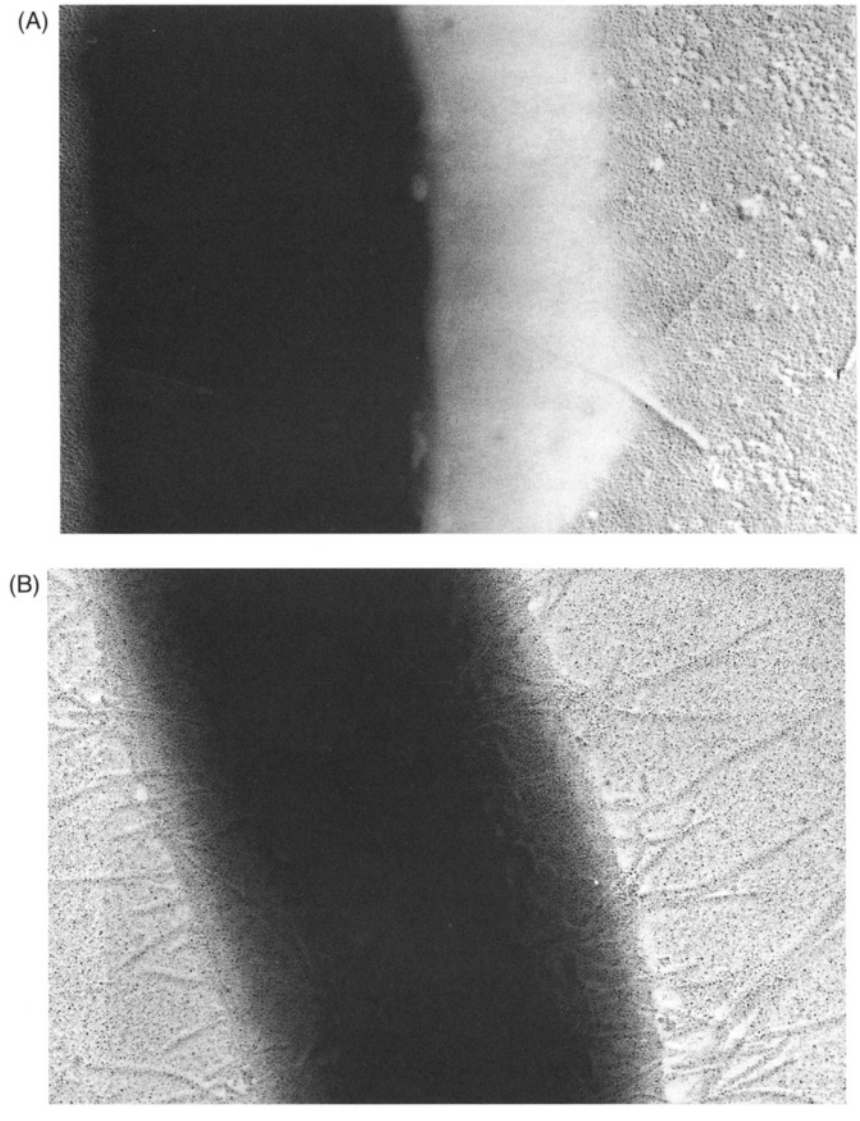

Figure 165. *Escherichia coli* coated with platinum–palladium. (A) Low-angle, fixed-direction coating. 51,474×. (B) Low-angle, rotary coating. 65,337×.

2. Materials Needed

- Vacuum evaporator
- Carbon electrodes
- Metal electrodes of choice
- Specimen (dried or, in the case of freeze-fracture, frozen)
- Grids
- Pieces of 3 × 5 in. (7.6 × 12.7 cm) card stock
- Carbon electrode sharpener
- 400-grit emery paper

3. Procedure

Carbon Electrode Preparation

1. Polish the ends of both carbon electrodes by first sanding them on a piece of 400-grit emery paper on a counter top and then polishing the sanded surface on a piece of cardboard or card stock until the sanded surface is shiny.
2. Use the electrode sharpener to sharpen the polished end of one electrode so that the final electrode has a reduced-diameter end about 5 mm long (Fig. 160).
3. Install the carbon rods with the sharpened rod in the driven electrode and the other attached to the fixed electrode. The rods should meet midway between the two electrodes, which are spread as far apart as possible. After the rods are installed, make sure that the driven electrode is free to travel when the carbon rods are evaporated.

Wire Evaporation (Platinum–Palladium)

1. Ball up 1.5 cm of platinum–palladium wire with a pair of coarse-tipped forceps.
2. Place the wire into a tungsten basket attached to a set of electrodes.
3. Load the specimen and place a small piece of 3×5 in. (7.6×12.7 cm) card stock for monitoring coating thickness near the specimen. The card should have been dried previously in a resin polymerizing oven so that no residual atomospheric moisture remains, which would slow down the pumping speed of the vacuum evaporator. Pump down the vacuum system as specified in the vacuum evaporator instructions.
4. Once the vacuum evaporator has reached high vacuum (1.3×10^{-2} Pa or better), slowly turn up the electrode current with the electrode rheostat until the wire in the basket melts. It is important to do this slowly enough so that the wire fuses with the tungsten basket. If the current is raised too quickly without careful visual monitoring, the noble metal wire can simply be cut by the heated tungsten and fall in large lumps to the vacuum chamber floor, producing no coating on the specimen. *Caution: Wear welder's goggles to prevent eye injury from the bright electrodes.*

Firing the Wire Electrodes

1. For a fixed-angle burn, once the platinum–palladium is welded to the tungsten basket, continue raising the electrode current slowly until the card stock begins to darken. When this is noted, do not increase the current any further. Observe the lumps of platinum–palladium welded to the basket. After they have evaporated, return the electrode rheostat to the off position.
2. For a rotary burn, the procedure is identical except that the rotary specimen holder should be turned on prior to the burn. The specimen should rotate at about 100 rpm.

Firing the Carbon Electrodes

1. Carbon rods are fired alone to coat polymer film-coated grids or to produce pure carbon films as specimen supports. They are also fired after the platinum–palladium has been evaporated onto a specimen surface to add electron-transparent physical support to the metal coat. To fire the electrodes, switch the electrode control to the set bearing the carbon rods, and slowly turn up the electrode rheostat until the pointed carbon rod begins to evaporate. Some sparking during this process is acceptable, but excessive sparks indicate that large chunks of the carbon rod are being discharged, which can result in debris on the specimen.
2. When coating a plastic support film or evaporating carbon onto a metal layer previously evaporated onto the specimen surface, a very thin carbon coat (light brown) is adequate. If coating a mica substrate to produce a carbon support film, a thicker (black) film is needed, so burn the electrodes until the sharpened tip has been consumed.

4. Results Expected

The evaporated metal coat from a fixed-direction shadowing run will have a fine grain and will produce a shadow where no metal has been deposited behind a specimen area with topography. A rotary coating run will produce a specimen with increased bulk but without much evident shadow. A carbon coating will not be noticeable under the electron beam, but will have contributed structural stability and electrical conductivity to the specimen.

5. Cautionary Statements

Always protect your eyes with welder's goggles during electrode firing, as the high-intensity light from the electrodes can damage the retina. The use of card stock to monitor coat thickness works well in the absence of an expensive crystal film monitor that can actually record the number of nanometers of film being deposited during electrode firing. Some workers use immersion oil or diffusion oil drops on a piece of broken white porcelain crucible lid to monitor film thickness. The vacuum may cause vaporization of the oil, however, coating surfaces within the vacuum chamber, including the specimen, and leading to problems for developing a good vacuum over time and to poor coating of the specimen surface. If oil is used, diffusion oil is preferred, because it is already part of the pumping system and has a lower vapor pressure than immersion oil.

DNA (Plasmid) Preparation for TEM[1]

1. Application and Objectives

This is a quick method for the preparation of purified short segments of nucleic acids (e.g., plasmids) for visualization in a transmission electron microscope. The technique confers sufficient bulk and contrast to isolated short pieces of nucleic acids for the purpose of measuring their length or assessing whether they are single-stranded or double-stranded utilizing a transmission electron microscope.

2. Materials Needed

- 1 mg/ml of cytochrome C (Sigma 7752, Type VI) in distilled water
- 0.25 M ammonium acetate in distilled water, pH 7.5
- Distilled water
- 50% ethanol
- 0.5–5.0 μg/ml of nucleic acid in distilled water
- Parafilm™
- Petri dishes
- Micropipets (2–10 μm and 10–100 μm adjustable) and tips
- 4% uranyl acetate stock (alcoholic or aqueous)
- 200-mesh Formvar-coated grids
- Vacuum evaporator with flat rotary stage
- Double-stick tape
- 1.5-cm platinum–palladium wire
- Microfuge tubes
- Shell vial or scintillation tube for mixing uranyl acetate
- Forceps
- Whatman™ No. 1 filter paper (9-cm disks)

[1] Special thanks are due to Chris Dykstra, College of Veterinary Medicine, Auburn University, for introducing us to this technique.

3. Procedure

1. Mix the following in a microfuge tube:
   - 40 μl of 0.25 M ammonium acetate, pH 7.5
   - 10 μl of 0.5–5.0 μg/ml of DNA in distilled water
2. Let the mixture sit for 1 min in the microfuge tube.
3. To the microfuge tube, add 1.0 μl of 1 mg/ml of cytochrome C (Sigma 7752, Type VI) in water. Invert the capped tube several times.
4. Place 51 μl of solution from microfuge tube onto Parafilm™ in a Petri dish, cover the dish, and wait for 1 min.
5. Touch the Formvar-coated side of a grid to the drop. More than one grid can be touched to the same drop.
6. Immediately stain in dilute uranyl acetate in 50% ethanol prepared by adding one drop of normal poststain stock to 20 ml of ethanol in a shell vial. Dip the grid into the shell vial of uranyl acetate in ethanol for 5 sec.
7. To destain the stained grid, dip the stained grid into 50% ethanol for 5 sec immediately after it is removed from the staining mixture.
8. Dry the destained grid quickly and completely with a piece of filter paper after destaining (see section in Chapter 4 on grid drying procedure).
9. After 15 min, stick the edge of the grid specimen-side up to a piece of double-stick tape previously applied to the surface of the horizontally rotating specimen support in the vacuum evaporator. Put the grid near the center of the rotating stage, and situate the center of the stage 1.5 cm below and 8 cm horizontally away from the platinum-palladium source. This gives a 10° shadowing angle.
10. Pump the vacuum evaporator chamber down to 1.33×10^{-3} Pa, and then fuse the platinum–palladium wire with the tungsten basket, as described in the instructions for shadowing.
11. Turn on the rotary stage and allow to rotate at 100 rpm.
12. Fire the platinum–palladium-coated tungsten basket, as described under shadowing, and remove the grid from the vacuum chamber.
13. Examine the coated nucleic acid with a TEM. The nucleic acids should be easily seen at a TEM screen magnification of 12,000× or above.

4. Results Expected

The nucleic acids should be well spread out on the surface of the coated grid and should have adequate bulk to be seen easily (Fig. 166). The metal coating should not be objectionably grainy.

5. Cautionary Statements

All cytochrome C is not the same. The cytochrome C is used to spread the nucleic acid over the drop to which the coated grid is touched. If the nucleic acid is not evenly spread over the grid surface, try another production batch of cytochrome C. Once a satisfactory stock of cytochrome C is demonstrated, it is good practice to make up aliquots of appropriate quantity in microfuge tubes and to store them frozen at −20 °C until needed.

Before proceeding with this method, review the instructions for shadowing and the specific instructions for your vacuum evaporator. Also, review the cautionary statements about uranyl acetate provided in the section on poststaining in Chapter 4.

Negative Staining

Before negative staining, particulate samples must generally be concentrated (see the sections on viral preparation and agar embedment of particulates for methods). The actual final concentration of specimens prepared for negative staining is often empirical, but some starting points are available. With bacteria, a faintly turbid suspension is desired. Harris and Horne (1991) suggest that 10^6 to 10^9 virions/ml will provide

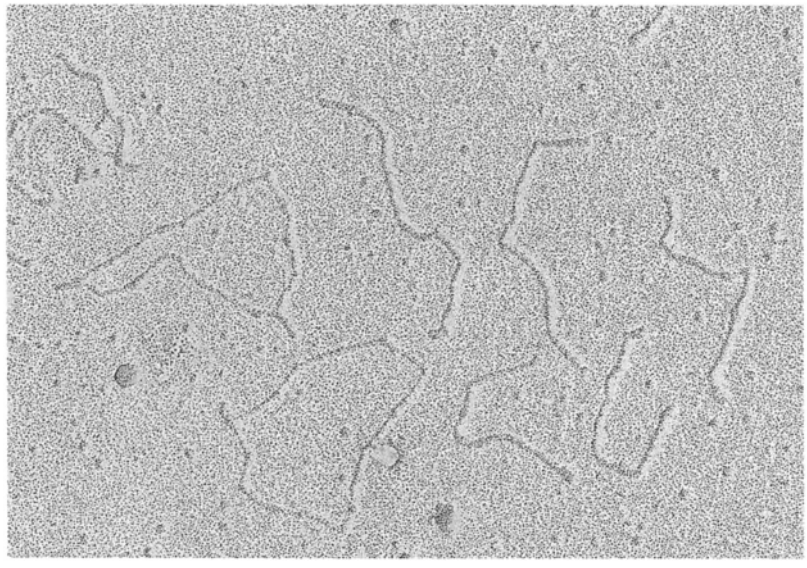

Figure 166. Plasmid DNA stained with uranyl acetate and shadowed with platinum–palladium. 68,654×.

a good preparation, while protein solutions should contain 0.1–0.2 mg/ml, lipid suspensions should be concentrated to 0.1–0.5 mg/ml, and cell membrane suspensions should contain 0.5–1.0 mg/ml.

Materials can be suspended in 5–10 mM saline or buffer, but should not be suspended in sucrose from sucrose gradients because it will interfere with negative staining.

Negative Staining with Phosphotungstic Acid

1. Applications and Objectives

Negative staining with slightly alkaline PTA is commonly used for many types of particulate samples. Nermut (1982) reports that this stain is most appropriate for the proteinaceous capsomeres of viruses, while uranyl acetate at acidic pH is superior for the membranous components and glycoprotein spikes associated with the surfaces of enveloped viruses.

The objective is to produce a finely electron-dense coating over the entire surface of a film-coated grid bearing particulate materials, with only slight stain pooling around the particulates, allowing easy visualization of surface structures of the particulate samples (viral capsomeres, bacterial pili or flagella, protozoan cell surface scales, etc.).

2. Materials Needed

- Sodium phosphotungstate
- 1 N NaOH
- 100-ml stock bottle
- Distilled water
- Pasteur pipets
- pH meter
- Formvar-coated grids
- Concentrated particulate sample suspended in a small volume of fluid
- Forceps
- Whatman™ No. 1 filter paper (9-cm disks)

(A)

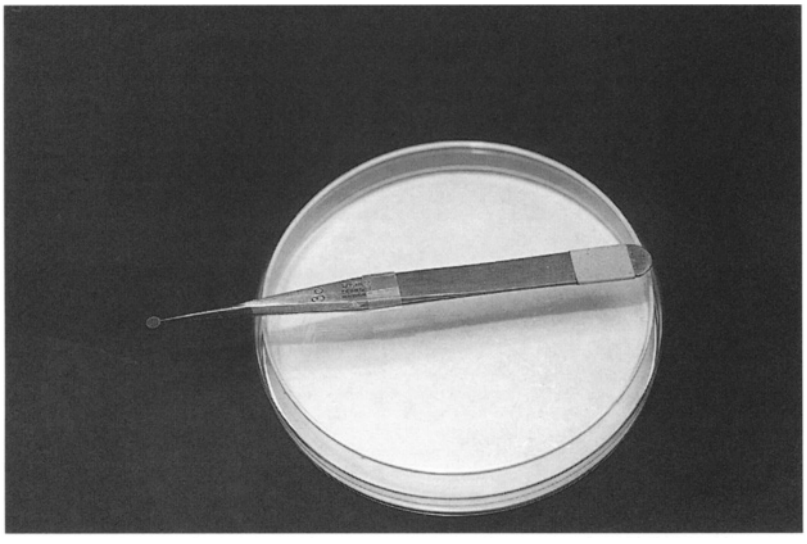

Figure 167. Negative stain procedure. (A) Forceps lying on a Petri dish lid with the grid held in jaws kept closed with forceps locking ring.

3. Procedure

Stain Preparation. Add 1 g of sodium phosphotungstate powder to 50 ml of distilled water in a 100-ml stock bottle. Check the PTA solution pH with the pH meter, and adjust the pH to 7.2–7.4 with the 0.1 N NaOH.

Staining Method

1. Pick up a Formvar-coated grid with forceps and push the forceps locking ring down so that the grid is held firmly. Lay the forceps down on the Petri dish lid with the tips extending over the edge with the grid held coated-side up (Fig. 167A).
2. Add one drop of concentrated particulate suspension to the grid with a Pasteur pipet (Fig. 167B). See the section on preparing viral samples for negative staining for preparation suggestions.
3. After 3–5 min, remove the suspension by touching the ragged, torn edge of filter paper to the edge of the forceps jaws where they contact the grid (Fig. 167C) until the grid surface is nearly dry. Never let the grid surface totally dry out because it will produce a coating of culture or sample materials and yield an excessively dirty grid.
4. Add one drop of 2% PTA to the grid.
5. After 1 min, dry the grid as before with the ragged torn edge of filter paper, except, this time, dry the grid quickly and completely. Immediately touch the sample side of the grid to a clean piece of filter paper in the bottom of a Petri dish. Slide a fresh piece of filter paper down between the forceps jaws to push the dried grid out of the forceps tips and onto a clean, dry part of the filter paper in the Petri dish.
6. Let the grid dry for 15 min in the Petri dish (covered) and then examine with the TEM.

4. Results Expected

The grid will have a finely granular electron density over the entire surface, with slightly darker regions surrounding the particulate sample, but the stain will be generally excluded from intact particulate materials (Fig. 168).

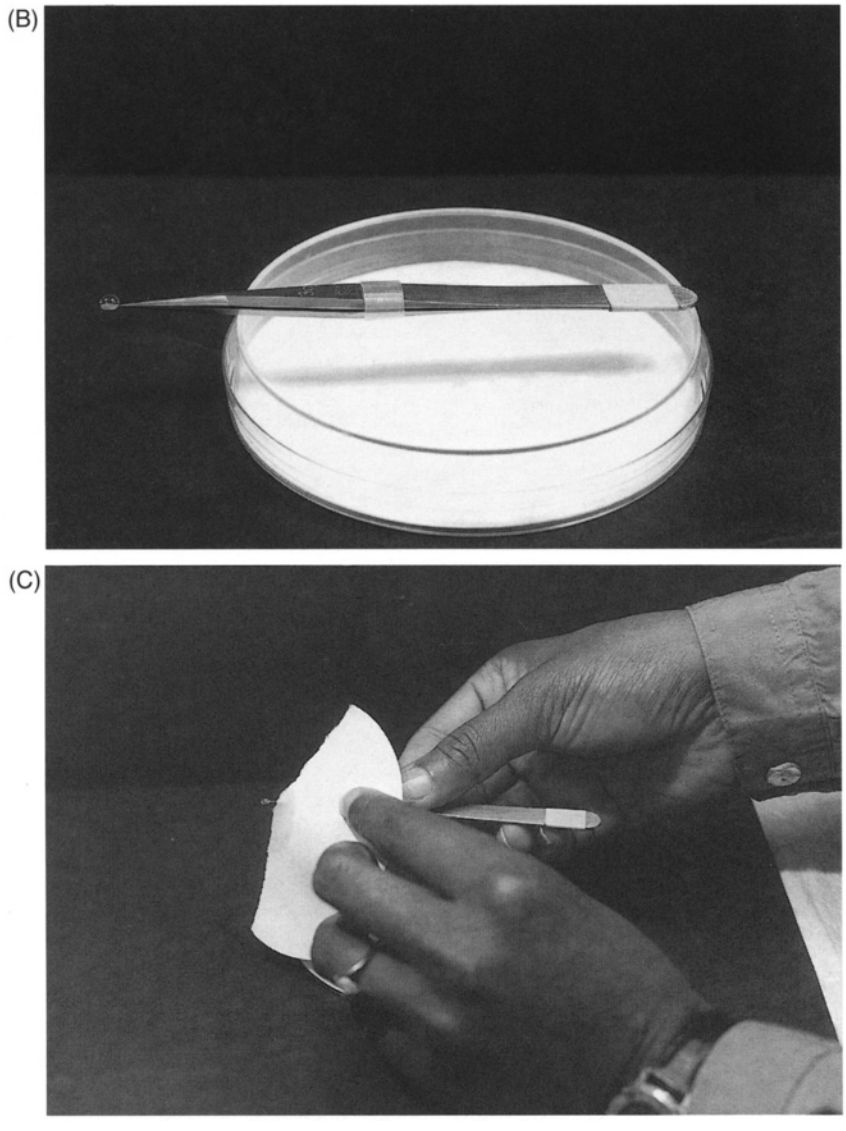

Figure 167. (B) Addition of one drop of particulate suspension to film-coated grid with Pasteur pipet. (C) Wicking grid almost to dryness by means of a piece of Whatman™ No. 1 filter paper.

5. Cautionary Statements

Negative stains are all heavy metals and thus should be handled as the toxic and hazardous materials that they are. Dried droplets of stain should be handled with care to avoid inhalation. All wastes should be disposed of according to the institutional guidelines for hazardous wastes.

If working with pathogenic viruses or bacteria, it should be noted that negative staining does not kill all pathogens. Thus, the infectious agent should be inactivated prior to negative staining, or the grid should be sterilized by gas or ultraviolet radiation prior to being handled or put into an electron microscope. If the viability of a pathogen is in question, proper safety precautions should be employed, and, following negative staining, the grid should be tested for pathogen viability before determining the necessary safety procedures to be employed in future studies of the agent.

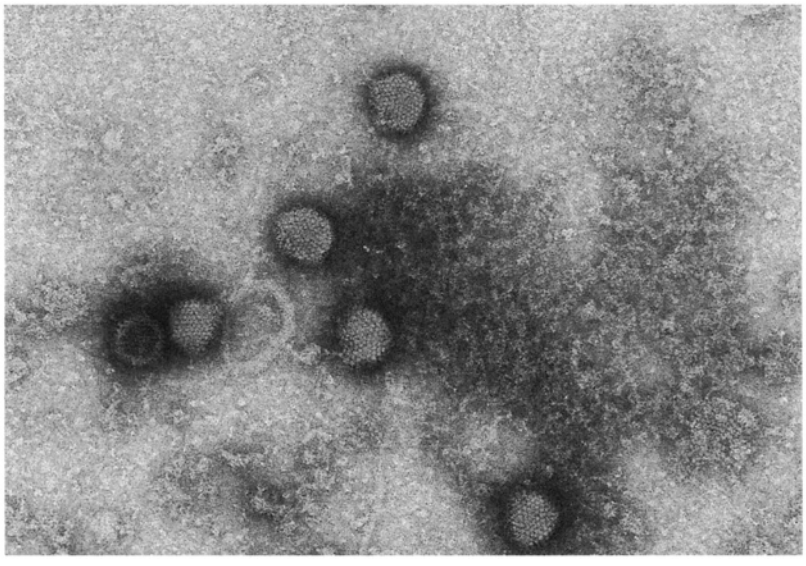

Figure 168. Adenovirus particles negatively stained with 2% PTA. 81,731×.

Some older papers and procedure manuals suggest the use of nebulizers to produce a fine mist of viral suspension that is directed toward a coated grid. This procedure should not be used under any circumstances, since atomizing a suspension of viral particles does not conform to safe laboratory practices.

A PTA solution will keep at 4°C for at least 3 years.

Negative Staining with Uranyl Acetate

1. Applications and Objectives

Uranyl acetate used as a negative stain at an acidic pH is superior for the demonstration of glycoprotein spikes and knobs associated with enveloped viruses, and develops a greater contrast than ammonium molybdate and PTA. The grain size of the uranyl acetate stain is greater than that of these other two negative stains (Nermut, 1982).

Uranyl acetate negative staining is also successful for staining ultrathin frozen sections produced by the Tokuyasu technique (see Chapter 2).

Proper staining with uranyl acetate will produce a faint electron density over the entire Formvar-coated grid surface, with minimal pooling around the particulate sample and minimal evidence of uranyl acetate crystals.

2. Materials Needed

The same materials are needed as listed for the PTA staining method, except that a 0.2–4.0% aqueous solution of uranyl acetate with a pH of 4–5 is used in place of PTA.

3. Procedure

The procedure is identical to that used for PTA negative staining.

4. Results Expected

The grid surface will be slightly electron-dense overall. The particulate sample will be revealed by negative contrast where the uranyl acetate is excluded. Some of the particulate sample will also exhibit positive staining from the uranyl acetate.

5. Cautionary Statements

A 4% aqueous solution of uranyl acetate is saturated, so large crystals of insoluble uranyl acetate will be found on the bottom of the storage bottle. For this reason, it is important not to pipet the stain from the bottom of the container to avoid the presence of numerous needle-like crystals of uranyl acetate on the surface of the negatively stained grid.

A solution of uranyl acetate will keep for weeks at room temperature in a dark bottle. If the solution appears turbid, do not use it. Hayat and Miller (1990) state that uranyl acetate stains are not stable above pH 6.0 and that a 1% aqueous solution is good for visualizing macromolecules.

Uranyl acetate is a toxic heavy metal and should be used and disposed of accordingly.

Negative Staining with Ammonium Molybdate

1. Applications and Objectives

Ammonium molybdate is an ideal fine-grain negative stain that will confer electron density and contrast to ultrathin frozen sections.

2. Materials Needed

This technique requires the same materials as called for with PTA negative staining, except that instead of PTA, a 3% aqueous solution of ammonium molybdate is used. This solution will have a pH of 6.5 without any adjustment.

3. Procedure

The staining procedure is identical to that described for PTA.

4. Results Expected

Sections stained with ammonium molybdate will have a reasonable contrast and a fine grain structure, revealing details of the frozen tissue/cell structures as a negative image.

5. Cautionary Statements

As with all the negative stains, this heavy metal should be handled and disposed of with methods appropriate to hazardous materials. The effect of this metal on the viability of negatively stained samples is not thoroughly documented, so it should be assumed that pathogens are still viable after staining unless they have been specifically tested.

Wetting Agents Used for Negative Staining

1. Applications and Objectives

If negatively stained preparations exhibit uneven spreading of the stain or sample, or have excessive pooling of the negative stain around the perimeter of the sample particulates, or if large structures such as protozoan wall plates (scales) roll up rather than remaining flat (Dykstra, 1976), wetting agents may help.

The most commonly utilized wetting agents are the antibiotic bacitracin (Gregory and Pirie, 1973) or BSA. Both of these substances are proteins and are, in themselves, visible after negative staining. These agents cause the sample and/or the negative stain itself to spread evenly on the film-coated grid surface.

2. Materials Needed

- 500 μg/ml of bacitracin in distilled water or 0.01–0.02% BSA in distilled water
- Formvar-coated grids
- Forceps
- Pasteur pipets
- Parafilm™
- Whatman™ No.1 filter paper (9-cm disks)
- Petri dishes (10-cm)

3. Procedure

For Spreading the Negative Stain

1. Place a suspension of the particulates on the surface of the filmed grid for 3–5 min and then wick almost to dryness.
2. Immediately replace with a drop of the chosen negative stain mixed 1:1 with either of the wetting agents (bacitracin, BSA) just before use.
3. After 30–60 sec, wick the grid quickly and completely to dryness, as described for the PTA negative stain procedure.

For "Relaxing" Large Specimens

1. Mix one drop of bacitracin solution with one drop of concentrated particulate suspension on a piece of Parafilm™.
2. Place one drop of mixture on a Formvar-coated grid for 3–5 min.
3. Wick almost to dryness, add the negative stain of choice, and wick to total dryness after 30–60 s, as previously described.

4. Results Expected

The negative stain should be evenly spread on the Formvar-coated grid surface, with minimal pooling around the particulate sample. Any large structures in the particulate sample should be well relaxed and spread out (Fig. 169).

5. Cautionary Statements

All normal precautions for negative stain procedures listed under negative stains should be observed. Both bacitracin and BSA will be seen after negative staining as small white dots excluding the negative stain. Bacitracin is a smaller molecule than BSA, so the dots will be smaller with the former wetting agent.

Preparation of Virus Samples for Transmission Electron Microscopy

The preparation of viral samples for negative staining and examination with the transmission electron microscope may be accomplished by the application of several different techniques. If large amounts of virus can be harvested and an ultracentrifuge is available, ultracentrifugation techniques work quite well. If only small amounts of virus are available from the sample being examined, immune electron microscopy techniques may be the best approach.

Viruses that cannot be grown in tissue culture can be negatively stained after isolation from the host tissues or body fluids. Viruses also can be passed through cell cultures and then negatively stained.

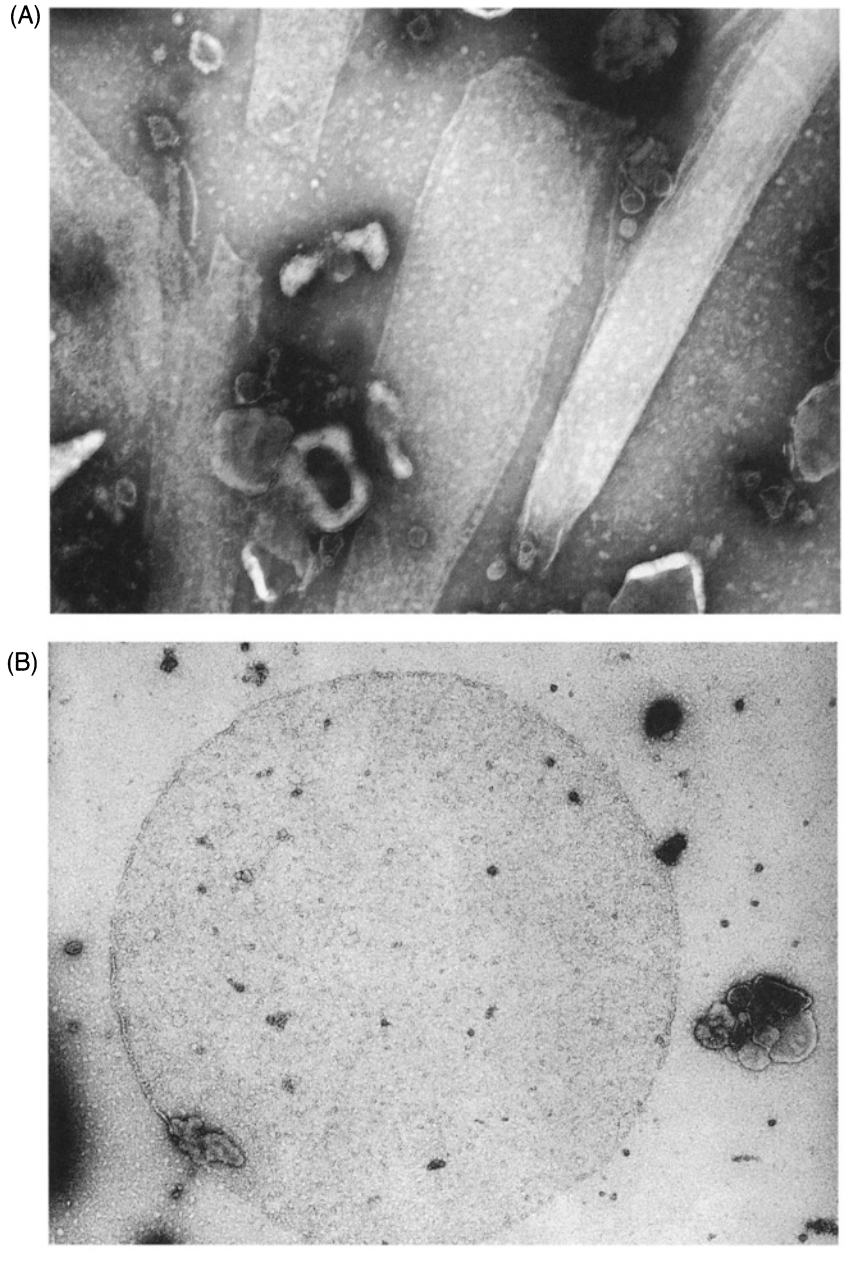

Figure 169. Cell wall scales of the protozoan *Sorodiplophrys stercorea*. (A) Negatively stained scales before using a wetting agent. 37,340×. (B) Scales after being "relaxed" by exposure to bacitracin. 28,938×.

Ultracentrifugation Technique for Viral Sample Preparation

1. Applications and Objectives

This technique is utilized to concentrate viral particles from infected cell cultures, tissues, or body fluids. For this technique to be highly successful, the number of viral particles needs to be fairly high.

2. Materials Needed

- Pasteur pipets
- 15-ml clinical centrifuge tubes
- Ultracentrifuge tubes
- Clinical centrifuge
- Ultracentrifuge
- Distilled water

3. Procedure

1. Collect the sample, dilute about 1:10 with PBS, and store frozen if necessary. Do not sonicate cell samples or scrape mucosal linings to release viral particles from cells. Sometimes, it is useful to freeze (at −20 °C) and thaw infected cell cultures several times to release viral particles.
2. Centrifuge the sample at approximately 1,000 rcf for 5 min or until clarified on a clinical centrifuge.
3. Centrifuge the supernate from step 2 at 10,000 rcf for 30 min.
4. Centrifuge the supernate from step 3 at 40,000 rcf for 60 min.
5. Discard the supernate from step 4, and resuspend the remaining pellet in about 0.1 ml of distilled water or PBS. If a pellet can be seen after the final centrifugation, remove all but about 0.1 ml of the supernate very gently with a Pasteur pipet.
6. Negative stain the resuspended pellet material (or 0.1-ml droplet) according to the instructions for the negative stain of your choice.

4. Results Expected

Viral particles will be visible after negative staining procedures.

5. Cautionary Statements

All normal precautions for dealing with potential viral pathogens should be observed, and all cautions for handling and disposal of the heavy metal negative stains should be followed.

Sonication is not recommended at any time for cells containing viral particles, since membranes tend to become disorganized, and many will reanneal with each other to produce extremely small vesicles that can be confused with some viral particles. Freeze–thawing will release virions from cells without producing vast numbers of small vesicles.

Immune Electron Microscopy for Concentrating Viruses
(King and Lecce, 1980)

1. Applications and Objectives

If an antibody has been raised against a virus, it can be used to concentrate and identify the virus prior to negative staining. In addition to providing a technique to specifically identify the viral isolate involved, the technique can be used to concentrate relatively small amounts of virus for negative staining.

2. Materials Needed

- Antibody against virus (IgG fraction against rotavirus, for example)
- Formvar-coated grids
- Negative stain of choice
- Forceps
- Whatman™ No.1 filter paper (9-cm disks)
- Pasteur pipets
- Petri dishes (10-cm)

3. Procedure

1. Prepare antibody to the virus.
2. Pipet a drop of antibody suspension onto a Formvar-coated grid, let sit for 5 min, dip briefly in distilled water, and then wick to dryness with a piece of filter paper.
3. Pipet a drop of fluid suspected of containing virus onto the antibody-coated grid. After 3–5 min, dip briefly in distilled water and wick almost to dryness with filter paper.
4. Negative-stain as described for PTA (or stain of your choice) for 30–60 sec and dry.

4. Results Expected

If the virus is recognized by the antibody, the virions will be bound to the coated grid and will be visible after negative staining (Fig. 170).

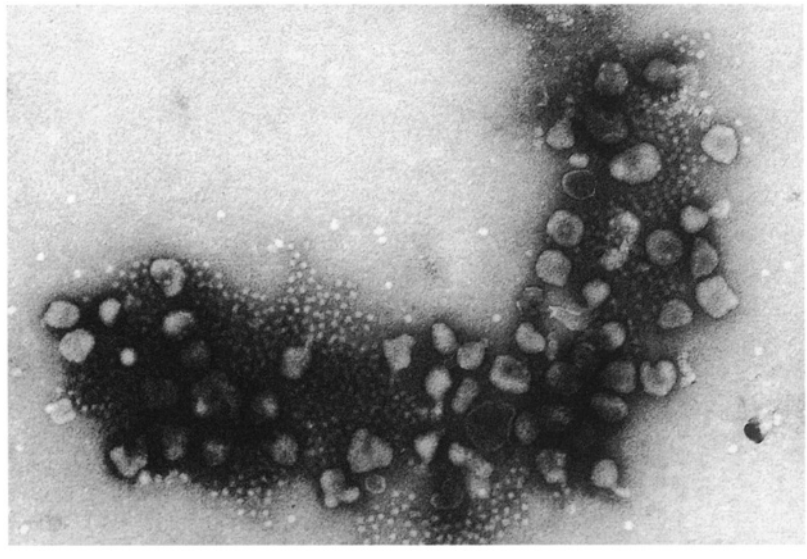

Figure 170. Immunoelectron microscopy of virus showing a coronavirus and a smaller helper virus coaggregated with specific antibody raised against the viruses. Negatively stained with PTA. 48,894×.

5. Cautionary Statements

Handle the viral suspension and the heavy metal stain with all the necessary precautions called for with potential pathogens and heavy metals.

If the grid is not dipped briefly after the antibody is bound to the Formvar coat, excessive negative stain may be bound to nonspecific serum proteins dried to the Formvar surface.

An alternative method involves mixing the antibody and viral suspension prior to placing it on a Formvar-coated grid. This would reveal clumps of antibody/virus after negative staining.

Viral Concentration with the Beckman Airfuge[2]

1. Applications and Objectives

This is a quick method to prepare viral samples from fecal samples or fractionated cell cultures for negative staining and transmission electron microscopy.

[2] Special thanks are due to Dr. William Steffens, College of Veterinary Medicine, University of Georgia, for introducing us to this technique.

2. Materials Needed

- Beckman Airfuge with 4 Position rotor
- 1.5-ml polycarbonate tubes ($^5/_{16} \times 1^3/_8$, 0.8×3.5 cm)
- 15-ml conical centrifuge tubes
- Clinical centrifuge
- DPBS or appropriate buffer
- Vortexing device
- Pasteur pipets
- Forceps
- Whatman™ No. 1 filter paper (9-cm disks)
- Petri dishes (10-cm)
- Negative stain

3. Procedure

1. If working with cells, freeze–thaw them several times (alternating −20 °C and room temperature) to fractionate the cells.
2. Place the fractionated cells or fecal sample (the latter diluted approximately 1:15 with DPBS) in a 15-ml conical centrifuge tube.
3. Centrifuge the samples at top speed on a clinical centrifuge for 5 min (or approximately 1,000 rcf).
4. Remove the supernate with a Pasteur pipet, and centrifuge for 2 min at half speed on a Beckman Airfuge in polycarbonate tubes.
5. Remove the supernate with a Pasteur pipet, and centrifuge for 2 min at full speed on the Beckman Airfuge.
6. Remove all but one drop of supernate with a Pasteur pipet.
7. Resuspend the "pellet" in the drop of supernate remaining by vortexing the tube.
8. Remove a single drop and place this on a Formvar-coated grid, leave for 4–5 min, wick almost to dryness, and negative-stain with the appropriate heavy metal, as described under the section on negative staining.

4. Results Expected

The virions will be sufficiently concentrated so that negative staining will reveal them on the Formvar-coated grids.

5. Cautionary Statements

All the normal precautions for handling potential pathogens and heavy metals should be observed.

References

Dykstra, M.J. 1976. Wall and membrane biogenesis in the unusual labyrinthulid-like organism *Sorodiplophrys stercorea. Protoplasma* 87: 329.

Gregory, D.W., and Pirie, J.S. 1973. Wetting agents for biological electron microscopy: I. General considerations and negative staining. *J. Microsc.* 99: 261.

Harris, R., and Horne, R. 1991. Negative staining. In: J.R. Harris (ed.), *Electron microscopy in biology. A practical approach* (pp. 203–228). Oxford University Press, New York.

Hayat, M.A., and Miller, S.E. 1990. *Negative staining*. McGraw-Hill, New York.

King, M.W., and Lecce, J.G. 1980. Immune affinity electron microscopy: A rapid method for the detection of rotavirus in fecal suspensions. *Proc. Southeast Electron. Microsc. Soc.* 3: 28.

Nermut, M.V. 1982. Advanced methods in electron microscopy of viruses. In: C.R. Howard (ed.), *New developments in practical virology*. Alan R. Liss, New York.

9

Transmission Electron Microscopy

I. HISTORICAL REVIEW OF MICROSCOPY (1590–2003)

Microscopy tools for direct visualization of cytological details include the light microscope, the confocal scanning microscope, and the transmission electron microscope (TEM). The scanning electron microscope involves circuitry that processes electronic signals into an indirect image seen on a cathode ray tube or digital screen. All of the direct visualization methods involve light or electrons interacting with specimens and utilize either glass or magnetic lenses to project an image to the eye, to a screen, or to film. When considering the development of electron microscopes, it is useful to recognize the antecedents from the realm of light microscopy. The concepts of electron optics underlying electron microscopes are primarily extrapolations from the physics of light optics.

The first compound light microscope was developed in 1590 by the Janssen brothers and led to the rapid rise in interest in microscopic life forms and microscopic structures found in multicellular organisms as described in the work of Malpighi, Hooke, and Leeuwenhoek in the 1600s. By the 1800s, countless improvements in optical microscopes had taken place, and important discoveries concerning cell structures had been reported. Brown had identified the nucleus of eukaryotic cells, Schleiden and Schwann had independently posited that all life was made up of cells, which was the basis of the cell theory, and mitosis had been described. In 1886, the maximum resolution available with glass optics and visible light had been achieved by coupling the contributions of Carl Zeiss and Ernst Abbe to produce a compound light microscope that was corrected for spherical aberration and chromatic aberration. With careful Köhler illumination and the use of matched substage condenser lenses, oculars, and apochromatic objectives corrected for three wavelengths of light, an ultimate point-to-point resolving capability of 0.1 μm was achieved, as predicted from theoretical calculations concerning light optics. It was not until 1934 that the resolution capabilities of light microscopes were improved upon by the electron microscope developed by Driest and Müller.

The first electron microscope was described by Knoll and Ruska (1932), as the culmination of Ernst Ruska's graduate work. This prototype for our modern instruments had an electron source and two magnifying lenses but no condenser lens, and actually had less resolving power than the contemporary light microscopes of the day. By 1934, Ruska had added a condenser lens to improve illumination. By 1938, von Borries and Ruska reported resolving capabilities of 10 nm. The German electronics firm of Siemens, under the direction of Halske, produced the first commercially available TEM in 1939 at the same time that Burton, Hillier, and Prebus were producing an experimental electron microscope in Canada. Hillier and Vance built the RCA type B in 1941, which delivered 2.5-nm resolution. By 1946, Hillier's group had produced an instrument capable of 1.0-nm resolution. This remains beyond the practical resolution needs of 2.0 nm, or one third of a mitochondrial unit membrane, the standard necessary for almost all biological work with chemically fixed specimens (Ghadially, 1985).

During the 1950s and 1960s, power supplies were refined, while lenses, vacuum systems, and mechanical controls were improved, and electronic stability was increased. Microscopes were produced with sliding objective lenses (Philips 75) and phosphor-coated glass viewing screens pointed almost horizontally at the viewer reminiscent of television screens (Philips 100).

Eventually, the standard TEM had a vertical column with electronic magnification steps, and images were projected onto phosphorescent screens that could be viewed through glass ports in the base of the column. Lens alignment progressed from methods requiring beating on the outside of the electron microscope column with a rubber mallet, as with the RCA 3, to every column element being physically adjusted with set screws, as with the Philips 200, to a mixture of mechanical alignments and electron alignment capabilities, as seen with the Hitachi HU-11E. Power supplies became increasingly smaller as solid-state circuitry replaced vacuum tube technology. Column vacuum improved from a level barely in diffusion pump range of 1.3×10^{-2} Pa to 1.3×10^{-4} Pa, with the addition of a liquid nitrogen cold trap.

The 1970s brought further improvement in all of the operational systems of the electron microscope and also saw the development of high voltage (1-meV) electron microscopes, microprobe analysis in the form of energy dispersive spectroscopy (EDS), scanning transmission electron microscopes, and an industry-wide standard of 0.344-nm resolution for TEMs sold in the latter part of the decade.

The 1980s saw further instrument system refinements. Instruments capable of less than 0.2 nm resolution became available, and intermediate voltage (300–400 keV) electron microscopes were produced. Cleaner vacuum systems were made possible by better diffusion pump oils, turbomolecular pumps, and ion getter pumps. At the same time, microanalytical capabilities such as energy dispersive spectroscopy (EDS) improved, and new techniques such as electron energy loss spectroscopy (EELS) and distantly related imaging methods such as scanning tunneling microscopy (STM) and atomic force microscopy (AFM) were invented. Computer-assisted microscopes became a reality, resulting in instruments capable of improved self-diagnostic capabilities, improved ease of alignment in various operational modes, and improved ease of use by minimally trained individuals. By the end of this decade, the theoretical resolving capability of electron optics through direct imaging techniques had been realized.

The 1990s saw incremental improvements in electronics and vacuum systems for TEMs and further refinements in intermediate voltage electron microscopes, leading to their wider acceptance in the biological community. The most important development of this decade was the result of coupling intermediate voltage electron microscopes, digital image acquisition, computerized motor-driven goniometer stages, and computer manipulation and analysis of images to support the new field of electron tomography described in Chapter 12.

The TEMs available from all major manufacturers in 2003 are actually driven by computer software, though an operator usually can usually choose between turning analog-like knobs or using a computer mouse or keyboard. Direct image acquisition through attached digital cameras is becoming ever more prevalent, and the manipulation of acquired digital images is easily done, requiring a new look at what constitutes an "original" image. Improvements in microanalytical methods (EDS, EELS, and ESI), reduction in probe sizes with consequent increased resolution, as well as improved sensitivity to lower atomic number elements are continuing, as discussed in Chapter 14.

Excellent sources for further information concerning the history of electron microscopy are *The Beginnings of Electron Microscopy* edited by Hawkes (1985) and Haguenau *et al.* (2003).

II. THEORY OF ELECTRON OPTICS

A. Light Microscopes versus the TEM

A comparison of schematic diagrams of the image-forming components of a compound light microscope (LM) and a TEM (Fig. 171) shows marked similarities between the two. With

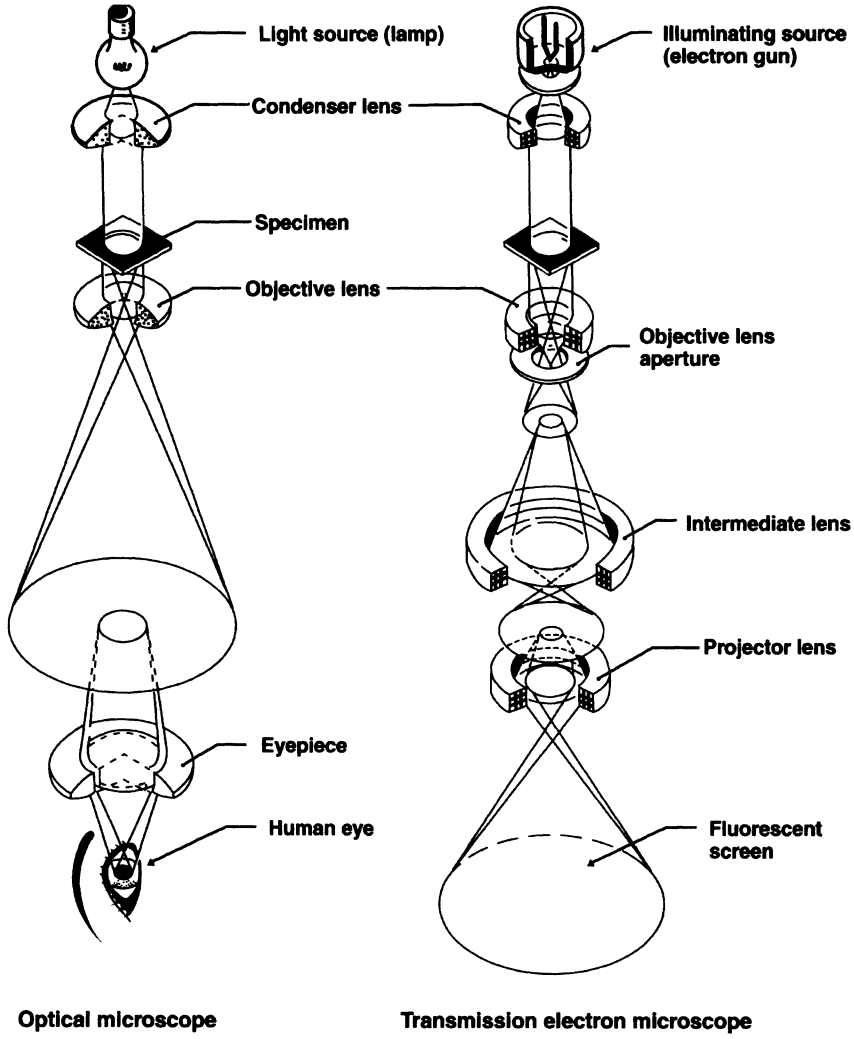

Figure 171. A comparison of the optical systems of a LM and a TEM. (Courtesy of JEOL USA, Inc.)

both conventional TEMs and those equipped with field emission guns (FEGs), as well as light microscopes, a tungsten filament is used as a source of illumination, though the LM utilizes photons emitted from the heated filament, while the TEM utilizes electrons released at the same time. Both utilize objective, condenser, and projector (ocular) lenses to magnify and focus the illumination source and projected images. The LM uses glass elements to bend the light waves, while the TEM utilizes electromagnetic lenses to bend the electron beam. The TEM requires more lenses than the LM to achieve adequate illumination and high magnification. In addition, the TEM must manipulate the electron beam in a high-vacuum environment within the microscope column, since molecules comprising air would otherwise deflect the electrons, interfering with illumination and the image-forming process. In both microscopes, the condenser lens(es) focus the imaging beam (light, electrons) on the specimen, while the objective lens focuses and magnifies the image of the specimen. Further magnification is provided by the projector (ocular) lens system that projects the final specimen image onto film, a phosphor-coated screen that can be viewed with a binocular microscope or the naked eye, or to a digital camera.

B. Resolution

Before discussing resolution, it is useful to review the units of measurement that apply to ultrastructural research. Historically, electron microscopists spoke in terms of angstrom (Å) units, but since the majority of the world deals strictly in metric units in modern times, the nonmetric angstrom unit is being abandoned. The relationship of measurement units encountered in cytological literature is shown below:

- $1\ \text{Å} = 1 \times 10^{-7}\,\text{mm} = 1 \times 10^{-10}\,\text{m}$
- $1\ \text{nm} = 1 \times 10^{-6}\,\text{mm} = 1 \times 10^{-9}\,\text{m}$
- $1\ \mu\text{m} = 1 \times 10^{-3}\,\text{mm} = 1 \times 10^{-6}\,\text{m}$

An average person with 20/20 vision can resolve (distinguish) two points located 0.1 mm apart. With the best compound light microscope, a theoretical resolution of 0.1 μm can be achieved. Some transmission electron microscopes can discern two points less than 0.127 nm apart. This means that large macromolecules such as hemoglobin and certain enzymes can be viewed directly with the electron microscope. A short film laboriously compiled by Al Crewe and his graduate students shows individual atoms of uranium moving about through a series of time-lapse photographs taken with a transmission electron microscope.

Resolution is generally defined as the ability to identify two points or lines as separate structures. The resolution of films is generally given as lines per millimeter, while point-to-point resolution is used to describe optical systems. The resolution formula can be used to calculate the theoretical resolution (d):

$$d = \frac{0.61 \times \lambda}{n \sin \alpha}$$

in an optical system wherein the refraction of the medium between the illumination source and the lens is defined as n, α is one half the cone of illumination entering the front of the objective lens after interaction with the specimen, and λ is the wavelength of the image-forming radiation. Objective lenses of light microscopes are usually marked with the numerical aperture (NA), which is equal to $n \sin \alpha$.

Using the formula to calculate the resolution available utilizing a light microscope equipped with an illumination source of 500-nm wavelength (using a green filter) and a numerical aperture of 1.4 (an oil immersion 100× objective and a 1.4-NA condenser lens with oil between both lenses and the specimen slide), two points approximately 0.2 μm apart could be distinguished:

$$d = \frac{0.61 \times 500\,\text{nm}}{1.4\ \text{NA}} = 217.85\ \text{nm} = 0.217\,\mu\text{m}$$

In 1924, De Broglie calculated that the wavelength of an electron is approximately 0.005 nm, thus suggesting a theoretical TEM resolution 100,000 times better than that possible with the light microscope. Spherical and chromatic aberration as well as diffraction artifacts prevent us from reaching this theoretical resolution limit. Both Meek (1976) and Slayter (1976) have excellent in-depth discussions of light and electron optics.

C. Electron Lenses

Electron lenses may be either electromagnetic or electrostatic in design, though the former are the only type encountered in commercially available TEMs. Electromagnetic lenses are similar

to simple solenoids used to operate such items as water shut-off valves in washing machines and starter engagement mechanisms for automobile engines. The basic principle is that a current applied to a coil of wire will produce a magnetic field at right angles to the current flow (Fig. 172). This magnetic field can either move a piece of metal located in the field (opening up the washing machine water source) or deflect small charged particles such as electrons passing through the field in the electron microscope. The more turns of wire in an electromagnetic lens, the stronger the magnetic field developed, because more flux lines are produced, by which magnetic strength is measured. Wrapping the copper wires conducting the electrical current around a soft iron core will further increase the magnetic field. Thus, there are three ways to increase the strength of an electromagnetic lens: (1) Increase the number of turns of copper wire in the lens; (2) Increase the amount of iron in the lens, either by enlarging the core or adding a pole piece (see below); and (3) Increase the amount of current applied to the windings of the lens.

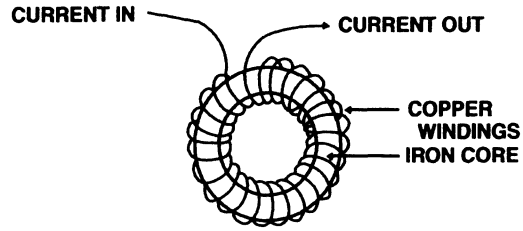

Figure 172. A simple solenoid.

D. Properties of Electron Lenses

1. Focal Length

The focal length of a lens is determined by the accelerating voltage of the electron beam (kV) and the magnetic field strength in the lens under consideration. Both of these factors determine where the electron beam comes into focus. At each different accelerating voltage, the lenses of the TEM must be adjusted to maintain the same focus. Modern microscopes use computer programs to increase lens current as accelerating voltages increase to keep the focal length constant.

2. Depth of Focus and Depth of Field

Photographers know that using a smaller aperture when focusing on a given object will bring more of the foreground and background into focus than when using a larger aperture. This phenomenon is known as depth of field. The mathematical expression for calculating depth of field (D_{fi}) is as follows:

$$D_{fi} = \lambda/NA^2$$

Meek (1976) calculated that a TEM operating at 50 kV (resulting in a wavelength of 0.004 nm) with an objective lens with a NA of 10^{-3} would provide a depth of field of 4 μm. Since this depth is over four times the thickness of a normal thin section (80–90 nm), every feature in a conventional

ultrathin section will be in focus. This great depth of field explains why a slightly bent grid will not be grossly out of focus from one point to another.

A similar phenomenon, known as depth of focus, is also important to consider. The small apertures used in electron microscopes result in the projected specimen image being brought into acceptable focus over a great distance. The formula for determining depth of focus, where M is the magnification, RP is the resolving power (in meters), and NA is the numerical aperture, can be used to calculate the depth of focus for a TEM. According to Meek (1976) the numerical aperture for a typical TEM objective lens is 10^{-3}. If the microscope is capable of 0.5 nm (5×10^{-10} m) resolution at a magnification of 100,000, then the depth of focus (D_{fo}) is 5,000 m:

$$D_{fo} = \frac{M^2 \cdot RP}{NA} \quad \text{or} \quad D_{fo} = \frac{100{,}000^2 \cdot (5 \times 10^{-10})}{10^{-3}} = 5{,}000\,\text{m}$$

This means that TEMs have sufficient depth of focus that an in-focus image can be easily projected onto a 35-mm camera inserted above the viewing screen, onto the viewing screen, onto sheet film in a camera below the viewing screen, and onto a digital camera located below the sheet film camera. If illumination is adequate and vacuum can be maintained to keep air from scattering the electrons, the image can be projected below the floor holding the electron microscope. At each viewing level, the magnification would be different, but the focus would be the same.

3. Diffraction

A limiting feature of aperture size is the phenomenon of diffraction. When an aperture becomes small enough, the wave front of illumination (photons or electrons) bends around the edge of the aperture, causing image degradation. With a light microscope at low magnification, where resolution is not critical, decreasing the aperture of the substage condenser results in greater contrast. However, if the aperture is made too small, the image becomes increasingly grainy and distorted. At high magnifications where resolution becomes critical, it is imperative that the substage condenser be used in the wide-open position to eliminate any possibility of image degradation due to diffraction. Diffraction degrades the image in the form of decreased resolution by producing spurious images through the formation of haloes and fringes. The formation of these fringes in an electron microscope (Fresnel fringes, Fig. 173) around small holes in plastic films is used to correct astigmatism in objective lenses. The effect of different aperture sizes on wave fronts of photons or electrons (Fig. 174) is similar to the effect of openings of different widths at the top of a dam restricting water flow. The objective aperture in an electron microscope is the point at which effects of diffraction are most easily noted. Electron microscopes are equipped with discrete objective apertures (10–100 μm in diameter in most cases), and the smallest of these results in minimal diffraction at the magnifications used with the preponderance of biological specimens.

4. Hysteresis

The strength of electromagnetic lenses is not strictly due to the current flowing through them, but also depends to some extent on the previous magnetic history of the lens. The soft iron core around which the copper windings are formed retains some of its magnetism, even when current is no longer flowing. This is called remnance. The easiest way to remove the effect of remnance is to reverse the current flow to the lens briefly. Some TEMs have a button labeled *normalizing* that does this. Hysteresis can cause magnification errors of 10% or more in some of the older TEMs, though most modern microscopes are designed essentially to eliminate this problem for practical purposes.

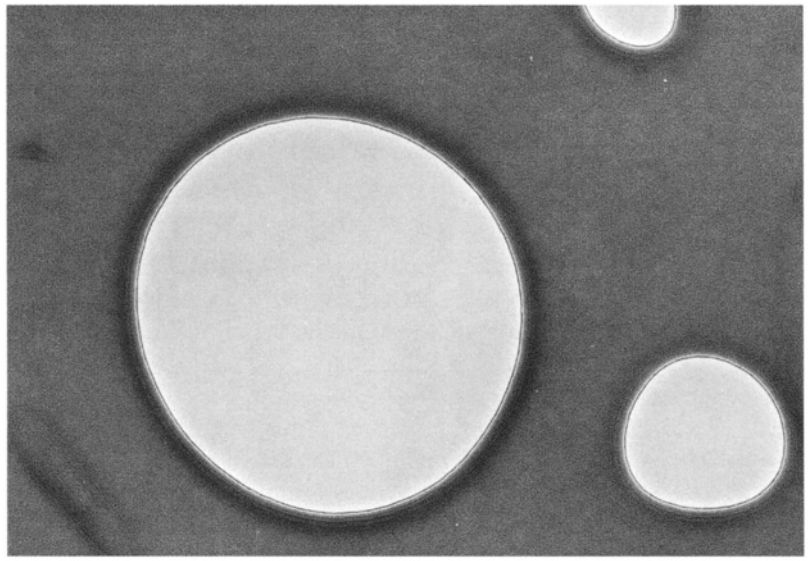

Figure 173. A Fresnel fringe.

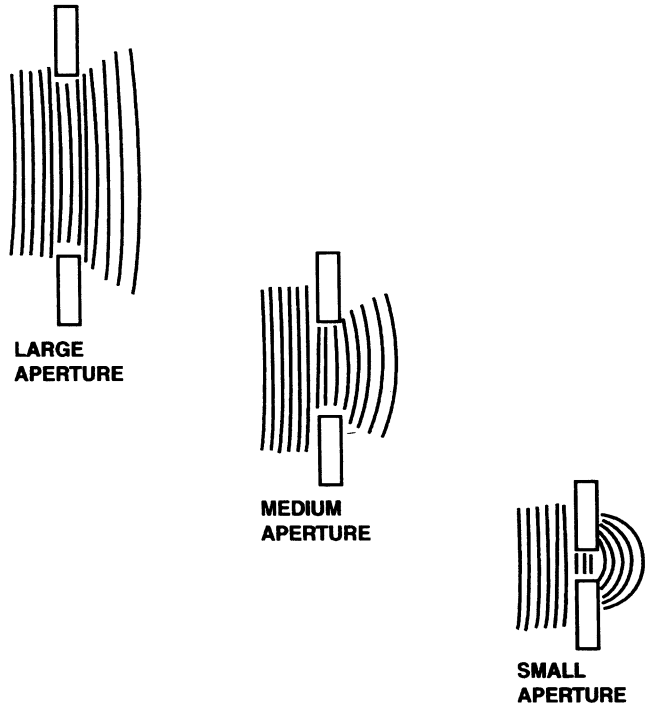

Figure 174. The effect of varying aperture size on a wave front.

5. Pole Pieces

A pole piece assembly consists of an upper and a lower short cylindrical iron piece separated by a small gap. The lines of magnetic flux are concentrated in the gap between the upper and

lower elements and exert a force at right angles to electrons passing through the bore of the lens (Fig. 175). Changing the focal length of a lens is usually accomplished by altering the current flow to the lens, but changing pole pieces is another less convenient method to change lens focal length.

6. Image Rotation

Stepping through image magnifications in a TEM causes slight image rotations at each change in magnification. At certain steps, the image may rotate up to 180°. This rotation also occurs during focus shifts, although it is less evident. Newer microscopes are less prone to this behavior because of better computer programs that simultaneously control the energy levels in all of the lenses to minimize the image shifts. Computer control of lenses also can permit intentional image rotation to better align points of photographic interest with the fixed film orientation.

Image rotation is often utilized during the column alignment procedure to center the optical axis within the column. The phenomenon of image rotation results from the path described by electrons being acted upon by electromagnetic lenses. As the electrons that are initially accelerated in a straight line by the high accelerating voltage encounter an electromagnetic lens, they are directed into a spiral path. Electrons moving through a magnetic field are exposed to a force at a right angle to the original direction of motion (Fig. 176), resulting in electrons exhibiting a spiral path during the remainder of their journey to the viewing screen or film plane. As the magnification increases or decreases, the diameter of the spiral electron path increases or decreases.

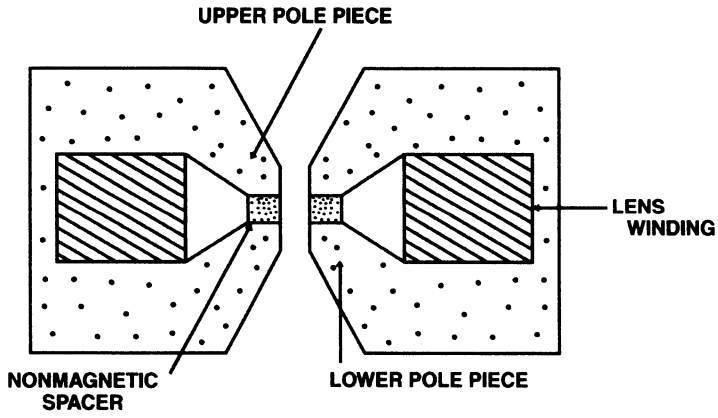

Figure 175. A pole piece.

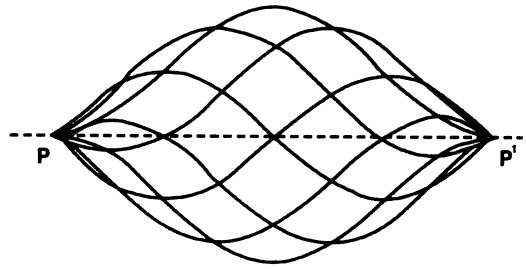

Figure 176. The spiral path of electrons induced by an electromagnetic lens. (Courtesy of JEOL USA, Inc.)

The velocity of unscattered electrons remains essentially constant until they are stopped by cameras or the viewing screen. However, if a lens is strongly energized, it will compress the spiral electron path more than when it is deenergized. An electron traveling in a straight line for 1 m will reach the screen at a certain point. Another electron traveling in a small spiral will arrive at a different point on the screen, while yet a third electron traveling in a comparatively large spiral will hit the screen at still another point. By examining a diagram of these different paths (Fig. 177), it becomes evident why an image rotates on the screen as the current delivered to one of the lenses in the imaging system (objective or projector lenses) is altered. The largest rotations (180°) occur when one of the projector lenses is turned on or off.

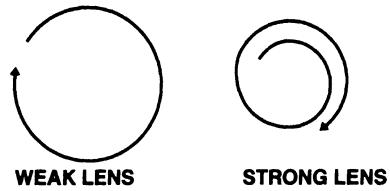

Figure 177. The effect of electromagnetic lens strength on the position of electrons reaching the viewing screen.

7. Lens Strength

As mentioned above, in a vacuum, the electron beam does not change velocity while passing through a magnetic field unless it hits something (the specimen). However, it is diffracted by the magnetic field of the lens. The objective lens changes focus by altering the current to the lens, which varies the focal length of the lens (Fig. 178). A more energized lens causes more refraction of the electron beam, resulting in a shorter focal length for that lens.

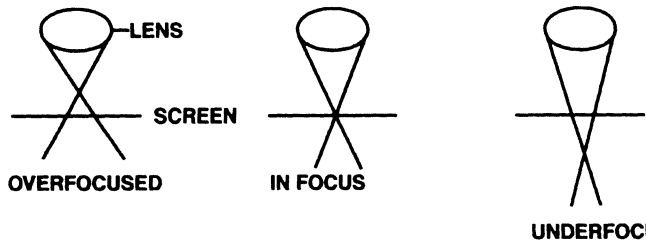

Figure 178. Comparison of an overfocused lens, a focused lens, and an underfocused lens.

8. Fresnel Fringes

Fresnel fringes (Fig. 179) occur when the electron beam strikes an opaque or semiopaque edge such as the edge of a hole in a plastic film. When the image is overfocused, a black fringe is visible around the outside of the hole. When the image is underfocused, a white fringe is visible inside the hole. In addition to Fresnel fringes, an over- or underfocused image has a grainy background. A truly in-focus image has no Fresnel fringe, exhibits little grain, and has minimal contrast. Most users tend to underfocus slightly, because this results in a higher contrast image that is more appealing to the eye. JEOL even provides an optimal under focus (OUF) control to allow

the user to take a slightly underfocus photograph after finding true focus. An underfocus image does not provide the highest resolution, however.

9. Spherical Aberration

Spherical aberration is the inability of a lens to focus all the incident beam from a point source to a point. It is important to remember that axial magnification is not equal to peripheral magnification, but all points of the image will be in focus due to the great depth of focus possible in the TEM.

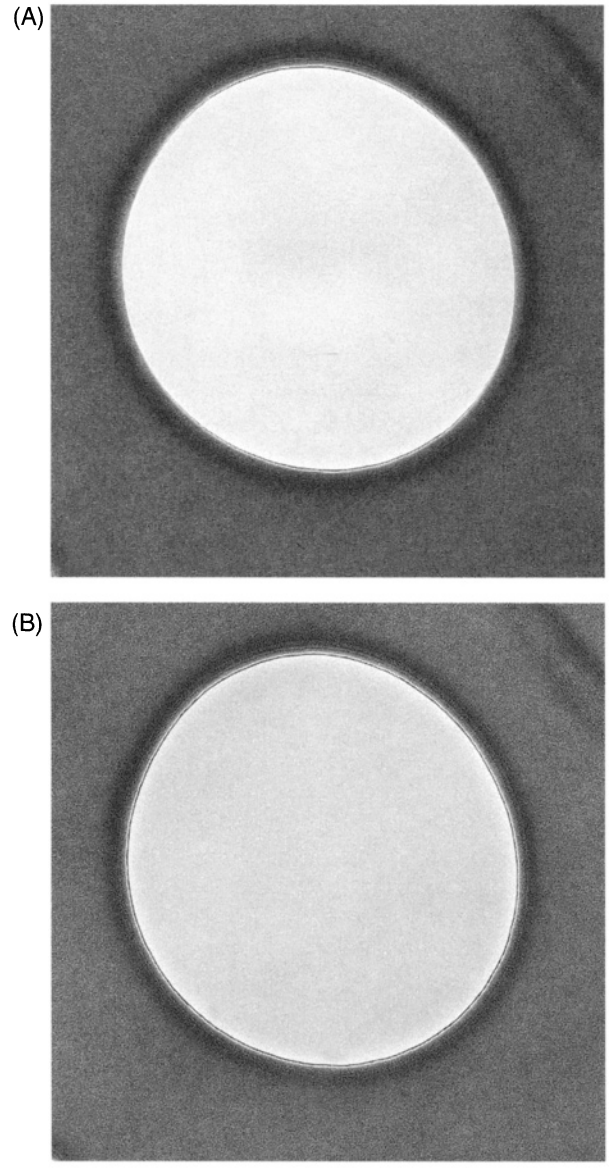

Figure 179. A through-focus series illustrating Fresnel fringes. 63,000 ×. (A) Astigmatic, overfocus. (B) Overfocus.

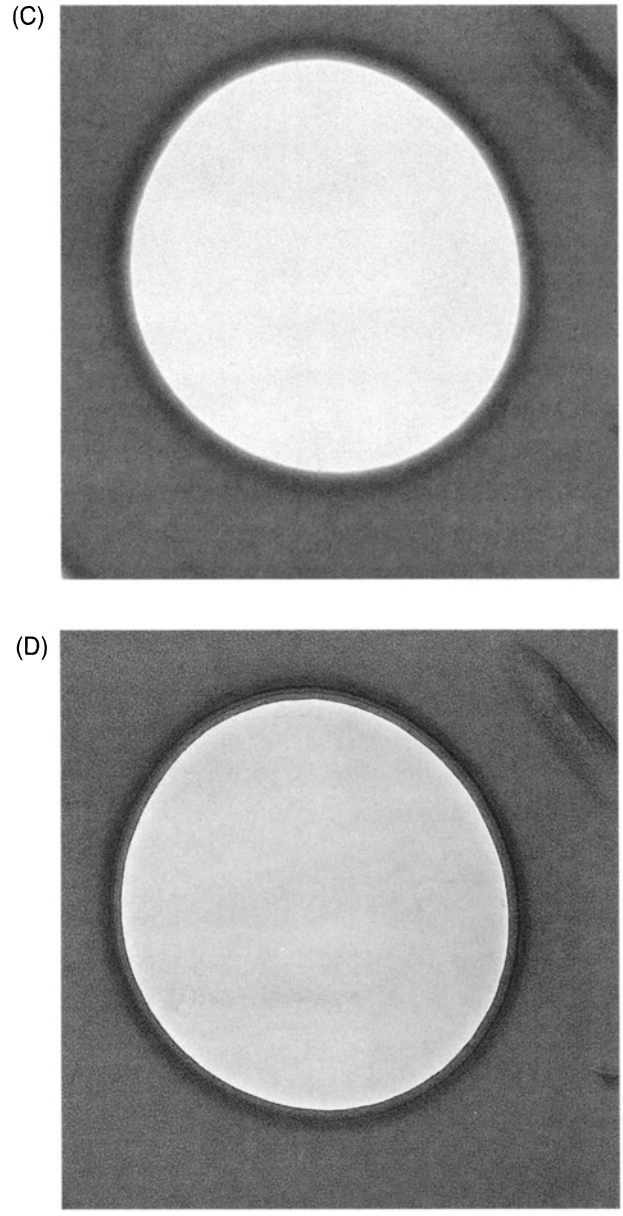

Figure 179. (C) Near Focus. (D) Underfocus.

If one examines a simple glass magnifying lens (Fig. 180), it is clear that the light striking the lens edge will be refracted (bent) more than the light striking the center (axial) portion of the lens. Consequently, information from the peripheral part of the light path will focus in a different plane from information from the axial part of the light path without correction. In a high-quality compound light microscope, this problem is compensated for by having convex and concave lens elements, or positive and negative lenses, coupled together.

In an electromagnetic lens, the flux lines are strongest near the electromagnet (peripherally) and become weaker near the central axis of the lens. Thus, electrons passing near the edge

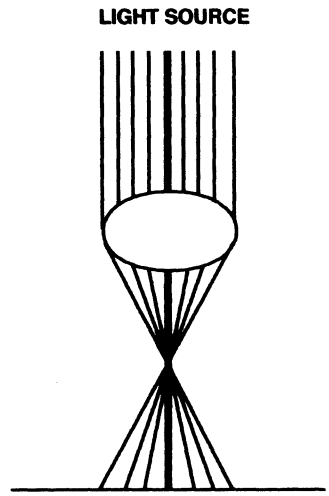

Figure 180. Refraction caused by a glass lens.

of the lens are subject to more lateral force from the lens magnetism and are refracted more than those passing through the center of the lens. Once again, due to the extreme depth of focus in a TEM, the whole specimen will be in focus, but the magnification of the image will not be the same for axial versus peripheral parts of the image. The electronic circuits and lens design of modern TEMs virtually eliminate evidence of spherical aberration, but older instruments still in use can exhibit barrel and pincushion distortion (Fig. 181) at low magnifications. The former results in parallel lines such as grid bars converging at the periphery of the viewing field, while the latter is seen as parallel lines diverging at the edge of the field.

Figure 181. Undistorted image of a grid compared with barrel and pincushion distortion (spherical aberration).

10. Chromatic Aberration

This phenomenon can be seen with inexpensive glass lenses, which give rise to colored fringes in the image due to the different focal lengths for photons of different wavelengths (Fig. 182). The greater the difference in wavelengths, the greater the problem of getting them to focus in the same plane. With light optics, various coatings are employed to minimize the defect. Achromatic objectives are corrected to allow blue and red light to focus in the same plane. Apochromatic lenses allow blue, red, and yellow light to focus in the same plane. One of the reasons for using green filters for black-and-white photomicrography is to provide monochromatic light to the lenses so that chromatic aberration will not be a problem.

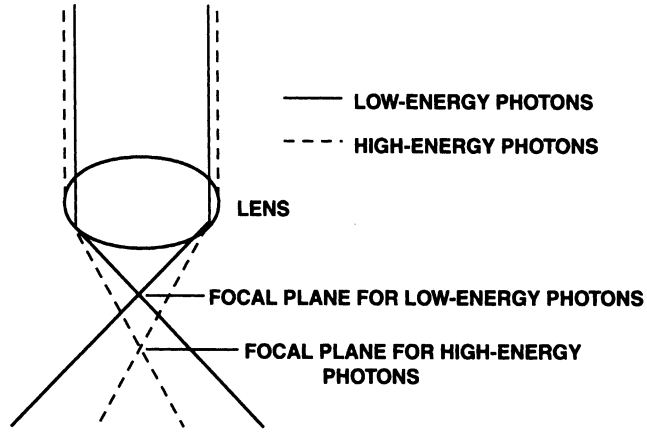

Figure 182. Chromatic aberration, resulting in photons of different wavelengths being focused at different planes.

Since the electron microscope does not provide color images, it is not intuitive that chromatic aberration can be a problem. However, there are actually three sources of chromatic aberration in an electron microscope (Slayter, 1976). Electrons liberated from an electron source (the heated filament) emerge from its surface with different energy levels (variation in thermal velocity). When the electrons are accelerated by the high-voltage field, they do not all achieve the same velocity (fluctuation in accelerating potential). The practical effect of this phenomenon is that minor fluctuations in the high-voltage supply result in a number of images at slightly different magnifications and focal levels, which are superimposed, producing decreased resolution. Thus, the sharpest image is produced in the central axis (voltage center) of the lens. To help minimize chromatic aberration due to accelerating voltage fluctuations and to realize the resolution capabilities of contemporary TEMs, it is necessary to have electronic stability in the high voltage supply allowing variations of only a few parts per million.

The third source of chromatic aberration in the TEM are energy losses within the specimen. The process of image formation is dependent on electron scattering caused by the specimen, particularly the various heavy metals with which it is impregnated during fixation and poststaining. Inelastic electron scattering due to the primary electrons being deflected over wide angles without significant energy loss is usually due to interactions with heavy metal atoms such as uranium, lead, or osmium in the specimen. Inelastic scattering essentially eliminates some of the electrons from the image-forming process, producing dark areas in the projected image because no electrons reach the phosphorescent screen or camera. Elastic scattering of electrons, when primary electrons from the electron gun displace specimen electrons, causes secondary electrons to be liberated from the specimen. These secondary electrons have less energy than the primary electrons originally impinging upon the specimen. Even in areas of the sections containing only pure resin with no biological material, some scattering of the electron beam will occur. Thus, some of the primary beam will pass through the specimen undeviated and with undiminished energy, some electrons will never reach the screen (elastically scattered), and still other electrons in the primary beam will produce secondary electrons, which have less energy than the primary beam but still reach the screen. Those electrons that have lost energy can focus in a different plane from the undeviated electrons. Any electrons that suffer energy loss but still reach the screen or a camera thus contribute to chromatic aberration. The thicker the specimen, the greater the chance that electrons in the beam will be deviated, thus leading to greater chromatic aberration.

Higher accelerating voltages decrease the likelihood of this problem because a higher energy beam is scattered less by the specimen.

11. Astigmatism

One definition for this phenomenon is the inability of the lens to form a point image of an object point. Astigmatism can also be thought of as instrument-induced radial asymmetry. Astigmatism is caused by a defect in the magnetic field symmetry resulting in different lens strengths exhibited at different points at right angles to the lens axis (Fig. 183). It can be caused by imperfect machining of pole pieces, imperfection of distribution of magnetic material within the lens itself, unevenness in the quality of windings within the lens, or aperture irregularities.

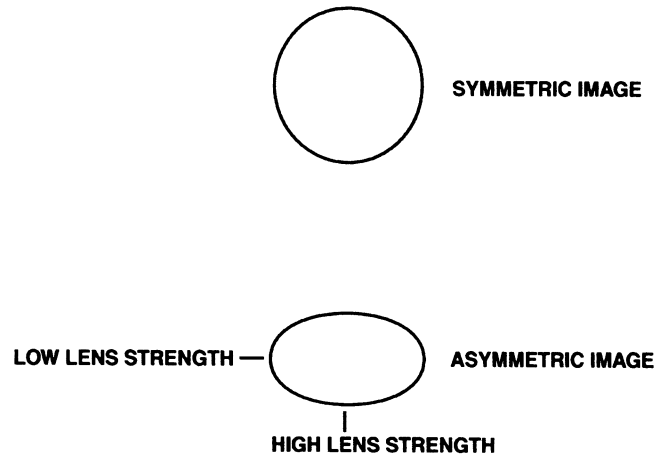

Figure 183. Diagram of asymmetric lens strengths.

III. FOUR ASPECTS OF IMAGE FORMATION (MEEK, 1976)

A. Absorption

Absorption gives rise to amplitude contrast, or differences in intensity, to which the eye is sensitive. This is the most important image-forming process with light microscopy.

B. Interference

Interference gives rise to phase-shift effects, to which the eye is insensitive. In most cases, interference can give rise to amplitude contrast (phase contrast), thereby contributing to image formation.

C. Diffraction

Diffraction, in general, results in degradation of the image by the formation of haloes and fringes that decrease resolution. With light microscopy at low magnifications where resolution is

not critical, the substage condenser diaphragm may be stopped down to increase contrast resulting from induced diffraction. At higher magnifications, this procedure is not advisable because of the concomitant decrease in resolution. In the typical range of magnifications used with biological materials in conjunction with the aperture sizes usually employed, diffraction is not a significant feature in TEM image formation.

D. Scattering

Scattering is, by far, the most important factor in image formation with the TEM and the least important in light microscopy. There are two types of scattering that take place as an electron beam interacts with the specimen: (1) Nuclear interactions (elastic scattering) which result in deflection of the primary beam electrons through a large angle, with little or no energy loss to the primary electrons. The bulk of these electrons do not contribute to information on the viewing screen. (2) Electron interactions (inelastic scattering) when the primary electrons encounter electrons within the specimen. The primary electrons dislodge secondary electrons from the specimen. The effect of this interaction is that parts of the primary electron beam are removed from image formation and are replaced by secondary electrons with considerably less energy, which are scattered easily and do not reach the phosphor on the viewing screen. Statistically, the large number of electrons compared to the number of nuclei in a specimen make it most likely that inelastic collisions will occur when the primary beam encounters the specimen. Thus, inelastic scattering is the most important aspect of image formation in a TEM, even though the electrons widely scattered due to elastic scattering also contribute. Electrons scattered by either mechanism do not reach the viewing screen, and thus, a dark spot remains on the screen where the phosphor would have emitted a photon if an undeviated electron had impinged upon it.

IV. GENERAL TEM FEATURES

Now that we have seen how electromagnetic lenses work and have discussed the theoretical aspects of image formation in a TEM along with the various aberrations that can detract from accuracy and clarity of the image, we can begin looking at the parts and operational parameters of a conventional TEM.

A. Operating Voltage

A conventional TEM operates up to 100–120 kV, usually with several lower steps (e.g., 40, 60, 80 kV). Intermediate voltage microscopes operate in the 200–400-kV range, while the high voltage instruments can generate 1–3 million volts.

B. Resolution

All currently manufactured TEMs guarantee 0.344-nm resolution, as judged with a graphitized carbon lattice. Certain instruments are actually capable of resolving less than 0.2 nm, but this

is of little use to most biologists, since conventionally prepared materials rarely yield better than 2-nm resolution (one third of a mitochondrial membrane).

C. Magnification

Most instruments can provide at least 200,000 × magnification, which is necessary to produce the manufacturer's guaranteed 0.344 nm resolution. More expensive units offer magnifications up to 500,000×, though this is of little practical value to most biologists. A picture taken at 35,000× and magnified three times when printed is within the enlargement range wherein no image-quality reduction will be noted. This magnification will resolve one third of a mitochondrial membrane (2 nm). Inexpensive microscopes (JEOL JEM-100S) have various steps of magnification up to 50,000×, followed by one step of 100,000× and one of 200,000×. The two highest steps are achieved through the activation of a "mini" lens only used for these magnifications. In operation, this means that the microscope is aligned for use with the lenses for 50,000× and below, and either of the high-magnification steps must be aligned separately. On a day-to-day basis, it usually means that the two highest magnification steps are not used. Despite the fact that the higher magnifications available on more expensive instruments are of little use to a biologist, the more gradual incremental increases in magnification (more intermediate steps between low and high magnifications) make them more usable throughout their magnification range.

Another feature of more expensive instruments is a more complex and flexible condenser system. In old microscopes like the Zeiss 9A or Philips 201, only one condenser lens was utilized, limiting the amount of illumination available. Microscopes capable of 500,000× magnification need two or three condenser lenses to provide adequate illumination, since image intensity is inversely proportional to the square of magnification.

D. High Vacuum, Electronic, Magnetic, and Physical Stability

The higher the vacuum, the less chance there is for scattering of electrons from gases in the column, resulting in increased illumination and image contrast. As previously mentioned, extremely high stability in power supplies for high voltage and lens currents is necessary to produce an instrument with minimal levels of spherical and chromatic aberration.

V. PARTS OF THE ELECTRON MICROSCOPE: FUNCTIONAL ASPECTS

Periodic reference to Fig. 184 will be helpful in the discussion of the TEM column and of the function and adjustment of the various parts.

A. The Electron Gun

There are three common sources for generating electrons that are accelerated by the high-voltage field of the electron gun. The simplest electron source is a tungsten wire (filament) with

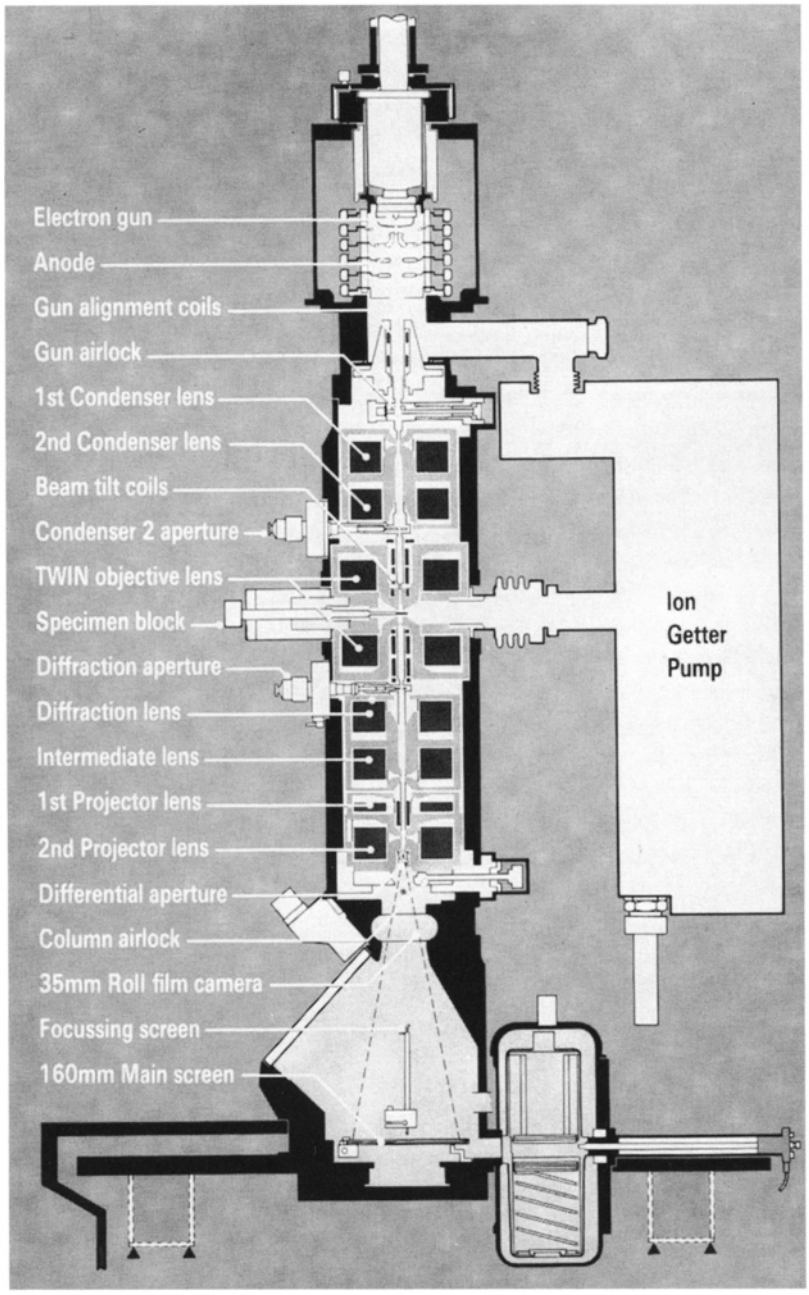

Figure 184. Diagrammatic sketch of the column components of a modern TEM. (Courtesy of Philips Electronic Instruments, Inc.)

an acute bend at the tip (Fig. 185), where the highest resistance to current flow is found. The tip of the filament is a small point from which most electrons will be liberated from heat generated when current is passed through the tungsten wire. Some of these filaments may actually be slightly melted during manufacture and pulled out to a thin point to further reduce the cross-sectional profile for an even more discrete source of electrons.

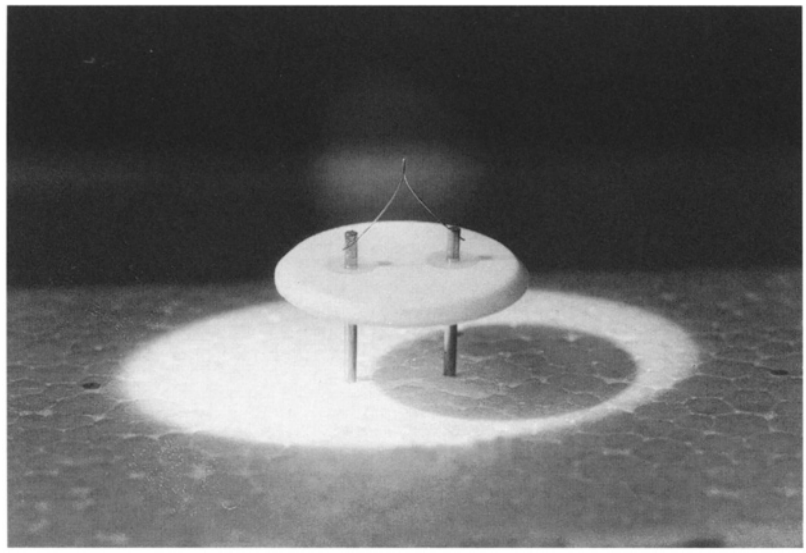

Figure 185. A typical tungsten filament assembly.

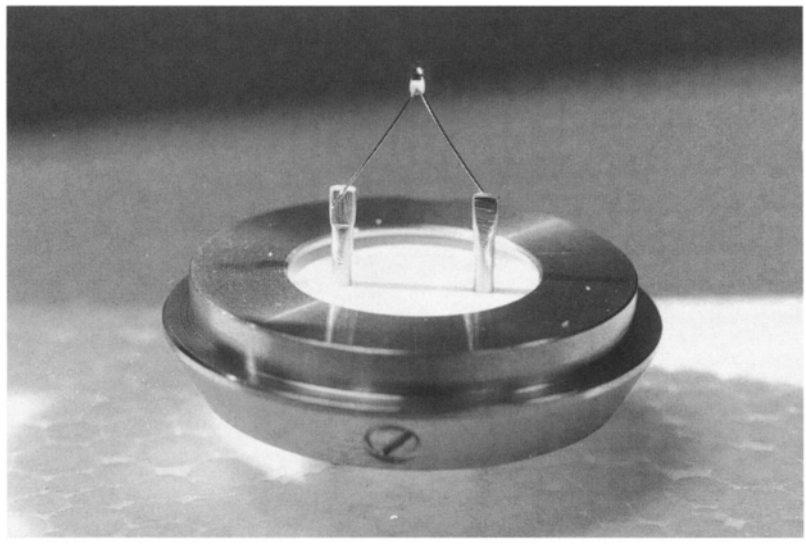

Figure 186. A lanthanum hexaboride (LaB_6) electron source.

Higher resolution microscopes equipped with extremely high-vacuum pumping systems (ion getter pumps) may be fitted with the second type of electron source known as a lanthanum hexaboride (LaB_6) cathode (Fig. 186). A single, pointed crystal of lanthanum hexaboride is positioned within a cup formed at the end of a tungsten filament so that when current is passed through the cup, and electrons are liberated, they transfer their kinetic energy to the lanthanum hexaboride crystal, thereby causing it, in turn, to release electrons. The advantages of this type of electron emitter are that it lasts longer (400–600 hr vs 100–200 hr for a tungsten filament) and produces a brighter image than that of a conventional tungsten filament. The disadvantages to

a LaB_6 emitter are higher costs (about 20 times higher than tungsten filaments) and the need for a higher vacuum (1.3×10^{-5} Pa or better, vs 1.3×10^{-2} Pa for tungsten).

The final type of electron emitter is a the field emission gun, or FEG (Fig. 187). A cold-cathode FEG consists of a tungsten filament whose tip has been etched to a radius of 20–30 nm placed near an anode at a potential of 3–5 kV. The small radius of the filament tip and the proximity of the positively charged anode causes electrons to be pulled from the filament tip. Thus, they are liberated through electrostatic forces rather than thermionic forces, as with the other two emitter types. The extremely fine tip of the filament allows electrons to be released from a very small area, forming an extremely coherent beam of electrons with a very narrow bandwidth of energies, resulting in a greater brightness and less spherical aberration compared with the other two types of emitters mentioned (Hainfeld, 1977). Once emitted, the electrons are accelerated by the high positive voltage of the anode (60–120 kV) at the bottom of the electron gun. Like the LaB_6 source, a very high vacuum must be maintained through the use of ion getter pumps for field emission guns to function properly.

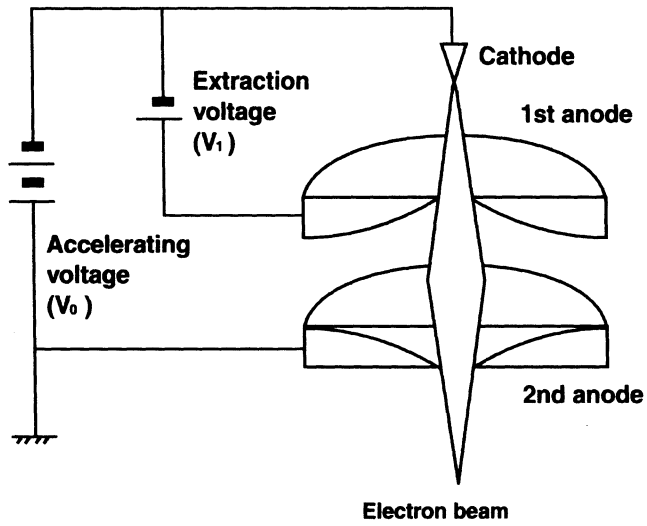

Figure 187. A field emission electron gun. (Courtesy of Hitachi Scientific Instruments.)

In a conventional tungsten filament electron gun, brightness is proportional to accelerating voltage, the distance of the filament behind the aperture in the Wehnelt assembly (Fig. 188), and the current passing through the filament. An electron cloud is produced as the filament is heated, with electrons (and photons) being emitted from the heated surface in all directions. Higher filament temperatures (current) dramatically reduce the filament life because of evaporation of the tungsten filament. Proper saturation of the filament is essential for optimal illumination coupled with optimal filament life. Saturating a filament may be compared with running water through a garden hose. To be most efficient, the water pressure is turned up as high as possible. If the hose can pass only 1 gallon (3.8 l) per minute, any increase in pressure beyond that flow rate is futile. In fact, further increases in pressure may cause the hose to burst. In a similar fashion, a tungsten filament can pass only so many electrons through it over a given period of time (current). If the current flow is below a critical rate, maximum heating and electron release are not achieved, and if the current is above this critical rate, excessive erosion of the tungsten wire will take place. As a filament ages, it thins due to metal evaporation, as shown on the right side of Fig. 189. As the current-bearing wire thins, its resistance increases. In practical terms, this means that an older

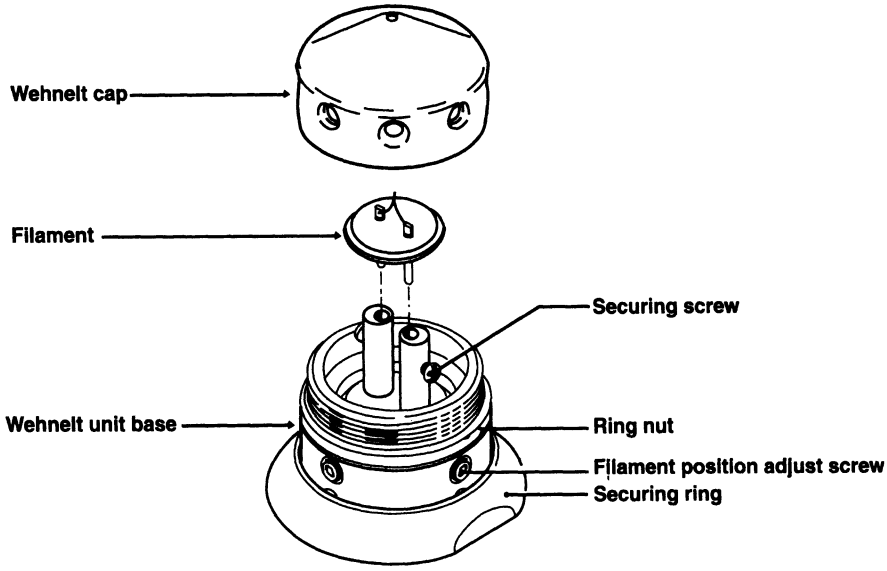

Figure 188. A typical Wehnelt assembly with a tungsten filament. (Courtesy of JEOL USA, Inc.)

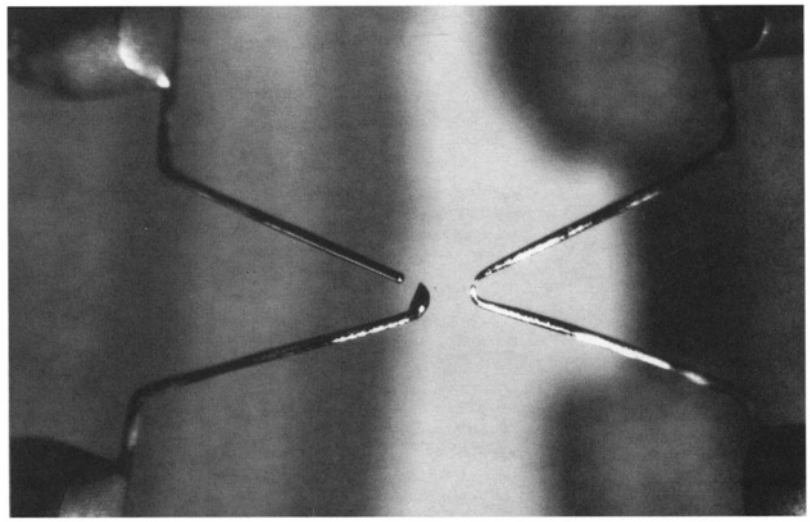

Figure 189. The filament on the left was massively oversaturated after 96 hr of operation and failed catastrophically. Note the large blob of melted tungsten on the lower half of the upper wire without evidence of reduced wire diameter. The filament to the right failed after 172 hr of operation, which is good filament life for the microscope. Note that the tip of the wire on both sides of the break has become attenuated through normal tungsten lost during filament aging.

filament needs a lower current to achieve the same illumination it produced when the wire was newer and thicker. It also means that the point of filament current saturation (the point at which a further increase in current does not yield an increase in electron emission) becomes oversaturation as the filament ages. If the filament current is increased considerably past the saturation point, catastrophic failure of the filament occurs. The characteristic melting of the filament tip following such an occurrence is shown on the left side of Fig. 189.

Most contemporary electron microscopes have self-biased electron guns. A resistor is put into the circuit providing current to the filament. It is connected between one leg of the filament and the Wehnelt cap (Fig. 190). As the current is increased to the filament, which heats it and causes electrons to be released, a voltage drop occurs at the resistor, producing a slightly negative polarity at the Wehnelt cap. Since the emitted electrons have a negative charge, they are repelled by the negative charge of the Wehnelt cap. Thus, as the current is increased to the filament and more electrons are emitted, the bias voltage (100–500 V) supplied to the Wehnelt cap increases, and the increased negativity forces the electrons toward the center of the Wehnelt assembly. At a low beam current (see Fig. 191), there is a low bias voltage, and electrons from the rear of the filament as well as from the filament tip can be imaged, resulting in multiple spots of illumination on the screen. Further increases in current result in an increased bias and a smaller area at the tip of the filament from which electrons can be emitted, producing an image on the screen of a central spot (produced from filament tip emissions) surrounded by a halo (emissions from areas back from the tip of the filament). At saturation, the spot of illumination is smaller than the original spot and halo, as the two have merged. This is the point at which maximum illumination is achieved, and filament structure is no longer visible.

Once the current flow to the filament is properly adjusted, the electron cloud is located primarily at the tip of the filament, which has been precentered over the aperture in the Wehnelt assembly during installation of the filament. Thus, most of the electrons are poised over the aperture and can be pulled through the aperture by the high voltage (40–120 kV) potential generated between the Wehnelt assembly and the anode above the condenser lens assembly.

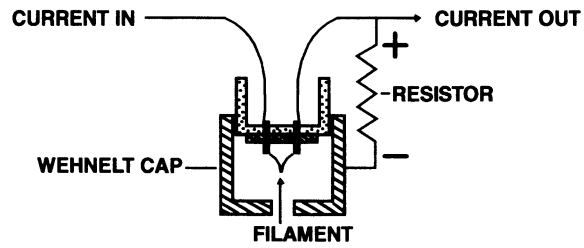

Figure 190. A self-biased Wehnelt assembly.

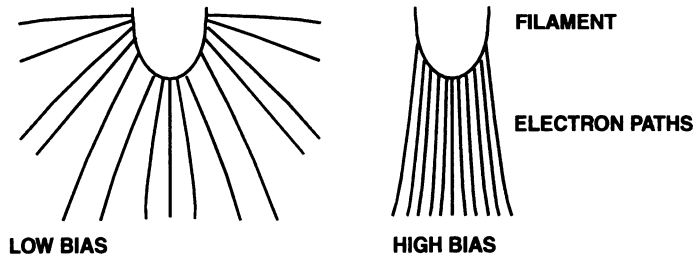

Figure 191. The effect of bias voltage on an electron cloud.

B. Condenser Lens System

The purpose of the condenser lens system is to focus the electrons produced and accelerated by the electron gun into a coherent beam for illumination of the specimen. In the first microscope designed by Ruska (Knoll and Ruska, 1932), there was no condenser lens system, so illumination was severely limited. Microscopes with only one condenser lens (e.g., the Zeiss 9A and Philips 201) have restricted magnification capabilities resulting from an inability to focus the beam into a spot small enough for high magnification illumination. As mentioned earlier, illumination is inversely proportional to the square of magnification, so with each doubling of image size, illumination decreases by a factor of two unless the condenser lens system can increase the number of electrons focused on the area of the specimen being viewed. Modern microscopes typically have two condenser lenses. The upper lens (C1) is a strong lens with a fixed aperture and is capable of producing a crossover image (smallest beam spot) of the beam that is about 9 μm in diameter.

The lower lens (C2) projects the crossover image of the first lens onto the specimen plane. The final focused beam can be adjusted to 2–3 μm in diameter. The lower condenser lens has a series of apertures (e.g., 50, 100, 150, 200 μm) that can be inserted and stigmated.

Under normal conditions, the C1 lens, which has a discontinuous series of settings, is set for the same current for all magnifications, while the C2 lens, which has a continuously variable current range, is adjusted for each magnification setting during use. The two apertures in the system limit the electrons striking the specimen to those from the most coherent part of the electron beam. This protects the specimen from excessive heating and generation of X-rays. The largest aperture gives a greater illumination at the expense of image quality if larger than about 250 μm.

C. Deflector Coils

Beam alignment is effected by deflector coils located below the condenser lens assembly but above the objective lens. These are small electromagnets capable of deflecting the focused electron beam and, thus, centering it over the specimen area being viewed. There are typically two sets of deflector coils. If the upper and lower coils are energized the same amount in the same direction, beam shift (pure translation of the beam) occurs (Fig. 192). If the upper and lower coils are not adjusted equally, beam tilt occurs (Fig. 193).

D. Objective Lens

After the beam is produced by the gun, focused by the condenser lens system, and centered with the deflector coils, it interacts with the specimen, which is inserted into the objective lens assembly. The objective lens both focuses and magnifies the specimen image.

Located below the specimen plane, there is an objective aperture assembly that contains a series of user-selectable apertures of different diameters (e.g., 15, 30, 50, 70 μm). Large objective apertures give little contrast and are not subject to much contamination. Small objective apertures offer increased specimen contrast but become contaminated more readily. The objective aperture eliminates the most widely scattered elements of the electron beam emerging from the specimen, which would cause something similar to flare in the glass optical system of a 35-mm camera from

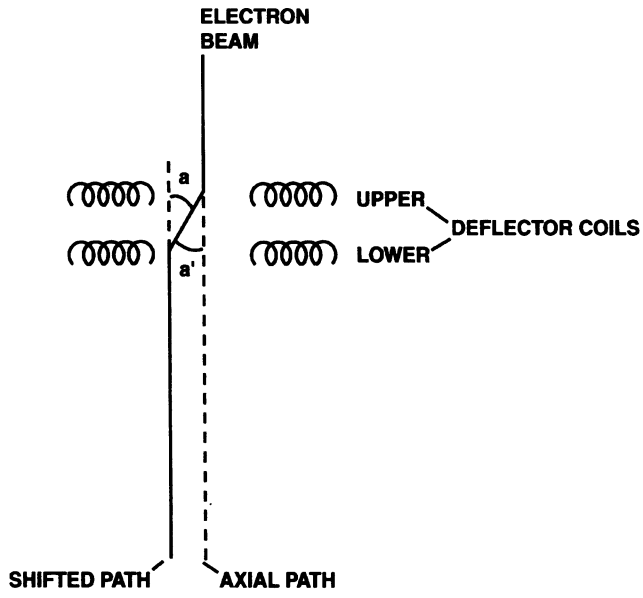

Figure 192. Beam translation. The upper deflectors move the beam through angle a, while the lower deflectors move the beam through an exactly equal but opposite angle a′.

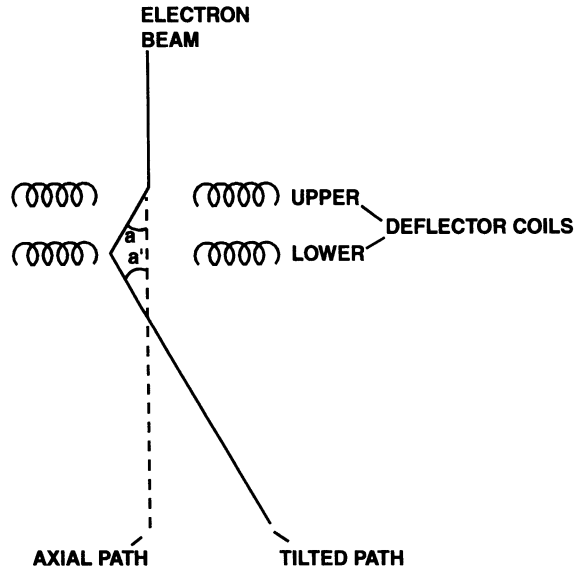

Figure 193. Beam tilt. The upper deflectors move the beam through angle a, while the lower deflectors move the beam through an exactly equal angle a′ in the same direction.

light being reflected by internal lens surfaces, leading to decreased image contrast. If a plastic section is viewed in a TEM with no objective aperture in place, the contrast will be extremely low, and the section will likely be severely damaged by the electron beam, often "popping" as it is examined.

An objective lens astigmatism corrector is associated with the objective lens (Fig. 194) and typically consists of a series of eight electromagnetic coils that are energized in pairs to adjust for any inherent asymmetry in the lens or the objective aperture being used.

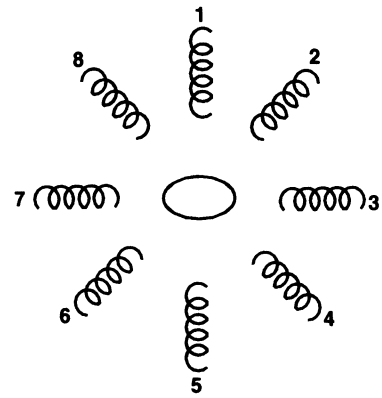

Figure 194. Objective lens stigmator. Eight concentrically arranged deflector coils are shown around a beam path that is normal to the page and in the center of the coils. More current is provided to coils 1, 2, 4, 5, 6, and 8, and less to coils 3 and 7 to achieve the asymmetric beam distribution shown in the center.

As objective apertures are used, they are subject to minute amounts of contamination from materials that outgas from lubricants and seals within the microscope column as well as materials vaporized from the specimen itself. If the electron beam is brought to a fine spot on an average plastic section, producing adequate illumination at high magnification, subsequent examination of the exposed area with a low magnification will reveal that the area under the intense, focused beam at a high magnification, appears lighter than the surrounding area. This effect may be caused by the electron beam evaporating part of the section, thus thinning the plastic. Some of the evaporated specimen can contaminate the objective aperture, which affects the electron beam, but this contamination can be compensated for by the use of the objective lens stigmator if not too severe.

Two types of stigmators may be encountered. The older, less frequently seen type consists of a set of knobs called the azimuth and amplitude controls. The former selects the direction of applied astigmatism, while the latter determines the magnitude of the applied effect.

Most current microscopes have a simple X–Y type of astigmatism correction system. By adjusting two knobs (X and Y), thereby adjusting the amount of applied astigmatism in the X and Y directions, inherent astigmatism is countered with applied astigmatism to produce a symmetric image.

E. Diffraction Lens

The first lens in the projection system (those lenses that magnify but do not focus the image of the specimen) is called a projector lens, an intermediate lens, or a diffraction lens. This lens is capable of producing an extremely low-magnification image such that the objective aperture can be viewed. This procedure allows the objective aperture to be centered around the electron beam and is the most common use of the diffraction setting for biologists. In addition, this lens can be used to produce low-angle diffraction patterns of crystalline structures to help identify their chemical composition (see Beeston *et al.*, 1972, for further discussion).

F. Projector System

This system typically is considered to consist of all lenses that magnify the image produced by the objective image. Lenses have names such as diffraction, intermediate, projector, mini-lens or supplementary lens. The semantics are less important than the functional characteristics. All of these lenses magnify the specimen image produced by the objective lens. It is important to remember that each lens inverts the image it receives from a previous lens. Thus, as lenses are turned on and off, the image can be rotated up to 180°. Most magnification is achieved by altering the strength of the intermediate lens (usually the first projector lens). High magnification is possible with a TEM because of the multiplying effect on the image size of each magnifying lens in the system. With a TEM possessing an objective lens and two projector lenses, the total magnification (MT) can be calculated:

$$MT = MO \times P1 \times P2$$

where MO is the magnification of the objective lens, P1 is the magnification of the first projector lens, and P2 is the magnification of the second projector lens. If MO is 50, P1 is 250, and P2 is 40, then MT is 500,000.

G. Camera System

Most TEMs sold in the United States employ a camera system consisting of metal film cassettes designed for $3\frac{1}{4} \times 4$ in. (8×10 cm) sheet film with a plastic base or, formerly, glass plates coated with the same film emulsions. These fine-grain, large format negatives suffer no loss in resolution when enlarged up to 3–4 ×, allowing sharp 8×10 in. (20×25 cm) prints to be produced. The camera is located below the viewing screen and may contain over 50 sheets of film.

Another camera available for many microscopes is a 35-mm system located above the viewing screen. This system is commonly found on older microscopes with a limited sheet film capacity. The smaller-format film cannot be enlarged to 8×10 in. (20×25 cm) size without any evident loss in sharpness and increased graininess. In addition, defects on the negative surface such as scratches and dust are more evident than with large format film.

Zeiss developed a fiber optic plate for the Zeiss 109 introduced in the early 1980s. In conventional camera systems where the film is put into the vacuum of the column, the gelatin of the photographic emulsion can become somewhat hydrated from the air and cause problems for the high-vacuum system in a conventional TEM. To solve this problem and to maintain an extremely clean column, Zeiss designed their camera system so that the film was outside the vacuum system. Photographs were taken with common 120-size films, allowing quick adjustments for materials of differing contrast by changing to different types of readily available emulsions. The film was firmly pressed against the fiber optic plate at the bottom of the viewing chamber, and electrons striking the plate caused photons to be emitted from the bottom of the plate, thus exposing the film. Various microscopes are now equipped with digital cameras that allow direct acquisition of digital images. These can be archived in computers and manipulated with various software programs. At the present time, digital images still have about 10-fold lower resolution (fewer pixels per unit area) than are obtainable with film. There are also some practical limitations to the number of high-resolution images that can be stored and quickly retrieved with various common media, such as CDs and Zip™ disks. As storage-device size and image-retrieval time improve, photographic emulsions will probably be supplanted by digital methods for most applications.

H. Specimen Holders

Specimens are inserted into the TEM column with either top-entry or side-entry holders (Fig. 195). The former allows greater stability and resolution while the latter offers easier specimen manipulation within the column. Some microscopes have goniometer-equipped stages that allow the specimen to be tilted in one plane over 60° to produce stereo pairs and an oblique section to be moved until it is normal to the beam. If the tissue section has a smudged tangential section of a membrane, it often can be tilted sufficiently to give a cross-sectional view that has

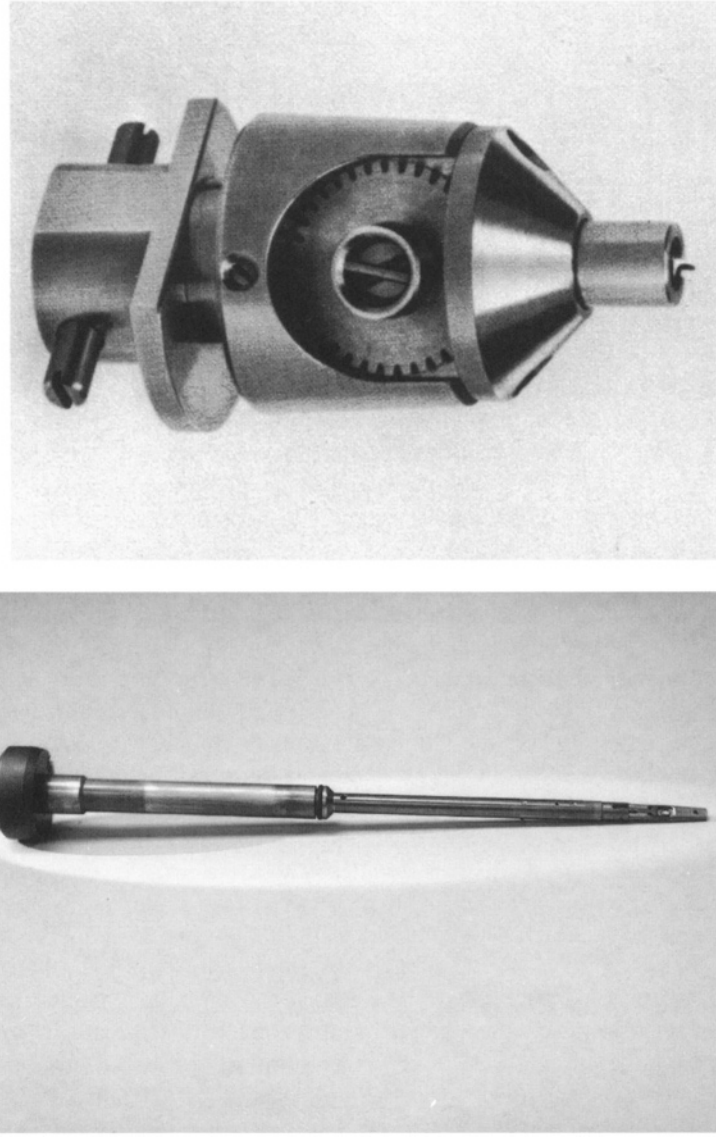

Figure 195. Top versus side-entry specimen holders. Top: A top-entry holder for a Zeiss EM-900 TEM (Courtesy of Carl Zeiss, Inc.) Bottom: A side-entry specimen holder from a Philips 410LS TEM.

a clear dark–light–dark "railroad track" membrane image. Microscopes with simple biological stages also usually have provisions to tilt the specimen up to 10°. Goniometer stages can also be provided with specimen holders that will rotate a grid through 360°, so that an item of interest can be effectively located at the proper position to take advantage of the tilting plane of the goniometer.

I. Viewing System

Different TEMs have a variety of small focusing screens, large viewing screens, and phosphor screen coatings. Some of the phosphors exhibit a finer grain than others. Some have a yellowish color, and some are greenish. Screens have scribe marks to show the approximate outline of the boundaries of the film in the camera beneath and various marks to designate the center of the screen, which can also be used as size references when calibrated properly. Unfortunately, the screens become less bright with time, and the various markings on them can become indecipherable. It is recommended that the viewing ports be covered between use to prevent fading of the phosphor screen coating.

The screens are used as meters for the camera system to provide reproducible exposures. In most systems the large viewing screen can be used to meter the entire field of view, or the small focusing screen can be used as a "spot" meter to read a specific portion of the field being viewed. These systems determine exposures based on electrons hitting the screen and the current they generate as they flow to ground potential. Other systems have photoelectric sensors above the viewing screen that read light emitted from the phosphor on the screen after electrons impinge upon it. Both types of metering systems work quite well.

The binocular microscopes provided for focusing on the viewing screen generally magnify the image projected onto the screen an additional 10 times. Thus, when the microscope is set for a 31,000× enlargement on the film plane, the magnified image viewed with the binoculars will be approximately 310,000×. The image on the viewing screen will not be quite 310,000 because it is above the film plane, which is the basis for the magnification calibration in most microscopes. Unfortunately, the grain size of the phosphor decreases the actual resolution possible with the viewing system. Agar (1957) reported that the actual resolution of the viewing system is limited to approximately 35 μm because of the size of the phosphors on screens. This explains why photographs reveal more detail than can be perceived while actually viewing specimens with the microscope.

J. Detectors

A variety of add-on units can be attached to TEMs to detect secondary and backscattered electrons, characteristic X-rays (energy dispersive spectroscopy, or EDS), or losses in electron energy after interaction with the specimen (electron energy loss spectroscopy, or EELS). They are attached to various ports on the microscope column and will be discussed in the chapter on microanalysis.

VI. OPERATION OF THE TEM: DECISION MAKING

Now that all the basic components in the illumination, imaging, and viewing system have been described, it is possible to examine the various adjustable components and to decide what settings are useful for general TEM operation when working with typical biological specimens.

A. Accelerating Voltage

With a typical microscope equipped to provide accelerating voltages from 40 to 100 (120) kV, it is useful to consider what will happen when the accelerating voltage is raised or lowered. The highest voltage allows the best specimen penetration, least specimen heating and damage (because of decreased inelastic electron scattering), and the brightest screen image, but the lowest contrast with an average specimen. At the same time, there is a greater possibility of decreased stability at a high voltage because of contaminants within the electron gun, leading to high-voltage discharge.

Both the screen phosphors and the photographic emulsions used for electron microscopy are optimally efficient at about 80 kV, so most microscopes are operated at this potential. Thicker specimens often require a higher voltage, while low-magnification work with specimens of low contrast where ultimate resolution is not critical can be improved by utilizing a lower voltage.

B. Choice of Beam Current and Bias

For the greatest filament life, the current should be adjusted to a point just slightly below saturation. Most microscopes have self-biased filaments, so the bias will automatically be adjusted properly as the current is increased. If the bias is selectable, keep the bias as low as possible while maintaining a good filament saturation and adequate illumination. An increased beam current will significantly lower the filament life, so a minimal current is recommended (10–20 μA). At higher magnifications where illumination becomes critical, it is often necessary to increase the beam current.

C. Condenser Settings

As previously mentioned, the upper condenser lens is generally set for maximum illumination, and the aperture is nonadjustable. The lower condenser, which is often labeled intensity or brightness, is continuously variable and is frequently adjusted during microscope operation. As magnification is increased, the lower condenser is adjusted for a smaller spot (of illumination) size. At a lower magnification, the spot is spread to cover the screen to prevent undue erosion of the specimen or damage to the screen from excessive beam intensity. The lower condenser lens is equipped with apertures of several sizes. An aperture of about 150 μm provides good image quality and good illumination.

D. Objective Settings

Like the second condenser lens, the objective lens has a series of apertures. They may be small holes bored in molybdenum or platinum strips or discs. Alternatively, they may be plastic films coated with a noble metal (e.g., gold) known as thin-film apertures. The latter are self-heating and are reputed to stay cleaner longer than metal apertures.

The second to the largest aperture (usually 50–70 μm) is used for most samples, providing sufficient contrast and adequate illumination. If the specimen suffers from too little contrast, a smaller aperture may be selected to increase contrast. If small apertures are used routinely,

however, they tend to become contaminated and eventually cannot be stigmated. They will then have to be removed and replaced or cleaned (if they are metal apertures) by heating in a vacuum evaporator to evaporate contaminants. Increased contrast can also be achieved by lowering the accelerating voltage of the TEM.

Every time the microscope is used, it is important to center the objective aperture because an off-center aperture can cause astigmatism in the image.

The focus controls on the TEM regulate the current to the objective lens. There may be a series of focusing knobs (typically six) with pairs nested together. On one end of the series will be the coarsest focusing knob, and on the other will be the finest. A novel system introduced by Philips has only two knobs, one selecting the size of the focus step, and the other selecting how many of those steps to make. At low magnifications, large focus steps are selected, while at high magnifications, small focus steps are used.

E. Alignment

In order to produce the illumination and image clarity expected from modern high-resolution TEMs, the microscope column must be carefully aligned, particularly after a filament change. Each manufacturer has different instructions for this procedure that are fairly instrument-specific, but a general outline of the procedure can be applied to all microscopes. Older microscopes have more mechanical adjustments than current instruments, which have some mechanically prealigned components that are left untouched except in the unlikely event that the column is disassembled. Modern microscopes are electronically user-aligned on a regular basis except for mechanical filament and aperture centering. The latest generation of microscopes has computers that are capable of evaluating their alignment parameters and to adjust them appropriately after self-diagnosis. At the least, an attached computer can record all the user-selected operational parameters for the microscope, allowing the users to switch rapidly between apertures, accelerating voltages and operational parameters while maintaining optimal optical characteristics. This is a vast improvement on older systems where a user interested in changing accelerating voltage to alter contrast would have to totally realign all the adjustable settings on the microscope visually, which could take an hour or two. A simple aperture change would also require some realignment.

It is critical to center the filament image, center the condenser aperture, stigmate the condenser lens, center the objective aperture, and stigmate the objective lens to obtain a high image quality. All of the other alignment steps are used to keep the image and/or illumination from sweeping all around the screen or completely off of the screen when changing magnification, focus, or illumination intensity. These latter adjustments do not affect image quality.

1. Filament Installation

Each manufacturer gives instructions for mounting a new filament within the Wehnelt assembly. The filament height is specified and should be adjusted carefully, as this setting will have an effect on the total illumination possible by determining how many of the liberated electrons will be able to enter the high-voltage field. Centering the filament over the aperture in the Wehnelt cap will also ensure that the maximum number of electrons will be accelerated down the column. Some manufacturers provide precentered filament assemblies, eliminating one of the preliminary alignment procedures for the user.

2. Finding the Beam

After installing a new filament, the high voltage is generally brought up stepwise through the various accelerating voltage settings, waiting until any high-voltage discharges are completed before moving up to the next higher setting. The discharges, which are caused by contamination such as dust in the gun area, are frequently audible but also can be monitored by observing the beam current meter. As the voltage is increased, the "dark" current on the meter will increase, which represents a small current induced in the filament by the high-voltage field. If the meter shows a large increase in current (typically the needle deflects to the stop at the high end of the scale), this large discharge should not continue for more than a few seconds. If it does, the voltage should be reduced to the next lowest setting until the current stabilizes. A momentary deflection several times over a minute or so is satisfactory, but the voltage should not be raised until the activity stops. Once the voltage has been brought to the maximum value (100 kV) and discharge has ceased, the voltage should be reduced to the operating value (80 kV). Then, the beam current is slowly brought up until illumination is visible on the screen. It is sometimes difficult to see any screen illumination because the filament is grossly misaligned or the beam is overly tilted. If the high voltage and current knob are turned up, but the current meter shows no current flow, the filament is either blown, or the filament contacts are not properly positioned. If the high voltage is turned on, and the beam current meter is showing increasing current flow as the beam current (filament) knob is turned up but the screen still does not show illumination, turn off all the lenses; this should yield a small, extremely intense spot of light projected onto the viewing screen. Do not leave this on the screen any longer than necessary, as it will burn the phosphor coating. Once this spot is located, the lenses can be turned on one at a time from the top of the column down until the spot vanishes again, which indicates that the last lens needs to be realigned until the illumination reappears. After illumination has been established with all the lenses turned on, return to the top of the column to continue the alignment procedures.

3. Beam Alignment

Once illumination is visible, bring the second condenser lens (intensity, C2, spot size) to crossover, which is the smallest, most intense spot of illumination visible on the screen. Next, increase the magnification to 3,000–5,000× for better visualization of the beam spot. Adjust the gun shift controls until the illumination on the screen is as bright as you can make it, then decrease the beam current until the spot of illumination breaks up into more than one image. Slowly bring the beam current up again until the spots begin to merge. If there is not a central spot with a halo around it, use gun tilt controls to center the illumination around the central spot. You may have to increase the beam current to keep the nonaxial component of the illumination visible as you center the halo around the central spot (Fig. 196). Once the halo is centered, increase the beam current until the halo converges with the central spot. Decrease the beam current slightly until a slight decrease in illumination is noted somewhere in the spot of illumination, which indicates slight undersaturation (thereby ensuring a longer filament life). At this point, the beam is aligned in relationship to the condenser lens assembly. Spread the beam (C2) until it fills the viewing screen.

4. Deflector Controls

Bring the beam near crossover by adjusting C2, and center the spot of illumination on the screen with the deflector controls.

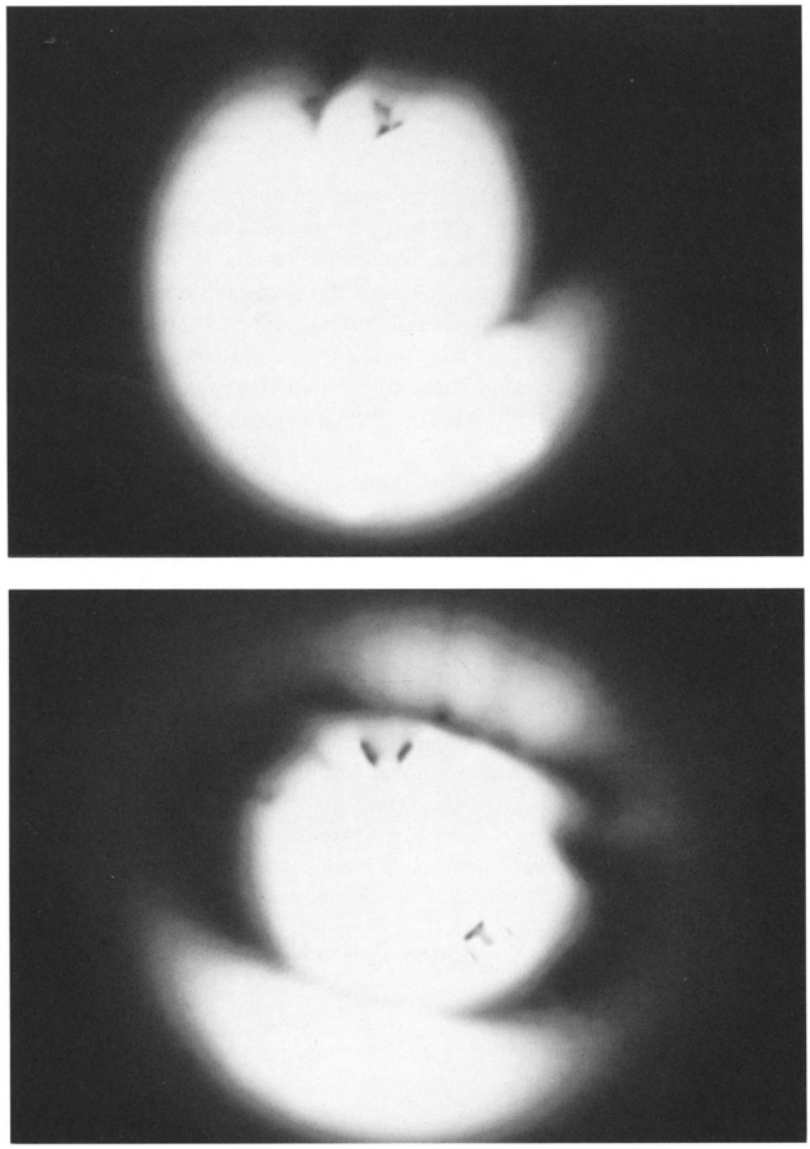

Figure 196. Image of an undersaturated filament. Top: Undersaturated and not centered. Bottom: Undersaturated, nearly centered. The dark spots in the center of the filament are defects in the tungsten filament due to aging (it had approximately 130 hr of use).

5. Condenser Assembly

Insert an appropriate condenser aperture into C2. The second to the largest is usually a good choice. Desaturate the filament so that the halo is once again visible at crossover, and make the image as sharp as possible by adjusting the condenser stigmator controls. Check to see if the condenser aperture is centered properly by sweeping C2 through crossover. If the spot of illumination on the screen moves from side to side, use the two condenser aperture centering controls to minimize

this motion. The spot should become larger and smaller as you sweep through crossover but should not move to the side if the aperture is centered. Spread the beam to cover the screen with C2.

6. Objective Lens

Insert the aperture of choice, usually the second aperture or one about 50–70 μm in diameter. Next, introduce a specimen of some sort. Bring the beam to crossover. Switch the lenses into the selected area diffraction (sometimes just called diffraction) mode. The carbon contained in the specimen will produce a diffraction pattern, which will be a series of concentric rings around a central, bright electron beam. The objective aperture then can be easily centered around the beam utilizing the centering controls on the objective aperture assembly on the column. Switch back to the nondiffraction (magnification) configuration for normal viewing.

After the aperture is centered, the lens and aperture can be stigmated as a unit. This is typically done at a magnification above where photographs are expected to be taken so that any minor astigmatism that remains will be imperceptible at the lower magnifications routinely used.

There are two major methods to stigmate the objective lens assembly. The first requires the insertion of a plastic film with minute holes in it (a holey grid, which can be commercially purchased or made as described in Chapter 7). The image is overfocused until a Fresnel fringe is visible around a hole in the plastic, and the stigmators are used to produce an even fringe around the hole.

If the microscope has the azimuth/amplitude type of stigmators, the stigmator is turned off so that the inherent astigmatism in the system is revealed (Fig. 197). Then, the stigmator is turned on, and the amplitude is turned up high enough so that the applied astigmatism is evident (Fig. 198). The orientation control is adjusted until the applied astigmatism is at 90° to the original inherent astigmatism. At that point, the amplitude knob is used to reduce the strength of the applied astigmatism until the Fresnel fringe around the hole is the same thickness all around the hole. Bring the image closer to focus (narrower Fresnel fringe) and repeat the process. Ideally, the barest perceptible fringe should vanish uniformly from around the hole with one click of a very fine focus step.

If using an X/Y type of stigmator, the same rules apply, except that the fringe is adjusted with the X/Y controls until it is even around the hole.

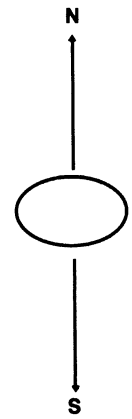

Figure 197. Inherent astigmatism.

Figure 198. Applied astigmatism.

Another, more universally applicable method for stigmation can be done at any time with any kind of specimen. Take the magnification above the normal working level to approximately to 100,000 ×, and focus on the grain of the plastic or some graininess in the specimen. Adjust the objective stigmators until the grain is as sharp as possible. Go closer to focus and repeat. Ideally, the grain should appear as points rather than short streaks. This technique is known as grain focusing.

7. Projector Lenses

In older microscopes, the projector lenses have to be aligned to be in the same axis as the previously aligned gun, condenser and objective lens assemblies, but most modern microscopes have these elements prealigned at the factory, so they do not need adjustment unless the column is disassembled. Any apertures within these lenses are generally fixed and therefore require no separate adjustment. The only exception to this is the diffraction lens aperture, which must be adjusted for critical low-angle diffraction studies.

8. Voltage Center and Current Center

The generalized alignment procedure described above will result in a microscope capable of producing high-quality images. However, without a few supplementary steps to align the voltage center (high voltage) and current center (lenses), the image will suffer from slight chromatic aberration (voltage center misalignment) and spherical aberration (current center misalignment). Under most conditions with biological specimens, these will not be perceptible.

As mentioned before, another set of alignment procedures specified for particular instruments does not actually improve image quality but makes the instrument more user friendly. Thus, when the image is swept through focus, the image stays in the center of the screen, and when the magnification is changed, the image and illumination stay centered.

F. Taking a Photograph

Taking a photograph requires attention to detail, as any omission in the following steps can seriously compromise the quality of the images produced. The first step is to focus the ocular system on some detail (dust) on the focusing screen. Make sure that focusing is *not* done on the specimen image. Next, the magnification is selected, and the image is focused using the electronic focusing controls. Wobblers are sometimes useful to determine focus at low magnifications where the eye tends to compensate, suggesting that images are in focus in more planes than they truly are. High-magnification focusing is generally not helped by the use of wobblers. The image is then framed within the scribed marks on the viewing screen describing the dimensions of the film format being used. The beam is brought toward crossover with the intensity (spot size) controls so that the periphery of the illumination can be seen, which is centered with the deflection controls. Next, spread the beam until the metering system indicates a proper illumination level for a photograph to be taken. Take the photograph.

Negative density (darkness) can be determined by exposure settings on the microscope or processing details such as developer strength, amount of agitation, type of developer, and the temperature of the developer. To ensure consistent results, film should be exposed and developed consistently (see Chapter 15 on photography). The microscope photographic metering system should be set such that an average specimen consisting of silver–gold sections of a typical tissue stained in a normal fashion produces a negative of average density. This means that the negative will print well on a middle-grade paper. Since slight variations in staining procedures and section thickness can produce materials with different levels of contrast, a microscope set to produce an "average" negative will yield a product that can be printed with more or less contrast to accommodate these slight specimen variations.

G. Specimen Radiation Dose

Grubb and Keller (1972) examined the beam damage to certain polymers in the TEM and the consequent damage to image quality. Keller was also quoted by Agar (1974) as having determined that 4,000 Mrad of radiation exposure results from the following conditions:

1. 0.01 sec at high beam current in a TEM
2. 20 min at low beam current in a TEM
3. 5 weeks inside a nuclear pile
4. 5 years near a 1-Curie cobalt 60 source of X-rays
5. Exploding a 10-megaton hydrogen bomb 30 yds away.

These numbers should make it clear that a TEM is a source of intense irradiation that can cause severe specimen damage. In addition, the production of X-rays makes it imperative that, whenever the integrity of a TEM column is disturbed, a check for radiation leakage is performed immediately.

H. Microscope Calibration

At various times, particularly with older TEMs, it becomes necessary to check the accuracy of the magnification steps on a particular instrument. It is also sometimes necessary to have

a specimen that will show clearly if the TEM is exhibiting any slight spherical aberration. As mentioned previously, when a microscope is installed, the usually guaranteed 0.344-nm resolution must be established by photographing a resolution standard (graphitized carbon).

There are a variety of resolution standards (shadowed metals such as gold–palladium, silicon monoxide gratings, biological crystals, graphitized carbon, etc.) available from most of the vendors for electron microscopy supplies. Each vendor supplies detailed instructions on how to utilize the individual standards. The most commonly used ones are described below.

1. Grating Replicas Mounted on Grids

Silicon monoxide grating replicas mounted on grids may be purchased with 1,134 parallel lines/mm, 2,160 lines/mm, or 2,160 crossed lines/mm. The first two replicas are usually photographed at several magnifications, and then the distance between the lines on the negatives is measured with an ocular micrometer to see if the actual magnification agrees with that shown on the magnification readout on the TEM. If the actual values are within 5–10% of those indicated on the TEM, the microscope can be considered to be within normal tolerance limits. If it is suspected that the microscope is exhibiting some sort of electronic stability problem resulting in the magnifications varying from photograph to photograph, suspensions of fragments of the silicon monoxide replicas can be put directly on specimens being examined, and a photograph can be taken, showing the item of interest alongside the replica for absolutely accurate magnification calibration directly on the specimen.

The crossed grating replicas will clearly show spherical aberration (pincushion or barrel aberrations will be clearly evident).

2. Catalase Crystals

Suspensions of these protein crystals may be purchased from some vendors and utilized much like the suspensions of silicon monoxide gratings, except that they exhibit 17.2-nm spacings between the lattice elements for higher resolution work.

3. Latex Beads

These are available in numerous sizes (e.g., 0.087 μm, 0.091 μm, ..., 25–55 μm), but are usually too large to be of much use in TEM work (they are very useful in scanning electron microscopy applications).

4. Graphitized Carbon

Grids may be purchased from various vendors consisting of a polymer film substrate upon which carbon black has been dispersed. These specimens exhibit 0.34-nm lattice spacing and are used most frequently to test the ultimate resolution of newly installed TEMs.

REFERENCES

Agar, A.W. 1957. On the screen brightness required for high resolution operation of the electron microscope. *Br. J. Appl. Phys.* 8: 410.

Agar, A.W. 1974. Operation of the electron microscope. In: A.W. Agar, R.H. Anderson, and D. Chescoe (eds.), *Principles and practice of electron microscope operation* (pp. 166–190). North-Holland, Amsterdam.

Beeston, B.E.P., Horne, R.W., and Markham, R. 1972. Electron diffraction and optical diffraction techniques. In: A.M. Gauert (ed.), *Practical methods in electron microscopy* (Vol. 1). North-Holland, Amsterdam.

Ghadially, F.N. 1985. *Diagnostic electron microscopy of tumors*, 2nd edn. Butterworths, London.

Grubb, D.T., and Keller, A. 1972. Beam induced radiation damage in polymers and its effect on the image formed in the electron microscope. *Proc. 5th Eur. Conf. Electron Microsc.*, Manchester, p. 554.

Haguenau, F., Hawkes, P.W., Hutchison, J.L., Satiat-Jeunemaître, B., Simon, G.T., and Williams, D.B. 2003. Key events in the history of election microscopy. Microsc. Microanal. 9:96.

Hainfeld, J.F. 1977. Understanding and using field emission sources. *Scan. Electron Microsc.* 1: 591.

Hawkes, P.W. (ed.). 1985. *The beginnings of electron microscopy*. Academic Press, New York.

Knoll, M., and Ruska, E. 1932. The electron microscope. 2. *Physik*. 78: 318.

Meek, G.A. 1976. *Practical electron microscopy for biologists*, 2nd edn. John Wiley & Sons, New York.

Robinson, D.G., Ehlers, U., Herken, R., Herrmann, B., Mayer, F., and Schurmann, F.-W., 1987. *Methods of preparation for electron microscopy*. Springer-Verlag, Berlin.

Slayter, E.M. 1976. *Optical methods in biology*. Robert E. Krieger, Huntington, New York.

10

Vacuum Systems

Vacuum is crucial to the proper operation of an electron microscope since electrons, the illumination source, are easily deflected by molecules of gas and thus are lost to the image-forming process. In order to have a working understanding of the vacuum system, it is necessary to examine the different types of vacuum sensors, or gauges, and vacuum pumps utilized in electron microscopy. This is especially important because various gauges and pumps can sustain damage if connected to the system being evacuated at an improper vacuum level.

To begin our discussion, we need to consult Table 16, which illustrates the various units for vacuum and indicates their relationships. Historically, the field of electron microscopy has expressed vacuum primarily in terms of Torr, while most vacuum physicists have used Pascal units (Pa). Another vestige of the past is found with some sputter coaters, which are calibrated in microns (μ), which is also an outdated unit of vacuum measurement. The field of electron microscopy is rapidly converting to adopting the language of the vacuum physicists, so this text has attempted to make this conversion, with reference to the older vacuum terminology so that those of us trained in earlier times can still quickly grasp the vacuum information. Two good books on vacuum technology as it applies to electron microscopy are those by Stuart (1983) and O'Hanlon (1980).

A typical transmission electron microscope produces a vacuum inside the column that exceeds 1.33×10^{-3} Pa (10^{-5} Torr), and instruments with ion getter pumps can achieve 1.3×10^{-7} Pa (10^{-9} Torr). In addition to indicating a high-vacuum (low-pressure) condition, what does this range mean in terms of imaging electrons and of their journey to the viewing screen and the phosphors that they excite? One cubic centimeter of air at 1.33×10^{-4} Pa (10^{-6} Torr), in a conventional TEM column, contains 3×10^{10} molecules of various types (Table 17). At this pressure, an electron has a mean free path of at least 50 m at room temperature. In other words, an electron can be

Table 16. A Comparison of Vacuum Units

760 Torr = 1 atmosphere
1 Torr = 1 mmHg
1 μ (of Hg) = 10^{-3} Torr
1 Pa = 133.3 Torr
100 mbar = 1 Pa

Table 17. Major Constituent Molecules of Air

Constituent	% (of Volume)
Nitrogen (N_2)	78.08
Oxygen (O_2)	20.95
Carbon dioxide (CO_2)	0.03
Argon (Ar)	0.93
Other moieties	0.01
	100

expected to travel a distance of at least 50 m without encountering and interacting with any other electrons or atomic nuclei. Of course, when the specimen is inserted into the electron beam, the probability of a specimen/electron encounter is quite high, and the electrons that penetrate the specimen will ultimately encounter the viewing screen. What is important is that random scattering of the electrons is very unlikely under the vacuum conditions described.

I. TYPES OF GAUGES

A. Direct Reading

Direct-reading gauges are used to monitor the water pressure feeding the cooling system for diffusion pumps and electromagnetic lenses. They also monitor positive air pressure used to hold various valves open in many electron microscopes or the low vacuum produced in holding tanks devoted to valve operation in other microscopes.

Diaphragm-type gauges have a needle attached to a flat membrane of metal or polymer that moves as pressure increases or decreases. Bourdon-tube gauges are found in the same applications and consist of a curved, thin-walled metal tube attached to a needle. As pressure increases or decreases in the tube, the needle is deflected. With both gauges, the deflection of the needle is read on a scale on the meter face to monitor pressure. Neither of the gauges are instruments of significant precision, but they provide enough information to fulfill the needs of their applications.

B. Indirect Gauges

1. Thermoconductivity Gauges

These gauges measure vacuum by monitoring a pressure-dependent quality of gas, the capability of air to conduct heat. This type of gauge is used at relatively low vacuum and is based on two principles: (1) heat will be conducted away from a heated wire by molecules of air and (2) current flow in a wire is inversely proportional to the heat of the wire. In other words, a higher heat results in a greater resistance and thus less current flow in a wire. Thermoconductivity gauges are used to monitor vacuum systems from a pressure of one atmosphere down to about 1.33×10^{-1} Pa, or 10^{-3} Torr. They are not damaged by exposure to atmospheric pressure.

Thermocouple gauges (Fig. 199) are the least complicated thermal gauges, consisting of a solid-state thermocouple device attached to a wire through which a constant current is being passed. The passage of current through the wire heats the wire. The more air present, the more heat is conducted away from the wire, and the thermocouple conductivity decreases, causing the DC microammeter needle to move to the bottom of the scale. As air is evacuated from the system, the heat of the wire cannot be conducted away as effectively, so the wire temperature increases, the thermocouple passes more current to the DC microammeter, and the meter needle swings toward the high end of the scale.

A slightly more complicated version of the simple thermocouple gauge is the Pirani gauge (Fig. 200). This gauge also measures the capability of air to conduct heat away from a heated wire. In this case, the heated wire is one of four resistances (the other three are constant-value resistors)

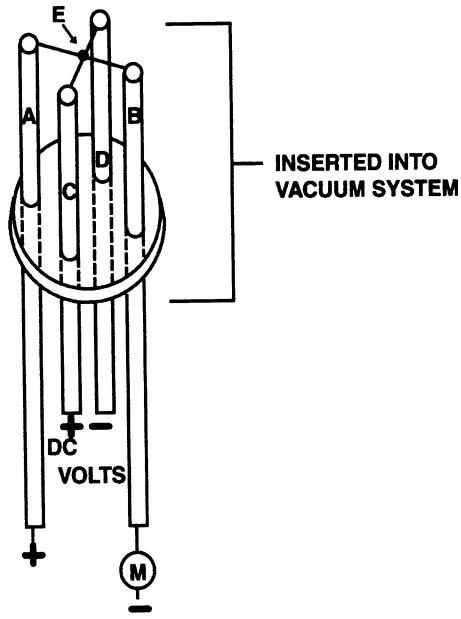

Figure 199. Diagrammatic sketch of a thermocouple gauge. The solid-state thermocouple device (E) is electrically connected to terminals A and B. It is also in thermal contact with the wire connected to terminals C and D, which is heated. The microammeter (M) reads the amount of current flow through the thermocouple.

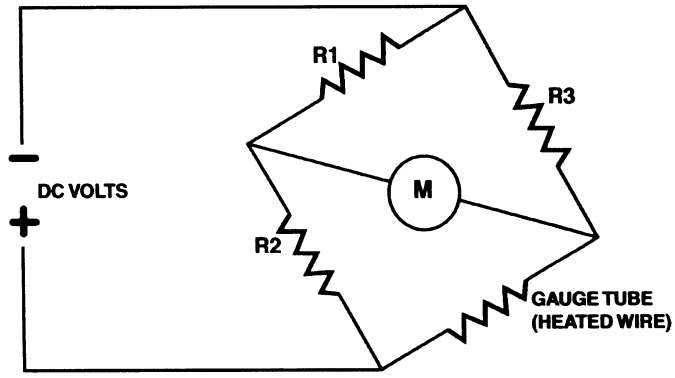

Figure 200. Diagrammatic sketch of a Pirani gauge. Resistors at R1, R2, and R3 are balanced by the heated wire in the gauge tube at atmospheric pressure. The microammeter (M) measures current flow as the Wheatstone bridge becomes unbalanced when higher concentrations of atmospheric gas in the gauge tube conduct heat away from the gauge wire.

in a Wheatstone bridge with an attached DC microammeter. Usually, a constant voltage is supplied to the Wheatstone bridge, and the fixed resistors are selected so that the meter registers very low current flow at high vacuum. When the chamber is at atmospheric pressure, the heat is removed from the wire and transferred to air molecules, which unbalances the Wheatstone bridge. The more air present, the cooler the wire becomes, and the more current it will pass, causing the microammeter gauge to deflect to the high end of the scale.

2. Ionization Gauges (Cold Cathode Ionization Gauges)

Ionization gauges are used to monitor ultimate vacuum in a TEM by measuring another quality of gases: the capability of air molecules to conduct an electrical current. The standard type encountered is the Penning gauge (Fig. 201). It is used in a high vacuum range (greater than 1.33×10^{-1} Pa, or 10^{-3} Torr) produced by diffusion pumps, turbomolecular pumps and ion getter pumps. Exposure to atmospheric pressure can damage an ionization gauge, so it is important to turn an ionization gauge on only after the chamber has been switched over to high vacuum. The gauge consists of a wire anode loop maintained at a potential of about 2–10 kV in relationship to the grounded cathode electrode, typically the outside of the sensing tube. The whole tube is inserted into the vacuum chamber and is surrounded by a strong permanent magnet. The high voltage causes electrons to be emitted from the cathode, which ionize any gas molecules in the tube. The positive ions formed follow a spiral path to the cathode because of the external magnet. This spiral path increases the path length to the cathode, thus causing more collisions with gas molecules and the production of more ions, consequently increasing current flow between the electrodes. As the vacuum increases, ionizable molecules decrease in number, and current flow in the ionization chamber decreases, as shown by the Penning gauge.

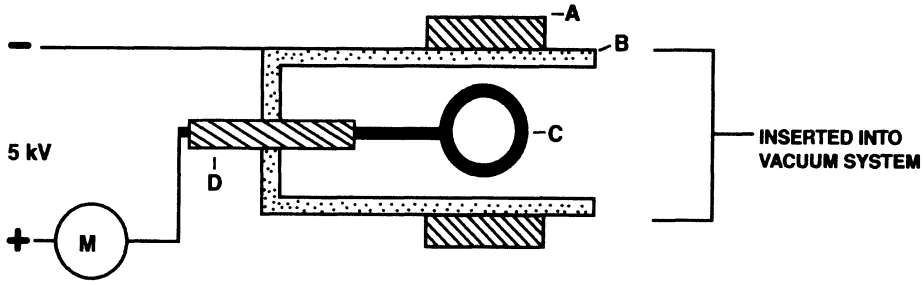

Figure 201. Diagram of a Penning (cold cathode discharge) gauge. A permanent magnet (A) surrounds the grounded gauge tube (B) connected to the vacuum chamber. The positively charged wire loop anode (C) is connected to a microammeter (M) and passes into the tube through the vacuum-sealed insulator (D).

II. VACUUM PUMPS

A. Types of Pumping Systems

Compressive, or mechanical, pumps function by compressing a given volume of gas, reducing its volume, and then expelling the compressed gas through an exhaust port. An example of this type of pump is the rotary (often called mechanical) pump, which is used to "rough out" a chamber before connecting the chamber to a high-vacuum pump. Roughing is the process by which a chamber is brought from atmospheric pressure down to about 1.33×10^{-1} Pa (10^{-3} Torr), at which point a pump capable of achieving a higher vacuum is attached to the chamber immediately after disconnecting the rotary pump.

A second type of compressive pump, the scroll pump, has been introduced in recent years to substitute for a conventional oil-filled rotary pump when an absolutely oil-free pumping system is needed.

A third type of compressive pump is the turbomolecular pump, which can reach the ultimate high vacuum level necessary for proper operation of an electron microscope. In a typical system, a rotary or scroll pump evacuates the compressed gas molecules from the exhaust port of the turbomolecular pump.

Entrapment is a totally different mechanism to remove air molecules from a chamber. Rather than compressing the gas into a small volume by mechanical means and expelling it from the system, air is entrapped within microscopic oil droplets within the diffusion pump and is ultimately removed by another lower vacuum pump.

Entrainment pumps, such as ion getter pumps, function by ionizing and accelerating gas molecules with high voltage and causing them to strike and attach to the sides of a chamber at high velocity, or by condensing gases onto a cold surface to which they stay attached until the chamber warms up (cryopumps).

These three entrapment or entrainment systems require other pumps, typically mechanical pumps, ultimately to remove the entrapped molecules from the entire system. When a pump is used to remove air from another pump, the latter can be said to be "backed" by the former. In some systems, a mechanical pump produces a vacuum on a holding, or buffer tank which is, in turn, used to back a pump producing a higher vacuum on the vacuum chamber.

B. Mechanical/Rotary Vane Pumps

These pumps consist of a rotor in which are housed two spring-loaded scraper blades. The edges of the blades are typically faced with Teflon™. The blade edges run within an eccentric chamber whose walls are lubricated from a reservoir of oil. One side of the eccentric chamber is attached to the chamber to be evacuated, while the side where the gas is exhausted has a small flapper valve, which is opened by the pressure of the gas, thus allowing it to be discharged from the pump.

A single-stage pump has one rotor, allowing it to achieve a vacuum of about 1.33×10^{-1} Pa (10^{-3} Torr) as shown in Fig. 202. These are typically belt driven from an electric motor.

A more efficient configuration is the two-stage mechanical pump wherein two rotors are connected in a series, one attached to the chamber being evacuated, which in turn is backed by the second rotor (Fig. 203). Two-stage pumps are typically directly driven by electric motors due to the high load on the motor. They can achieve vacuum of up to 1.33×10^{-2} Pa (10^{-4} Torr).

A rotary pump will pump about 500 l/s from a chamber. Such pumps most frequently contain hydrocarbon oils, but they may have more complex synthetic lubricants containing silicone, chlorofluorocarbons or fluorocarbons (O'Hanlon, 1980). If the pumps are to be used in situations (plasma etching) utilizing oxygen, they must have appropriate oils to avoid the risk of explosion.

Both single- and two-stage mechanical pumps are subject to contamination by any solvents being evacuated such as acetone, alcohols, and water. As the gases are evacuated from the vacuum chamber and compressed within the rotor assembly, they become cooled and can condense on the pumping chamber walls and finally mixed with the pump's lubricating oil. The first symptom of a problem is usually less pumping efficiency in the system. If the oil in the pump's sight glass appears turbid or discolored, the oil has become contaminated. If pumping efficiency has dropped but the oil still looks reasonably clean, the pump may be "ballasted" if so equipped. These pumps possess a ballasting valve located just before the pump's exhaust port. The valve is opened slightly for 30 min to an hour to help the system purge the contaminating substances. When this valve is opened a small amount, it admits air just before the exhaust side of the pump, thereby decreasing the ultimate vacuum of the system. However, at the same time, the solvents dissolved in the

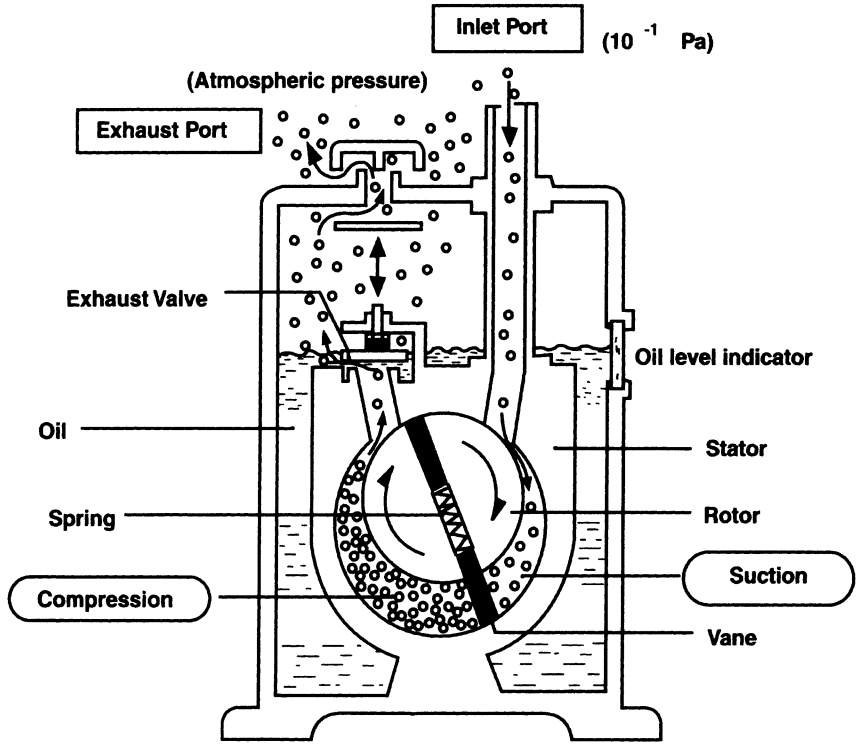

Figure 202. Diagram of a single-stage rotary pump. (Courtesy of JEOL USA, Inc.)

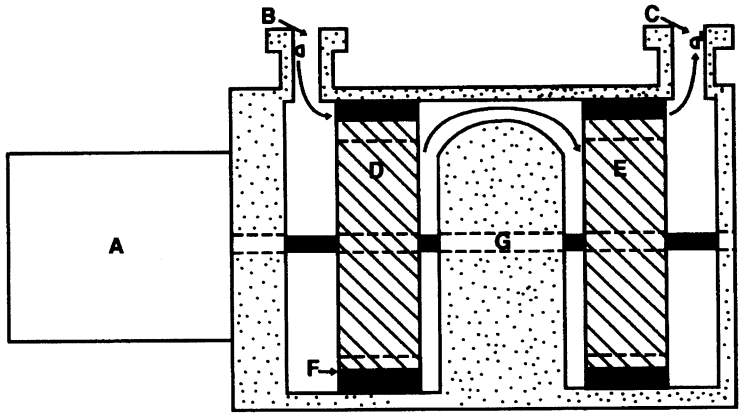

Figure 203. Diagram of a two-stage rotary pump. A direct-drive motor (A) with a long drive shaft (G) drives two rotors (D, E) located in two eccentric chambers containing oil through which spring-loaded scraper blades (F) pass. Gas enters through port B (a), is compressed by the first rotor (D), passes into the second chamber, and is further compressed by the second rotor (E) before being exhausted (a′) through port C.

lubricating oil will be vaporized and exhausted from the system. When it is determined that most of the solvents have been pumped out, the ballasting valve is closed, at which time the vacuum system should return to normal values. If the chamber still cannot be brought to the proper advertised value, the oil may be hopelessly contaminated with solvents, necessitating removal of the pump oil and replacement with high-quality mechanical pump oil. If a pump has difficulty starting after being stopped even though it has been properly vented, it usually indicates that the

oil should be changed even if it looks all right. Always vent mechanical pumps that are not turned on. If they are attached to a vacuum chamber below ambient air pressure, the pump oil will be sucked into the vacuum chamber.

A last problem to consider is "backstreaming." All pumps, when they are close to their pumping limits and have achieved their maximum vacuum on a chamber, are capable of actually releasing their oil into the vacuum chamber in minute quantities. Mechanical pumps with worn scraper blades can backstream badly, indicated by an oil film in the chamber being evacuated. When roughing a chamber, it is good practice to disconnect the mechanical pump shortly after reaching its ultimate vacuum to decrease the likelihood of backstreaming.

C. Diffusion Pumps

Diffusion pumps are deceptively simple in construction (Fig. 204). They consist of a metal can containing a stack of inverted funnels held on a central core. Directly below the flange that bolts to the chamber to be evacuated, the pump may have a series of angled baffles surrounded and thermally connected to a water source for cooling. Other pumps have a baffle at the top of the diffusion pump into which liquid N_2 can be introduced to entrap gas molecules (cold trap). Wrapped around the outside of the pump chamber wall is copper tubing through which runs cooling water or oil. Near the bottom of the chamber is an exhaust port, also usually surrounded by coils containing coolant. This port can be attached to a mechanical pump or buffer tank that backs the diffusion pump. At the bottom of the pumping chamber, typically bolted to the outside, is an electrical heating element.

A diffusion pump contains a small amount of high-grade synthetic lubricant (Table 18). Hydrocarbon and silicone oils are not used much because of potential column contamination. The oil is boiled by the external heater and rises as a vapor toward the top of the pump chamber. The oil vapor hits the central stack of inverted funnels, and microscopic oil droplets are ejected outward and downward toward the chamber walls at supersonic speeds. Any gas molecules in their path are adsorbed. When the oil droplets with adsorbed gas molecules hit the water- or oil-cooled chamber walls, they condense and run down the walls to the base of the chamber. As the cooled oil with entrapped gas molecules is reheated by the electric heater, the oil vaporizes and releases the entrapped molecules, which are removed from the diffusion pump by the backing system. The cooling coils on the pump

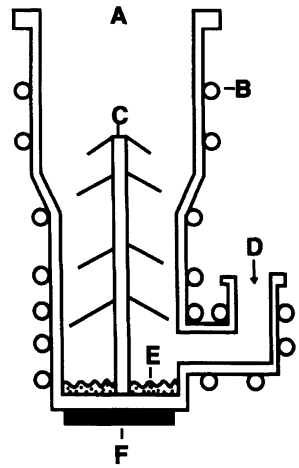

Figure 204. Schematic diagram of a diffusion pump showing the top of the pump that would be connected to the vacuum chamber (A), the cooling coils (B) wrapped around the pump and the port (D) to the backing pump, the stack of inverted cones (C) that direct the oil vapors to the wall of the pump, and the heater (F) that boils the oil (E).

Table 18. Chart of Some Pump Lubricants

Name	Chemical Name	Prices in 2002 ($)
Oils for mechanical pumps		
Edwards Supergrade A	Mineral oil derivative	11.00/l
Fomblin Y LVAC 25/5[a]	Perfluorinated polyether[a]	54.55/100 ml
Silicone oils for vacuum evaporators (not for use in microscopes)[b]		
Dow Corning 704	Tetramethyltetraphenyltrisiloxane	28.65/100 ml
Dow Corning 705	Pentaphenyltrimethyltrisiloxane	55.95/100 ml
Oils for microscope diffusion pumps		
Fomblin® Y HVAC 25/9[a]	Perfluorinated polyether[a]	295.35/100 ml
Octoil-S®	Dioctylsebacate	25/100 ml
Santovac 5®	Five-ring polyphenylether	225/100 ml

[a] If Fomblin oils are used, they should be used in *both* the mechanical and diffusion pumps (they do not mix with oils with other bases).
[b] The reason that these oils are not recommended for electron microscopes is that if an accident occurs, resulting in oil being introduced to the column, silicone-based oils are much harder to clean off column components than other types of oils.

wall, the cooled baffle at the top of the diffusion pump, and the coils around the exhaust port usually prevent oil from escaping the diffusion pump. Diffusion pumps have a pumping speed of about 2,160 l/s, considerably faster than the 8 l/s of a mechanical pump (Stuart, 1983). They rarely achieve a greater vacuum than 1.33×10^{-4} Pa (10^{-6} Torr) when attached to electron microscopes.

Diffusion pumps should not be used unless the chamber to be evacuated has reached about 1.33×10^{-1} Pa (10^{-3} Torr). If a heated diffusion pump is brought to atmospheric pressure, the oxygen present can react with the boiling oil, thus oxidizing it. This is known as "cracking" the oil. Most modern oils can withstand brief exposure to atmospheric pressure at operating temperature, but repeated venting to atmospheric pressure can eventually result in oxidation of the oil. If the pumping efficiency of the pump drops considerably, check to see if the heater is still heating. The electrical wires to the heaters often corrode and break, preventing current from reaching the heating coils. If the heater is hot, shut the instrument down, vent the pump according to the manufacturer's recommendations, and check that the pump contains a relatively uncolored pump oil, typically 100–200 ml. If there is an appropriate quantity of unoxidized oil in the pump, remove the heater from the pump, disconnect cooling lines and the backing line, and then unbolt the upper flange from the vacuum chamber. Then examine the central tower with its inverted cones. If it looks like the bottom of a camping skillet as shown in Fig. 205, the oil has been severely cracked. No liquid diffusion pump oil was found in the pump when it was disassembled. If the diffusion stack looks like that in the photograph, the central core should be removed and cleaned or replaced, and then the pump refilled with the proper kind and quantity of oil before being reinstalled. Before removing a diffusion pump from a vaccum chamber, make sure you have a new "o" ring for the upper flange, since it is frequently difficult to put the used "o" ring back into its groove.

As mentioned, most modern diffusion pumps have cooling baffles or cold traps at the upper end of the pump to prevent backstreaming. Even so, if a microscope column is suddenly brought to atmospheric pressure from high vacuum, oil from the diffusion pump may backstream into the column.

D. Turbomolecular (Turbo) Pumps

Turbo pumps have been around since the 1950s but have been incorporated into electron microscope designs for only about two decades. They consist of a series of variably sized and

Figure 205. A diffusion stack with dark, oxidized (cracked) oil on its surface, next to a new diffusion stack with clean metal surfaces.

pitched blades on a shaft that is spun within the pump chamber at 20,000–60,000 rpm, supported by high-quality metal, magnetic, or air bearings external to the pumping chamber (Fig. 206). The momentum of the rapidly rotating blades is transferred to the gas molecules, and the cascaded series of blades directs the gas toward the exhaust port of the pump while simultaneously compressing the gas into an ever smaller volume. As O'Hanlon (1980) stated, "The relative velocity between the alternate slotted rotating blades and slotted stator blades makes it probable that a gas molecule will be transported from the pump inlet to the pump outlet." These pumps are usually attached to a chamber previously evacuated to 1.33×10^{-1} Pa (10^{-3} Torr) or better and can

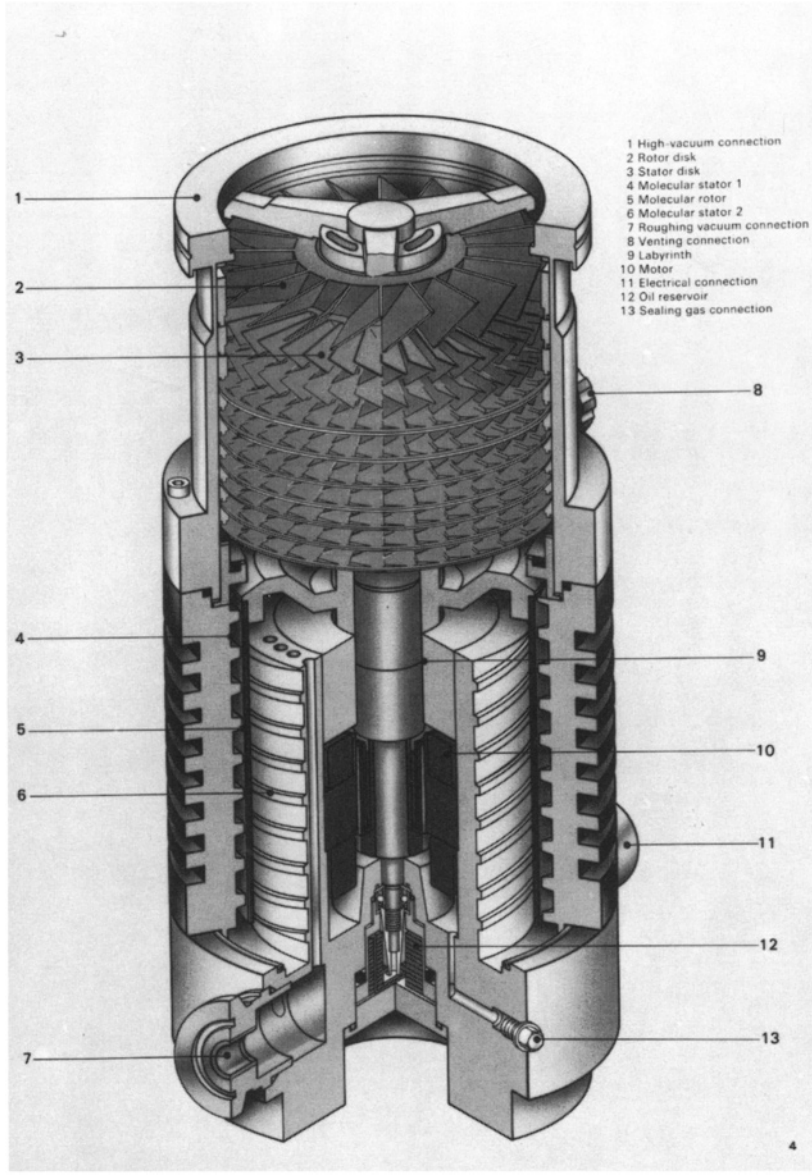

Figure 206. Diagrammatic sketch of a turbomolecular pump. (Courtesy of Balzers.) 1: High-vacuum connection; 2: rotor disk; 3: stator disk; 4: molecular stator 1; 5: molecular rotor; 6: molecular stator 2; 7: roughing vacuum connection; 8: venting connection; 9: labyrinth; 10: motor; 11: electrical connection; 12: oil reservoir for bearings; 13: sealing gas connection.

achieve a vacuum of about 1.33×10^{-4} Pa (10^{-6} Torr) when attached to an electron microscope. The pumping speed is in the range of 100–500 l/s.

Turbo pumps are usually used in lieu of diffusion pumps and have the distinct advantages of not being subject to backstreaming or oil cracking. Unfortunately, they are also considerably more expensive than diffusion pumps due to the high mechanical precision necessary to sustain the high speeds utilized. They are of particular importance to the SEMs produced for the microelectronics

industry. The microscopes are used to examine semiconductor wafers for defects, and any backstreaming of oil would contaminate the wafer surfaces before they could be "doped" with further layers of material during the manufacturing process.

E. Sputter Ion (Ion Getter) Pumps

With the advent of lanthanum hexaboride (LaB_6) guns and, more recently, FEGs, a higher vacuum than that achieved by diffusion pumps or turbomolecular pumps alone is needed. Ion getter pumps (Fig. 207) fulfilled this need, producing 1.33×10^{-7} Pa (10^{-9} Torr) in restricted areas of an electron microscope column, typically in the area from near the specimen up to the top of the column. Ion getters are usually metal chambers lined with titanium containing a high-voltage (5 kV) cathode and surrounded by strong permanent magnets. The theory of operation is virtually identical to that of a Penning gauge, as discussed earlier. Gas molecules within the chamber are ionized by electrons liberated from the cathode. The ionized gas molecules are accelerated toward the cathode and directed into a spiral path by the external magnets. They eventually impinge on the chamber walls, where they become entrained. Some ion getter pumps are designed to be externally heated and baked out periodically to release the molecules entrapped by the titanium walls so that they can be pumped out of the ion getter by other pumps. In other cases, the chambers are merely removed from the microscope, when they are no longer working efficiently, and replaced with new or reconditioned pumps. The removed pump is then baked out and reconditioned by the manufacturer.

Ion getters can pump air at about 500 l/s but work poorly unless the system is prepumped by a diffusion or turbomolecular pump. If these pumps are connected to a system at atmospheric pressure, they will arc audibly. The arcing of electricity from the cathode to the anode surfaces across air molecules will result in excessive heating of, and possible damage to, the pump.

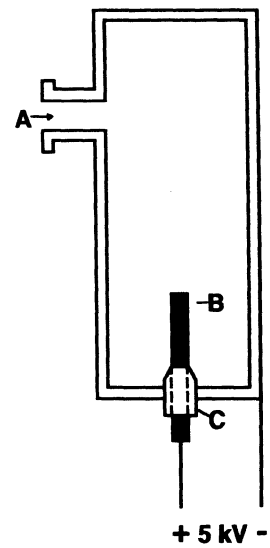

Figure 207. Diagrammatic sketch of an ion getter pump showing the inlet port (A) and high-voltage anode (B) insulated (C) from the titanium-lined pump housing cathode.

F. Cryopumps and "Cold Fingers"

Cryopumps are typically filled with liquid nitrogen or the colder but much more expensive liquid helium. They are located below the chamber to be pumped and often used in conjunction with diffusion pumps, being located above the flange connecting the diffusion pump to the chamber being pumped. Liquid nitrogen is contained in a large chamber external to, but in intimate contact with, the top of the diffusion pump. After most of the air is removed from the system by a diffusion or turbomolecular pump, the cryopump is filled, and the extremely cold surface produced on the walls of the evacuated chamber (microscope column, etc.) causes any remaining gas molecules to be securely bound until the liquid nitrogen evaporates from the cryopump, at which time all the adsorbed molecules are liberated and are usually pumped out by the diffusion pump.

Cold fingers are small cages located around specimens within the objective lens in TEMs that are in thermal contact with an external source of liquid nitrogen or helium. Any contaminants produced by the interaction of the electron beam with the specimen will tend to condense on the cold surface of the cold finger, where they will remain as long as it is kept cold. When the cold finger reaches room temperature, the trapped gas molecules are released and are evacuated by the diffusion pump.

Some microscopes are equipped with cold specimen stages that are cooled with liquid nitrogen or liquid helium. These are used to maintain frozen sections for viewing in the frozen, hydrated state and are not designed as pumps *per se*. These are frequently utilized in conjunction with electron tomography.

Cold fingers, cold stages, and cold traps can cause major problems for systems that are brought to atmosphere without first emptying cryogen containers and bringing them to room temperature. If these devices are not warmed up above ambient temperature, they may condense water vapor from the air, which then can result in water droplets in a microscope column. Water droplets or vapor are extremely difficult to remove from the column.

Currently, the cleanest microscope columns are needed by the microelectronics industry. Wafers composed of numerous microelectronic chips are examined with scanning electron microscopes prior to various steps in the manufacturing process as a form of quality control. Any traces of oil left on the surface of these wafers would compromise later steps in the manufacturing process. A microscope set up for this application would probably have a scroll pump used for roughing out the specimen chamber and for backing a turbomolecular pump that attains operational vacuum on the specimen chamber. Additional ion getter pumps typically would be attached to the gun and the upper portion of the column as well. The system comprising these three types of pumps working in concert exposes the microscope specimen chamber and column to no oils, and so it is the cleanest system that can be manufactured with current technology.

III. SEQUENTIAL OPERATION OF A COMPLETE VACUUM SYSTEM TO ACHIEVE HIGH VACUUM

Figure 208 shows an electron microscope pumping system illustrating the various pumps, pumping lines, and valves. Before beginning pumping on a chamber, the chamber should be isolated from the diffusion pump by the main valve. The mechanical pump should also be isolated from the chamber by a valve. The diffusion pump may have some residual vacuum, but the mechanical pump should be at atmospheric pressure.

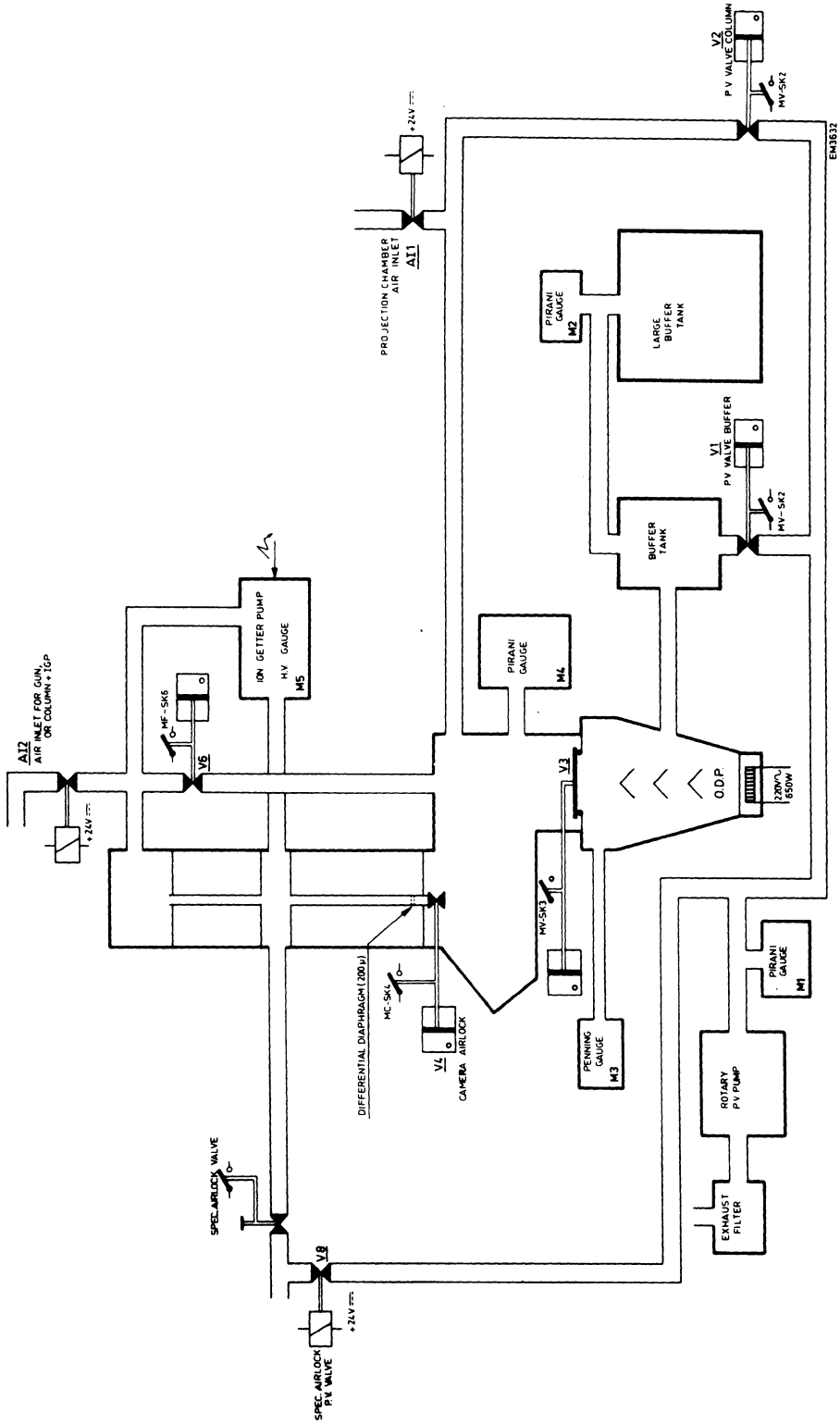

Figure 208. Complete TEM pumping system of a Philips 410LS. (Courtesy of Philips Electronic Instruments, Inc.)

The typical sequence of events to reach high vacuum from atmospheric pressure begins with the mechanical pump being turned on and attached to the chamber to be evacuated by opening a valve. The mechanical pump is left attached until the chamber has reached approximately 1.33×10^{-1} Pa (10^{-3} Torr).

In the meantime, the diffusion pump is being backed by either a buffer tank previously evacuated to 1.33×10^{-1} Pa or another mechanical pump. Once the diffusion pump has reached 1.33×10^{-1} Pa, the heater is activated. The buffer tank or mechanical pump remains actively backing the diffusion pump while it is on. After about 20 min, the oil in the diffusion pump will be boiling. The mechanical pumping on the chamber should then be stopped by closing a valve, and the diffusion pump connected to the chamber by opening up the main valve between the chamber and the diffusion pump. It is imperative that the mechanical pump never be connected to the chamber at the same time as the diffusion pump because the higher vacuum developed by the diffusion pump would pull the mechanical pump oil into the chamber.

After the diffusion pump evacuates the system to approximately 1.33×10^{-4} Pa (10^{-6} Torr), the microscope or vacuum evaporator is ready for use unless it is an electron microscope equipped with a LaB_6 gun or a field emission gun. In those cases, once the highest vacuum is reached with the diffusion pump (see above), the ion getter pump is attached to the gun area through another valve. A differential aperture allows the upper part of the column from above the specimen to the gun area to reach a very high vacuum, while the lower part can be at a lower vacuum. The viewing chamber and camera systems, which have a large number of "o"-rings, and/or moving parts are all sources of small, unavoidable leaks. Some microscopes are equipped with two diffusion pumps, each pumping on a different part of the column. This increases the overall pumping speed of the system but probably does not affect the ultimate vacuum in most cases.

If a microscope or vacuum evaporator is equipped with a cold trap or cryopump, it should be filled *after* the chamber has been brought below mechanical pump range (1.33×10^{-1} Pa).

IV. LUBRICATION OF VACUUM SEALS AND LEAK DETECTION

Leaks may be caused by lint, hairs, dust or small cuts in o-ring seals, or even by dry o-rings rolling slightly as metal parts are pulled across their surfaces. Every time a microscope column is brought to atmospheric pressure to change a filament or a camera is vented to change film, there is a possibility that repumping the system will draw dirt from around o-rings under seal areas. The glass viewing ports on a column usually sit on o-rings, and dust is continually falling between the glass and the metal part of the column around the glass. When the system is vented, the vacuum pulling the glass tightly onto the o-ring relaxes, and the o-ring rounds up slightly, allowing dust to get under the edge of the ring. When the chamber is pumped down again, the dust may be drawn completely under the o-ring. Repeated cycling as one changes several cameras will probably draw dust under the o-ring and into the camera chamber. You will note that the screen develops lint and dust over time from this process. It is thus important to keep the area around windows and column joints as free of dust as possible.

Moving parts that extend into the vacuum system should be lubricated with silicone-free greases such as Fomblin®. The object is to let the o-ring around the part move freely from lubrication and to prevent the o-ring from rolling and twisting. The grease is strictly a lubricant and is not meant to provide a seal, so use it sparingly. Any column component that merely sits on

an o-ring and never moves laterally does not need to be greased. If too much grease is used, it will eventually become a contaminant within the column.

Leak detection becomes an issue when the vacuum system takes longer to pump down than usual or does not reach the expected ultimate vacuum. As O'Hanlon (1980) points out in his section on leak detection, keeping a good log for an instrument including information on normal pumping speed and ultimate vacuum is good practice for becoming aware of leaks.

A common confounding factor is wet film. The gelatin layer of film is hydrophilic and will readily absorb enough atmospheric moisture to cause problems for a microscope pumping system. If film is not thoroughly dried, vacuum systems can have great difficulties. Microscopes equipped with ion getter pumps are particularly sensitive to this phenomenon. If the film is not held in a separate drying chamber provided with a Petri dish of phosphorous pentoxide to remove minute amounts of water vapor, a new load of film may make it impossible to use the microscope for hours. Some workers vent the film storage chamber with dry nitrogen to try and eliminate contact of atmospheric air with film.

A common method of leak detection is to isolate an area of the microscope through use of the valves and to read the appropriate vacuum sensors to determine if the isolated area is the source of leakage. Some workers (Stuart, 1983) recommend using a syringe to apply minute amounts of methanol to suspect seals while observing the vacuum gauge for perturbation, but methanol can actually dissolve paint and plastics in some cases and might be injurious to certain microscope components. Sensitive helium leak detector devices are commercially available but are rarely found in electron microscopy laboratories.

REFERENCES

O'Hanlon, J.F. 1980. *A user's guide to vacuum technology*. John Wiley, New York.
Stuart, R.V. 1983. *Vacuum technology, thin films, and sputtering. An introduction*. Academic Press, Orlando, FL.

11

High-Voltage Transmission Electron Microscopes (HVEM)

I. HISTORY

The first high-voltage electron microscope (HVEM) capable of generating 1,000 kV was put into operation in Toulouse, France in the laboratory of Dr. G. Dupouy in 1960 (Dupouy, 1985). In 1969, Dupouy installed a 3,000-kV instrument, which offered improved specimen penetration and reduced chromatic aberration, but did not offer significant advantages over the original 1,000-kV instrument.

In the United States, federal funding helped several laboratories purchase and install HVEMs in the 1970s. In 1971, Dr. Hans Ris installed an AEI instrument at the University of Wisconsin; this was followed by the installation of a JEOL instrument at the University of Colorado in Dr. Keith Porter's laboratory and the installation of a HVEM instrument in Albany, NY in 1978. All of the instruments listed above that are in the United States are available free of charge to American investigators because they are national resources and are subsidized by federal funds. To gain access, one should contact the laboratories about the availability of the instruments and proposal guidelines.

The original expectation was that the high accelerating voltage of these instruments would permit the examination of living materials in small closed environmental chambers. However, Dupouy demonstrated that radiation damage was so severe that HVEMs have been mostly limited to the examination of fixed biological specimens and various types of nonbiological samples.

Intermediate voltage electron microscopes (IVEMs) capable of 200–400 kV were subsequently developed that could perform many of the same tasks of HVEMs but required less initial capital expenditure, less space, had a greater stability, and were generally easier to operate. Recent developments in the design and application of IVEMs allow most of the work formerly done with HVEMs to be accomplished with less expensive, more versatile, and more stable IVEMs.

Buseck *et al.* (1988) edited a text with thorough discussions of the physics of high-resolution TEM and HVEM from a materials scientist's point of view. Johnson *et al.* (1986) edited another collection of chapters on HVEM applications to materials.

II. PURPOSE

After the initial attempts to examine living material in environmental chambers met with failure, investigators developed other uses for HVEMs. The superior beam penetrating capability of these instruments permits an examination of much thicker specimens (up to 10 μm in thickness) than is possible with conventional TEMs. When stereo pairs of these materials are prepared, the great depth of field possible from electron optics delivers impressive three-dimensional images of these specimens.

Chromatic aberration is reduced when greater accelerating voltages are employed because less beam spreading caused by multiple inelastic and elastic scattering events within the specimen occurs. This improves X-ray signals that are measured point by point with EDS. EELS also can be performed on thicker specimens than in a conventional TEM because the mean free path of an electron between two inelastic scattering events is greater as a result of the higher accelerating voltage of the primary electrons.

The advantages of HVEM are all related to the increased accelerating voltage. There is greater specimen penetration along with greater resolution with thick specimens. The former leads to greater brightness for a given specimen, and the latter is mostly the result of reduced chromatic aberration because of reduced beam spreading. In addition, the specimens suffer less ionization damage and thus less heating.

The disadvantages of HVEMs are largely the result of physical parameters. The instruments are extremely costly (the original instruments in the 1970s cost millions of dollars when a conventional 100-kV instrument could be purchased for less than $100,000), they require space specifically designed for them, since they are several stories tall and occupy more than the floor space of a conventional laboratory, and they are physically less stable than conventional TEMs because of their size.

As already mentioned, HVEMs caused considerably more specimen damage due to atomic displacement than originally expected, so living materials have eluded significant investigation with these instruments. These instruments are also not very useful for examination of conventional specimens, since they suffer from reduced contrast and inferior image quality at low operating voltages.

III. FUNCTIONAL ASPECTS OF HVEMs

A. Resolution

Chromatic aberration is a major source of decreased resolution with all electron microscopes. This phenomenon can be initiated at the electron gun, resulting from the broad spectrum of energies exhibited by electrons emitted and accelerated from a tungsten filament. A smaller source provides less chromatic aberration (LaB_6, FEG), and the latest generation of FEGs provides the most focused electron beams with the least chromatic aberration available today

The most important source of chromatic aberration is energy losses of the incident electron beam within the specimen. As the image-forming electrons emerge from a specimen, some have become widely scattered from elastic collisions; they consequently strike the objective aperture and do not reach the imaging plane. Some electrons experience inelastic collisions within the specimen with the result that electrons of greatly reduced energy levels emerge from the specimen and enter the projector lens system. Finally, some electrons emerge from the specimen having undergone neither elastic nor inelastic collisions. Chromatic aberrations result from the inelastic collisions occurring in the specimen, which produce electrons with varying energies. As imaging electrons pass through the projector lens system, those with higher energies are refracted less than those with lower energies, producing several planes of focus for the image and resulting in decreased resolution. Since higher voltages produce electrons that pass through the specimen at higher velocities, less inelastic scattering occurs, leading to less chromatic aberration and a higher resolution.

The practical side of this feature is that for a given specimen, a higher resolution is possible with a higher accelerating voltage. Of course, chromatic aberration is directly proportional to section thickness. Since most investigators use HVEMs to examine specimens much thicker than those used for conventional TEM work, the final resolution achieved for very thick specimens does not approach that for ultrathin sections examined with a conventional TEM. For biological specimens, chromatic aberration will be reduced by at least 20 times in going from 100 kV to 1,000 kV. In other words, it should be possible to achieve 0.5-nm resolution in a 1-μm-thick specimen imaged at 1,000 kV.

B. Radiation Damage

Radiation damage arises from several different types of interaction between the electron beam and atoms within the specimen. Any structural changes that are induced in the sample can result in artifacts or, at the very least, a decrease in resolution.

At high accelerating voltages (over 100 kV), an accelerated electron can transfer enough energy to a specimen atom to displace the atom. This relatively rare event, however, is probably a negligible factor in terms of final image quality.

The most important source of biological specimen damage from an electron beam is ionization damage. This type of damage is of little consequence with metallic specimens because any electrons ejected from the specimen are replaced by others flowing up from the normally grounded specimen holder. If, however, areas of a specimen are inadequately grounded (as is often encountered with poorly conductive biological specimens embedded in nonconductive plastic resins), charging can result, thus degrading the image. In addition, covalently bonded structures found in biological specimens may incur permanent changes after electron bombardment because of electron rearrangements (often accompanied by atomic rearrangements within molecules). The amount of specimen damage theoretically varies inversely to the square of the incident electron velocity. Thus, increasing the accelerating voltage from 100 to 1,000 kV should reduce ionization damage by one third.

Beam heating can also damage specimens. For a specimen of a given thickness, beam heating effects should be about three times less at 1,000 kV than at 100 kV. However, in practice, a HVEM is used to look at specimens at least 10 times thicker than those examined with conventional TEMs, so the amount of heat damage is still greater with HVEM than with conventional TEM.

C. Contrast

Contrast is essentially a signal-to-noise problem. A thin specimen without added contrast-building materials (osmium, uranium, lead) produces a small amount of beam scattering and thus a low contrast. For a given specimen thickness, scattering by the sample decreases as the incident electron energy increases. If a small feature is of a low contrast, the signal-to-noise ratio (SNR) may not be high enough to detect the feature. In this case, resolution is limited by a lack of contrast. As explained previously, with HVEM, the high accelerating voltages employed produce excellent specimen penetration and brightness but also reduce contrast. One possible solution to this problem is dark-field imaging. By using an off-center aperture or electromagnetic deflection to eliminate the axial component of the beam following specimen interaction, the scattered components of the electron beam can be used to produce a dark-field image of materials with low contrast (Ottensmeyer, 1982).

IV. MICROSCOPE CONSTRUCTION

Microscopes designed for HVEM work are in all ways larger than conventional TEMs. They must have larger electromagnetic lenses to control the more energetic electron beam, the column is at least 3-m tall, and the high-voltage generator is itself larger than most conventional TEMs (Figs. 209 and 210).

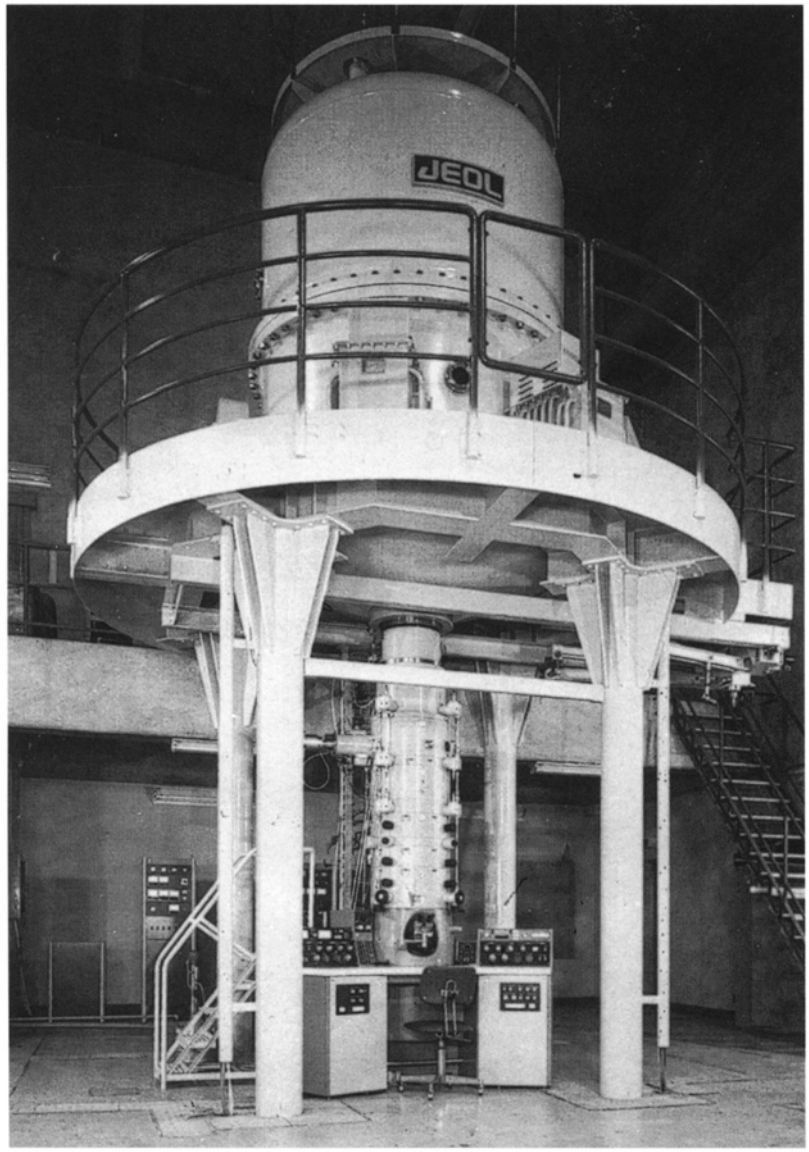

Figure 209. JEOL JEM-1000. The platform supporting the high-voltage generator is supported on steel pillars above the microscope column. Note the size of the operator chair for proper perspective. (Courtesy of JEOL USA, Inc.)

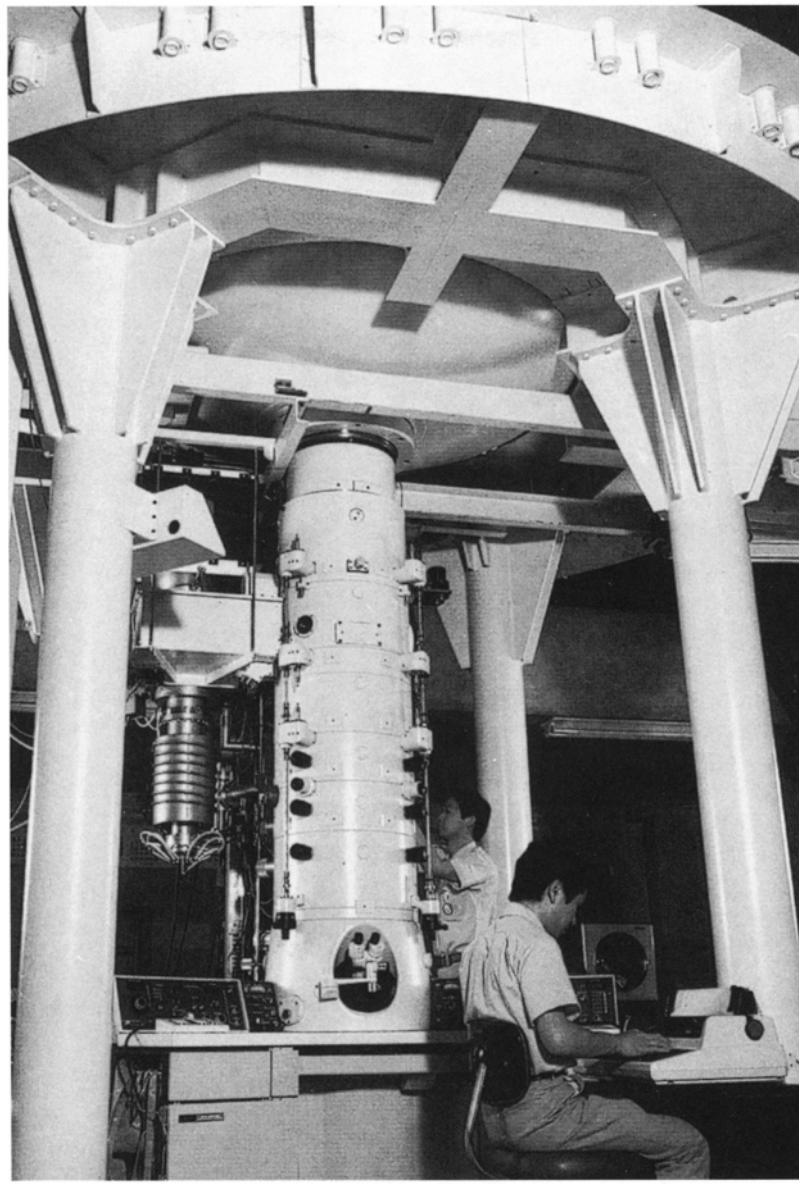

Figure 210. A close-up view of the JEOL Atomic Resolution Microscope (JEM-ARM1000). (Courtesy of JEOL USA, Inc.)

The high-voltage generators and accelerators in most commercial HVEMs are gas insulated, occupying about 20 m^3 of space. These large chambers are designed to prevent arcing of the high voltage.

The stages are larger than those found in conventional TEMs and thus suffer from more drift and vibration problems. The sheer height of the column makes all mechanical controls longer, bulkier, and less exact than those on conventional TEMs.

V. SAMPLE PREPARATION

Preparation of samples up to 1-μm thick can be done with conventional TEM techniques, but thicker samples often require selective staining methods to prevent confusion. As with all electron optics, such a great depth of field exists that all materials within a section even 5-μm thick will be in focus at the same time. Being unable to optically section by focusing up and down through the specimen as one does with light microscopy, the flood of information presented simultaneously is extremely difficult to interpret. Selective staining has been used by Franzini-Armstrong and Peachey (Franzini-Armstrong and Peachey, 1982; Peachey, 1986; Peachey and Franzini-Armstrong, 1978) to stain the sarcoplasmic reticulum (SR) in muscle in thick sections so that its branching networks could be deciphered without confusion caused by muscle proteins with which the SR is associated. Even with selective staining, however, the SR patterns within a thick section were difficult to decipher, so Peachey employed stereo pairs, allowing three-dimensional viewing of the SR.

Using HVEM, Wolosewick and Porter (1979) revealed a complicated network of cytoplasmic proteins, which they termed the microtrabecular lattice, in whole cells grown directly on coated grids. The cells were cultured directly on polymer film-coated grids, allowing them to spread out so that they were thin enough to be penetrated easily by the HVEM electron beam.

Wolosewick (1980) also developed a technique utilizing PEG specimen embedment. Sections cut from fixed and PEG-embedded samples were placed on grids for subsequent removal of the PEG medium, followed by critical point drying. This allowed Wolosewick to examine thick sections of biological samples with conventional TEM and HVEM without having to deal with the electron-scattering (and contrast-robbing) aspects of nonbiological support media (embedding resins).

VI. APPLICATIONS

As mentioned above, sections of biological materials 1–10-μm thick can be examined with HVEM. Stereoscopy is usually applied to these materials to help reduce confusion caused by all the cellular structures being in focus at the same time (Peachey, 1978). With selective staining of cellular components and/or stereoscopy methods, a true understanding of three-dimensional relationships between cellular structures is possible. With conventional TEM, the specimen is essentially two-dimensional and extremely thin, so a large number of pictures of serial sections must be taken and analyzed to discern relationships revealed in one HVEM photograph (or stereo pair). As discussed in Chapter 12, electron tomography methods have produced an easier method for 3-dimensional analyses than either HVEM or serial section analysis with conventional TEMs.

Another type of preparation used extensively to study cells as described above is produced by growing cells directly on grids, which are then subjected to fixation and critical point drying prior to HVEM examination. This technique is limited to those cells that will adhere to a plastic film and spread out sufficiently to allow beam penetration. Large, multinucleated cells such as myofibers or thick-walled cells such as those of plants are not suitable for this technique.

Immunocytochemical techniques, particularly postembedment localization in conjunction with cryosectioning are another potential application of HVEM (see Chapter 6).

The dream of examining living cells with HVEM has only occasionally been realized because of the problems with radiation damage already mentioned. Over the years, various thin-film chambers and differentially pumped wet chambers were developed for these purposes, but little work continues in the area.

REFERENCES

Buseck, P., Cowley, J., and Eyring, L. (eds.). 1988. *High-resolution transmission electron microscopy and associated techniques*. Oxford University Press, New York.

Dupouy, G. 1985. Megavolt electron microscopy. In: P.W. Hawkes (ed.), *The beginnings of electron microscopy* (pp. 103–165). Academic Press, New York.

Franzini-Armstrong, C., and Peachey, L.D. 1982. A modified Golgi black reaction method for light and electron microscopy. *J. Histochem. Cytochem.* 30: 99.

Johnson, J.E., Jr., Hirsch, P., Fujita, H., Shimizu, R., and Thomas, G. 1986. *High resolution and high voltage electron microscopy*. Alan R. Liss, New York.

Ottensmeyer, F.P. 1982. Scattered electrons in microscopy and microanalysis. *Science* 215: 461.

Peachey, L.D. 1978. Stereoscopic electron microscopy. Principles and methods. *EMSA Bull.* 8: 15.

Peachey, L.D. 1986. The extraction of three-dimensional information from stereo micrographs of thick sections using computer graphics methods. *Ann. NY Acad. Sci.* 483: 161.

Peachey, L.D. and Franzini-Armstrong, C. 1978. Observations on the T system of rat skeletal muscle fibers in three-dimensions using high voltage electron microscopy and the Golgi stain. *Biophys. J.* 21: 61a.

Wolosewick, J.J. 1980. The application of polyethylene glycol (PEG) to electron microscopy. *J. Cell Biol.* 86: 675.

Wolosewick, J.J. and Porter, K.R. 1979. The microtrabecular lattice of the cytoplasmic ground substance: Artifact or reality? *J. Cell Biol.* 82: 114.

12

Intermediate Voltage Electron Microscopes (IVEM), Electron Tomography, and Single-Particle Electron Microscopy

I. INTERMEDIATE VOLTAGE ELECTRON MICROSCOPES

Contemporary IVEMs as typified by those from JEOL (JEM-2010 and JEM-3010) and FEICO/Philips (Tecnai T20 and Tecnai T30) possess most of the advantages of beam penetration of HVEMs without most of the disadvantages associated with HVEM cost, stability, and space requirements. The original IVEM units did not provide images at low accelerating voltages (100–120 kV) that were comparable with conventional TEM images, but modern IVEMs are considerably more flexible. It is now possible to achieve high resolution for both ultrathin sections and semithin sections in excess of 3 μm with IVEMs, particularly if equipped with energy filtration systems.

In the 1990s, there were comparatively few IVEMs available for the biological community, which was primarily using them to look at tilt pairs of semithin sections, often utilizing specific staining to define structures within cells, since all of the material in the section was in focus at the same time, making it difficult to understand spatial relationships from a single section (Peachey, 1986).

Lower-voltage IVEMs (200 kV) offer several configurations that can be chosen for different applications. When the JEOL JEM-2010 was introduced, it could be outfitted with one of two pole pieces, one permitting limited specimen tilting but offering high resolution (0.19 nm) and the other designed for high tilt capacity for analytical purposes, which had slightly less resolution (0.25 nm). In addition, the instrument could be provided with a conventional tungsten filament or a thermal FEG. The FEG would be chosen if microanalytical applications were desired because FEGs provide a high beam density and narrow energy bandwidth ideal for producing a fine probe diameter (1 nm with 1 μA of current) with high coherence for microanalytical purposes.

The JEOL JEM-3010 (300 kV) can be thought of as a 300-kV instrument with a 2010 built in. A 300-kV instrument such as the 3010 is probably most versatile for IVEM work with biological specimens because it has better specimen penetrating capabilities with the standard pole piece, allowing visualization of thicker sections, as well as having a high tilt stage that can be tilted up to 40°. The 3010 thus obtains almost the same resolving capability (0.21 nm) available with the high-resolution pole piece available for the 2010 and simultaneously can do high tilt work.

The development of electron tomography has produced a demand for IVEMs that can be operated remotely, have high-precision motorized goniometer stages, and which are operated by computer programs that can compensate for specimen drift, as well as focus and spatial

aberrations induced as the specimen is tilted through the viewing axis. Images are typically recorded by high-resolution CCD cameras, then analyzed and assembled by powerful computer software programs to produce three-dimensional (3D) images. FEICO/Philips have produced the Tecnai G^2 Sphera, and JEOL offers the JEM-2010F FasTEM to address these needs.

As described by Glaeser (1982), when the accelerating voltage is increased, the specimen exhibits reduced stopping power in regard to the electron beam. This means that less scattering occurs, resulting in reduced spherical aberration, reduced chromatic aberration, and increased brightness. The first two features are responsible for the increased resolving power of IVEMs.

As the section thickness increases, higher accelerating voltages are required to maintain the same resolving capabilities. Thus, depth of field (section thickness) helps define the need for IVEM and HVEM. Table 19 (Glaeser, 1982) shows these relationships.

As mentioned previously for HVEM, using tilting stages (goniometers) to produce stereo pairs helps reduce the potential visual confusion caused by all structures in a thick section being in focus at the same time. Peachey (1986) discusses the relationships between section thickness and magnification when determining the proper tilting angles for stereo image production.

Lewis *et al.* (1988) discuss practical resolution as dependent on accelerating voltage, section thickness, magnification, and stereoscopy (Table 20).

According to van Heel *et al.* (2000), there were approximately thirty 200-kV FEG TEMs in use at the time of their paper. A large number of these instruments were found within materials sciences departments, though the biological field is rapidly installing this type of instrumentation for elucidation of the 3D structure of cellular organelles (Golgi apparatus, mitochondria, and septal pore caps in fungi), cellular protein and nucleic acid arrays (chromatin, spindle pole bodies, centrioles, ribosomes), as well as viruses, bacterial surface layers, whole prokaryotic cells, and macromolecules (Frank, 1996; McEwen and Marko, 2001).

In the early 1990s, there were a handful of IVEM facilities available sponsored, at least in part, by the National Institutes of Health (NIH). Since then, additional NIH-sponsored facilities

Table 19. Depth of Field at Selected Accelerating Voltages in Relation to Resolution[a]

	Depth of Field (μm)		
Resolution (nm)	100 kV	300 kV	1,000 kV
1.5	0.6	1.1	2.6
2.5	1.7	3.2	7.2
4.0	4.3	8.1	18.4

[a] From Glaeser (1982).

Table 20. Factors Associated with Practical Resolution[a]

Accelerating Voltage	Section Thickness	Image Quality	Useful Magnification
100–120 kV	60–120 nm	Excellent	150,000+
	0.5–1.5 μm	Good with 3D	5,000–15,000
300–400 kV	Up to 1.5 μm	Excellent	15,000–40,000
	2.5–3.5 μm	Excellent with 3D	25,000–35,000
1,000 kV	3.5 μm+	Excellent with 3D	25,000+

[a] From Lewis *et al.* (1988).

have been equipped for IVEM, so it is possible to gain access to the equipment at a number of sites around the United States when a research project requires this type of instrumentation (Table 21). In addition, the biological research community has been purchasing IVEMs and installing them at a number of universities, particularly to support electron tomography research.

Table 21. Some of the NIH Resources for IVEM[a]

Contact	Location	Name of Facility
Ms. Linda Batlin	Department of MCD Biology University of Colorado Boulder, CO (http://bio3d.colorado.edu/userinfo.html)	Laboratory for 3-D Fine Structure
M.H. Ellisman, PhD	Department of Neurosciences University of California, San Diego La Jolla, CA (http://ncmir.ucsd.edu/us.html)	National Center for Microscopy and Imaging Research
W. G. Jerome, PhD	Wake Forest University Baptist Medical Center Winston-Salem, NC (www.wfubmc.edu/research/micromed.html)	MICROMED
C. R. Jefcoate, PhD	EHS Center for Development and Molecular Toxicology University of Wisconsin-Madison Madison, WI (http://www.niehs.nih.gov/centers/fac-core/mad-fac3.htm)	Imaging Facility and Services Core

[a] Additional facilities can be located by accessing the website http://cimewww.epf.l.ch/EMYP/lab_ame.html.

II. ELECTRON TOMOGRAPHY AND SINGLE-PARTICLE ELECTRON MICROSCOPY

Tomography is a method for visualizing 3D structures by examining slices through an object. The imaging source and recording medium can be rotated about the specimen, as is found with computerized axial tomography (CAT) scans and magnetic resonance imaging (MRI) used in medicine, or the specimen can be tilted and/or rotated through a fixed imaging source, as is found with electron tomography. Two books by Frank (1992, 1996) are valuable resources for gaining an overview of electron tomography and have in-depth discussions of the physics, mathematical and statistical concepts, computer algorithms, etc. involved in this discipline.

The basic idea of using 3D reconstructions to help elucidate ultrastructural details was first described in three papers published in 1968 (DeRosier and Klug, 1968; Hart, 1968; Hoppe *et al.*, 1968). The advent of modern IVEMs, along with the development of computers and software capable of driving goniometers with precision, has made electron tomography practical. The hardware and software make it possible to acquire the assemblage of images while compensating for specimen drift, changes in focus, changes in illumination as the electron beam path through the specimen increases with tilt angle, image elongation caused by tilting, and image registration problems when many images with different viewing angles are assembled into 3D displays. In addition, low-dose methods had to be developed to minimize specimen damage from the electron beam during the numerous exposures needed for electron tomographic methods.

Two major techniques are used for true electron tomography: single-axis tilt and conical tilt. With the first technique, the specimen is tilted in one axis in reference to the electron beam, while recording numerous images, or *projections*. Single-axis tilt electron tomography is used primarily to record images of resin-embedded or native-frozen cellular structures such as the Golgi apparatus and mitochondria, which are not uniform in structure and which are relatively large (Ahting *et al.*, 1999; Deng *et al.*, 1999; Nicastro *et al.*, 2000; Perkins *et al.*, 1997a, 1997b). Usually, approximately 50–100 images are recorded, resolution in the range of 5 nm is realized, and the specimen receives a total electron dose of approximately 1,000 $e^-/Å^2$. Conical tilt methods tilt and also rotate the specimen while projections are recorded, an approach that adds more data points to the data set that is produced by tilting on a single axis.

A quasi-tomographic technique known as random conical tilting is used to examine a large number of macromolecular specimens in a field of view that are randomly oriented on a grid, with one image recorded of the specimen field normal to the electron beam and, typically, a second image of the field tilted in reference to the electron beam.

Finally single-particle electron microscopy (van Heel *et al.*, 2000) methods can be used to produce zero-tilt 3D reconstructions of randomly oriented particles.

A. Single-Axis Tilt Electron Tomography

Medalia *et al.* (2002) discussed three major problems associated with electron tomography of intact cells. First, resolution is dependent on the number of images collected and the angular range covered as they are recorded. As wide a tilt range as possible is desired, with the smallest increments between each projection as possible. Second, specimen exposure to the electron beam should be minimized to decrease radiation damage. Third, and perhaps most important in relation to examining whole cells, is specimen thickness. When the specimen thickness is greater than the mean free path of the electrons from the electron beam, multiple inelastic scattering will significantly degrade the quality of the recorded images, even with an accelerating voltage of 300 kV and the use of energy filters to remove the scattered electrons from the image-forming process. Because of this, they concluded that samples over 1-μm thick cannot be studied intact and, consequently, must be cryosectioned for analysis.

Medalia *et al.* (2002) studied whole cells of *Dictyostelium*, a cellular slime mold, that were grown on carbon-coated copper grids, plunge-frozen, and viewed with an IVEM that had a cryostage to hold the cells in a vitrified state during examination. Their primary interest was to view the actin filament network of intact cells without any pretreatment (other than plunge freezing) that might alter the natural association of the actin filaments with cellular membranes. Looking at the specimens without electron tomographic methods produced two-dimensional images that were hard to interpret because cellular structures were layered on top of each other (superposition problems). Through the use of electron tomographic techniques, they produced easily understood 3D images of branching actin filaments with clear associations with other cellular structures.

B. Random Conical Tilt Electron Tomography

Random conical tilting methods are generally applied to negatively stained or frozen hydrated macromolecules that are uniform in structure, but randomly oriented (Frank, 1996;

van Heel *et al.*, 2000). Resolutions of less than 1 nm are currently being achieved. Typically, many individual images are recorded from a relatively large array of virtually identical molecules on a grid by capturing an image normal to the beam, and then a second, tilted image, producing a low total specimen irradiation by the electron beam in the range of $10\,e^{-}/Å^2$. As discussed in the excellent review article by Burmeister *et al.* (1999), the numerous repeated orientations of nearly identical molecules present in a single image on a grid are used to generate a "virtual" set of tilted projections. They explain that "... many particles assume a preferred orientation when adsorbed to a carbon film, except for in-plane rotations. Therefore, the particle projections in a single tilted image correspond to a conical tilt series with a random distribution of the projection vectors on the cone."

In a comparison of negative staining methods for electron tomography of macromolecules with the direct examination of frozen hydrated samples, Frank (1996) pointed out that negative staining is variable, resulting in incomplete staining of some molecules and uneven stain thickness, with the additional problem that the specimen structure may be deformed due to the air drying inherent in the process. When frozen hydrated specimens are examined with a cryostage-equipped electron microscope, there is no specimen distortion due to drying, all image contrast seen is due to the specimen itself, rather than from an applied stain, and the cooled stage helps minimize beam irradiation damage to the specimen.

C. Three-Dimensional Reconstruction of a Microtubule

Microtubules are constructed of aggregations of α–β tubulin heterodimers. Li *et al.* (2002) produced a 3D reconstruction of an intact microtubule at a resolution of about 0.8 nm, utilizing cryoelectron microscopy and computerized reconstruction of multiple images of segments of a microtubule. They polymerized microtubules *in vitro* from tubulin, placed suspensions of the material onto coated grids, and plunge-froze them in liquid ethane. The grids were then examined with a cryostage-equipped 400-kV transmission electron microscope. Multiple images along the length of a tubule were recorded with film. Complex computer analysis and reconstruction of 89 images of a microtubule gave rise to the 3D reconstruction shown in Fig. 211. The complex relationship of the heterodimers to each other in the 13 protofilaments constituting the microtubule is discussed in depth in the paper.

D. Irradiation Issues

The issue of specimen electron beam irradiation and the ionization of organic materials leading to the production of free radicals, ions, bond breakage and molecular fragmentation is discussed at length by Luther *et al.* (1988) and Luther (in Frank, 1992). Luther states that less than $1\,e^{-}/Å^2$ can damage the secondary structure, and higher doses can change the tertiary structure, but the main concern is that there is mass loss and shrinkage in the specimen in the plane normal to the beam, potentially causing losses in information in the final 3D image. He reports that there is a reduction in plastic section thickness of about 30% within the first three minutes of beam exposure but that the rate of shrinkage then levels off, indicating that the specimen can then effectively dissipate the beam energy at that dose rate.

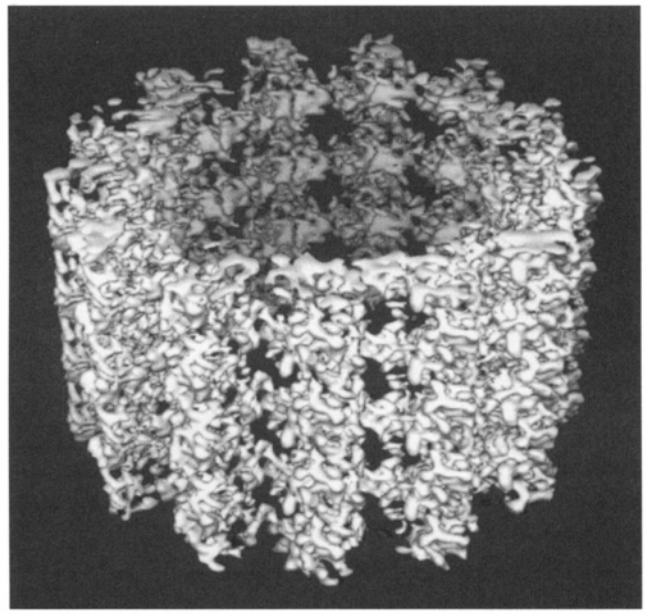

Figure 211. A three-dimensional reconstruction of a microtubule, showing the helical arrangement of the α–β tubulin heterodimers comprising the 13 parallel protofilaments from which the microtubule is constructed. Reproduced from Li *et al.*, 2002 with permission from Elsevier.

Lamvik (1991) found that a 70-fold improvement in shrinkage rates with epoxide sections was possible if the specimen was held at liquid helium temperatures by a cryostage, thus allowing a complete tilt series of images to be recorded, while incurring radiation damage similar to recording one image at room temperature. He recommended irradiating the specimen at low illumination until it becomes stable and "clears," followed by recording the tilt series with low doses.

Trachtenberg *et al.* (2000) studied the cell surface glycoprotein layer of *Halobacterium salinarum*. They examined isolated and flattened negatively stained envelopes as well as cryofixed intact cells that were subsequently cryosubstituted, epoxide embedded, and sectioned prior to electron tomography. They found that the epoxide-embedded materials suffered from dimensional distortion due to compression during sectioning as well as mass loss due to electron irradiation during image recording. By holding the specimen at −170 °C, the initial mass loss was about 20 times smaller than at room temperature. The total mass loss of 45–50% occurred quickly, and after a dose of about $100\,e^{-}/Å^2$, the mass loss became fairly negligible, and specimen movement consequently ceased. They compared araldite resin and Spurr resin in terms of mass loss and found that the former lost about 25%, while the latter lost 45% mass.

E. Resolution Issues

McEwen and Marko (2001) state that "resolution in the depth dimension cannot exceed twice the section thickness." They give the example that a 10-nm-thick section cannot provide over 20-nm resolution in the depth dimension with conventional TEM examination, while electron tomography methods can yield 5- to 10-nm resolution with the same specimen. They point

out that serial section analyses with conventional TEM still have their place for 3D analyses. In their example, since serial sections are rarely cut thinner than 40–50 nm, resolution in the depth dimension would be limited to 80–100 nm, even though resolution in the plane of section (laterally) could be as good as 2 nm. They found that it was easier to study the thin, fibrous structure of an entire kinetochore using serial sections, because it was difficult to cut one section suitable for electron tomography that would include the entire structure. Thus, they used serial sections and conventional TEM to see how many microtubules were bound to the kinetochores, while they used electron tomography to determine how far into the kinetochores the microtubules penetrated.

F. Issues Related to Specimen Tilting during Electron Tomography

As mentioned above, the electron path through the specimen changes in length as the specimen is tilted. This causes changes in illumination and contrast in the recorded images, as well as potential problems with chromatic aberration with high-angle tilts. Inelastic scattering, leading to increased noise, will obscure fine details in the specimen image as the beam passes through greater specimen thickness at higher tilt angles. This can be counteracted, to some extent, by increasing the kilovolts, or by using energy filters and/or FEGs that have greater beam coherence.

In addition, since most workers use microscope goniometers with a maximum tilt angle of 60–70°, a typical tilt series will be missing 20–30° of specimen information between the maximum tilt angle possible and 90°. This results in changes in resolution in 3D reconstructions that are dependent on viewing direction (tilt direction) as well as a distortion in reconstruction due to the missing information, known as the elongation factor (Koster *et al.*, 1997).

G. Drift Correction

Dr. Barbara Armbruster (JEOL USA, Inc.) recently explained (personal communication) the problems with inherent specimen drift in relationship to electron tomography, and the instrumentation and software provisions that have been developed to deal with this problem. The basic problem is that mechanical and/or thermal instability within the specimen, the specimen holder, and the goniometer manipulating the specimen can cause resolution losses due to drift, or specimen movement. Hardware modifications in the form of piezo drives built into the X and Y motor drives of the goniometer can control specimen holder movement to a level of 0.01-nm precision. A digital camera is then employed to record the movement of the specimen and to provide a feedback loop for the motors controlling specimen holder movement. This is accomplished by drift-correction software that utilizes a sequential pair of digital images to analyze the vector and speed of drift. Once this information is collected, the software activates the goniometer piezo drives to counteract the measured movement. Current software is so "smart" that it can perceive the minute variations found in virtually featureless low-dose images, such as those of amorphous carbon, and effectively counteract drift. For further information about how such systems operate, see Pulokas *et al.* (1999).

H. Fiduciary Markers

Plastic-embedded sections of cells and cellular structures examined with single-axis tilt methods suffer from lateral movement of structures as the specimen is tilted. Depending on the

specimen holder and goniometer design, accumulated specimen shifts of 1–3 μm are seen (Koster *et al.*, 1997). Fiduciary markers, typically 10-nm colloidal gold particles applied to the surface of the sections, are used as reference points that allow alignment algorithms within computer software to calculate shift vectors and rotations necessary to bring images into proper register, as well as correcting for the small magnification changes that are associated with refocusing the image throughout the tilt series (McEwen and Marko, 2001). These markers are not needed for random conical tilting approaches, since the macromolecules typically examined can serve as their own fiduciary markers.

I. Back-Projection

McEwen and Marko (2001) explain the utility of back-projection used for producing 3D images from electron tomography methods. As shown in Fig. 212A, a tilt image records the amount of mass density encountered by the electron beam (projection ray) at different points in the specimen. Back-projection algorithms are used to distribute the known specimen mass evenly over the calculated back-projection rays, thus retracing the path of the imaging rays. This, in effect, projects the specimen mass back into a reconstruction volume. When all the images recorded from the various tilt angles are processed in this way, the different images intersect, and the various structures (mass) reinforce one another, as shown in Fig. 212B, helping to make up for information lost due to the incomplete sampling of the specimen inherent in electron tomographic methods.

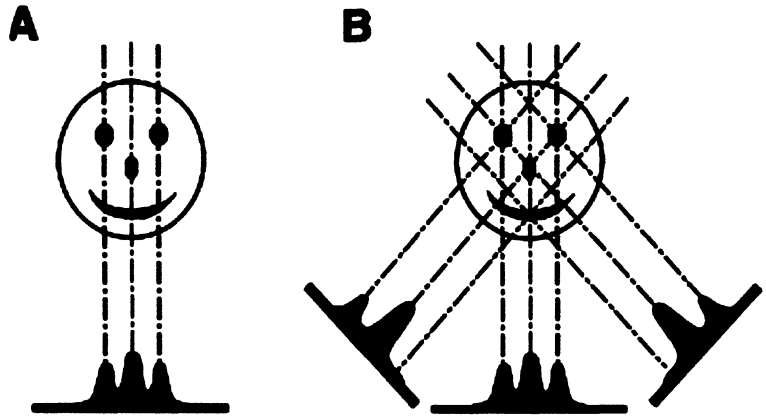

Figure 212. An example of projection imaging and reconstruction via back-projection, explained below by McEwen and Marko (2001): (A) Projection of a two-dimensional structure onto a one-dimensional line. The broken lines indicate selected projection rays. In transmission imaging, the projection rays also indicate the path taken by photons, electrons, etc. The graph along the solid line indicates the amount of specimen mass traversed by electrons that reach each point in the projection image (note that the actual number of electrons reaching the film is inversely proportional to the specimen mass traversed by the beam). Peaks of mass are recorded where the beam goes through the "eyes," "nose," and "mouth" of the face. (B) Projection from a different direction. Note that the shape of the projected mass plot changes with the direction of projection, that is, at the angle of the tilted projections, some rays traverse both an eye and the nose. For reconstruction via back-projection, the mass recorded at each point in the projection image is smeared uniformly along the projection ray. Such "back-projection rays," arising from areas of high recorded mass in different tilt views, intersect and reinforce one another at the locations of the main features in the two-dimensional structure. In this way, the two-dimensional structure is "reconstructed" from a series of one-dimensional projections. (Figure and legend reproduced with permission from McEwen and Marko, 2001 and the Journal of Histochemistry & Cytochemistry.)

REFERENCES

Ahting, U., Thun, C., Typke, D., Nargang, F.E., Neupert, W., and Nussberger, S. 1999. The TOM core complex: The general protein import pore of the outer membrane of mitochondria. *J. Cell Biol.* 147: 959.

Burmeister, W., Grimm, R., and Walz, J. 1999. Electron tomography of molecules and cells. *Trends Cell Biol.* 9: 81.

Deng, Y., Marko, M., Buttle, K.F., Leith, A., Mieczkowski, M., and Mannella, C.A. 1999. Cubic membrane structure in amoeba (*Chaos carolinensis*) mitochondria determined by electron microscopic tomography. *J. Struct. Biol.* 127: 231.

DeRosier, D.J. and Klug, A. 1968. Reconstruction of three-dimensional structures from electron micrographs. *Nature* 217: 130.

Frank, J. (ed.). 1992. *Electron tomography: Three-dimensional imaging with the transmission electron microscope.* Plenum Press, New York.

Frank, J. 1996. *Three-dimensional electron microscopy of macromolecular assemblies.* Academic Press, New York.

Glaeser, R.M. 1982. A critique of the theoretical basis for the use of HVEM in biology. *EMSA Proc.* 40: 2.

Hart, R.G. 1968. Electron microscopy of unstained biological material: The polytropic montage. *Science* 159: 1464.

Hoppe, W., Langer, R., Knesch, G., and Poppe, C. 1968. Protein-Kristallstrukturanalyse mit Electronestrahlen. *Naturwissenschaften* 55: 333.

Koster, A.J., Grimm, R., Typke, D., Hegerl, R., Stoschek, A., Walz, J., and Baumieister, W. 1997. Perspectives of molecular and cellular electron tomography. *J. Struct. Biol.* 120: 276.

Lamvik, M.K. 1991. Radiation damage in dry and frozen hydrated organic material. *J. Microsc.* 161: 171.

Lewis, J.C., Jones, N.L., O'Toole, E.T., Grant, K.W., and Jerome. W.G. 1988. Intermediate voltage electron microscopy in biomedical research. *EMSA Bull.* 18: 2.

Li, H., DeRosier, D.J., Nicholson, W.V., Nogales, E., and Downing, K.H. 2002. Microtubule structure at 8 Å resolution. *Structure* 10: 1317.

Luther, P.K., Lawrence, M.C., and Crowther, R.A. 1988. A method for monitoring the collapse of plastic sections as a function of electron dose. *Ultramicroscopy* 24: 7.

McEwen, B.F., and Marko, M. 2001. The emergence of electron tomography as an important tool for investigating cellular ultrastructure. *J. Histochem. Cytochem.* 49: 553.

Medalia, O., Weber, I., Frangakis, A.S., Nicastro, D., Gerisch, G., and Baumeister, W. 2002. Macromolecular architecture in eukaryotic cells visualized by cryoelectron tomography. *Science* 298: 1209.

Nicastro, D. Frangakis, A.S., Typke, D., and Baumeister, W. 2000. Cryo-electron tomography of *Neurospora* mitochondria. *J. Struct. Biol.* 129: 48.

Peachey, L.D. 1986. The extraction of three-dimensional information from stereo micrographs of thick sections using computer graphics methods. *Ann. N. Y. Acad. Sci.* 483:161.

Perkins, G., Renkin, C., Martone, M.E., Young, S.J., Ellisman, M., and Frey, T. 1997a. Electron tomography of neuronal mitochondria: Three-dimensional structure and organization of cristae and membrane contacts. *J. Struct. Biol.* 119: 260.

Perkins, G.A., Renken, C.W., Song, J.Y., Frey, T.G., Young, S.J., Lamont, S., Martone, M.E., Lindsey, S., and Ellisman, M.H. 1997b. Electron tomography of large, multicomponent biological structures. *J. Struct. Biol.* 120: 219.

Pulokas, J., Green, C., Kisseberth, N., Potter, C.S., and Carragher, B. 1999. Improving the positional accuracy of the goniometer on the Philips CM series TEM. *J. Struct. Biol.* 128: 250.

Trachtenberg, S., Pinnick, B., and Kessel, M. 2000. The cell surface glycoprotein layer of the extreme halophile *Halobacterium salinarum* and its relation to *Haloferax volcanii*: Cryo-electron tomography of freeze-substituted cells and projection studies of negatively stained envelopes. *J. Struct. Biol.* 130: 10.

Van Heel, M., Gowen, B., Matadeen, R., Orlova, E.V., Finn, R., Pape, T., Cohen, D., Stark, H., Schmidt, R., Schatz, M., and Patwardhan, A. 2000. Single-particle electron cryo-microscopy: Towards atomic resolution. *Quart. Rev. Biophys.* 33: 307.

13

Scanning Electron Microscopy

I. HISTORY

Scanning electron microscopy (SEM) has a history almost as old as TEM, but the development of a commercial product took much longer. Von Ardenne (1938) built the first SEM, and Zworykin *et al.* (1942) produced an SEM with a 50-nm probe. A group in Cambridge, England headed by Oatley began work in 1948 that led to the first commercial SEM (the Cambridge Stereoscan) in 1965. Pease (1963) achieved a beam diameter of 5 nm, which resulted in 10-nm resolution. With the introduction of the Cambridge Stereoscan in 1965, the biological community immediately began exploiting the tool to examine numerous tissues and cells. During the 1970s, resolution was improved to 5–6 nm, microprobe analysis (EDS) was applied to SEMs, freeze-fracture methods were explored (Haggis, 1972), and magnifications of over 100,000 × became a reality. The 1980s saw the introduction of FEGs in commercially produced SEMs offered by Hitachi and then JEOL, which allowed lower accelerating voltages and increased magnification and resolution (under 1 nm) and which were immediately adopted by materials scientists. A major technological advance occurred in 1986, when Cambridge Instruments introduced the first digital SEM. This allowed images to be stored and transmitted as digital files, allowed several independently captured images to be averaged to minimize charging artifacts, and led to the contemporary assortment of SEMs operated through a Microsoft Windows™ environment, which has provided a user platform that is accessible to most scientists at work today. By the late 1980s, biologists had discovered FEG instruments and were examining tissues and cells at low voltages with high magnifications previously possible only with sectioned material viewed with a TEM (Ris, 1991). The 1980s and 1990s also saw improvements in probe diameters for microanalysis along with better instrument sensitivity, allowing recognition of elements with lower Z-numbers than previously possible (see Chapter 14).

In the late 1980s, an instrument called the environmental scanning electron microscope (ESEM) was introduced that allowed hydrated specimens to be visualized. The advantage of this instrument was that specimens could be dehydrated and hydrated while being observed, and samples could be observed in the native state, without fixation, dehydration, and critical point drying. This instrument has been used to look at raw plant tissue, untreated pharmaceutical powders, and sensitive or valuable samples such as dinosaur teeth and forensic specimens that cannot be chemically treated or coated with metals before viewing. When the ESEM became part of the line produced by FEICO/Philips in the late 1990s, the relative cost of the instrument came down, along with improvements in ease of operation. A logical outgrowth of the ESEM has been the assortment of current low-vacuum SEMs that provide a more limited capability to examine samples that may not be totally dry at relatively low kV with both backscatter and secondary electron imaging modes at a reasonable cost.

Three excellent general reference books on SEM instrumentation and specimen preparation, though somewhat dated, are those by Goldstein *et al.* (1992), Hayat (1978), and Postek *et al.* (1980).

II. THE USE OF SEM IN BIOLOGICAL RESEARCH AND MEDICINE

The SEM can be thought of as a high-resolution dissecting microscope, since it is used to examine surfaces of specimens. It has been used to study cell surface receptors for lectins (Kan, 1990), to compare normal tracheal epithelium with tissues from cases of immotile cilia syndrome leading to respiratory abnormalities (Edwards *et al.*, 1983), and to assess the effect of various compounds on cellular motility and cellular polarity. For these types of studies, the SEM has advantages over the TEM because serial reconstructions are not necessary, the sample size is generally much larger, and the 3D view with great depth of field is easy to comprehend, even for viewers not trained in electron microscopy.

Chondrocytes from the growth plate of a bone (Fig. 213) are a good illustration of how SEM can offer understandings not available from other types of microscopy. With light microscopy, chondrocytes appear to be embedded in an amorphous matrix that stains pale blue in hematoxylin and eosin preparations. This matrix appears faintly granular with TEM preparations (Fig. 213A). When a sample is fixed and dehydrated in the same way as for TEM and is then critically point dried and examined with an SEM (Fig. 213B), it becomes obvious that the "amorphous" material is really quite structured and forms distinct chambers around the chondrocytes. Thus, SEM has given us an understanding of the relationship of the cells to their surrounding matrix not available with other tools.

As Humphreys *et al.* (1975) described, cells can be fixed and dehydrated up to 100% ethanol, quickly frozen in liquid nitrogen, fractured with a cold razor blade, and placed inside a vacuum evaporator bell jar until the ethanol has sublimed. Once sputter-coated, this freeze-fractured material provides excellent intracellular detail, particularly now that FEG SEMs are available.

(A)

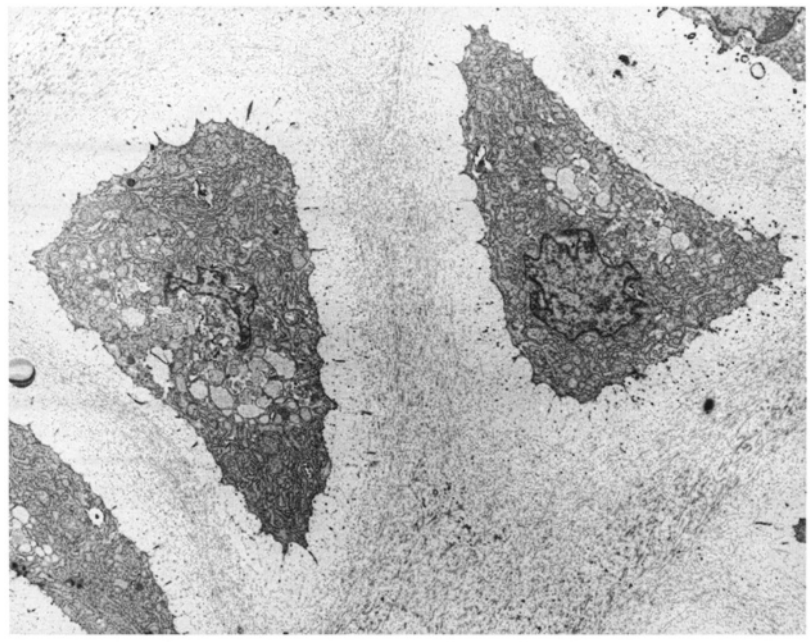

Figure 213. (A) Canine chondrocytes from femur growth plate. TEM image. ×2,500.

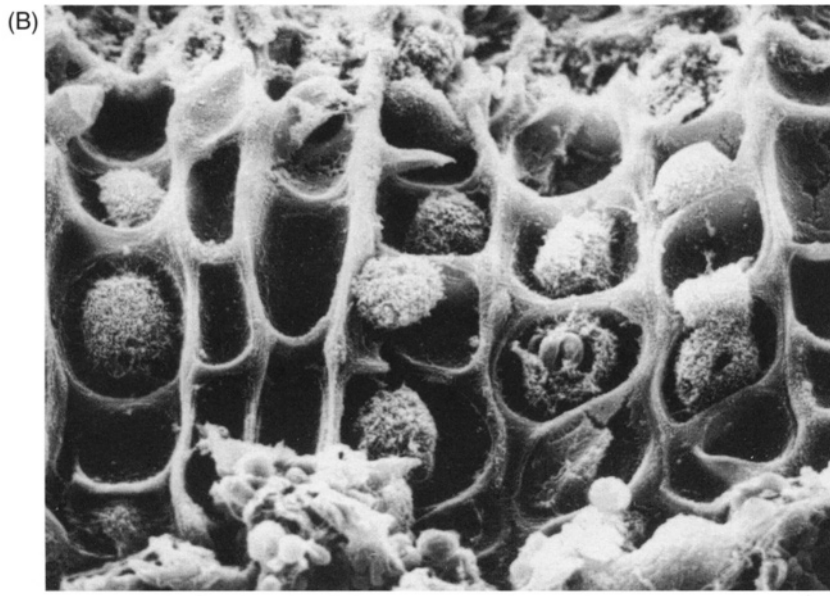

Figure 213. (B) Rabbit chondrocytes from femur growth plate. SEM image. ×750.

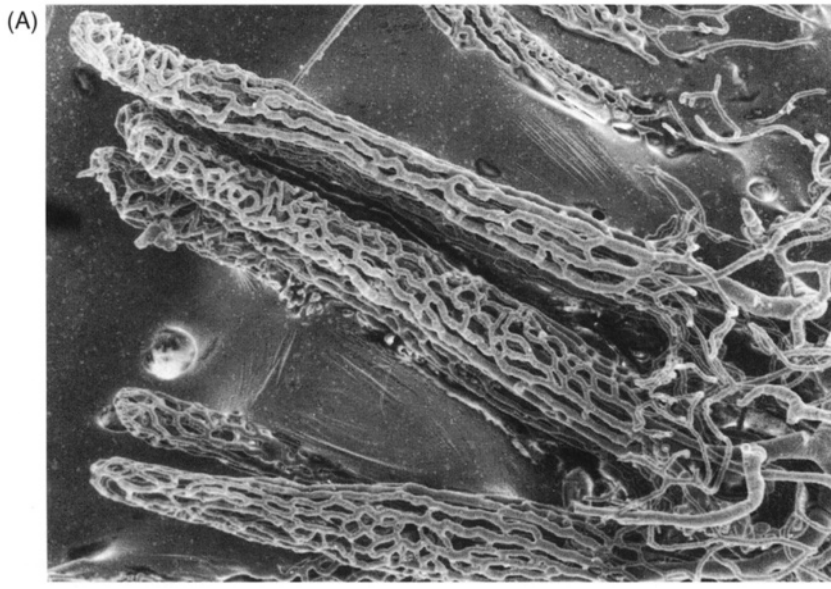

Figure 214. (A) Mercox™ resin cast of microvilli of equine small intestine revealing ultimate capillary bed. ×85.

To make use of another unique capability of the SEM, the vasculature must be perfused with various resins (Hanstede and Gerrits, 1982; Hossler and Douglas, 2001; Motta *et al.*, 1992; Okada and Schraufnagel, 2002; Suzuki, 1982). After the tissue is corroded from the sample, casts of the vasculature remain. These can provide 3D information about the smallest capillary beds (Figs. 214A and B) and can also reveal vascular accidents (leakage) and neovascularization associated with

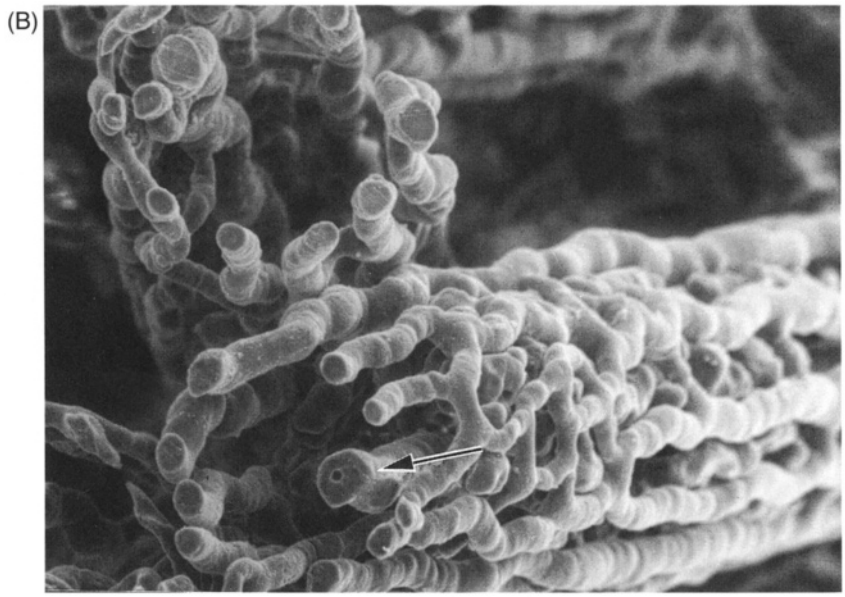

Figure 214. (B) Mercox™ resin cast of microvilli of equine small intestine cut across the tip with a razor blade to reveal the central arteriole (arrow). ×385.

certain disease processes. These casts can be easily manipulated and dissected while in liquid, though they become quite brittle when dried.

Evaluation of epithelial layers and their response to injury can be done easily with SEM. Normal chicken tracheal epithelium (Fig. 215A) possesses ciliated cells interspersed with mucus cells, which have only short microvilli on their surfaces. When challenged by *Mycoplasma gallisepticum*, the epithelial cells become round, lose their intercellular connections, and exfoliate (Fig. 215B). Scanning electron microscopy provides a much better view of this dynamic process than TEM or light microscopy.

Intricate details of microorganismal surfaces and topographic information about pollen, plant epidermal layers, and bryozoans revealed by SEM may be used for taxonomic, morphologic, and ontogenetic studies (Claugher, 1990).

III. PRINCIPLES OF THE SEM

The SEM employs electromagnetic lenses, vacuum systems, apertures, and electron guns similar to those described in the chapter on TEMs. Figure 216 illustrates the basic parts of an SEM. Unlike the TEM, which passes electrons through a thin specimen, the SEM accelerates electrons and collimates them into a narrow beam that is then impinged upon the specimen surface, producing several different imaging possibilities. Because of the small aperture sizes used and the short wavelength of electrons, a tremendous depth of field can be realized. The magnification chosen may be no more than that achievable with a light microscope, but much more of the specimen will be in focus at one time, thereby resulting in one SEM photograph conveying the same information that would require a series of optical sections and computer reconstruction with light microscopy.

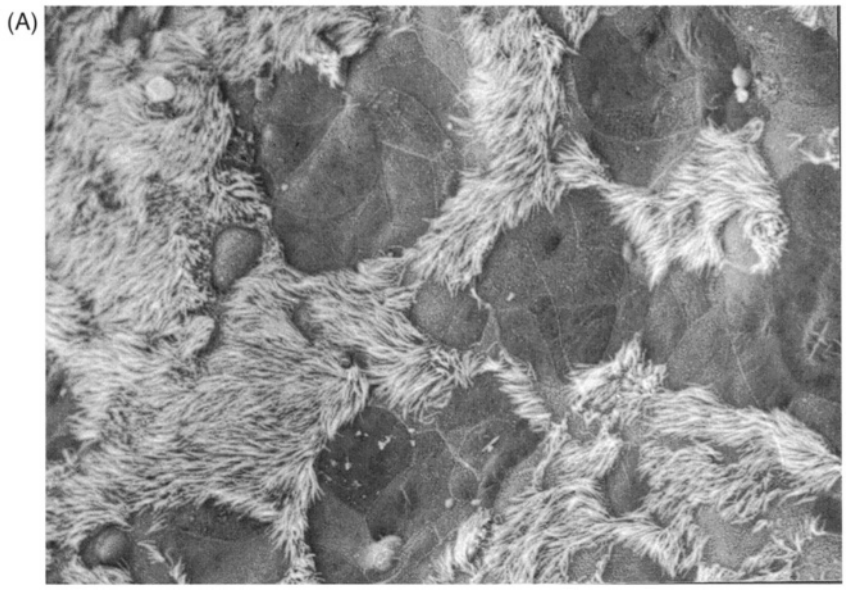

Figure 215. (A) Normal chicken tracheal epithelium. ×514.

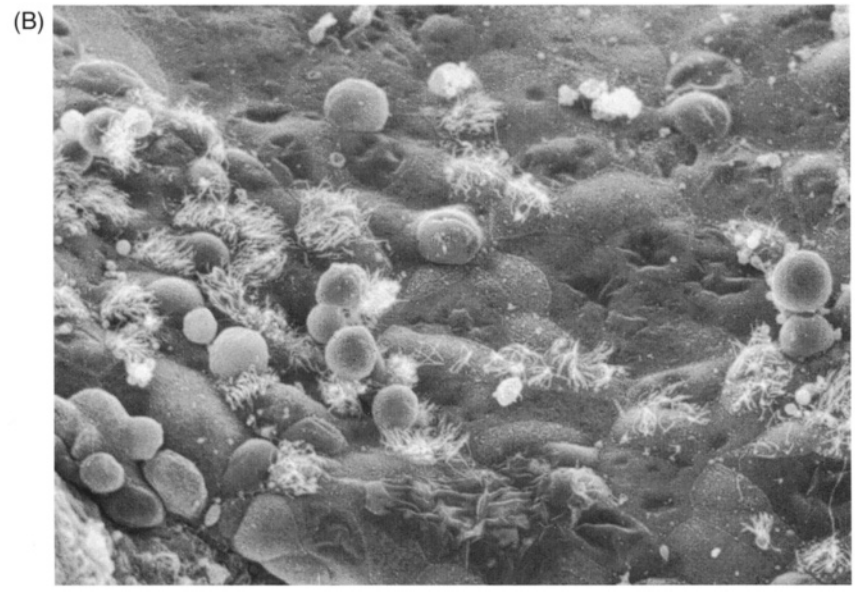

Figure 215. (B) Chicken tracheal epithelium exposed to *Mycoplasma gallisepticum*. × 654.

A narrow beam of electrons from the electron gun is focused by electromagnetic lenses into a small spot less than 10 nm in diameter on the surface of the specimen. Deflector coils then scan the beam across the specimen. In the most common imaging mode, secondary electron imaging (SEI), the high-energy primary beam dislodges electrons from atoms near the surface of the specimen (secondary electrons), some of which then strike the SEI collector. Those electrons that

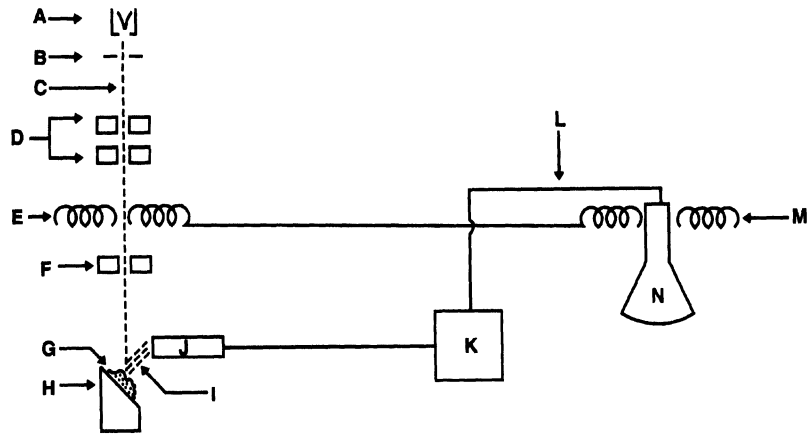

Figure 216. Diagrammatic sketch of an SEM showing Wehnelt assembly with filament (A), anode aperture (B), electron beam (C), condenser lenses (D), deflector coils on column (E) connected to deflector coils (M) of CRT (N), final condenser lens, called an objective lens in most descriptions (F), specimen (G) on stage (H), producing secondary electrons (I) striking collector (J) connected to amplifier (K) feeding voltage through cable (L) to CRT.

contact the collector produce photons that then are processed by a photoamplifier circuit connected to a cathode ray tube (CRT) or converted directly into a digital signal that can be sent to a printer or saved as a digital file. An electron that interacts with the collector produces a voltage applied to the gun of the CRT or a digital signal, which produces a point of illumination on the viewing screen. The scan generator that operates the scanning coils controlling the electron beam within the SEM column also is connected to the scan generator of the viewing screen. Thus, as the SEM beam is scanned over the specimen, the image is simultaneously produced on the viewing screen.

The output of the photoamplifier (voltage) is employed to modulate the brightness on the viewing screen in synchronization with the SEM electron beam. The current of secondary electrons recorded by the collector at a given point in time produces a given voltage after processing by the photomultiplier circuit, determining the brightness of the spot on the viewing screen. Any variation in elemental composition, texture, or topography can result in variations in the current reaching the collector. Specimen magnification is determined by the relationship between the distance scanned on the specimen surface by the primary beam and the distance scanned on the viewing screen during the same time period. Unlike the TEM, where the image is recorded over the entire screen simultaneously, the SEM image is collected and displayed point by point.

IV. OPERATION OF THE SEM

An SEM may have any of the three types of electron source (tungsten filament, LaB_6 source, FEG) described in Chapter 9. The type of gun determines the type of vacuum system needed. Most SEMs have accelerating voltages adjustable from 0 to 35 kV and have three electromagnetic lenses, the first two of which defocus the beam, while the third is used to determine the final diameter of the beam striking the specimen surface. The final lens has apertures of various sizes, the smallest of which gives the greatest depth of field but also decreases the amount of secondary electrons produced (signal). At low magnifications, there is a comparatively high

signal-to-noise ratio (SNR), while at high magnification, the SNR is lower, resulting in "noisier" images showing "snow" (noninformational, resolution-decreasing emissions).

As stated earlier, magnification is achieved by changing the relationship between the distance scanned over the specimen surface and the distance scanned over the viewing screen. If 5 μm of specimen surface is scanned at the same time that 5 mm of the viewing screen is scanned, the specimen magnification would thus be 1,000.

Working distance can be varied, placing the specimen higher or lower in the column, which also places the specimen nearer or farther from the electron source and collector, respectively. Moving the specimen farther away from the lenses and collector increases the depth of field and can reduce charging to some extent.

Several types of collectors may be located within a given SEM. The most commonly encountered types are designed to be receptive to either secondary electrons emitted from the specimen surface with energies of 50 eV or less (selected by biasing the collector with +10 kV), backscattered electrons (energies from 50 eV up to the energy of the primary electron beam), or X-rays (EDS collectors).

V. INTERACTION OF THE ELECTRON BEAM AND SPECIMEN

With most biological materials, an accelerating voltage of 10–15 kV is used. This voltage results in the specimen surface being penetrated to about 10 μm and gives rise to five major types of radiation (signal): secondary electrons, backscattered electrons, Auger electrons, X-rays, and cathodoluminescence (Figs. 217a and b).

A. Resolution

The concept of resolution is more complex in the SEM than in the TEM because time is an integral part of SEM image formation. In addition, the various types of electron interactions with specimen atoms have an effect on SEM images, unlike the relatively simple beam scattering used to produce TEM images.

Resolution is affected in a point-by-point recording system in a temporal sense (*when* a signal is recorded). As shown in Fig. 218, if the primary beam impinges on a part of the specimen (point A) that results in the release of electrons (or X-rays) that are shown virtually simultaneously on the viewing screen, good resolution has been achieved. However, if interactions within the specimen result in signals being received by the collector some time after the primary beam has scanned on to a different area of the specimen (point B), the viewing screen will show an event at point B, even though the beam interaction that ultimately produced the signal happened at point A. This clearly produces an image of lower resolution than one generated by a signal resulting from the beam interacting with the specimen at point A and being recorded at point A.

This problem is of particular significance when working in the SEI mode. When the primary, high-energy beam strikes the specimen surface, it can penetrate up to several micrometers at the 10–15 kV commonly used for SEI work on biological specimens. When the primary beam interacts with an atom, such that an orbital electron is released, this electron is called a type I secondary electron. Secondary electrons dislodged from atomic orbits can be emitted in any direction.

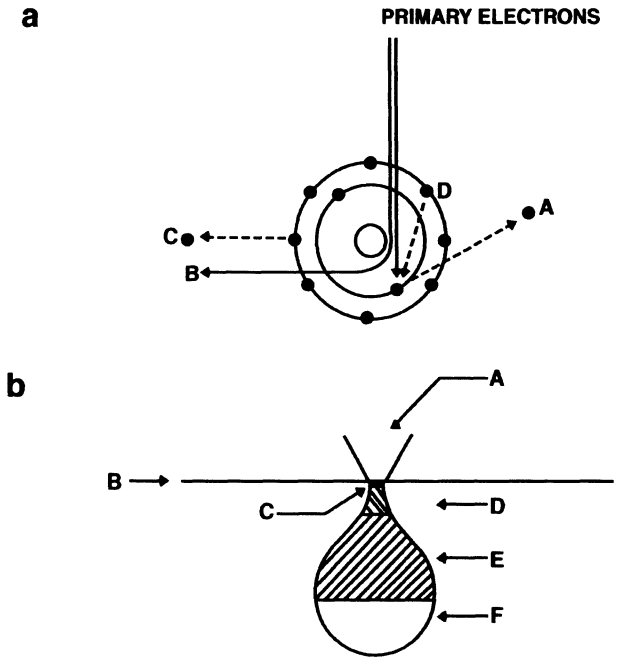

Figure 217. (a) Diagram of the sources of signal types produced from primary electron beam interaction with a specimen. The primary electrons may displace an orbital electron (A), which becomes a type I secondary electron, or may pass by the nucleus to become backscattered electrons (B). After a secondary electron is produced, a high-energy outer shell electron (D) will shift to the electron-deficient lower energy inner shell. The excess energy from this shift may be liberated as cathodoluminescence or an X-ray photon, or may cause a further electron rearrangement leading to the release of an Auger electron (C). (b) Specimen surface (B) penetrated by an electron beam (A). Auger electrons (C) are produced from near the specimen surface, while type I secondary electrons (D), backscattered electrons (E), and X-ray photons (F) are produced from deeper in the specimen.

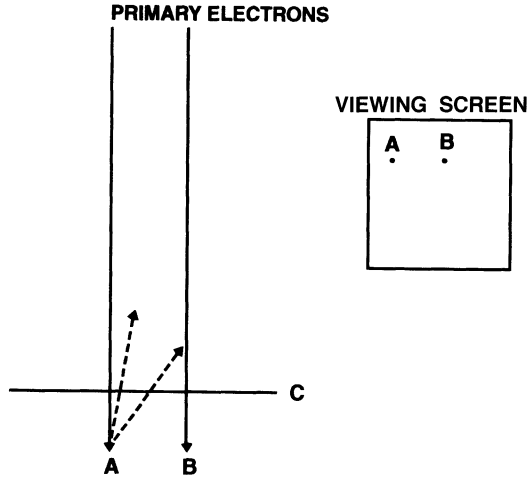

Figure 218. The relationship between time and resolution. The primary electron beam enters the specimen surface (c) at point A to produce type I secondary electrons (dotted arrows), while the beam produces no type I secondary electrons at point B on the specimen. The viewing screen shows a bright spot at *both* points A and B, corresponding to points A and B on the specimen. The secondary electron has emitted almost normal to the specimen surface is recorded at point A on the viewing screen, while the more oblique secondary electron emerges from the specimen surface at a later time and is recorded at point B, even though no emission took place at point B on the specimen.

Only those electrons that have enough energy to emerge from the specimen surface and reach the collector will be recorded. Thus, only those secondary electrons produced near the specimen surface and directed toward the collector will result in recorded information with a high resolution. The temporal relationship between production of these secondary electrons and their imaging will be almost coincident, leading to a high resolution.

Unfortunately, backscattered electrons are also produced at the same time secondary electrons are produced. Backscattered electrons can interact with the SEI collector and other components of the specimen chamber, causing the release of type III secondary electrons, which contribute to noise. Backscattered electrons produced by interactions several micrometers from the sample surface still have a high energy and can interact with further atoms until their energy is spent. If they are scattered back toward the sample surface and interact with an atom, causing the release of a secondary electron that escapes from the sample, this electron is known as a type II secondary electron. If the type II secondary electron strikes the detector and is recorded (Fig. 219), loss of resolution will be a probable outcome. The backscattered electron has traveled some distance through the specimen before causing the ejection of a type II secondary electron from the specimen surface. Thus, an electron has been released some distance from the original point of primary beam interaction with the specimen surface, resulting in a loss in resolution from spatial and temporal inaccuracies. It is important to remember that a number of different signals are being produced simultaneously from an SEM sample, even though only one or two are usually recorded at a time. The fact that events not being recorded can affect those that are being recorded should not be overlooked.

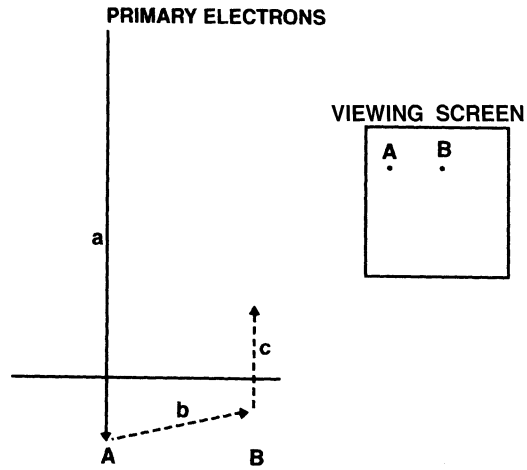

Figure 219. Production of secondary electrons (type II) by backscattered electrons, resulting in loss in resolution. No type I secondary electrons are produced from the interaction of the primary electron beam (a) with the specimen at point A. A backscattered electron (b) is produced from the specimen interaction at point A, which travels obliquely through the specimen. At point B, the backscattered electron produces a type II secondary electron (c) that emerges from the specimen surface and is recorded at point B on the viewing screen.

B. Secondary Electrons

SEI is the main method for examining structural characteristics of specimens. Inelastic collisions between the high-energy primary electron beam and the specimen result in orbital electrons being ejected from atoms located no more than 5–10 nm from the specimen surface. The latest generation of FEG SEMs are capable of 0.5-nm resolution under carefully controlled conditions.

By convention, secondary electrons are those with less than 50 eV of energy (the upper limit set for the secondary electron collector), though most fall within the range of 2–5 eV and about 75% are less than 15 eV (Hayat, 1978). The number of secondary electrons emitted depends on the voltage of the primary electron beam, the angle of impingement on the specimen surface, and the electron density of the specimen (based on its elemental composition). The number of secondary electrons emitted is directly proportional to the number of primary electrons contacting the specimen. The probability of inelastic scattering varies inversely with the accelerating voltage, with the highest yield potentially at 1 kV. Higher accelerating voltages penetrate more deeply into the specimen, and any secondary electrons produced at more than 10 nm from the surface have little statistical probability of having sufficient energy to emerge from the specimen for subsequent collection.

The secondary electron collector (scintillator) in a conventional SEM has a slightly positive bias to attract secondary electrons, but this bias is not strong enough to collect backscattered electrons. The surface of the scintillator is coated with aluminum to reflect photons produced by the secondary electrons toward the photomultiplier tube to which the scintillator is affixed.

Pawley (1988) described the importance of specimen coating, charge accumulation on specimen surfaces, and surface topography on imaging for low-voltage SEM:

> Although there is a danger that this metal coating may decorate or obscure small details on the specimen surface, it does increase the amount of signal produced near the point of beam impact, and it also provides a degree of conductivity which prevents the accumulation of a negative surface charge which might displace or defocus the beam or interfere with the secondary electron collection field...Charge accumulation occurs because on most specimens viewed at 10–20kV, more electrons enter the surface than leave it. Because on flat samples, the total secondary and backscattered electron yield increases to unity at lower voltages, it is widely believed that charging artifacts should always be less important at low voltage...it is not true for geometrically complex samples. On these materials, even though the absorbed current averaged over the area viewed may equal zero, marked variations within and adjacent to the scanned area can produce serious charging effects...To sum up, coating is needed at low voltage for conductivity and at high voltage for contrast.

Factors Increasing Signal (2° Electrons Collected)

The lower, or more oblique, the angle of primary beam impingement on the specimen surface, the more secondary electrons will be emitted. If the specimen appears to have little contrast, tilting it in relationship to the primary beam will increase the signal, resulting in improved contrast.

More electrons will be emitted from a specimen surface that is rough or pointed, with edges producing strong emissions, a condition known as *relief contrast*. A flat epidermal surface will produce little signal compared with a pointed surface (e.g., villi in small intestine, trichomes on plant leaves).

More secondary electrons will be produced from a negatively charged area than from a positively charged area within a specimen, which is known as *potential contrast*.

The closer the specimen is to the collector, the more secondary electrons will be recorded. Variation of the specimen working distance allows adjustment for this factor, depending on the amount of signal emanating from the specimen.

Lower accelerating voltages yield greater emission of secondary electrons. Different accelerating voltages can also alter the depth from which the image is generated. Boyes (2000) explains that low-voltage scanning electron microscopy benefits from the high stopping power of the

sample for low-energy electrons with concomitant restricted penetration of the beam into the sample. Figure 220 shows a copper grid that is coated with Formvar, to which some circular diatoms are attached. Both images were taken at a working distance of 10 mm, but Fig. 220A was taken with an accelerating voltage of 25 kV. In this image, the copper grid is producing a strong signal (it is very light in the photograph), and the thin Formvar film directly below the grid and the

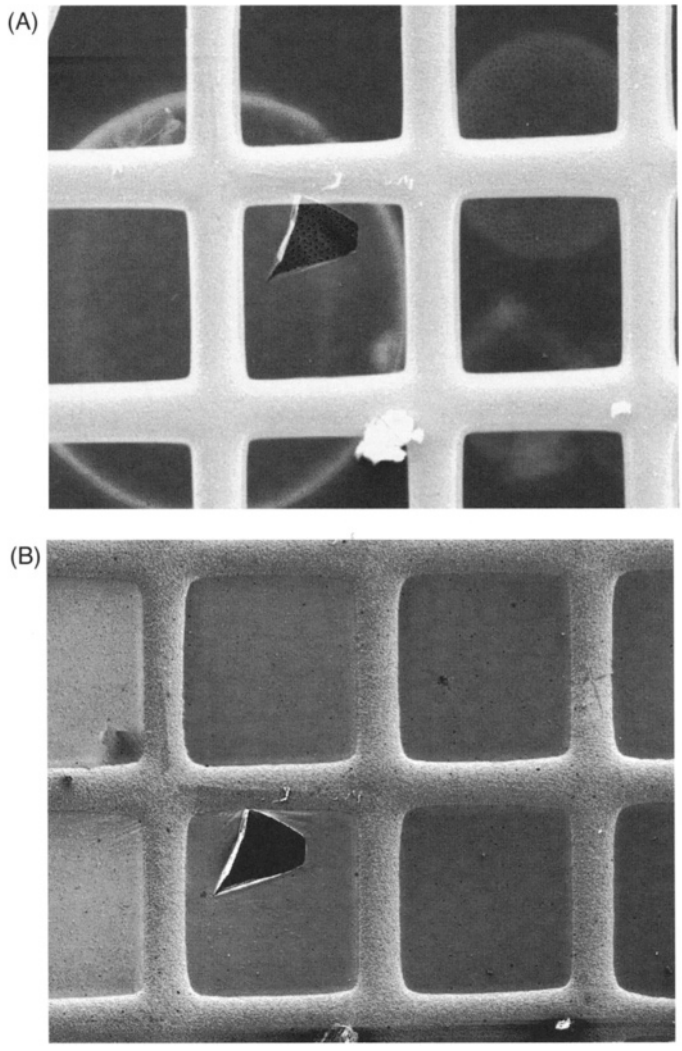

Figure 220. Secondary electron imaging (SEI) of Formvar-coated grid, with diatoms attached to one side of the Formvar film. (Courtesy of Vernon Robertson, JEOL USA, Inc.) (A) Working distance of 10 mm, 25 kV accelerating voltage. Grid bars are bright white, indicating a large amount of signal. The Formvar film on the underside of the copper grid and the frustules of the circular diatoms attached to the underside of the film are visible. A tear in the Formvar film reveals the punctuate nature of the diatom frustule. (B) Working distance of 10 mm, 3 kV accelerating voltage. The grid bars are no longer exhibiting the strong signal characteristics found at 25 kV, above. In addition, the ghost-like images of diatoms are not visible through the Formvar coat, and the punctuate surface of the frustule is not visible through the hole in the Formvar film.

diatoms on the opposite side of the Formvar are producing far less signal (they are darker). A small rip in the Formvar shows the intricate pattern of the diatom frustule surface beneath the Formvar film. Figure 220B was taken with an accelerating voltage of 3 kV, which resulted in the beam generating signal only from near the surface of the sample so that the Formvar film and the copper grid are clearly seen, but the indistinct diatom outlines visible through the Formvar in Fig. 220A and the diatom surface directly below the torn Formvar are no longer visible.

In all SEM imaging modes, more signal is produced by concentrating the beam to produce a smaller spot on the specimen. With SEI, when working at low magnifications, a higher beam collimation achieved by increasing the current to the final condenser lens results in more contrast and more noise. For high magnification, there is inherently less signal and less contrast if the condenser lens is left at the setting used for low magnification. As a rule of thumb, as the magnification increases, the current to the final condenser lens should be increased, and the SEI collector contrast should be increased. As the magnification is decreased, the condenser lens should be deenergized, or spread, and the SEI collector contrast should be decreased.

Field emission gun (FEG) filaments have a tip diameter of only 3–5 nm, producing a beam that is more coherent and thus 1,000 times brighter than a conventional tungsten filament. The same number of electrons are generated in both cases, but a much higher electron density is possible with the FEG. In addition, the energy spread in an FEG beam is much narrower than that of a conventional tungsten filament, resulting in less chromatic aberration in the former (Hainfeld, 1977). A typical FEG source size is 1,000 times smaller than the typical tungsten filament of a thermionic emitter while being 100 times brighter. Thus, an FEG produces greater brightness and increased signal from a given specimen as well as a lower chromatic aberration due to the decreased energy spread of the electron beam, compared with a conventional thermionic emitter.

There are two types of FEGs available: *hot*-(Schottky) and *cold*-cathode FEGs (see Table 22). A *cold*-cathode FEG is useful at lower kilovolts (e.g., 1 kV) because the low energy spread of the beam produces a better resolution under low kilovolt conditions. With a *hot*-cathode FEG, the energy spread of the beam is greater, so resolution suffers at low kilovolts, while the effect of the energy spread in the beam is masked at higher kilovolts. The hot-cathode FEG also has a larger probe size than a cold-cathode FEG but produces a higher beam current for analytical work. It has higher beam stability than a cold-cathode FEG because it operates at approximately 1,800° K, yielding a beam stability of more than 1% per hour. The higher temperature of operation allows it to remain largely contamination free. A cold-cathode FEG, however, produces a smaller spot size and consequently a better resolution at low kilovolts because of the lower energy spread in the beam than for a hot-cathode FEG. Unfortunately, a cold-cathode FEG suffers from contamination by adsorbed gas molecules, which causes emissions to decrease and the stability of emissions to decrease over hours to days of use. According to Goldstein *et al.* (1992), brief periods of unstable emission can occur following the adsorption of a single gas molecule to the emitter. To restore

Table 22. Comparison of Different Types of Electron Sources (Courtesy LEO Electron Microscopy)

Emitter Type	Thermionic	Thermionic	Cold FEG	Hot FEG (Schottky)
Cathode material	W	LaB_6	W	ZrO-coated W
Operating temperature (°K)	2,800	1,900	300	1,800
Cathode radius (nm)	60,000	10,000	≤ 100	$\leq 1{,}000$
Effective source radius (nm)	15,000	5,000	2.5	15
Operating vacuum (Pa)	$\leq 1 \times 10^{-5}$	$\leq 1 \times 10^{-6}$	$\leq 1 \times 10^{-10}$	$\leq 1 \times 10^{-8}$
Cathode regeneration	Not required	Not required	Every 6–8 h	Not required

high and stable emission, a cold-cathode FEG is "flashed" at 2500° K approximately daily. For some analytical techniques requiring long periods of beam exposure to acquire sufficient signal, a cold-cathode FEG is contraindicated, since the continual tip contamination results in current changes over time and, thus, changes in the signals collected. Literature provided by LEO Electron Microscopy (from which Table 22 was abstracted) for their LEO 1500 series SEMs with their GEMINI column compares different electron source performance in reference to a variety of operational parameters.

C. Backscattered Electrons

Backscattered electron imaging (BEI) records events due to elastic collisions. When electrons of the primary electron beam entering the specimen surface are deflected through large angles as a result of electron/nuclear interactions without energy loss, the electrons may escape from depths of several micrometers. Resolution in the backscattered mode is now approximately 10 nm less than with secondary electron imaging (40 nm versus 30 nm, respectively, with conventional SEMs with thermionic emitters). Backscattered electrons may have energies equal to the accelerating voltage of the primary beam or lower. By convention (and adjustment of the BEI collector circuitry), any electron with more than 50 eV of energy is classed as a backscattered electron. Composition (contrast between elements of significantly different atomic number) and topography (contrast between areas with different surface structures) are the two imaging modes used.

1. Factors Increasing Signal

With BEI, the elemental composition of the specimen is a major factor in developing contrast. Major differences in atomic number and their effect on contrast can be utilized in cytochemical procedures. For example, if it were useful to localize lysosomes in a monolayer of cells attached to a coverslip, a lead-capture procedure could be used on aldehyde-fixed cells to label the hydrolytic enzymes present. After dehydration and critical-point drying, the cells could be coated with carbon so that the only high atomic number moiety present would be lead in lysosomes. In the BEI mode, primary electrons would penetrate several micrometers beneath the cell surface and would produce a strong backscatter signal from the lead.

As with SEI imaging, the angle of the primary beam striking the specimen can be manipulated by tilting the specimen stage. A higher beam angle produces more image contrast in BEI. Topographic changes in adjacent areas also contribute to the development of contrast. Edge effects result in more signal from edges and pointed structures within a specimen. Some workers impregnate the specimen with a heavy metal such as osmium or osmium/thiocarbohydrazide combinations to increase the overall backscatter signal.

Backscatter electron imaging has less resolution than SEI because of the depth from which signal can be produced. High-energy backscattered electrons passing through the specimen at a very oblique angle (Fig. 221) can emerge from the specimen surface and be recorded a short time after the primary beam interaction with the specimen. However, during this time, the primary beam and the viewing screen scan have moved on to a new part of the specimen. Thus, the obliquely emergent electron will result in a bright spot on the viewing screen when the scanning beam may actually be over a specimen area producing no signal, thus causing a spurious signal and consequent loss in resolution.

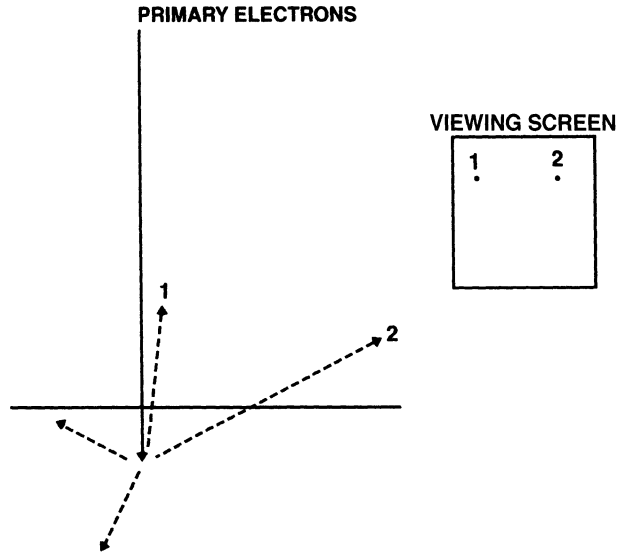

Figure 221. Oblique path of backscattered electrons, resulting in loss of resolution in the backscatter mode. All of the dashed lines with arrows represent backscattered electron paths resulting from the interaction of the primary electron beam with the specimen. Backscattered electrons 1 and 2 will be recorded, though at different times during the scan.

D. Auger Electrons

When a primary electron strikes an atom and causes an electron from an inner orbit to be ejected, an electron from a higher level fills the resulting void. When an electron from a higher-energy outer shell moves to a lower-energy inner shell, an amount of energy equal to the difference in energy levels between the two shells must be released, as dictated by the laws of physics. This energy adjustment can be accomplished by emission of an X-ray, a photon of light (cathodoluminescence), or the release of a low-energy Auger electron.

Auger electron imaging (AEI) measures low-energy electron emissions. The average depth below the specimen surface from which Auger electrons can escape without appreciable energy loss is between 0.5 and 2 nm. Similar to the other signals considered, numerous Auger electrons are produced deep within a specimen that are not recorded because the emissions never escape the specimen surface to strike a collector.

Hayat (1978) defines Auger electrons as secondary electrons with energies from 1 to 2,000 eV released from the specimen surface when the primary beam is set at about 3 kV. The signal is measured in electron volts and allows the elemental composition to be determined. Anything above lithium in the periodic chart can be detected.

A miniscule quantity of backstreaming diffusion oil can result in a total loss of Auger electron signal, since any signal produced would originate in the thin film of oil deposited on the specimen surface rather than from the sample itself.

E. Energy-Dispersive Spectroscopy (EDS)

In almost all cases, EDS, which records characteristic X-rays emitted by specimens exposed to a high-energy electron beam, can provide elemental analysis that is more easily

accomplished than with AEI. As described above, displacement of an inner shell electron results in an electrically unbalanced atom, leading to shifts of outer orbital electrons to fill inner shells. As these shifts take place, energy is often released in the form of X-rays. If an electron is dislodged from the innermost shell of an atom with three filled electron shells, a variety of rearrangements can take place (Fig. 222). The innermost (K) shell will be filled by an electron shifting inward from the L shell, resulting in energy being released in the form of a characteristic X-ray. The hole left in the L shell will be filled by an electron from the M shell, with an energy release in the form of an X-ray with an energy level characteristic of that orbital shift.

Thus, the bigger the atom, the more possible characteristic X-rays that can be produced, depending on the orbit from which the secondary electron is dislodged. Chapter 14 will discuss the utilization of this type of imaging in detail.

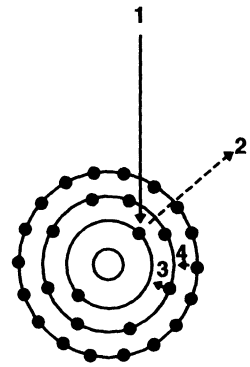

Figure 222. Orbital rearrangements following an inelastic collision between the primary electron beam and an electron in the K shell of an atom. The primary electron beam (1) causes the ejection of a secondary electron (2) from the innermost orbital, followed by the shift of an electron (3) from the next orbital to fill the vacancy, resulting in a shift of an electron (4) from the next orbital to fill the vacancy caused by the shift of electron 3.

F. Cathodoluminescence

In order to detect photons released as a result of atomic rearrangements following secondary electron emission, either the scintillator over the SEI photomultiplier tube can be removed or a second photomultiplier tube can be incorporated in the SEM. Cathodoluminescence is weak, requiring a great deal of signal amplification, but Postek *et al.* (1980) state that 80-nm resolution is possible. They suggest that the primary use for this technique is to examine compounds for impurities. Hayat (1978) provides a series of references for the use of cathodoluminescence in biological research while pointing out the technical difficulties in some of these applications.

VI. SPECIMEN PREPARATION

A. Fixation

Sample preparation for SEM requires the same thought and consideration that were described for TEM samples in Chapter 1. Aldehyde fixation is frequently adequate, but some

investigators use a postfixation with osmium to try to improve bulk conductivity of the specimen. Another technique (Kelley *et al.*, 1975) utilizes a rinse in thiocarbohydrazide (TCH) prior to osmication, because the TCH serves as a mordant for osmium, allowing increased osmium binding to the tissue.

Samples should be made as small as practical to reduce dehydration and drying problems as well as to reduce the thickness of tissue attached to the grounded specimen support. Dried tissues and cells act as electrical insulators under most circumstances. When the primary electron beam enters the surface of the specimen, much of the electron beam energy encounters difficulty reaching ground potential. In extreme cases where specimens are quite thick, the specimen can be seen to bulge under the SEM beam as the subsurface tissues heat up and expand from the electron beam energy that cannot reach ground and be dissipated. Osmium or osmium/TCH treatment along with reduction in specimen thickness can help reduce this problem.

Complex spore-bearing structures found in fungi are typically difficult to fix without losing the spores or developing handling artifacts. In particular, masses of fungal hyphae and sporophores bearing spores can be extremely difficult to wet adequately. Vapor fixation with osmium prior to immersion in aldehydes can help preserve these delicate structures (King and Brown, 1983).

Needless to say, if native samples being examined are already naturally dry (e.g., an aged seed, fossil, or egg shell surface), fixation is generally unnecessary. In some cases, fixation might even be contraindicated because it would change the character of the specimen to rewet it with processing fluids. The use of an LV SEM or an ESEM to examine native samples or frozen samples is another way to investigate samples such as fossils or forensic samples that cannot be processed in any way without potentially damaging their integrity.

B. Dehydration and Transition Fluids

Dehydration may be accomplished with the same agents typically employed for TEM preparations (ethanol, acetone), but the final method for drying the specimen should be considered before choosing the agent. If the specimen is to be critical point dried, ethanol is usually the best choice because some of the seals in most critical point dryers may be damaged by acetone. In some cases, a transition solvent such as amyl acetate may be used between the dehydration agent and the critical point dryer fluid (e.g., CO_2 or Freon™). This was originally done so that the investigator could tell when the dehydration agent in the specimen had been completely purged and replaced by liquid CO_2 in the dryer (the banana smell of amyl acetate would no longer be present as the dryer chamber was vented and drained during the purging process).

C. Drying

The conventional SEM operates with a vacuum in the diffusion pump range or better, depending on the type of gun used, so it is necessary to dry a specimen thoroughly before introducing it into the high-vacuum system. In the early days of SEM, certain insect samples were examined live without fixation and dehydration, because insects with thick cuticles and air passageways (spiracles) that can be closed have an unusual ability to withstand the harsh environment within an SEM for a limited time. Since the late 1980s, ESEMs and LV SEMs have finally allowed

the examination of a wide range of unprocessed or minimally processed materials as described later in this chapter.

Samples that are air-dried may be exposed to surface tensions during the process as high as 2000 lb/in^2 (13.8 MPa), which can result in up to 45% shrinkage of embryonic and fetal tissues (Hayat, 1978). Hayat also showed two figures of slime mold spores (*Badhamia utricularis*) to support the contention that air drying can crush biological structures. Unfortunately, his example illustrates a totally different point as well: Slime mold spores in nature become air dried as they mature and are then dispersed by breezes. If field-collected material is examined without mounting in any fluid, spores are clearly collapsed. Hayat shows these as an example of an air-drying artifact. Hayat's second figure shows perfectly inflated, round spores following fixation and critical point drying, which he identified as a superior image. The second case is clearly an artifact of specimen preparation. This example is offered to make the reader aware that an examination of a specimen by light microscopy in its native state may be of use prior to SEM sample preparation so that such preparation-induced artifacts can be avoided.

1. Critical Point Drying

Critical point drying (CPD) is based on the principle that under certain temperature and pressure conditions, a fluid and its overlying vapor phase will become indistinguishable (the critical point). At this point, the surface tension on a specimen originally in the fluid phase will be zero. As pointed out by a flyer describing the EMS850 critical point dryer (Electron Microscopy Sciences, Fort Washington, PA), our main concern is to remove water from a biological sample, however "... the critical point for water of +374°C and 3212 psi is inconvenient, and would cause heat damage to the specimen."

To avoid these harsh conditions, samples may be dehydrated up to 100% ethanol, put into a critical point dryer, and then purged repeatedly with liquid CO_2 until all the ethanol has been replaced with CO_2. Next, the chamber is sealed and heated until the critical point for CO_2 is reached [31°C and 1,072 lb/in^2 (7.4 MPa)].

As the chamber temperature is raised above ambient, the liquid CO_2 begins to evaporate at a greater rate. At the same time, the pressure inside the critical point dryer increases. The increased chamber pressure causes the vapor to condense back into liquid. The process is based on two principles: (1) Higher temperatures turn liquids into vapors; and (2) Higher pressures turn vapors into liquids. Above the critical point (critical temperature and pressure), the density of the liquid phase becomes equal to that of the vapor phase and thus only one phase remains, with no surface tension. If the temperature of the chamber is maintained above the critical temperature (36–38°C), the chamber can be vented to release CO_2 gas without any danger of recondensation into liquid CO_2 to produce surface tension on the specimen. The chamber should be vented slowly, and the temperature gauge must be closely observed. Allowing gas to escape through a small orifice (the venting valve) at high velocity will cause a temperature drop. If the temperature drops below the critical point, specimen surfaces can become rewetted and suffer surface tension damage.

Critical point drying is not a perfect technique. Shrinkage is still observed, resulting in a 10–15% size reduction in central nervous system materials, 12–13% shrinkage with embryonic and fetal tissues, and up to 20% shrinkage for lung, kidney, liver, and skin (Hayat, 1978). Much of this shrinkage may be due to the fixation and dehydration process itself. One way to monitor this potential problem is to cut frozen sections of the same material with a cryostat, omitting dehydration and drying. If the dimensions of structures in frozen sections and dried specimens are

similar, shrinkage is probably not a serious problem. If they vary considerably, a stepwise comparison of both frozen and dried sections of tissue during the preparative process may yield some clues about how to circumvent the difficulty.

Once samples are dried, they should be mounted on specimen stubs, coated, and examined as quickly as possible. If the samples must be stored, they should be put in chambers with Drierite® to minimize rehydration from atmospheric humidity. In particular, a coated specimen is subject to decreased image quality if the specimen swells hygroscopically and develops hairline fractures in the thin metal coating sputtered onto it to increase conductivity.

Critical point dryers are usually provided with various safety interlocks to prevent overheating or overpressurization of the chamber. It is potentially possible to overpressurize and explode the chambers, hence the common nickname "bomb" often applied to CPD devices. Thus, it is important never to leave a critical point dryer that is in operation and to monitor chamber pressure at all times. Sight glasses in the chambers have been known to fail explosively, so it is a good practice not to sit directly in front of the chamber without some sort of plexiglass safety barrier in place. I have been unable to document any actual cases of CPD failure resulting in serious injury, but failure resulting in unpleasant moments for investigators can be documented from my own laboratory.

2. Freeze-Drying

Freeze-drying was introduced because, in theory, less shrinkage should occur than with a CPD. Also, freeze-drying avoids the perceived danger of the CPD process. The processing schedule is identical through dehydration. Once the specimen is in 100% ethanol, it may be frozen in liquid nitrogen-cooled Freon™ 12 (−158°C) or the sample may simply be cryofixed from its native state. The sample is then placed on a precooled specimen stage held at −40 to −80°C, put under mild vacuum (1.33×10^{-2} Pa or less) and left for 6–8 hr with most specimens. Monolayers need only 1–2 hr, while a 1–3-mm-thick specimen might need 3 days. When frost is no longer visible on the cooled stage, indicating that all the fluids have sublimed, the specimen is warmed gradually over a period of 6 hr or so. When the stage and specimen temperatures are slightly above ambient conditions, the chamber may be vented. The specimen should be mounted on a specimen support, coated, and examined as soon as possible.

3. Specialized Drying Agents

Chemical drying agents have been suggested to eliminate the need for capital investment in a CPD or freeze-dryer as well as the need for facing the "bomb." The published photographs of materials produced with hexamethyldisilazane (Bray *et al.*, 1993; Nation, 1983; Oshel, 1994) and tetramethylsilane (Dey *et al.*, 1989) are quite convincing, but results in our laboratory have been somewhat variable with both techniques. Peldri II™, a proprietary fluorocarbon, was easy to use and gave good results (Kan, 1990), but is no longer available because of regulations imposed by the U.S. Environmental Protection Agency.

Both the hexamethyldisilazane and tetramethylsilane drying techniques require sample fixation followed by dehydration. After the final dehydration step, the dehydration agent is replaced with the drying agent, which is then allowed to evaporate at room temperature (hexamethyldisilazane) or 27–32°C (tetramethylsilane) before the specimen is mounted.

D. Mounting Specimens

Specimens must be mounted onto holders for the specific SEM being used. Most specimen mounts are made of aluminum. They can also be obtained in brass, though brass is more expensive than aluminum and confers no added advantage. If microanalysis of samples is desired, specimens are usually put on pure carbon stubs to avoid spurious readings that might be produced from metal stubs.

Particulate samples are best attached to poly-L-lysine-coated coverslips (Mazia *et al.*, 1975), which are, in turn, attached to stubs. If microanalysis is to be performed, glass is contraindicated as a support because its numerous impurities might give rise to spurious readings with EDS.

Specimens or coverslips with adherent material may be attached to stubs with colloidal silver paint, colloidal silver paste, colloidal carbon paint, carbon tape, or double-stick tape. If double-stick tape is used, some conductive paint or paste must bridge from the stub to the surface of the specimen, since the tape is an insulator. Coverslips are also insulators, so they must be treated in the same fashion. The various pastes and paints must be allowed to dry before being introduced into the specimen chamber of a conventional high-vacuum SEM, otherwise outgassing of the vehicle for the conductive materials will prevent development of adequate vacuum. If microanalysis is to be attempted, tape, coverslips, and metal pastes or paints are contraindicated because they can all result in spurious signals.

E. Coating Specimens

As previously noted, biological tissues are generally good insulators and, if not coated with a conductive material, will build up charge, though this problem is alleviated to a large extent in an ESEM or LV SEM, as will be described in the discussion of such instruments below. In conventional high-vacuum SEMs, the primary electron beam current will have no way to reach ground potential, so if the net specimen current (1° current minus 2° current) is not conducted to ground, image distortion results because the specimen builds up a negative charge from the beam, and the beam is repelled by the negative specimen charge.

In the early days of SEM, vacuum evaporators were used to coat specimens. Since vacuum evaporators are directional coaters, specimens were placed on motorized holders within the vacuum system in order to coat surfaces of variable topography evenly. These holders spun a disc containing the specimens at an angle while the whole disc was quickly rotated around a central axis, thus causing the specimens to go up and down in a clockwise direction while being rotated away from and toward the source (Fig. 223). This procedure frequently heated the specimen to an unacceptable level while not producing a truly even metal coating on specimens with much topography.

Sputter coaters were introduced to solve these problems. The earliest units still heated the specimens, but the ion cloud of argon and the metal atoms dislodged to coat the specimen produced well-coated surfaces for any topography. Later sputter coaters with a triode design, consisting of a permanent magnet installed in the center of the metal target, reduced specimen heating to negligible levels.

Specimens are usually coated with gold or gold–palladium because the fine grain size necessary for TEM resolution is not required with conventional SEMs. However, the introduction of high-resolution (0.5 nm) FEG SEMs led to the design and production of sputter coaters

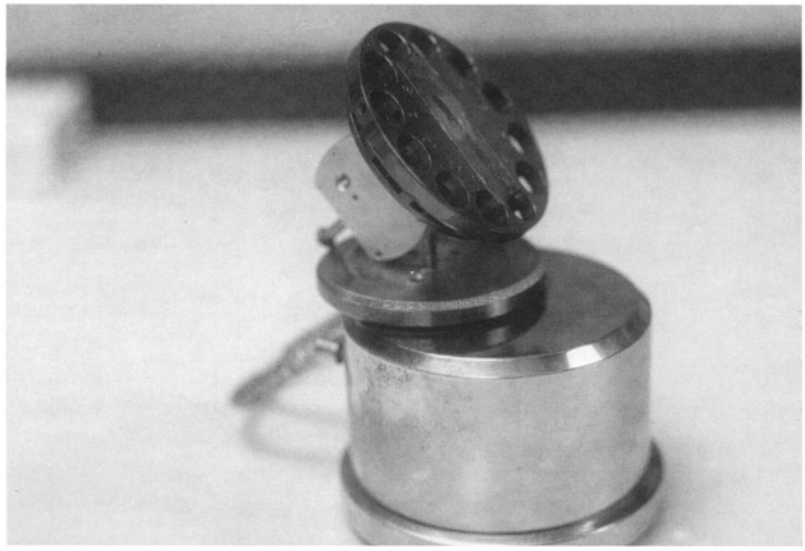

Figure 223. Specimen holder for coating SEM samples in a vacuum evaporator (from a Ladd Vacuum Evaporator).

capable of depositing 1.0-nm chromium metal coatings, in contrast to the usual 20-nm gold–palladium coatings used with conventional SEMs as described by Apkarian (1989).

Specimens prepared for microanalysis (EDS) should not be coated with metals because the metal may cause overlapping emissions with areas of interest within the specimen. Carbon coating can be used in place of metal, and as mentioned above, the specimen is normally placed onto pure carbon stubs with colloidal carbon rather than onto coverslips or aluminum stubs to reduce the chance for spurious readings.

VII. ARTIFACTS AND THEIR CORRECTION

Some artifacts are inherent in specimens of a given type but can be minimized by instrument adjustments. Other artifacts are caused by improper instrument handling. Hayat (1978), Postek *et al.* (1980), and Crang and Klomparens (1988) show a number of examples of SEM artifacts along with explanations concerning their derivation.

Charging occurs any time a negative charge builds up in the specimen. It can result in areas of strikingly different brightness in the specimen or movement of the specimen, particularly if the specimen has long thin processes such as fungal filaments extending above the specimen mount surface. Charging can also lead to blurred images in photographs of the subject. To minimize charging, specimens should be freshly coated with a good conductive material such as gold–palladium (about 20 nm thick), the coating should be grounded to the specimen mount, and the specimen mount should be grounded to the SEM chamber. For high-resolution work, coating with chromium would be necessary, because the grain structure of coarser coatings like gold–palladium obscure the details visible with high-resolution SEMs. If charging is still severe despite application of a conductive metal coating, the specimen can be moved to the farthest working distance and/or the accelerating voltage can be reduced. A flat specimen produces less signal and less potential charging than a tilted specimen. If none of these suggestions helps, reduce the size and

height of the specimen and consider increasing the bulk conductivity in future preparations of the particular specimen type by incorporating osmium during fixation.

Specimen burning can be a problem in situations that produce charging, as just described. In addition, nonconductive materials such as wax coatings on leaf epidermal surfaces can heat up sufficiently during bombardment with the beam to actually melt (Hayat, 1978). In these cases, a heavier coating of conductive metal may help, as well as decreasing the accelerating voltage. Vascular casts made of nonconductive methacrylate plastic resins are also prone to beam damage. If the magnification is increased significantly above 2,000× at 15 kV, the plastic casts will actually begin cracking. This happens because the beam is concentrated over a smaller amount of the specimen at higher magnifications, leading to greater specimen heating. A lower accelerating voltage or better conductive coatings can decrease the problem, but taking photographs at lower magnifications will also alleviate the problem. For some reason, thin layers of corneal tissues often are damaged by the beam, particularly when a line scan is used to saturate the SEM filament. If filament adjustment is not done quickly enough, the line scan may be burned into the specimen surface, even at low magnification. Since the more highly focused electron beam used at higher magnifications can damage the specimen, it is wise to record low-magnification images of beam-sensitive samples prior to going to higher magnification. It is very disappointing to take a high-magnification photograph and then to decrease magnification in order to take a survey photograph, only to find that the specimen has a square burned into it where the high-magnification area was scanned by the beam.

Edge effects occur frequently. If villi of small intestinal surfaces are being observed, the pointed tips will tend to produce excess signal. If a cut surface of tissue is examined, the edges of open spaces will tend to be much brighter than the surrounding flat areas. Decreasing high voltage, spreading the beam by turning down the condenser setting, moving the specimen farther from the collector by increasing working distance, and making sure that the specimen is not tilted can decrease these effects. Minimizing the bulk of the specimen below the surface viewed, as well as osmicating the sample during processing, may reduce bulk charging effects. Working with brightness and contrast controls on the collector may also allow the operator to decrease an edge effect by adjusting the brightness and contrast of the edge to desired levels, disregarding the concomitant decrease in illumination and contrast of the surrounding area, if it is not the area of true interest.

Some specimens consisting of long filamentous structures, such as algal or fungal filaments or fruiting structures that extend well beyond the specimen stub surface, will tend to move when exposed to the electron beam, making them difficult to record. One solution to this problem is to lay such structures down on a substrate like double-stick tape so that they are closer to the specimen stub surface and, thus, better grounded.

VIII. SPECIALTY SEMS: FEG, LV, AND ESEM INSTRUMENTS

A. Field Emission Gun SEMs

The use of a FEG with its improved coherence and ability to work well at low accelerating voltage allows 1.5- to 0.5-nm resolution with biological materials, permitting detailed examination of structures, such as the component parts of nuclear pores, previously possible only with a TEM (Ris, 1991). This technology is a major breakthrough for biologists because we can now examine structures with an SEM at the same level of resolution that has been standard for years

with chemically-fixed TEM samples (2 nm). Both types of microscopes have resolving capabilities that exceed our current conventional chemical fixation capabilities (see Chapter 1).

B. Environmental Scanning Electron Microscopes (ESEMs)

The ESEMs now supplied by FEICO/Philips have already been mentioned as a major breakthrough in the SEM business because of their ability to examine hydrated specimens or specimens near atmospheric pressure. They can operate at pressures of up to 50 Torr (or 6.7 kPa; atmospheric pressure is 760 Torr, 101.3 kPa) with specimen temperatures up to 1,500°C. Two pressure-limiting apertures are located at the bottom of the column, which limits the distance the beam travels through gases in the chamber to a few millimeters and thus minimizes the interactions between the electron beam and the gas molecules in the chamber (Fig. 224). In addition, the patented Gaseous Secondary Electron Detector (GSED) operates on a different principle than the standard Everhart–Thornley detector found in conventional SEMs, which converts secondary electrons into photons that are further processed by a photomultiplier tube and which will not operate in a gaseous environment. The GSED (Fig. 225) is a conical electrode located directly above the sample, through which the electron beam passes. Secondary electrons dislodged from

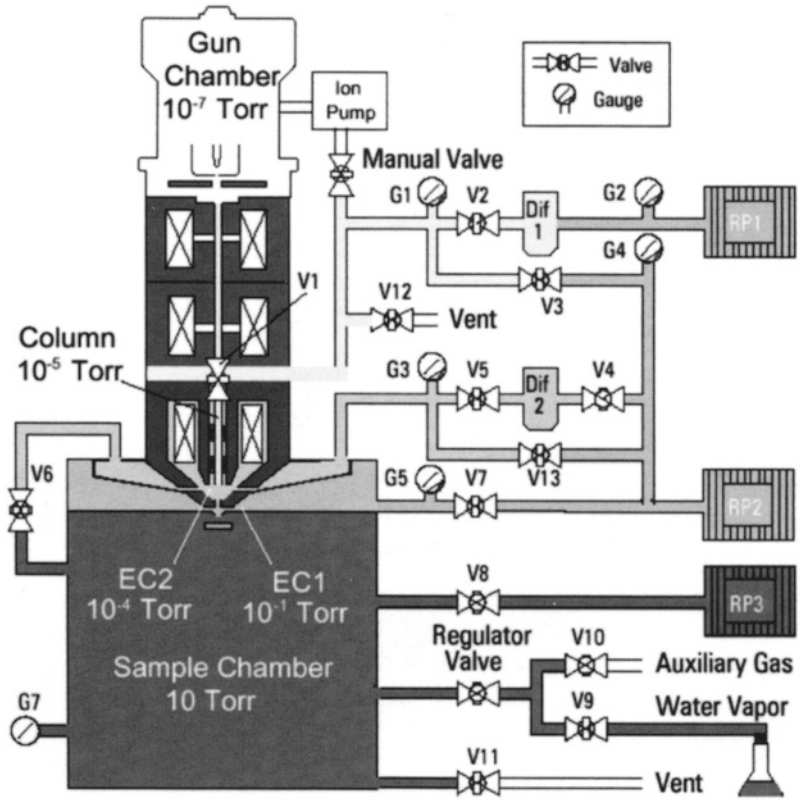

Figure 224. Diagram of the ESEM column. (Courtesy of FEI Company.)

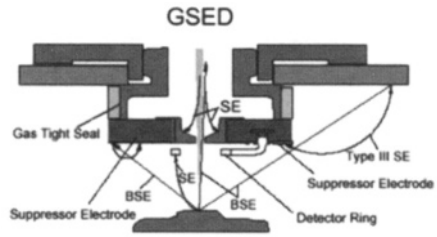

Figure 225. Diagram of Gaseous Secondary Electron Detector (GSED) from ESEM. Secondary electrons (SE) are collected by the detector ring. Back scattered electrons (BSE) impacting the suppressor electrode can produce type III secondary electrons. The suppressor electrode is positively biased to trap the type III secondary electrons (Type III SE) generated from the suppressor electrode or other components in the specimen chamber to reduce noise in the secondary electron image. (Courtesy of FEI Company.)

the specimen by the primary electron beam are attracted to the positive potential of a few hundred volts applied to the detector. As secondary electrons move toward the detector, they collide with gas molecules in the chamber, ionizing the gas molecules and resulting in the release of further electrons, called environmental secondary electrons (ESE) and positive ions. This process is repeated many times, resulting in an amplification of the original secondary electron signal, which is received by the detector and transmitted to an electronic amplifier and further processed into a visual image. A second advantage to this process is that the positive ions produced during signal amplification are attracted to the sample as charge accumulates, resulting in the suppression of specimen charging due to the accumulation of negative charge from the initial impingement of the primary electron beam. Thus, specimen coating to decrease specimen charging is not necessary.

C. Low-Vacuum SEMs (LV SEMs)

Since the early 1990s, the first LV SEMs produced by Hitachi and quickly followed by LV SEMs from JEOL have been joined by multiple LV SEM models produced by LEO, Hitachi, and JEOL. FEICO/Philips has chosen not to produce LV SEMs, since their ESEMs can be used under conventional high-vacuum conditions as well as for hydrated, extremely low vacuum conditions that overlap the operating parameters of LV SEMs (see Fig. 226 for a comparison of vacuum ranges of the different types of SEMs). At the present time, the patents held by FEICO associated with the ESEM design limit the operational parameters of LV SEMs being produced by other manufacturers. The ESEM has multiple differential apertures (Fig. 227) controlling the pressure differences between the column and the specimen chamber as well as their patented GSED described above, while LV SEMs are limited to one differential aperture and have only recently been provided with secondary electron detectors for use in the LV mode that are based on a different design than those found in the ESEM.

Even with these limitations, the LV SEM allows the examination of a much broader group of specimen types than a conventional high-vacuum SEM. Low-vacuum SEMs have the basic capabilities of a high-vacuum SEM, while offering the opportunity to leak air into the specimen chamber to reduce vacuum to the 2–4 Torr (267–533 Pa) range.

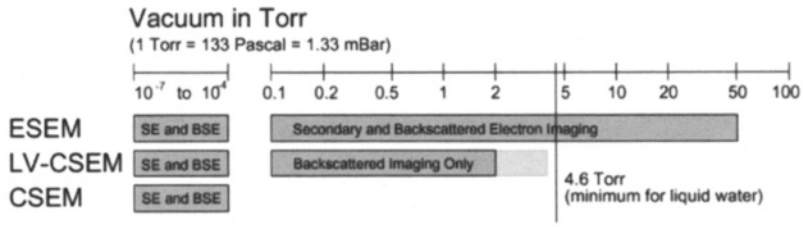

Figure 226. Vacuum in Torr produced by conventional SEMs (CSEM), low-vacuum SEMs (LV-CSEM), and environmental SEM (ESEM) and the type of imaging possible in each vacuum range, secondary electron imaging (SE) and backscatter electron imaging (BSE). (Courtesy of FEI Company.)

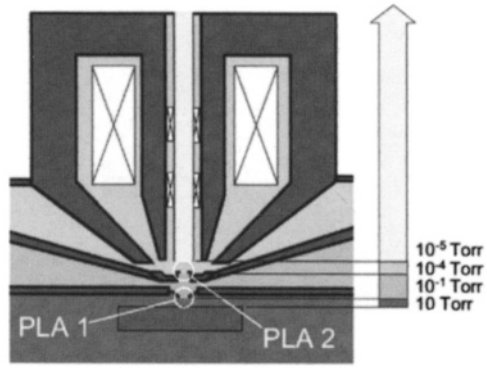

Figure 227. Patented multiple differential aperture assembly, with pressure-limiting apertures 1&2 (PLA1 and PLA 2) directly below final electromagnetic lens in ESEM column, showing vacuum in Torr at various locations. (Courtesy of FEI Company.)

Since the vapor pressure of water is 4.6 Torr (613.3 Pa) at 0°C, a wet sample cannot maintain its hydrated state in an LV SEM but will become dried over a relatively short period of time, with consequent structural damage (see Fig. 228). This feature has been turned to advantage by some workers (Suzuki *et al.*, 1995) who have effectively used the LV SEM to conduct studies of materials under "poor-man's cryo" conditions, as recently demonstrated to us by Donna Guarrera and Vernon Robertson at JEOL USA, Inc. in Peabody, MA.

Vernon Robertson had a simple specimen stub (Fig. 229A) machined, consisting of a brass blank with clips secured by screws to the upper surface, and nylon screws protruding slightly from the base of the holder, to effect thermal isolation of the stub from the specimen holder (Fig. 229B). To minimize backscatter signal from the brass stub, carbon tape is placed on the stub. The clips shown in Fig. 148A are used to secure the tape, which will otherwise detach when the stub is placed in liquid nitrogen. The stub is placed into a small container filled with liquid nitrogen and left until the stub surface quits bubbling violently, indicating that the stub is cooled to −196°C. At that point, the stub is quickly removed from the liquid nitrogen, the specimen is loaded onto the black tape, and the stub is quickly inserted into the LV SEM specimen holder, put into the LV SEM specimen chamber, and pumped down to 2–4 Torr (267–533 Pa) and examined in the backscatter mode.

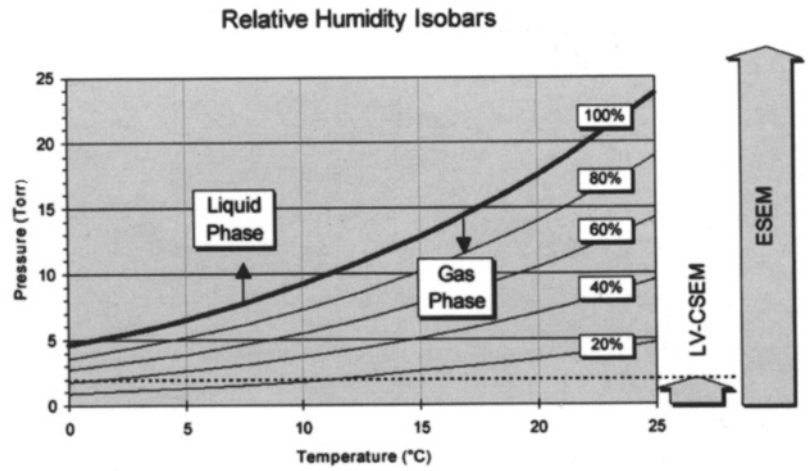

Figure 228. Graph showing the behavior of water at various pressures, in Torr. Note that at 0°C, water becomes gaseous at approximately 4.6 Torr. ESEM: environmental SEM; LV SEM: low-vacuum SEM. (Courtesy of FEI Company.)

During our visit to the JEOL lab, we examined "green pond scum" kindly provided by Dr. David Domozych (Department of Biology, Skidmore College). Small paper-punch-sized filter paper disks covered with green material were picked up directly from a Petri dish filled with freshwater pond scum, put on the liquid nitrogen-cooled specimen stub, and pumped down as described above. Initial examination of the specimen revealed a relatively featureless, smooth surface that was the frozen water in which cells were embedded. Within a minute or so, the ice sublimed to reveal algal cells with surface decorations. The cells were subsequently identified by Dr. Domozych as *Penium* sp. (Fig. 230). In the background, a vast lawn of bacilliform bacteria can be seen. After

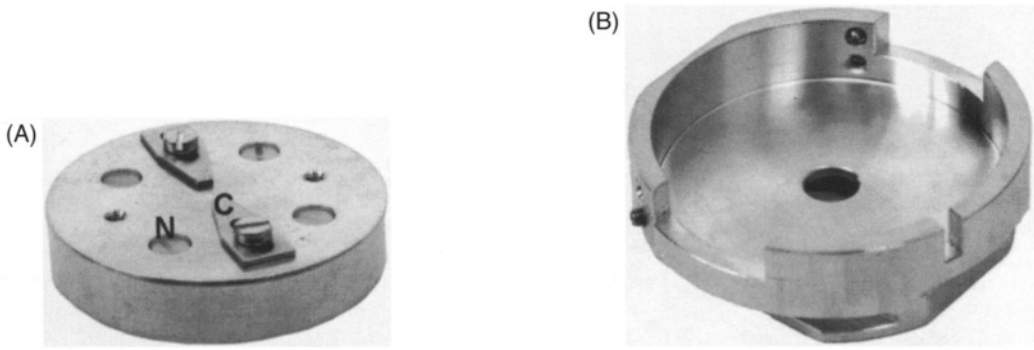

Figure 229. Cryo specimen stub and specimen holder available from JEOL USA, Inc. for their JEOL JSM-6460LV scanning electron microscope. (Courtesy Vernon Robertson, JEOL USA, Inc.) (A) Cryo specimen stub, with two clips (C) to hold carbon tape to stub during liquid nitrogen immersion. Nylon screws (N) are screwed through the brass stub and protrude slightly from the bottom so that the bulk of the brass stub does not contact the specimen holder shown in Fig. 148B. The carbon tape is placed on the brass stub to prevent excessive backscatter signal from the brass stub when viewing specimens in the backscatter mode. (B) Specimen holder for the JEOL JSM 6460LV SEM. When the cryo specimen stub is placed into the specimen holder, thermal contact is limited to the grounding screw visible near the top center of the photograph and the edge of the holder directly opposite.

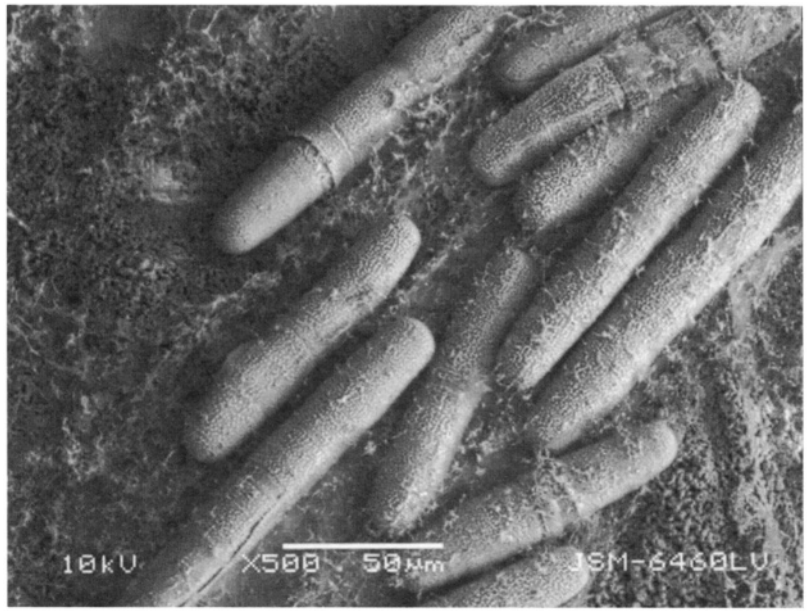

Figure 230. Cryofixed sample of pond scum examined with a JEOL JSM-6460LV SEM, utilizing the cryo stub prepared as described in the text. The large tubular cells are the alga, *Penium*, and the much smaller bacilliform cells in the background are bacteria. ×42. (Courtesy of Donna Guarrera, JEOL USA, Inc.)

a short time, the continued sublimation process led to the extraction of frozen water from the interior of the *Penium* sp. cells and their eventual collapse. The inevitable dehydration of frozen hydrated samples under LV SEM conditions necessitates fairly rapid examination and image recording, but still allows the examination of frozen-hydrated specimens that heretofore required specialized, expensive cryostages attached to conventional SEMs or the use of expensive ESEMs.

REFERENCES

Apkarian, R.P. 1989. Condenser/objective lens SE-I imaging of chromium coated biological specimens using a Schottky field emission source. In: *Proc. 47th Ann. Meeting Electron Microsc. Soc. Am.* (p. 68). San Francisco Press, San Francisco.

Boyes, E.D. 2000. On low voltage scanning electron microscopy and chemical microanalysis. *Microsc. Microanal.* 6: 307.

Bray, D.F., Bagu, J., and Koegler, P. 1993. Comparison of hexamethyldisilazane (HMDS), Peldri II and critical-point drying methods for scanning electron microscopy of biological specimens. *Microsc. Res. Tech.* 26: 489.

Claugher, D. (ed.). 1990. *Scanning electron microscopy in taxonomy and functional morphology*. Clarendon Press, Oxford.

Crang, R.F.E., and Klomparens, K.L. 1988. *Artifacts in biological electron microscopy*. Plenum, New York.

Dey, S., Basu Baul, T.S., Roy, B., and Dey, D. 1989. A new rapid method of air-drying for scanning electron microscopy using tetramethylsilane. *J. Microsc.* 156: 259.

Edwards, D.F., Patton, C.S., Bemis, D.A., Kennedy, J.R., and Selcer, B.A. 1983. Immotile cilia syndrome in three dogs from a litter. *J. Am. Vet. Med. Assoc.* 183: 667.

Goldstein, J.I., Newbury, D.E., Echlin, P., Joy, D.C., Romig, A.D., Jr., Lyman, C.E., Fiori, C., and Lifshin, E. 1992. *Scanning electron microscopy and X-ray microanalysis*, 2nd edn. Plenum, New York.

Haggis, G.H. 1972. Freeze-fracture for scanning electron microscopy. In: *Proc. Fifth Eur. Congress Electron Microsc.* (p. 250). The Institute of Physics, London.

Hainfeld, J.F. 1977. Understanding and using field emission sources. *Scan Electron Microsc.* 1: 591.

Hanstede, J.G., and Gerrits, P.O. 1982. A new plastic for morphometric investigation of blood vessels, especially in large organs such as the human liver. *Anat. Rec.* 203: 307.

Hayat, M.A. 1978. *Introduction to biological scanning electron microscopy*. University Park Press, Baltimore.

Hossler, F.E., and Douglas, J.E. 2001. Vascular corrosion casting: Review of advantages and limitations in the application of some simple quantitative methods. *Microsc. Microanal.* 7: 253.

Humphreys, W.J., Spurlock, B.O., and Johnson, J.S. 1975. Transmission electron microscopy of tissue prepared for scanning electron microscopy by ethanol-cryofracturing. *Stain Tech.* 50: 119.

Kan, F.W.K. 1990. Use of Peldri II as a sublimation dehydrant in place of critical-point drying in fracture-label cytochemistry and in backscattered electron imaging fracture-label. *J. Electron Microsc. Tech.* 14: 21.

Kelley, R.O., Dekker, R.A.F., and Bluemink, J.G. 1975. Thiocarbohydrazide-mediated osmium binding: A technique for protecting soft biological specimens in the scanning electron microscope. In: M.A. Hayat (ed.), *Principles and techniques of scanning electron microscopy: Biological applications, Vol. IV*. Van Nostrand-Reinhold, New York.

King, E.J., and Brown, M.F. 1983. A technique for preserving aerial fungal structures for scanning electron microscopy. *Can. J. Microbiol.* 29: 653.

Mazia, D., Schatten, G., and Sale, W. 1975. Adhesion of cells to surfaces coated with polylysine. Applications to electron microscopy. *J. Cell Biol.* 66: 198.

Motta, P.M., Murakami, T., and Fujita, H. 1992. *Scanning electron microscopy of vascular casts: Methods and applications*. Kluwer Academic, Boston.

Nation, J.L. 1983. A new method using hexamethyldisilazane for preparation of soft insect tissues for scanning electron microscopy. *Stain Tech.* 58: 347.

Okada, S., and Schraufnagel, D.E. 2002. Microvasculature of the olfactory organ in the Japanese monkey (*Macaca fuscata fuscata*). *Microsc. Microanal.* 8: 159.

Oshel, P. 1994. Hexamethyldisilazane (HMDS) as a substitute for critical point drying. *Microsc. Today* 97–4: 19.

Pawley, J.B. 1988. Low voltage scanning electron microscopy. *EMSA Bull.* 18: 61.

Pease, R.F.W. 1963. *High resolution scanning electron microscopy*. Ph.D. dissertation, Cambridge University.

Postek, M.T., Howard, K.S., Johnson, A.H., and McMichael, K.L. 1980. *Scanning electron microscopy. A student's handbook*. Ladd Research Industries, Burlington, VT.

Ris, H. 1991. The three-dimensional structure of the nuclear pore complex as seen by high voltage electron microscopy and high resolution low voltage scanning electron microscopy. *Electron Microsc. Soc. Am. Bull.* 21: 54.

Suzuki, F. 1982. Microvasculature of the mouse testis and excurrent duct system. *Am. J. Anat.* 163: 309.

Suzuki, T., Shibata, M., Tanaka, K., Tsuchida, K., and Toda, T. 1995. A new drying method: Low-vacuum SEM freeze drying and its application to plankton observation. *Bull. Plankt. Soc. Japan* 42: 53.

Von Ardenne, M. 1938. Das Elektronene-rastermikroskop, praktische ausfuhrung. *Z. Tech. Phys.* 19: 407.

Zworykin, V.K., Hillier, J., and Snyder, R.L. 1942. A scanning electron microscope. *Am. Soc. Test. Mater. Bull.* 117: 15.

CHAPTER 13 TECHNIQUES

Fixation of biological samples for SEM, in general, utilizes the same principles and materials as described for preparing samples for TEM in Chapter 1. Osmium tetroxide postfixation can usually be omitted, though samples that have "charging problems" leading to image distortion can frequently benefit from osmication. Subsequent dehydration in an ethanol or acetone series followed by critical point drying, freeze-drying, or drying with one of the chemical techniques described in this section produces a sample suitable for viewing with a conventional high-vacuum SEM. Preparation of samples for ESEM or LV SEM viewing may not require dehydration, drying, and coating protocols used for high-vacuum SEM, while materials destined for microanalytical techniques may necessitate specialized techniques to avoid spurious signal generation.

Poly-L-Lysine Technique for Attaching Particulates to Coverglasses for SEM

1. Applications and Objectives

Poly-L-lysine can effectively bind particulates from the size of bacteria to sperm, large protozoa, and pollen grains to coverglasses for scanning electron microscopy. This procedure was modified from Mazia *et al.* (1975).

2. Materials Needed

- 0.1% solution of Sigma Poly-L-lysine (70,000–150,000 Da) in 0.1 M Sorenson's sodium phosphate buffer, pH 7.2–7.4
- 12-mm round coverglasses, washed in detergent, rinsed thoroughly in distilled water, and dried before use
- Petri dish
- Glass microscope slides

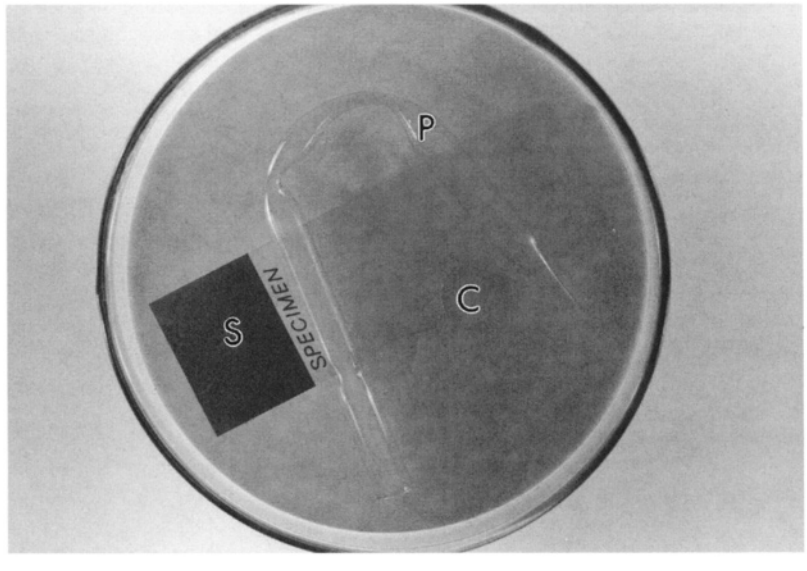

Figure 231. Moist chamber for Poly-L-lysine procedure showing a bent Pasteur pipet (P) supporting the glass slide (S) beneath round coverslips (C).

- Whatman™ #1 filter paper (9-cm disks)
- Bent Pasteur pipet to support glass slide
- Forceps

3. Procedure

1. Place a drop of Poly-L-lysine on a precleaned 12-mm round glass coverglass, and then place this on a glass slide supported by a bent Pasteur pipet (Fig. 231) in a moist chamber consisting of a Petri dish containing distilled water-soaked filter paper. Close the chamber and leave at room temperature for 10 min to 1 hr.
2. Rinse the Poly-L-lysine-coated coverglass with distilled water, dry by touching edge to filter paper, and immediately load sample (see step 3). Alternatively, the coated coverglasses can be dried and stored in a covered Petri dish at 4°C for at least a year.
3. Place a drop of the cell or particulate suspension of living or aldehyde-fixed material onto the coated coverglass. Incubate the coverglass in a moist chamber at room temperature for 10 min to 1 hr.
4. Rinse the coverglass briefly in buffer.
5. Dehydrate the coverglass in a holder that will keep it from turning over during processing so that the side with the sample material can still be identified by its position in the holder following critical point drying as described for standard SEM preparation.

4. Results Expected

Cultured eukaryotic cells, prokaryotic cells, subcellular organelles, protozoans, and other particulates will usually adhere easily and securely to Poly-L-lysine-coated coverglasses. This method is generally superior to impinging such materials onto filters for processing because the samples will generally stick better to the coverglasses, and distracting filter fibers (e.g., those of cellulosic Millipore filters) will not be imaged. This also avoids the potential problems with pulling or pushing fragile materials onto filters of any kind.

5. Cautionary Statements

If sufficient numbers of cells do not adhere to the coverglasses or there is evidence that they fall off during subsequent processing, the organosilane coverglass/slide procedure might be more appropriate.

Reference

Mazia, D., Schatten, G., and Sale, W. 1975. Adhesion of cells to surfaces coated with polylysine. *J. Cell Biol.* 66: 198.

Organosilane Coverglass/Slide Treatment

1. Applications and Objectives

Organosilane treatment is used to prepare glass surfaces for the attachment of biological materials. The surface hydroxyl groups of glass can covalently bind amino groups of aminopropyltriethoxysilane, which then can bind to a number of reactive groups on cell and tissue surfaces through a Schiff-type reaction. This type of molecular binding has greater strength than the Poly-L-lysine procedure for preparing particulate samples for SEM.

2. Materials Needed

- Glass coverglasses
- 1% aqueous 3-aminopropyltriethoxysilane (Sigma A-3648), pH 3.45, adjusted with concentrated HCl

- 10% glutaraldehyde in 0.1 M sodium phosphate buffer, pH 7.2
- 0.1 M aqueous sodium metaperiodate
- Petri dishes
- 0.1 M Sorenson's sodium phosphate buffer, pH 7.2–7.4

3. Procedure

Coating Coverglasses

1. Acid-wash the coverglasses and rinse in distilled water.
2. Put the coverglasses into a glass Petri dish with 1% aqueous 3-aminopropyl-triethoxysilane at 70 °C overnight.
3. Wash thoroughly in distilled water for at least 2 hr.
4. Bake the coverglasses at 100°C overnight. After this, the glass substrate will have free amino groups available for activation.

Coverglasses can be stored at room temperature for up to 6 months before activation.

Activation of Coverglasses, to be done no more than 2 Weeks before Use

1. Soak the coverglasses in 10% glutaraldehyde in 0.1 M sodium phosphate buffer for at least 30 min. Aldehyde groups will then be attached to the organosilane, and free aldehyde groups will be available for attaching to amino groups in cells/tissues.
2. Rinse thoroughly in distilled water.
3. Soak the coverglasses in 0.1 M sodium metaperiodate in distilled water at room temperature for at least 15 min. This is thought to keep the free aldehyde groups functional.
4. Rinse in 0.1 M sodium phosphate buffer.

Attachment of Tissues/Cells

1. Place fixed or unfixed tissues/cells on a coverglass for 1–2 hr in a moist chamber.
2. Rinse the coverglass in 0.1 M sodium phosphate buffer to remove unattached material or peel off tissue, if membranes are wanted, and then rinse.
3. Dehydrate according to routine method for SEM preparation and critical point dry. Mount, sputter coat, and view with an SEM.

4. Results Expected

Cells and particulates adhere to the glass with great avidity.

5. Cautionary Statements

Observe all customary precautions for dealing with solvents and fixatives, and carefully read the MSDS sheet (see Appendix D) for the organosilane product before proceeding.

Reference

Clayton, D.F. and Alvarez-Buylla, A. 1989. *In situ* hybridization using PEG-embedded tissue and riboprobes: Increased cellular detail coupled with high sensitivity. *J. Histochem. Cytochem.* 37: 389.

Critical Point Drying for SEM

1. Application and Objectives

This technique is used for samples of soft tissue that are hydrated. If the sample is already dry, such as bone, prosthetic bone implants, air-dried field samples of pollen, or spores, critical point drying is often

inappropriate. In such cases, the dried sample can be mounted immediately on SEM stubs, sputter coated, and examined with the SEM. As mentioned earlier, if an ESEM or LV SEM is available, many materials do not need to be critical point dried.

A hydrated biological sample should be fixed and dehydrated as described for routine SEM preparation. The dehydration fluid (ethanol) must be removed from the specimen prior to sputter coating and viewing with an SEM. As mentioned earlier, if the sample is allowed to air-dry, pressures of up to 2000 lb/in^2 (13.8 MPa) can be generated, resulting in major distortion of specimen surfaces. Critical point drying is based on the concept that, at a certain temperature (31°C) and pressure (1,072 lb/in^2, 7.4 MPa), the vapor and liquid phases of carbon dioxide become indistinguishable.

Liquid CO_2 from a siphon-tube tank is introduced into the chamber and used to replace the 100% ethanol in the specimen. After the ethanol has been totally replaced by the CO_2, the critical point drying chamber (CPD) is brought above the critical point of 31°C, 1,072 lb/in^2 (7.4 MPa). The temperature is kept above the critical point while the gaseous CO_2 is vented from the chamber. The process is finished when the CPD is returned to atmospheric pressure.

After critical point drying, the specimen should be totally dry, contain neither ethanol nor carbon dioxide, and have minimal distortion or shrinkage artifacts caused by the drying process. Once the sample has been dried, it is ready to be introduced to the vacuum systems of the sputter coater and SEM.

2. Materials Needed

- Critical point dryer
- Fixed specimen in 100% ethanol
- Siphon tube CO_2 tank
- Specimen containers for CPD

3. Procedure

1. Before proceeding, carefully read the specific instructions for the CPD available in your laboratory.
2. Close the drain, fill, and vent the valves on CPD. Make sure that the chamber door is securely sealed. Open the main valve on the CO_2 tank. Listen for any leaks, and correct them by tightening fittings or replacing seals.
3. Slightly open the vent valve on the CPD, and then open the fill valve and watch the sight glass on the CPD. The chamber should fill with liquid. If it fills slowly or appears excessively gaseous, reduce the chamber temperature. If the liquid CO_2 is vented quickly from the chamber, the chamber temperature will usually drop a few degrees. Once the chamber is partially filled, close all of the valves and check again for leaks. Correct any before proceeding. Depressurize the CPD and open the chamber door.
4. Remove samples from vials of 100% ethanol and quickly load them into appropriate CPD sample holders previously submerged in 100% ethanol in a deep dish or beaker. Close the sample holders and quickly transfer them to the CPD.
5. Immediately close the CPD chamber door, tighten the screws securing the door, slightly vent the chamber, and open the fill valve completely to rapidly fill the chamber with liquid CO_2. If the vent is not slightly open, the chamber may not fill properly.
6. When full, close the vent valve and wait for 3 min.
7. Open the drain valve and slightly open the vent valve. Watch the sight glass on the CPD and be careful not to vent and drain the chamber so fast that the fluid level drops below the surface of the specimen holder(s). After 3 min, close the drain and vent valves.
8. Repeat the filling and draining steps (steps 6 and 7 above) three times. Draining the chamber removes the heavier ethanol, which settles to the bottom of the CPD. Filling the chamber produces considerable turbulence, thoroughly mixing the liquid CO_2 and ethanol. The 3-min resting period after the CPD has been filled allows the mixture to stratify, with the ethanol sinking to the bottom to be drained subsequently.
9. Close the drain and the fill and vent valves. Close the main valve on the CO_2 tank.

10. Open the drain valve slightly until a meniscus is seen at the top of the liquid CO_2 through the chamber sight glass.
11. Begin heating the chamber.
12. As the chamber is heated, the meniscus will usually rise toward the top of the sight glass. If the meniscus rises above the sight glass, vent the CPD slightly to bring it back into view. As the chamber pressure rises, monitor it carefully. If it rises above 1,350 lb/in^2 (9.3 MPa), vent the chamber slightly to bring the pressure back down to 1,300 lb/in^2 (9.0 MPa).
13. Once the chamber temperature is well above the critical point (36–38°C) and a pressure of 1,300 lb/in^2 (9.0 MPa) has been reached, open the vent valve and release the chamber pressure at a controlled rate of about 100 lb/in^2 (689 kPa) per 30 sec. If the temperature begins to drop, the venting rate is too rapid.
14. When the CPD pressure has dropped to 0, turn off the CPD if it is an automatic device, or turn off the external heater and recirculator.
15. Open the chamber door and remove the dried specimens.

4. Results Expected

The specimens should be dry and beige to white in color, unless they have been osmicated. They should have no odor of ethanol.

5. Cautionary Statements

The CPD is a pressurized device and should never be left alone during the heating process. All commercially produced CPDs have features to prevent overpressurization leading to catastrophic failure, but it is best not to rely on these features. There have been some cases where CPDs have failed because of overpressurization, reportedly resulting in death in at least one instance. For the same reason, it is advisable not to stand directly in front of the sight glass of the CPD.

It is of utmost importance that the specimen in 100% ethanol not air-dry at any time, to avoid consequent crushing. Thus, transferring the specimen to the CPD quickly, sealing the chamber door quickly, and filling the chamber with liquid CO_2 quickly are imperative.

Drying Samples with Hexamethyldisilazane

1. Applications and Objectives

This method is designed to dry specimens previously fixed and dehydrated to 100% ethanol prior to sputter coating and viewing with an SEM without having to use a CPD device.

2. Materials Needed

- SEM sample previously fixed by routine methods and dehydrated to 100% ethanol contained in a sample vial
- Hexamethydisilazane
- Glass Petri dish
- Pasteur pipet

3. Procedure

1. Fix tissue by routine methods.
2. Dehydrate tissue to 100% ethanol.

3. Remove 100% ethanol with a pipet and replace with hexamethyldisilazane. Do not let the hexamethyldisilazane come into contact with skin; it is *toxic*. After 5 min, replace with fresh hexamethyldisilazane.
4. Place specimens in hexamethyldisilazane in a Petri dish under a fume hood at room temperature. Partially cover container to keep air-borne debris off of the sample surface.
5. After samples are completely dry (usually overnight), mount on SEM stubs, sputter-coat, and examine with an SEM.

4. Results Expected

The samples should be dry and show no evidence of shrinkage or crushing artifact.

5. Cautionary Statements

As mentioned above, the hexamethyldisilazane is a toxic compound that should be handled carefully in accordance with recommendations on the MSDS sheets provided by EM supply houses with chemical purchases. Bray *et al.* (1993) suggest that highly vacuolated specimens, such as plants and fungi, tend to show considerable shrinkage and distortion with this technique, so CPD methods should be used.

References

Bray, D.F., Bagu, J., and Koegler, P. 1993. Comparison of hexamethyldisilazane (HMDS), Peldri II and critical-point drying methods for scanning electron microscopy of biological specimens. *Microsc. Res. Tech.* 26: 489.

Nation, J.L. 1983. A new method using hexamethyldisilazane for preparation of soft insect tissues for scanning electron microscopy. *Stain Tech.* 58: 347–351.

Oshel, P. 1997. Hexamethyldisilazane (HMDS) as a substitute for critical point drying. *Microsc. Today* 97-4: 19.

Sputter Coating

1. Applications and Objectives

Sputter coating is a technique for depositing a nondirectional metal coating on specimen surfaces to be examined with an SEM. It employs a relatively low vacuum (1.3×10^{-2} Pa) and introduces an inert gas (argon) into a high-voltage field. The gas molecules are accelerated into the target, typically gold–palladium, resulting in metal atoms being dislodged. These dislodged molecules continue interacting with the argon gas, producing an energetic "cloud" of argon/metal that is visible as a purplish glow in the sputter coater chamber. This cloud of metal atoms condenses on all surfaces within the chamber. If the stage bearing the specimens to be coated is cooled, the condensation process will occur preferentially on the cooler surfaces in the chamber. Because of all the molecular interactions between the dislodged metal atoms and the argon gas within the high-voltage field, the metal is deposited nondirectionally, allowing even coating of all surfaces of the specimen, regardless of topography, unlike the directional coating process of vacuum evaporation. Less specimen heating is developed during sputter coating than with vacuum evaporation.

The recent development of high-resolution field emission gun SEMs, some of which can resolve 0.5 nm, has necessitated the development of chromium target sputter coaters capable of producing metal coats with a grain structure fine enough not to interfere with the microscope resolution capabilities. Chromium sputter coaters use higher vacuum and cleaner pumping systems than conventional sputter coaters and are considerably more expensive. They are not indicated for conventional SEM specimen preparations to be viewed with conventional 4–5-nm-resolution SEMs.

2. Materials Needed

- Gold–palladium target
- Sputter-coating device
- Dry specimens mounted on SEM stubs with tape or conductive colloidal carbon, silver paste, or silver paint
- Argon tank and pressure regulator

3. Procedure

1. Open the chamber and load the specimens onto the specimen platform. If the platform has screws to secure the specimen stubs, tighten them until they lightly touch the stubs. They are meant to ground the specimen stubs, not to lock them into place.
2. Turn the main power switch on, turn on the pump, if controlled by a separate control, and wait until the chamber has reached the pressure suitable for sputtering specified by the instrument instructions, usually 1.3×10^{-1} to 10^{-2} Pa. This usually takes 2–5 min. If the chamber is pre-pumped for 5 min before specimens are introduced, it will pump down faster. This is particularly helpful if a number of specimens are introduced at the same time. Extended pumping times may allow backstreaming, which could interfere with metal coating.
3. Purging the system with argon also helps produce a better vacuum more quickly. Open the main valve on the argon tank on the top of the tank. Adjust the regulator on the argon tank to a pressure of 2–4 lb/in^2 (13.8–27.6 kPa). Open the gas-pressure control knob on the sputter coater and admit argon until the chamber pressure is 2.6×10^{1} Pa. Leave the control knob at that setting for about 1 min. Close the argon control knob. Wait for about 1 min, then repeat the process. After several cycles of admission of argon gas followed by closing the system to return to a higher vacuum, the ultimate vacuum of the sputter coater will have improved.
4. If, after purging the system with argon, the vacuum is close to, but still not within, the acceptable sputtering range, turn on the high-voltage switch and slowly raise the voltage until 5 mA is indicated on the current meter. This passes a small amount of current through the chamber gas, ionizing the gas. When the voltage is turned off, the vacuum should have improved. Do not exceed 5 mA of current during this procedure or sputtering will take place in an atmosphere containing small amounts of residual air in addition to the introduced argon, resulting in an inferior specimen coating.
5. Once the vacuum in the sputter-coater chamber has reached the sputtering pressure specified by the manufacturer, turn on the high-voltage switch and begin raising the voltage until it reaches the point specified by the sputter-coater manufacturer.
6. Gradually open the argon control knob until 10–15 mA current is indicated on the current meter. Note the purple cloud produced during the sputtering process.
7. Set the timer switch to 2 min. This should produce a coat about 20 nm thick on the specimen surfaces.
8. After 2 min of sputtering, turn off the high voltage, close the argon control knob, and vent the sputter-coater chamber.
9. Remove the specimens and examine them with an SEM.
10. Clean the chamber glass with 95% ethanol and paper towels when it becomes hard to see the specimens through the glass. Excessive residual metal deposits make it more difficult to achieve a good vacuum.

4. Results Expected

The specimens should be evenly coated with a grayish silver coat of gold–palladium.

5. Cautionary Statements

If the specimens are not properly dried or if the chamber is loaded with a large number of specimens, it may be impossible to achieve a sufficient vacuum to make a sputter coating run despite purging the system

with argon and burning the system with a low voltage current. In such cases, either put fewer specimens in the chamber for the run or dry the specimens further by packing them into an airtight chamber with Drierite™ until they do not compromise the vacuum system.

Vascular Casting with Mercox CL-2B™ Resin

1. Applications and Objectives

This is an excellent acrylic resin with which to fill vasculature. After the resin polymerizes, which takes about 10 min, the resulting vascular cast is relatively rigid, and resists most chemicals used to corrode (digest) the surrounding tissue, such as Clorox™, sulfuric acid, chromic acid, and nitric acid. The rigidity of the resulting casts allows the three-dimensional relationship among the elements (Fig. 232) to be observed, unlike latex casts, which can collapse, become tangled, and defy interpretation. This technique will produce a negative cast of the vascular spaces, revealing nuclei, vascular networks, and any abnormalities present, such as occlusions, neovascularization, and leakage.

The resin can be injected directly into living tissue and allowed to polymerize, injected immediately following a flush of the tissue with buffer and/or aldehyde fixatives, or injected into tissues months after an aldehyde fixative such as 4F:1G has been injected if the tissues are stored at 4°C. All three treatments provide casts that appear identical. The limitation to this resin is that, under the conditions described, about 10-ml of resin can be injected before the resin begins to polymerize. This restricts the amount of vasculature that can be injected at one time to a 10-ml volume.

2. Materials Needed

- Two empty saline drip bottles and tubing for attaching to catheters
- 10-ml plastic syringes
- 4F:1G fixative

Figure 232. Mercox™ resin cast of a rat glomerulus. ×375.

- Catheters and tubing for attaching them to syringe tips, with appropriate diameters for the vasculature being injected with resin
- Mercox CL-2B™ resin
- Storage containers to hold injected tissues
- Clorox™
- 50% ethanol (or methanol)
- Tap water
- SEM specimen stubs
- Colloidal silver paste or paint
- Sputter coater
- DPBS
- 100-ml disposable beakers
- 10-ml disposable graduated pipets
- Rubber bulb for filling graduated pipets
- Applicator sticks
- Sage Syringe Pump or other controlled-pressure delivery system (optional)
- Suture

3. Procedure

1. Isolate the tissue segment with a 10-ml vascular volume or less to be perfused with Mercox CL-2B™ resin from surrounding tissues with clamps and cannulate the appropriate arteries to reach the final segment of vasculature which is of interest. Securely tie the catheter in place with a suture. Open a vein in the general area for outflow of fixative and resin.
2. Remove the cannulated segment and perfuse it with 20 ml of DPBS from a drip bottle, followed by 50 ml of 4F:1G fixative from another drip bottle. The drip bottles containing DPBS and 4F:1G should be located as close to the ceiling as possible, and the perfusion fluids should be at room or body temperature, never chilled, to prevent vascular spasms. Once the vasculature has been thoroughly flushed with the fixative, put the segment into a sample container holding some of the same fixative, where it may be stored for 1 hr to several years at 4°C. The fixative volume in the container should be five to 10 times the tissue volume.
3. To prepare the Mercox CL-2B™ resin for injection, place 10 ml of the blue resin in a 100-ml disposable beaker with a 10-ml disposable pipet controlled with a large pipet bulb. Never pipet by mouth.
4. Add 0.6 ml of the resin hardener (MA) and mix the hardener and resin quickly and thoroughly with a wooden applicator stick.
5. Pull the stirred mixture into a 10-ml disposable syringe and *quickly* put it into the cradle of a Sage Syringe Pump or similar device preadjusted to inject at the rate of 30 ml/min at the 30-ml syringe setting. Many papers have been published where "hand pressure" has been used to infiltrate the vasculature, so that method is possible.
6. Once the resin components have been mixed, about 5 min is available for the injection process before the resin begins to set up. Injection of more than 10 ml of the plastic resin mixture is generally unsuccessful because the resin begins hardening before all of it is injected.
7. After the tissues have been injected, they may be stored in fixative for several years without further treatment. Wait at least 1 hr for the resin to polymerize completely. To corrode the tissue away from the resin cast of the vasculature, place the tissue in 100% Clorox™. Change the Clorox™ several times over 2–3 days or until all the tissue has been digested. During the digestion process, keep the tissues in loosely capped containers under a fume hood, because a lot of gas is generated.
8. Once the tissue is gone, rinse the vascular cast several times with tap water and then pass it through several changes of 50% methanol or 50% ethanol. The casts may be stored indefinitely in alcohol.
9. To prepare the casts for SEM examination, remove pieces small enough to fit onto the appropriate SEM stubs and air-dry them. Any cutting of the casts should be done while they are still submerged

in the alcohol to prevent excessive fracturing. The casts may be blotted gently with filter paper to speed up the drying process. Mount the dried casts on SEM stubs with colloidal silver, carbon tape, or double-stick tape and sputter coat them with gold–palladium.

4. Results Expected

The vascular casts produced will have sufficient rigidity to preserve proper three-dimensional relationships among the vascular elements. Endothelial nuclei will be obvious as round depressions in the casts.

5. Cautionary Statements

The use of a Sage Syringe Pump is suggested to provide carefully controlled, reproducible conditions of injection. However, Suzuki's (1982) original paper stated that the injection was delivered under hand pressure, without any further details. Cold buffer or fixative may cause vascular constriction, and should not be used. As noted above, the casts are quite brittle when dried, so any cutting to select specific areas to be examined should be performed before they are air-dried. Finally, the casts are quite susceptible to beam damage, particularly at magnifications over 2,000× at 15 kV accelerating voltage. Decreasing the accelerating voltage can decrease the damage to some extent. The best procedure is to minimize specimen beam exposure prior to photography.

The designation 2B in the product description is for the blue-colored resin. When it polymerizes, it turns brownish red. The blue color makes it easier to see if a good fill has been achieved. The resin keeps for at least 1–2 years at 4°C, but the accelerator tends to dry out.

References

Motta, P.M., Murakami, T., and Fujita, H (eds.). 1992. *Scanning electron microscopy of vascular casts: Methods and applications*. Kluwer Academic, Boston.

Suzuki, F. 1982. Microvasculature of the mouse testis and excurrent duct system. *Am. J. Anat.* 163: 309–325.

14

Microanalysis

In electron microscopy, the term microanalysis has historically referred to X-ray microanalysis (energy dispersive spectroscopy, or EDS), electron diffraction, and electron energy loss spectroscopy (EELS). Materials scientists have utilized these techniques longer and more extensively than biologists, so their applications are most thoroughly discussed in texts on the subject (Chandler, 1978; Egerton, 1989; Goldstein *et al.*, 1992; Morgan, 1985; Newbury *et al.*, 1986; Russ, 1984).

Electron optical imaging and X-ray analysis were first combined in the late 1940s, and since the early 1960s, X-ray microanalysis has been widely used in physics, electronics, metallurgy, mineralogy, and more recently, biology.

I. ENERGY DISPERSIVE SPECTROSCOPY (EDS)

X-ray microanalysis (EDS) provides a method to identify elements within thin and thick specimens with high sensitivity and precise location, particularly with thin specimens examined with a field-emission gun-equipped TEM. Electrons are arranged in a series of shells (K, L, M, etc.) around an atom's nucleus, with the shells nearest the nucleus having the least energy. If an electron is removed from the shell of an atom by an elastic collision of an electron from the primary beam, an ion is produced (Fig. 233). To stabilize the ion, an electron from a higher-energy orbit (outer shell) must fill the gap formed when the electron is ejected from the atom. An amount of energy equal to the difference in energy between the outer shell and the inner shell is released in the form of an auger electron, a photon of light, or an X-ray photon. The X-ray energy is the potential energy difference between the two shells. In an atom with a large number of electrons, the initial electron loss can lead to a cascade of orbital electron shifts and the potential release of a large spectrum of different X-rays. A heavy atom such as uranium (atomic number 92) has a large number of possible spectral emissions, while a smaller atom like sodium (atomic number 11) will exhibit far fewer. However, quantum theory principles predict that a number of the expected transitions cannot occur.

With EDS, the X-rays generated by the interaction of the primary beam with the specimen are sorted electronically. This technique is usually sensitive to elements with a Z number of 11 or above and to elemental concentrations of 1% or below in a given sample (Vaughan, 1989). An X-ray photon that reaches the semiconductor detector first produces a current, which is then converted electronically into a voltage whose amplitude is directly proportional to the energy of the X-ray signal (Fig. 234).

The voltage is then converted into a digital signal, which is, in turn, recorded as a count by a multichannel analyzer. The counts accumulated from a sample over time produce an X-ray spectrum for the specimen.

X-ray microanalysis units can be attached to SEMs, TEMs, and scanning transmission electron microscopes (STEMs). The advantage of STEMs over standard TEMs for this work is that STEMS are designed to produce a more finely focused beam that is scanned over a thin

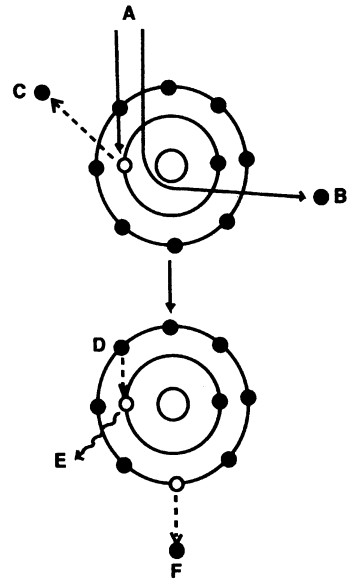

Figure 233. Diagram of the possible energetic events following primary electron beam interaction with a specimen atom. A: primary electrons; B: backscattered electron; C: secondary electron; D: electron shift to fill vacancy following release of secondary electron C; E: photon of light or X-ray photon; F: release of auger electron after shift D.

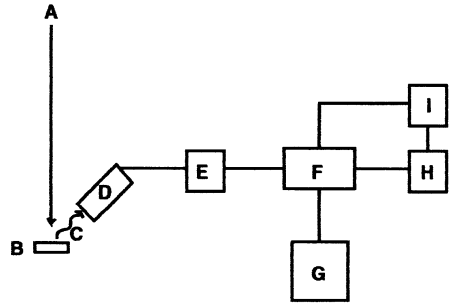

Figure 234. Diagrammatic representation of the signal-handling components of an EDS unit. The electron beam (A) interacts with the specimen (B), causing the release of characteristic X-rays (C), which reach the detector (D). The signal is amplified by the amplifier (E), passes through the multichannel analyzer (F), and then can be viewed on the display (G), stored in the computer (H), or can be fed to the data output device (I) by either the computer or the multichannel analyzer.

section, which gives more signal and higher resolution than with the less finely focused beam of a conventional TEM. FEGs produce a more coherent beam and a finer probe diameter than a typical tungsten gun or one equipped with a LaB_6 emitter. As explained in Chapter 13, a Schottky (*hot* cathode) emitter is preferred for most microanalytical work because of the stability in beam current, compared with a *cold* cathode type of emitter.

Vacuum systems of microscopes devoted to EDS need to have the capability of producing a vacuum of better than 6.7×10^{-3} Pa (5×10^{-5} Torr) or better to prevent condensation of gas molecules on the detector, which is operated at cryogenic temperatures. If gases condense onto the detector window, they can potentially absorb incoming X-rays, thus degrading the signal-detecting capabilities of the instrument. The accumulation of contaminants resulting from the interaction of the electron beam with the specimen under suboptimal vacuum conditions can also lead to the absorption of X-rays generated from beneath the contaminating material and the

appearance of nonspecimen generated X-rays. Absorption of X-rays by surface contaminants can compromise quantitative studies. Low energy X-rays generated by light elements are more likely to be absorbed by surface contaminants and not reach the detector surface.

A. The Detector

The X-ray detector is a solid-state device consisting of a silicon–lithium crystal (Fig. 235) with a surface area in the range of 5–200 mm^2. It is sandwiched between two metal electrodes across which a bias voltage is applied. The detector crystal is kept under high vacuum and cooled with liquid nitrogen. The crystal is either part of a windowless detector or, more commonly, is covered with a thin (approximately 7-μm-thick) radiation-transparent beryllium window. In this latter configuration, elements below atomic number 11 are not detected because their X-rays are absorbed by the beryllium. Each electron in the silicon portion of the collector can absorb 3.8 V. The negative charge on the detector is directly proportional to the energy of the incident X-ray. The X-ray is thus converted into an electron signal by the detector, which is then amplified and processed by a multichannel analyzer that separates the energy pulses in terms of amplitude and stores them in memory.

B. Emission Analysis

Emissions, or characteristic X-ray lines, vary in intensity. Those that are the easiest to detect because they have the greatest intensity are generally used for characterizing an element within a sample.

X-rays generated by transitions from the E_L to the E_K shell are called K lines. These transitions are the source of the most intense emissions, followed by E_M to E_L transitions (L lines) and so forth. Even within a given shell, a variety of electron jumps can take place, designated by Greek letters along with numerical designations (α 1, α 2; β 1, β 2; γ 1, etc.). Higher numbers and letters further from the beginning of the alphabet indicate a greater intensity.

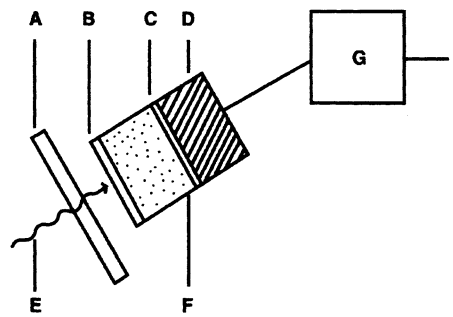

Figure 235. Diagrammatic sketch of an X-ray detector showing the characteristic X-ray (E) passing through the beryllium window (A), where it interacts with the solid-state detector composed of a positive layer (B), the silicon–lithium semiconductor (F), a negative layer (C), and the field effect transistor (D), which serves as a preamplifier for the signal that is then conveyed to the amplifier (G).

Moseley (1914) calculated the relationship between X-ray frequency (V or energy) and atomic number (Z), as follows:

$$V = 0.248\ (Z - 1)^2 \times 10^{16}$$

The X-ray frequency has been determined for all elements, which allows an element to be identified by the energy of the X-ray emissions generated by a given sample.

C. Electron Ionization

In order to produce an X-ray, the primary electron beam must have enough energy to remove an electron from an inner shell of a specimen atom. This energy is known as the critical excitation potential or the absorption edge and has a discrete value for each orbital electron energy level (K shell electrons need more energy than L shell electrons, etc.). The energy needed also tends to increase with increasing atomic number.

As mentioned previously, X-ray photon production does not always follow ionization of atoms. Auger electrons or photons of light may also be released.

D. X-Ray Fluorescence

As discussed in Chapter 13, the interaction of an electron beam with a specimen produces a myriad of events that take place simultaneously following the initial ionization event. We selectively record specific aspects of the signals generated, and the instruments are provided with several mechanisms to assist us with this selectivity. X-rays produced following ionization can cause other atoms within the sample to be secondarily ionized, leading to generation of further X-rays. This phenomenon is known as X-ray fluorescence and may lead to quantitation errors, since the additional fluorescent X-rays can enhance or reduce the primary X-ray signal.

E. X-Ray Absorption

Absorption accompanies X-ray fluorescence. Some X-rays are stopped en route to the detector or are scattered away from the detector, and are thus lost to the image-forming system. As previously mentioned, X-rays from higher Z-number atoms have a higher energy and are thus less likely to be absorbed within the specimen or within the detector window. Those with a Z-number of 11 or lower have a very low energy and will be absorbed by the specimen or by the beryllium detector window, so no signal can be recorded from these elements. To increase the likelihood of recording low-energy X-rays, the detector is usually placed at a high angle in relationship to the specimen (Fig. 236). This reduces the chance for X-rays from the sample to be self-absorbed.

F. Bremsstrahlung, Continuum, White Radiation

A primary electron that is scattered inelastically by the Coulomb field of an atomic nucleus can lose some or all of its energy. The amount of energy lost may vary from zero up to the initial

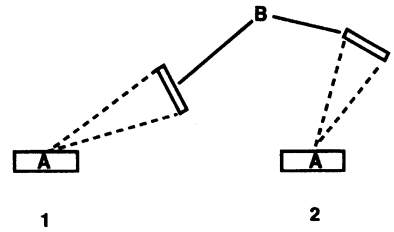

Figure 236. Location of an X-ray detector (B) in relationship to the specimen (A). If the detector is located at a low angle in relationship to the specimen (1), the resolution will be lower than if it is located at a higher angle (2).

energy of the primary electron beam. This lost energy may be released in the form of X-rays called bremsstrahlung (braking radiation), continuum, or white radiation. The amount of bremsstrahlung is directly related to the total number of atoms of all kinds within the sample, unlike the characteristic X-rays that are specific to one type of atom. Thus, bremsstrahlung is a source of specimen noise during qualitative analysis (elemental analysis). However, bremsstrahlung is a source of information concerning the mass thickness of a specimen, an important factor if quantitative analysis of thin sections is being performed.

G. Signal Analysis

Our discussion so far should make it clear that the X-ray spectrum of a given element is a complex signal with a number of different characteristic X-ray lines of different intensities (energies) against a background of bremsstrahlung. Thus, it is necessary to utilize a computer attached to the multichannel analyzer to determine which parts of the broad spectrum of signals are meaningful. In addition, a knowledgeable operator can select which part of the spectrum to evaluate, depending on the information being sought by the investigator.

With heavier elements, it is not always possible to excite K lines; thus, the L lines generated would need to be evaluated. Another factor that is of concern is the sensitivity of the X-ray detector. Various detectors are available, many of which will detect one line (M) more easily than another (L) even if the intensity of the L line is greater. Overlapping spectral lines are produced when a number of elements are present in the specimen. If this overlapping prevents clear analysis, another part of the spectral range can be selected where the lines of the originally overlapping elements are farther apart.

H. Sensitivity and Resolution

Sensitivity can be increased by placing the detector closer to the specimen, thus increasing the count rate. Moving the detector closer to the specimen also reduces specimen damage because less beam exposure time is necessary to produce a usable spectrum. If too much signal is generated, however, more background will be recorded as well, leading to the potential for reduced resolution as the system becomes overloaded with signals.

Higher accelerating voltages penetrate more deeply into the specimen, causing more beam spreading and, thus, less resolution, even though there is a simultaneous increase in excitation of

the specimen. The high-density, finely focused (3–5 nm) beam generated by field emission guns is well suited to high-resolution EDS work, since the larger the probe diameter, the more beam spreading takes place within a sample, and the less resolution produced.

I. Specimen Preparation

The best instrumentation for EDS work is generally found associated with engineering or materials science laboratories. The technicians who maintain and operate these instruments typically are very knowledgeable about the spectra of various elements and their overlaps, and about how to adjust the multichannel analyzer and computer analysis to separate elements with similar spectral characteristics for commonly read lines. At the same time, they generally have no knowledge of fixation, embedment, staining, and general preparative methods employed by biologists as well as the interpretation of morphological features of biological materials. These matters have been discussed in detail by Coleman (1975) and Hall *et al.* (1974).

To work effectively with materials laboratories, it is necessary to communicate what chemicals with *Z*-numbers over 11 were used in specimen preparation, such as osmium, lead, uranium, and so on. In addition, the chemical composition of the substrates (stubs, grids, coverslips, polymer films) used as specimen supports should be provided.

If a TEM or STEM unit is employed for EDS, it is necessary to choose a grid material that will not interfere with the analysis desired. Grids are manufactured from copper, nickel, gold, molybdenum, titanium, chromium, platinum, beryllium, carbon-coated nylon, and so on. If the biological sample is not expected to contain materials with spectra overlapping those of copper, copper grids will be adequate. Beryllium grids are generally considered to be good substrates for EDS work because of their electron transparency, but they are extremely hydrophobic, making section pick-up very difficult. In addition, they should never be cleaned with any solvents since beryllium is extremely toxic and must not be solubilized in any fluids that might come into contact with living things. Grids coated with polymer films like Formvar or collodion can have a significant silicon, chlorine, and sulfur content, so many microanalytical laboratories use grids coated only with carbon.

If there is any danger of solubilizing elemental components of cells or tissues during processing for conventional chemical fixation and embedment, cryotechniques can be applied. Native frozen sections and cryotransfer to a microscope equipped with a cryostage can preserve soluble electrolytes such as sodium, potassium, and chlorine for subsequent microanalysis. Cryosubstitution also has advantages over conventional chemical fixation procedures because substitution of methanol or acetone for water at low temperatures results in less extraction of water-soluble cellular components. Cryofixation followed by freeze-drying can also preserve small soluble ions that otherwise would be leached from the specimen during conventional chemical processing, and thus would be eliminated from possible detection by EDS.

With preparations intended for SEM EDS work, carbon stubs are usually used to reduce spurious signals that would be generated from metal stubs. For the same reason, specimens are typically coated with carbon rather than gold–palladium or other metals. Carbon will still allow excess electrical current to be conducted to ground potential and will decrease specimen heating without producing conflicting signals from the heavy metals used for coating specimens for conventional secondary electron imaging. In addition, it should be remembered that any conductive coating has some capacity to absorb X-rays generated from the specimen. If samples are mounted on glass coverslips, there may be further problems with spurious readings, since glass can contain magnesium, copper, and, of course, silicon.

Coleman (1975) offers a brief discussion of sample preparation for biological fluids containing soluble ions. He also discusses the problems of drying samples obtained from buffered media. In the latter case, if a sample soaked in buffer is dried, the buffering salts tend to precipitate as the sample is dried, thus obscuring detail for SEI examinations as well as producing large domains of crystals capable of being recorded by EDS.

J. Qualitative versus Quantitative Work

Most EDS work performed on biological specimens is qualitative in nature and determines the presence of different elements within a sample. In some cases, it is desirable to ascertain the amount of a specific element within a specimen. In these cases, quantitative analysis is necessary. As mentioned above, this is made possible by utilizing the bremsstrahlung to determine the mass of the sample based on the nonspecific radiation arising from the beam interactions with all the different atoms in the specimen. Once the mass of the specimen is recorded by the computer, the relative quantity of a given element of interest can be determined, and then the computer can make a quantitative analysis for that element. This method is discussed more thoroughly in the texts cited at the beginning of this chapter.

II. ELECTRON ENERGY LOSS SPECTROSCOPY (EELS)

When the electron beam of a TEM interacts with an ultrathin section, three events occur. Most of the primary beam electrons pass through the specimen without significant interaction, eventually striking the phosphor-coated viewing screen, photographic film, or CCD array in a digital camera. Primary electrons that experience elastic scattering within the specimen are swept through large angles, scattered behind the objective aperture opening, and prevented from reaching the viewing screen. Primary electrons experiencing inelastic collisions within the specimen suffer an energy loss (ΔE) but have only small changes in direction. Thus, the monoenergetic primary electron beam becomes a polyenergetic beam after interacting with the specimen due to electron scattering. Those electrons that suffer an energy loss because of one or more inelastic collisions within the specimen but that still arrive at the viewing chamber may be imaged in a different plane from the undeviated primary beam and become a source of chromatic aberration in the specimen image. Egerton (1989), Hezel (1988), and Zaluzec (1986) discuss the instrumentation and theory behind EELS. Specimen analysis with EELS is more sensitive for elements at the lighter end of the spectrum such as sodium and potassium, compared with EDS.

Electromagnetic spectrometers are placed either in the column below the specimen, as in the Zeiss EM902 TEM, or at the bottom of column, below the screen. The energy filtration system found in the Zeiss EM902 incorporates an imaging electron energy spectrometer into the lens system. The unscattered part of the primary electron beam is bent through a 90° angle in the magnetic field of the prism (Fig. 237), reflected back through the electrostatic field of the mirror, and then deflected again by the prism back onto the optical axis. The slower electrons produced by inelastic collisions are less energetic and thus are more easily deflected as they pass through the magnetic field of the prism. As the electrons are refracted, they strike the spectrometer slit and thus are prevented from reaching the viewing screen. The thicker a specimen, the greater the fraction of inelastically scattered electrons caused by multiple scattering within the specimen.

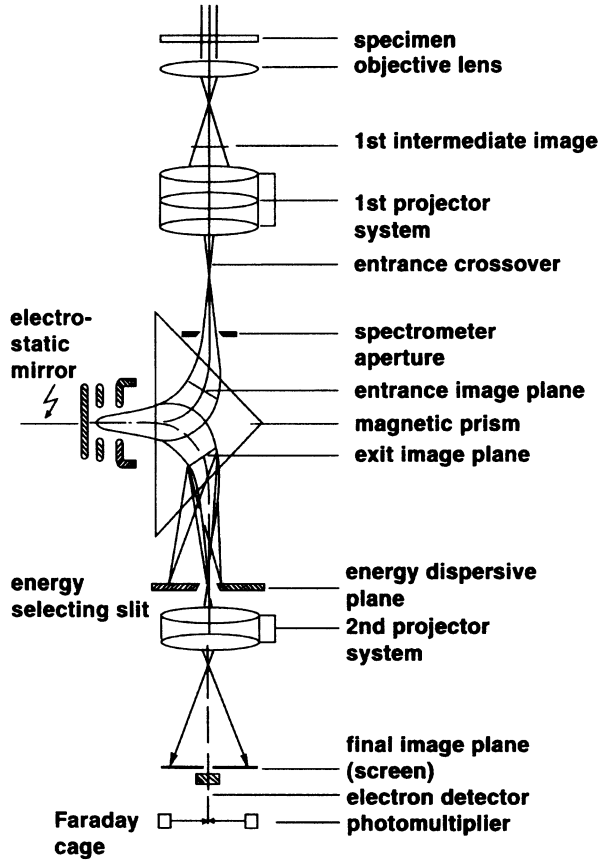

Figure 237. Diagram of the electron paths within a Zeiss EM902 TEM. (Courtesy of Carl Zeiss, Inc.)

Thus, a thicker specimen will generate a broader electron energy spectrum. With the Zeiss EM902, a 0.75-μm-thick section viewed at 80 kV will produce a sharper image than that produced from the same sample in a 200-kV instrument, and it will be virtually as sharp as that produced from a 1,000-kV unit due to the reduction in chromatic aberration facilitated by the energy filter. The Zeiss EM902 works like a conventional 80-kV TEM when the slit filter is turned off.

A procedure called contrast tuning can change the contrast of the specimen image by selecting electrons for imaging that have experienced various energy losses. If the spectrum is swept across the spectrometer slit, multiple scattered electrons with specific energy losses can be imaged.

A mode, called electron spectroscopic imaging by Zeiss, images through an electron energy spectrometer, always using electrons of defined energy and a narrow bandwidth to visualize a specific atomic element. Each element within a specimen has its own characteristic capability to scatter the electron beam, both elastically and inelastically, largely due to the element's *Z*-number, which allows this mode of elemental visualization.

REFERENCES

Chandler, J.A. 1978. X-ray microanalysis in the electron microscope. In: A.M. Glauert (ed.), *Practical methods in electron microscopy* (Vol. 5, Part 2). North-Holland, New York.

Coleman, J.R. 1975. Biological applications: Sample preparation and quantitation. In: J.I. Goldstein and H. Yakowitz (eds.), *Practical scanning electron microscopy. Electron and ion microprobe analysis* (pp. 491–527). Plenum Press, New York.

Egerton, R.F. 1989. *Electron energy-loss spectroscopy in the electron microscope*. Plenum Press, New York.

Goldstein, J.I., Newbury, D.E., Echlin, P., Joy, D.C., Romig, A.D., Jr., Lyman, C.E., Fiori, C., and Lifshin, E. 1992. *Scanning electron microscopy and X-ray microanalysis*, 2nd edn. Plenum Press, New York.

Hall, T., Echlin, P., and Kaufmann, R. (eds.). 1974. *Microprobe analysis as applied to cells and tissues*. Academic Press, New York.

Hezel, U.B. 1988. Electron spectroscopy for imaging and analysis in the transmission electron microscope. *Am. Lab.* September: 51.

Morgan, A.J. 1985. X-ray microanalysis in electron microscopy for biologists. In: *Royal Microscopical Society handbook 5*. Oxford University Press, New York.

Moseley, H.G. 1914. The high frequency spectra of the elements, part II. *Phil. Mag.* 27: 703.

Newbury, D.E., Joy, D.C., Echlin, P., Fiori, C.E., and Goldstein, J.I. 1986. *Advanced scanning electron microscopy and X-ray microanalysis*. Plenum Press, New York.

Russ, J.C. 1984. *Fundamentals of energy dispersive X-ray analysis*. Butterworths, London.

Vaughan, D. (ed.). 1989. *Energy-dispersive X-ray microanalysis. An introduction*. Kevex Instruments, San Carlos, CA.

Zaluzec, N.J. 1986. A beginner's guide to electron energy loss spectroscopy. Part II—Electron spectrometers. *EMSA Bull.* 16: 58.

15

Photography

Despite the rapid ascendancy of digital imaging for scientific information delivery, photography remains a discipline that offers the highest resolution and, in some ways, the most flexible product. The digital imaging medium is powerful but still retains some problematic issues. Digital images generated in high numbers in many electron microscopy laboratories still represent a storage issue if they are all saved at the highest resolution (file size). The current types of image files in use (JPEG, TIF, GIF, BMP, etc.) may not be universally recognized 10 years or more in the future, whereas a negative filed away over 100 years ago still can be printed easily. Another problem is that digital images currently deliver approximately one tenth to one twentieth the resolution available from the best recording films. Buonaquisti (1994) stated that typical EM film can display a feature size as small as 10 μm, which is equivalent to having a $3\,^1/_4 \times 4$ in. (8.3×10.1 cm) negative with a pixel display of $10{,}400 \times 7{,}800$ pixels, or slightly more than 81 million pixels, compared with a little over 4 million pixels for a $2{,}048 \times 2{,}048$ digital pixel display. One of the risks associated with the ease of working with digital images is that we will learn to accept a slightly less sharp image for convenience, and the market will not push the computer hardware producers to improve digital recording devices to the point where the difference in resolution between the two media will be erased.

In addition, once a high-resolution photographic image is recorded, it is easy at a later time to produce images of different sizes, whereas decisions have to be made at the outset as to what the eventual use of a digital image will be. If the image is to be sent over the internet, it usually has to be relatively small (100–300 kb), which also works pretty well for a Powerpoint™ presentation. However, if the image needs to be printed for a poster at approximately 8×10 in. (20.3×25.4 cm), then a much larger file in the range of 5–12 Mb is needed for visual sharpness. If every image collected is stored at the highest resolution, they can always be changed to files of lesser resolution, but it takes an enormous amount of media space to store the typical libraries of images that an electron microscopy laboratory has on file. Our laboratory, for example, has been open for 19 years and has over 36,000 images on file, which, at 5 Mb per image for decent resolution, would amount to 180,000 Mb of information, and some digital imaging experts would argue that a 5 Mb file would not be large enough to produce a truly excellent 8×10 in. (20.3×25.4 cm) print (see Chapter 16).

Finally, photographic negatives have been manipulated in the darkroom since the beginnings of photography to produce images that are lighter or darker or have lesser or greater contrast, as well as to lighten up or darken specific areas within the overall image. Needless to say, this and more can be done with digital images through such programs as the ubiquitous Adobe Photoshop™, which also raises the issue of scientific honesty in images. Film images have always been manipulated as stated above, but it is so much easier to change images with digital imaging programs that we now have a greater obligation to maintain vigilance to guard against the improper use of doctored images and consequent falsification of scientific data.

Thus, photography still has an edge in ultimate resolution for scientific imaging, and photographic materials have such stability and longevity that they remain, for at least the near future, a powerful medium for recording scientific information. In our laboratory, we still rely heavily on photographic media to record high-resolution electron micrographs in black and white,

while using digital imaging methods to produce color renditions of photomicrographs. It is considerably costlier and more difficult, in general, for scientific and commercial photographic laboratories to produce printed color images of sufficient quality for presentation. This is because many of our scientific images, particularly images of stained sections of materials viewed with light microscopes (like a standard hematoxylin- and eosin-stained preparation of tissue), do not have the normal diversity of colors that the color analyzers used by color print laboratories need to balance the printing parameters during print production.

The early history of photography and its antecedents is recounted admirably in the book *The keepers of light* (Crawford, 1979). This text also provides details about different types of papers and chemistry used over the last 150 years or so, including recipes and instructions for their use. Other extremely useful texts on technical aspects of photography are Adams (1980, 1981, 1983), Engel (1968), Lefkowitz (1979), and Stroebel *et al.* (1986).

Photography is an important partner to any form of microscopy utilized in the sciences. It is rare enough just to observe something in science, but we are compelled by the nature of microscopy to record events and to share them with students and colleagues. The first recording method was to draw freehand the images observed through a light microscope, but the result was frequently inaccurate. In 1807, the physicist and chemist, William Wollaston, invented the camera lucida, which projected an image from an ocular onto a surface, where the projected image could be traced by the observer. One of the two prime developers of photography, the mathematician William Henry Fox Talbot, was frustrated in his efforts to produce accurate images with a camera lucida and began pursuing methods to produce a photographic image. He coated papers with sodium chloride, let them dry, and then coated them with silver nitrate, thus producing a silver chloride emulsion. He placed objects such as leaves and lace on the surface of paper and produced a negative image called a *photogenic drawing*. His writings note the production of a negative photographic image for the first time in 1834 (Crawford, 1979). In the meantime, Louis Daguerre in France was producing positive photographic images, which were first reported to the Academy of Sciences in Paris in 1839, thus starting a longstanding conflict between the British Talbot and the French Daguerre. In 1885, George Eastman introduced film with a cellulose nitrate base that was flexible and could be rolled up inside a camera for multiple photographs (Collins, 1990). At that point, the modern age of black-and-white photography had come into existence.

Electron microscopy utilizes specialized films to record images and various photographic papers upon which the images are printed. Understanding how to use these two types of products is enough to produce photographs that can be shared, but an important part of scientific communication is to produce photographs of proper quality for slide presentations, poster presentations, and journal publication. The objective of this chapter will be to introduce the reader to the mechanistic foundation of the photographic process and to introduce a variety of photographic materials and approaches specifically devoted to scientific illustration. A great deal of printed information concerning photographic techniques and products available from the two biggest suppliers, Kodak and Ilford, used to be available, but both manufacturers have reduced their scientific product line over the years and, at the same time, the number of useful pamphlets. Most of the information is still available over the internet, so searching www.kodak.com or www.ilford.com yields much of the information formerly available in print.

I. EMULSION COMPOSITION

A photographic emulsion consists of silver halide (usually silver bromide) crystals suspended in a matrix of gelatin attached to a substrate consisting of plastic, glass, paper, or

resin-coated paper stock. Films often have an anti-halation backing to prevent photons of light from bouncing off the camera back and being reflected back through the emulsion, which would produce "fog" (non-informational silver grains in the final image) and reduce resolution.

A considerable number of photographic materials are available for color and black-and-white work. One of the reasons that high-resolution scientific photography is done primarily with monochromatic materials is that images produced on a single layer of emulsion will be slightly sharper than equivalent images recorded on color films, which usually have three layers of emulsion stacked on top of each other.

With black-and-white materials used to record electron microscope images, we are concerned only with density and contrast, not actual hue. Even getting these two factors the way you want them can be a problem unless you print your own materials. The rest of this chapter will be directed toward producing your own illustrations with minimal esoteric chemicals or equipment.

II. FILM TYPES

Films for scientific use are available in various formats such as 35 mm, 120, and sheet films of various dimensions. Most of the films used in scientific applications in the United States are produced by Kodak or Ilford. A list of their film products, along with their characteristics, can be found on the internet at www.kodak.com/cgi-bin/webproducttypes.pl?type = films and www.ilford.com/html/us_english/products.html, respectively. Emulsions can be categorized on the basis of their spectral sensitivities: (1) "ordinary," which is essentially color blind and sensitive to only blue light; (2) panchromatic, which is sensitive to essentially the same colors as the human eye; (3) orthochromatic, which is sensitive to all colors except red; and (4) color, which is sensitive to roughly the same spectral bands as panchromatic film and is capable of recording the individual hues themselves. Special-purpose films such as infrared films are also available. It is worth noting that most films have sensitivity to ultraviolet radiation, which the human eye does not perceive. This explains why those views of crystal-clear fall foliage taken on sunny days in the mountains come back from the processor with a somewhat washed-out, lower contrast image than remembered. Ultraviolet radiation decreases the overall contrast of the image on the film compared with what the eye perceives.

Films are also rated as to their speed (ISO) or their exposure index (EI) under specified conditions. Both the ISO speed and the EI numbers are a measure of the emulsion's sensitivity to light and are used to set light meters for determining proper exposure. The higher the ISO, the "faster" a film is. This means that less light is required to cause exposure, a feature generally related to the fact that faster films have larger silver halide crystals that are more likely to be hit by a photon than smaller ones. Thus, higher ISO products are associated with a larger developed silver grain size and, thus, more graininess in the printed image.

The ISO for each film is determined utilizing very specific exposure, developer, and developing conditions in a laboratory setting. Exposure indexes (EI) are based on different developers and procedures from those dictated for ISO ratings. A film such as Kodak Technical Pan (Tech Pan) can be used for a variety of purposes and has several EIs, even though it can have but one ISO number.

Another way to categorize films is to divide them between two major applications: pictorial work (panchromatic films) or graphic arts work (orthochromatic/process films). In reality, some films share characteristics of both groups. Electron microscope films and Tech Pan are two examples that have characteristics of both film classes. Electron microscope films have high

contrast and are red-light insensitive like graphics films. At the same time, they can produce continuous tone negatives, with numerous levels of gray between black and white, a characteristic of panchromatic films. Tech Pan is actually more sensitive to red light than a typical panchromatic film but, if developed with high-contrast panchromatic film developer (D-19), exhibits a strong contrast suitable for line drawings (no significant gray is seen).

Finally, films can be described on the basis of their sensitometric curves (characteristic curves, Hurter & Driffield curves). These curves are published for each film produced (DeCock, 1985) and provide information that helps determine to which application the film should best be directed. The curves for different films under different use conditions are available at the two websites listed above. Panchromatic films have gradual curves (Fig. 238), indicating that they have a fairly wide latitude for exposure and development. In practical terms, this means that satisfactory images can be produced, even with slightly inaccurate exposure times, developer strengths, development times, and with slightly uneven illumination. However, graphic arts films have steep curves (Fig. 239), indicating that precise exposure, even illumination, and critical development procedures are necessary. Most panchromatic films must be processed in the dark because of their broad spectral sensitivity, while graphic arts films typically have orthochromatic characteristics and thus may be processed under dim red safelights. Just remember that the term "safelight" is a bit of a misnomer, since all photographic emulsions will eventually become fogged by exposure to safelights. Some films are just more insensitive than others, so they do not usually fog during normal processing times.

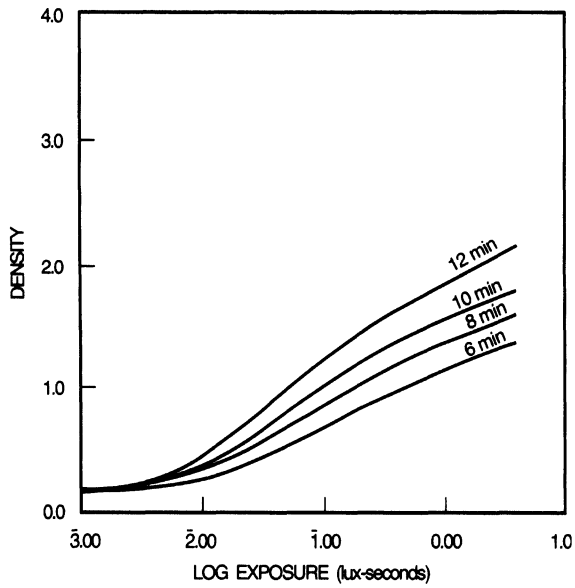

Figure 238. Sensitometric curve for a panchromatic film (Kodak T-max 100). Kodak D-76 developer, 20°C. (Reprinted courtesy of Eastman Kodak Company.)

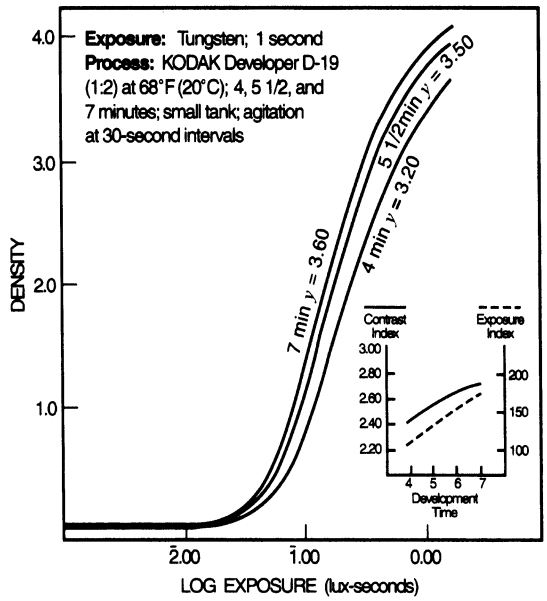

Figure 239. Sensitometric curve for a high-contrast film (Kodak Technical Pan). Kodak D-19 developer, 20°C. (Reprinted courtesy of Eastman Kodak Company.)

III. PRODUCING A LATENT IMAGE

A latent image is formed when a sensitivity speck has been converted to atomic silver. Latent images are produced when film is exposed to light, electrons, radioactive emissions, cosmic rays, certain chemicals, and mechanical pressure. Any form of energy has the potential to reduce ionic silver in the silver halide crystals to metallic silver.

A sensitivity speck is a flaw in the crystal lattice of a silver halide crystal (Fig. 240). An electron is released from bromine in silver bromide emulsions when the crystal is struck by a photon or other source of energy. The electron travels through the crystal lattice to the sensitivity speck where it produces one reduced silver atom. Metallic silver at the sensitivity speck tends to draw other silver ions toward it and reduces them in turn, given enough time.

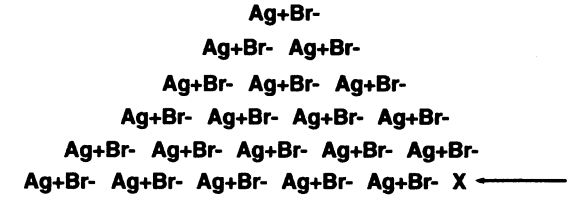

Figure 240. Silver halide crystal with a sensitivity speck (arrow).

IV. FILM PROCESSING

Silver bromide will be converted to metallic silver in about 2,000 years at an aperture opening of f8 in a camera, even without development, a form of the process known as *printing out.*

Chemical development is used to speed up this process about 1 billion times by providing the photographic emulsion with a ready source of electrons, the developer.

Before discussing the chemical components for film processing, a warning must be provided concerning the toxicity of the chemicals encountered. Film developers are basic and are thus more reactive with tissues than the acidic stop bath or fixers encountered. Severe contact dermatitis may result from repeated exposure to photographic chemicals. Some workers who have moved prints through trays of chemicals by hand for years, rather than with print tongs, have no apparent problems, while others may develop severe allergic reactions to the same chemicals after only a few exposures. Some individuals develop skin reactions or respiratory allergies sufficiently debilitating to prevent any further darkroom work.

A. Developer

All developers are complex solutions containing water, developing agents, preservatives, activators, and restrainers. Developer is used to provide electrons to all silver halide crystals containing latent images, catalyzing the conversion of the remainder of the crystal to metallic silver.

Water is used as a solvent for the other constituents and also causes the gelatin of the emulsion to swell, allowing the developer chemistry to reach the silver halide crystals of the emulsion more easily.

The developing agents, as mentioned, are electron donors, almost all of which are benzene derivatives. Developers will ultimately reduce *all* silver ions to metallic silver, but work preferentially on silver halide crystals containing latent images. Film development is performed under controlled time and temperature conditions to selectively develop primarily the silver halide crystals with latent images. Some of the common developing agents are Elon® (metol), hydroquinone, and phenidone. The developing agent(s) used and their concentrations are dependent on the type of emulsion being processed. Panchromatic film developers such as Kodak D-76 and D-19 are mixtures of metol and hydroquinone. These developers exhibit a short inertial time with gradual grain development. What this means is that very shortly after a film is immersed in the developer, silver grains begin appearing from the conversion of all of the exposed silver halide crystals into metallic silver. As time goes on, the crystals enlarge as the process continues. The practical side to this feature is that cutting development time or lowering development temperature allows most exposed crystals to begin development, even though most will be slightly underdeveloped. The silver grains will be smaller than if they were fully developed, thus sacrificing the ultimate "speed" of the film, or sensitivity, for smaller grain size. The development time and temperature are frequently manipulated to produce images with a smaller grain size to improve the enlargement capabilities for a given panchromatic film.

Graphic film developers such as Kodalith developer, however, are composed primarily of hydroquinone. These developers exhibit a long inertial time followed by rapid development. Cutting the development time will thus yield a loss of apparent film speed with no decrease in grain size or graininess. If the film is underdeveloped significantly, few silver halide crystals will be turned into reduced silver, and so little image will be produced.

Knowing the characteristics of a given film based on its sensitometric curve will give some clue as to the type of developer to use. Films with steep curves usually utilize developers such as Kodalith developer, while panchromatic films identified by shallow curves utilize lower activity developers. The steep-curve films tend to produce high-contrast images with true white and true black, with little or no grays. The shallow-curve films typically produce continuous-tone images with a number of gradations of gray between true white and true black.

Preservatives are included in developers to retard oxidation of the development agent. One typical preservative is sodium sulfite (which is also used as an activator for the developer). Developers are stored in full, tightly stoppered bottles in the dark to help prevent oxidation and photodegradation. As developers become oxidized, they usually become brownish in color. Oxidized developers also develop a characteristic chemical odor somewhat reminiscent of ammonia. Any time a developer has colored noticeably or has a strong smell, it should be discarded. Paper developer is the only possible exception, since it can be tested by printing and developing one photograph and, if it does not develop properly, another can be quickly printed from the negative with new chemicals. Films, however, offer only one chance for development, and bad chemistry will result in the irretrievable loss of an image.

Restrainers serve to reduce the tendency to develop unexposed silver halide crystals, resulting in fog (non-informational silver deposits). Potassium bromide is a common restrainer. The development process itself produces restrainers in the form of bromide ions. As metallic silver atoms are formed, bromide is released from the emulsion into the developer solution. If film is not agitated during processing, two things occur: (1) fresh electron donors (developing agent) do not come into contact with the emulsion, and (2) the bromide ions released from silver halide crystals in the emulsion remain on the surface of the film, thus serving as restrainers for the development process. However, excessive agitation is to be avoided. The surfaces of plastic film racks, the holes on the edges of individual metal sheet film holders, and the edges of film reels are all places of high-velocity fluid flow during agitation compared with the center of a sheet or roll of film. Excessive agitation, therefore, results in overdeveloped film edges. Such negatives will be difficult to print because the edge of the print will be light due to excessive negative density on the edge compared with the central area of the print. Kodak and the other film manufacturers give specific instructions for agitation that should be followed explicitly. Most films should be agitated every 30 sec during development. Reels should be rotated in both directions within the tank of chemistry and inverted once during each agitation cycle, if possible. The sheet film should be raised vertically from the tank and tipped at 45° in one direction before being returned to the chemistry. At the end of the next 30-sec period, the film should be tipped in the opposite direction. Kodak has published a short pamphlet (Kodak, #E-57) describing how to set up a nitrogen burst system that is recommended for electron microscope negative processing to make sure that even development is achieved.

B. Stop Baths

Stop bath solutions usually contain about 4% acetic acid. Kodak Indicator Stop Bath contains a color indicator that turns the fresh yellow–orange solution to a purple hue as it becomes neutralized. The purpose of stop baths is to neutralize any of the basic developer clinging to emulsions prior to exposing the film or paper to acidic fixer. Stop baths are generally needed only for paper development series. Films have plastic or glass backing materials incapable of retaining much developer chemistry, so rinsing with water for 1 min between the developer and fixer steps is usually adequate. However, fiber-based papers soak up significant amounts of developer during the typical 90–120-sec development process. If the developer is carried into the fixer, it will quickly render the fixer inactive by raising the fixer pH. Resin-coated papers do not retain as much liquid as fiber-based stock as long as minimal chemistry bath times are maintained. Excessive times will allow chemicals to penetrate the cut edges of the resin-coated stock, and it will be difficult to remove the absorbed chemistry during subsequent steps.

C. Fixer

Fixer is typically a solution of sodium thiosulfate, also known as sodium hyposulfate, hence the common name "hypo." After the silver halide crystals containing latent images are converted into metallic silver, the remaining unexposed silver halide crystals must be removed by the fixer so that future light exposure will not result in their development. Thus, the fixer solubilizes the unexposed crystals and converts them into stable salts that do not decompose during the final washing step and that can be effectively removed from contact with the film or paper. Depleted fixer contains significant quantities of silver and should not be put down the drain to enter the water supply since silver is toxic to most organisms. There are various businesses that reclaim silver from spent fixer and usually can be located through local photographic supply houses.

V. DEVELOPMENT CONTROLS

A. Time

With most panchromatic film developers, longer development times will yield greater negative density, greater contrast, greater fog (noninformational density), and greater granularity. If development continues long enough, the film surface will become completely covered with silver grains. Remember, development preferentially develops silver halide crystals with latent images but ultimately will develop *all* silver halide crystals.

B. Temperature

Since film development is a catalytic chemical process, it is obvious that higher temperatures will result in faster development. What is not necessarily intuitive is that more granularity and fog also are generated at higher temperatures. These two features are objectionable in scientific images, where maximum resolution and sharpness are paramount. Most films are processed at 20°C, which allows reasonable development times in the 4–15-min range, depending on film, application, developer, and developer dilution. Within these time constrains, there is minimal grain and fog. Films developed above about 25°C can exhibit a phenomenon known as reticulation, which is sometimes intentionally produced to make interesting artistic photographs with crazed images somewhat similar to old varnished surfaces. Reticulation is caused by the continuous gelatin layer developing cracks from the elevated temperature. In tropical climates without chilled water supplies, this problem can be dealt with by cooling the developer with ice prior to use. Developer temperature is the only absolutely critical temperature to maintain during processing. Other chemical and washing steps can have temperature fluctuations of several degrees without any dire consequences.

C. Agitation

As mentioned in the section on developers, agitation is a critical aspect of film processing. Overagitation will result in uneven development, while underagitation can result in inadequate or uneven development because of the restraining action of bromide ions released from the emulsion.

D. Developer Choice

The section on developers in this chapter describes the general differences between orthochromatic developers for process (graphic arts) films and panchromatic film developers. Within each category, however, several choices can be made. In addition, there are films that share characteristics of both film types, which can be manipulated by developer choice to produce steep-curve, high-contrast, graphic arts types of negatives or relatively shallow curve, panchromatic type negatives.

Tech Pan was designed to replace a previous high-contrast, low-grain product. It has the usual panchromatic spectral sensitivity, being a broad-spectrum film with a peak in the green region, similar in response to the human eye. The film has a second sensitivity peak in the red portion of the spectrum, which means that it cannot normally be used in portraiture, since Caucasian skin color appears darker than normal.

Shortly after Tech Pan appeared, pictorial photographers discovered its extremely fine grain characteristics and experimented with developers high in phenidone to produce a negative with a broader gray scale, providing more gradations of gray between strictly black and strictly white. Kodak eventually marketed a phenidone-based developer under the name Technidol specifically for the pictorial use of this film. During the last decade, this film has been used for continuous-tone photomicrography (using an EI of 50 and developing in Kodak HC-110 developer diluted 4:246), pictorial work (using an EI of 100 and phenidone developer), and high-contrast graphic work (using an EI of 25 and Kodak D-19 developer). This film can be manipulated more than most other films, and the choice of developer is a significant variable that must be considered.

VI. PAPER TYPES

Fiber-based papers are produced by various manufacturers such as Kodak and Ilford. Each manufacturer has a different set of codes to classify their surfaces. Kodak produces a variety of products, among them F surface papers (gloss finish), N surface papers (flat finish), papers with pearl or textured surfaces, single weight and double weight papers, papers with blue–black blacks (Kodabromide™), and papers with deep sepia tones (Ektalure™). Some are even designed to make black-and-white prints from color negatives (Panalure™). Fiber-based papers are tray processed and must be handled carefully to make sure that undue amounts of the absorbed chemistry are not carried from the developer into the fixer resulting in inadequate fixation. Prints must then be washed extensively for about 1 hr with tumbling in running water. Hypo eliminators such as Permawash® or Kodak Hypo Clearing Agent™ can reduce washing times considerably and simultaneously improve image permanence. Products such as Edwal Hypochek™ can be used to check fixer. If the fixer is spent (contains excessive amounts of complexed silver), this agent will produce a precipitate (silver nitrate) that is easily seen.

Resin-coated papers appeared in the 1970s and offered a coated paper stock that absorbed minimal chemistry, thus allowing relatively shorter processing times in trays. There are two varieties available. Papers with activator incorporated in the emulsion could be processed in machines without heated chemicals, but the chemicals were more toxic than conventional photographic chemicals, and so these processors are no longer on the market. The remaining machines heat both the developer and fixer tanks, allowing them to process resin-coated papers that do not have the activator included in the emulsion. The number of photographic print processors available to EM laboratories has decreased in recent years, particularly since Kodak abandoned the market. Ilford still offers the 2150 RC processor for medium- to reasonably high-output operations, while

the Mohr 8 processor (Mohr Industries) is adequate for lower-output laboratories. Other manufacturers still produce small print processors, but they are less commonly found in scientific laboratories. Using these processors, the resin-coated papers emerge in about 90 sec as dried, fixed prints. The ability to control print density by altering developing time as can be done with paper-based materials in trays is not possible. Of course, prints should actually be developed to completion, unlike the situation for films, so print density should ideally be determined strictly by exposure, not development.

Since the popular market that drives the photographic products industry is based on photofinishing shops dedicated to rapid production techniques, resin-coated papers are more readily available than fiber-based products from photographic supply stores. The surfaces available for resin-coated papers are not as varied as with fiber-based products, and the long-term archival properties of resin-coated stocks are not as well known (after all, we have fiber-based prints dating from the mid-1800s).

Both resin-coated and fiber-based papers are available as single-grade papers, each with different contrast characteristics. The Kodak line has five levels of contrast available, from #1 (lowest contrast) to #5 (highest contrast). Each has a slightly different sensitometric curve. When processed in trays, the lowest grade begins showing an image shortly after immersion in the developer and develops continuously until it is completed at about 2 min. However, the highest grade (#5) has a long inertial time followed by rapid image development during the last 30 sec or so.

Both major paper types are also available as polycontrast (Kodak) or multigrade (Ilford) materials. These papers can produce various degrees of contrast, depending on the colored filter used during printing. Five or six major grades of contrast are available with half-steps between them. The original variable-contrast products did not have quite the contrast range available from the series of single-grade papers, but the current versions of both are virtually identical. The only limitation is that fewer surface types are available in polycontrast papers.

If archival-quality prints with good storage characteristics are desired, prints should be made on fiber-based stock followed by development, stopping, and careful fixation, preferably in two fixer baths. The prints then should be washed thoroughly, subjected to a fixer-killing chemical (Kodak Hypo Clearing Agent™, Permawash®), and then rinsed again. Finally, increased permanence can be gained by toning the prints in a selenium or gold agent, which will prevent oxidation (tarnishing) of the silver image. In most cases, scientific images do not require this much effort, since they will be used in a publication long before archival quality will be a factor. If, however, a long-term display of micrographs under continuous institutional lighting is desired, it might be wise to use methods for archival-quality prints.

VII. KEEPING PROPERTIES OF CHEMICALS AND PRECAUTIONS

As mentioned earlier, photographic chemicals, particularly developers, are capable of producing contact dermatitis in some individuals. The liquid solutions should not be allowed to come into extensive contact with the skin. If contact does occur, quickly rinse the exposed surface with water. In addition, the powdered chemicals should be handled carefully when mixing up photographic solutions. Minimize exposure to the chemical dust by pouring the powders slowly into mixing containers. Read all packages for precautionary notes and also for specific mixing instructions, since various chemicals are to be dissolved at different temperatures.

Kodak's darkroom data guide (Kodak #R-18) has guidelines describing the shelf life of chemicals once in solution as well as information on film types, processing, paper types, and so on.

Developer chemicals are the most labile, having a tray life of only a few hours before oxidation degrades them significantly. Most of Kodak's developer solutions have a shelf life of about 2–3 months when stored in full, tightly stoppered bottles to reduce exposure to oxygen in the air. Often, the shelf life is considerably longer than is stated in Kodak literature, and developer that is several months out of date, uncolored, and nonodiferous is most likely usable but should not be used for negative development. As mentioned, old paper developer is worth trying, since it can be discarded with only the loss of one print if it proves to be bad.

VIII. SHARPNESS

Sharpness, as defined by good contrast and good resolution, is usually the objective in scientific illustration. When processing film, diluted developer used at 20°C will typically produce the smallest grain size for a given emulsion/developer combination. The photographic guide from Morgan and Morgan (DeCock, 1985) gives details concerning proper developers to be used, dilutions possible, and development times. A smaller grain size allows greater resolution and greater enlargement without any objectionable graininess. Overexposure in the camera and/or overdevelopment will produce a larger grain size and, hence, less resolution. In most cases, the most information can be gained from a negative that is "exposed for the shadows and developed for the highlights" (Adams, 1981). If a high-contrast graphic arts material is used to reproduce line drawings, a slight underdevelopment will result in crisper lines. To minimize background, these thinner negatives (underdevelopment decreases the amount of silver left on the film) should be printed with high-contrast (F5) papers or filters.

IX. FILMS COMMONLY USED IN THE EM LABORATORY

As already stated, our purpose in biological electron microscopy is to record images from light and electron microscopes as we study cells and tissues. High-quality prints suitable for viewing at a distance (posters) as well as prints for reproduction in journal articles (publication prints) are also needed. Projection slides for presentations (2×2 in., 5.1×5.1 cm) are usually produced from color slide film (Ektachrome, Fujichrome), or more recently in the form of digital Powerpoint™ slides, projected directly from computers. Since a publication or poster may include light micrographs, electron micrographs, line drawings, views of anatomical specimens, radiographs, and photographs of gels containing DNA or proteins, the list of photographic materials utilized in the laboratory can be fairly extensive.

A. Negative-Release Films

These films produce negative images, which must, in turn, be printed to produce a positive image. They encompass electron microscope films, Polaroid products like Type 55 film used for SEM and copy work, sheet films for large-format copy work, 35-mm panchromatic films for photographs of experimental set-ups and anatomical materials, and films for photomicroscopy or for copying high-contrast materials such as Kodak Tech Pan and Kodalith.

Sheet film for electron microscopy comes in a variety of sizes for the various instruments on the market. Emulsions were originally coated onto glass to produce an extremely rigid, flat surface to prevent image degradation, which is theoretically possible if the film plane is not precisely

flat. Since the projected TEM image is in focus at a variety of levels above and below the plane of the film, an uneven recording height (slightly buckled film) could produce an image with minute variations in magnification, even though all areas would be in focus, causing inaccuracies in image recording. In practical terms, this is of little concern, so glass plates have vanished from the photographic market. The current polymer-based products are easier to store and less fragile than the old glass plates. Most U.S. laboratories use either Kodak 4489 or Kodak SO-163 electron microscopy films. These products are high-contrast, fine-grain emulsions coated onto stiff, thick (0.007 in., 0.178 mm) plastic stock. They do not have anti-halation backings as found with films for photography with light, since electrons cannot penetrate the plastic base, much less reflect from the back of the film holder back through the film. Of the two Kodak films, SO-163 film produces a higher-contrast image. Kodak 4489 film is widely used and has a tough Estar base.

A variety of 35-mm (and 120) format films are available for photomicrography and recording of other subjects examined in the electron microscopy laboratory. The T-max™ films produced by Kodak are designed for minimal graininess for their ISO rating when compared with the previous products such as Pan-X™, Plus-X™ and Tri-X™. Ilford produces a variety of products equivalent to the T-max™ films, designated Delta™ films. They also offer a line of non-Delta films equivalent to the Kodak-X series. Ilford invented chromogenic film, with Kodak bringing out a similar line shortly afterward. Chromogenic films are actually color negative films requiring development with color negative film developer (C-41 processing). Once the negatives are processed, however, they are printed onto black-and-white papers. The advantage to these products is that they can be exposed over a wide range of EI. A film rated at 400 ISO can be used up to EI 1600. In addition, they produce very fine-grain images so that they are ideal for low-light photomicrography situations as encountered with certain fluorochromes (Texas red).

If low-contrast materials are to be utilized in photomicrography, Tech Pan used at EI 50 and developed in HC-110 as previously described is to be recommended. The negatives can be enlarged up to 28 × without any objectionable grain, though they will become fuzzy because of the empty magnification this represents as explained later in terms of copying images. The only problem with this Tech Pan film is that it is very unforgiving of improper exposure or uneven illumination because it has a steep sensitometric curve (Fig. 239). If photographed materials have a high inherent contrast, the recorded images may have too much contrast to print well.

Polaroid products such as Type 55 (4 × 5 in., 10.2 × 12.7 cm single sheet film) and Type 665 $3\frac{1}{4} \times 4$ in. (8.3 × 10.2 cm) sheet film in packs of eight sheets have been used extensively in SEM work and for making copies with a copy stand. They offer the advantage of producing an image that can be examined 30 sec after the photograph is made (the positive) as well as producing a high-resolution negative that can be processed and stored for future use. Other Polaroid products are available that yield only positive images (Type 53, among others), but these do not allow further prints to be made unless the original is copied first.

Various manufacturers such as Kodak and Ilford produce both panchromatic and graphic arts (process, or litho) films in 4 × 5 in. (10.2 × 12.7 cm) format and larger to produce negatives of continuous tone and line-drawing types of materials, respectively.

B. Positive-Release Black-and-White Films

When these films are developed, a positive image is produced that is suitable for mounting in slide binders and for projection to an audience. These are rarely used now, but were quite popular for producing projection slides before the dominance of Powerpoint™ slides. Some of these films are quite slow (low ISO) products and so are unsuitable for direct photomicrography

and are generally used to copy materials on a well-lit copy stand. Kodak discusses making slides with film for presentations (Kodak publication #M3-106) and provides useful guidance for designing projected images in the standard "slide" format (2×2 in., 5.1×5.1 cm), even if they are produced and projected from computers. They suggest that all slides should be made to be projected horizontally, since that is usually the way projectionists set up screens at meetings. If slides are projected vertically, they will often go over the top or bottom of the screen. In addition, all the material on a slide should be capable of being read in less than 30 sec. Finally, the font used for a 2×2 in. (5.1×5.1 cm) slide should be large enough to be read with the naked eye. We have all seen slides projected at meetings that do not conform to these rules and recognize that they are difficult to read and understand.

Black-and-white projection slides can be made with Ektachrome (T64, with 3,200° K floodlights) or Fujichrome 100 daylight films under 3,200° K lights, with the addition of adequate blue filtration. The resulting slides will exhibit more contrast than the original prints, but they will seem quite sharp. Unfortunately, any materials copied on a typical light box (radiographs, gels) will often take on the greenish cast characteristic of most fluorescent tubes.

Kodak Tech Pan has been used to copy electron microscope negatives on a light box, but because it increases the contrast of the original, a series of negatives made from different sections will be unlikely to have identical contrast. Any slide series made from these negatives may have widely varied contrast and density characteristics.

X. COPY WORK

Lefkowitz (1979) covers copying and duplicating in black-and-white as well as in color. Copy work is used to reproduce images, often those that are actually composites made from several media (e.g., gels with added lettering). When preparing figures for publication, often you will need three copies of the illustrations, one for the printer and two for the reviewers. An increasing number of publishers are requesting electron submissions, including files of images, so photographic copies are not used for the submission process. However, if given the opportunity to provide original photographs of images, we still prefer to do so. The rationale is that every reproduction of an image, by whatever method, degrades the image. If a primary digital file is sent to the printer, the printed product will probably be as good as the image resulting from the printer digitizing a photograph. However, if you send the printer a hard copy of a digitized image that is then digitized again for the printing process, it is likely that the image will be degraded to some extent.

When printing publication photographs, a paper containing a number of illustrations, particularly if they have labeled cellular structures, can lead to a large amount of darkroom work if multiple copies are needed for reviewers. It is usually simpler to make one perfect and complete set of camera-ready illustrations, printed at exactly the size used in the journal, for the printer and then to make a copy negative of them grouped together. The copy negative can be used to make multiple copies quickly and easily for the reviewers. It is also usually easier for the reviewers to handle one sheet of photographic paper with several illustrations on it rather than numerous loose photographs, and a happy reviewer is typically a generous one. In addition, if someone requests a preprint of the paper, further copies of the figures can be quickly printed from the copy negatives, rather than having to locate the original negatives and to print them all over again, carefully trying to get them to match. Finally, relabeling all the prints is not necessary.

Copy negatives are also useful when the original illustration (a photograph of a gel) is subsequently labeled, and then copies of the assembled labels and original material (the gel) are needed.

A. Films

Copy negatives of line drawings can be made with a high-contrast film such as Kodak Tech Pan in the 35-mm format, but the camera lens must be stopped down, and the material to be copied must not fill over two-thirds of the viewing field. If the lens is used wide open (largest aperture) and/or the material fills the camera frame to the edges, letters in the corners will appear discontinuous, unevenly illuminated, and unsharp when printed because of spherical aberration.

These two cautions (fill only two thirds of the field, and stop the lens down to at least the middle of its f-stop range) apply to any film and camera but are particularly important in the 35-mm format, since the negatives will usually be considerably magnified.

Polaroid types 55 and 665 positive/negative films are ideal for copy-stand work because they are both high-resolution films designed for continuous tone work. Since they are processed quickly, it is possible to know at once if the copy negative contains the desired information. If the films are used for line drawings, underexposing them slightly and then printing them on a high-contrast paper (Kodak F5 or polycontrast paper with a #5 filter) will result in crisp letters and lines.

B. Improving Copy Stand Images

In order to produce copy negatives or 2×2 in. (5.1×5.1 cm) slides that contain all the information possible, it is imperative that exposures are accurate and reproducible and that developing is done accurately and consistently. Several aids are available to help us achieve these ends.

1. Gray Cards

Gray cards known as 18% gray cards may be purchased from Kodak to allow accurate metering of light. Light meters, whether hand-held or built into single-reflex cameras, are calibrated to average the viewing area and to call for an exposure that would represent an "average" mixture of black and white with grays in between. This mixture averages out to an 18% gray, and meters are adjusted to see this gray as a mid-scale reading for a given ISO setting. Metering on copy stands is done by reading reflected light. Clearly, a printed page has much more white (reflectance) under a given set of floodlights than does a continuous-tone electron micrograph that consists mostly of grays and blacks, with very little white (except where holes exist in plastic sections). Since the meter actually is calibrated to see 18% gray, the electron micrograph will be metered properly, while the line drawing will tend to be underexposed to make it 18% gray. To avoid this problem, after the ISO for the film is set on the meter, a gray card is read to determine the f-stop (lens opening) and the exposure time. After this is set on the camera, any automatic metering capability on the camera should be disengaged so that the camera metering system cannot adjust to the levels of reflected light encountered because the camera would reset its exposure parameters continuously depending on whether line drawings or continuous tone drawings were being metered. If this precaution is taken, the camera will be insensitive to the type of material being photographed, since the exposure is based just on the amount of light reflected off the surface of the 18% gray card and will take consistently exposed photographs of any kind of material (line drawings or continuous tone photographs) put onto the copy stand.

2. Gray Scale

Gray scales are another aid designed to help determine if all the potential grays available in a photographic print (about eight gradations of gray are usually possible) are being reproduced on a negative. Since various materials have different levels of gray, the scales (available from Kodak) have bars of different density, ranging from black, through a series of gray, to white. If a copy negative showing all the gradations of gray seen on the original scale can then be printed on paper and can reproduce the various grays seen in the test scale, the exposure and development processes for that copy have been successful.

3. Focusing Aids

These devices (Fig. 241A and B) typically consist of targets of closely spaced lines or other devices containing lines with well-defined edges. Some of these devices are also used to determine lens quality, since they can show astigmatism, sharpness, flare (loss of contrast), and spherical aberration. They can be placed alongside the print to be copied and in the same plane so that true focus can be determined by observing the edges of the target lines (Fig. 241B). Continuous-tone photographs are difficult to focus on at times because they rarely exhibit many sharp, dark lines.

4. Stopping Down for Sharpness

Photographs of high-resolution materials such as the engraver's lines on a $1 bill (Fig. 242) will exhibit improved sharpness if the lens is closed down to somewhat less than midway on the f-stop scale. If the largest aperture (typically around f1.8) is used, spherical aberration may be noted; if the smallest aperture is used (typically f22), diffraction may degrade the image. Midscale is a good compromise.

5. Depth of Field as a Function of f-Stop and Magnification

The smaller the f-stop, the greater is the depth of field. However, magnification is inversely proportional to depth of field, so the higher the magnification, the less the depth of field. Most copy-stand materials are absolutely flat, since they consist of a print underneath a glass plate. In those cases, the f-stop selected is not critical for depth of field, though it can still affect sharpness due to potential spherical aberration. If an illustration is being copied from a journal or book for presentation, any slight curvature of the original may result in part of the image being out of focus compared with another part if the lens opening is large (f 1.8) or the magnification factor is large. In addition, materials with three-dimensional aspects may be difficult to get into focus unless the lens is stopped down (Fig. 243).

6. Copy Lenses

Macro lenses are designed to focus on materials close to the lens and are, thus, ideal for copy-stand work. A relatively good aftermarket 50-mm macro lens for a 35-mm camera can cost from about $200 and up. A 50-mm macro lens may focus closely enough to produce a 1:1 copy, while some manufacturers make lenses that enlarge up to 1:2 but need an added extension tube to produce 1:1 copies. If you might use a macro lens in a surgical or field setting, a 100-mm macro

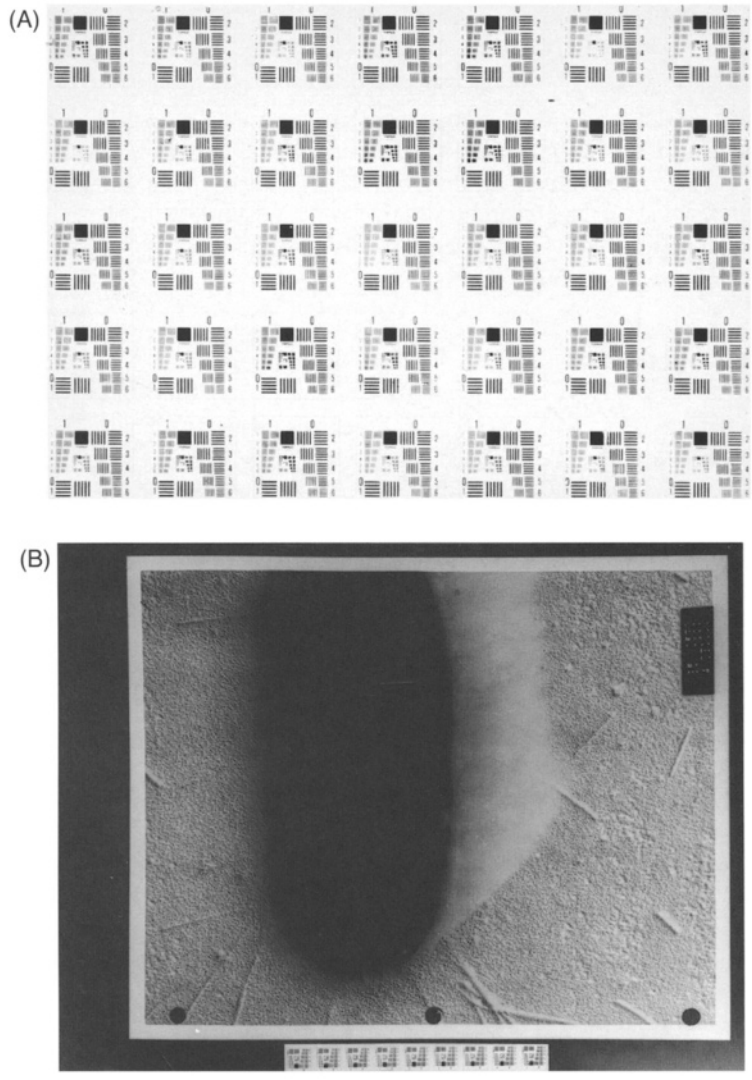

Figure 241. A focusing aid. (A) Detail of the focusing aid made by printing a portion of a lens resolution-checking target. (B) Focusing aid in the image copied, which is cropped out when the copy negative is printed.

lens might be worth considering. They are more expensive than 50-mm lenses, but they allow you to stand back farther from the subject and to gain a bit more depth of field.

Bellows or extension tube sets can also be purchased that are placed behind the primary lens. These decrease the amount of illumination available, so through-the-lens metering is necessary to avoid having to recalculate exposures based on the decreased illumination.

Finally, inexpensive diopter lenses in sets of +1, +2 and +3 or +6 may be purchased (for under $60). These screw onto the front of the prime lens, may be stacked up in different combinations, do not decrease illumination, but do cause a drop in contrast due to flare, since they are not thoroughly coated like the primary lenses. They are also not as sharp as normal focal length or macro primary lenses. Unless photographs produced with diopter lenses are placed beside products of macro lenses, it is difficult to detect variations between them in many cases.

It is probably useful to mention the concept of empty magnification at this point. For example, a 100 × enlargement can be produced from a negative that contains an image enlarged 50 times with microscope optics that is then enlarged 2× further when printed. However, a 100× enlargement can also be produced by enlarging the same image 10 times with a microscope when the original negative was produced, followed by another 10× enlargement when printed. When the two prints are put side by side, the differences in sharpness and resolution will be glaring. Even when viewed alone, it will be evident that the print enlarged 10× cannot be viewed as closely without noting lack of clarity when compared with the 2× print enlargement. The 10× enlargement suffers from empty magnification (Fig. 244). Most black-and-white films can be enlarged 3–5× without any loss in resolution or objectionable increase in grain size at any viewing distance.

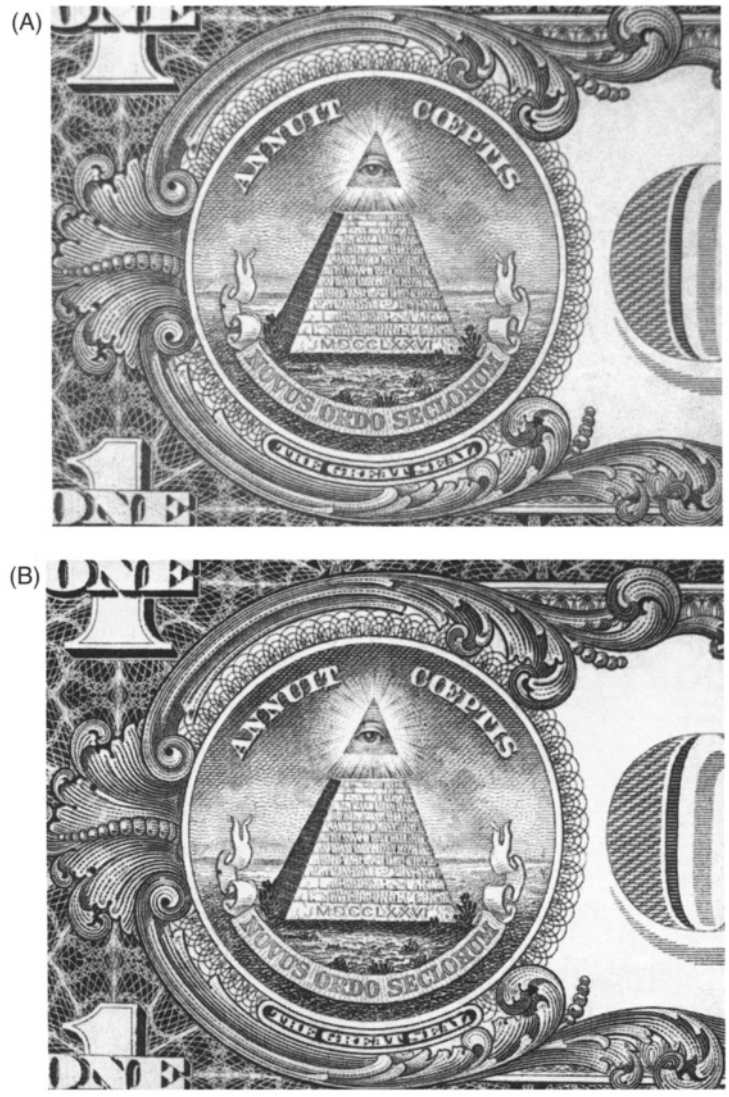

Figure 242. The effect of aperture size (f-stop) and lens type on sharpness. (A) Portion of dollar bill photographed with a 50-mm macro lens at f2.8. (B) Portion of dollar bill photographed with 50-mm macro lens at f16.

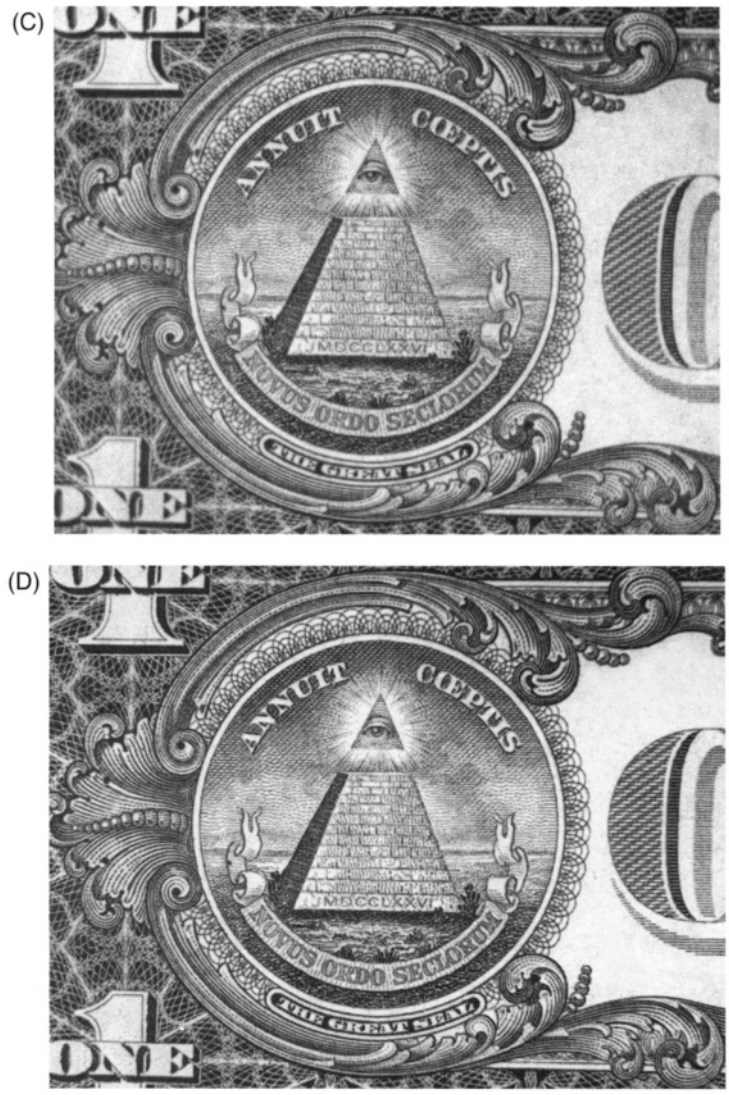

Figure 242. (C) Portion of dollar bill photographed with 50-mm standard lens with +6 diopter lenses attached, f2.8. (D) Portion of dollar bill photographed with 50-mm standard lens with +6 diopter lenses attached, f16.

XI. TYPES OF ENLARGERS

There are three types of enlargers used in photography: diffusion (cold light), condenser, and point light source. Condenser enlargers are the most commonly encountered, while diffusion enlargers are primarily used for pictorial work, particularly portraiture. Point light source enlargers are most useful in graphic arts and electron microscopy settings.

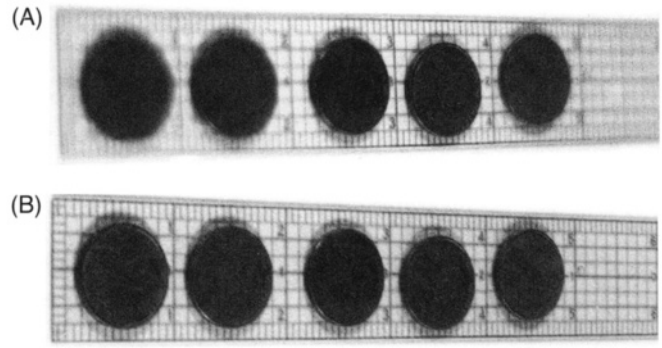

Figure 243. Depth of field as related to f-stop. (A) Pennies photographed at an angle with a 50-mm standard lens, f1.8. (B) Pennies photographed at the same angle with a 50-mm standard lens, f16.

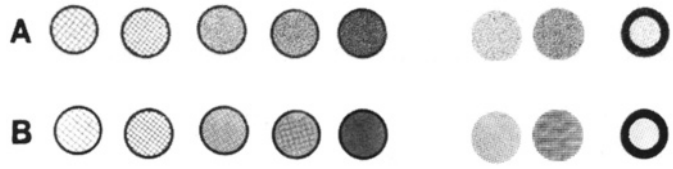

Figure 244. An illustration of empty magnification. (A) Electron microscope grids enlarged 17.5 × from size on a negative taken with a 50-mm standard lens, f16. (B) Electron microscope grids enlarged 3 × from size on a negative taken with a 50-mm macro lens, f16.

A. Diffusion Enlargers

This type of enlarger utilizes diffuse light, generally produced by a circular fluorescent tube. There is no lens before the enlarging lens, so the film is illuminated from an unfocused, scattered light characteristic of fluorescent tubes. The image produced is soft and lacks the contrast and sharpness produced by the other types of enlargers. These are obviously unsuitable for the crisp, high-resolution photographs we expect of scientific materials.

B. Condenser Enlargers

These enlargers are equipped with heavily frosted incandescent bulbs (opal bulbs) and condenser lens assemblies designed to optimally focus the beam of light on the negative being printed. Enlargers such as the Bessler 45, which can print negatives of all sizes up to and including 4 × 5 in. (10.2 × 12.7 cm), have a movable condenser lens enabling the illumination to be properly focused for negatives of various sizes. More condenser enlargers are manufactured and used than any other kind because they offer good illumination (in other words, reasonable exposure times), good contrast (compared with a diffusion enlarger), and moderate expense, since most of them have one condenser lens that is moved around to accommodate various negative formats. Furthermore, relatively inexpensive enlarging lenses may be used with them by stopping them down considerably to avoid the spherical aberration characteristic of cheap lenses.

C. Point Light Source Enlargers

Of the three enlargers, this type is capable of producing prints with the most contrast and the most apparent sharpness. These enlargers are found almost exclusively in settings where these characteristics are required, so they are rarely found outside of scientific and, more specifically, electron microscopy darkrooms. They are typically more expensive than their condenser enlarger counterparts, probably because fewer are produced. They consist of a small, unfrosted incandescent bulb (usually 12 V) whose filament (the "point") is focused by a condenser lens assembly onto the film plane. Because stopping the lens down produces an image of the light source, the lenses must be used at their largest opening. Thus, very expensive enlarging lenses are necessary so that they are optically excellent, even at their largest aperture.

Point light source heads may be purchased for a Bessler 45, allowing easy conversion from a straight condenser enlarger to a point light source enlarger. Many electron microscopy laboratories still have enormous Durst Laborator enlargers equipped for point light source work, even though the enlarger has been out of production since about 1986. The last one purchased by our laboratory in 1983 cost more than $10,000 when equipped for all possible formats up to 4 × 5 in. (10.2 × 12.7 cm) negatives. The chassis is massively built, and the head contains a front-surface mirror from which the filament image is projected down through the condenser lens assembly. It is critical that the light source be centered, or uneven illumination will be a problem. Unlike the case for most other condenser enlargers, the Durst has individual upper and lower condenser lenses that are paired, depending on negative format being used, the enlarging lens being used, and the level of magnification desired for the negative. At the time this enlarger was last produced, the condenser lenses used with 4 × 5 in. (10.2 × 12.7 cm) negatives cost over $500 each, but the Durst enlarger is probably the most flexible and precise manual enlarger ever produced. The Durst can also be set up for 110 V operation with an opal bulb as a straight condenser enlarger, which is useful for printing 35-mm negatives because a point light source enlarger will reveal every speck of dirt, every piece of lint, every scratch and every grain in the emulsion with sufficient enlargement. Used as a straight condenser enlarger, prints show fewer of these common defects. With large-format negatives that typically are not enlarged as much as 35-mm negatives, these defects are generally not noticed.

XII. VIEWING A PRINT IN PERSPECTIVE

Kodak's pamphlet #M-15 explains the concept of viewing a print in perspective. What this means is that the use for a photograph should be determined before the print is prepared. A print to be published, meant to be viewed from 12–18 in. (30.5–45.7 cm), demands a degree of resolution and clarity that is considerably different from one made for a billboard intended to be viewed at 60 miles (97 km) an hour from 100 ft (30 m) away.

The proper viewing distance is determined by the formula:

$$D = F \times N$$

where D = viewing distance, F = focal length, and N = enlargement. Since normal reading distance is about 15 in. (400 mm), a rearrangement of the formula can determine the optimal enlargement of a photograph taken with a standard lens on a 35-mm camera (50-mm focal length) to be viewed in, say, a journal:

$$N = \frac{D}{F}; N = \frac{400}{50}; N = 8\times$$

Thus, a 35-mm negative should not be enlarged more than 8× for normal reading-distance viewing. In normal practice, as previously mentioned, negatives for publication are rarely enlarged more than 3–5× to prevent overemphasis of grain structure and to avoid any decrease in sharpness.

In the case of posters, it should be considered that prints will not be viewed from much closer than 72 in. (182.9 cm), so a photograph taken with a 50-mm lens could be enlarged 36× for use in a poster:

$$N = \frac{72}{4};\ N = 36\times$$

However, if the photograph were taken with a 100-mm lens, it could be enlarged only 18× for viewing at that distance:

$$N = \frac{72}{4};\ N = 18\times$$

Table 23 shows some of the relationships between the focal length of lenses using 35-mm and 4 × 5 in. (10.2 × 12.7 cm) film and the maximum advisable enlargements along with print sizes possible.

Table 23. Relationship Between Film Size, Lens Focal Length, and the Maximum Suggested Print Size

Film	Focal Length of Lens (mm)	Enlargement	Print Size
35 mm	35	11×	11 × 15 in. (27.9 × 38.1 cm)
	50	8×	8 × 10 in. (20.3 × 25.4 cm)
	100	4×	4 × 5.5 in. (10.2 × 14.0 cm)
4 × 5 in. (10.2 × 12.7 cm)	100	4×	16 × 20 in. (40.6 × 50.8 cm)
	180	2.2×	9 × 11 in. (22.9 × 27.9 cm)
	270	1.5×	6 × 8 in. (15.2 × 20.3 cm)

Adapted from Kodak Publication #M-15, with permission.

REFERENCES

Adams, A. 1980. *The camera.* Little, Brown and Company, Boston.

Adams, A. 1981. *The negative.* Little, Brown and Company, Boston.

Adams, A. 1983. *The print.* Little, Brown and Company, Boston.

Buonaquisti, A.D. 1994. Digital imaging for TEM Part 2-Pros and Cons. *Microsc. Today* 94–9: 10.

Collins, D. 1990. *The story of Kodak.* Harry N. Abrams, New York.

Crawford, W. 1979. *The keepers of light: A history and working guide to early photographic processes.* Morgan & Morgan, Dobbs Ferry, NY.

DeCock, L. (ed.). 1985. *PhotoLab index. Lifetime edition.* Morgan & Morgan, Dobbs Ferry, NY.

Engel, E.E. (ed.). 1968. *Photography for the scientist.* Academic Press, New York.

Lefkowitz, L. 1979. *The manual of close-up photography.* American Photographic Book Publishing Co., Garden City, NY.

Stroebel, L., Compton, J., Current, I., and Zakia, R. 1986. *Photographic materials and processes.* Focal Press, Boston.

CHAPTER 15 TECHNIQUES

As previously mentioned, most of the latest photographic product sheets with descriptions of applications and information concerning different exposure and processing regimens are most easily found on the websites for Kodak (www.kodak.com) and Ilford (www.ilford.com).

Kodak Electron Microscope (TEM) Film 4489

1. Description

The most widely used TEM films are Kodak 4489 and Kodak SO-163. Kodak 4489 film delivers a relatively high-contrast image with sufficient speed for reasonable exposure times in contemporary electron microscopes. Kodak SO-163 film has greater contrast and is twice as fast as 4489 film. We have tested both products and found that we could produce negatives with adequate contrast using Kodak 4489 film, judged by our ability to produce prints with good contrast on a medium contrast-grade paper, and chose not to use SO-163 because it is more expensive than 4489 film.

Electron microscope films have characteristics of both panchromatic films and graphic arts (orthochromatic) films. They produce good gray scales similar to typical panchromatic films while maintaining a high contrast similar to graphics arts films under recommended developing conditions. In addition, they exhibit relative insensitivity to red or orange–red safelights (Kodak 1A, OA or OC, respectively), which is normally a characteristic of graphic art high-contrast emulsions.

The Kodak films are available in several sizes, although the most common size purchased in the United States is $3\frac{1}{4} \times 4$ in. (8.3×10.1 cm) sheets. This film provides relatively high-contrast images from typical exposures with a TEM operated at an accelerating voltage of 80–100 kV.

2. Processing

- Developer: Kodak D-19, diluted 1:2 with tap water
- Temperature: 68°F (20°C)
- Time: 4 min; every 30 sec, remove rack from the developer tank and tip it at a 45° angle, alternating sides every other time (i.e., tip it toward yourself first, then away from yourself the next time)
- Rinse: 1 min in running tap water
- Fix: Kodak fixer for 4 min; no agitation is necessary
- Wash: 5 min in running tap water
- Photo-Flo: dip in Kodak Photo-Flo (6.5 ml/4 l water) for 30 s and dry

3. Notes

After the darkroom for negative processing is set up, it is advisable to leave a sheet of the film out on the processing counter for 15–30 min to produce a test strip. Put something opaque over the sheet of film and expose a small strip of the film to the safelights for 5 min. Move the opaque material and expose another strip of the film for 5 min. Continue exposing more strips of the film for 5 min until the 30 min exposure period is completed. Develop the film under standard conditions to determine how many minutes of exposure produce objectionable fog, which is the noninformational background of exposed silver grains, seen as a gray haze.

Developed negatives should have no discernible dust, and edges with no observable fog. The edges covered by the TEM negative holders should be completely clear. You should be able to just barely read a page of type through a negative resting on the page. Adjust negative density by changing the exposure conditions in the TEM, not by altering developer strength, development time, or development temperature. Electron microscope film does not produce adequate images unless developed at the temperature and for the time specified. The development process is not as linear as it is for typical pictorial films because this type of film has the long inertial time, followed by rapid development, characteristics of orthochromatic, or graphic arts films.

Change the photographic chemicals every 150 negatives ($3^1/_4 \times 4$ in., 8.3×10.1 cm) or 30 days. Always keep a floating lid on the developer tank when not developing film to prevent excess oxidation of the developer.

Reference

Anon. 1973. *Electron microscopy and photography. Kodak data book P-236.* Eastman Kodak, Rochester, NY.

Films in 35-mm Format

A broad range of 35-mm-format films are available from various manufacturers for pictorial or graphics applications. As discussed earlier, the black-and-white films that we commonly use in the electron microscopy laboratory are either positive release, providing a projectable positive image (transparencies), or negative release, which are printed onto paper to give a positive image.

As previously mentioned, a second way of categorizing these emulsions is based on their sensitometric curves. High-contrast products generally have steep sensitometric curves (Fig. 239), with a consequent narrow exposure and development latitude for error. Products with broader gray scales capable of recording more tonal gradations between black and white have flatter sensitometric curves (Fig. 238) and are less sensitive to lighting unevenness, slight under- or overexposure, and developing errors.

With any of the negative-release products, including the electron microscope film previously described, enlarger magnifications up to 5× will show no obvious degradation of image sharpness. Most prints with a greater magnification show both excessive grain and loss of resolution. Kodak Technical Pan 2415 film can be enlarged over 20× without evident grain, but resolution still suffers.

Very few color films are used in our laboratory, but Kodak Ektachrome balanced for use with tungsten lights (Ektachrome T-64 or T-160) is used for copying color illustrations and gross specimens as well as photomicrography of histological specimens. This film is generally sent out for E-6 processing. If the light microscope you are using has proper filtration, Fujichrome daylight films (100 ISO) are recommended over the Ektachrome products because reds and greens as well as contrast appear to be improved over the Ektachrome emulsions. If the lighting source is an unfiltered tungsten bulb, Ektachrome T-64 or T-160 remains the best choice for color slides.

The various emulsions that we commonly use are listed below with comments on their specific applications and handling precautions. Most films have a single set of instructions, but the first film, Kodak Technical Pan 2415, has two applications listed, with different exposure and development instructions. There are even more applications for this film in pictorial photography involving still other processing methods described in the instructions provided by Kodak for the product.

Kodak Technical Pan 2415 Film for Photomicrography

1. Description

This film is a high-resolution (250–400 lines/mm), high-contrast product yielding a negative image that can be developed for moderate contrast if processed as described below. Processing must be in total darkness.

2. Uses

This film is excellent for photomicrography where contrast-building is needed. Prints produced from the negatives will have no noticeable grain with enlarger magnifications below 20×.

3. Exposure

Set the photomicroscope metering system for ISO 50 for materials with a good inherent contrast such as hematoxylin/eosin-stained histological preparations, or to ISO 100 for low-contrast materials such as immuno-stained or phase-contrast images.

Table 24. Chart For Mixing Working Developer Solutions of HC-110

	Stock (ml)	Concentrate (ml)	Water (ml)
Dilution F	12.5	0 or 3	237.5
	0		247
Dilution D	25	0 or 6	225
	0		244

4. Processing

- Developer: Prepare Kodak HC-110 stock (see Table 24) by combining 473 ml of concentrate with 1,427 ml of water to make a total volume of 1,900 ml; to make working dilution F, used for film exposed at EI 50, mix one part HC-110 stock with 19 parts water; alternatively, add 3 ml of HC-110 concentrate to 247 ml of water; to develop film exposed at EI 100, develop film with working dilution D made by mixing one part HC-110 stock with 9 parts of water; to prepare dilution D directly from HC-110 concentrate, add 6 ml of concentrate to 244 ml of water; one 36-exposure roll of 35-mm film in a stainless steel developing tank can be processed with 250 ml of developer solution
- Temperature: 68°F (20°C)
- Time: 8 min for dilution F, 7 min for dilution D[1]
- Rinse: 1 min in running water
- Fix: 4 min in Kodak Fixer with frequent agitation
- Wash: 10 min in running water
- Photo-Flo: Dip in Kodak Photo-Flo (6.5 ml/4l water) for 30 sec and hang to dry

5. Notes

This film helps to build contrast in naturally low-contrast images encountered in photomicrography. Unfortunately, because of its steep sensitometric curve, it has a very narrow exposure latitude. Development is also extremely unforgiving because of this film's sensitometric curve. If exposures are even one f-stop off, the negative may be unacceptable. Concomitantly, uneven field illumination will be dramatically accentuated. Recording phase-contrast materials with the camera meter set at EI 50 will produce a better contrast than at EI 100. The HC-110 stock will last for one month in a tightly stoppered bottle, while the concentrate will last indefinitely.

Reference

Anon. 1985. *Kodak Technical Pan 2415/6415. Kodak Publication #P-255.* Eastman Kodak, Rochester, NY.

Ilford Pan-F and FP-4

1. Description

Both of these panchromatic films must be developed in total darkness. They yield excellent continuous-tone negatives. These films have a broad latitude of exposure and development and are thus forgiving of errors and will still yield usable negatives when 1–2 stops off proper exposure. This characteristic also tends to forgive uneven illumination.

[1] Agitation is extremely critical with this film because of its steep sensitometric curve. After loading the tank with film, quickly add the developer. Agitate for 15–20 sec, rap the tank on the counter a couple of times to dislodge air bubbles. Thereafter, agitate 5 sec every minute. More frequent agitation will cause overdevelopment along the edges of the reel and consequent light edges on prints.

2. Uses

These are both excellent films for photomicrography, copy work, and general pictorial work.

3. Exposure

The ISO rating of Pan-F is 50, and that of FP-4 is 125. If doing copy work, use an 18% gray card for metering.

4. Processing

- Developer: Kodak D-76, full strength
- Temperature: 68°F (20°C)
- Time: Pan-F, 6 min; FP-4, 6.5 min, with agitation every 30 sec
- Rinse: 1 min in running tap water
- Fix: 4 min in Kodak fixer with periodic agitation
- Wash: 30 min in running tap water
- Photo-Flo: Dip in Kodak Photo-Flo (6.5 ml/4 l of water) for 30 sec and hang to dry

5. Notes

Longer exposures give darker negatives. If used for photomicrography, develop the film for 150% of the recommended times above to help build contrast in the negatives. Do not dilute the developer, because these films react differently to diluted D-76 than do Kodak products.

Kodak T-Max 100 Film

1. Description

This is a general-purpose pictorial film producing negative images exhibiting fine grain and high resolution. Its panchromatic nature and relatively gradual sensitometric curve accommodate minor lighting unevenness and exposure errors. This film must be processed in total darkness.

2. Uses

This product is recommended for indoor and outdoor pictorial work as well as photomicroscopy of materials with adequate inherent contrast.

3. Exposure

Light meters should be set for the rated ISO of 100. If the film is being used for copying a series of line drawing materials and continuous-tone materials, the f-stop and shutter speed should be set by using the meter to read an 18% gray card. Develop photomicrographs for 150% of the recommended time to build contrast in the resulting negatives.

4. Processing

- Developer: Kodak D-76 developer
- Temperature: 68°F (20°C)

- Time: For pictorial work, 9 min in full-strength D-76 , or 12 min 1:1 D-76 for finer grain; for photomicroscopy, 13 min in full-strength D-76, or 18 min 1:1 D-76 for finer grain; the film tank should be agitated every 30 sec during development for 5 sec
- Rinse: 1 min in running tap water
- Fix: 8 min in Kodak fixer; agitate periodically
- Wash: 15 min in running tap water
- Photo-Flo: 30 sec in Kodak Photo-Flo (6.5 ml/4 l of water); hang to dry

5. Notes

If the processed film has a faint magenta cast to it, the film can be returned to the fixer for a few more minutes. Overagitation will cause uneven development, with the edges of the negatives becoming denser (more developed) than the center. The use of diluted developer and longer exposure times will reduce the size of developed silver grains, resulting in less grainy prints.

Reference

Anon. 1991. *Kodak T-Max professional films. Kodak Publication #F-32*. Eastman Kodak, Rochester, NY.

Kodak Kodalith Film

1. Description

Kodak Kodalith films are high-contrast graphic arts negative-release films that yield an image with no midgray tones and an extremely fine grain. This film is relatively insensitive to Kodak 1A, OA, and OC safelights.

2. Uses

This film can be used to make negative title slides with white letters on a black background or copies of line drawings and graphs for projection. The film may also be used to produce high-contrast negatives of graphs and charts from which to make prints.

3. Exposure

Set the exposure meter to ISO 8 when using Kodalith developer and 25 when using Kodak D-11 developer.

4. Processing

- Developer: Kodak D-11 or Kodalith developer
- Temperature: 68–70°F (20–21°C)
- Time: Develop for 2–3 min with continuous agitation; the film should be developed to the maximum density possible without filling in the lines of the type or graphs
- Rinse: 1 min in running tap water
- Fix: 5 min in Kodak fixer
- Wash: 15 min in running tap water
- Photo-Flo: Dip in Kodak Photo-Flo (6.5 ml/4 l of water) for 30 sec and hang to dry

5. Notes

This film is available only in 100 ft (30-m) rolls in the 35-mm format and as sheet film. A test strip of film should be exposed to determine proper exposure times with individual copy-stand lighting systems so that maximum line sharpness is obtained.

Kodak LPD4/Precision Line Film

1. Description

This product is a positive-release, high-contrast graphic arts film that is relatively insensitive to Kodak 1A, OA, or OC safelights.

2. Uses

This film is used for making positive black-and-white projection slides of line work such as graphs, charts, and line drawings.

3. Exposure

Set the light meter ISO to 3.2, when developing with Kodak D-11, and to 5 for Kodalith developer. Copy stands with four 250 W photoflood bulbs require about 4 sec of exposure at f 4.

4. Processing

- Developer: Kodak D-11 or Kodalith
- Temperature: 68–70°F (20–21°C)
- Time: Develop in Kodak D-11 diluted 1:1 with water for 3 min; developing in Kodalith developer requires visual inspection under safelights during development to determine proper development time, which is typically 2–3 min
- Rinse: 1 min in running tap water
- Fix: Kodak fixer for 5 min
- Wash: 15 min in running tap water
- Photo-Flo: Dip in Kodak Photo-Flo (6.5 ml/4 l of water) for 30 sec and hang to dry

5. Notes

LPD4 is available only in 150-ft (46-m) rolls in 35-mm format.

Kodak Rapid Process Copy 2064 Film

1. Description

Rapid process copy film is a positive-release film that is relatively insensitive to red or yellow (1A, OA, or OC) safelights. The film was designed to copy radiographs and has a relatively low resolution and a bluish cast. When used for copying, contrast in the copy is lower than in the original.

2. Uses

This film is best for copying radiographs but can be used for copying continuous-tone materials. It is contraindicated for line drawings due to its lack of resolution and sharpness.

3. Exposure

The EI of this film is less than 0.1 and thus cannot be metered by most users. An alternative way to obtain a starting point for exposures is to set a meter for ISO 100 and to adjust the copy-stand lights to obtain a gray card reading that indicates an exposure of 1 sec at f1.4. Once this light level is achieved, set the lens at f3.5 and expose the film for 3 sec. For copying radiographs, meter the light transmitted through the radiograph, and set the camera for an exposure equivalent to that calculated for light reflected from the gray card above.

4. Processing

- Developer: Kodak Dektol diluted 1:2
- Temperature: 68°F (20°C)
- Time: 4 min with slight agitation *only* at the beginning of development
- Rinse: 1 min in running tap water
- Fix: 4 min in Kodak fixer with agitation
- Wash: 10 min in running tap water
- Photo-Flo: Dip in Kodak Photo-Flo (6.5 ml/4 l of water) for 30 sec and hang to dry

5. Notes

To make the resulting slides lighter, increase the exposure time.

Tungsten-Balanced Kodak Ektachrome

1. Description

The tungsten-balanced Ektachrome films are color reversal films yielding positive transparencies. They are only available as professional films, which are meant to be refrigerated until used and processed immediately to maintain the best color rendition. They are designed to be used with tungsten illumination (3,200° K), unlike daylight-balanced films, which require about 5,500° K for proper color balance.

2. Uses

These films are used when a positive color transparency is needed for projection. They can be used for copy work with tungsten lights (3,000–3,200° K photofloods) or for photomicroscopy with tungsten light sources adjusted to 3,200° K.

3. Exposure

After adjusting the lighting temperature, set the exposure meter. Trial exposures may be necessary. Start with the ISO setting recommended by Kodak. Two tungsten Ektachrome films are available, ISO 64 and 160. The former is preferred for best color rendition and finest grain. Underexposure of $\frac{1}{4}$ to $\frac{1}{2}$ stops yields slides with a better color saturation in some cases.

4. Processing

Processing chemicals (E-6 kits) are available from Kodak, but it is usually most cost-effective for local film processing labs to do the work.

5. Notes

As with all color films, the temperature of the lighting source is critical to proper color rendition. If a color–temperature meter is available, it is best to check all potential light sources and to determine what,

if any, supplementary filtration is needed to achieve the optimum 3,200° K color temperature. Copy-stand lights and nonhalogen tungsten light bulbs slowly yellow with age as the inside of the glass bulb becomes coated with vaporized tungsten, lowering the color temperature of the lights. If it is not possible to measure the light-source color temperature, adjust the voltage of the light source to that specified by the manufacturer to produce 3,200° K, and change bulbs before they begin yellowing, if halogen sources are not used. With light microscopes, monitor the light-source transformer during use, because some transformers will slowly decrease the bulb voltage during a microscopy session, producing color shifts toward yellow–red in the resulting slides. As mentioned above, slight underexposure of color slide films produces more saturated, richer-looking colors, which is usually recommended. As with all positive-release materials, a longer exposure time yields lighter slides.

Polaroid Copy Negatives Using Type 55 P/N Film

1. Description

This film yields continuous-tone 4 × 5 in. (10.2 × 12.7 cm) negatives as well as positives, and exhibits high resolution (150–160 line pairs/mm).

2. Uses

This film is recommended for copying either line drawings or continuous-tone materials. Contrast usually increases slightly over the originals. The resulting large-format negative can be enlarged easily to produce prints as large as usually necessary without any loss in resolution or detail.

3. Exposure

This film has an ISO rating of 50. For copy-stand work, use an exposure meter to read an 18% gray card after the meter has been set to ISO 50. Set the camera f-stop and shutter speed to the settings indicated on the meter. If the original line drawings and continuous-tone materials are properly printed, a whole series of images may then be photographed without resetting the camera.

4. Processing

- Developer: Follow the instructions on the Polaroid camera back to crush and spread the developer pod
- Temperature: 70°F (21°C)
- Time: 20 sec to 2 min
- Clear: Strip the positive image from the negative, and detach the negative from the film sleeve; attach to clips or place in a sheet film holder, and immerse in 18% aqueous sodium sulfite for 2–5 min, preferably with a vigorous up-and-down agitation to dislodge the developer gel
- Wash: 5 min in running tap water
- Photo-Flo: Dip in Kodak Photo-Flo (6.5 ml/4 l of water) for 30 sec and hang to dry

5. Notes

This film has a very delicate emulsion, particularly before it is dried. Be extremely careful not to touch it while processing. If copying a line drawing, a slightly thinner negative (darker positive) will yield crisper line edges. When copying continuous-tone materials, the positive Polaroid image should be slightly lighter than looks good to produce a negative with good contrast. If the film is not processed promptly after

the chemical pod has been spread over the emulsion, the chemicals dry out somewhat and become very difficult to clear in the sodium sulfite solution. If processing is delayed, presoak the film for 15 or 20 min before putting it into sodium sulfite to help the clearing process. When making up the sodium sulfite, be sure to stir it continuously until it goes into solution. If any of the powder settles to the bottom of the processing tank, it will become rock hard and will not go into solution.

Film packs that have been sitting at room temperature for weeks or months tend to be reluctant to release the developer gel. If, after sodium sulfite treatment and washing for 5–10 min, the gel is still attached to the film, dip them in Photo-Flo and hang them to dry. The remaining developer gel, when dried, rarely causes printing problems.

This same emulsion is available in eight-sheet packs as Type 665. The film size in the packs is reduced to $3\frac{1}{4} \times 4$ in. (8.3 × 10.2 cm) The pack film is less expensive, and the slight reduction in image size is insignificant for copying purposes.

Making Photographic Prints

1. Description and Uses

Black-and-white photographic papers with various surface, tone, and contrast characteristics are available. Fiber-based photographic paper is not used as much as in the past but still offers the greatest archival potential and is most appropriate for photographs that will be exposed to light for a long period of time. Resin-coated paper has the advantage of rapid processing times compared with fiber-based stock, particularly if a processing machine is available.

Different paper surfaces (textures) are available. Electron microscopists usually desire the sharpness provided by a glossy surface such as Kodak F-surface papers, but photographs to be viewed under strong overhead lighting, as for posters displayed at large meetings, are easier to see if printed on a nonglossy surface such as Kodak N-surface paper.

As mentioned, many modern electron microscopy darkrooms have automatic processors into which a piece of exposed photographic paper is inserted and from which, about 90 sec later, a dried print emerges that can be expected to last for many years. These processors require resin-coated paper stocks.

Other laboratories choose to tray-process prints made on either fiber-based or resin-coated stocks. The former materials have the greatest archival capability, while the latter can be processed more quickly through the trays of chemicals and can be hung to drip-dry or put through a resin-coated paper dryer to allow relatively short times to elapse before the print can be filed. Never put a piece of resin-coated stock through a print dryer designed for fiber-based stock, because the high temperature of a fiber-based stock dryer drum will melt the resin-coated stock surface, transferring resin to the dryer drum and also ruining the print.

Kodabromide paper is the hardest (most blue–black) paper produced by Kodak. When purchased with an F-surface, it produces a high-gloss image with excellent contrast and sharpness. Five different contrast grades are available, from low contrast ("1") to high contrast ("5"). Higher-contrast papers have more grain and have a long latency period during development. In other words, it takes longer for the image to become visible in the developer tray than with lower contrast papers, but once the image begins to appear, it reaches the end of development very quickly compared with low-contrast papers. Polyfiber paper available from Kodak is slightly warmer (browner) than Kodabromide but can be used with a series of colored filters to produce different grades of contrast from a single negative. The colored filters allow one sheet of paper to be exposed for a range of contrast from 0 to 5, with $\frac{1}{2}$ grade increments.

Resin-coated stocks, such as Kodak Polycontrast and Ilford Multigrade papers, are designed for quick processing in automated equipment and use filters to vary contrast as was discussed for Polyfiber paper. As previously mentioned, they can also be tray-processed with reduced times in each tray of chemicals compared with fiber-based products.

2. Exposure

Exposure times from 5 sec to several minutes will work adequately. Shorter exposure times are most convenient and lessen the possibility of fogging the photographic paper with the darkroom safelights or developing darker print borders because of the enlarger light reflecting off the easel edges. However, exposures of less than 5 sec are not always consistent because the warm-up time for an enlarger bulb changes slightly, dependent on how long it was off between exposures. A cold tungsten filament warms up slightly more slowly than one that has recently been used because the recently used filament is still warm, causing slightly more resistance to current flow in the wire filament, resulting in a quicker heating time than is characteristic of a cold filament.

If a condenser enlarger is used, install the appropriate lens for the negative size and adjust the condenser lenses for the negative size and degree of magnification according to the manufacturer's instructions. Stop the lens down to a middle f-stop (about f8 or f11) for maximum sharpness.

If a point-light-source enlarger is used, install the appropriate enlarging lens and condenser lenses, or set the condenser lens height at the appropriate level for the negative format and enlargement desired. Focus the image. Remove the negative and stop the lens down (reduce the aperture size) to reveal a bluish halo. Center this halo and then open the lens to its largest aperture. No dark frame corners or blue halo should be visible and the illumination should be even across the printing frame. Reinstall the negative and expose the photographic paper.

As mentioned above, the higher the number of the paper/filter, the higher the contrast of the print. Exposure times also have to be increased with a higher filter number using the same negative. If no filter is in the enlarger, it is the equivalent of a 2 or 2.5 filter. The high-contrast portion of the emulsion in Polyfiber, Polycontrast, and Multigrade papers is red-sensitive, while the low-contrast portion is yellow-sensitive. Thus, an unfiltered light source possessing the yellow–red color of a tungsten bulb produces a medium contrast ($2–2\frac{1}{2}$ filter equivalent) with multi-grade printing papers.

When determining which paper/filter contrast grade to employ, it is important to realize that increased print density (increased exposure/print darkness) is perceived as increased contrast. Thus, altering the amount of exposure, which changes print density, should not be confused with changes in paper grades/filters to achieve a different contrast. A TEM negative should be printed so that there is a barely perceptible gray background anywhere there is the plastic resin of the section. In other words, plastic section areas containing plastic devoid of biological material such as the luminal space of an empty kidney tubule should be slightly gray, while a hole through the section should be as white as the unexposed print border.

With Ilford Multigrade resin-coated paper, if there is sufficient illumination to produce a proper print density with no filter after a 5 sec exposure, adding a filter in the range of 0, 1, 2, 3, or 4 will require about a 1.5–2 × increase in time of illumination. The number 5 filter will require a little more than a 3 × increase in illumination or time over the no filter situation. In other words, if a 5-sec exposure works for no filter in place, an exposure of 7.5–8 sec will work with all the other filters except number 5, which will require about 18 sec for an equivalent print density. Kodak Polycontrast papers and filters behave in a similar fashion, though the times for equivalent density from different filters should be determined empirically.

3. Tray Processing

Fiber-Based Papers

- Expose the photographic paper: Try to keep the exposure time between 5 and 15 sec
- Develop the print: Use Dektol developer diluted 1:2 with water; develop with constant agitation for 1.5–2 min; do not control the final density (darkness) of a print by altering the developing time because it can cause uneven development; control the final print density by varying the exposure time with the enlarger
- Stop Bath: Leave the print for 10–30 sec in Kodak Stop Bath (16 ml of indicator stop bath in 1 l of water); the stop bath turns purple when it is no longer functional; if stopped for over 5 min, the print will become permanently acidic

- Fix: Leave the print for 5–7 min in Kodak fixer, with intermittent agitation; if prints are left in fixer for hours, the emulsion will eventually separate from the stock; divide the time between used fixer saved from a previous processing run (but still usable based on checking it with Edwal Hypo-Chek™) and a final bath of fresh fixer; Edwal Hypo-Chek™ will form a cloudy white precipitate when a drop is put into spent fixer because excess silver in the fixer causes the formation of a cloudy silver chloride precipitate; do not dilute the fixer.
- Wash: Tumble the print in the print washer with running water for a minimum of 1 hr. If Perma-Wash™ is available, make it up according to the instructions on the bottle of concentrate; after prints have had an initial 5 min wash in tumbling in running water, put them into Perma-Wash™ diluted from concentrate for 5 min with constant agitation, and then wash them again for 5 min in tumbling running water; use 1 liter of Perma-Wash™ for up to 35 prints (8 × 10 in., 20.3 × 25.4 cm) and always discard after use.
- Soak prints in dilute PakosolL™: See the bottle of concentrate for instructions for mixing up solution; soak for 5 min with constant agitation.
- Dry: Follow the instructions on using the print dryer you have; it takes about 30 min for most dryers to reach operating temperature before use; again, never run resin-coated stock through a dryer designed for fiber-based prints; doing so will melt the resin onto the polished-metal of the platen, which will be extremely difficult to clean up

Resin-Coated Papers. Tray-processing resin-coated papers is similar to working with fiber-based papers, except that the processing times are shorter.

- Develop the print: 15–20 sec in dilute Dektol (1:2)
- Stop bath: Kodak indicator stop bath for 10–20 sec
- Fix: Kodak fixer for a total of 2.5–4 min in two baths.
- Wash: 4 min in running tap water; drain and hang with wooden or plastic clothespins on a line until dry or stand on end in the darkroom sink until dry; print dryers designed for resin-coated papers are also commercially available.

4. Chemical Disposition

- Dektol: Always make up diluted Dektol stocks right before use; when finished, pour the contents of the developing tray down the sink with a copious water flush, if permitted by your local waste management advisor; dilute Dektol does not keep; use the diluted Dektol in the tray until it no longer develops prints
- Stop bath: Make fresh stop bath for each processing run; it does not keep, so pour it down the sink with a water flush when finished or if the stop bath turns purple.
- Fixer: When finished processing, check both fixer baths with Edwal Hypo-Chek™. If either bath is still usable, pour the fixer into a bottle labeled "used fixer" using a funnel. This used fixer can be used as the first fixer bath during the next darkroom session. If the fixer is spent, save it for collection by institutional waste management personnel.

5. Useful Quantities of Chemicals for 20 Prints (8 × 10 in. 20.× 25.4 cm or Equivalent)

- Kodak Dektol: 750 ml (250 ml of Dektol + 500 ml of water).
- Kodak Indicator Stop Bath: 1,000 ml (16 ml of concentrate per liter of water).
- Kodak Fixer: 1,000 ml per tray. Used fixer in the first tray, fresh in the second tray.

Poster Preparation

The ever-increasing number of participants at scientific meetings has caused many scientific societies to institute or increase the number of poster sessions. Poster prints present a few challenges that are different from preparing images for publication or utilizing 2×2 in. (5.1×5.1 cm) transparencies or computer-generated Powerpoint™ images for platform presentations.

The majority of posters prepared today are assembled in computer programs and output to a printshop to produce a single flexible print that is the poster. Nonetheless, it still can be helpful to produce posters by strictly photographic methods for certain applications, and the cost is generally considerably less than commercially generated posters if you do the photographic work yourself.

In general, images for posters are much larger than those used for publications and typically have a mixture of continuous-tone and line-drawing/typescript materials. Color prints are often added as well. Advice on making a succinct presentation of an elaborate experimental design to support a scientific hypothesis and organizing the results and discussion is beyond the scope of this manual. However, some tips about how to produce the most effective images are appropriate.

1. Image Size

The size of prints for a poster is determined to some extent by the space available for the poster being presented. A few rules of thumb should be considered, however. Prints should be easily seen and interpreted from an 8–10 ft (2.4–3.0 m) viewing distance. This may mean that enlargements exceed the $5 \times$ rule for publication prints (meant to be scrutinized from 10–18 in., 25.4–45.7 cm). To determine the level of magnification that is acceptable, refer to Table 23 about viewing a print in perspective earlier in this chapter.

2. Color Prints

As explained earlier, color prints of scientific materials photographed with color negative films can be extremely disappointing. Automatic processing facilities utilize machines to evaluate "average" color rendition for a given photograph. Most of our preparations are skewed heavily to red and blue (hematoxylin and eosin-stained tissues) or blue only (toluidine blue O-stained semithin sections). When the automatic machines are confronted with such nonaverage materials, they produce underexposed, overexposed, or strangely color-balanced prints. Even if these negatives are hand-printed by a professional laboratory, it is difficult for the technician to realize what the material should look like unless they are extremely familiar with the type of preparations with which your laboratory works.

The best solution to this problem is to import color image into a program such as Adobe Photoshop™, adjust the color rendition, brightness, and contrast to acceptable levels, and then print out the image to a decent digital color printer. This generally is cheaper and faster, and produces better images than trying to find a photo lab that can make proper high-quality color prints from film.

3. Paper Surface

Paper surfaces can be shiny, matte, pebbled, or screened in appearance. The different types of surfaces alter the appearance of continuous-tone images such as electron micrographs, high-contrast images such as graphs and line drawings, as well as color prints. For most poster presentations, high-gloss surfaces such as F-surface Kodak papers will do quite well for all of these materials. High-gloss surfaces appear to have the most contrast and sharpness of the various surfaces available. If lighting conditions are expected to produce a large amount of glare, as with bright overhead incandescent lights, it may be better to use a nonglare surface such as Kodak N-surface papers. This is particularly recommended for areas of typescript on the poster.

4. Mounting Photographs

As with publication prints, borders are normally trimmed from the prints to be mounted. Dry-mount tissues consisting of heat-activated adhesive paper are available from Kodak or Seal Products, Inc. These are more permanent than methods employing liquid or sprayed glue products to effect adhesion. There are also cold-mount tissues using laminating presses to attach photographs to surfaces.

When using dry-mount tissues, select a piece slightly larger than the print to be mounted. Make sure that dry-mount tissue designed for fiber-based prints is not used for resin-coated prints. The former requires a temperature of 220°F (104°C) to fuse it with the print and matte board, a temperature that will melt the surface of resin-coated papers.

Put the print face-down on a clean piece of paper, center the mounting tissue on the print, and attach it by quickly making an "X" in the center of the tissue over the print with a tacking iron. Test the temperature of the tacking iron on a scrap print first to make sure that the resin-coated print does not melt from the heat but that the iron is hot enough to melt the tissue to the print.

Trim the border from the print with a paper cutter. When you are finished, the dry-mount tissue should still be attached to the print and should be flush with all edges of the print.

Place the print face-up on the piece of matte board or poster board where it is to be affixed. Carefully raise a corner of the print so that the dry-mount tissue remains lying on the matte board. Tack the tissue to the matte board with the tacking iron. Repeat the process at another of the print corners.

After all the poster prints have been tacked to the matte board in their appropriate locations, place the matte board print-side up into a dry mount press heated to the appropriate temperature (about 180°F, 82°C, for any color prints or resin-coated black-and-white papers). Cover the prints with a product such as Seal Release Paper (Catalog #928, Seal Products, Inc., Naugatuck, CT), close the platten of the dry-mount press and heat for 10–12 sec. Open the press and remove the release paper and poster. The release paper is reusable.

Prints can also be attached to posters by 3M adhesive or adhesives like rubber cement as alluded to above. However, the 3M adhesive is not recommended because the spray can produces an aerosol that can be inhaled if not used in proper hoods, which are not usually available in electron microscopy laboratories. Neither of these adhesives will hold prints to the boards as well as dry-mount tissue, and changes in heat and humidity will cause the prints to curl off the boards.

16

Digital Imaging and Telemedicine

I. GENERAL CONCEPTS CONCERNING DIGITAL IMAGING

Digital imaging has become an important aspect of image acquisition, storage, and output in all arenas of cytological investigation and analysis, particularly since the late 1980s, when computer storage media and computational speed began their rapid improvement that continues through the present time. Even though photographic materials still hold more pixels, or picture elements, than digital media, the ease with which images can be captured, manipulated, and output to Microsoft Powerpoint® presentations, emails, web pages, and photographic-quality computer prints has led to the widespread acceptance of digital images for scientific presentation. Some journals currently request electronic submission of papers, including illustrations, in digital format, totally bypassing hard copy of either text or images. Finally, telemedicine (Weinstein *et al.*, 2001; Williams *et al.*, 2001) allows pathologists and other medical personnel to send images quickly to other scientists and doctors for examination to help determine the cause of pathology and the treatment that should follow for the patient. This subdiscipline of digital imaging is guiding the way for biologists to share images and the information contained within them quickly with colleagues throughout the world.

Numerous papers and books have been written about digital imaging and processing of digital images, and the books by Baldock and Graham (2000), Inoué and Spring (1997), and Russ (2002) provide in-depth discussions of the subjects treated below. The web page by Davidson *et al.* (2002) is also a useful resource.

A. Pixels, DPI, File Types, and File Size

To take full advantage of digital technology, it is useful to understand basic definitions of the terminology associated with file resolution, file size, and file types. First, a digital image is created when an analog image is converted into a format that a computer can read, display, and process. To accomplish this conversion, the analog image is divided into specific brightness values arranged as individual points, each containing specific information about brightness or contrast and each described by a specific digital brightness value. The digital image is composed of picture elements or pixels, each containing one or more bits of information forming an array with a vertical and a horizontal dimension. The pixel size of an image, not to be confused with the file size of an image, is calculated by multiplying the number of vertical pixels by the number of horizontal pixels.

Pixels define not only the dimensions of an image but also the detail. Pixel depth defines the detail in the image by adding or subtracting gray levels. The number of gray levels is determined by the binary number assigned to each pixel. The basic unit of computer information is a binary digit or a bit. Each bit has two values, either on or off (0 or 1). Therefore, there are two values associated with a bit. What this means in terms of an image is that a 1-bit image has just

two levels, black or white. Thus, a 1-bit image assigns either black or white (no grays) to each pixel (Fig. 245D). A 2-bit image contains two values for each bit (2×2), resulting in an image with four levels of gray (Fig. 245C). A 4-bit image also contains two values for each bit ($2 \times 2 \times 2 \times 2$), resulting in an image with 16 levels of gray (Fig. 245B). Finally, an 8-bit image again contains two values for each bit ($2 \times 2 \times 2 \times 2 \times 2 \times 2 \times 2 \times 2$), resulting in an image that assigns one of 256 levels of gray (0–255) to each pixel (Fig. 245A). Thus, the greater the bit depth, the greater the number of gray levels. An image with a high bit depth corresponds to increased useful information acquired when the image was digitized. Since the human eye can discern about 50 discrete levels of gray, the minimum choice for pixel depth should be about 6-bit ($2 \times 2 \times 2 \times 2 \times 2 \times 2$), or 64 levels of gray. However, since digital images are typically enhanced through image processing, they should be of at least 8-bit resolution to prevent any loss in gray levels.

In addition to resolution achieved through pixel depth, the dots (or pixels) per inch (dpi) of an image is another way to describe the resolution of a digital image. Retention of fine details present in an original analog image when it is converted to a digital image is directly associated with the number of pixels used while acquiring and rendering the digital image. That pixel number depends on how finely the image is sampled during acquisition. Increasing resolution means increasing the number of pixels per unit area. Therefore, the desired resolution should be determined by the intended use for the image. Once the image has been acquired, the dpi cannot be

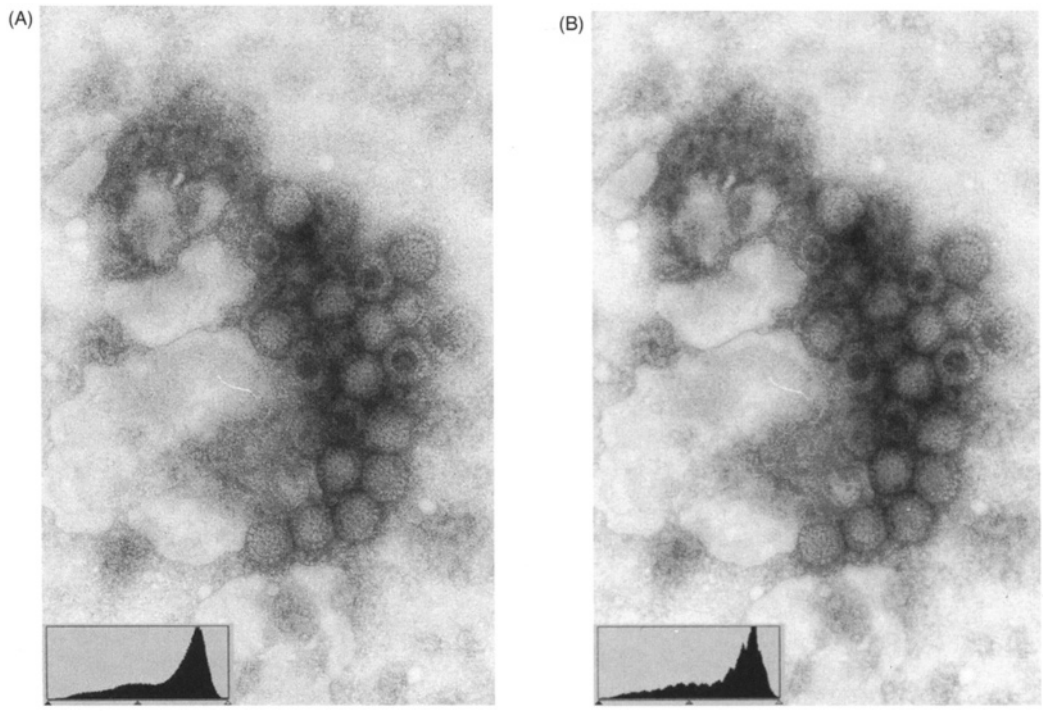

Figure 245. A comparison of grayscale images of a TEM photograph of negatively stained viral particles showing different gray levels with corresponding histograms shown as insets. (A) An 8-bit image that contains 256 gray levels (0–255) and provides a pleasing continuous tone picture. The corresponding histogram depicts a range of grays from black (0) to white (255). (B) A 4-bit image that contains 16 gray levels. The image is not significantly degraded from that shown in (A). Note that the histogram transition from black to white is not as smooth as that shown in the (A) inset due to gaps between peaks resulting from fewer available gray levels.

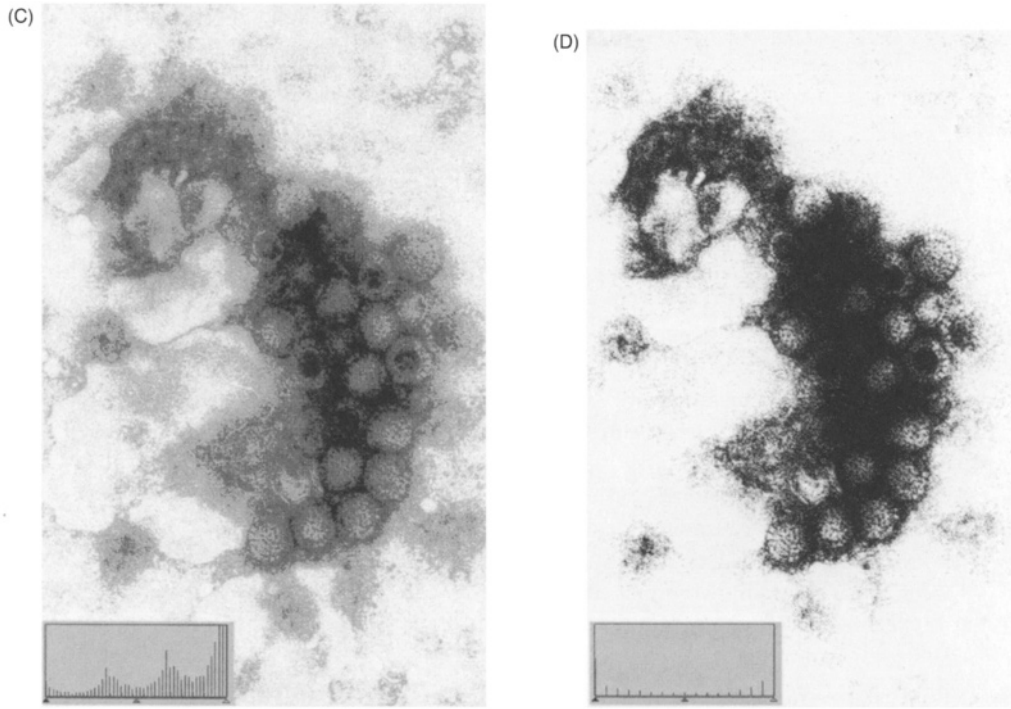

Figure 245. (C) A 2-bit image that only contains four gray levels. The image is significantly different from those shown in (A) and (B). The histogram still ranges from black to white, but at this bit depth, the gaps between peaks are more evident than those in (B). (D) A 1-bit image that contains just two gray levels. While the histogram still ranges from black to white, the gaps here are much more evident, and the major peaks correspond to black and white at either end of the histogram, with only minor spikes in between. This accounts for the extremely high contrast and loss of information in the image.

increased within a file without obvious loss of information. In general, images to be used on a web page or sent via email can be digitized at 72 dpi, characteristic of the resolution of most screens, whereas images meant for print should be acquired at a much higher resolution. Most current desktop printers print at 600dpi, while some photo-quality printers produce 1,200 dpi or higher. An image should be acquired based on the dpi of the output device. Acquiring images with an excessive dpi is not only unnecessary; it produces larger files, which can create storage problems (Table 25). As illustrated in Fig. 246, the higher the resolution, the larger the file size.

Note that Fig. 246 shows images produced from TIFF files that were saved at a size of 3.4×4.4 in. (8.6×11.1 cm) If the 600 dpi file (4.8 Mb) was a full page or an 8×10 in. (20.3×25.4 cm) image, the saved TIFF file would increase to 28.1 Mb, and if it was a full-color 8×10 in. (20.3×25.4 cm) image, the saved TIFF file would be further increased to 84.3 Mb. This concept becomes important when saving files to different media and building archives of images.

When saving image files, it is obvious that there are numerous file types available (Davidson *et al.* 2002). Some of these file type are:

- TIFF (Tagged Image File Format) files are the current industry standard, which means that it is the most widely supported file format, represents a good format for image processing, and is ideal for archiving raw data image files that may subsequently be output to a variety of devices; the downside of TIFF files is that they are quite large

Table 25. Memory Requirements for Some of the Different Digital File Formats (from Davidson *et al.*, 2002)

Pixel Dimensions	Grayscale (8-Bit)	Bitmap File (24-Bit)	JPEG File (24-Bit)	TIFF File (24-Bit)
16 × 16	2 kb	2 kb	2 kb	2 kb
256 × 256	66 kb	193 kb	22 kb	193 kb
640 × 480	302 kb	901 kb	56 kb	902 kb
1280 × 1024	1.28 Mb	3.84 Mb	147 kb	3.84 Mb
3840 × 3072	11.52 Mb	34.56 Mb	611 kb	34.56 Mb

- GIF (Graphics Interchange Format) files are used for Internet exchange and screen viewing
- PSD (PhotoShop Document) files are used only by Adobe PhotoShop™ but preserve all image layers and channels for further editing
- EPS (Encapsulated PostScript) files are read by PostScript printers
- BMP (Bitmapped file format) files are the standard bitmapped graphics format used in Microsoft Windows® environments
- JPEG (Joint Photographic Experts Group) files are a compression format for email and web pages; the compression is "lossy," which means when an already-compressed JPEG file is converted to an uncompressed format, such as a TIFF, the final image will result in less information than that contained in the original JPEG file; the advantage of a JPEG file is that the saved file is much smaller than any uncompressed file format; different programs allow different degrees of compression when creating JPEG files.

B. Digital Cameras

Digital image acquisition is primarily accomplished with either charge-coupled device (CCD) cameras or complementary metal oxide semiconductor (CMOS) cameras. The CCD camera may be operated at ambient temperature or may be cooled below ambient temperature to improve the signal-to-noise ratio (SNR) by reducing the dark current. Dark current is the noise produced in a digital camera image by thermal agitation of electrons in the chip sensors, rather than by excitation of the chip sensors by photons. Since electrons become more energized at higher temperatures, dark current increases with the operating temperature of a digital camera.

As explained by Russ (2002), the CMOS camera contains a chip manufactured by processes similar to those for computer memory chips and can be built with other circuits attached, potentially leading to single-chip cameras that would be quite inexpensive and compact. Unfortunately, the CMOS chip produces a higher dark current and thus more noise than a CCD camera chip. In addition, each pixel has its own amplifier, producing nonuniformity of signal between different pixels. This is known as fixed pattern noise, or FPN, resulting in a reduced dynamic range (Russ, 2002). Thus, at the present time, CMOS cameras tend to be limited to the lower end of the consumer market and do not find significant application to the scientific market, which is dominated by CCD cameras.

The solid-state silicon chip that is found within a CCD camera is opaque to wavelengths under 400 nm (ultraviolet light) and is transparent to wavelengths above 1,100 nm (infrared), with a maximum sensitivity of approximately 1,050 nm. This represents a spectral sensitivity quite different than that found in the human eye (approximately 400–700 nm) and engineered for most films (Fig. 247). To counteract the increased sensitivity to infrared light, a blocking filter is

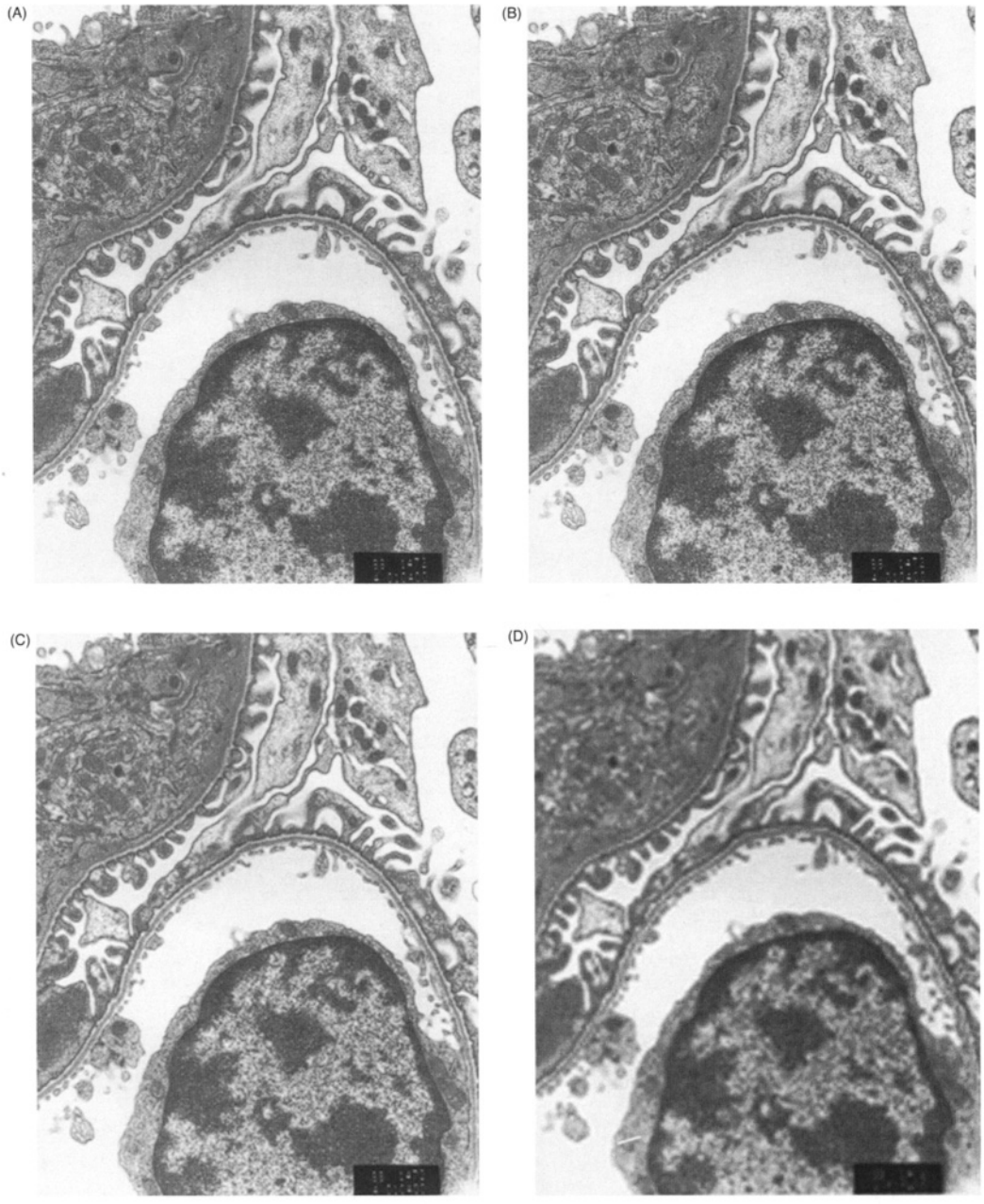

Figure 246. A comparison of grayscale images of a TEM photograph of a kidney glomerulus acquired at different file resolutions and corresponding file sizes. All images were acquired and printed as 3.4×4.4 in. (8.6×11.1 cm) images. (A) A 600-dpi file that produced a 4.8-Mb file when saved in the TIFF format. (B) A 300-dpi file that produced a 1.2-Mb file when saved in the TIFF format. This image is virtually identical to (A). (C) A 150-dpi file that produced a 311-kb file when saved in the TIFF format. The image shows an obvious decrease in resolution when compared with (A) and (B). (D) A 72-dpi file that produced a 76-kb file when saved in the TIFF format. This image is unusable due to the total loss of resolution.

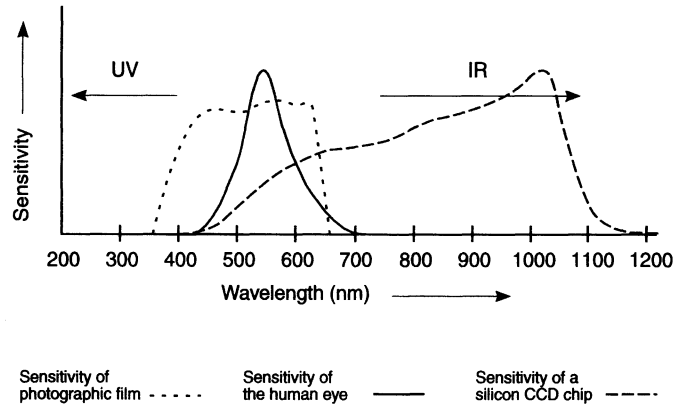

Figure 247. A comparison of the spectral sensitivities of photographic film, the human eye, and a CCD silicon chip.

usually installed to exclude infrared light. Since infrared light has a longer wavelength than visible light, the infrared parts of the image would be focused in a different plane than the parts of the image generated from visible light. If a blocking filter were not installed, blurred or fogged images would result (Russ, 2002).

A digital camera designed for scientific recording typically has smaller pixels, for greater resolution, compared to a low-end consumer market camera. A large pixel has a higher SNR but less resolution. For example, a scientific camera with pixels measuring $6.8 \times 6.8\,\mu m$ has a SNR or 45 dB, while a camera with pixels measuring $23 \times 23\,\mu m$ has a SNR of 56 dB (Baldock and Graham, 2000). As mentioned above, cooling the silicon chip of a CCD digital camera below ambient temperature increases the SNR by decreasing the dark current, allowing an acceptable SNR even with the smaller pixel dimensions needed for high-resolution work. Finally, cooling the CCD camera to decrease dark current noise makes it possible to record images from situations of very low light levels, such as those characteristic for epifluorescent microscopy. A typical noncooled CCD video camera produces a very "speckled" image, due to the recorded noise, while a cooled-CCD digital camera records very little of this noise.

There are several approaches to producing color images from the broad spectrum CCD chips found in digital cameras. In some cameras, a prism separates incoming light into red, green, and blue, each is recorded separately by a dedicated CCD chip, and the three outputs are combined to produce a video image. This type of camera is made more affordable by reducing the numbers of pixels in the CCD chips and typically has resolution levels below those needed for scientific recording (Russ, 2002).

Scientific cameras are generally of the Color Mosaic, or one-shot type, or are three-shot cameras. In the former, all of the colors are recorded at the time a single image is "grabbed" because each pixel in the CCD array has an R, G, or B filter bonded to it, allowing sampling of only one color at each location.

Some Color Mosaic cameras have a row of red receptors next to a row of green receptors, followed by a row of blue receptors. This pattern is continued across the entire face of the CCD chip and is known as the Stripe pattern. An alternate arrangement of the sensors is known as the Bayer pattern, where there are twice as many green receptors as there are blue or red, which produces a recording sensitivity similar to the human eye, which is more sensitive in the green region (Russ, 2002). In both types of Color Mosaic camera, the overall resolution of the camera is reduced, because subpopulations of pixels are restricted to recording information of only one color.

The three-shot camera utilizes the entire CCD chip to record the image. The image is recorded by placing one colored filter over the entire CCD chip and recording the image (e.g., red), followed by the recording of a second image after insertion of a blue filter, and finishing by recording an image with a green filter in place. The three separate images are then combined electronically to produce a single image. An example of this type of camera is the Spot RT Slider Camera (Diagnostic Instruments, Inc., Sterling Heights, MI). It can be purchased with a Kodak CCD chip with an imaging area of 11.8×8.9 mm, with 7.4 μm^2 square pixels providing a single-pass display of 1,920,000 pixels ($1{,}600 \times 1{,}200$ pixels). A full-color image produced from three passes is three times bigger, since the entire image has been recorded three times, each with a different color of monochromatic light. Thus, an 8-bit monochrome image producing a file size of 1.83 Mb is turned into a 24-bit RGB image by the sequential insertion of three filters and produces a file size of 5.49 Mb.

C. Image Manipulation

After acquiring an image and saving the raw data file, the next step is to enhance the image through image processing techniques using a program such as Adobe PhotoShop™ (PhotoShop). In general, most images need a few basic adjustments to contrast, brightness, and overall sharpness. To alter the contrast of the image, the best tool is the histogram utility. The histogram of an image is the graphic depiction of pixel intensity of the image (Fig. 245, insets). The gray levels (0–255) are depicted along the x-axis of the histogram. The number of pixels that represent each of the gray levels are stacked vertically (along the y-axis). Therefore, the peaks of a histogram represent gray levels that occur most frequently within the image. An image with a good dynamic range contains true black (gray level 0) and true white (gray level 255) as well as intermediate gray levels. When adjusting the histogram of an image, the goal is to extend the image histogram to include true black and true white. In PhotoShop, for example, to access the histogram of an image, click on *Image > Adjust > Levels*. The dialog box that opens contains the histogram with three arrowheads below the x-axis. To create a true black, click and drag the left arrowhead inward (right) toward the left-hand edge of the histogram. To create a true white, click and drag the right arrowhead inward (left) toward the right-hand edge of the histogram. Then click "OK" to apply the changes made.

Another useful tool for image enhancement is gamma adjustment. Gamma controls the overall brightness of an image. In color image files, varying the amount of gamma correction changes not only the brightness but also the ratios of red to green to blue. In PhotoShop, click on *Image > Adjust > Levels*, to open the dialog box that contains the gamma curve. Gamma is a logarithmic curve representing brightness. This line can be manipulated by placing the cursor over the line and clicking and dragging to the desired brightness.

Most photo manipulation programs provide a variety of filters for image enhancement. In PhotoShop, for example, clicking on *Filter > Sharpen* will locate filters such as Sharpen (which can improve the appearance of soft or blurry images) and Unsharp Mask (which can improve the appearance of the image by removing haze and enhancing contrast where fine details are lost against a diffuse background). The Sharpen filter accentuates the edges of the image by finding the edges and increasing the contrast between adjacent pixels at that location. The Unsharp Mask filter compares the contrast between neighboring pixels and then increases the contrast between those pixels according to the values provided by the user, thus enhancing details lost in shadows without sacrificing bright objects in the image. The Unsharp Mask filter provides more control

than the Sharpen filter, using three separate menus to adjust for *Amount, Radius*, and *Threshold. Amount* determines the level of sharpening. Selecting a higher percentage provides a higher degree of sharpening. *Radius* determines how much information is included during the application of the filter. Selecting a larger value for Radius produces more intense changes in contrast. *Threshold* limits the application of sharpening to certain areas. The user specifies how far apart the contrast of two pixels must be before the filter will affect them. Excessively high values for the Amount, Radius, and Threshold under the Unsharp Mask menu produce a very grainy image. It is best to start with low numbers and increase them until the desired result is achieved. The dialog box provides a preview, which is useful for observing different combinations before applying the filter to the image. It is also useful to view the image at 100% when applying filters so that changes are seen accurately.

To summarize, when using PhotoShop or other programs to manipulate digital images, determine the use for the image beforehand. Once the use is determined, select the desired resolution (dpi) in the scanner or digital image software program. After acquisition, select an appropriate pixel depth (at least 8-bit), crop the image as desired, adjust the histogram and/or gamma, and sharpen as desired.

D. Image Output

As mentioned above, saving an image as a high-resolution file in every case will create storage problems and can yield images inappropriate for some applications. Microsoft PowerPoint® presentations will often slow down as RAM is filled with large TIFF files that must be downloaded before new images may be subsequently loaded into RAM during the presentation. Sending attachments larger than JPEG files over the Internet is usually difficult, and some email programs have more problems than others transmitting images. Local area network (LAN) transmissions of large images are usually easily accomplished because the network has its own broadband sufficient to handle transmission of large files.

II. TELEMEDICINE/TELEPATHOLOGY CONSIDERATIONS

Most of the information for this section was provided by Dr. Bruce Williams, who heads the Telemedicine Department of the Armed Forces Institute of Pathology (AFIP). All three types of imaging systems described below are currently in operation at the AFIP and can be accessed by contacting Dr. Williams (williams@afip.osd.mil). Static images on the AFIP site may be viewed at www.afip.org/departments/telepathology/archive/index.html.

The Telemedicine Department of the AFIP reviews pathology cases submitted by physicians and veterinarians from around the world via the Internet. The AFIP attempts to provide a 4-h turnaround time for submitted cases. Physicians and veterinarians provide text files describing the background of the cases and actual images of tissues exhibiting pathology for review by AFIP pathologists. In order to ensure successful analysis of the digitized images submitted to the AFIP, the sender needs to understand some basic rules of thumb concerning electronic submission of images.

Telemedicine/telepathology needs are currently helping to drive the development of instrumentation and software for the acquisition and electronic transmission of scientific images.

As this technology is utilized by an increasing number of medical sites, we can look forward to the technology becoming more affordable so that applications to image communication between basic science laboratories will become more routine.

A. File Size

There are three common types of image files produced (Table 26): those for general imaging on a computer screen or for inclusion in a Microsoft PowerPoint® presentation, those minimally suitable for diagnostic work, and those suitable for publication. A relatively inexpensive CCD video camera with a 640 × 480 pixel display will produce a small image that can be somewhat challenging for diagnostic pathology because of the limited resolution available. A digital camera capable of recording a 1,280 × 960 pixel display delivers sufficient resolution for good diagnostic pathology work (Dr. B. Williams, personal communication).

For pathological diagnosis, which is primarily based on pattern recognition, resolution is more important than color. When an image is small, and detail is lost, diagnosis is difficult. However, the variability in staining found in histological preparations from different labs or staining runs does not usually impact the ability to interpret the slides. A color depth of 8 bits is adequate for most pathology work, yielding 256 colors for RGB output, but 24-bit color depth would be preferred, since it provides truly photorealistic quality with the 16 million colors available. Some cameras can provide 36-bit color depth, but the standard is not recognized by many computer programs at this time, so is not recommended for images that must be conveyed to others.

As mentioned previously, some file formats compress image files, making them easier to transmit over the Internet. JPEG files are the most common type of transmitted image file and can be compressed to different degrees. Once they are compressed over 14 times, the difference is clearly visible. It is important, once again, to remember that a compressed file cannot be uncompressed. If the image is to be put to other uses, it should be saved initially as an uncompressed file. Then, a second compressed version of the file can be created for transmission over the Internet.

At the present time, most users will have trouble sending electronic video files over the Internet because of the sheer size of even compressed images. Video presentations are based on 30 frames (images) per second. Even at a minimal 640 × 480 pixel image size, the video file will be approximately 30 Mb/sec in full color:

$$640 \text{ pixels} \times 480 \text{ pixels} \times 3 \text{ (RGB)} \times 30 \text{ (frames/sec)} = 27.648 \text{ Mb}$$

Files of this size cannot be transmitted with less than T1 bandwidth, to which most physicians and veterinarians do not have access. Thus, televideo currently is not a very relevant aspect of telemedicine/telepathology.

Table 26. Applications for Images of Different File Size[a]

640 pixels by 480 pixels	1,280 pixels by 960 pixels	2,560 pixels by 1,920 pixels
X3 (colors)	X3 (colors)	X3 (colors)
0.9 Mb	4 Mb	14 Mb
Small image	Diagnostic image (pathology)	Minimal publication quality

[a] Dr. B. Williams, personal communication

B. Types of Telemedicine/Telepathology Systems

There are three fundamental types of systems for electronic image transmission produced today. Static systems can send individual images of preselected areas of a histological slide, for example, across the Internet. Robotic, or real-time, systems can control a microscope from a remote location, leading to the capture and transmission of images from that remote location over the Internet. Finally, the most elegant, expensive, and complicated systems produce virtual slides for examination and transmission.

1. *Static systems* can cost as little as $5,000–6,000 to set up on an existing microscope. They are in wide use and require only the microscope, a digital camera with appropriate image-handling software, and access to an Internet connection. These systems are relatively inexpensive, support low bandwidth and Internet transmission of images, and can be used for real-time and offline diagnostic purposes. As mentioned above, a CCD camera with a 640×480 pixel chip can produce an image to view on a computer screen but may not produce an image of sufficient detail for diagnostic work, so it is advisable to invest in a camera with a chip with at least $1,024 \times 768$ pixels. In a typical situation, the captured image that is being transmitted to another site contains about 0.2% of the entire glass slide. If you need to view a large area at low magnification, the low-end video camera will rarely provide sufficient resolution to be of much use. The major limitation to static systems is that the image that is conveyed to another viewer is preselected by the person capturing the image, who may not have noticed some other aspect of pathology that the pathologist viewing the transmitted image might have found, were they to have access to the entire histological slide.

2. *Robotic (real-time) systems* require a dedicated microscope, software, and hardware, and the total cost for such a system is in the range of $65,000–100,000. Another $5,000 or so is needed for a dedicated server, and about $3,000 monthly will have to be spent on the necessary bandwidth to support the operation of the instrument. These systems cannot work across the Internet because the connection must be uninterrupted during microscope operation. These systems will work well on LANs. Even with a dedicated broadband, there is a 1- to 2-sec lag time for changing objectives and moving the field of view. The pathologist at a distance that is viewing a slide on the microscope at the laboratory maintaining the equipment and worldwide web access can examine the entire slide and zoom in on areas of pathology for diagnostic assessment, but the process is clearly slower than looking at a histological slide on a microscope on your own desk.

3. *Virtual slide systems* are the most complex and expensive but represent the state of the art for distributing images of slides over the worldwide web. Bacus Laboratories, Inc., Lombard, IL manufactures a system for somewhat over $100,000 that costs about $20,000 a year to maintain. In addition, the costs for a dedicated server and monthly fees for the bandwidth are the same as for a robotic system. This approach scans a histological slide automatically, taking high-magnification images of the entire slide, with all of the images ultimately tiled together. Once the images are all tiled, an image of the entire slide can be viewed at one time, or the viewer who has accessed the site where the slide image(s) reside can select areas of the slide (individual units of the tiled image) and examine them at a higher magnification. This presents the most realistic way to view a histological slide from a distance, since the viewer can scan the entire slide to look for evidence of a lesion and can then zoom in on the lesion to make an assessment, which is what a pathologist would normally do with a histological slide on their own microscope. At the present time, scanning in an image of a single histological slide of a liver can take 1–2 hr. In addition, the file size necessary to store an image of a single histological slide can be quite large. For example,

a virtual slide of a single 1- to 2-mm needle biopsy produces a digital file of approximately 60 Mb, while a virtual slide of a whole liver slice could produce a 2.6-Gb file. In general, a 2-Gb file for a single virtual slide would be needed to provide an image at high magnification of large slices of tissue, while an image stored only at low magnification or an image of a small piece of tissue, like the aforementioned needle biopsy, would require a smaller file. As these systems undergo further development, image acquisition times should decrease dramatically, and the mechanical aspects of automatically transporting, scanning, and focusing on slides should continue to improve, resulting in machines that can store images of numerous virtual slides relatively quickly without human intervention, except to load the hopper containing the slides to be scanned.

REFERENCES

Baldock, R., and Graham, J. 2000. *Image processing and analysis. A practical approach*. Oxford University Press, Oxford.

Davidson, M.W., Abramowitz, M., Olympus America Inc., and The Florida State University (eds.). July 30, 2002. http://micro.magnet.fsu.edu/primer/digitalimaging/index.htm

Inoué, S., and Spring, K.R. 1997. *Video microscopy. The fundamentals*. Plenum Press, New York.

Russ, J.C. 2002. *The image processing handbook*, 4th edn. CRC Press, Boca Raton, FL.

Weinstein, R.S., Descour, M.R., Liang, C., Bhattacharyya, A.K., Graham, A.R., Davis, J.R., Scott, K.M., Richter, L., Krupinski, E.A., Szymus, J., Kayser, K., and Dunn, B.E. 2001. Telepathology overview: From concept to implementation. *Hum. Pathol.* 32: 1283.

Williams, B.H., Mullick, F.G., Butler, D.R., Herring, R.F., and O'Leary, T.J. 2001. Clinical evaluation of an international static image-based telepathology service. *Hum. Pathol.* 32: 1309.

17

Morphometry and Stereology

Most biologists interested in morphometric analysis and stereology purchase programs to do the work, and a specific knowledge of all the algorithms and statistical calculations behind their operation is not critical. The programs are booted up, the menus are consulted to see what functions are possible, and the operator instructs the computer to perform certain operations from the menu. At the same time, if the operator does not possess knowledge concerning the types of questions that may be asked, the limitations inherent in the sampling techniques being used, and the general underlying assumptions necessary for morphometric analyses, the software may not be used to its ultimate extent. The purpose of this chapter is to give an overview of the capabilities and a few of the shortcomings of morphometric analysis programs used today. Several texts (Baldock and Graham, 2000; Hader, 1991; Howard and Reed, 1998; Mouton, 2002; Russ, 1986, 1990, 2002; Russ and Dehoff, 2000) cover most aspects of the mechanics behind morphometric analysis and stereology and address specific applications in great detail. They are recommended reading prior to embarking upon a project requiring morphometric or stereologic analysis methods. The text by Misell (1978) was written prior to the currently available software, but deals extensively with the principles and methods for image enhancement and analysis not confined to computers.

I. PURPOSE

Morphometric and stereological analysis methods encompass techniques devoted to image acquisition (photography, digitizing, and storage of digitized images), image manipulation (changing grayscales, sharpening edges, smoothing edges, dilation, erosion, skeletonization, and colorization), and subsequent image analysis. Most of these techniques were originally developed without the benefit of computers, but with the beginning of the desktop computer industry in the 1970s, the disciplines of morphometry and stereology became more focused on the digitized images from which computers could derive information concerning size, volumes, frequency of occurrence, spatial distribution, and color of objects within digital images. While humans are still more proficient at making subjective comparisons between structures, computers are best at measuring objects, performing statistical analyses, and acquiring vast stores of numerical data, provided that the parameters defining the data sets collected are sufficiently clear to the computer software.

Typical images of use to cell biologists are acquired from transmission electron microscopes, scanning electron microscopes, or light microscopes and may be either black-and-white images or color images. Measurements are usually made from real or optical sections and projected images wherein a once three-dimensional structure is viewed as a more-or-less two-dimensional structure.

The various software packages available are designed for object counting, measuring the percent area occupied by features within a field of view, and describing the position, shape, and size of objects within an image. Computers are particularly suited to these tasks because they are capable of seeing all the details in an image and have no inherent interest in noninformational trivia within the image, unlike the human observer. Of course, humans are far better at understanding incomplete or unusual objects, discriminating between contiguous objects, and mentally

turning objects over in order to view them from different angles than those actually presented (a standard component of psychological testing). Computer-assisted design programs have only begun to approach human capabilities in this regard.

II. RESOLUTION AND DISCRIMINATION

Computers typically convert an analog image into a digital signal composed of pixels (picture elements), which then can be stored easily and manipulated on a pixel-by-pixel basis. A relatively inexpensive digital camera records 640×480 pixels, and high-resolution digital cameras producing images of over $1{,}600 \times 1{,}200$ pixels are becoming more affordable. The latter camera allows 5,760,000 pixels to be measured per RGB (color) image. The actual image resolution is usually less than the pixel count because more than two pixels are typically required to discriminate a feature or boundary. A 512×512 pixel image consists of 262,144 pixels, which clearly discriminate less than the human eye with its 150 million individual receptors. However, the human eye can only distinguish approximately 50 different levels of gray in a monochrome image, while a computer can discriminate between 256 brightness levels (gray levels).

Another aspect to be considered is the resolving capability of the original image-capture device. A typical inexpensive video camera has a spectral sensitivity similar to the human eye and consists of 525 lines per image, seen at 30 frames/s. Sixty interlaced 1/2 frames/s are produced, each consisting of 262 lines. Some of the newer video cameras can produce 1,000–2,000 lines in a video image, but when this is compared with photographic films, which can produce images with 100–200 lines/mm, it is clear that video images have far less resolution than photographic images. In addition, video cameras can suffer from pincushion and barrel distortion, uneven coatings, vignetting and blooming (bright objects or edges will cause adjacent areas to develop brightness, resulting in bright objects appearing larger than they really are). Cameras with CCDs (charge-coupled devices) consist of a receptive surface covered with transistors. Some cameras have over 10 million receptors across their surface. With CCDs, signals are passed to the right on the screen on clock-based time and read out a line at a time. CCD units are smaller and more rugged than the analog units that preceded them. Cooled CCDs have a high SNR (signal-to-noise ratio) and thus can record dim images more easily, making them ideal for immunofluorescence studies, wherein the fluorochromes may not produce bright images. Resolution of all digital cameras is limited by the spacing of the individual solid-state detectors that make up their receptive surfaces. In some cameras, a third of the receptors are restricted to recording reds, a third to greens, and a third to blues (RGB), thus yielding a true resolution for color images to a third of the total pixels available. Some manufacturers utilize movable red, green, and blue filters that are sequentially put in front of the CCD chip, so that each color is recorded by the entire CCD display, and then all three color images (RGB) are superimposed, thus providing an image in full color that has three times the resolution found with the former camera design.

III. IMAGE PROCESSING

Image processing can be used to make an image more appealing or can be used to extract meaning, data, or numbers from an image. There are several data, or numbers that may be extracted from an image. These data then may be manipulated in several ways, as outlined below as described by Russ (1990). As we go down the chart, there is a reduction in the amount of data remaining at each level. Any lateral movements in the chart change the form of the data but do not change the amount present.

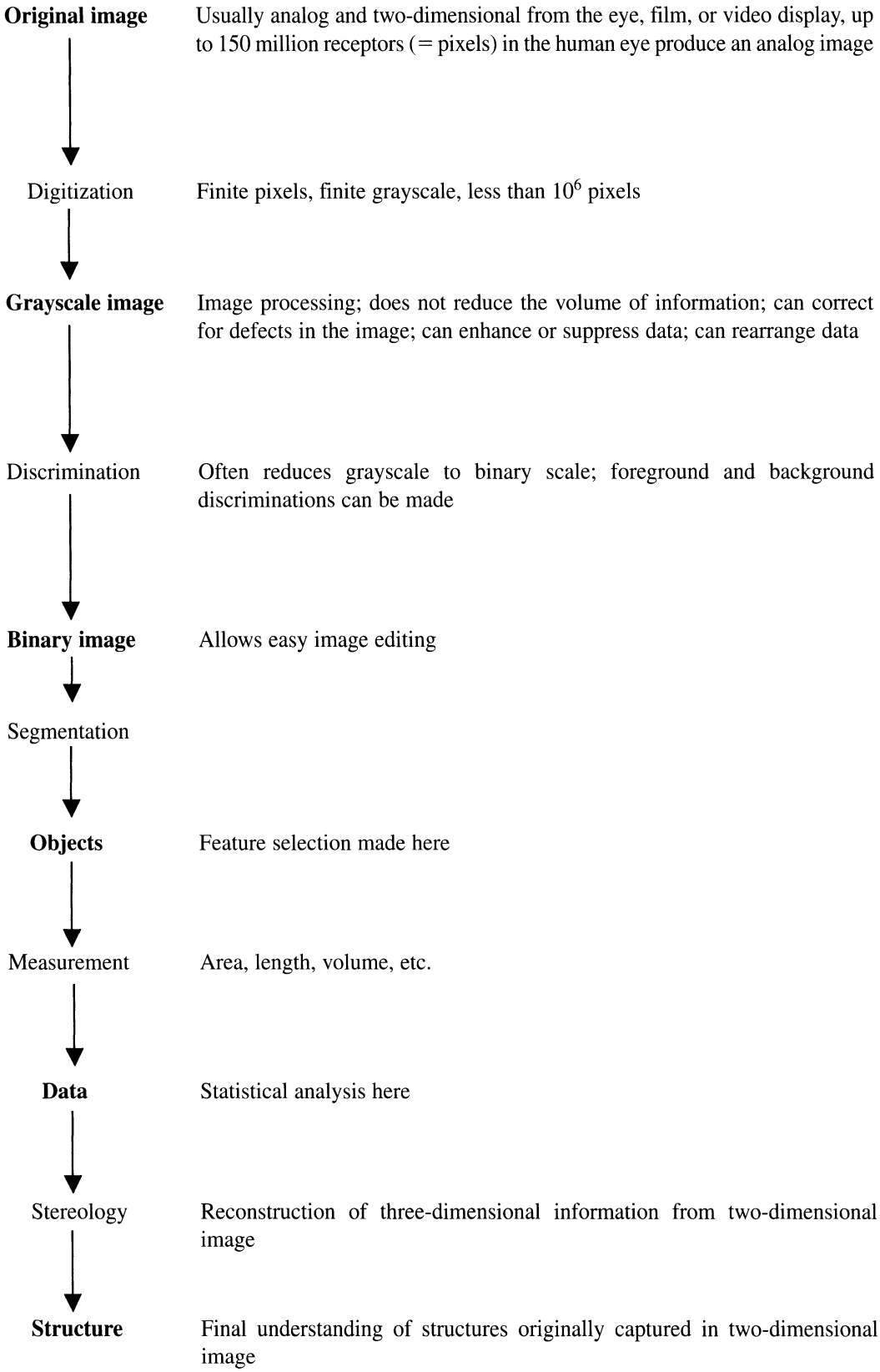
Original image
Usually analog and two-dimensional from the eye, film, or video display, up to 150 million receptors (= pixels) in the human eye produce an analog image
Digitization
Finite pixels, finite grayscale, less than 10^6 pixels
Grayscale image
Image processing; does not reduce the volume of information; can correct for defects in the image; can enhance or suppress data; can rearrange data
Discrimination
Often reduces grayscale to binary scale; foreground and background discriminations can be made
Binary image
Allows easy image editing
Segmentation
Objects
Feature selection made here
Measurement
Area, length, volume, etc.
Data
Statistical analysis here
Stereology
Reconstruction of three-dimensional information from two-dimensional image
Structure
Final understanding of structures originally captured in two-dimensional image

Image processing can be used to correct defects in the image caused by uneven illumination, excess charging (as with SEM images), or noninformational noise. Averaging techniques can be used to reduce random noise (e.g., "snow" in a video image). To do this, many images are averaged, thus averaging out the noise that appears in different locations of individual successive images. This technique, of course, is only applicable to stationary images.

If only one image with excessive noise is available, the values of nine nearest-neighbor pixels can be averaged, and then each pixel value can be replaced with the average value for the array to decrease the noise.

A set of nine pixels with brightness from low levels (1) to high levels (9) is:

2	4	6	
1	7	9	averaged = 5.88 (rounded to 6)
8	8	8	

The display after the "smoothing" operation is:

6	6	6
6	6	6
6	6	6

The programs that perform this sort of operation are actually much more sophisticated than the example given, but they still tend to decrease the sharpness of real edges or discontinuities within the image. For this reason, another method, known as applying a median filter (Russ, 1990), is preferred. This procedure uses the same array of pixels shown above, consisting of a 3×3 square of pixels. The nine pixels are ranked in order of brightness, and then the median brightness is assigned to the central pixel, 7 in the case cited above. An image can have median filtering applied to it repeatedly until no further changes are noted. Since the isolated random noise pixels will rarely have the median brightness value with which they are replaced, filtering will smooth out noisy, but uniform, areas. Surface edges or discrete object boundaries will not be moved, made broader, or have contrast reduced by this technique.

Image processing can be used to separate foreground information from background information, usually on the basis of brightness. Processing can also quickly reveal changes in the location of objects by subtracting a later image from an earlier image, a method used for tracking motion as in studies of sperm motility. Objects that remain in the same place are effectively subtracted from the combined image, leaving only those that have moved.

Other common operations are erosion, dilation, and skeletonization. Erosion removes any pixel that has a preassigned character (i.e., black color) that touches more than a selected number of neighbors. Dilation is used to fill in spaces, essentially by a reverse of the process of erosion. Dilation can decrease noise in an image by filling in spaces in a broken-up image but will increase the size of features. Skeletonization is a form of severe erosion effected by producing lines of pixels that define the midline of a feature. This can allow the operator to segregate touching objects that would normally be counted as one object into two objects that can be separately scored. Producing a skeleton can also be useful to analyze branching patterns more easily within a structure.

The methods, statistical bases, and applications of these and other image processing operations performed to improve images and to prepare them for analysis are discussed thoroughly in texts on image analysis by Russ (1986, 1990) and Hader (1991). The first two texts deal extensively with the statistical and mathematical models behind the operations upon which image analysis is based, but the second is more devoted to specific applications in the analysis of problems.

Once a two-dimensional image is digitized and subjected to the variety of image enhancement techniques briefly alluded to above, the image can be analyzed. Analysis can yield information about the brightness or color of an object. Thus, analysis can locate the color of Coomassie blue in protein gels or can record the density of bands (levels of gray) in a DNA gel.

The specific position of objects also can be ascertained, as well as information about the number of objects per unit area, the amount of space occupied per unit area, any preferred orientation of the objects, and the distribution of the objects (are they evenly spaced or clustered?).

Distance measurements can be made to determine the distance from one object to another as well as the distance between a given object and a specific boundary. Size measurements can be taken that describe an object's area, its perimeter, the center of balance for the object (centroid feature), the equivalent diameter (a circle of the same area as the entire feature), and the longest and shortest chords of the feature.

Shape analyses are possible with most programs that are based on form factors such as dimensional ratios, topological information (e.g., links, nodes, ends, branches), roundness, solidity, convexity (ratio of taut string to perimeter), and aspect ratio (length to breadth).

IV. STEREOLOGY

An essential problem of quantification in biological studies is that most of the images with which we work are two-dimensional, while most biological structures are three-dimensional. We are thus faced with the problem of interpreting the true three-dimensional structure from a two-dimensional image.

Stereology is the science which derives three-dimensional information from the analysis of two-dimensional images. Morphometric techniques are first used to derive spatial information from the two-dimensional images, and then further mathematical manipulations extrapolate three-dimensional images from the two-dimensional constructs. All known practical counting rules (e.g., the rules for counting red blood cells with a hemocytometer) that are over a few decades old are biased. Gundersen *et al.* (1988a) state that "counting on certain edges and corners of the counting frame ... systematically overestimates the number" of objects in the field of view. The fundamental principles employed in programs for computer-assisted stereology correct for this source of error. See Gundersen *et al.*, 1988a, 1988b for a discussion of the mathematical and statistical basis for stereological methods.

There are a number of parameters that biologists attempt to measure with stereological techniques such as the volume occupied by a given structure (e.g., the number of cells present per unit area of a liver as a measure of hypertrophy of the organ), the number of structures within a unit volume (e.g., the number of peroxisomes present in a hepatocyte exposed to a drug that causes upregulation), and the size of individual structures such as mitochondria in the field of view (volumetric analysis).

Stereological methods provide information about two types of geometrical properties of structures: topological and metric. Topological properties include the number of disconnected features in a set and their connectivity (the number of redundant connections in the structure of a network). Metric properties are more commonly studied and encompass the collective volume of the set of features, the area of the surfaces of the structures in the set, the length of any lineal feature of interest within the structure, and the total curvature of the structure surface.

To perform a stereological analysis, certain fundamental assumptions must be made: (1) the structures counted must be randomly oriented; (2) the structures must be randomly

distributed; and (3) the sample must be representative. In short, the sample must be isotropic, uniform, and random (unbiased). Naturally, biological structures rarely possess all three of these attributes, so stereological techniques must be used with caution.

Stereological methods are based on the assumptions that the volume of an object within a given specimen volume is proportional to the area of a given object within a given specimen area, which is proportional to the number of points (from a grid) resting on an object out of the number of points over the entire field of view of the specimen, which is proportional to the length of an object in relation to the length of the field of view of the specimen. In other words, $V_V = L_L = P_P = A_A$ where V = volume fraction, L = lineal fraction, P = point fraction, and A = areal fraction.

When spherical objects in a field are either physically sectioned or optically sectioned (e.g., a high-magnification light microscope image of a thick specimen, with little depth of field), what one sees is a collection of circular profiles with different chord lengths (diameter) (Fig. 248). The Swartz–Saltikov diameter method (Russ, 1990) may be used to determine the true size distribution of spherical or nearly spherical objects from two-dimensional images. The chord lengths (diameters) of the two-dimensional structures are measured, or, if the objects are not circular, the major and minor axes are measured (a and b, respectively), and the diameter, d, of the structure is determined by the formula:

$$2\times\sqrt{a}\times b$$

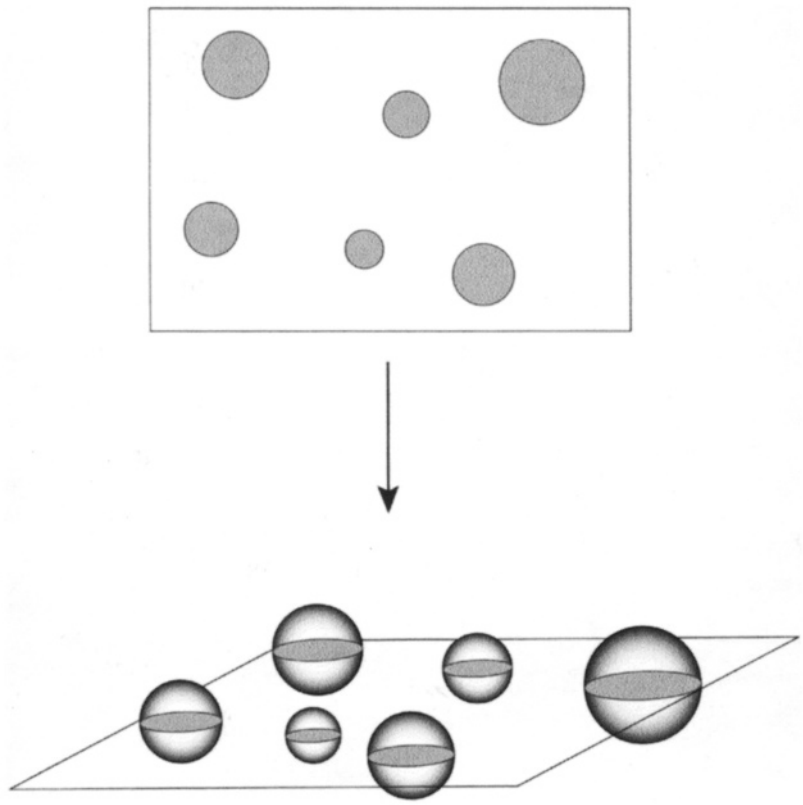

Figure 248. Illustration of an optical section through a three-dimensional volume containing spherical structures.

The measured diameters are then divided into 10–15 equal groups, and the number of objects in each size category (N_A) is calculated. The results of this calculation are used to calculate the number per unit volume in each size class in the original three-dimensional sample.

As previously mentioned, to calculate the volume fraction, V_V, of objects within a specimen, the assumption is made that the volume fraction of the objects within a volume of sample is equal to the areal fraction, A_A, of the objects, and both of these are proportional to the fraction of points on a grid striking the objects compared with the number of points within the whole specimen volume (P_P). The volume of a particular object or set of objects within a selected specimen volume may be determined by two major methods: point counting and planimetry.

In planimetry, the calculated area of objects subjected to the application of algorithms in the computer program is used to calculate the volume fraction of the objects. Point-counting methods require several decisions by the computer operator. The general rule of thumb is to have no more than 0.6–1 points striking the object's profile. The correct grid spacing is thus dependent on the magnification of the image being analyzed and on the number of object profiles present within the image. It is also necessary to calculate how many "hits" are necessary to assure that P_P will predict V_V within reasonable limits of confidence. To achieve a confidence limit of 5%, 400 independent hits must be recorded. Finally, if an average of 40 independent hits are recorded per photograph, 10 photographs will be necessary to estimate V_V within a 5% confidence limit. It should also be remembered that the point counting must be done on 10 different photographs, and not just by placing a grid randomly on a given photograph 10 different times. The latter case would not yield 400 independent hits.

The classic sterological methods discussed above, which are geometry based and best used to evaluate cylinders, spheres, and so on, that are isotropic and randomly oriented, relate surface area to unit volume work, in many instances, but fall short with anisotropic objects. Modern methods of stereology (see Gundersen *et al.*, 1988a, 1988b for thorough discussions of these methods) were developed to accommodate objects typically encountered with biological specimens, which are not randomly oriented or uniform. Modern methods are geometry independent, which allows nonrandomly oriented material to be evaluated as if it were isotropic, uniform, and random.

V. COMPUTER-ASSISTED ANALYSIS OF MOVEMENT

A final area of general interest to biologists to which computer-assisted methods are applied is the analysis of the movement of objects within a field of view. The analysis of sperm motility after exposure to therapeutic compounds of interest to the pharmaceutical industry and the chemotactic movement of bacteria, which involves changes in direction of cell rotation, represent two typical applications. In both situations, the number of cells and the speed of movements make human analysis difficult. Live digital image acquisition followed by computer analysis easily delivers information concerning the rotational movements of individual cells and their track lengths over selected time periods. For this application, a CCD camera requiring the field to be recorded three times (once for each of the RGB filters) would not be suitable. A simple CCD video camera that can record in what appears to be real time (30 frames/sec) would have less resolution than a high-end cooled CCD camera with three different color filters but can record an image of a moving object that would be blurred and that would show three separate bands of color (RGB) if recorded with a digital camera utilizing three passes (each with a separate color filter) to produce the final full-color image. Takahashi (1991) discussed automated measurement of movements of halobacteria. He used computer programs to quantify the percent of reversing cells

(those cells changing direction from clockwise to counterclockwise and *vice versa*) in a population and to calculate the average number of reversals occurring in a population at a given time point. Finally, he calculated the latency period between the application of a chemotactic stimulus and the subsequent reversals exhibited by the cells.

The programs available for tracking cellular motion can evaluate populations by measuring changes in population density resulting from cells migrating toward or away from chemical or environmental stimuli. Computers also can be used to track individual cells, which allows a greater time resolution than population methods. Cells therefore can be exposed to stimuli for shorter time periods than with population analysis methods.

REFERENCES

Baldock, R., and Graham, J. (eds.). 2000. *Image processing and analysis. A practical approach*. Oxford University Press, Oxford.

Gundersen, H.J.G., Bagger, P., Bendtsen, T.F., Evans, S.M., Korbo, L., Marcussen, N., Moller, A., Nielsen, K., Nyengaard, J.R., Pakkenberg, B., Sorensen, F.B., Vesterby, A., and West, M.J. 1988b. The new stereological tools: Disector, fractionator, nucleator and point sampled intercepts and their use in pathological research and diagnosis. *Acta Pathol. Microbiol. Immunol. Scand.* 96: 857.

Gundersen, H.J.G., Bendtsen, T.F., Korbo, L., Marcussen, N., Moller, A., Nielsen, K., Nyengaard, J.R., Pakkenberg, B., Sorensen, F.B., Vesterby, A., and West, M.J. 1988a. Some new, simple and efficient stereological methods and their use in pathological research and diagnosis. *Acta Pathol. Microbiol. Immunol. Scand.* 96: 379.

Hader, D.-P. 1991. *Image analysis in biology*. CRC Press, Boca Raton, FL.

Howard, C.V., and Reed, M.G. 1998. *Unbiased stereology. Three-dimensional measurement in microscopy*. BIOS Scientific, New York.

Misell, D.L. 1978. *Image analysis, enhancement and interpretation*. North-Holland, New York.

Mouton, P.R. 2002. *Principles and practices of unbiased stereology. An introduction for bioscientists*. The Johns Hopkins University Press, Baltimore.

Russ, J.C. 1986. *Practical Stereology*. Plenum Press, New York.

Russ, J.C. 1990. *Computer-assisted microscopy: The measurement and analysis of images*. Plenum Press, New York.

Russ, J.C. 2002. *The image processing handbook*, 4th edn. CRC Press, Boca Raton, FL.

Russ, J.C. and Dehoff, R.T. 2000. *Practical stereology*, 2nd edn. Kluwer Academic/Plenum Press, New York.

Takahashi, T. 1991. Automated measurement of movement responses in halobacteria. In: P.-P. Hader (ed.), *Image analysis in biology* (pp. 315–378). CRC Press, Boca Raton, FL.

18

Photomicroscopy

Photomicroscopy employs a variety of optical microscopes, some of which look through sectioned material (upright and compound light microscopes), and some of which allow views of the surface of samples (dissecting, or operating microscopes) or image light emitted from the specimen (epifluorescence or confocal laser scanning microscopes). Illumination of the sample may utilize focused light from an incandescent bulb or diffuse light from a fluorescent bulb. Epifluorescence microscopes employ arc lamps to produce high luminance levels and short-wavelength or ultra-violet light. Confocal microscopes generally use laser-derived illumination sources. Compound microscopes can be set up for standard bright-field viewing, dark-field viewing, phase-contrast microscopy, differential interference contrast (DIC) microscopy, epifluorescence, and polarization microscopy. Each type of microscope requires a variety of alignments and adjustments. Recording an image with modern photomicroscopes requires little more than focusing and pushing the shutter button, but producing an excellent photographic image requires considerable effort, whether using film or digital media for image storage. Producing a high-quality image is dependent on choosing proper optics, proper films, proper filtration or light temperatures (for color films), and making sure that Köhler illumination has been set up for the highest resolution and uniformity of illumination. This chapter provides an introduction to the various choices available for optics, lighting, and films and shows how to adjust a microscope to produce the best images. A large number of books and chapters in books have been written about light microscopy and photomicroscopy, but the texts by Bradbury (1991), Delly (1988), Rawlins (1992), Slayter (1976), and Slayter and Slayter (1992) provide a broad base of information and have served as the fundamental sources for this chapter.

I. LIGHT-MICROSCOPE OBJECTIVE LENSES

Objectives both magnify and focus the image of the specimen. They are described on the basis of their general optical design (bright-field, phase-contrast, DIC), numerical aperture, working distance, and degree of correction for spherical aberration and chromatic aberration (achromat, semiapochromat, apochromat). They may bring the specimen image to focus at a specific plane 160 mm from the nosepiece hole into which they are screwed, shown by the number 160 inscribed on the barrel of the objective, or they may contain a lens in between the objective and the ocular (a tube lens) that allows the image to be focused at any distance past the tube lens without the need for supplementary lenses, as found in older photomicroscopes. Some lenses are designed to be immersed in oil or water (immersion lenses), some need to have coverglasses over the sectioned sample, while others require no coverglasses. Finally, the best lenses for photomicroscopy are designed to give flat-field views from edge to edge and are usually designated as *plan* lenses if they have this feature. Each manufacturer has slightly different designations for the different classes of lenses they produce, so it is necessary to talk with their sales representatives to determine which group of lenses offers the features desired.

A. Numerical Aperture

The numerical aperture (NA) of a lens is a measure of its light-gathering ability and its capacity to capture image-forming rays of light that have been highly diffracted by the specimen. The latter ability makes high-resolution microscopy possible. The NA of a lens is described by the formula:

$$\text{NA} = n \sin \alpha$$

Thus, the NA of a lens is the product of the refractive index (Table 27) of the medium (n) and the sine of one half the angular aperture of the lens (α). The *resolving power* of a lens is described by the formula:

$$R = \frac{0.61\lambda}{\text{NA}}$$

With a given wavelength of an illumination source (λ), a higher NA will provide a higher resolution. Resolution is also dependent on the wavelength of the illumination source. An oil-immersion lens with an NA of 1.4, utilizing green light for illumination ($\lambda = 546\,\text{nm}$) will yield a theoretical resolution of 237.9 nm, or 0.24 μm:

$$\frac{0.61 \times 546\,\text{nm}}{1.4} = 237.9\,\text{nm}$$

Using the same lens with blue light provides a theoretical resolution of 190 nm, or 0.19 μm, indicating that shorter wavelengths of visible light will yield greater resolution:

$$\frac{0.61 \times 436\,\text{nm}}{1.4} = 189.97\,\text{nm}$$

B. Degree of Optical Correction

Spherical aberration is the inability of a lens to bring the peripheral portion of the specimen image to focus in the same plane as the axial portion of the specimen image. This is caused by greater refraction of the image at the edge of a curved lens than at the center of the lens (Fig. 249).

Chromatic aberration exists when light with different wavelengths is refracted by the curved lens as it passes through the same point on the lens (Fig. 250). Light of longer wavelengths, such as red light, comes to focus after refraction by a lens at a more distant point from the lens

Table 27. Refractive Indices of Various Media (Baldock and Graham, 2000)

Medium	Refractive Index	Maximum NA
Air	1.00	0.95
Water	1.33	1.2
Glycerin	1.44	1.3
Oil	1.52	1.4
Glass	1.52	1.4

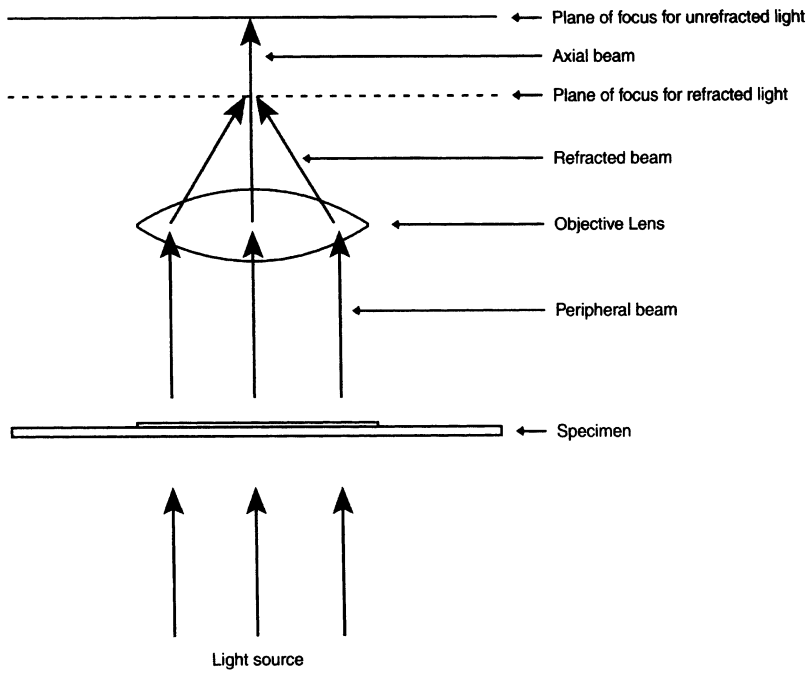

Figure 249. Spherical aberration causing the axial and peripheral portions of the light beam to focus at different planes.

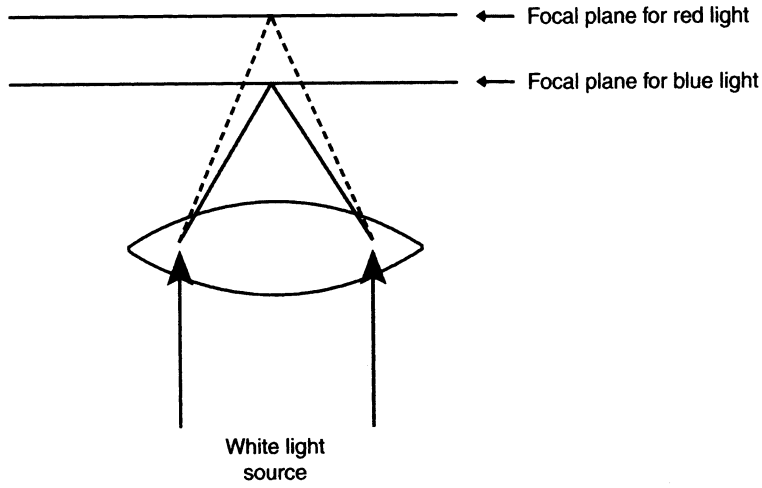

Figure 250. Chromatic aberration, where white light, containing blue and red light, passes through the same point of a curved lens. The blue light, with a shorter wavelength, comes to focus nearer the lens than the red light, which has a longer wavelength.

than blue light passing through the same point in the lens, since blue light has a shorter wavelength and is focused nearer the lens.

Both of these phenomena were addressed in the early 1800s by coupling so-called positive lenses (Fig. 251) and negative lenses (Fig. 252) together to form doublet lenses (Fig. 253) or triplet lenses. Coating lenses with a variety of materials also reduces chromatic aberration.

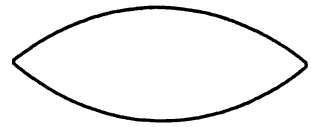

Figure 251. A positive lens.

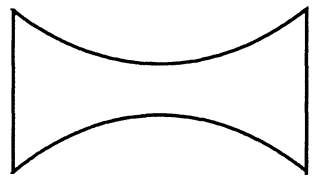

Figure 252. A negative lens.

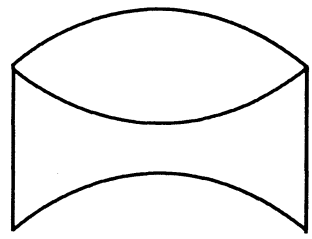

Figure 253. A doublet lens combining a positive and negative lens.

Flat-field or *plan* lenses made before the advent of infinity optics required matched compensating oculars to achieve the edge-to-edge flatness necessary for photomicroscopy. Modern flat-field infinity optics may be used with noncompensating oculars, so they can be easily adapted to various camera systems, without having to resort to specific oculars to project the image into the camera system.

C. Working Distance

Lenses from different microscope manufacturers exhibit different working distances, and lenses of different quality from the same manufacturer will also exhibit different working distances. This can be a critical feature when assembling a microscope, depending on the use to which it will be put. A microscope that will always be used to examine xylene-cleared histological slides with #1.5 coverglasses does not need great working distances. However, microbiologists who periodically examine Petri dish cultures with an upright compound microscope at relatively low magnifications (e.g., with 4 × or 10 × objectives) benefit from having microscopes with long-working-distance objectives. At the present time, the Nikon line of objectives offers the greatest working distances for each class of objectives in the industry.

Working distance can be a factor in lens selection because it is associated with the quality (and cost) of the different objectives. From a given manufacturer, inexpensive achromat lenses of a given magnification will have the greatest working distance, while apochromats have the least, and semiapochromats (fluorite) lenses are in between.

The greater the magnification of an objective, the shorter the working distance, and the more optical sectioning will take place when examining anything but the thinnest sections. What this means in practical terms is that a 40× lens will be capable of focusing on several different planes within a specimen. This can be a problem with epifluorescence microscopy, since out-of-focus specimen fluorescence above and below the plane of section will still be seen, but will not be from the plane of section being viewed and thus will produce extraneous noise.

D. Types of Objectives

As already mentioned, there are three major classes of objectives, with different degrees of correction for chromatic and spherical aberration, differing numerical apertures, working distances, and cost.

Achromats are the least expensive and have the greatest working distances, in general. This type of lens is typically found on student microscopes and is not recommended for photomicroscopy. They have the highest degree of chromatic and spherical aberration. Chromatic aberration is corrected for red and blue, while spherical aberration is corrected for yellow–green, which is the range of greatest spectral sensitivity for the human eye. Color fringes may appear at the margins with white light, which can decrease the resolution with black-and-white and color recording media. Using a green filter with black-and-white film can improve images, since both chromatic and spherical aberrations are minimized by using monochromatic light.

Semiapochromats or *fluorite* lenses are made from calcium fluorite, rather than glass, and provide a refractive index not possible with glass. They are generally two to three times more expensive than achromats, tend to have a shorter working distance, and are coupled with compensating oculars for the best image quality. They are corrected for two colors for chromatic aberration like achromats but have been corrected for two colors for spherical aberration, unlike the single color characteristic of achromats. A final advantage of this class of lens is that they transmit ultraviolet light more efficiently than glass lenses. If using the fluorescent dye DAPI, which is excited by ultraviolet light, fluorite lenses are recommended (Rawlins, 1992). With dyes such as FITC, which are excited by other wavelengths of light, glass lenses work well.

Apochromats are the most expensive type of objectives, and generally cost five to six times more than achromats. They are used with compensating oculars, and have chromatic correction for red, green, and blue light and spherical correction for red and blue light. Apochromats have the shortest working distance of the three types of objectives, the highest numerical apertures, and provide the least contrast.

Flat-field or *plan* lenses are produced for all three classes of objectives. The addition of this capability raises the price of a given objective considerably due to their added complexity and number of lens elements. For example, a 100× achromat lens may contain six glass elements, while a 100× planapochromat lens may contain 18 or more elements (Delly, 1988). Plan lenses are necessary for photomicroscopy to ensure edge-to-edge flatness needed for sharp photomicrographs but are not necessary for microscopes used merely for observational purposes.

Even though the maximum resolving capability for glass lenses was reached in the 1880s, manufacturers have continued to improve the contrast, the width of field of view, and the image brightness by improving glass composition, lens coatings, light sources, and glass element manufacturing methods, particularly since the advent of computer-design and manufacturing methods. In recent years, the development of so-called infinity optics has made it easier for manufacturers to produce photomicroscopes with multiple ports to which images can be sent without the

addition of various internal supplementary lenses to refocus the specimen image to the different focal planes represented by the various ports. The addition of various adapters to fit a variety of film and digital cameras has been simplified by the use of these optics. Carefully matched compensating oculars are no longer necessary to preserve the qualities of chromatic and spherical aberration correction, as well as flatness of field, that have been engineered into infinity objectives. As mentioned above, once the image is focused by the objective and projected through the tube lens, the image is focused at any further point in the system. For example, planapochromat and planfluorite (semiapochromat) infinity optic (UIS) objectives currently provided on Olympus microscopes not only offer excellent flatness of field, width of view, and contrast but are corrected for longitudinal chromatic aberration for four wavelengths (violet, blue, yellow–orange, and red) as explained by Abramowitz (1994). These lenses are also corrected for four wavelengths for spherical aberration. Achromat lenses in the UIS line are corrected for three wavelengths for chromatic and spherical aberration.

1. Objectives with focusing collars: When examining thick samples such as bone sections or gelatin-mounted immunostained preparations with standard high-dry objectives (40×, 50×, or 100×), the images frequently appear fuzzy or out of focus. This may also be a problem with coverglasses of unknown thickness. A standard high-dry objective is meant to be used with a flat, 4- to 10-μm-thick section under a #1.5 coverglass (nominally 0.15–0.18 μm thick). If these conditions are not met, a sharp image cannot be obtained because the narrow focal length of the lens at this high a magnification range produces a very narrow focal depth. When faced with routine work utilizing slides from various sources, such as received by diagnostic laboratories where section thickness and coverglass thickness cannot be controlled, it is wise to spend the extra money required to buy a high-dry objective with a focusing collar.

2. Objectives with internal diaphragms: Some oil-immersion objectives have adjustable collars that control an internal diaphragm but do not change the focus of the objective. We prefer using the substage condenser diaphragm (explained below) to increase the contrast and depth of field slightly, rather than using the diaphragm on the objective, which we leave wide open at all times.

3. Proper use of oil with oil-immersion lenses: In our experience, the proper use of oil and condenser lenses for high-resolution, high-magnification light microscopy seems to be fairly confusing to many light-microscope users. The first concept that comes into play concerns the purpose of immersion oil.

If a stick is pushed down into a clear pond, the part of the stick below the surface of the water appears to bend away from the straight line defined by the part of the stick above the water. This is a result of the phenomenon of refraction, which results in the image being bent as light passes from a medium of one refractive index (air, at 1.00) into a medium with another refractive index (water, at 1.33).

The glass of slides and coverglasses has a refractive index of 1.52, which is significantly different than the refractive index of air at 1.00. As shown in Table 27, the maximum numerical aperture possible with light passing through air is 0.95, while the maximum numerical aperture of glass is 1.4. The lowest numerical aperture is the limiting step in determining the potential resolution available with an optical system.

The highest resolution achievable with a light microscope (1.4, with an oil immersion lens) is thus available in a system where the light leaving the condenser assembly passes through nothing with an effective numerical aperture less than 1.4. Thus, the numerical aperture of the uppermost element of the condenser lens assembly must be 1.4. In addition, the light leaving the condenser assembly must not pass through air (with a numerical aperture of only 0.95), because

refraction and image degradation would result. Since immersion oil has a refractive index of 1.52, as do the glass slide and coverglass, a numerical aperture of 1.4 can be maintained if oil fills the space between the upper element of a 1.4 NA condenser assembly and the glass slide, and if oil also fills the space between the upper surface of the coverglass and the front of a 1.4 NA objective.

Some lenses primarily designed for epifluorescence work are designated *water-immersion* objectives. These are limited to the numerical aperture of water (1.2) because of the refractive index of water (1.33). To achieve the highest resolution with these lenses, a substage condenser assembly with at least 1.2 NA must be used (typically a 1.4 NA assembly) and both the space between the condenser assembly and slide and the space between the slide and the objective must be filled with drops of water. Again, if the illuminating light or image-containing light passes through air at any point between the upper condenser lens and the lens at the tip of the objective, the effective numerical aperture will be limited to 0.95.

II. LIGHT-MICROSCOPE OCULARS

Oculars, or eyepieces, magnify the image previously magnified and focused by the objective lens, may further correct aberrations in the image caused by the objective lens (compensating oculars), and frequently serve as a place to house reticles for measuring or counting objects being viewed. There are two major types of eyepieces found on light microscopes: *Huygenian* and *Ramsden* oculars.

Huygenian oculars are found most frequently on inexpensive microscopes fitted with achromat objectives. They contain two planoconvex lenses, a field lens closest to the objective, and an eye lens closest to the eye (Fig. 254). The diaphragm that limits the field of view and also is the plane at which a reticle may be placed is between the two lenses, both of which have their curved surfaces facing the objective.

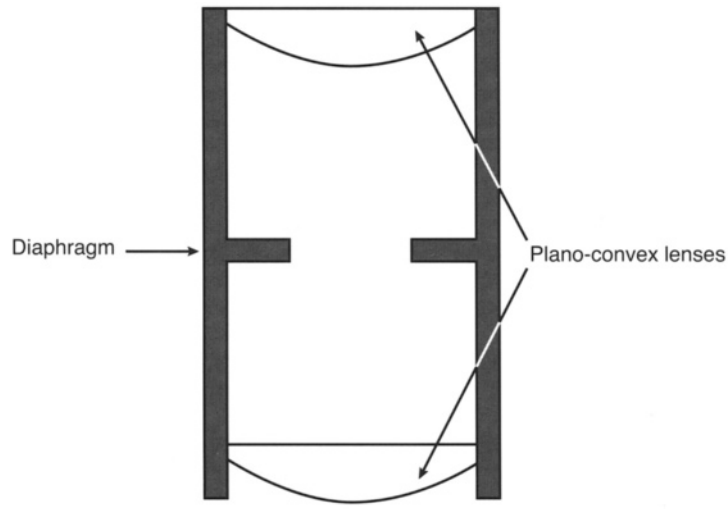

Figure 254. A Huygenian ocular consisting of two plano-convex lenses, each with the curved surface facing the objective. The diaphragm in the center is the point where a ocular micrometer would be placed.

Ramsden oculars are found on microscopes equipped with semiapochromat or apochromat objectives. They contain two sets of lenses like the Huygenian oculars, but the field lens closest to the objective has the curved surface facing away from the objective, while the eye lens has the curved surface pointing away from the eye (Fig. 255). Highly corrected Ramsden oculars have eye lenses constructed as doublet lenses. The limiting diaphragm where a reticle may be installed is located below the field lens.

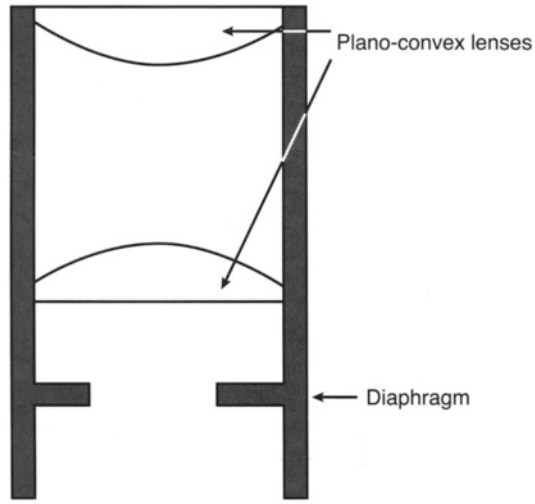

Figure 255. A Ramsden ocular consisting of two plano-convex lenses. The field lens, which is closest to the objective, has its flat side facing the objective. The eye lens, which is farthest from the objective, has its curved side facing the objective. The diaphragm below the field lens is the point where an ocular micrometer would be placed.

Some oculars of both types are designed as *high-eyepoint* eyepieces, suitable for users who wear their glasses while using microscopes. Oculars designed for wide-field viewing are ideal for surveying large areas quickly and are useful for laboratories doing diagnostic light microscopy, such as medical laboratories screening blood smears.

There are several reasons why it is useful to identify the type of ocular found on a given microscope. Highly corrected Ramsden oculars have compensating functions, as mentioned above, and are often carefully matched by the manufacturer to a type of objective in their line of microscope lenses. It is rare that using a compensating ocular from one manufacturer with the objectives from another manufacturer will produce good results. Properly placing reticles so that they can be focused sharply in the field of view necessitates placing them in the proper position, which may be in the middle of the ocular (Huygenian), or below the field lens (Ramsden). The Ramsden type of ocular produces sharper reticle images because the focal plane of the eyepiece lies below the field lens (Bradbury, 1991). A compensating eyepiece can be identified by looking through it toward a white light source. A red–orange color will be noted at the edge of the ocular field of view. A noncompensating (simple) ocular will show a blue ring around the edge of the field of view.

III. LIGHT-MICROSCOPE CONDENSER ASSEMBLIES

A typical substage condenser assembly contains the condenser lens, a substage condenser diaphragm (aperture assembly) and either an additional lens below the condenser that can be

brought into the light path to spread the beam of light for low-magnification objectives, or a mechanism for swinging the uppermost element of the condenser lens assembly out of the illumination field for the same purpose. The condenser assembly also has some means to move it up and down in relationship to the sample, for purposes of focusing the light beam at the plane of the specimen to produce the most even lighting and best resolution, as described by August Köhler in 1893. Finally, the condenser assembly may contain annular rings for dark-field or phase-constrast microscopy.

Condenser assemblies are designed for different purposes and must be matched with appropriate objectives to achieve the highest image quality. Abbe condensers are the simplest and least expensive. They typically contain two or three glass elements and are uncorrected for spherical or chromatic aberration. Aplanatic condensers are corrected for spherical aberration, and aplanatic–achromatic condensers are corrected for both spherical and chromatic aberration.

Dark-field condensers are designed to deliver only the light scattered by the specimen to the objective. The substage condenser diaphragm must be opened to its maximum diameter, and the numerical aperture of the condenser assembly must be greater than that of the objective being used to avoid direct light entering the image. The upper element of the dark-field condenser must have oil between it and the bottom of the glass slide.

The substage condenser diaphragm can be used to increase depth of field and specimen contrast, at some cost to resolution. At low magnification, where resolution is usually not an issue, the substage condenser can be closed down so that it intrudes approximately one quarter to one third into the field of view. This is monitored by removing an ocular and looking down the ocular tube. If the diaphragm is closed down too far, the image will exhibit unacceptable graininess due to diffraction, causing each point in the specimen to become artificially enlarged. The substage condenser diaphragm also can be used to increase contrast at higher magnifications (40 × to 100 ×), but there will be a decrease in ultimate resolution due to the numerical aperture being reduced by the intrusion of the aperture edges into the cone of light from the condenser assembly.

IV. SLIDE THICKNESS

Glass slides may be purchased from a variety of sources, in a variety of configurations. Slides may have chamfered edges to decrease the risk of cuts from handling them, and they may have frosted ends to make them easy to label. Another often-overlooked variable is the thickness of a slide. Except for special purposes, glass slides should have a nominal thickness of 1 mm (0.96–1.06 mm thick). Because condensers of high numerical aperture suitable for high-resolution microscopy with high numerical aperture objectives have short working distances, it may be impossible to focus the light source on the image plane as described by Köhler with a slide over 1 mm thick (Delly, 1988).

V. LIGHT SOURCES

Older microscopes have either 6 or 12 V incandescent bulbs with a glass globe and a tungsten filament. Both of these suffer from an aging phenomenon, whereby the slowly evaporating tungsten of the heated filament condenses on the relatively colder part of the bulb, the inside of

the glass globe. Over time, the globe becomes increasingly grayer because of tungsten deposition, and the color temperature of the light that started out at 3,200° K slowly shifts to increasingly lower temperatures. This results in the light source becoming increasingly redder as the filament ages. Color films such as Kodak Ektachrome T-64 produce proper color rendition when used with a new tungsten bulb adjusted to its maximum rated voltage of either 6 or 12 V. As the bulb ages, images captured on T-64 film will be more yellow–red than those produced with a new bulb. When a Kodak 80 A color-conversion filter, or equivalent, is used to boost the color temperature of the light source to the 5,500° K needed for daylight-balanced films such as Kodachrome, daylight Fujichrome, or daylight Ektachrome, excellent color rendition will be possible with a new bulb but will suffer the same color shifts noted above as the bulb ages.

Modern halogen light sources found on newer photomicroscopes avoid the aging phenomenon associated with old tungsten bulbs, and consequent color temperature shifts are not a problem with halogen bulbs. The quartz envelope of a halogen bulb operates at a much higher temperature than does the glass envelope of a standard tungsten bulb. Thus, the evaporating tungsten does not readily coat the inside of the bulb envelope, essentially eliminating color changes as the bulb ages. A halogen bulb produces 3,200° K when first installed, and continues to do so until the filament blows, requiring bulb replacement. *A halogen bulb should not be touched with bare hands.* The oil from fingertips will adhere to the surface of the bulb, and the high operating temperature of the bulb will cause the residual oil to degrade the surface of the bulb, resulting in premature bulb failure. If the bulb is touched with bare fingers, carefully remove the fingerprint oils from the surface with an alcohol-soaked tissue and let the bulb dry thoroughly before installation.

Fluorescent microscopes typically use mercury arc lamps that have a recommended bulb life of several hundred hours. The power supplies for these bulbs have elapsed time counters to help guide the user to change the bulb prior to the recommended time limit for the bulb, since a shattered bulb would disperse vaporized mercury into the room housing the microscope, creating a health hazard.

Finally, laser light sources of several types are coupled to confocal scanning microscopes. They produce an intense monochromatic light, which is necessary to produce sufficient signal when collecting images point by point from specimens. True color cannot be recorded by these microscopes, but false colorization of the computer-derived images is often used to produce color images.

VI. TYPES OF OPTICAL SYSTEMS

Compound light microscopes used to look through specimens are available as upright microscopes traditionally used to examine histological slides and as inverted microscopes designed to look through the bottom of culture dishes and flasks. Bright-field microscopes that can perform dark-field analyses with a simple condenser change are the most commonly encountered light microscopes. Phase-contrast and DIC microscopes are utilized extensively by microbiologists and other investigators looking at unstained materials with little inherent contrast. Most microscopes can be easily adapted to polarization sufficient to demonstrate oriented fibers, crystals, or other anisotropic substances within samples by the addition of a polarizing filter in the light path preceding the specimen, and another polarizing filter located above the objectives. Epifluorescence microscopy capabilities can be coupled to most bright-field microscopes with the addition of an arc lamp assembly with a dedicated power supply, a light tube to direct light through the light microscope objectives, and a set of filters to narrow the bandwidth of the light needed to

excite various naturally fluorescent materials in specimens or fluorochromes incorporated into the samples. Finally, confocal scanning light microscopes that scan a beam of light across a sample can be used to collect images from a very narrow plane of section within a specimen and achieve levels of resolution with fluorescence microscopy techniques that are not possible with standard epifluorescence microscopes.

A. Bright-Field Microscopes

These microscopes are the most widely used in biological light microscopy and can be extremely inexpensive instruments if they are used only to view specimens, without any intention of recording images. An inexpensive basic bright-field microscope used to observe, but not record, images of samples can be purchased for approximately $2,000. However, a bright-field photomicroscope with a motorized condenser assembly and nosepiece, along with autofocus and multiple output ports, can cost upwards of $75,000. The difference in cost between these two extremes represents increasing complexity in mechanical design and increased complexity in the optical components such as objectives, condensers and oculars, and filtration systems necessary to produce high-contrast, high-resolution images that are easily recorded through automated exposure and focusing systems standard with the high-end microscopes. In addition, the more expensive microscope stands are easily upgraded with the addition of a variety of different lighting systems, optical systems, and recording devices.

For photomicroscopy, a basic bright-field system with an automatic camera, a full set of semiapochromat plan lenses (4×, 10×, 20×, 40× and 100×), and an appropriate condenser assembly can be purchased for about $10,000–$15,000. The resolving power of such a system would be slightly lower than that available if equipped with plan apochromats. Microbiologists would probably need to add the expense of the plan apochromat objectives and matched substage condenser assembly to reach the level of resolution that they customarily need. One further point to consider is the fact that semiapochromat objectives actually exhibit higher contrast than apochromats. Unless a slightly higher resolution is a critical issue, semiapochromat lenses will probably do a better job than apochromats for most investigators. This represents a case where buying the best product may actually decrease the quality of the photographs produced, in terms of contrast.

Recommended options include a set of built-in neutral density filters that can decrease illumination intensity, primarily for viewing comfort, without changing color values in the specimen. Built-in color-balancing filters to bring the light source to the proper color temperature for daylight films (5,500° K) and tungsten films (3,200° K) are very useful if the light source is properly calibrated for their use. If a contemporary 12 V halogen light source is provided with 12 V (3,200° K), a Kodak 80A filter (blue), or equivalent, introduced into the light path allows the use of daylight color films. Tungsten-based films (T-64) can be used with no filtration. A green filter is recommended for black-and-white film work because it provides a monochromatic light in the middle of the visible spectrum that is in the most sensitive portion of the spectral sensitivity curve for most black-and-white films. In addition, the use of monochromatic green light eliminates any possibility of chromatic aberration and tends to build contrast in a typical hematoxylin- and eosin-stained histological sample because it accentuates its complementary color, red. Red areas (eosin-stained areas) in the specimen are shown in higher contrast to the bluish areas produced by the hematoxylin with the use of a green filter.

B. Dark-Field Microscopy

As mentioned above, dark-field microscopy can be achieved with a conventional bright-field microscope by adding a dark-field condenser assembly. On some microscopes, the substage condenser assembly is provided with a dark-field annulus that can be placed into the light path to allow dark-field work without changing condenser assemblies.

This optical method allows detection of objects such as bacterial flagella (0.02 μm in diameter) that are below the resolution limits of light optics (Slayter and Slayter, 1992). The dark-field stop occludes the central part of the cone of illumination (Fig. 256), such that the specimen is illuminated by a hollow cone of light. The oblique light rays that emerge from the condenser lens interact with the specimen, and those that are deviated by specimen structures then are collected by the objective lens and produce the dark-field image. Undeviated light rays cannot enter the objective lens and are subtracted from the specimen image. Thus, specimen structures appear as bright areas against a black background. For *dark-field microscopy, immersion oil needs to be put between the top lens of the condenser assembly and the bottom of the microscope slide.*

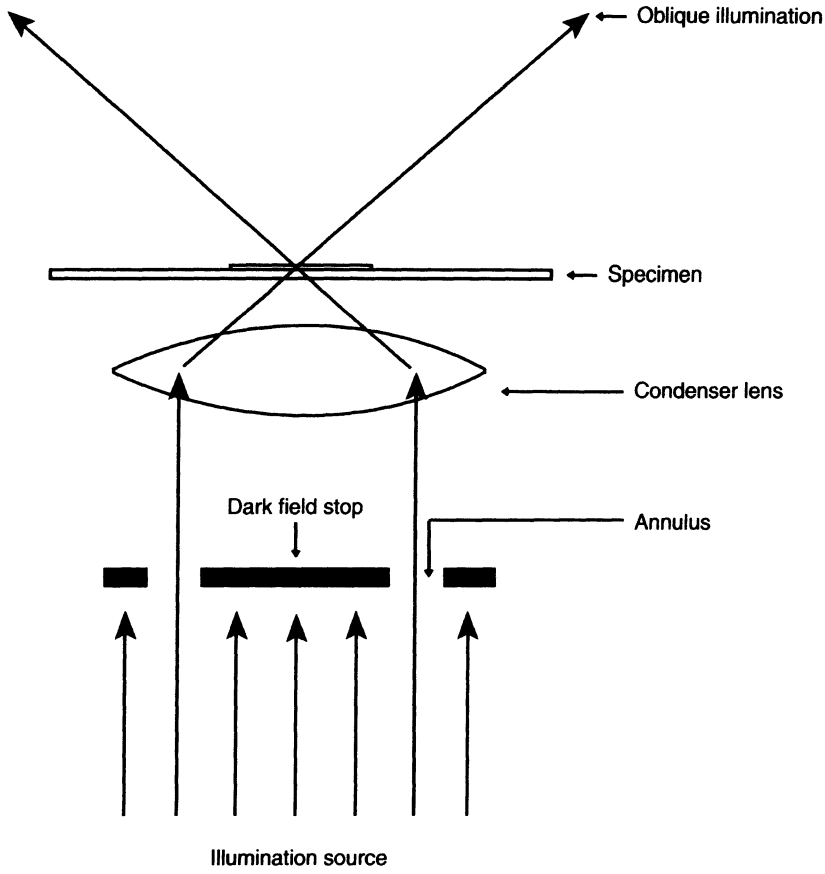

Figure 256. A dark-field condenser. The condenser has a central opaque disk, allowing only oblique rays of light passed by the annulus to interact with the specimen.

C. Phase-Contrast Microscopy

As explained by Delly (1988), phase-contrast microscopy provides contrast to specimens with little inherent contrast by producing interference between light rays. If a ray of light from a single point source is split into two light rays, and both are then passed through the same medium, they can be recombined without interference because the respective peaks and valleys of the waveform will coincide with each other. However, if the two light rays are passed through media of different refractive indices, their relative speeds will change. The difference in speed between the two rays may result in their being out of phase when recombined. When the phase differences are less than one wavelength, a decrease in illumination intensity is observed. If one light ray is exactly one half wavelength out of phase with the other, the peak and valleys of the two wave forms will cancel each other out, causing extinction of the illumination.

A set of annular apertures are located in the condenser assembly. These annular apertures must be matched to phase-contrast objectives containing complementary phase plates (Fig. 257). The phase plate in an objective has an annular groove that is visually superimposed over the annular aperture in the condenser assembly by looking through the microscope with an ocular removed and moving the condenser assembly adjusting screws until the groove and aperture are coincident (Fig. 258). Once that relationship is established, the oblique illumination provided by the annular aperture which is undeviated by the specimen passes through the annular groove, which typically retards the light rays one quarter of a wavelength. At the same time, the light rays deviated by interactions with the specimen will pass through the phase plate in locations other than at the annular groove. Because the rest of the phase plate is thicker and has different coatings on it than the annular groove, the light rays deviated by the specimen will be retarded more than those light rays that remain undeviated by specimen interactions and subsequently pass through the

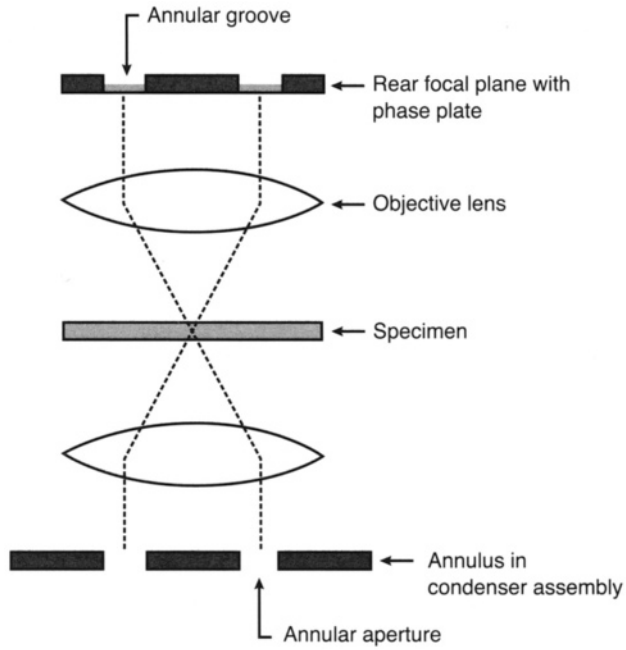

Figure 257. Optical elements in a phase-contrast microscope.

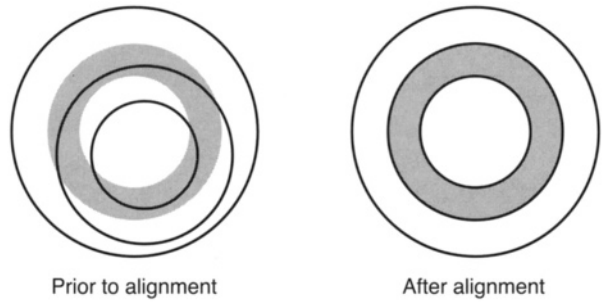

Figure 258. Alignment of the phase plate and the phase annulus with a phase-contrast microscope.

annular groove on the phase plate. Thus, the undeviated light ray speeds up relative to the deviated light rays that pass through the thicker portion of the phase plate after specimen interactions. When the difference between the deviated and undeviated light rays is 180° out of phase, the specimen details will appear dark due to extinction of the illumination, and the enhanced specimen contrast makes the detail of an unstained sample more apparent (see Slayter and Slayter, 1992). Spurious haloes around the specimen details are common (Fig. 259).

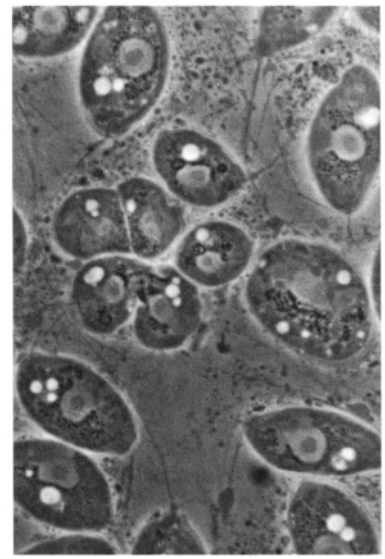

Figure 259. Phase-contrast photograph of the protozoan, *Sorodiplophorys stercorea* taken with a 100× oil objective.

D. DIC Microscopy

As succinctly described by Abramowitz (1987), DIC systems as developed by Nomarski employ a polarizing filter to produce light vibrating only in a plane perpendicular to the direction of the light beam. This light is passed through a modified Wollaston prism that splits the light beam into two rays perpendicular to each other. The two light rays then pass through the condenser

lens and emerge as two parallel beams that are extremely close together but have a slight path difference. The shear, or distance between the two rays, is below the resolving capabilities of the objectives. The split beam then enters the specimen, and the two beams are deviated according to their interactions with specimen features. The two beams of light altered individually by their interactions with the specimen pass into the objective in use and then are recombined with the beam-combining modified Wollaston prism above the objectives. The light beams then pass through another polarizing lens (the analyzer). When the two beams of light with slightly different path lengths are recombined by the modified Wollaston prism and brought into the same plane and axis by the upper polarizing lens, differential interference occurs between the formerly independent beams of light. Differences in light intensity or color seen are dependent on variations in refractive indices and/or specimen thickness. When the upper prism is set to produce the grayest image, the most evident three-dimensional view of the specimen is provided (Fig. 260). Rotating the specimen 180° can turn areas perceived as raised to areas that seem to be depressed.

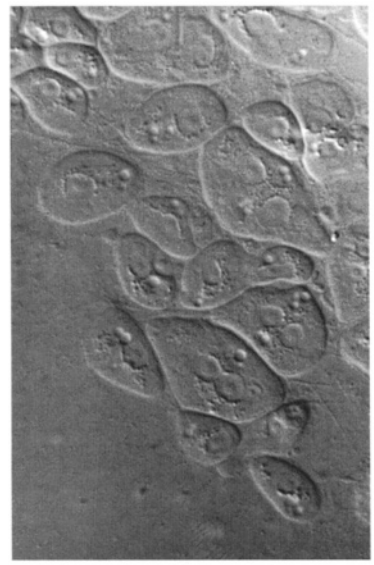

Figure 260. Nomarski interference (DIC) photograph of the protozoan, *Sorodiplophrys stercorea* taken with a 100× oil objective.

E. Epifluorescence Microscopy

Epifluorescence microscopy utilizes a high-intensity light source to excite primary, or autofluorescent, materials in a specimen and areas containing fluorescent dyes such as fluorescein isothiocyanate (FITC), resulting in secondary fluorescence. Two types of light sources are used: high-pressure mercury vapor arc lamps that produce light in the ultraviolet to short blue wavelength area of the spectrum, and xenon arc lamps that produce light across the visible spectrum as well as ultraviolet light (Abramowitz, 1993). These high-intensity light sources are needed to produce adequate fluorescence for imaging, since the majority of the light impinging on the specimen is lost to the imaging process.

Modern epifluorescence microscopes (Fig. 261) conduct light from the light source through an excitation filter that limits the wavelength of light reaching the specimen (Table 28). The light passed by the excitation filter then passes down through the objective and interacts with the specimen. Those illuminated areas containing fluorochromes or exhibiting autofluorescence will emit fluorescent light in all directions, some of which will be collected by the objective and transmitted through a barrier filter that passes the emitted light, but not the original transmitted, or excitation, light. The filtered emitted light is delivered to the ocular that subsequently projects the image to the eye or a suitable recording device.

There are four fundamental problems for epifluorescence microscopy. First, specimens exhibiting significant autofluorescence can obscure the signal from introduced fluorochromes. Second, fluorescent emissions from the specimen are many orders of magnitude dimmer than the

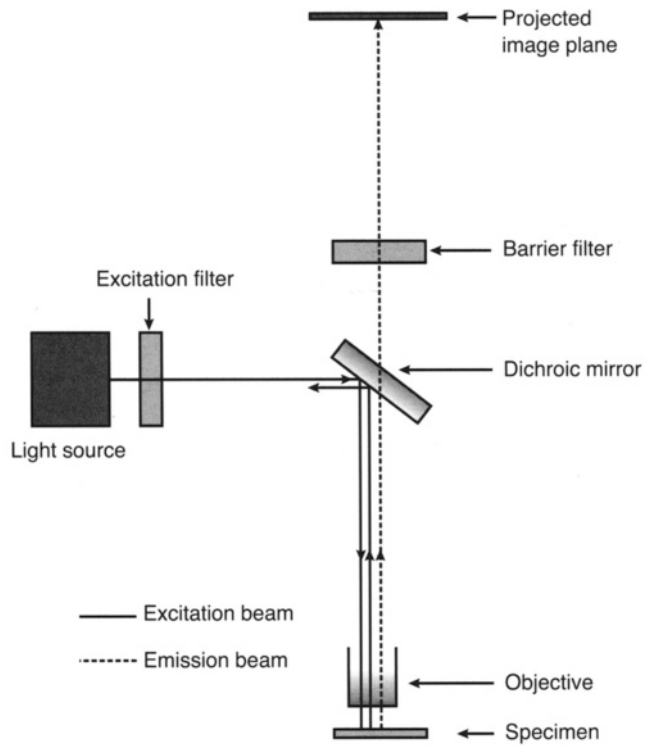

Figure 261. Optical elements of an epifluorescence microscope. (Redrawn from Rawlins, 1992, with permission of BIOS Scientific Publishers Ltd.)

Table 28. Common Excitation Filters and the Wavelengths Passed

Fluorochrome	Excitation (nm)	Emission (nm)	Color Observed
Fluorescein (FITC)	495	525	Green
Hoechst 33258	360	470	Blue
R-Phycoerythrin (PE)	488	578	Orange–red
Rhodamine (TRITC)	552	570	Red
Quantum Red	488	670	Red
Texas Red	596	620	Red
Cy3	552	570	Red

original illumination source, necessitating high-speed films and/or long exposure times for recording images. Modern cooled CCD digital cameras with high SNRs make recording of these low-luminance images easier in most cases. Third, fluorescent emissions in all directions from the source as well as emissions from areas of the specimen not in the plane of focus at higher magnifications can degrade the spatial resolution potential of the optical elements in the microscope. Confocal scanning microscopes have helped alleviate this problem by allowing very narrow planes of focus, eliminating the effects of out-of-focus fluorescence from above and below the imaged portion of the specimen. Fourth, many fluorochromes lose their capacity to fluoresce over time, particularly if illuminated with high levels of light typical of epifluorescent light sources. A variety of anti-quenching agents (Table 29) will lessen, but not eliminate, this phenomenon. In some cases, the rapid quenching of the signal (fluorescence) will make it difficult to record images from weakly emitting specimens because the length of time necessary to record sufficient signal will be hampered by the destruction of the fluorescence capacity of the specimen.

Table 29. Several Common Anti-Quenching Agents Available from Sigma Chemical Co. (St. Louis, MO)

Catalog Number	Name	Instructions for Use	Reference
P 3130	*n*-Propyl gallate	Used as a 0.1 M solution in 90% glycerol in PBS	
P 6001	*p*-Phenylenediamine, free base		*J. Immunol. Meth.* 43: 349–350 (1981)
P 1519	*p*-Phenylenediamine, dihydrochloride		*J. Immunol. Meth.* 43: 349–350 (1981)
D 2522	1,4-Diazabicyclo [2,2,2] octane (DABCO)	Added to mounting medium to 2.5% concentration	*Antibodies: A Laboratory Manual*, Harlow and Lane, Cold Spring Harbor (1988); *J. Histochem. Cytochem.* 33: 755 (1985)

Most epifluorescent microscopes are equipped with excitation filters capable of passing wavelengths of light (ultraviolet, blue, green) suitable for a variety of individual fluorochromes. Dichroic filters are interference filters that have coatings designed to reflect shorter wavelengths of light (e.g., ultraviolet light at 330–370 nm) used for excitation while transmitting longer wavelengths emitted by the excited fluorochromes, which are ultimately imaged. Most modern microscopes incorporate the exciter filter, dichroic filter, and barrier filter into single cubes for specified groups of fluorochromes.

F. Polarizing Microscopy

Polarizing filters are used to differentiate between isotropic substances with a single refractive index and anisotropic materials that have two or three principal refractive indices. When the azimuths of the polarized light being passed through two polarizing filters are parallel, the maximum amount of light is passed. When the azimuths of polarized light are perpendicular to each other, the polarizers are "crossed." This is also known as a position of extinction, and no light is passed unless it interacts with an anisotropic substance. Viewing isotropic materials with crossed polarizing filters shows a dark field, while anisotropic materials are revealed as illuminated areas (they exhibit birefringence). Examples of isotropic substances would be water, unoriented polymers, and the cytoplasm of cells. Anisotropic materials would include bone containing

crystallized calcium, asbestos fibers in lung sections, and cellular components consisting of oriented fibers such as mitotic spindles and cellulosic cell walls.

Polarizing microscopes can detect and then measure the amount of birefringence. As described in detail in Slayter and Slayter (1992), polarizing microscopes are used by crystallographers to determine the sign and type of birefringence of materials for analytical purposes. Most biologists examine materials only to detect birefringent areas. The more complex and expensive analyzers and polarizers needed for crystallographic analyses are generally not needed for biological work, and the addition of one fixed polarizing filter (analyzer) above the specimen and a rotatable polarizing filter located below the specimen will usually suffice. Limited budgets have led some labs to buy a pair of cheap plastic polarized sunglasses from which two pieces of the lens material are cut to serve as the analyzer and polarizer, respectively. The former is inserted somewhere above the nosepiece, and the latter is placed on the exit pupil for the light tube on the base of the microscope and rotated in relationship to the stationary analyzer. These less than optically perfect lenses generally would be contraindicated for photographic purposes, but they certainly work well for the diagnostic detection of birefringence in a specimen.

G. Confocal Microscopy

As alluded to above, confocal microscopy has greatly improved fluorescence microscopy because of its ability to image an extremely narrow plane within a specimen, while eliminating any spurious out-of-focus information from above and below the plane of section being viewed (Fig. 262). Numerous books and papers have been published concerning the physics, instrumentation designs, and applications of confocal microscopy. The books by Diaspro (2002), Inoué and Spring (1997), Kriete (1992), Paddock (1999), Pawley (1995), and Shotten (1993) are devoted to confocal microscopy or provide chapters with good treatments of the subject. In particular, the two major types of confocal instruments, laser scanning and Nipkow disk-based tandem scanning reflected light microscopes, are discussed by Inoué (1995) and Kino (1995), respectively.

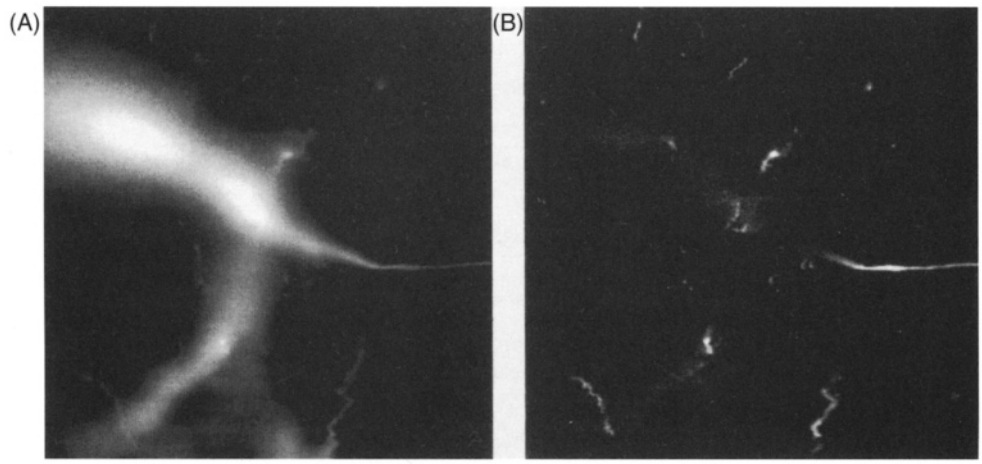

Figure 262. Comparison of an image of a fluorescently labeled neuron taken with an epifluorescence microscope (A) to an image of the same neuron taken with a confocal laser scanning microscope (B). In the epifluorescent image, both in-focus and out-of-focus areas of the specimen contribute to the image and degrade resolution. In the confocal image, only the in-focus areas are imaged, leading to greater resolution. (Image from Wallén *et al.*, 1992, with permission from VCH-Wiley Publishers.)

The original scanning reflected light microsope conceived by Nipkow in 1884 (Inoué, 1995) was based on a Nipkow disk with a series of square holes arranged in single series into an Archimedean spiral toward the center of the disk (Fig. 263). This was modified by Petran *et al.* (Kino, 1995) to produce a path consisting of interleaved Archimedean spirals (Fig. 264). Light is passed through holes in the spinning perforated disk and focused onto the specimen by the objective lens. The light reflected or scattered by the specimen is then focused by the objective lens onto a centro-symmetric portion of the disk (Inoué, 1995). The second set of pinholes exclude light originating from the specimen areas not illuminated by the first set of pinholes.

The real-time scanning optical microscope described by Xiao and Kino in 1987 (Kino, 1995) had a glass disk coated with a layer of specularly reflecting black chrome, which produced a narrow reflected light beam that was effectively eliminated with a light trap (Fig. 265). In addition, the input light was polarized, and then the light reflected by the specimen was passed through an analyzer (another polarizing filter) to further decrease illumination from the light source that was not contributing to image formation. The disk was rotated at 2,000 rpm, which produced up to 700 frames/sec containing 5,000 lines per image, if sufficient light intensity could be delivered. The images exhibited depth of focus characteristics comparable with the best mechanically scanned confocal laser images. Kino (1995) showed images of a rabbit eye examined with a 50 × water-immersion lens on his real-time scanning optical microscope that revealed endothelial cells 400 μm below the tear film.

Nipkow disk-based microscopes produce real-time images in true color, but since approximately 99% of the disk is opaque (Kino, 1995), a very strong light source (mercury arc lamp) is needed. In addition, the critical nature of alignment of the disk and the various optical elements make for a mechanically complex instrument that is expensive and difficult to maintain, compared with a confocal laser scanning microscope.

The most significant aspect of the confocal laser scanning microscope is the short depth of focus, which makes it well suited for optical sectioning of specimens. These microscopes produce a high illumination intensity and a better transverse definition and contrast than that possible with a conventional light microscope. The precise optical sectioning produced, along with computer-assisted assembling of the optical sections, allows three-dimensional reconstructions of samples

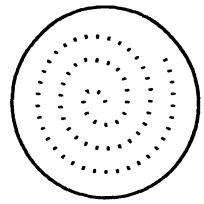

Figure 263. Nipkow disk. Note the single Archimedean spiral of holes.

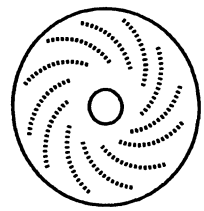

Figure 264. Modified Nipkow disk with interleaved Archimedean spirals of holes. (Redrawn from Kino, 1995 with permission from Kluwer Academic Plenum Publishers.)

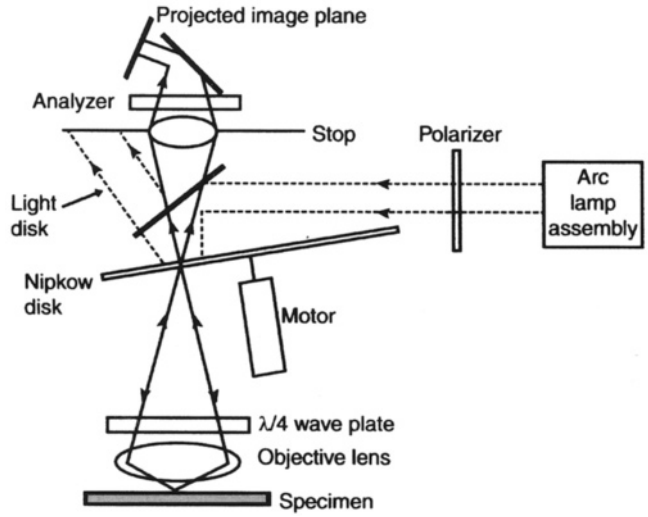

Figure 265. Optical components of a real-time scanning optical microscope. (Redrawn from Kino, 1995 with permission from Kluwer Academic Plenum Publishers.)

with a speed and accuracy previously unattainable. The major disadvantage for this instrument is that the point-by-point acquisition of the image results in a scan time too slow to produce an image allowing real-time viewing. In addition, the typical monochromatic laser light source prevents true color images of a specimen.

Confocal laser scanning microscopes either move the specimen stage relative to the light beam (stage or object scanning) or scan a light beam over the specimen (beam scanning). The latter type of instrument is the most commonly manufactured system on the market today because it can be adapted to virtually any microscope, is less expensive to manufacture than a stage-scanning system, and has fewer mechanical difficulties. With typical systems, the optical pathway is similar to that found in conventional epifluorescent microscopes. The scanned laser light source is delivered to the microscope via a fiber optic cable, and the images are stored as digital files that can be reassembled into three-dimensional images by software supplied by the manufacturer of the confocal laser scanning system.

In a typical confocal laser scanning microscope, a minute spot of laser light is scanned across the sample, with a pinhole placed conjugate to the spot being scanned, which eliminates any light originating from other areas on the specimen or from light scattered from within the optical system. The volume of the sample that is imaged point by point is around 0.02 μm^3 (Diaspro and Sheppard, 2002). This reduces the impact of out-of-focus light scattering and fluorescence, leading to much crisper images than with standard epifluorescence microscopy (Inoué and Spring, 1997). As explained by Diaspro and Sheppard (2002), one of the disadvantages to standard confocal laser scanning microscopy is that the whole section thickness within an hourglass-shaped region is affected by each scan, even if no image is collected from the out-of-focus regions. In practical terms, this means that three-dimensional imaging may be compromised because of photo bleaching of the fluorescent label in the sample within this hourglass-shaped region.

A variety of different laser light sources are currently available, and their characteristics and applications are thoroughly discussed by Gratton and vandeVen (1995). As they explain, there are two major classes of lasers, continuous-wave and pulsed, with a number of subcategories

in each. These different types of lasers vary widely in cost, power, stability, maintenance requirements, and breadth of wavelength produced (Table 30). Consideration of all of these factors will help to determine which laser package is most appropriate for an individual laboratory.

Table 30. Wavelengths Produced from Lasers Commonly Used for Confocal Laser Scanning Microscopy (Gratton and vandeVen, 1995)

Wavelength (nm)	Type of Laser
325 or 442	Helium–cadmium laser
351	Water-cooled argon laser with UV option
364	Air-cooled argon-ion laser
457–514.1	Small-frame argon-ion laser
543.5	Green helium–neodymium laser
630	External cavity semiconductor laser
630	Colliding pulse dye laser
632.8	Helium–neodymium laser
700–1,100	Titanium–sapphire laser
1,152	Helium–neodymium laser

REFERENCES

Abramowitz, M. 1987. *Contrast methods in microscopy. Transmitted light.* Olympus Corporation, Lake Success, NY.

Abramowitz, M. 1993. *Fluorescence microscopy. The essentials.* Olympus America, Lake Success, NY.

Abramowitz, M. 1994. *Optics, a primer.* Olympus America, Lake Success, NY.

Baldock, R., and Graham, J. (eds.). 2000. *Image processing and analysis. A practical approach.* Oxford University Press, New York.

Bradbury, S. 1991. *An introduction to the optical microscope*, rev. edn. Oxford University Press, Oxford.

Delly, J.G. 1988. *Photography through the microscope*, 9th edn. Kodak, Rochester, NY.

Diaspro, A. (ed.). 2002. *Confocal and two-photon microscopy.* Wiley-Liss, New York.

Diaspro, A., and Sheppard, C.J.R. 2002. Two-photon excitation fluorescence microscopy. In: A. Diaspro (ed.), *Confocal and two-photon microscopy.* Wiley-Liss, New York.

Gratton, E., and vandeVen, M.J. 1995. Laser sources for confocal microscopy. In: J.B. Pawley (ed.), *Handbook of biological confocal microscopy*, 2nd edn (pp. 69–97). Plenum Press, New York.

Inoué, S. 1995. Foundations of confocal scanned imaging in light microscopy. In: J.B. Pawley (ed.), *Handbook of biological confocal microscopy.* 2nd edn (pp. 1–17). Plenum Press, New York.

Inoué, S., and Spring, K.R. 1997. *Video microscopy. The fundamentals.* Plenum Press, New York.

Kino, G.S. 1995. Intermediate optics in Nipkow disk microscopes. In: J.B. Pawley (ed.), *Handbook of biological confocal microscopy*, 2nd edn (pp. 155–165). Plenum Press, New York.

Kriete, A. (ed.). 1992. *Visualization in biomedical microscopies. 3-D imaging and computer applications.* VCH, New York.

Paddock, S.W. (ed.). 1999. *Confocal microscopy. Methods and protocols.* Humana Press, Totowa, NJ.

Pawley, J.B. (ed.). 1995. *Handbook of biological confocal microscopy*, 2nd edn. Plenum Press, New York.

Rawlins, D.J. 1992. *Light microscopy.* BIOS Scientific, Oxford.

Shotten, D. (ed.). 1993. *Electronic light microscopy.* Wiley-Liss, New York.

Slayter, E.M. 1976. *Optical methods in biology.* Krieger, Huntington, NY.

Slayter, E.M., and Slayter, H.S. 1992. *Light and electron microscopy.* Cambridge University Press, New York.

Wallén, P., Carlsson, K., and Mossberg, K. 1992. Confocal laser scanning microscopy as a tool for studying the 3-D morphology of nerve cells. In: A. Kriete (ed.), *Visualization in biomedical microscopies. 3-D imaging and computer applications* (pp. 109–143). VCH, New York.

CHAPTER 18 TECHNIQUES

Köhler Illumination

1. Applications and Objectives

To achieve the highest resolution, maximum illumination, and even illumination required for excellent photomicrographs, it is necessary to focus the light source carefully onto the plane of focus of the specimen. *This procedure must be performed for each objective prior to photomicroscopy on any nonmotorized light microscope.* Motorized microscopes may have different procedures specified by the manufacturer due to the complexity of the condenser assemblies supplied.

2. Procedure

1. Focus the ocular(s) on the built-in or projected reticle image by turning the ocular exit pupil in reference to the ocular barrel.
2. Choose the objective desired and focus it on the specimen.
3. Close the field diaphragm located somewhere near the light exit port in the microscope base until the edges of the diaphragm blades become visible.
4. Find the knob that raises and lowers the condenser assembly, and adjust it up or down until the edge of the field diaphragm blades are sharp.
5. Center the field diaphragm image with the adjusting screws on the substage condenser assembly.
6. Open the field diaphragm until it is just beyond the field of view. If it is opened any wider, noninformational, widely scattered light from the condenser assembly may be captured by the objective, leading to *flare*, which can decrease image contrast.
7. For low-power objectives, typically 10 × or below, it is necessary to swing the front element of the substage condenser assembly out of the light path or to remove the substage condenser assembly completely in the case of some low-magnification objectives. Some inexpensive microscopes may have a supplementary lens below the substage condenser assembly that is moved into the light path to spread the light for full coverage of the field of view. When this is done, it may not be possible to effect proper Köhler illumination.
8. If dust appears at the plane of focus for the specimen following Köhler illumination, either clean the optics in the illumination system or defocus the condenser assembly slightly until the dirt is no longer focused in the same plane as the specimen image.

Use of the Substage Condenser Diaphragm

1. Applications and Objectives

Proper adjustment of the substage condenser diaphragm at low objective magnifications will enhance the depth of field and contrast in the specimen. At higher objective magnifications (40× to 100×), the aperture should be adjusted so that it does not impinge on the cone of light leaving the condenser assembly, since it would decrease the numerical aperture of the optical system, leading to decreased resolution. With most microscopes, decreasing the aperture diameter with objectives below 25× is recommended to increase contrast, since contrast is a more critical issue than resolution at lower magnifications. If the substage condenser is closed down to too small a diameter, diffraction will cause the specimen image to become unacceptably grainy.

2. Procedure

After Köhler illumination is set up as described above, remove an ocular and close the substage condenser diaphragm located in the condenser assembly until it is about a quarter to a third of the way into the field of view. Replace the ocular.

Focusing Using a Focusing Telescope (Bertrand Lens)

1. Applications and Objectives

At low magnifications, typically using a 10 × or lower objective, it can be difficult to see true focus. The human eye, particularly prior to the need for bifocal lenses, has a remarkably pliable lens that can be focused such that even out-of-focus images can be brought into satisfactory focus. At the same time, a camera attached to a photomicroscope has only one plane of focus. Thus, it is frequently useful to use a Bertrand lens to further magnify both the image of the reticle and the image of the specimen for critical focusing.

2. Procedure

1. Focus the Bertrand lens (focusing telescope) on some object at infinity, such as the bumps on concrete blocks at a distance of about 15–20 ft (4.6–6.1 m).
2. Place the focusing telescope on an ocular and refocus the ocular reticle image and then focus on the specimen. Avoid squinting, closing the nonfocusing eye, or focusing for too long a time, since straining can cause the eye to change focus, resulting in improperly focused photographs.
3. Take the photograph.

Using a Stage Micrometer and Ocular Scale to Measure Objects or to Calibrate Microscopes and Morphometry Programs

1. Applications and Objectives

It is often useful to be able to measure an object on a slide being examined, particularly in a diagnostic setting. For example, identifying narrow (5-μm-diameter) versus wide (10–20-μm-diameter) hyphae can help differentiate between "higher" and "lower" fungi seen in histological sections and thus help determine which type of antifungal therapy would be dictated to treat the infection in humans and other animals.

A second application allows calibration of the microscope so that the magnification on the film plane is positively known or to calibrate each objective for a morphometry program so that the program can provide accurate morphometric assessment of linear measurements.

2. Procedures

Determining Final Magnifications at the Film Plane. A typical stage micrometer obtained from scientific supply houses consists of a glass slide containing a 2-mm scale marked off in 0.1-mm units, with the terminal 0.1-mm unit further subdivided into 10 units of 0.01 mm. Place the stage micrometer on the photomicroscope stage, and photograph it with each objective and supplementary magnification lens on the microscope in all combinations possible. Develop the negatives and then use a loupe with a calibrated scale

(also available from scientific supply houses) to measure the photographed scale. Record the magnification factor for each lens combination so that all future negatives or 2 × 2 slides taken with specific lens combinations can be given a specific magnification factor from the chart you have created. For example, if the negative of the micrometer scale shows five markings that were originally 0.1 mm apart on the stage micrometer and the loupe scale shows the five marks to now span 1.0 mm, the magnification factor on film for that particular lens combination would be 2 × and would be recorded for that specific set of magnification lenses on your table.

Calibration of an Ocular Scale for Measuring Objects Being Viewed Live. Place a stage micrometer on the microscope stage and insert a micrometer scale (available from scientific supply houses) into the proper location for the specific ocular you have, such that the scale is in sharp focus. Ramsden oculars will have a ring to hold the scale below the lowest glass element, while a Huygenian ocular will have a ring to locate the scale between the two glass elements of the ocular. For each objective lens, record the number of lines in the ocular scale that span a known distance on the stage micrometer. Divide the known distance on the stage micrometer by the number of lines in the ocular scale that covers the distance to determine the distance measured between two lines on the ocular scale. Thus, if six lines on the ocular scale fall on or between the beginning of the scale on the stage micrometer and the 0.03-mm mark, each of two adjacent lines in the ocular scale spans 0.005 mm and should be recorded as such. If a fungal spore is observed with the same lens combination, and the spores touch two lines of the ocular scale, the spores are 5-μm in diameter (0.005 mm).

Calibration of Morphometry Programs. Turn on the microscope, digital camera, and computer to which the camera is attached. Place a stage micrometer onto the microscope stage and open the morphometry software. Find the calibration utility, which typically will specify that you focus on the stage micrometer with a given objective, and then open the calibration utility. From there, select fixed end-points on the stage micrometer scale, put a calibrating line across them, and enter the distance spanned into the program, along with a designation for the objective in place when the measurement was performed. After this is done for all of the objectives on the microscope, the program will typically provide a look-up table from which you would select the appropriate objective being used (e.g., 10 ×) before future morphometric measurements are taken or scale bars produced for inclusion in images stored by the morphometry program. Unless the software, camera, or objectives are replaced, these measurements will be accurate for all future morphometric work.

Reading an Objective Lens

1. Applications and Objectives

Manufacturers provide several critical pieces of information on the barrels of their objectives. Knowing how to decipher their inscriptions will ensure that an objective can be used to its best advantage.

2. Procedure

Look at the inscriptions on the lens barrel. The following information will be noted:

1. *Apochromat*, or *apo*, means that the lens is color-corrected for three or four colors. As mentioned in the main text of this chapter, these lenses are the most expensive and have the highest numerical apertures, the least working distance, and the lowest contrast. *Semiapochromat*, or

some designation with *fluor* incorporated, indicates fluorite lenses and means that the lens has an intermediate numerical aperture, working distance, and color correction, and gives good contrast. *Achromat*, or *achro*, identifies the least expensive category of objective, with the greatest working distance, least color correction, and the lowest numerical apertures.

2. *Plan*, or *plano*, designates a flat-field objective suitable for photomicroscopy, since the edge-to-edge flatness of the field of view is critical to good photomicrographs. This designation can be associated with all three classes of lenses above.
3. An objective inscribed with *160/-* or *160 NC* indicates a lens meant for a microscope with a 160-mm mechanical tube length that focuses the image of the specimen 160 mm from the nosepiece surface to which the objective is attached. The "-" or NC designation indicates that a coverglass is not needed to produce a good image. The marking *160/0.17* means that the lens is meant for a microscope with a 160-mm tube length and that a #1.5 coverglass (nominally 0.15–0.18 mm thick) is needed over the specimen to produce sharp images. Finally, an inscription of an infinity symbol indicates an infinity optic that focuses the image at any distance beyond the point where the tube lens focuses the image.
4. *OEL*, or *oil*, indicates that the lens should be immersed in immersion oil, while *W* indicates the lens is intended for immersion in water. Some lenses meant for dedicated fluorescence microscopy have the latter designation.
5. The numbers *1, 10, 25, 40, 100*, and so on, with or without *X* indicate the magnification provided by the objective. Remember that the final magnification of the image is dependent on the objective, any tube lenses present, any internal "photo" lenses, and the specific ocular, if any, projecting the image onto the recording instrument. *The magnification factor of viewing oculars has no effect on the magnification of recorded images in the microscope.*
6. Designations such as *PH* or *Phaco* indicate a lens containing a phase plate for phase-contrast microscopy. Reading the objective shown in Fig. 266 indicates that it is a phase-contrast objective meant to be used with the #3 phase annulus in the substage condenser assembly (PHACO 3). In addition, the lens is a semiapochromat lens (FLUOTAR), is meant to be used on a microscope with a 160-mm tube length and with a #1.5 coverglass (160/0.17), and magnifies 100 × with a numerical aperture of 1.32 and must be used with immersion oil (100/1.32 OEL).
7. Finally, numbers such as *0.32, 1.25*, and *1.4* indicate the numerical aperture of the lens, which helps the user determine how critical coverglass thickness will be to image quality. High-numerical-aperture dry lenses demand the coverglass thickness designated on the lens barrel. Knowing the numerical aperture of a high-resolution objective helps a user to make sure that the condenser assembly is properly matched to the objective. *If the numerical aperture of the objective lens is greater than that of the front element of the condenser assembly, the resolution will be limited by the lowest numerical aperture found in the optical system.* In other words, if a 0.9 NA condenser lens is used with a 1.4 NA objective, the actual numerical aperture for the optical system would be 0.9.
8. A high-dry lens with a movable collar and numbers from approximately 0.11 to 0.23, with a line scribed onto the stationary portion of the objective barrel, can be adusted for various coverglass or specimen thickenesses. Figure 267 shows a variable-focus flat-field 40× apochromat (SPlanApo 40) objective with a numerical aperture of 0.95 (0.95), meant for a microscope with a 160-mm tube length and coverglass thicknesses from 0.11–0.23 mm (160/0.11–0.23).

Use of Focusing Collars on High Dry (40×) Objective Lenses

1. Applications and Objectives

The proper use of these objectives allows adjustment of depth of focus for differing coverglass and/or specimen thickness.

Figure 266. A 100× semiapochromat phase-contrast objective intended for use on a microscope with a 160-mm tube length. The numerical aperture of the oil-immersion lens is 1.32, and the lens is meant to be used with a #1.5 coverglass.

2. Procedure

Examine the focusing collar on a lens so equipped and note that it will have a range of numbers printed on the barrel, with a reference mark above them. Typically, the range will be from about 0.1 to 0.2. These numbers refer to the thickness, in millimeters, of the coverglass to be used on the slide. A typical H&E preparation with a #1.5 coverglass attached with a Permount™ type of mounting medium over a xylene-cleared section should yield the sharpest images with the focusing collar set at about 0.16–0.17, since the #1.5 designation refers to a coverglass of approximately 0.15-mm thickness. However, some thicker preparations, such as a glycerin-mounted immunostained slide or a bone section will be significantly thicker. Using a 40 × dry lens without a focusing collar will make it unlikely that a sharp image can be obtained. With the focusing collar adjusted to somewhere around 0.2, a noticeably sharper image will be seen. *In addition, if the substage condenser diaphragm is closed down until diffraction is seen (the image becomes grainy) and then opened slightly until the graininess disappears, the image will potentially appear even sharper because this adjustment further increases contrast in the specimen, as well as increasing the depth of field.*

Using Oil- or Water-Immersion Objectives

1. Applications and Objectives

The purpose of immersion media is to decrease refraction of the light beam as it passes from one medium (air) into another (the glass slide), and then back into air before entering the glass of the objective

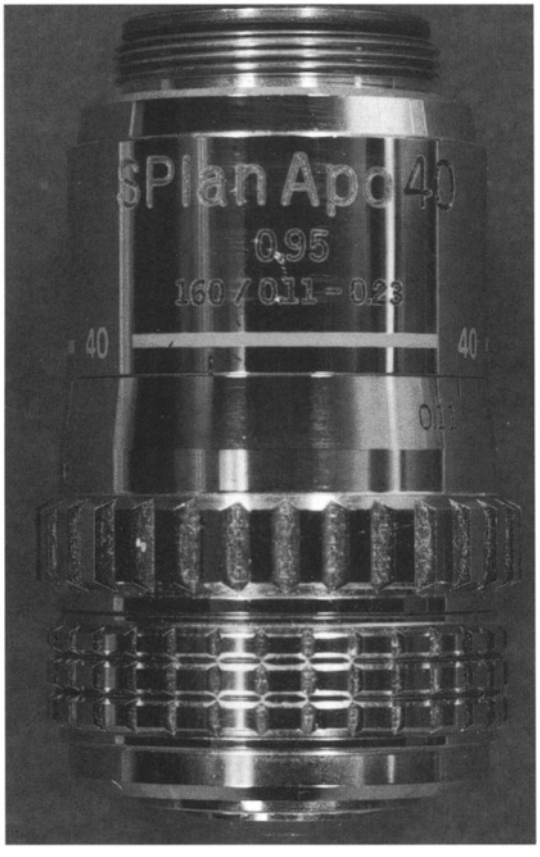

Figure 267. A flat-field 40× apochromat objective intended for use on a microscope with a 160-mm tube length. The numerical aperture of the lense is 0.95, and the high-dry lens may be used with #1, #1.5, and #2 coverglasses, as well as for specimens of various thickness. The focusing collar should be adjusted empirically for various specimens, until the image is as sharp as possible.

lens. This phenomenon decreases resolution. In addition, dark-field observation requires immersion oil between the condenser lens and the slide.

2. Procedure

A lens designated for use with water or oil, as described above, should have the appropriate liquid placed on the surface of the slide, with or without a coverglass, based on the designation after the mechanical tube length on the objective. The objective lens is then brought into contact with the liquid. *Do not allow these liquids to come into contact with objectives designated for dry work.* Any lens with a NA above 0.95 should also have the immersion medium placed between the front element of the condenser lens and the bottom of the glass slide. If the condenser assembly has a numerical aperture of 0.95, it is not useful to put immersion media on the front element of the condenser assembly, since air limits the numerical aperture to 0.95.

Use of Filters with Black-and-White Films

1. Applications and Objectives

Filters can be used to increase the overall contrast in an image or to accentuate or diminish certain colors in the original polychromatic specimen as well as to improve the image quality by eliminating the effects of chromatic aberration.

2. Procedure

Filters are customarily placed over the exit port of the light tube in the base of a photomicroscope but may be placed in slots near the light housing and could be introduced above the objectives if a suitably shaped filter holder is available. When possible, filters should be placed slightly out of the plane of focus after Köhler illumination adjustments so that any minor imperfections, scratches, or dust are not focused in the plane of the image.

Green Filter. This filter delivers monochromatic light to the film, eliminating the possibility of chromatic aberration causing decreased resolution. Black-and-white films are typically most sensitive in the middle of the visible light spectrum (green). In addition, hematoxylin and eosin (H&E) preparations will develop added contrast with the use of this filter, since the complementary red of the eosin-stained areas will be enhanced with a green filter.

Filters of Other Colors. Colored filters diminish their own color in the specimen and accentuate the complementary color. In other words, a red filter will diminish the eosinophilic, or reddish areas in an H&E preparation, while enhancing the basophilic, or bluish areas. Semithin plastic sections stained blue with Toluidine Blue O will exhibit a greater contrast if photographed with complementary orange or yellow filters in place.

Neutral Density Filters. Neutral density filters will diminish illumination without altering the colors of a specimen. They are primarily used to diminish light levels to comfortable viewing levels for the microscopists. Most modern camera metering systems can take perfectly exposed photographs at essentially any illumination level set up on a microscope.

Use of Filters with Color Films

1. Applications and Objectives

Three classes of filters are used with color films: light balancing filters, color compensating (CC) filters, and neutral density filters.

2. Procedure

Light Balancing (Color Temperature) Filters. Unless the photomicroscope comes with specific filters designated for use with tungsten- and daylight-balanced films, it will often be necessary to expose several test rolls of film with various filter combinations until perfect exposures are obtained. Once the standard filter package that delivers images with proper color rendition is identified, it should produce consistent results with a halogen-based illuminator. As mentioned previously, glass light bulbs darken over time, dropping the color temperature of the light source, with resulting shifts in color rendition. If using an older photomicroscope, the state of the light bulb should be monitored regularly, and any darkening of the globe due to tungsten deposition should suggest that it is time to change the bulb.

Tungsten-balanced films such as Kodak T-64 Professional film are designed to be exposed with lights exhibiting a color temperature of 3,200° K, which is produced by a new glass tungsten bulb at its maximum rated voltage (6 or 12 V), or a halogen bulb of any age that is set at its maximum rated voltage (6 or 12 V). No filtration is required under such conditions. However, if this film is used under daylight or stroboscopic flash illumination conditions (5,500° K), an amber color must be added by a Kodak 85B filter, or equivalent, to decrease the color temperature to 3,200° K.

Daylight-balanced films such as Fujichrome 100 daylight, Ektachrome daylight, or Kodachrome are meant to be exposed under daylight or stroboscopic light conditions (5,500° K). If they are used with tungsten light (3,200° K), a blue Kodak 80 A filter, or equivalent, must be used to shift the color temperature from 3,200° K up to 5,500° K.

CC Filters. These filters come in varying densities of red, green, blue, cyan, magenta, and yellow. They can be used to compensate for minor color variations associated with lens coatings and other optical pieces (mirrors, prisms) within photomicroscopes. One Leitz microscope that was in our lab 20 years ago, and was probably 15–20 years old at the time, had optics that imparted a slightly greenish cast to color photographs. To correct the problem, a CCM (magenta) filter was used to diminish the green cast to the photographs.

Neutral Density Filters. As mentioned above, these filters are generally used to reduce illumination to comfortable levels for the microscopists, since the camera metering systems on modern photomicroscopes can cope with a wide variety of illumination levels and still take consistently exposed photographs. We have found that all neutral density filters are not created equal. Neutral density filters designed for photomicroscopy typically cost over $50 each, while neutral density filters to be screwed onto camera lenses can be purchased for less than half that amount. Unfortunately, our experience has shown us that inexpensive neutral density filters that appear to work well on cameras produce slight color shifts when used with photomicroscopes.

19

Laboratory Safety

It is a great testimony to the discipline of electron microscopy that our safety record is excellent. From the earliest days of biological electron microscopy, investigators have realized the toxicity and danger of the chemicals with which we routinely work, which include flammable liquids, potential carcinogens, strong oxidants, heavy metals, caustic substances, and skin and respiratory irritants. The industry has also made sure that the radiation generated from electron microscopes is shielded from the operator. In addition, even though we have all suffered minor cuts from the razor blades and glass from which we make glass knives, very few injuries necessitating hospital visits for stitches have occurred. We work with pressurized gas cylinders, extremely cold liquid nitrogen, hot plates, heated ovens, diffusion pumps, and equipment that can be a source of electrical shock hazard and injury from motor-driven belts, and so on.

This textbook has discussed safety issues throughout as they apply to the various techniques described. We are committed to conveying the concept that the laboratory setting provides exposure to a number of hazards. However, if common sense laboratory practices are followed, the laboratory should be no more dangerous in the short- or long term than any other workplace.

All chemicals should be treated as if they are toxic unless Material Safety Data Sheets (MSDS), available from suppliers, declares them harmless. The MSDS sheets should be maintained for each chemical within the laboratory, and all workers in the laboratory should be responsible for knowing the contents. Even though we work with many toxic chemicals, they are generally handled in small amounts, and the chance of personal injury is extremely small if the chemicals are properly handled, as suggested in the MSDS instructions. Hands and eyes should be protected at all times, and sinks for washing should be readily available as well as eye-wash stations and showers for major exposures. Spill and first aid kits should be provided within the laboratory and clearly marked. The Occupational Safety and Health Administration (OSHA) has published specific guidelines for the safe operation of workplaces (available from institutional administrations), including scientific laboratories. The guidelines mandate what manner of safety equipment should be present, what types of safety training need to be administered, and to whom it should be offered. All government, educational, and private laboratories are required to have a safety plan in place that describes how to deal with emergency situations.

It would be redundant to go into the broad principles of safety in an electron microscopy laboratory because of the federal regulations mandating compliance with the OSHA training rules. Sources of heat, cold, and electricity necessitate the same precautions that would be exercised in any workplace.

MSDS are available from all chemical suppliers today and should be requested whenever new chemicals are ordered. An overview of safety issues and chemical handling and disposal is offered in the books listed below:

Anon. 1981. *Prudent practices for handling hazardous chemicals in laboratories.* National Academy Press, Washington, DC.

Anon. 1983. *Prudent practices for disposal of chemicals from laboratories.* National Academy Press, Washington, DC.

Barber, V.C. and Mascorro, J.A. (eds.). 1994. *Electron microscopy safety handbook,* 2nd edn. San Francisco Press, San Francisco.

Matheson Gas Products. 1983. *Guide to safe handling of compressed gases.* Matheson Gas Products, Secaucas, NJ.

OSHA. 1990. Occupational exposure to hazardous chemicals in laboratories. *Code of federal regulations* (Vol. 55, No. 21).

20

General Sources for Information Concerning Microscopy

Throughout the text, various books and journal articles are listed. There are atlases on ultrastructure for insects, protozoans, fungi, mammals, and other organisms. The list below of journals and general books is not exhaustive but offers a starting point to begin researching questions about biological ultrastructure.

I. ATLASES

Beckett, A., Heath, I.B., and McLaughlin, D.J. 1974. *An atlas of fungal ultrastructure*. Longman, London.

Berner, T. (ed.). 1993. *Ultrastructure of microalgae*. CRC Press, Boca Raton, FL.

Fawcett, D.W. 1981. *The cell*, 2nd edn. W.B. Saunders, Philadelphia.

Ghadially, F.N. 1985. *Diagnostic electron microscopy of tumors*, 2nd edn. Butterworths, London.

Ghadially, F.N. 1997. *Ultrastructural pathology of the cell and matrix*, 4th edn in 2 Volumes. Butterworth-Heinemann, London.

Gunning, B.E.S., and Steer, M.W. 1975. *Ultrastructure and the biology of plant cells*. Edward Arnold, London.

Kessel, R., and Kardon, R.H. 1979. *Tissues and organs, a text-atlas of scanning electron microscopy*. W.H. Freeman, San Francisco.

Kurman, M.H., and Doyle, J.A. (eds.). 1994. *Ultrastructure of fossil spores and pollen: Its bearing on relationships among fossil and living groups*. Royal Botanic Gardens, London.

Lott, J.N.A., and Darley, J.J. 1976. *A scanning electron microscope study of green plants*. Mosby, St. Louis, MO.

Palmer, E.L., and Martin, M.L. 1988. *Electron microscopy in viral diagnosis*. CRC Press, Boca Raton, FL.

Rhodin, J.A.G. 1974. *Histology, a text and atlas*. Oxford University Press, New York.

Threadgold, L.T. 1976. *The ultrastructure of the animal cell*, 2nd edn. Pergamon Press, New York.

II. JOURNALS

There are numerous journals dealing with cell and molecular biology, with histochemistry and cytochemistry, with specialized tissues and groups of organisms, and with the physics of electron microscopy in addition to journals devoted to materials analysis. Those listed below comprise a short list of the most readily available journals that have the most concentrated focus on biological ultrastructure questions.

Acta Histochemica et Cytochemica
Biology of the Cell (Société Française de Microscopie)
Biotechnie and Histochemistry (Stain, before 1991)
Cellular and Molecular Biology
Histochemistry
Histochemistry and Cell Biology

Journal of Cell Biology
Journal of Cellular Biochemistry
Journal of Electron Microscopy (Japanese Society of Electron Microscopy)
Journal of Electron Microscopy Technique
Journal of Histochemistry and Cytochemistry
Journal of Structural Biology
Micron et Microscopica Acta
Microscopy, Microanalysis, and Microstructures (Société Française de Microscopie)
Structure
The Histochemical Journal
Ultramicroscopy
Ultrastructural Pathology

III. SOCIETIES

In the United States, the Microscopy Society of America (MSA) is composed of light and electron microscopists in both the biological and materials sciences. Numerous organismally oriented, or cyto/histochemically oriented societies also publish significant numbers of cytological papers. Membership in the MSA is encouraged, which allows the receipt of the MSA bulletin containing helpful technical hints and articles on ultrastructural techniques. The MSA bulletin also lists affiliated regional and state microscopy societies.

IV. NATIONAL RESOURCES (INSTITUTIONAL INSTRUMENTATION)

Some of the NIH Resources for IVEM[1]

Contact	Location	Name of Facility
Ms. Linda Batlin	Department of MCD Biology University of Colorado Boulder, CO (http://bio3d.colorado.edu/userinfo.html)	Laboratory for 3-D Fine Structure
M.H. Ellisman, PhD	Department of Neurosciences University of California, San Diego La Jolla, CA (http://ncmir.ucsd.edu/us.html)	National Center for Microscopy and Imaging Research
W. G. Jerome, PhD	Wake Forest University Baptist Medical Center Winston-Salem, NC (www.wfubmc.edu/research/micromed.html)	MICROMED
C. R. Jefcoate, PhD	EHS Center for Development and Molecular Toxicology University of Wisconsin-Madison Madison, WI (http://www.niehs.nih.gov/centers/fac-core/mad-fac3.htm)	Imaging Facility and Services Core

[1] Additional facilities can be located by accessing the website http://cimewww.epf.l.ch/EMYP/lab_ame.html.

21

Electron Microscopy Equipment and Supplies

Listed below are some of the suppliers, primarily in the United States, who can provide the products necessary for light and electron microscopy work. There are other suppliers, but this list will provide a starting point when in need of specific items.

I. EXPENDABLE SUPPLIES AND SMALL EQUIPMENT

BAL-TEC AG
Fohrenweg 16
FL-9496 Balzers
Principality of Lichtenstein
Tel: 423-388-1212
www.bal-tec.com

Electron Microscopy Sciences
321 Morris Road
Box 251
Fort Washington, PA 19034, USA
Tel: 800-523-5874
www.emsdiasum.com

Ernest F. Fullam, Inc.
900 Albany Shaker Road
Latham, NY 12110-1491, USA
Tel: 800-883-4024
www.fullam.com

Ladd Research
83 Holly Court
Williston, VT 05495, USA
Tel: 800-451-3406
www.laddresearch.com

Polysciences, Inc.
400 Valley Road
Warrington, PA 18976, USA
Tel: 800-523-2575
www.polysciences.com

Sigma Chemical Co.
P.O. Box 14508
St. Louis, MO 63178, USA
Tel: 800-325-3010
www.sigmaaldrich.com

SPI Supplies
P.O. Box 656
569 East Gay Street
West Chester, PA 19381-0656, USA
Tel: 800-242-4774
www.2spi.com

Ted Pella, Inc.
P.O. Box 492477
Redding, CA 96049-2477, USA
Tel: 800-237-3526
www.tedpella.com

II. LIGHT MICROSCOPES

Carl Zeiss MicroImaging, Inc.
One Zeiss Drive
Thornwood, NY 10594, USA
Tel: 800-223-2343
www.zeiss.com/micro

Leica Microsystems Inc.
2345 Waukegan Road
Bannockburn, IL 60015, USA
Tel: 800-248-0123
www.leica-microsystems.com

Nikon Inc.
Science and Technologies Group
Instruments Division
1300 Walt Whitman Road
Melville, NY 11747-3064, USA
Tel: 516-547-8500
www.nikonusa.com

Olympus America Inc.
2 Corporate Center Drive
Melville, NY 11747, USA
Tel: 800-446-5967
www.olympusamerica.com

III. ELECTRON MICROSCOPES

FEICO
7451 NW Evergreen Parkway
Hillsboro, OR 97124-5830, USA
Tel: 503-640-7500
www.feicompany.com

Hitachi High Technologies America
Electron Microscope Division
5100 Franklin Drive
Pleasanton, CA 94588-3355, USA
Tel: 800-227-8877
www.hitachi-hhta.com

JEOL USA, Inc.
11 Dearborn Road
Peabody, MA 01960, USA
Tel: 978-535-5900
www.jeol.com

LEO Electron Microscopy Inc.
One Zeiss Drive
Thornwood, NY 10594, USA
Tel: 800-356-1090
www.leo-usa.com

IV. DIAMOND KNIVES

Delaware Diamond Knives, Inc.
3825 Lancaster Pike
Wilmington, DE 19805, USA
Tel: 800-222-5143
www.ddk.com

DiATOME U.S.
P.O. Box 125
321 Morris Road
Fort Washington, PA 19034, USA
Tel: 215-646-1478
www.emsdiasum.com

Drukker Diamond Knives
Harris International
35 West 45th Street
New York, NY 10036, USA
Tel: 212-869-3037
www.harrisinternational.com

MicroStar Technologies Inc.
511 FM 3179
Huntsville, TX 77340, USA
Tel: 800-533-2509
www.microstartech.com

V. HIGH-VACUUM PUMPS

Alcatel Vacuum Products, Inc.
67 Sharp Street
Hingham, MA 02043, USA
Tel: 781-331-4200
www.alcatelvacuumus.com

BOC Edwards
Manor Royal
Crawley RH10 9LW, UK
Tel: 01293-603134
www.edwards.boc.com

DanVac, Inc.
P.O. Box 2592
Naperville, IL 60567-2592, USA
Tel: 630-355-8629
www.danvac.com

ULVAC Technologies, Inc.
401 Griffin Brook Drive
Methuen, MA 01844, USA
Tel: 978-686-7550
www.ulvac.com

Varian Vacuum Technologies
121 Hartwell Avenue
Lexington, MA 02421, USA
Tel: 781-861-7200
www.varianinc.com

VI. ULTRAMICROTOMES

Boeckeler Instruments, Inc. (formerly RMC)
4650 South Butterfield Drive
Tucson, AZ 85714, USA
Tel: 800-552-2262
www.boeckeler.com

Leica Microsystems Inc.
2345 Waukegan Road
Bannockburn, IL 60015, USA
Tel: 800-248-0123
www.leica-microsystems.com

MicroStar Technologies Inc.
511 FM 3179
Huntsville, TX 77340, USA
Tel: 800-533-2509
www.microstartech.com

VII. EQUIPMENT FOR CRYOTECHNIQUES

Available from various EM supply houses and:

BAL-TEC AG
Fohrenweg 16
FL-9496 Balzers
Principality of Lichtenstein
Tel: 423-388-1212
www.bal-tec.com

Boeckeler Instruments, Inc. (formerly RMC)
4650 South Butterfield Drive
Tucson, AZ 85714, USA
Tel: 800-552-2262
www.boeckeler.com

Gatan, Inc.
5933 Coronado Lane
Pleasanton, CA 94588, USA
Tel: 925-463-0200
www.gatan.com

Leica Microsystems Inc.
2345 Waukegan Road
Bannockburn, IL 60015, USA
Tel: 800-248-0123
www.leica-microsystems.com

MicroStar Technologies Inc.
511 FM 3179
Huntsville, TX 77340, USA
Tel: 800-533-2509
www.microstartech.com

VIII. SPUTTER COATERS AND VACUUM EVAPORATORS

Available from various EM supply houses and:

Anatech Ltd.
Hillcrest Plaza
90 New Athol Rd. Ste 4
Orange, MA 01364, USA
Tel: 800-566-9554
www.anatechltd.com

BAL-TEC AG
Fohrenweg 16
FL-9496 Balzers
Principality of Lichtenstein
Tel: 423-388-1212
www.bal-tec.com

Denton Vacuum
1259 North Church Street
Moorestown, NJ 08057, USA
Tel: 856-439-9100
www.dentonvacuum.com

Appendix A: Computing Micrometer Bar Sizes

Many journals request that internal micrometer bar references be added to electron micrographs to be published. The bars should be designed to be between 1 and 2 cm long. For example, if the final print magnification is 57,800 a line 57.8 mm long would represent 1 μm. Dividing the final print magnification by 1,000 will always give the line length, in millimeters, that would represent 1 μm. A 57.8-mm line would be too long, and a 5.78-mm line representing 0.1 μm would be too short, so it would be appropriate to make a line 11.6 mm and state in the figure legend that it represents 0.2 μm.

Another question that arises concerns determining the real size of an object in a photograph of known magnification. Divide the size of the object of interest in the print measured in millimeters by the print magnification to determine the true size of the object in micrometers. For example, if an object measures 30 mm in diameter in a photograph with a final magnification of 60,000, the true diameter of the object is 0.5 μm.

Appendix B: Calibrating the TEM and the SEM

I. TRANSMISSION ELECTRON MICROSCOPE

To calibrate the TEM, several commercially available size references may be purchased. Diffraction grating replicas with an array of parallel lines (2,160 lines/mm or 54,864 lines/in.) or crossed lines (2,160 lines/mm in both directions) can be photographed and the center-to-center distance between the lines measured on the negative. The size-determination procedure in Appendix A will then yield the actual magnified distance between the lines, which can be compared with that shown by the electron microscope magnification readout.

A suspension of catalase crystals spread on a Formvar-coated grid (or on sections, for an internal reference) and negatively stained will provide a lattice plane spacing of 8.75 and 6.85 nm, which can be photographed and measured as above.

Graphitized carbon may be purchased on grids to measure line-to-line spacing of 0.34 nm, which is the guaranteed resolution of most standard biological transmission electron microscopes sold today. Oriented gold crystals that have plane spacing of 0.204, 0.143, and 0.102 nm may be purchased on prepared grids for even more stringent resolution checking.

II. SCANNING ELECTRON MICROSCOPE

Polystyrene or latex spheres may be purchased from various electron microscopy supply houses in standard diameters from 0.085 to 1.091 μm. They can be attached to poly-L-lysine-coated coverglasses, air-dried, sputter-coated, and examined with the SEM. Photographing them at a specific magnification and then comparing the diameter calculated from measuring the photograph with the actual diameter specified by the manufacturer will establish the accuracy of the magnification readout of the SEM.

Appendix C: Materials and Methods Write-Up Suggestions for Standard TEM and SEM Preparations

The objective of the Materials and Methods section in publications is to provide the reader with sufficient information to duplicate the work. Writing up materials and methods sections for publications should provide a concise package of information that explains the critical details of the procedures used, with references where appropriate. At the same time, the reader should not be burdened with information about materials used that do not bear on the outcome of the study. For example, giving the brand name of a diamond knife used to cut sections is irrelevant. Any brand of diamond knife could be used to cut similar sections. By the same token, the type of ultramicrotome is not important. Similar sections could have been cut with any ultramicrotome. The type of electron microscope used might be relevant, but probably not, since all conventional TEMs produce relatively indistinguishable prints from a given specimen. However, if specialized techniques are employed that require an intermediate-voltage electron microscope, such as electron tomography, the class of instrument should probably be specified (e.g., "... images were recorded with a 400-kV IVEM."). However, the type of fixative used, the type of buffer (including molarity and pH), the type of dehydration agent, the poststaining methods, and the type of embedding resin can demonstrably alter the results of a study, and so should be described.

Examples of materials and methods sections for routinely processed TEM and SEM materials that include the necessary information are as follows.

I. MATERIALS AND METHODS FOR ROUTINE TEM PREPARATION

Tissues were excised, cut to 1-mm thickness in at least one dimension, and placed in 4F:1G fixative (McDowell and Trump, 1976) for 1 hr to several months at 4 °C. After two rinses in 0.1 M sodium phosphate buffer (pH 7.2), samples were placed in 1% osmium tetroxide in the same buffer for 1 hr at room temperature. Samples were then rinsed two times in distilled water, with subsequent dehydration in a graded ethanol series culminating in two changes of 100% acetone. Tissues were then placed in a mixture of Spurr (Spurr, 1969) resin and acetone (1:1) for 30 min, followed by 2 hr in 100% resin with two changes. Finally, samples were placed in fresh 100% resin in molds and polymerized at 70 °C for 8 hr to 3 days. Semithin (0.25–0.5 μm) sections were cut with glass knives and stained with 1% toluidine blue-O in 1% sodium borate. Ultrathin (70–90 nm) sections were cut with a diamond knife, stained with methanolic uranyl acetate followed by lead citrate, and examined with a transmission electron microscope.

References

McDowell, E.M. and Trump, B.F. 1976. Histologic fixatives suitable for diagnostic light and electron microscopy. *Arch. Pathol. Lab. Med.* 100: 405.

Spurr, A.R. 1969. A low-viscosity epoxy resin embedding medium for electron microscopy. *J. Ultrastruct. Res.* 26: 31.

II. MATERIALS AND METHODS FOR ROUTINE SEM PREPARATION

Tissues were excised and placed in 4F:1G (McDowell and Trump, 1976) fixative for 1 hr to several months at 4°C. After two rinses in 0.1 M sodium phosphate buffer (pH 7.2), samples were dehydrated in a graded ethanol series to 100% ethanol, at which time they were critical point dried with liquid CO_2. Finally, they were mounted on specimen stubs with colloidal silver, sputter-coated with approximately 20 nm of gold–palladium, and examined with a scanning electron microscope.

Reference

McDowell, E.M. and Trump, B.F. 1976. Histologic fixatives suitable for diagnostic light and electron microscopy. *Arch. Pathol. Lab. Med.* 100: 405.

Index